DESIGN ASPECTS OF THE HYDRODYNAMIC AND STRUCTURAL LOADING ON FLOATING OFFSHORE PLATFORMS UNDER WAVE EXCITATION

Atilla Incecik, B.Sc.

Submitted as a Thesis for the Degree of Doctor of Philosophy

Department of Naval Architecture and Ocean Engineering
Glasgow University, 1982

LIST OF CONTENTS

LIST OF FIGURES AND TABLES

CHAPTER 1:

Figure 1 shows the variation of geometries in some existing semi-submersible designs.

Table 1 illustrates the number of accidents involving floating platforms.

CHAPTER 2:

Figure 1 illustrates the wave and structure reference systems and the co-ordinates of motion displacements of a floating object.

Figure 2 illustrates the co-ordinates which are used in the source and Green functions.

Figure 3 shows the comparison of inertia and drag forces acting on a circular cylinder versus the ratio of wave height to cylinder diameter.

Figure 4 illustrates various regimes according to which wave forces are calculated.

Figure 5 illustrates the control and the member sufraces of a body placed in an unbounded fluid.

Figure 6 illustrates the cross-section of a submerged circular cylinder.

Figure 7 shows two circular cylinders placed in a stream.

Figures 8-19 show the interia coefficients of two closely situated cylinders versus the distance in between the cylinders.

Figure 20 illustrates the stream lines around a circular cylinder situated near to a wall.

Figure 21 shows the effect of a wall on inertia coefficients of a circular cylinder.

CHAPTER 2 (Cont'd)

Figures 22 and 22-A show the drag coefficients of circular cylinders situated in series (one behind the other).

Figure 23 shows the drag coefficients of circular cylinders situated side by side.

Figures 24-27 illustrate various methods of resolving the inertia and drag forces acting on an inclined circular cylinder.

Figure 28 illustrates stream lines due to the horizontal gradient of horizontal wave particle velocity.

Figures 29-32 show comparison of linear and non-linear theories for wave force calculations on surface piercing circular cylinders.

Figure 33 illustrates a cross-section of a circular cylinder on which second-order time independent forces are calculated.

Figure 34 shows the second-order time independent forces calculated on a submerged circular cylinder using the linear theory.

Figure 35 shows the second-order horizontal water particle velocities.

Figure 36 shows the second-order wave drift forces on a submerged circular cylinder.

Figure 37 illustrates oncoming and scattered wave potentials around a circular cylinder.

Figure 38 shows the variation of Bessel function of the first kind versus the ratio of cylinder diameter to wave length.

Figure 39 shows the variation of Bessel function of the second kind versus the ratio of cylinder diameter to wave length.

Figure 40 shows the variation of inertia coefficients versus the ratio of cylinder diameter to wave length.

CHAPTER 2 (Cont'd)

Figure 41 shows the wave inertia force on a vertical circular cylinder calculated using the diffraction theory.

Figures 42 and 43 show the comparison of wave forces calculated on the submerged circular cylinder using the linear and the diffraction theories.

Figure 44 shows the second-order time independent forces calculated on the submerged circular cylinder using the diffraction theory.

Figure 45 shows the comparison of second-order time independent forces calculated on the submerged circular cylinder using the linear and the diffraction theories.

Figure 46 illustrates a cross-section of a circular section on which second-order time dependent forces are calculated.

Figure 47 shows second-order time dependent forces calculated on the submerged circular cylinder using the diffraction theory.

Table 1 shows the coefficients of the series which represent Stokes' fifth-order oncoming wave potential.

CHAPTER 3:

Figure 1 illustrates the bottom of a vertical circular cylinder on which vertical wave acceleration forces are calculated using the strip-wise approach.

Figure 2 illustrates the wave, structure and member reference systems as well as co-ordinates of motion displacements of a floating object.

Figure 3 shows a cross-section of a circular cylinder in the member reference system.

Figure 4 illustrates continuous and intercostal members on a semi-submersible.

CHAPTER 3 (Cont'd)

Figures 5 and 6 illustrate identification of the joints in the case of more than one member passes through the same point.

Figure 7 illustrates the selection of the members which are to be used for correcting the wave loading calculations for covered-up areas.

Figure 8 illustrates the plane from which the structure is viewed.

Figure 9 illustrates the geometry and the main dimensions of the platform on which wave forces are calculated.

Figure 10 illustrates the space frame idealisation of the platform shown in Figure 9.

Figures 11 and 12 illustrate the space frame idealisation of the platform shown in Figure 9 from different view points.

Figure 13 shows the member reference systems on the members of the floating structure shown in Figure 9.

Figure 14 shows the distribution of wave loading on the nodal points of a twin circular hull design semi-submersible.

Figure 15 shows surge force per unit wave amplitude versus wave frequency.

Figures 16-A, 16-B and 16-C show Heave force per unit wave amplitude versus wave frequency.

Figure 17 shows Sway force per unit wave amplitude versus wave frequency.

Figure 18 shows Roll moment per unit wave amplitude versus wave frequency.

Figure 19 shows Yaw moment per unit wave amplitude versus wave frequency.

CHAPTER 3 (Cont'd)

Figure 20 shows Pitch moment per unit wave amplitude versus wave frequency.

Table I shows the member data to be provided as input to FILER.

Table II shows the joint data to be provided to FILER.

Table III shows the sample run of FILER.

Table IV illustrates the summary data produced by FILER.

Table V shows the sample run of BONES.

Table VI shows the sample run of WAVLOA.

Table VII illustrates the output data produced by WAVLOA.

CHAPTER 4:

Figure 1 illustrates displacement co-ordinates of an object oscillating in an unbounded fluid.

Figure 2 illustrates displacement co-ordinates of a circular cylinder oscillating in an unbounded fluid.

Figure 3 illustrates structure and member reference sustems as well as rigid-body velocity and acceleration components.

Figure 4 shows the geometry of a submerged horizontal circular cylinder oscillating in an unbounded fluid.

Figure 5 shows the added-mass values of a circular cylinder oscillating near to the free surface.

Figure 6 shows the measured values of inertia coefficients of various geometries oscillating near to the free surface in heave mode of motion.

Figure 7 shows the measured values of damping coefficients of various geometries oscillating near to the free surface in heave mode of motion.

CHAPTER 4 (Cont'd)

Figure 8 illustrates the space position vectors used in the calculation of rigid-body motion induced mass-inertia forces.

Figure 9 shows heave response per unit wave amplitude versus wave frequency for the semi-submersible model.

Figure 10 shows roll response per unit wave amplitude versus wave frequency for the semi-submersible model.

Figure 11 shows variation of phase angles between heave force and heave displacement.versus wave frequencies for the semi-submersible model.

Figure 12 shows variation of phase angles between roll moment and roll displacement versus wave frequencies for the semi-submersible model.

Figure 13 shows variation of magnification factors versus wave frequencies for the full scale semi-submersible design.

Figures 14-16 show variation of heave response per unit wave amplitude versus wave frequency for the full scale semi-submersible design.

Figure 17 shows variation of roll response per unit wave amplitude versus wave frequency for the full scale semi-submersible design.

Figure 18 shows variation of pitch response per unit wave amplitude versus wave frequency for the full scale semi-submersible design.

Figures 19-25 illustrate co-ordinate transformations.

CHAPTER 5:

Figure 1 shows the distribution of mass and loading along the ship length.

Figure 2 shows a floating structure on which structural response formulations are demonstrated.

Figures 3-17 illustrate plane frame representations of the structure shown in Figure 2 for the structural response formulations.

CHAPTER 5 (Cont'd)

Figures 18-20 illustrate a mass and a beam system which represents a single degree of freedom system.

Figure 21 illustrates two masses and a beam system which represents a two degrees of freedom system.

Figures 22-26 show idealised semi-submersible model for the calculation of structural response values under the dynamic loading.

Figures 27-28 illustrate a general view of two existing semi-submersible designs.

Figure 29 shows a general view of the semi-submersible model for structural response experiments.

Figures 30-32 show bending moment per unit wave amplitude versus wave frequency variations on the deck of a twin circular hulled semi-submersible model.

Figure 33 shows components of bending moment per unit wave amplitude versus wave frequency variations on the deck of a twin circular hulled semi-submersible model.

Figure 34 illustrates force-displacement relations on the beam.

Figure 35 illustrates force and displacement vectors of the beam defined in the member and in the structure reference systems.

Figures 36-37 show the structure used as an example for the demonstration of the stiffness method and the FRAN2 computer program.

Figure 38 illustrates a space frame representation of the semi-submersible model with bracing arrangements.

Figure 39 illustrates plane frame representations of the semi-submersible model shown in Figure 38 for the structural response formulations.

Figure 40 shows a general view of the semi-submersible model with bracing arrangements.

CHAPTER 5 (Cont'd)

Figure 41 shows bending moment per unit wave amplitude versus wave frequency variations on the deck of a twin circular hulled semi-submersible model with bracing arrangements.

Figure 42 shows axial force per unit wave amplitude versus wave frequency variations on the inclined bracing of a twin circular hulled model with bracing arrangements.

Figure 43 illustrates the geometry and the main dimensions of the full scale semi-submersible design.

Figure 44 illustrates the space frame representation of the full scale semi-submersible design shown in Figure 43.

Figures 45-49 show the structural response values versus wave frequencies on the strength members of the semi-submersible design shown in Figure 43.

CHAPTER 6:

Figure 1 shows the co-ordinates of the twin circular hulled semi-submersible model and the input data to program FLUID4A.

Figures 2 and 3 show the relation between drag and inertia coefficients.

Figures 4 and 5 show turbulence factors for circular cylinders.

Figure 6 shows roughness factors for circular cylinders.

Figures 7-9 show the drag coefficients of circular cylinders obtained from steady flow experiments.

Table 1 illustrates the hydrostatic characteristics of the twin circular hulled semi-submersible model.

Table 2 illustrates the overlay tree of program FLUID4A.

Table 3 summarises the units system used in the program FLUID4A.

Table 4 illustrates the output of the program FLUID4A.

APPENDIX 1:

Figure 1 shows general and detailed arrangements of twin circular hulled semi-submersible model for structural response experiments.

Figure 2 illustrates the general tank set-up for motion and structural response experiments.

Figure 3 shows strain-gauges on transverse beams.

Figure 4 shows strain-gauges on brass tubes.

Figure 5 illustrates the calibration of strain-gauges on the transverse beam of the semi-submersible model.

Figure 5-A illustrates the valibration of strain-gauges on the inclined bracings of the semi-submersible model.

Figures 6-9 show the wave, heave, roll, bending moment, and axial force amplitude variations versus time.

Table 1 illustrates the mass distribution of the twin circular hulled semi-submersible model.

Table 2 illustrates the structural properties of the twin circular hulled semi-submersible model.

Table 3 illustrates calculated and measured natural periods and damping coefficients in heave and roll modes of motion.

ACKNOWLEDGEMENTS

The research study reported in this thesis would not have been possible without the assistance of the members of the Department of Naval Architecture and Ocean Engineering at Glasgow University.

The author is deeply indebted to:

Professor D. Faulkner, Head of Department, for allowing him to carry out this research, and for his constructive guidance;

Mr. N.S. Miller, Acting Head of Department, for his continuous encouragement, stimulating discussions, and his tireless assistance with many aspects of the study;

Dr. A.M. Ferguson, Superintendent of the Hydrodynamics Laboratory, for making the tank testing facilities available to him;

Mr. M. Sharp and Mr. C. Bradley, for their continuous assistance during the development of the computer software routines;

Mr. R.B. Christison and Mr. J. Holmes, who constructed the model: Their skilful work enabled the experiments to run very smoothly;

Mr. T. Mellon, for providing him with well tried measuring systems;

Mr. D. Sinclair, who helped him during the rigging and calibration of the model;

the other members of the staff for very useful discussions on various matters associated with this study;

Miss I. Campbell, Secretary to the Head of Department, and to Mrs. M. Frieze for their excellent typing;

Mrs. A. McGowan and Mr. G. Kerr, for their careful tracing;

and to his wife, Janet, for her patient encouragement.

The author gratefully acknowledges the financial support for the N.A.T.O. Fellowship Programme, and the Marine Technology Directorate of the Science and Engineering Research Council, U.K.

DECLARATION

All the material presented in this thesis, unless it is otherwise stated, is the original work of the author.

SUMMARY

In this thesis an investigation into the wave loading, motion and structural response of floating offshore platforms is presented. The aim of the study was to develop an analysis procedure which could be applied by an offshore designer to various platform designs for accurate and safe calculations.

The investigation starts with a review of the basic hydrodynamic principles of wave loading on floating structures. In this part the effects of interference between the closely spaced circular cylinders, second-order forces, and the non-linear free surface conditions on load calculations are presented.

During the next part of the study, generalised calculation methods for circular cylindrical members of offshore platforms have been devised in order to determine the hydrodynamic and the structural loads under wave excitation. The wave and motion induced load calculations are also coupled with the structural analysis to predict the structural response of individual members of a floating platform. This load information provides basic input data for the accurate and safe determination of member scantlings.

The developed calculation procedures were implemented in various computer routines for practical applications. These methods were applied to model and full-scale semi-submersible designs for the determination of motion and structural response.

Finally, model tests have been carried out and the comparisons between the theoretical predictions and the test measurements are presented.

Chapter 1: INTRODUCTION

INTRODUCTION

The design and construction of floating offshore platforms for relatively calm waters started in the early 1960s. In the 1970s, with the discovery of oil and gas fields in the North Sea, a wide range of platforms (wide, that is, both in respect of underwater geometry and of column and bracing arrangements) was designed and built (Fig. 1). These structures, which were built for the purpose of drilling, production, storage, pipe-laying and installation of deck modules on fixed platforms, are operated in moderate weather conditions, and must survive most severe conditions.

During the early development of North Sea drilling activities, various investigators developed linearised methods to predict the motion response of semi-submersible type floating platforms. Details of these methods are given in References 1, 2, 3. The features common to all of these studies may be summarised as follows:

a) Airy wave theory is adopted. Amplitudes of wave and platform motions are assumed to be small so that linear hydrodynamic methods may be used. This assumption permits the linear superposition of the wave forces acting on the restrained structure due to the wave particle motions, and hydrodynamic forces acting on the structure due to the rigid-body oscillations of the structure in calm water. The relative motion concept is discussed in detail in References 4, 5, 6.

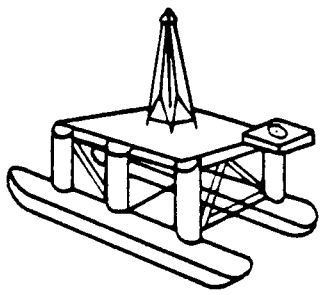

a

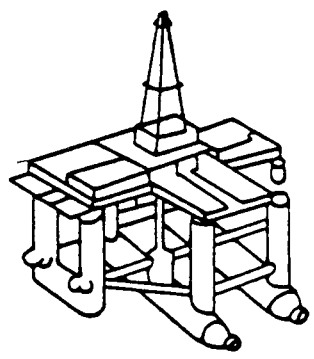

b

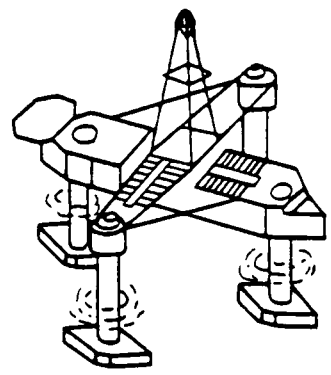

c

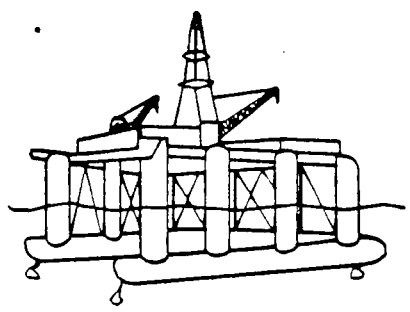

d

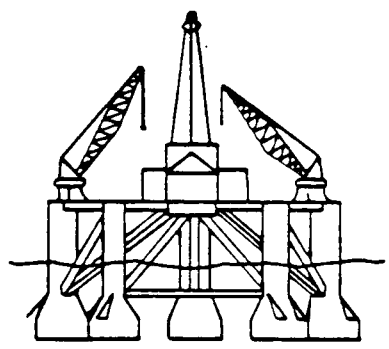

e

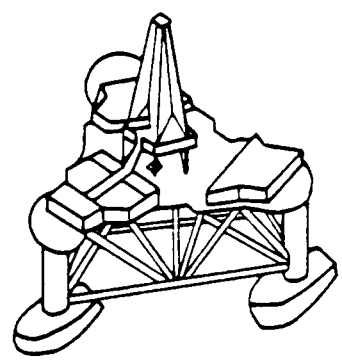

f

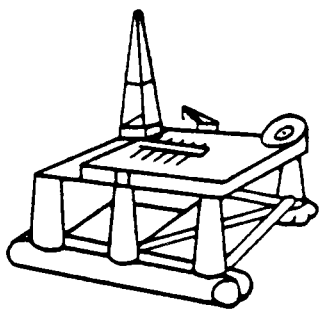

g

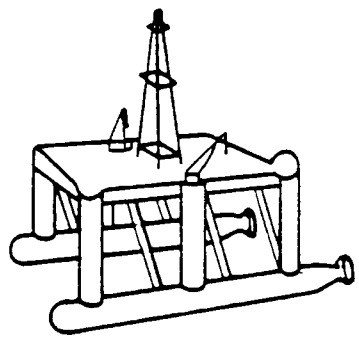

h

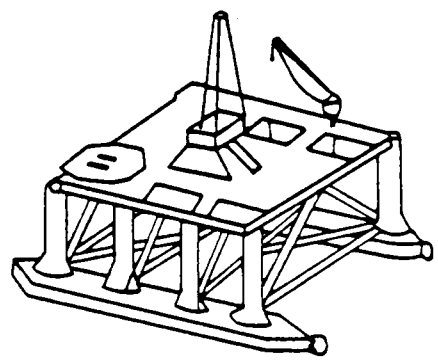

i

GEOMETRY OF SOME EXISTING SEMI - SUBMERSIBLES.

FIGURE 1.

b) Sectional dimensions of members of the floating structure are small compared to the wave lengths. The floating structure can be divided into small volume elements if the dimensions of these elements are less than about 1/5 of the wave length. The wave and motion induced forces can be assumed to be concentrated in the centre of these volume elements. If one of the dimensions of these volume elements is large compared to the wave length, the strip theory approach is adopted [4]. The wave and motion induced forces are calculated on each volume element, assuming that the rest of the structure is not present, in other words, the interference between the elements of the structure is not taken into account.

c) Since most of the volume elements of a floating structure are deeply submerged, the free-surface effects are neglected.

d) Hydrodynamic forces due to rigid-body velocity are linearised and the calculation methods derived in Refs. 2 and 3 neglect the wave forces due to wave particle velocities.

All these methods, reported in References 1, 2, 3, give a good estimation of the wave induced motions of semi-submersible type platforms.

Following the successful development of motion prediction methods, optimisation studies were carried out to find the best geometrical configurations from the point of view of minimum motion response [7,8,9,10,11].

Despite the significant progress achieved in the field of structural analysis with the development of various computer programs which were based on finite element methods, [12, 13, 14], there was not any agreed structural design philosophy to apply to this new generation of floating vessels. The wide range of structural arrangements in the existing designs (Fig. 1) indicates that insufficient interaction took place between the advanced fields of hydrodynamic and of structural analysis during the early development of floating platforms. The literature reveals that designers or classification societies carried out very refined finite-element analyses for a certain type of floating structure under loading conditions which are computed by poising the structure statically on a wave of a certain height and length [15]. (Wave length was usually taken to be half of the pontoon length and wave height corresponded to a significant wave height of in the area where the platform was operated).

As experience from the floating platforms operated in the North Sea gave evidence of the shortcomings in the design calculations, the need was felt for more rational design methodologies [16]. Towards the middle of the 1970s some large design and construction companies, as well as some classification societies, either sponsored research or in their own organisations initiated analytical studies in order to develop computational methods for the structural design of floating platforms [17,18,19,20,21 of chapter 5].

The features common to these new computational methods of structural analysis may be summarised as follows:

a) All members of the structure are assumed to deform in the elastic region under static and time-dependent quasi-static loading

b) The member forces are determined under static and time-dependent loading using finite element methods. The structure is usually represented with beam elements for the overall structural response analysis

c) The whole structure is analysed under time-dependent quasi-static loading to determine member forces in the frequency domain

d) These member forces are divided by the wave amplitudes to obtain the transfer functions which will be used for the statistical analysis. These transfer functions will be correct only if the member forces vary linearly with the wave amplitudes. This is largely true for the floating platforms which operate in most areas.

e) The transfer functions for each member are combined with the spectral characteristics of the operational environment of the platform to arrive at the member force and moment spectra for the critical locations of the structure

f) The response spectra for member forces and moments are analysed to obtain significant or extreme design stresses as well as the fatigue resistance of the joints. Details of the statistical analysis procedures can be found in References 21, 22 and 23.

g) Extreme design stresses on, and the fatigue resistance of, a member are compared with the existing design codes which take safety factors into account. These comparisons will enable the designer or the certifying authority to make the decision as to whether to retain the scantlings used throughout the design calculations or to modify the scantlings and repeat the calculations.

The conceptual philosophy for the overall structural response analysis, which is summarised above, can be accepted as a rational approach for the design calculations. The development of calculation routines based on this new structural analysis procedure was reported to be completed in late 1976 [24,25]. However, since they were the property of a small number of institutions, the calculation routines were inaccessible to a large group of designers who would have been able to understand and use them as design tools. On the other hand, these developed routines, as far as the author can conclude from the relevant published literature, were in any case restricted in use to design calculations on a limited range of geometry. The accidents involving floating platforms bear witness to the shortcomings of the developed design procedures [26,27]. Table 1, which was taken from Reference 27, shows the number of accidents, between 1970 and 1980, involving floating platforms in relation to the hydrodynamic and structural aspects.

As drilling activities are, in recent years, being extended to deeper waters and more hostile environments, it becomes

essential to develop and verify calculation procedures by merging the latest methods of hydrodynamic load calculations with the most modern and thorough structural analysis techniques. The calculation methods should be devised and documented in such a form that an offshore designer can successfully and safely apply them to different designs which may vary in geometrical and structural configuration, size and operational environment.

In this study an attempt is made to derive generalised calculation methods by which the hydrodynamic and the structural loading on a floating platform under wave excitation can be predicted.

The methods developed are suitable for use with any structural configuration which is composed of circular cylindrical elements.

Wave loading calculations are carried out for a model and a full-scale semi-submersible.

Model experiments were performed in order to compare the predictions of motion and structural response with the measurements.

TABLE 1

(From Reference 27)

FLOATING PLATFORMS						
Initiating Event	Structural Loss					SUM
	Total	Severe	Damage	Minor	No.	
Weather	3	10	22	17	8	60
Collision	2	2	11	18	12	45
Blow-out	5	7	9	7	6	34
Leakage	-	1	3	-	2	7
Machine, etc.	-	1	4	6	-	11
Fire(1)	1	2	12	12	-	48
Explosion(1)	-	2	4	6	-	12
Out-of-posit.	-	-	2	-	4	6
Foundering	1	-	-	-	-	1
Grounding	1	6	2	2	1	12
Capsizing	11	4	1	1	-	17
Structural Strength(2)	1	4	14	20	2	41
Other	-	-	-	8	10	18
SUM	25	40	84	97	45	291

Number of Accidents involving floating platforms operated world-wide during 1.1.1970-31.12.1980 (Records were obtained from Lloyd's Register of Shipping).

1) Fires and explosions occurring in connection with blow-outs do not belong to this category as the initiating event in this case is the blow-out.

2) This category includes structural failures that are not apparently indiced by rough weather or accidental loads. Hence accidents caused by a deficient structure belong to this category.

Chapter 2: WAVE LOADING ON CIRCULAR CYLINDRICAL MEMBERS OF OFFSHORE STRUCTURES IN DIFFERENT REGIMES

INTRODUCTION

This chapter summarises the methods used in the evaluation of wave loading on structures for different sizes of members on, or beneath the free surface. Throughout the report the geometry of circular cylinders is used for the numerical procedures and examples. At first, the general hydrodynamic problem is outlined and this is followed by a detailed analysis of the inertia and diffraction regimes. The analysis is primarily based on irrotational (no viscosity), incompressible potential flow theory. Allowances are made for small diameter members which give rise to the viscous forces. In addition, non-linear effects and the additional loading generated by linear potential are summarised and their importance in design calculations is shown.

1. BASICS OF THE HYDRODYNAMIC PROBLEM

Our concern is to estimate the wave loading on the cylindrical members of a structure which can be fixed or floating amongst the waves. In the simple case it may be assumed that the waves are plane progressive waves of small amplitude with sinusoidal time dependence. It is also assumed that the wave amplitude is sufficiently small to satisfy linearisation.

If the fluid motion is irrotational it was shown that the following relations exist between fluid particle velocity U(x,y,z,t) and a scalar potential which will depend on the three space co-ordinates (x,y,z) and times [1,2].

$$\vec{U} = \nabla\Phi(x,y,z,t) \ , \qquad \nabla = \frac{\partial}{\partial x}\vec{i} + \frac{\partial}{\partial y}\vec{j} + \frac{\partial}{\partial z}\vec{k} \tag{1}$$

where $\vec{U}$ denotes the velocity vector of the fluid, and

Φ denotes the velocity potential.

The time dependence of the fluid motion to be considered here is simple harmonic motion and therefore Φ may be expressed as:

$$\Phi = \mathrm{Re}[\phi(x,y,z,t)]e^{-i\omega t} \tag{2}$$

The mathematical condition specifying the incompressibility of the fluid is:

$$\nabla \cdot \vec{U} = 0 \tag{3}$$

If equation (1) is substituted in equation (3) the basic differential equation of irrotational, incompressible fluid is obtained:

$$\nabla^2 \Phi = 0 \tag{4}$$

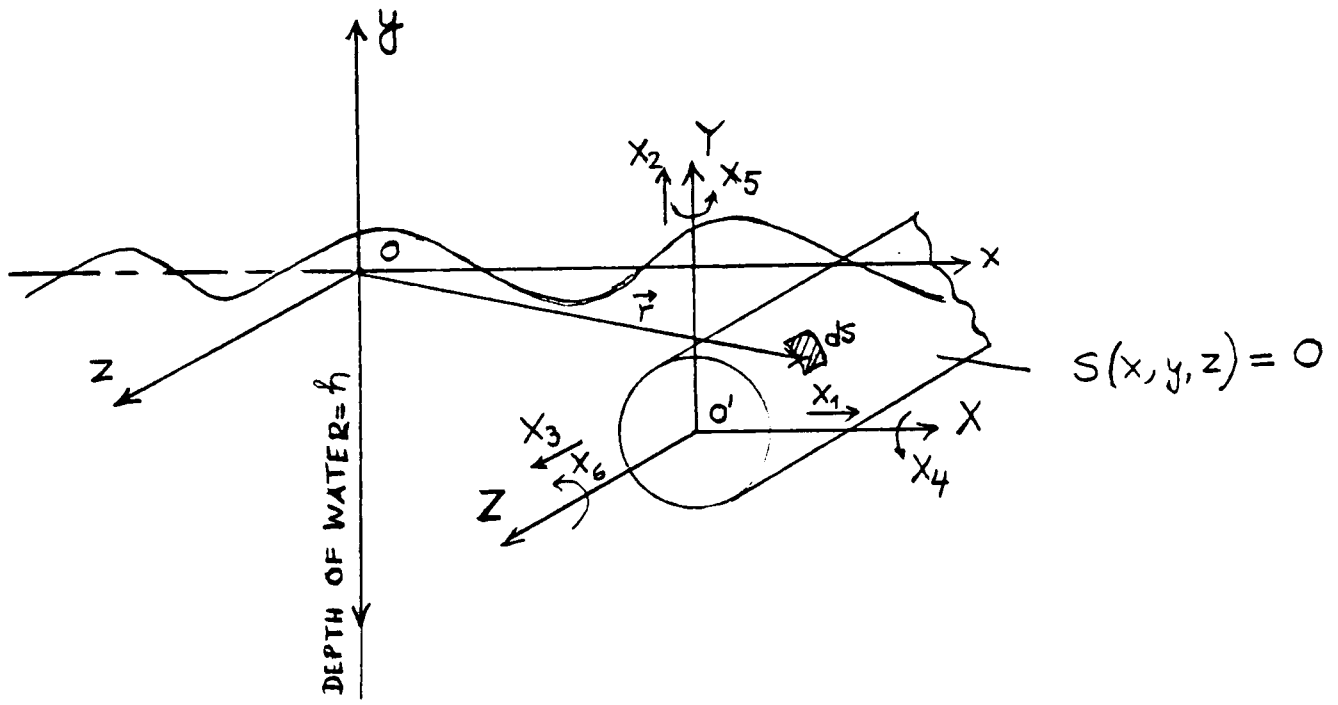

Fig. 1.

Since we assume that incident wave is sufficiently small in amplitude and the structure in the wave is stable, the resulting motions will be proportionately small. Then the velocity potential Φ for the floating structure amongst waves can be given as follows:

$$\Phi(x,y,z,t) = \mathrm{Re}\left\{\left[\underbrace{\phi_o(x,y,z) + \phi_s(x,y,z)}_{\phi_A} + \sum_{j=1}^{6} X_j \phi_j(x,y,z)\right]e^{-i\omega t}\right\} \tag{5}$$

or

$$\Phi(x,y,z,t) = \mathrm{Re}\left\{\left[\phi_A(x,y,z) + \sum_{j=1}^{6} X_j \phi_j(x,y,z)\right]e^{-i\omega t}\right\} \tag{5-A}$$

If the structure is fixed amongst the waves the velocity potential takes the following form:

$$\Phi(x,y,z,t) = \text{Re}\left\{\phi_A(x,y,z)e^{-i\omega t}\right\} \tag{5-B}$$

The first two terms in equation (5) are due to the incident waves and their interaction with the structure respectively. These potentials are independent of the body motions. The third term in equation (5) is due to the structure's rigid body motions in waves.

The velocity potential associated with an incident wave is given by:

$$\phi_o = -\,i\,\frac{0.5gH_w}{\omega}\,\frac{\text{Cosh}[k(h+y)]}{\text{Cosh}[kh]}\,e^{ikx} \tag{6}$$

for the deep water waves equation (6) becomes:

$$\phi_o = -\,i\,\frac{0.5gH_w}{\omega}\,e^{ky}\,e^{ikx} \tag{6-A}$$

On the surface of the structure elements the following boundary condition should be satisfied:

$$\frac{\partial\phi_A}{\partial n} = 0 \qquad \text{on} \qquad S(x,y,z) = 0 \tag{7}$$

where

$$\frac{\partial\phi_A}{\partial n} = \nabla\phi_A \cdot \vec{n} = \frac{\partial\phi_A}{\partial x}\,n_x + \frac{\partial\phi_A}{\partial y}\,n_y + \frac{\partial\phi_A}{\partial z}\,n_z$$

since

$$\phi_A = \phi_o + \phi_s \qquad \text{and} \qquad \frac{\partial\phi_A}{\partial n} = \frac{\partial\phi_o}{\partial n} + \frac{\partial\phi_s}{\partial n} = 0$$

$$\frac{\partial\phi_o}{\partial n} = -\,\frac{\partial\phi_s}{\partial n} \tag{8}$$

Equation (8) shows the kinematic boundary condition on the structure's surface.

In addition to the kinematic boundary condition given by equation (7) or equation (8) ϕ_s must also satisfy the following boundary conditions:

(a) Laplace equation:

$$\nabla^2 \phi_s = 0 \tag{9}$$

(b) Bottom boundary condition:

$$\frac{\partial \phi_s}{\partial y} = 0 \quad \text{at} \quad y \to -\infty \tag{10}$$

(or, at $y = -h$ for shallow water core)

(c) Free surface condition:

$$\frac{\partial \phi_s}{\partial y} - \frac{\omega^2}{g} \phi_s = 0 \quad \text{on} \quad y = 0 \tag{11}$$

(d) Radiation condition:

$$\lim_{r \to \infty} r^m \left(\frac{\partial \phi_s}{\partial r} - \frac{i\omega}{c} \phi_s \right) = 0 \tag{12}$$

where $m = (n-1)/2$ n: the number of dimensions

r : radial distance, $r = \sqrt{x^2+z^2}$

c : wave celevity, $c = \lambda/T$

It can easily be shown that the incident wave potential ϕ_o given by equation (6) satisfies the boundary conditions given by equations (9),(10) and (11).

The scattering potential, in the most general form, can be represented by a distribution of wave sources over the immersed surface of the structure using Green's function. The scattering potential function is given by Wehausen and Laitone [3] as follows:

$$\phi_s(x,y,z) = \frac{1}{4\pi} \iint_S f(\xi,\eta,\zeta)\, G(x,y,z,\xi,\eta,\zeta) \tag{13}$$

where $f(\xi,\eta,\zeta)$ represents the source strength,

(ξ,η,ζ) denotes a point on the surface of the structure,

$G(x,y,z,\xi,\eta,\zeta)$ shows Green's function, and

dS is the differential area on the immersed surface of the structure.

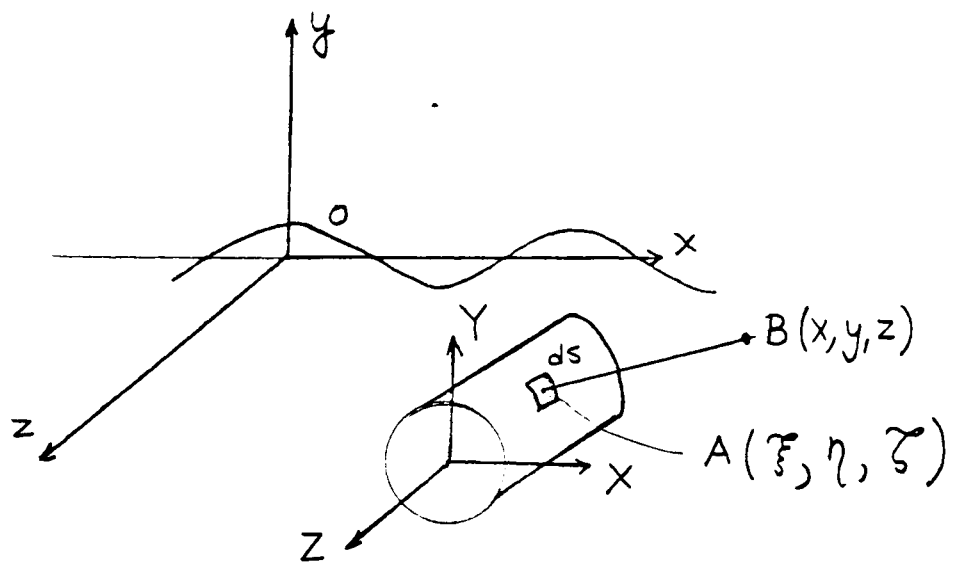

Fig. 2.

The Green function which satisfies the Laplace equation (9) is given by John [4] as:

$$G = \frac{1}{R} + G^* \tag{14}$$

where

$$R = [(x-\xi)^2 + (y-\eta)^2 + (z-\zeta)^2]^{\frac{1}{2}}$$

and

$$G^* = \frac{1}{R^1} + 2P.V. \int_0^\infty \frac{(\mu+\nu)e^{-\mu h}\,\mathrm{Cosh}[\mu(\eta+h)]\,\mathrm{Cosh}[\mu(y+h)]}{\mu\,\mathrm{Sinh}(\mu h) - \nu\,\mathrm{Cosh}(\mu h)} J_o(\mu r)\,d\mu$$

$$+ i\,\frac{2\pi(k^2-\nu^2)\,\mathrm{Cosh}[k(\eta+h)]\,\mathrm{Cos}[k(y+h)]}{k^2h - \nu^2h + \nu} J_o(kr)$$

(P.V. denotes the principal part of the above integration.)

where

$$\nu = \frac{\omega^2}{g} = k\tanh(kh), \quad R' = [(x-\xi)^2 + (y+2h+\eta)^2 + (z-\zeta)^2]^{\frac{1}{2}}$$

$$r = [(x-\zeta)^2 + (z-\zeta^2)]^{\frac{1}{2}}$$

An alternative form of the Green function in series form was given in reference [4] as follows:

$$G = \frac{2\pi(\nu^2-k^2)}{k^2h - \nu^2h + \nu}\,\mathrm{Cosh}[k(\eta+h)]\,\mathrm{Cosh}[k(y+h)][Y_o(kr) - iJ_o(kr)]$$

$$+ 4\sum_{m=1}^{\infty} \frac{(\mu_m^2+\nu^2)}{(\mu_m^2h+\nu^2h-\nu)}\,\mathrm{Cos}[\mu_m(y+h)]\,\mathrm{Cos}[\mu_m(\eta+h)]\,K_o(\mu r)$$

where J_o and Y_o are Bessel functions,

K_o modified Bessel function, and

μ_m is the real positive roots of the following equation.

$$\mu_m \tan(\mu_m h) + \nu = 0 \tag{16}$$

Equation (13) satisfies all the boundary conditions except the kinematic boundary condition on the immersed surface of the structure.

Substituting equation (13) into equation (8) and taking the integration around the source into account the following result is obtained:

$$-\frac{\partial \phi_o}{\partial n} = -\frac{1}{2} f(x,y,z) + \frac{1}{4\pi} \iint_S f(\xi,\eta,\zeta) \frac{\partial G}{\partial n}(x,y,z,\xi,\eta,\zeta)\, dS \tag{17}$$

From equation (6)

$$\frac{\partial \phi_o}{\partial n} = \frac{g0.5\ H_w k}{\omega} \left[n_y \frac{\text{Sinh}[k(y+h)]}{\text{Cosh}[kh]} + i n_x \frac{\text{Cosh}[k(y+h)]}{\text{Cosh}[kh]} \right] e^{ikx} \tag{18}$$

Finally the following Fredholm integration is obtained as follows:

$$-f(x,y,z) + \frac{1}{2\pi} \iint_S f(\xi,\eta,\zeta) \frac{\partial G}{\partial n}(x,y,z,\xi,\eta,\zeta)\, dS$$

$$= \frac{2g0.5\ H_w k}{\omega} \left[n_y \frac{\text{Sinh}[k(y+h)]}{\text{Cosh}[kh]} + i n_x \frac{\text{Cosh}[k(y+h)]}{\text{Cosh}[kh]} \right] e^{ikx} \tag{19}$$

Equation (19) may be solved numerically by subdividing the immersed surface into N panels and assuming the source strength $f(\xi,\eta,\zeta)$ remains constant over each panel. Numerical solution of this equation and estimation of ϕ_s are discussed in detail in reference [5].

Green's function method is very suitable in cases of complex geometries, and moreover for the definition of the flow field so as to be able to calculate wave forces on members of the structure taking the interaction between the members into account. It is worth noting that numerical solution of equation (19) to obtain ϕ_s takes up much computing time from the point of view of development, large storage space and it is quite costly to run.

Havelock [6] presented a scattering potential function as an infinite series using the polar co-ordinates diameter r, and angle θ for circular cylinder geometry in waves:

$$\phi_s(r,\theta,y) = -\frac{g0.5\ H_w}{\omega}\ \frac{\text{Cosh}k[y+d]}{\text{Cosh}(kd)}\ \sum_{m=0}^{\infty} A_m\ \text{Cos}m\theta\,[J_m(kr) + iY_m(kr)]e^{-i\omega t} \tag{20}$$

where A_m are numerical constants, and

$J_m(kr)$ and $Y_m(kr)$ are Bessel functions.

The application of equation (20) is given in Section 2.2 to calculate the wave forces on large diameter cylindrical members of offshore structures.

The last term in equation (5-A) $\phi_j(x,y,z)$ represents the velocity potential of a rigid body motion with unit amplitude in the absence of the incident waves. For example viz. Fig. 1, if the structure is forced to heave with unit amplitude in calm water, the resulting fluid field can be represented by potential $\phi_2(x,y,z)$. The appropriate boundary conditions can be obtained by equating the normal derivatives of the potential to the normal vector of the rigid structure velocity on the surface $S(x,y,z) = 0$:

$$\frac{\partial \phi_j}{\partial n} = i\omega n_j \qquad j=1,2,3 \tag{21}$$

$$\frac{\partial \phi_j}{\partial n} = i\omega(\vec{r}\wedge\vec{n})_{j-3} \qquad j=4,5,6 \tag{22}$$

In addition to the kinematic boundary condition on the body surface each potential ϕ_j should also satisfy the Laplace equation (9), the free surface equation (11) and the radiation condition (12).

The forced motion potentials ϕ_j can be obtained from the solutions of the radiation problem and they only depend on the structure geometry and the boundary conditions.

Having summarised the components of equation (5) we can easily achieve our main aim of the calculation of wave loading on the structure using Bernoulli's equation:

$$-\frac{1}{\rho}(p-p_A) = \frac{\partial\Phi}{\partial t} + \frac{1}{2}\nabla\Phi\nabla\Phi + gy \tag{23}$$

Substituting equation (5) into equation (23) the pressure can be obtained in terms of velocity potential:

$$\begin{aligned} p = \rho\omega\, \mathrm{Re}\Bigg\{ & \left[\phi_o(x,y,z) + \phi_s(x,y,z) + \sum_{j=1}^{6} X_j\phi_j(x,y,z)\right] ie^{-i\omega t} \\ & - \frac{1}{2}\left[\left(\frac{\partial}{\partial x}\left(\phi_o(x,y,z) + \phi_s(x,y,z)\right)\right)^2 + \left(\frac{\partial}{\partial y}\left(\phi_o(x,y,z) + \phi_s(x,y,z)\right)\right)^2\right. \\ & \left. + \left(\frac{\partial}{\partial z}\left(\phi_o(x,y,z) + \phi_s(x,y,z)\right)\right)^2\right] e^{-i2\omega t} \\ & - \frac{1}{2}\sum_{j=1}^{6}\left[\left(\frac{\partial}{\partial x} X_j\phi_j(x,y,z)\right)^2 + \left(\frac{\partial}{\partial y} X_j\phi_j(x,y,z)\right)^2\right. \\ & \left. + \left(\frac{\partial}{\partial z} X_j\phi_j(x,y,z)\right)^2\right] e^{-i2\omega t}\Bigg\} - \rho g y \end{aligned} \tag{24}$$

The second and third terms in equation (24) are neglected usually for the force and moment calculations on the structure, but since they give rise to the time independent forces they may be significant on some structures. The evaluation of steady-state forces will be given in Section 2.1.11.2.

The force F and moment M can easily be obtained using equation (24):

$$\begin{aligned} \vec{F} &= \iint_S p\vec{n}\,dS \\ \vec{M} &= \iint_S p(\vec{r}\wedge\vec{n})\,dS \end{aligned} \tag{25}$$

The mathematical background outlined in this section is based on linear theory, i.e. linear incident wave and linear surface conditions are assumed. Non-linear solutions for incident waves were given by Stokes [7]. These solutions are based on the systematic power series in the wave amplitude. But convergence of these power series is

restricted to certain values of the wave steepness H/λ and relative water depth. (Depth of structure/water depth.) Some applications of Stokes' higher order theory were given by Skjelbreia and Hendrickson in reference [8]. Non-linear effects can be significant on offshore structures which are working in shallow water. The gravity type platform can be a typical example whereby it may be important to consider non-linear forces. In Section 2.2 calculation of these forces are shown.

Finally, the theory for quadratic correction of the velocity potential $\Phi(x,y,z,t)$ and of the associated forces due to the assumption of a non-linear free surface condition was developed by Lighthill in reference [9]. The applications of Lighthill's theory in design calculations are shown in Section 2.1.11.

2. ESTIMATION OF WAVE FORCES ON THE MEMBERS OF OFFSHORE STRUCTURES

In this section the wave force calculations on the members of offshore structures are considered, basically in two flow regimes. These regimes are mainly controlled by the structure's characteristic length, such as diameter for circular cylinders and the wave length.

When the ratio between diameter and wave length is less than 0.2, force caltulations are carried out in the inertia regime. Within the inertia regime as the ratio between diameter and the wave height gets smaller viscous forces become significant. The inertia regime may be summarised from Fig. 3 as follows:

when $D/H > 0.2$, inertia increasingly dominant

$0.125 < D/H < 0.2$, inertia + drag significant

$D/H < 0.125$ drag predominant.

As the ratio between diameter and wave length gets larger ($D/\lambda > 0.2$ or $kR > 0.63$) the wave force calculations should be done in

COMPARISON OF INERTIA & DRAG FORCES

ACTING ON A CIRCULAR CYLINDER.

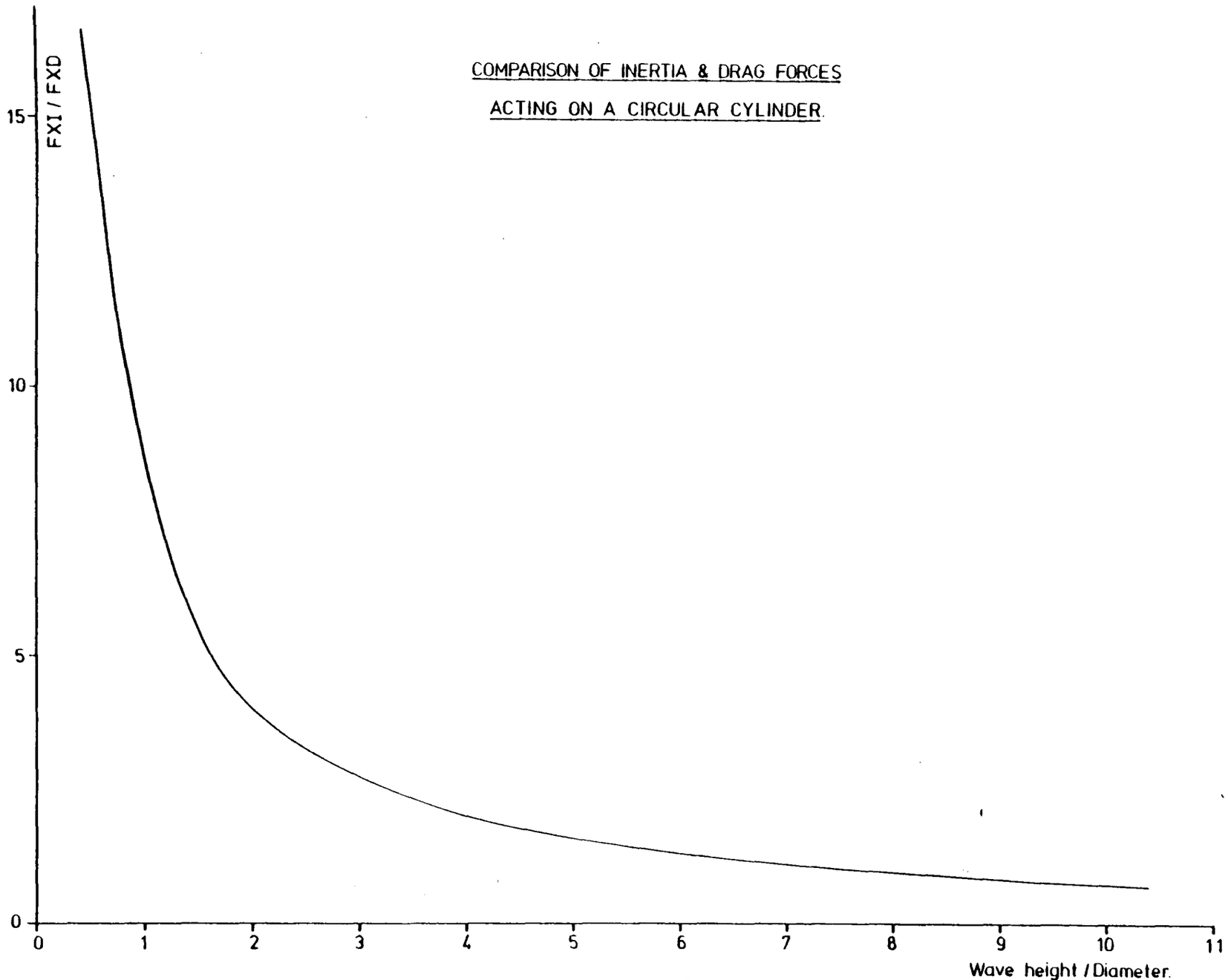

Fig. 3

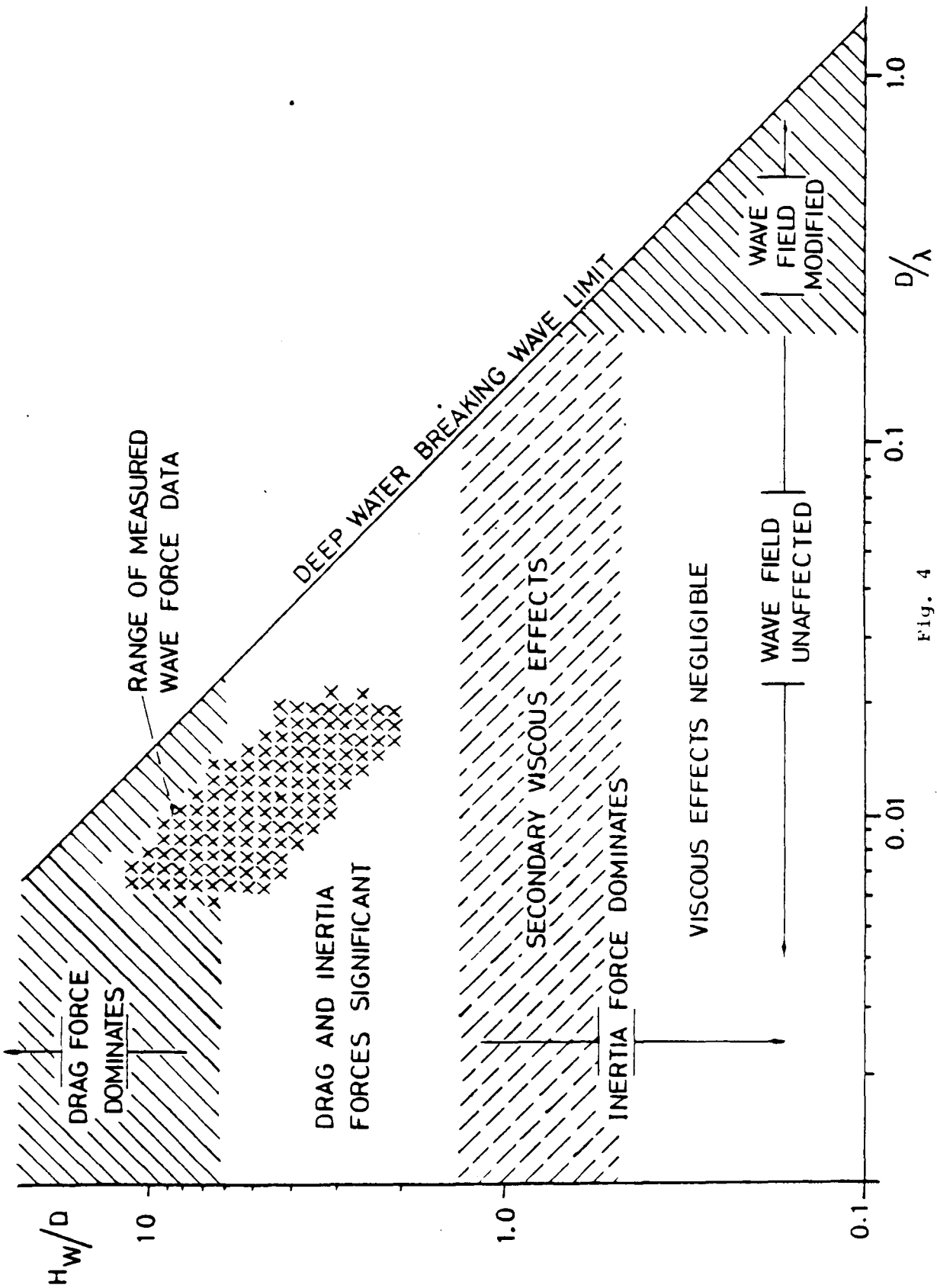
H_W/D
10
1.0
0.1
DRAG FORCE DOMINATES
RANGE OF MEASURED WAVE FORCE DATA
DEEP WATER BREAKING WAVE LIMIT
DRAG AND INERTIA FORCES SIGNIFICANT
SECONDARY VISCOUS EFFECTS
INERTIA FORCE DOMINATES
VISCOUS EFFECTS NEGLIGIBLE
WAVE FIELD UNAFFECTED
WAVE FIELD MODIFIED
1.0
0.1
0.01
D/λ

Fig. 4

diffraction regime. If we assume linear-free surface conditions, in other words the wave height is small compared to the wave length ($H/\lambda<0.14$ for deep water waves) in diffraction regime the viscous forces become negligible.

Various regimes are summarised as a function of D/λ and He^{ky}/D in Fig. 4.

2.1 Wave Forces on Small Diameter Members

2.1.1 Inertia force. The summarised results of the linear potential flow theory will be applied to calculate wave forces on small diameter members of offshore structures. In the absence of the structure the fluid motion can be described by a velocity potential $\Phi_o(x,t)$, here Φ_o is unsteady in time, but the change with time is slow and length scale $\Phi_o/|\nabla\Phi_o|$ is small compared to the characteristic length of a member and for simplicity it is assumed that the wave particles' velocity is $U_x = \frac{\partial\Phi_o}{\partial x}$ and is parallel to the x axis at a member and that the member has symmetry in respect to the whole reference axis. The disturbance of the wave flow due to a member, depends only on the relative flow between the member and the fluid. (Here a member of the structure is isolated from other members of the structure, in other words it is assumed that there is no interference due to the other members.) The total potential including the effect of the structure in the flow field is given by:

$$\Phi = \Phi_o + (U_x - U_1)\ \phi_1 \qquad (26)$$

Here U_1 is the velocity of a member and ϕ_1 the corresponding velocity potential. The second term in equation (26) identical to the rigid body velocity potential representation in equation (5). In equation (26) the velocity term was used to include the effect of interference between the structure velocity and fluid velocity. When the velocity potential of a rigid body is written in the above form the kinematic

boundary conditions on the body surface would also be different from those given in equation (21). They would take the following form:

$$\frac{\partial \phi_j}{\partial n} = n_j \qquad j=1,2,3$$

$$\frac{\partial \phi_j}{\partial n} = (\vec{r} \wedge \vec{n})_{j-3} \qquad j=4,5,6 \tag{27}$$

Substituting equation (23) in equation (25) the hydrodynamic force vector can easily be written in terms of velocity potential as follows:

$$\vec{F} = \iint_{S_M} p\vec{n}dS = -\rho \iint_{S_M} \left(\frac{\partial \Phi}{\partial t} + \frac{1}{2} \nabla\Phi\nabla\Phi \right) \vec{n}dS \tag{28}$$

Newman [10] gives two alternative forms to equation (28) as follows:

$$\vec{F} = -\rho \frac{d}{dt} \iint_{S_M} \Phi\vec{n}dS + \rho \iint_{S_M} \left(\frac{\partial \Phi}{\partial n} \nabla\Phi - \frac{1}{2} \nabla\Phi\nabla\Phi\vec{n} \right) dS \tag{29}$$

or

$$\vec{F} = -\rho \frac{d}{dt} \iint_{S_M} \Phi\vec{n}dS - \rho \iint_{S_C} \left[\frac{\partial \Phi}{\partial n} \nabla\Phi - \vec{n} \frac{1}{2} \nabla\Phi\nabla\Phi \right] dS \tag{29-A}$$

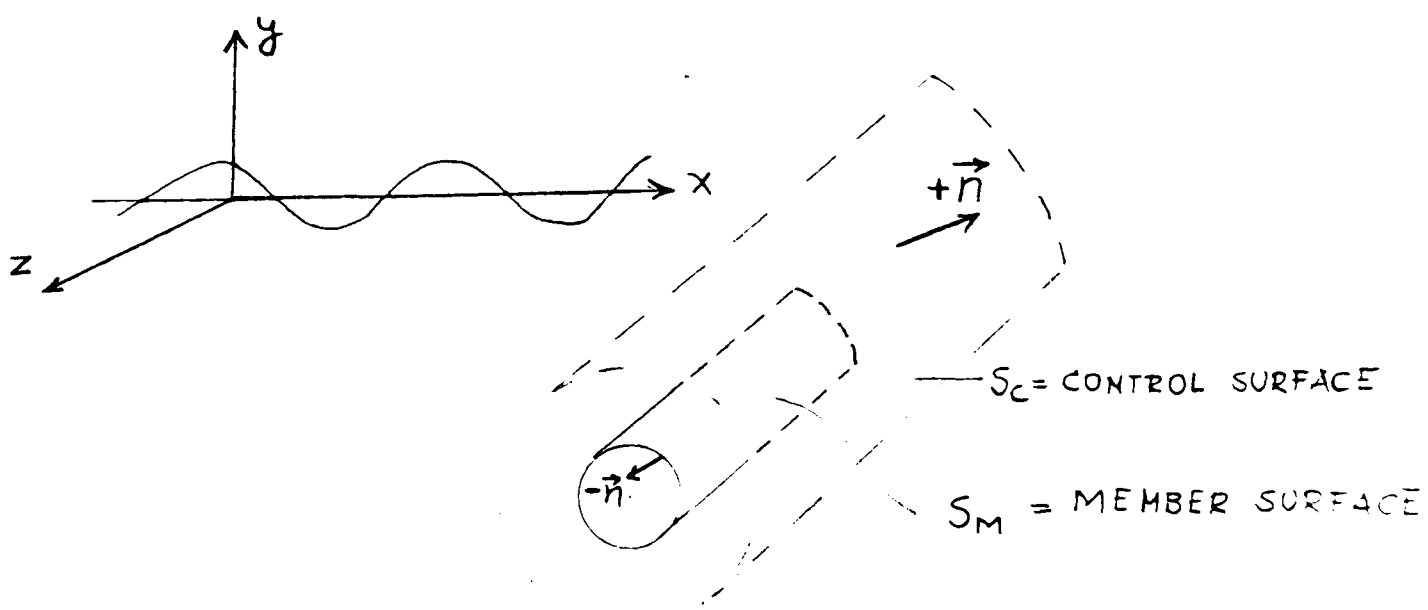

Fig. 5.

If we substitute equation (26) in equation (29-A) F_X becomes:

$$F_X = -\rho \frac{d}{dt} \iint_{S_C} (\Phi_o + (U_x - U_1)\phi_1) n_x dS - \rho \iint_{S_C} \left\{ \left[\frac{\partial \Phi_o}{\partial n} + (U_x - U_1) \frac{\partial \phi_1}{\partial n} \right] \right.$$

$$\left. \left[\frac{\partial \Phi_o}{\partial x} + (U_x - U_1) \frac{\partial \phi_1}{\partial x} \right] - \frac{1}{2} n_x \left[\nabla \Phi + (U_x - U_1) \nabla \phi_1 \right]^2 \right\} dS \qquad (30)$$

The following relations can also be used to estimate the value of F_X:

From the divergence theorem of Gauss:

$$\iiint_V \nabla a dV = \iint_S \vec{a} n dS \qquad (31)$$

In equation (27) if we multiply both sides by ϕ_i and integrate over S_M the following equation is obtained:

$$\iint_{S_M} \phi_i \frac{\partial \phi_j}{\partial n} dS = \iint_{S_M} \phi_i \, n_j \, dS \qquad (32)$$

If we suppose that we are only considering the value of the force due to the structure velocity potential substituting equation (26) into equation (28) and neglecting the second-order terms the following equation can easily be written:

$$\vec{F}_{T,M} = \rho \frac{d}{dt} \iint_{S_M} U_i \phi_i \vec{n} dS = \rho \frac{dU_i}{dt} \iint \phi_i \vec{n} dS \qquad (33)$$

If we substitute equation (32) into equation (33) $F_{T,M}$ becomes:

$$\vec{F}_{T,M} = \rho \frac{\partial U_i}{\partial t} \iint_{S_M} \phi_i \frac{\partial \phi_j}{\partial n} dS \qquad (34)$$

By analogy to Newton's second law equation (34) can be expressed in the following form:

$$\vec{F}_{T,M} = m_{ij} \frac{\partial U_i}{\partial t} \qquad (35)$$

From the definition it becomes clear that:

$$m_{ij} = \rho \iint_{S_M} \phi_i \frac{\partial \phi_j}{\partial n} dS \qquad (36)$$

Here m_{ij} is the added-mass tensor. Using the divergence theorem of Gauss:

$$m_{ij} = \rho \iint_{S_M} \phi_i \frac{\partial \phi_j}{\partial n} dS = \rho \iiint_V \nabla(\phi_i \nabla \phi_j)\, dV = \rho \iiint_V (\nabla \phi_i \nabla \phi_j)\, dV \qquad (37)$$

From the definition of kinetic energy of the fluid:

$$T = \frac{1}{2} \rho \iiint_V (\nabla \Phi \nabla \Phi)\, dV = \frac{1}{2} \rho \iiint_V U_i U_j\, \nabla \phi_i \nabla \phi_j\, dV \qquad (38)$$

Combining equations (37) and (38):

$$T = \frac{1}{2} \rho\, U_i U_j\, m_{ij} \qquad (38\text{-A})$$

This result is very useful for finding the added-mass values of different geometries.

As an example, the kinetic energy of the fluid in the case of a circular cylinder which is moving with U constant speed can be written using the definition of kinetic energy expression as follows:

$$T = \frac{1}{2} \rho \int_R^\infty dr \int_o^{2\pi} U^2 r d\theta = \frac{\pi}{2} \rho\, R^2 U^2 \qquad (39)$$

Equating (38-A) and (39) m_{uj} can easily be obtained for circular cylinders per unit length:

$$m_{ii} = \pi \rho R^2$$

In reference [11] the kinetic energy of flow is given for different geometries of moving or rotating bodies. Now we can use the results obtained in equations (31)-(39) to calculate the first integral in equation (30):

$$\begin{aligned} \iint_{S_M} [\Phi_o + (U_x - U_1)\phi_1]\, n_x dS &= \iiint_V \frac{\partial \Phi_o}{\partial x} dV + \frac{1}{\rho} m_{11}\, (U_x - U_1) \\ &= U_x V + \frac{1}{\rho} m_{11}\, (U_x - U_1) \end{aligned} \qquad (40)$$

or

$$-\rho \frac{d}{dt} \iint_{S_M} [\Phi_o + (U_x - U_1)\phi_1]\, n_x dS = (\rho V + m_{11})\, \dot{U}_x - m_{11} \dot{U}_1 \qquad (40\text{-A})$$

If we write the terms in the second integral after the multiplications of the terms in brackets the following form is obtained:

$$\rho \iint_{S_C} \left\{ \left[\frac{\partial \Phi_o}{\partial n} + (U_x - U_1) \frac{\partial \phi_1}{\partial n} \right] \left[\frac{\partial \Phi_o}{\partial x} + (U_x - U_1) \frac{\partial \phi_1}{\partial x} \right] - \frac{1}{2} n_x \left[\nabla \Phi_o + (U_x - U_1) \nabla \phi_1 \right]^2 \right\} dS$$

$$= \rho \iint_{S_C} \left\{ \left(\frac{\partial \Phi_o}{\partial x} \right)^2 n_x + (U_x - U_1) \frac{\partial \Phi_o}{\partial n} \frac{\partial \phi_1}{\partial x} + (U_x - U_1) \frac{\partial \phi_1}{\partial n} \frac{\partial \Phi_o}{\partial x} + (U_x - U_1)^2 \left(\frac{\partial \phi_1}{\partial x} \right)^2 n_x - \frac{1}{2} n_x \left[(\nabla \Phi_o)^2 + 2 (U_x - U_1) \nabla \Phi_o \nabla \phi_1 + (U_x - U_1)^2 (\nabla \phi_1)^2 \right] \right\} dS \qquad (41)$$

Since Laplace equations $\nabla^2 \Phi_o$ and $\nabla^2 \phi_1$ are satisfied throughout the entire region of S_C, equation (41) becomes:

$$\rho (U_x - U_1) \iint_{S_C} \left[\frac{\partial \Phi_o}{\partial n} \frac{\partial \phi_1}{\partial x} + \frac{\partial \Phi_o}{\partial x} \frac{\partial \phi_1}{\partial n} - n_x \nabla \Phi_o \nabla \phi_1 \right] dS \qquad (41\text{-A})$$

For sufficiently large radial distance r from the body, the potential due to the structure's rigid body motion can be written in terms of dipole moments:

$$\phi_i \simeq A_{ij} \frac{\partial}{\partial x_j} \frac{1}{r} \quad \text{as } r \to \infty \qquad (42)$$

Dipole moments A_{ij} were calculated using Green's theorem and given as follows [10]:

$$A_{ij} = \frac{1}{4\pi} (V \delta_{ij} + m_{ij}/\rho) \qquad i,j=1,2,3 \qquad (43)$$

From the symmetry of the structure $A_{ij} = 0$ if $i \neq j$ here:

$$\delta_{ij} = \begin{cases} 0 & i \neq j \\ \text{if} & \\ 1 & i = j \end{cases}$$

Assuming that control surface S_C is sufficiently distant from a member of the structure, we can then substitute equations (42) and (43) into equation (41-A) to obtain the following form for the second integration in equation (30):

$$\frac{1}{4\pi}\ (\rho V+m_{11})(U_x-U_1)\iint_{S_C}\left[\frac{\partial\Phi_o}{\partial n}\frac{\partial^2}{\partial x^2}\left(\frac{1}{r}\right)+\frac{\partial\Phi_o}{\partial x}\frac{\partial^2}{\partial n\partial x}\left(\frac{1}{r}\right)-n_x\nabla\phi\nabla\frac{\partial}{\partial x}\left(\frac{1}{r}\right)\right]dS \tag{44}$$

or

$$\frac{1}{4\pi}\ (\rho V+m_{11})(U_x-U_1)\iint_{S_C}\left[\frac{\partial^2\Phi_o}{\partial x^2}\frac{\partial}{\partial n}\left(\frac{1}{r}\right)-\frac{1}{r}\frac{\partial}{\partial n}\frac{\partial^2\Phi_o}{\partial x^2}-n_x\nabla^2\phi\frac{\partial}{\partial x}\left(\frac{1}{r}\right)\right]dS \tag{44-A}$$

Using Green's theorem inside the control surface S_C the velocity potential $\phi_i(x,y,z)$ can also be given as follows:

$$\phi_i(x,y,z) = -\frac{1}{4\pi}\iint_{S_C}\left[\phi_i\frac{\partial}{\partial n}\left(\frac{1}{r}\right)-\frac{1}{r}\frac{\partial\phi_i}{\partial n}\right]dS \tag{45}$$

Using equation (45) and the Laplace equation, the final form of the second integral in equation (30) will be:

$$-(\rho V+m_{11})(U_x-U_1)\ \frac{\partial^2\Phi_o}{\partial x^2} \tag{46}$$

If we replace equations (40-A) and (46) with the first and second integrals in equation (30) respectively, we obtain the total horizontal force F_x on a member in the following form:

$$F_x = (\rho V+m_{11})\dot{U}_x - m_{11}\dot{U}_1 + (\rho V+m_{11})(U_x-U_1)\frac{\partial U_x}{\partial x} \tag{47}$$

or

$$F_x = (\rho V+m_{11})\ \dot{U}_x + (U_x-U_1)\frac{\partial U_x}{\partial x} - m_{11}\dot{U}_1 \tag{47-A}$$

Similarly the F_y, F_z components of the force vector can be written as follows:

$$F_y = (\rho V+m_{22})\ \dot{U}_y + (U_y-U_2)\frac{\partial U_y}{\partial y} - m_{22}\dot{U}_2 \tag{47-B}$$

$$F_z = (\rho V+m_{33})\ \dot{U}_z + (U_z-U_3)\frac{\partial U_z}{\partial z} - m_{33}\dot{U}_3 \tag{47-C}$$

Equations (47-A),(47-B) and (47-C) are the fundamental expressions for the calculation of wave loading on the members of offshore structures.

We may interpret equation (47-A) to give the physical meaning of each component:

$$F_x = \rho V \dot{U}_x + m_{11} \dot{U}_x + (\rho V + m_{11})(U_x - U_1) \frac{\partial U_x}{\partial x} - m_{11} \dot{U}_1 \qquad (48)$$

The first term on the right hand side of equation (48) is the dynamic pressure force due to undisturbed wave field. This can easily be understood by comparing equation (40) or (40-A) with the first term in question. This force is also called the Froude-Krylov force.

The second term is the acceleration force due to the presence of a member in the wave field. The third term takes the interaction between water particle velocity and body velocity into account, as well as the variation of fluid particle velocity along the cross-section of a member. We may call this term a "correction force for disturbance of the wave field due to the body" and it has a second order effect. The third term is usually neglected in the practical calculations. The last term of equation (47-A) is due to the member's motion. If we set the sum of all F_x's for individual members equal to the product of the total mass of the structure and $\dot{U}_1$ we can also obtain the motion equation as:

$$M\dot{U}_1 = \sum_{i=1}^{m} F_{x_i} = \sum_{i=1}^{m} \left[(\rho V_i + m_{11,i}) \dot{U}_{x,i} - m_{11,i} \dot{U}_1 \right] \qquad (48)$$

or

$$\left(M + \sum_{i=1}^{m} m_{11,i} \right) \dot{U}_1 = \sum_{i=1}^{m} \left[(\rho V_i + m_{11,i}) \right] U_{x,i} \qquad (48\text{-A})$$

If we want to show the use of equation (47-A) by calculating the horizontal wave forces on a circular cylinder, if we assume that the cylinder is stationary and the wave field is described with a velocity potential given in equation (6-A):

$$\phi_o = \frac{-i\ 0.5g\ H_w}{\omega} e^{ky}\ e^{ikx} \qquad (49)$$

$$U_x = \mathrm{Re}\left\{ \frac{\partial}{\partial x} \left(\frac{-i\ 0.5g\ H_w}{\omega} e^{ky}\ e^{ikx}\ e^{-i\omega t} \right) \right\} \qquad (50)$$

$$U_x = 0.5\ H_w\ \omega\ e^{ky}\ \mathrm{Cos}(kx - \omega t) \qquad (50\text{-A})$$

$$\dot{U}_x = \frac{\partial U_x}{\partial t} = 0.5\ H_w\ \omega^2\ e^{ky}\ \mathrm{Sin}(kx-\omega t) \tag{51}$$

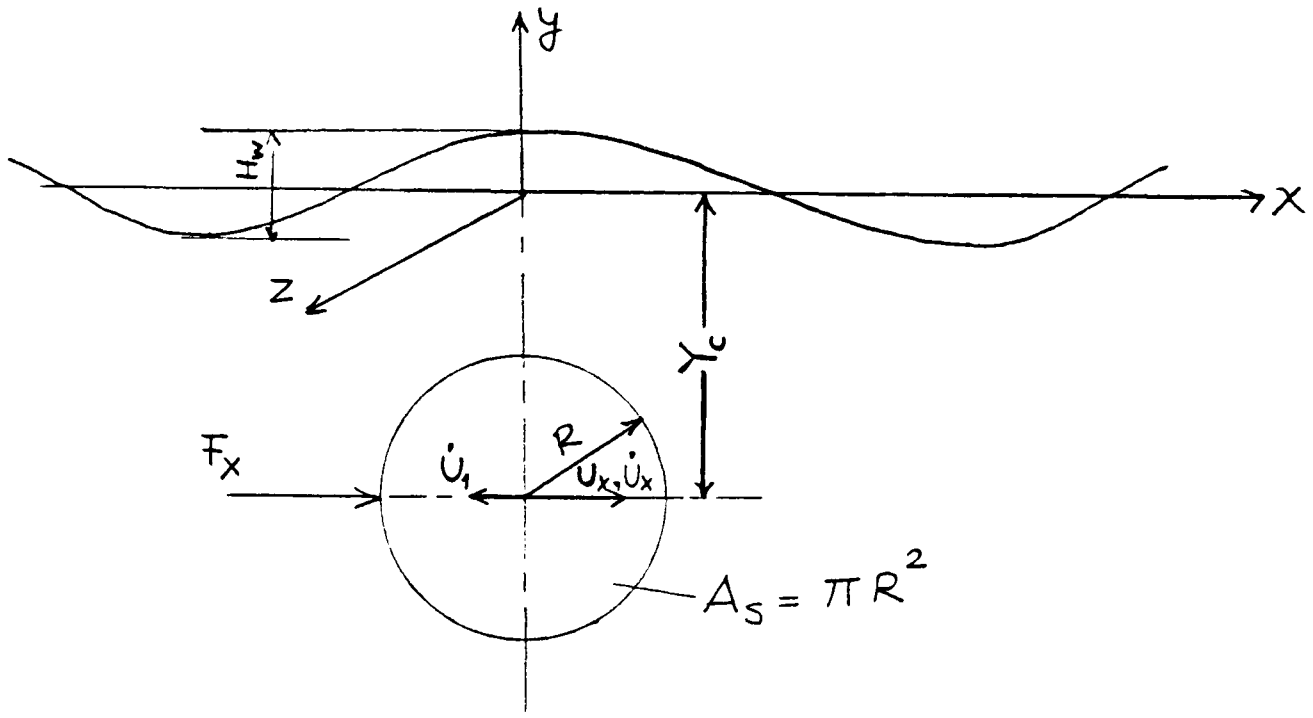

Fig. 6.

$$\frac{\partial U_x}{\partial x} = -\ 0.5\ H_w\ \omega\ k\ e^{ky}\ \mathrm{Sin}(kx-\omega t) \tag{52}$$

Since the member is assumed to be stationary:

$$U_1 = 0 \tag{53}$$

If we substitute the equations (50-A)-(53) into equation (47-A) F_x can be written as:

$$F_x = \int_o^{\ell} \Big\{ (\rho\pi R^2 + \rho\pi R^2)(0.5\ H_w\ \omega^2\ e^{ky}\ \mathrm{Sin}(kx-\omega t) - 0.5^2\ H_w^2\ \omega^2\ k\ e^{2ky}\ \mathrm{Sin}(kx-\omega t)\ \mathrm{Cos}(kx-\omega t) \Big\}\ dz \tag{54}$$

or

$$F_x = \int_o^{\ell} 2\rho\pi R^2\ 0.5\ H_w\ \omega^2\ e^{ky}\ \mathrm{Sin}(kx-\omega t)(1-0.5\ H_w\ k\ e^{ky}\ \mathrm{Cos}(kx-\omega t))\ dz \tag{55}$$

If we neglect the second term in brackets F_x becomes:

$$F_I = \int_o^{\ell} 2\rho\pi R^2\ 0.5\ H_w\ \omega^2\ e^{ky}\ \mathrm{Sin}(kx-\omega t)\ dz \tag{54-A}$$

Finally, equations (47) can be written as a function of wave properties and the geometry of a structure in waves:

$$F_x = \rho \int_0^{\ell} (A_s(1+k_{11})\,\dot{U}_x - A_s k_{11}\dot{U}_1)\,dz \qquad (55)$$

Here A_s : cross-sectional area of a structure

k_{11} : added mass coefficient.

Usually $1+k_{11}$ is written as C_M and therefore equation (55) takes the following form:

$$F_x = \rho \int_0^{\ell} (A_s\, C_M\, \dot{U}_x - A_s\, k_{11}\, \dot{U}_1)\,dz \qquad (55\text{-A})$$

If we substitute $A_s=\pi R^2$, $k_{11}=1$ or $C_M=2$, and $U_1=0$ for stationary circular cylinders into equation (55-A) we obtain an equation identical to the expression given in equation (54-A).

2.1.2 Drag force. The theoretical wave force predictions given in Section 2.1.1 use ideal potential fluid theory and are proportional to the local acceleration of the fluid relative to the body, hence they are "inertia forces". But as was mentioned earlier in Section 2, when the body's characteristic length becomes smaller compared to the wave amplitude (D/H<0.125), the situation in the flow field is fundamentally different and we should also include viscous forces which are due to the turbulent flow in the lee of a body. The wave force due to the viscosity of the flow can be represented as follows:

$$F_D = \int_0^{\ell} \frac{1}{2}\,\rho\, A_L\, U_x|U_x|\, C_D\, dz \qquad (56)$$

where $A_L = 2R$, U_x^2 is replaced by $U_x|U_x|$ to ensure that F_D acts in the same direction as the fluid velocity.

The main difficulty comes with C_D coefficients in the drag force calculations in waves, simply because C_D coefficients in waves are not only the function of the Reynolds Number which changes throughout one wave cycle, but they are also related to the inertia coefficients with the Keulegan-Carpenter Number which is defined as U_xT/D. (The details of C_M-C_D relation are discussed in Section 2.1.4.) Therefore the most

accurate viscous force prediction in the waves could be obtained from the experimental results with time averaging where flow is sinusoidally oscillating or from real wave data. In practice one tends to use steady flow results for estimating the C_D value for the prediction of drag forces in waves, although the published values of drag coefficients in waves show similarity to the drag coefficients in steady flow, where C_D decreases considerably with Reynolds Number over the approximate range $10^4<Re<10^6$. Care must be taken if steady flow results are applied to sea-wave flows, because of the two main flow phenomena which do not exist in steady flow or in the sinusoidally oscillating flow:

(a) The water particle motions are orbital, and

(b) Irregularities of sea-waves.

If a member of the structure is relatively large with respect to the wave height, the viscous drag coefficient becomes less sensitive to Reynolds Number and steady flow results may be more suitable.

2.1.3 Total wave force. As was mentioned earlier, in the region where $0.25<D/H_w<0.2$ inertia and drag forces both become significant. In this region despite the interaction between the inertia and drag forces, the total wave force on a cylindrical member of the structure may be assumed to be predicted as a summation of the inertia and drag forces which are given in equations (54-A) and (56).

$$F_T = F_I + F_D \qquad \text{or}$$

$$F_T = \rho \int_0^{\ell} \left(C_M A_s \dot{U}_x + \frac{1}{2} C_D A_L U_x |U_x| \right) dz \tag{57}$$

This form of total force was first proposed by J.R. Morison for the design of pile supported offshore structures [12]. If we replace $\dot{U}_x$ by $(\omega^2\ 0.5H_w)$ and replace U_x by $(\omega\ 0.5H_w)$ it follows that the ratio of maximum viscous forces to the maximum inertial forces is proportional to:

$$\frac{\frac{1}{2} \rho\ \omega^2\ (0.5H_w)^2\ C_D\ D}{C_M\ \rho\ \pi\ D^2/4\ \omega^2\ (0.5H_w)} = \frac{C_D}{\pi\ C_M} \frac{H_w}{D} \tag{58}$$

In Fig. 3 ratios of maximum inertia force/maximum drag force is given as a function of H_w/D. When equation (57) is used the coefficients should be chosen very carefully for the appropriate values of Reynolds Number, Keulegan-Carpenter Number ($=U_{x,max}\ T/D$), the relative roughness ($=k/D$) and instantaneous time ($=t/T$). In other words equation (57) can be generalised and written as:

$$F_T = f(U_{x,max},\ D,\ \rho,\ \nu,\ T,\ t,\ k) \tag{59}$$

A simple dimensional analysis of the equation (57) shows that total force F_T will be a function of the following variables:

$$\frac{F_T}{\rho\, D U_{x,max}^2} = f\left(\frac{U_{x,max}\ D}{\nu},\ \frac{U_{x,max}\ T}{D},\ \frac{k}{D},\ \frac{t}{T}\right) \tag{60}$$

Combining equation (60) with equation (57) the force coefficients C_M and C_D can take the following form:

$$C_M = f\left(\frac{U_{x,max}\ D}{\nu},\ \frac{U_{x,max}\ T}{D},\ \frac{k}{D},\ \frac{t}{T}\right) \tag{61}$$

$$C_D = f\left(\frac{U_{x,max}\ D}{\nu},\ \frac{U_{x,max}\ T}{D},\ \frac{k}{D},\ \frac{t}{T}\right) \tag{61-A}$$

2.1.4 Experiments for C_M and C_D values. As is seen from the equations (61) and (61-A) C_M and C_D can only be obtained from the experiments where flow is time dependent. For accuracy and easy usage of the experimental results one has to eliminate time dependence by introducing time-invariant averages. This was done by Keulegan-Carpenter using Fourier analysis [13]. Since F_T is periodic and flow has symmetry the following relations can be deduced:

$$F_T(\theta) = -\ F(\theta+\pi) \tag{62}$$

and from equation (60):

$$\frac{F_T}{\rho\ D\ U_{x,max}^2} = \frac{A_1\ \mathrm{Sin}\theta + A_3\ \mathrm{Sin}3\theta + A_5\ \mathrm{Sin}5\theta + \cdots\ +}{B_1\ \mathrm{Cos}\theta + B_3\ \mathrm{Cos}3\theta + B_5\ \mathrm{Sin}5\theta + \cdots} \tag{63}$$

where $\theta = \omega t = 2\pi\ \frac{t}{T}$

Observation of the force curve suggested that the best method for the determination of A_n, B_n coefficients in equation (63) will be the use of the Fourier analysis as follows:

$$A_n = \frac{1}{\pi} \int_o^{2\pi} \frac{F_T \, \mathrm{Sin}(n\theta)}{\rho \, U_{x,max}^2 \, D} \, d\theta$$

$$B_n = \frac{1}{\pi} \int_o^{2} \frac{F_T \, \mathrm{Cos}(n\theta)}{\rho \, U_{x,max}^2 \, D} \, d\theta \qquad (64)$$

Using equations (50-A) and (51) the total inertia and drag force equation can be written in the following non-dimensional form:

$$\frac{F_T}{\rho \, U_{x,max}^2 \, D} = \frac{\pi}{4} C_M \frac{D \, \omega}{U_{x,max}} \mathrm{Sin}\theta - \frac{C_D}{2} \mathrm{Cos}\theta|\mathrm{Cos}\theta| \qquad (65)$$

Since $\mathrm{Cos}\theta|\mathrm{Cos}\theta| = \frac{8}{3\pi} \mathrm{Cos}\theta + \frac{8}{15\pi} \mathrm{Cos}3\theta + ---$

equation (63) can also be written, taking the first terms only, as:

$$\frac{F_T}{\rho \, U_{x,max}^2 \, D} = A_1 \mathrm{Sin}\theta + --- \frac{3\pi B_1}{8} \mathrm{Cos}\theta|\mathrm{Cos}\theta| + --- \qquad (66)$$

Equations (66) and (65) are identical, therefore the following relation can be written to obtain C_M and C_D coefficients in terms of the total measured experimental wave force values:

$$A_1 = \frac{\pi}{4} C_M \frac{D \, \omega}{U_{x,max}} = \frac{\pi^2}{2} C_M \frac{D}{T \, U_{x,max}}$$

$$B_1 = - \frac{8}{3\pi} \frac{1}{2} C_D \qquad (67)$$

Using equations (64) and (67):

$$C_M = \frac{2}{\pi^3} \frac{U_{x,max} \, T}{D} \int_o^{2\pi} \frac{F_T \, \mathrm{Sin}\theta d\theta}{\rho U_{x,max}^2 \, D} \qquad (68)$$

$$C_D = - \frac{3}{4} \int_o^{2\pi} \frac{F_T \, \mathrm{Cos}\theta d\theta}{\rho U_{x,max}^2 \, D} \qquad (68\text{-A})$$

From equation (68) it becomes clear that C_M is related to C_D with Keulegan-Carpenter Number $\frac{U_{x,max} \, T}{D}$ and C_M, C_D can easily be obtained from

the experimental results using equations (68) and (68-A).

In the experimental towing tanks and in wind or water tunnels several experiments have been done to evaluate the inertia and drag coefficients on various geometries having different orders of surface roughness [13-15]. Experimental results are always at Reynolds Numbers, generally two to three orders of magnitude smaller than prototype Reynolds Numbers. It is strongly believed that coefficients obtained at relatively low Reynolds Numbers may not be applicable at higher Reynolds Numbers with linear interpolations. A review of the existing literature giving explicit C_M and C_D values has been made by Hogben [16]. In the same reference recommended values of inertia and drag coefficients for offshore structures are given. These values have been mostly used in this study. Some large oil companies have joint experimental programs to evaluate these coefficients for offshore structures in the real sea environment, but none of these data have been made available to the public as yet.

Still further experimental work is required to find out the interference effects between the neighbouring members, the effect of inclination and wall-proximity effect in the determination of wave force coefficients. The experimental study of wave and current combination and its results in the force coefficient is also one of the areas in which research is needed. However, a simple theoretical method has been developed by the author to determine inertia coefficients in the ideal fluid, taking into account the interference effects between neighbouring members and wall-proximity. The results are given in Sections 2.1.6 and 2.1.7. In Section 2.1.8 some experimental work to determine the effect of inclination on the wave force coefficients will be summarised.

2.1.5 Lift force. When a member is placed in a steady flow, or sinusoidally oscillating flow, or wavy flow, one might expect the resulting

flow to be steady and laterally symmetrical. In fact, these assumptions are not correct because when the KCN (Keulegan-Carpenter Number = $U_{x,max}\,T/D$) is sufficiently large, the eddies will form in the lee of the cylinder. The developed configuration of the eddies in the wake of the cylinder is assymmetrical. Because of this assymmetrical configuration of the vortices a lateral lift force will act on the cylindrical member with the same frequency as vortices shed. In the design of offshore structures, lift forces should be carefully taken into account for several reasons:

Firstly, they could be as large as drag forces under some circumstances. Secondly, they could give rise to the hydro-elastic oscillations and result in fatigue failure. This point may have more importance than the effect of drag forces, in particular when vortex shedding frequency becomes equal or approaches the structural mode of vibration of a member. The severe vibrations of cables or riser pipes and members of fixed offshore structures are the result of this phenomenon. This phenomenon may cause failure due to fatigue. Thirdly, lateral vibrations of a member in response to lift forces may cause a significant increase in the magnitude of in-line forces.

A non-dimensional form of lift force and vortex shedding frequency can be defined as follows:

$$F_{L,max} / \tfrac{1}{2} \rho\, U^2_{x,max}\, A_L\, C_L \qquad (69)$$

$$St = \frac{f_v\, D}{U_{x,max}} = \text{Strouhal Number} \qquad A_L = D \cdot \ell \qquad (69\text{-A})$$

Some experimental research has been carried out to find the lift coefficients, C_L, and Strouhal Number, St, for circular cylinders in the steady, and in the wavy or sinusoidally varying linear flows [14,15, 17,18]. The results may be summarised as follows:

Roshko [17] reports that the Strouhal Number for circular cylinders in a steady flow appears to be proportional to the inverse of the drag coefficients.

For Reynolds Numbers between 10^2 and 10^6 excluding the trans-critical region which is $Re \simeq 10^6$, the Strouhal Number is given as $S=0.23/C_D$.

Bidde [18] reports that, lift force is dependent on KCN rather than Reynolds Number and lift force frequency (or vortex shedding frequency) is twice the wave frequency. Bidde's results should be applied very carefully since, the submerged end of the cylinder was completely free to generate a complex three-dimensional flow and influence vortex shedding.

From Sarpkaya's [14,15] results it may be concluded that C_L depends on Keulegan-Carpenter Number, for the Reynolds Numbers smaller than about 2×10^4. For Reynolds Numbers which are between 2×10^4 and 1×10^5 C_L depends, to varying degrees, both on Reynolds Numbers and KCN. Above Re Numbers 1×10^5 the dependence of lift coefficient on both KCN and Re Numbers is negligible. Sarpkaya also reports that the Strouhal Number and the ratio of frequency of vortex vibration over flow vibration are functions of KCN and Re Numbers. Finally, he found that the vortex shedding frequency is not a pure multiple of the frequency of flow oscillation. Since Sarpkaya's results were obtained in the sinusoidally varying flow, one might expect lift coefficients to be different in an ocean environment because of the variation of velocity vector with time as well as the depth and orientation of a member.

2.1.6 Interference effects of closely spaced circular cylinders. Let two cylindrical members A and B having the radii R_1 and R_2 respectively be located along the x axes at a distance, d, from each other, and assume that R_1/d and R_2/d are small and a stream is approaching the

cylinders at an angle α. If we also assume that flow has circulations Γ_1, about cylinder A, and Γ_2 about cylinder B, the complex flow potential is written as the summation of the stream potential and the doublets which represent the two cylinders in the following form.

[Details of the theory were given in reference [1] and [36]].

$$W = U\left\{ze^{-i\alpha} + e^{i\alpha}\left(\frac{R_1^2}{z} + \frac{R_2^2}{z-z_1}\right) + \frac{i}{2\pi}\left[\Gamma_1 \ell nz + \Gamma_2 \ell n(z-z_1)\right]\right\} \qquad (70)$$

where $z = x+iy$, $z_1 = -d$

$$e^{i\alpha} = \cos\alpha + i\sin\alpha$$

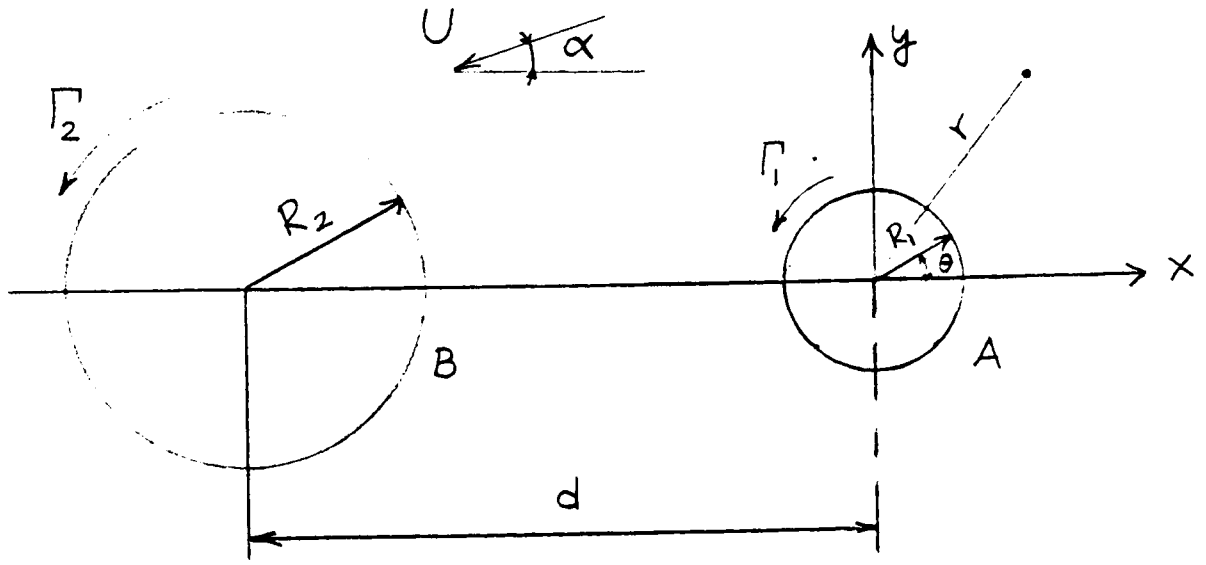

Fig. 7.

2.1.6.1 The calculation of wave force when α=0 and Γ_1 and Γ_2 are zero:

If we set α, Γ_1 and Γ_2 equal to zero, in equation (70) the complex flow potential becomes:

$$W = U_x\left[x+iy + \frac{R_1^2}{x+iy} + \frac{R_2^2}{(x+d)+iy}\right] \qquad (71)$$

or

$$W = \Phi_F + i\psi_F = U_x\left[x+iy + \frac{R_1^2(x-iy)}{r^2} + \frac{R_2^2[(x+d)-iy]}{(x+d)^2 + y^2}\right] \qquad (71\text{-A})$$

$$\Phi_F = U_x\left[x + \frac{R_1^2 x}{r^2} + \frac{R_2^2(x+d)}{(x+d)^2 + y^2}\right] \qquad (72)$$

$$\psi_F = U_x \left[y - \frac{R_1^2 y}{r^2} - \frac{R_2^2 y}{(x+d)^2 + y^2} \right] \tag{73}$$

In equation (72) the first term represents the potential of undisturbed flow, the second and third terms represent the effect on the flow field due to the existence of the first cylinder and second cylinder respectively.

The wave force on cylinder A can be written per unit length of the cylinder as follows:

$$dF_x = - \rho \iint_{S_M} \frac{\partial \Phi}{\partial t} \vec{n} dS \tag{74}$$

(from equation (28)), or

$$\vec{dF}_x = - \iint_{S_M} \rho \frac{\partial U_x}{\partial t} \left[x + \frac{R_1^2 x}{R_1^2} + \frac{R_2^2 (x+d)}{(x+d)^2 + y^2} \right] \vec{n} dS \tag{74-A}$$

The integration can easily be obtained on the circular cylinder using polar co-ordinates:

$$\left.\begin{aligned} x &= R_1 \, \mathrm{Cos}\theta \\ y &= R_1 \, \mathrm{Sin}\theta \\ \vec{n} dS &= -R_1 \, \mathrm{Cos}\theta d\theta \end{aligned}\right\} \tag{75}$$

Substituting the relations given at (75) into equation (74-A) the force equation becomes:

$$dF_x = \int_0^{2\pi} \rho \cdot \frac{\partial U_x}{\partial t} \left[2R_1 \, \mathrm{Cos}\theta + \frac{R_2^2 (R_1 \, \mathrm{Cos}\theta + d)}{R_1^2 + 2R_1 \, d \, \mathrm{Cos}\theta + d^2} \right] R_1 \, \mathrm{Cos}\theta d\theta \tag{76}$$

We can also derive modified C_M coefficient to suit conventional wave inertia force formulation for circular cylinders as follows.

Using equations (55-A) and (76) the following relation may be written for C_M taking the effect of neighbouring cylindrical members into account:

$$dF_x = \rho \, C_{M,A} \, \pi R_1^2 \frac{\partial U_x}{\partial t} = \rho \frac{\partial U_x}{\partial t} \left\{ 2R_1^2 \, \pi + \int_0^{2\pi} \left[\frac{\beta^2 \, R_1^2 (\mathrm{Cos}\theta + \alpha)}{(1 + 2\alpha \, \mathrm{Cos}\theta + \alpha^2)} \mathrm{Cos}\theta \right] d\theta \right\} \tag{77}$$

or

$$C_{M,A} = 2 + \frac{\int_0^{2\pi} \left[\frac{\beta^2 (\cos\theta+\alpha)\ \cos\theta}{1+2\alpha\ \cos\theta+\alpha^2}\right] d\theta}{\pi} \qquad (77\text{-A})$$

where $\alpha = \frac{d}{R_1}$, $\beta = \frac{R_2}{R_1}$

Similarly, wave forces on cylinder B may be written as follows:

$$dF_{x,B} = \rho \frac{\partial U_x}{\partial t} \left\{ 2R_2^2 \pi + \int_0^{2\pi} \left[\frac{\beta'^2\ R_2^2 (\cos\theta-\alpha')\ \cos\theta}{(1-2\alpha'\ \cos\theta+\alpha'^2)}\right] d\theta \right\} \qquad (78)$$

and C_M coefficient for the same cylinder can be written as follows:

$$C_{M,B} = 2 + \frac{\int_0^{2\pi} \left[\frac{\beta'^2 (\cos\theta-\alpha')\ \cos\theta}{1-2\alpha'\ \cos\theta+\alpha'^2}\right] d\theta}{\pi} \qquad (79)$$

where $\alpha' = \frac{d}{R_2}$, $\beta' = \frac{R_1}{R_2}$

The integrations in equations (77-A) and (79) have been carried out numerically to obtain C_M values and results for varying $\gamma=S/R_1$ and β (or β') values were plotted in Figure 8-19 where $S=d-(R_1+R_2)$.

2.1.6.2 The calculation of wave force when $\alpha=90°$ and Γ_1 and Γ_2 are zero: If we set $\alpha=90°$ and Γ_1 and Γ_2 equal to zero in equation (70) the complex flow potential becomes:

$$W = U_y \left[(-x-iy)i + i\left(\frac{R_1^2}{x+iy} + \frac{R_2^2}{x+iy+d}\right)\right] \qquad (80)$$

The velocity and stream potentials can be obtained from equation (80) as follows:

$$\Phi_F = U_y \left[y + \frac{R_1^2\, y}{r^2} + \frac{R_2^2\, y}{(x+d)^2+y^2} \right] \qquad (81)$$

$$\psi = U_y \left[-x + \frac{R_1^2\, x}{r^2} + \frac{R_2^2 (x+d)}{(x+d)^2+y^2} \right] \qquad (82)$$

The wave force on cylinder A and C_M coefficient for the same cylinder can be written using the procedure that has been followed

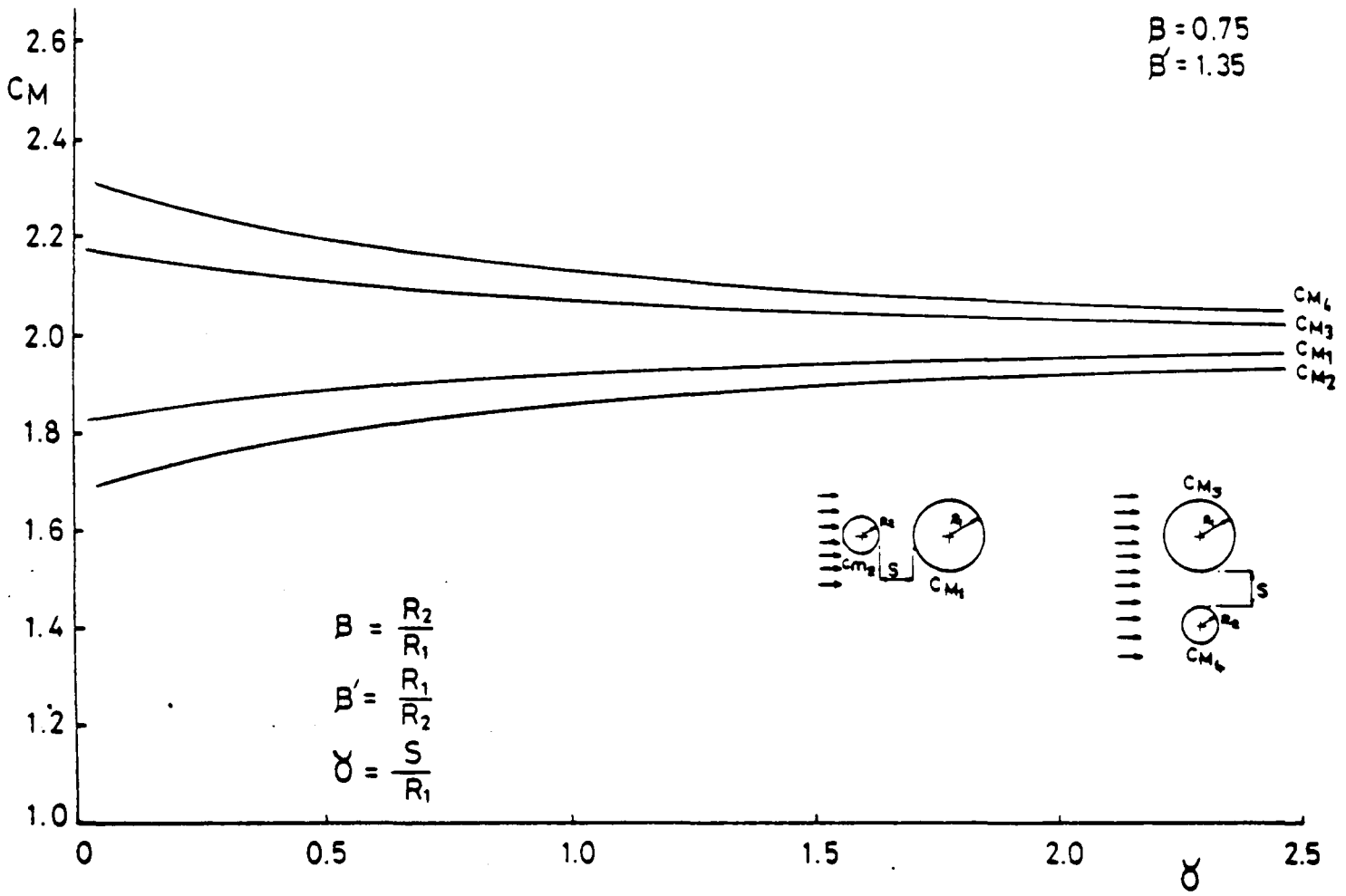

Figure 8

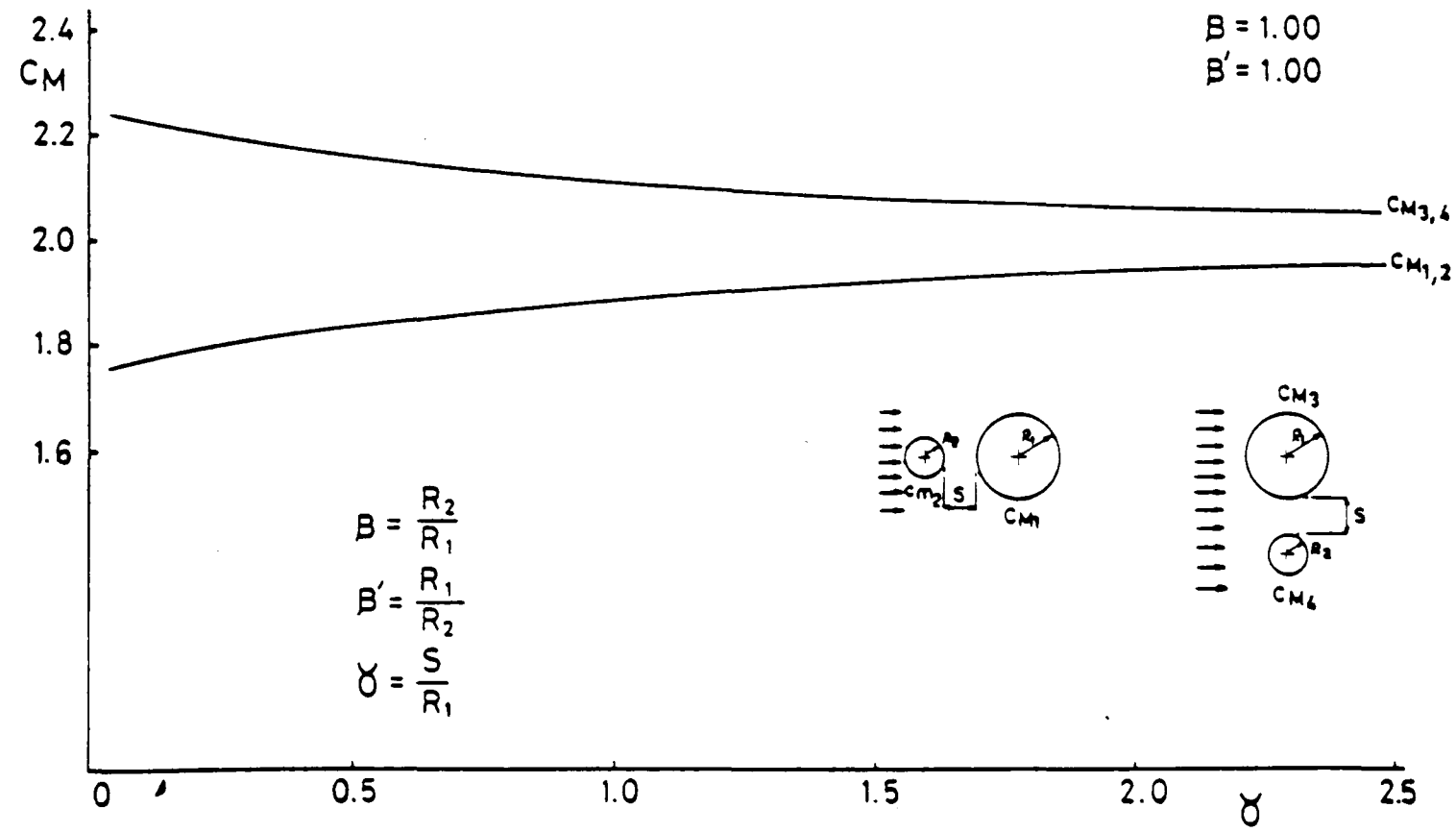

Figure 9

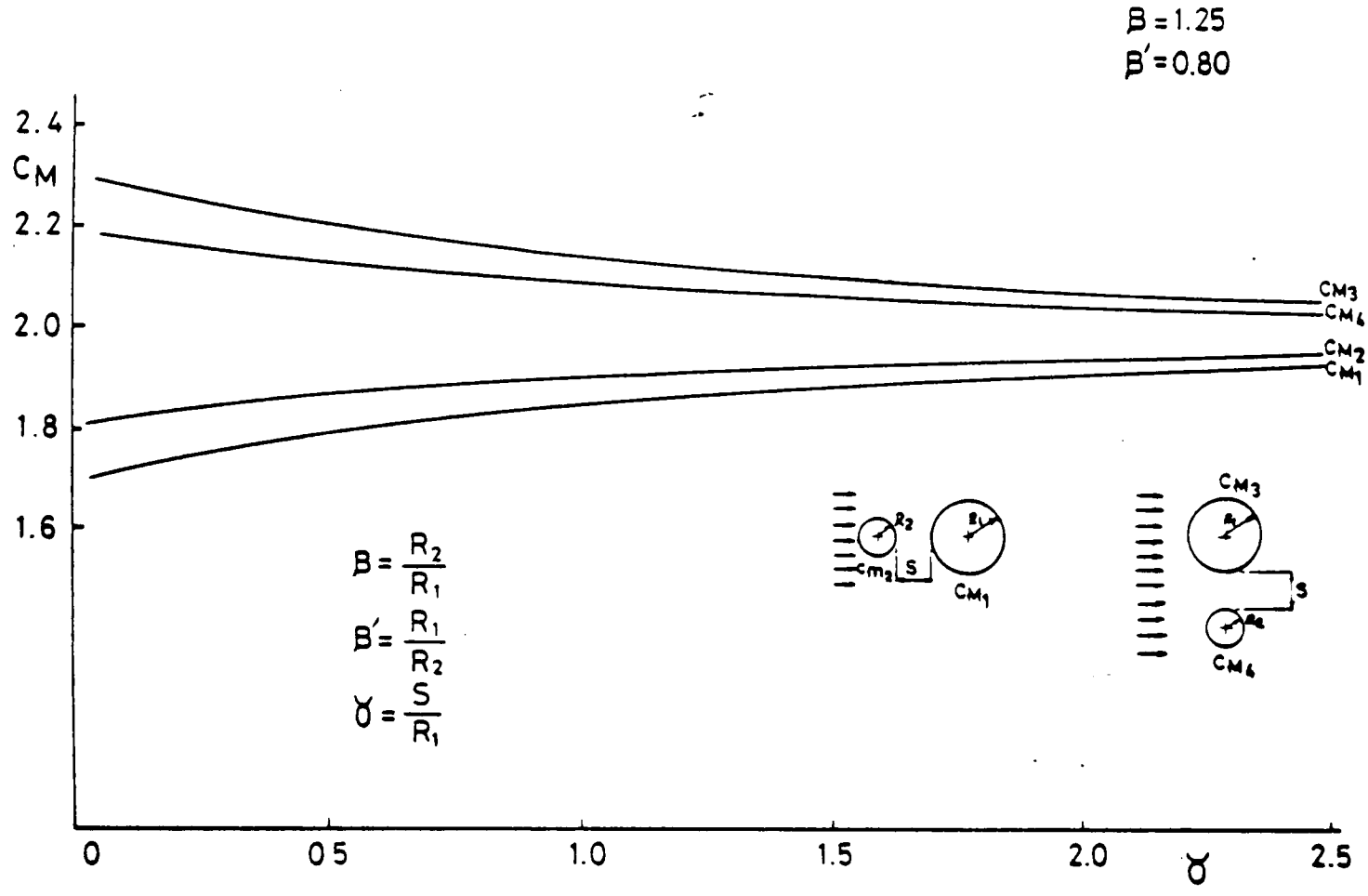

Figure 10

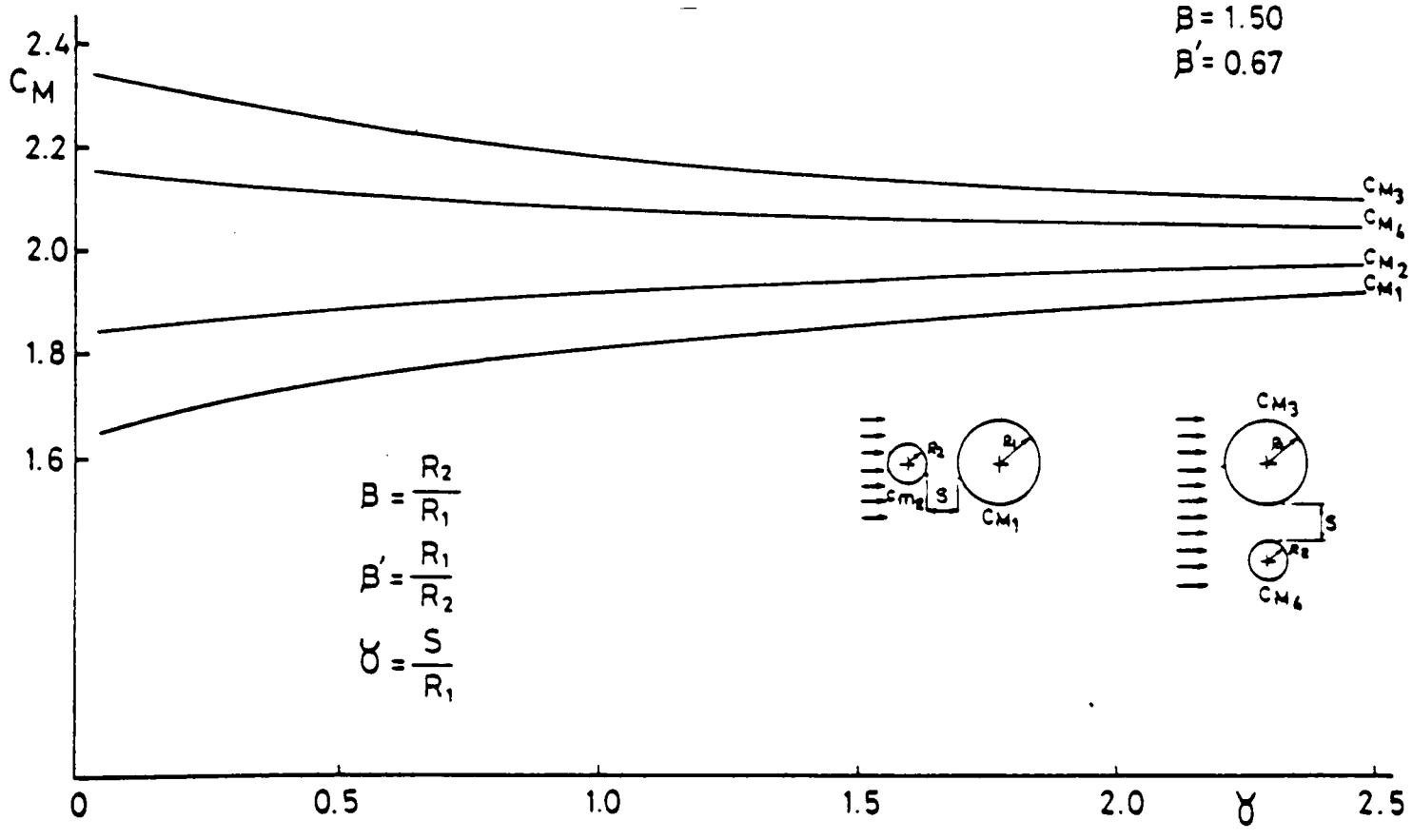

Figure 11

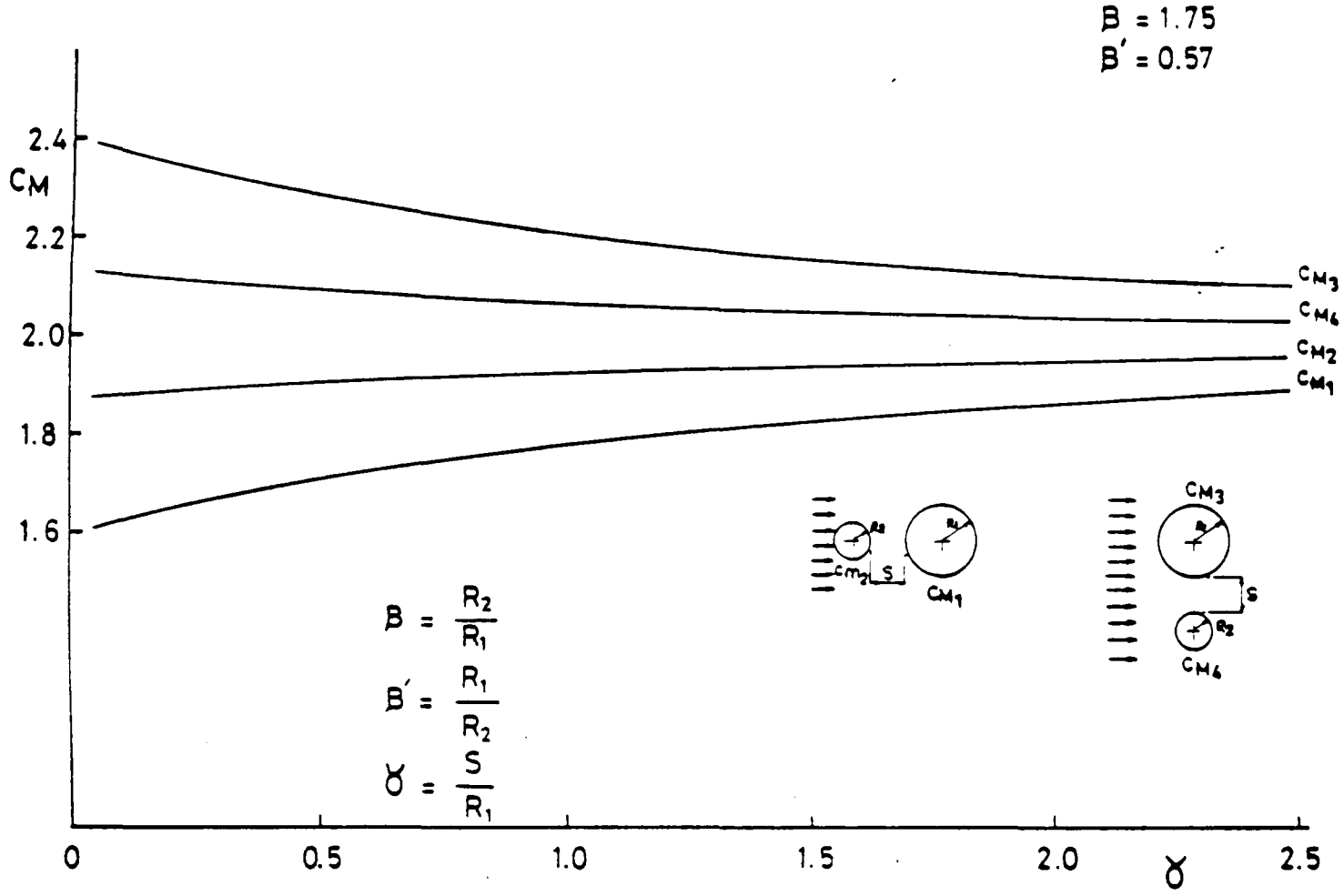

Figure 12

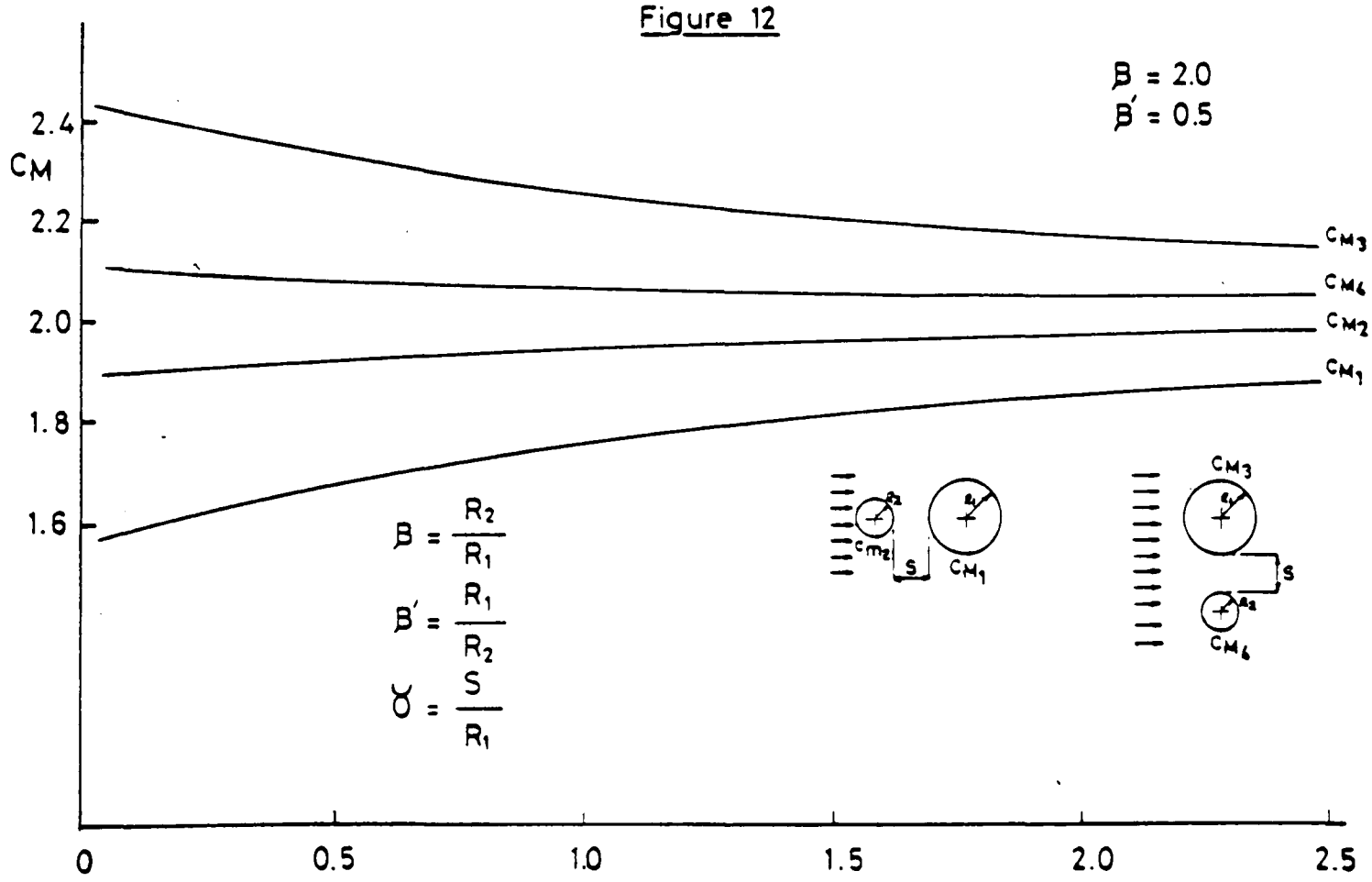

Figure 13

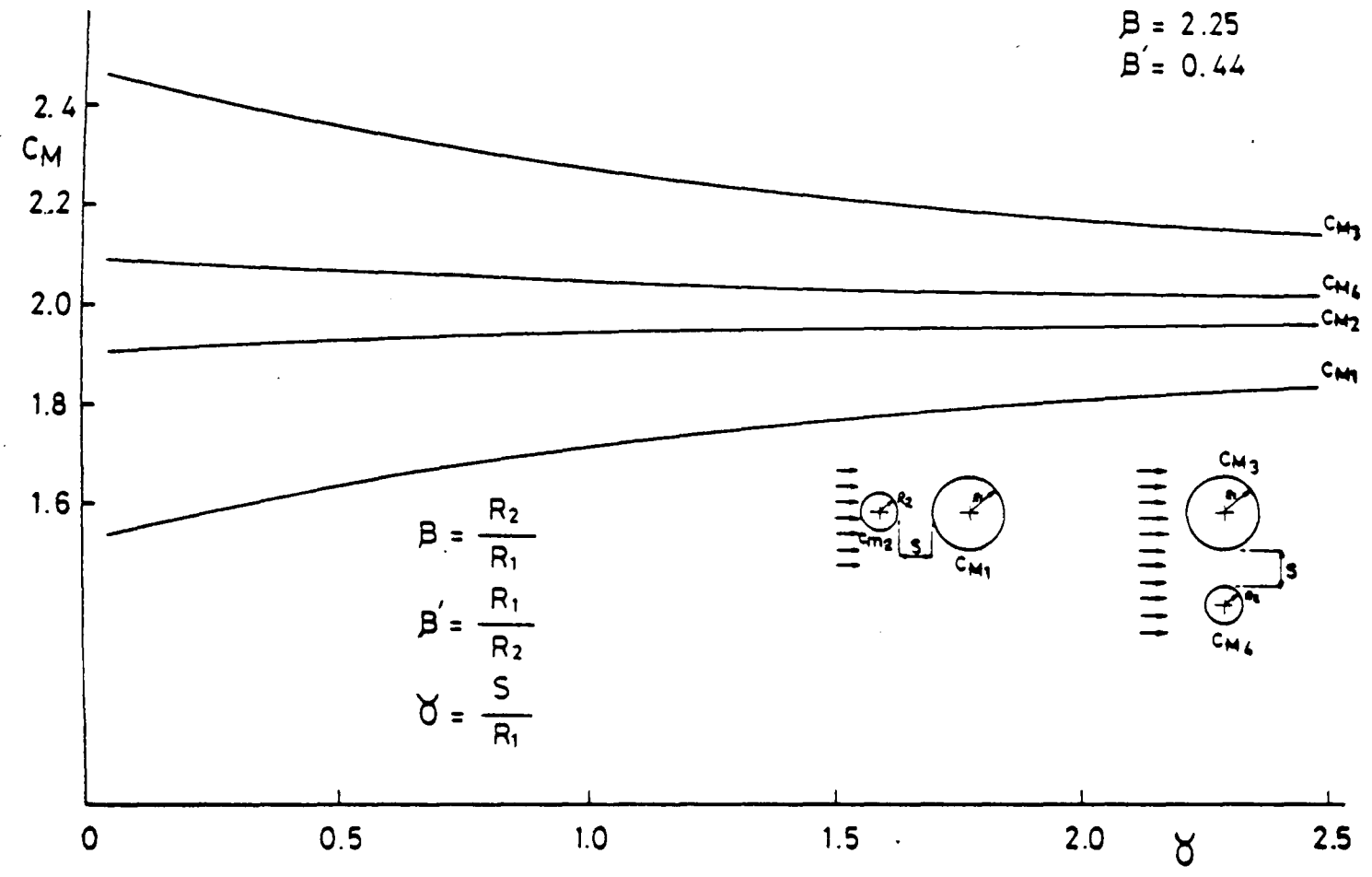

Figure 14

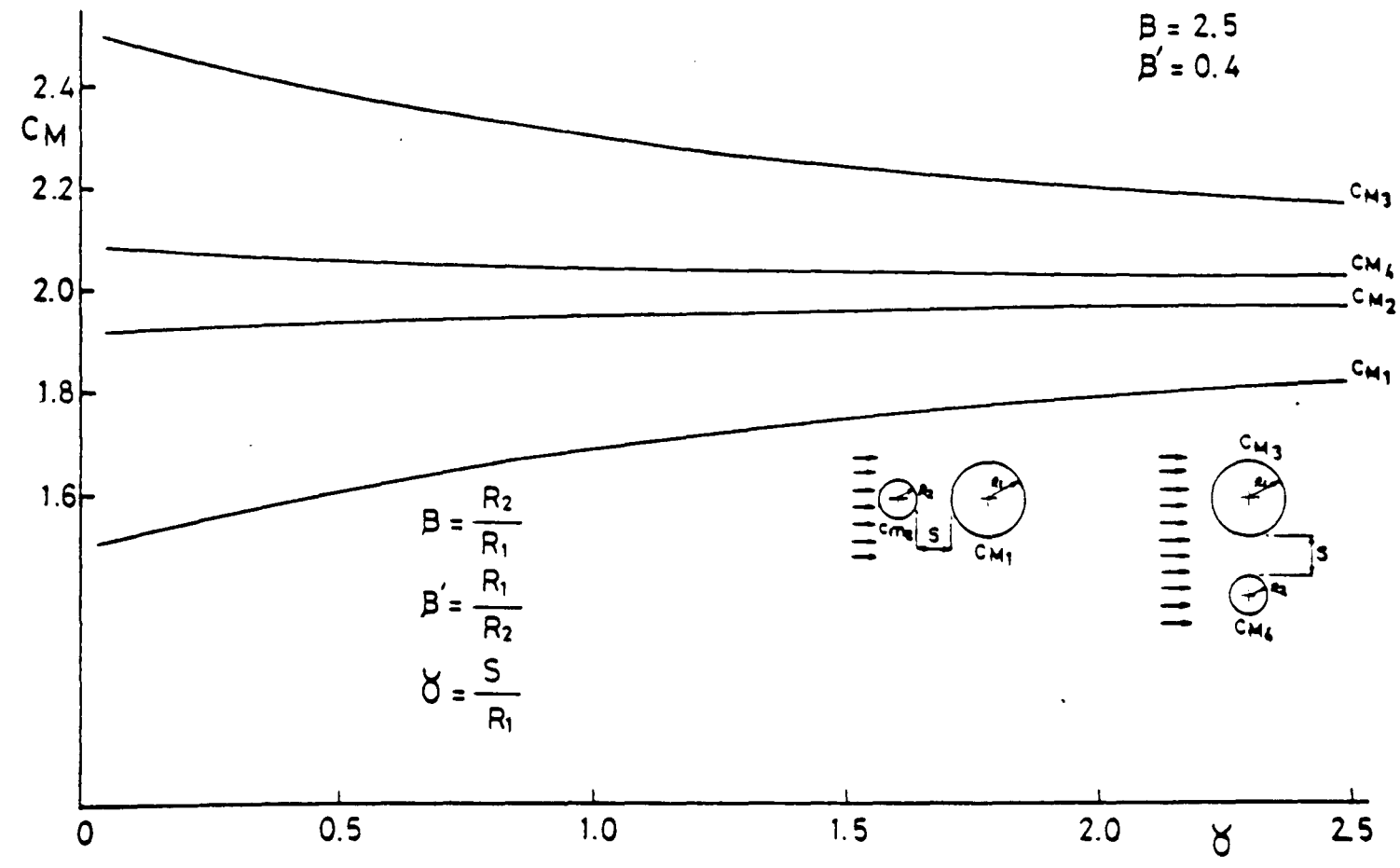

Figure 15

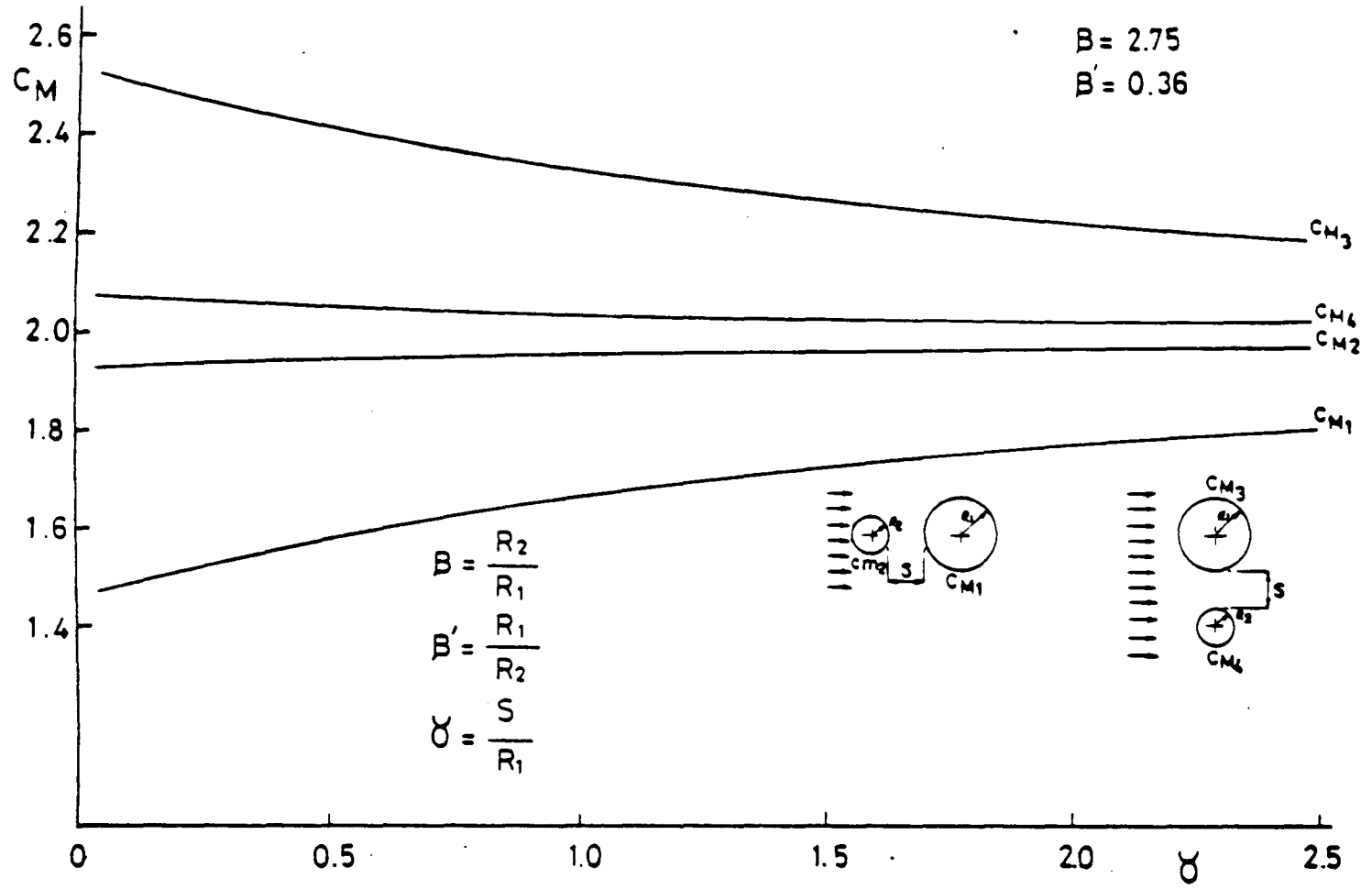

Figure 16

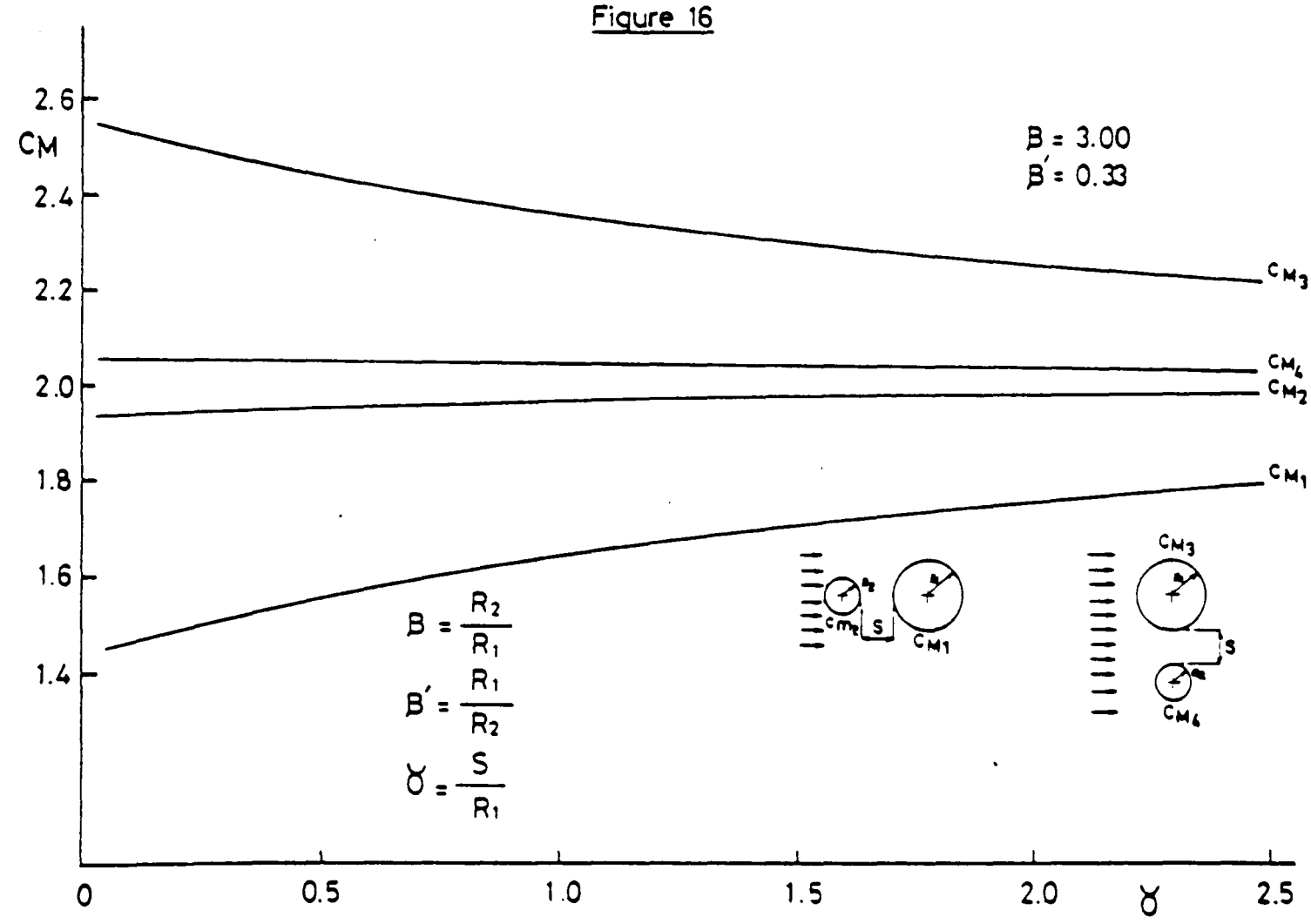

Figure 17

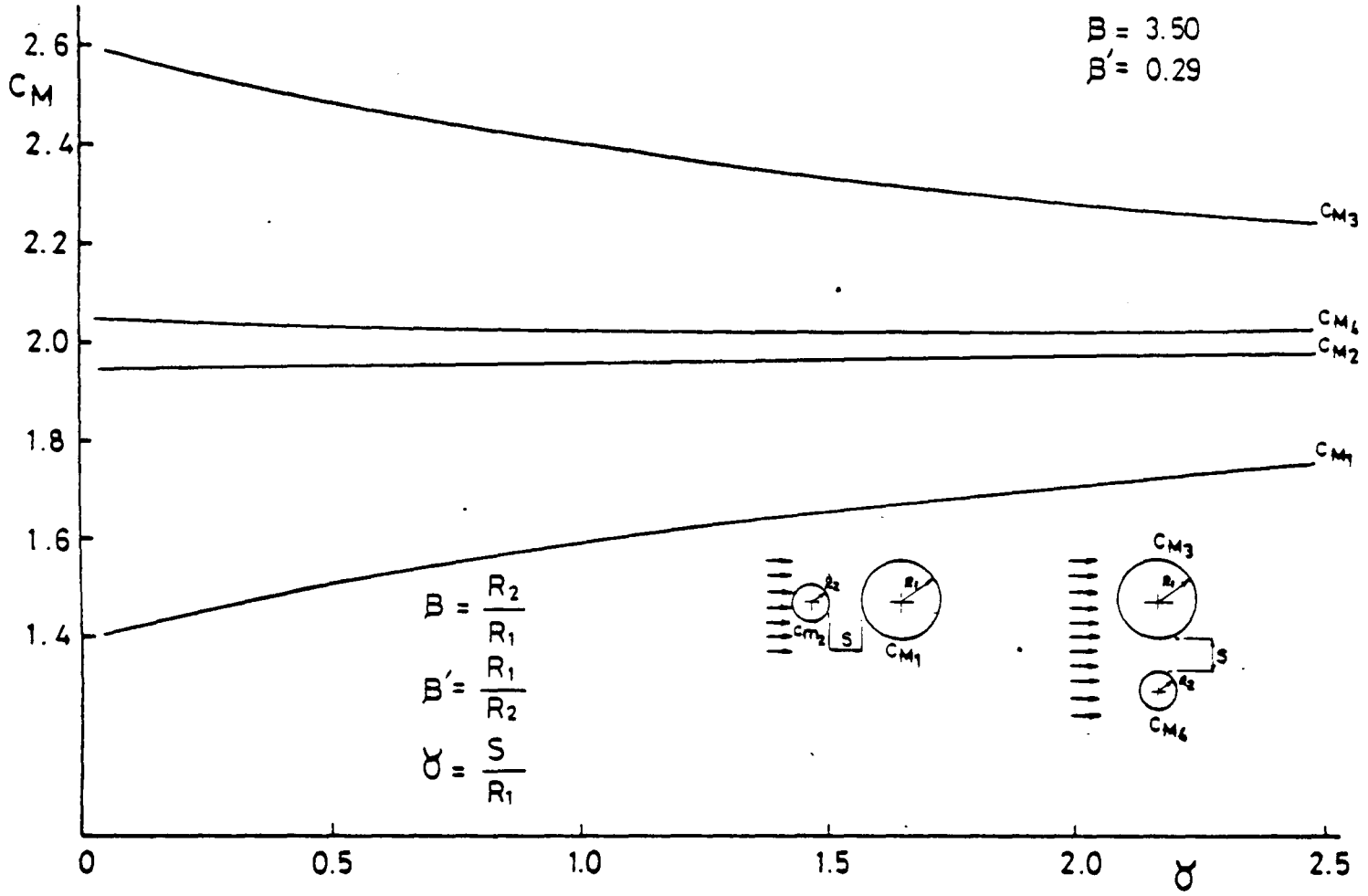

Figure 18

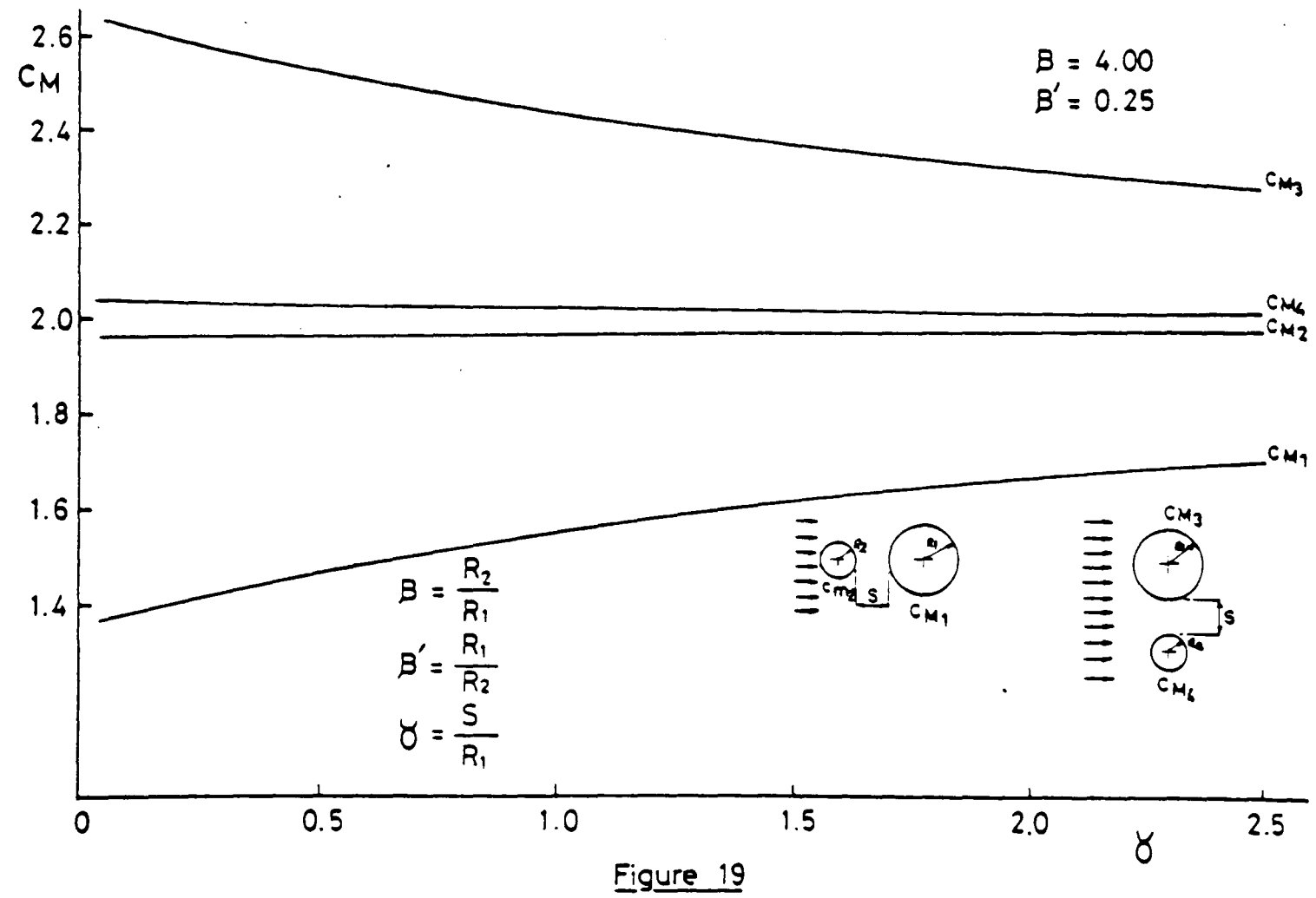

Figure 19

in the previous section

$$dF_{y,A} = \rho \frac{\partial U_y}{\partial t} \left\{ 2R_1^2 \pi + \int_o^{2\pi} \left[\frac{\beta^2 R_1^2 \sin^2\theta}{1+2\alpha \cos\theta+\alpha^2} \right] d\theta \right\} \tag{83}$$

$$C_{M,A} = 2 + \frac{\int_o^{2\pi} \left[\frac{\beta^2 \sin^2\theta}{1+2\alpha \cos\theta+\alpha^2} \right] d\theta}{\pi} \tag{84}$$

Similarly, the wave force and inertia coefficient take the following form for the second cylinder:

$$dF_{y,B} = \rho \frac{\partial U_y}{\partial t} \left\{ 2R_2^2 \pi + \int_o^{2\pi} \left[\frac{\beta'^2 R_2^2 \sin^2\theta}{1+2\alpha' \cos\theta+\alpha'^2} \right] d\theta \right\} \tag{85}$$

$$C_{M,B} = 2 + \frac{\int_o^{2\pi} \left[\frac{\beta'^2 \sin^2\theta}{1+2\alpha' \cos\theta+\alpha'^2} \right] d\theta}{\pi} \tag{86}$$

C_M values in equation (84) and (86) have been obtained numerically and results are shown in Figure 8-19 for various γ and β (or β').

2.1.7 The calculation of wall effect on the inertia coefficients. The results obtained in the previous section can easily be extended to calculate the effect of wall on the inertia coefficient calculations. If we consider two cylinders which have the same diameters and if the stream which has no circulation approaches perpendicular to the line of these cylinders' axes, then the stream surface which is normal to the line between the centres of the cylinders may be replaced by a rigid wall, see Fig. 20.

The inertia coefficient taking the wall effect into account can be calculated from equation (84) setting β equal to 1:

$$C_{M,W} = 2 + \frac{\int_o^{2\pi} \left[\frac{\sin^2\theta}{1+2\alpha \cos\theta+\alpha^2} \right] d\theta}{\pi} \tag{87}$$

In reference [19] added mass coefficient $k=C_M-1$ was calculated using kinetic energy of the fluid to take the effect of wall proximity

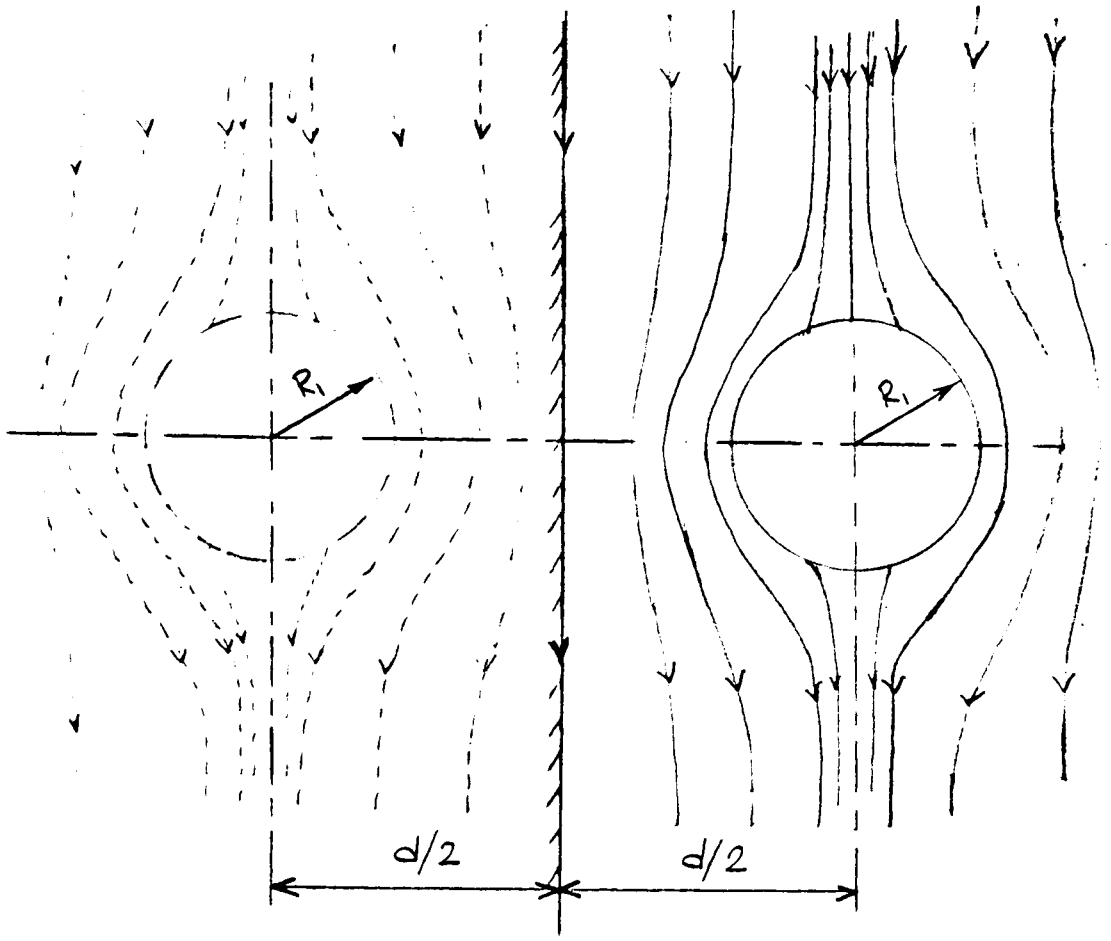

Fig. 20.

into account. Added virtual mass coefficient is given as follows:

$$k_{,w} = 1 + \frac{2}{\alpha^2} \tag{88}$$

The results of equations (87) and (88) have been plotted for various values of α in Fig. 21.

The results given in Fig. 21 may be used in the experimental work for the correlation of theoretical results with the experimental results.

2.1.8 The change of drag forces on closely spaced circular cylinders.

2.1.8.1 Drag force on circular cylinders in series (one cylinder behind the other): If a cylinder is placed in the wake of another cylinder the critical Reynolds Number for the rear cylinder reduces due to the high turbulence level of the wake. The experiments [20,21] carried out in a steady flow, show that the drag coefficient of the rear cylinder reduces considerably, while the drag coefficient of the front cylinder remains almost constant if $D/d > 0.25$, see Figs 22 and 22-A.

Wall Effect On Inertia Coeficients
For The Circular Cylinders

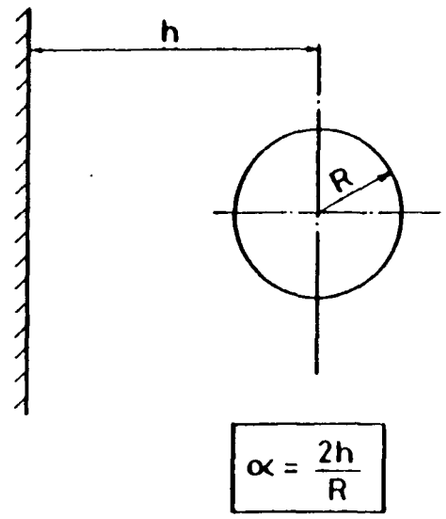

Figure 21

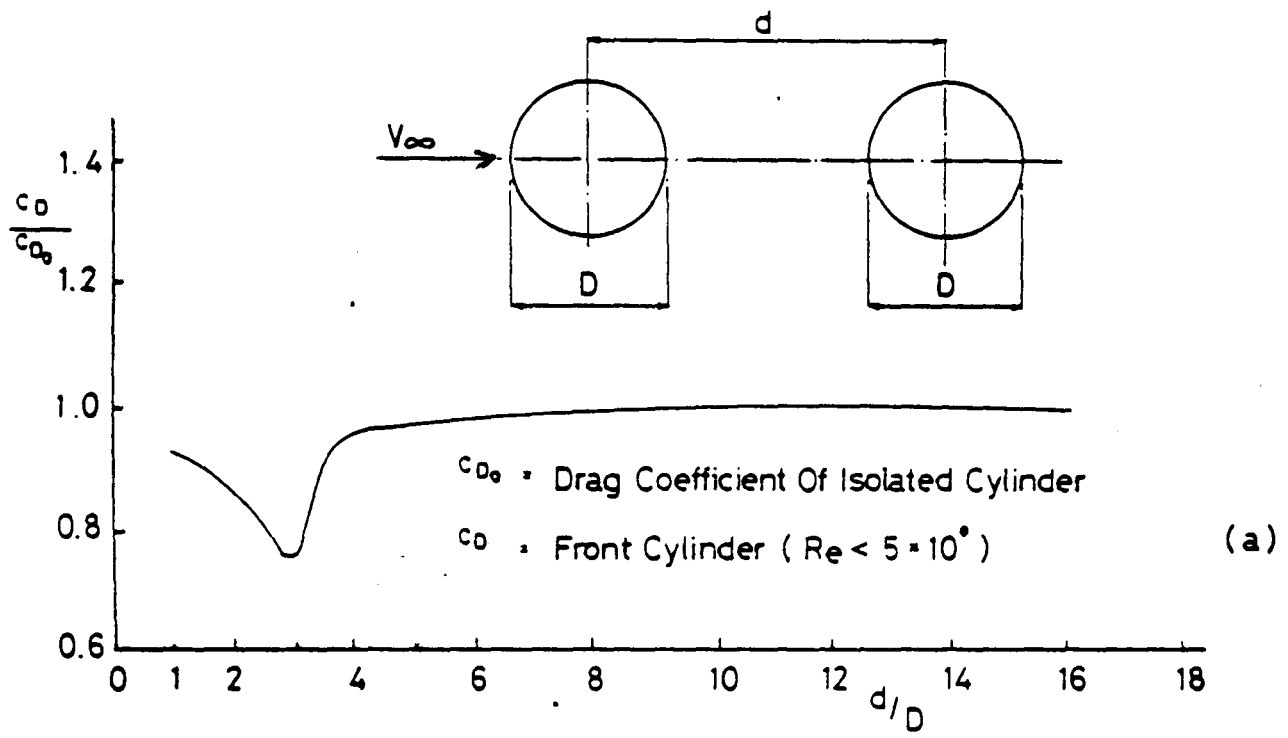
d
V∞
D
D
1.4
1.2
1.0
0.8
0.6
$\frac{C_D}{C_{D_0}}$
0 1 2 4 6 8 10 12 14 16 18
d/D
C_{D_0} = Drag Coefficient Of Isolated Cylinder
C_D = Front Cylinder ($Re < 5 * 10^5$)
(a)

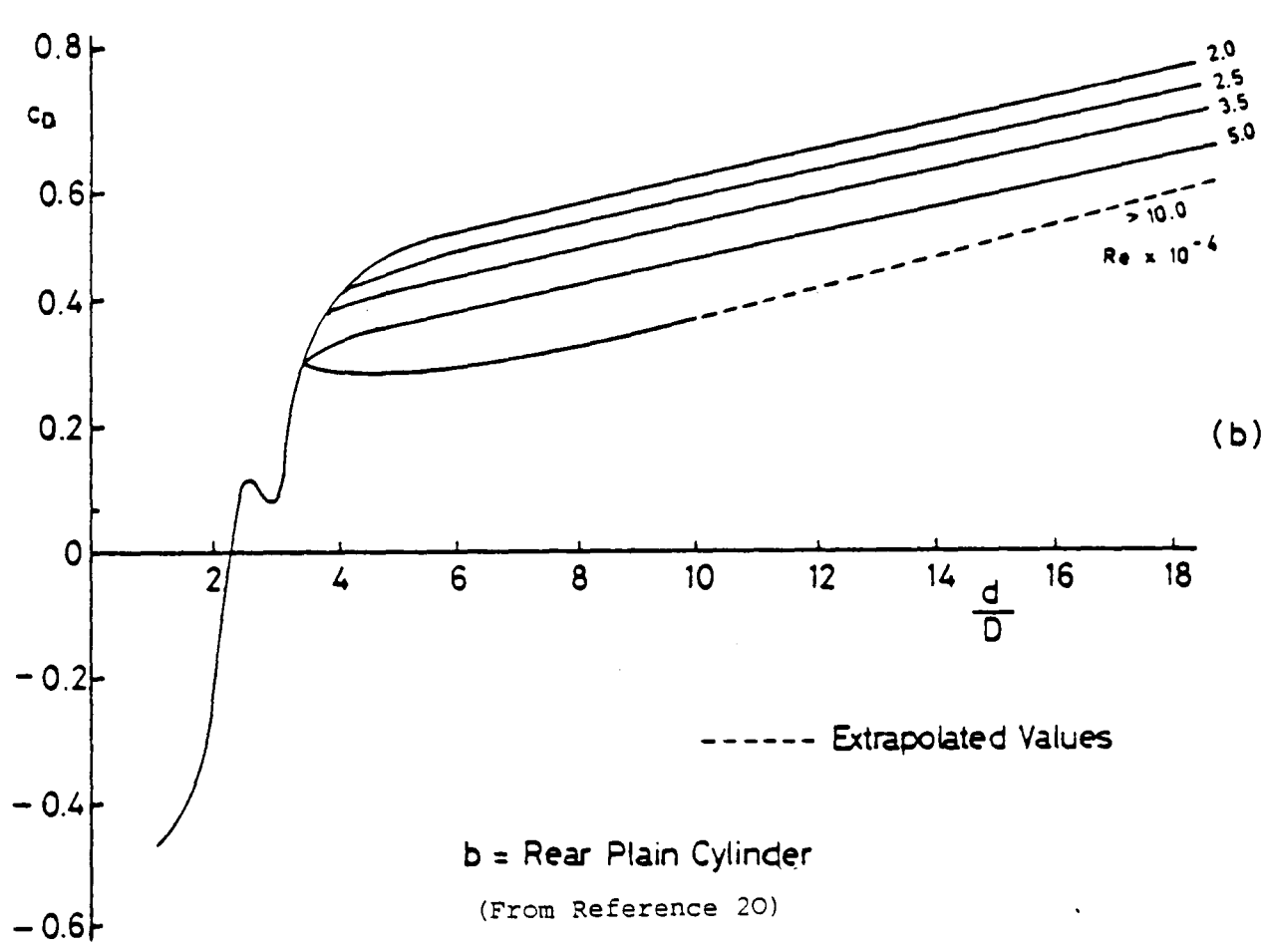
0.8
0.6
0.4
0.2
0
-0.2
-0.4
-0.6
C_D
2 4 6 8 10 12 14 16 18
$\frac{d}{D}$
2.0
2.5
3.5
5.0
> 10.0
Re x 10^{-6}
(b)
------ Extrapolated Values
b = Rear Plain Cylinder
(From Reference 20)

Figure. 22

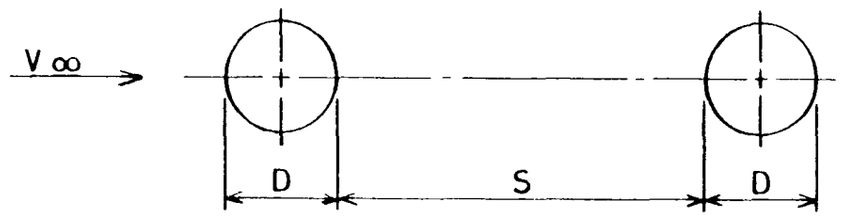

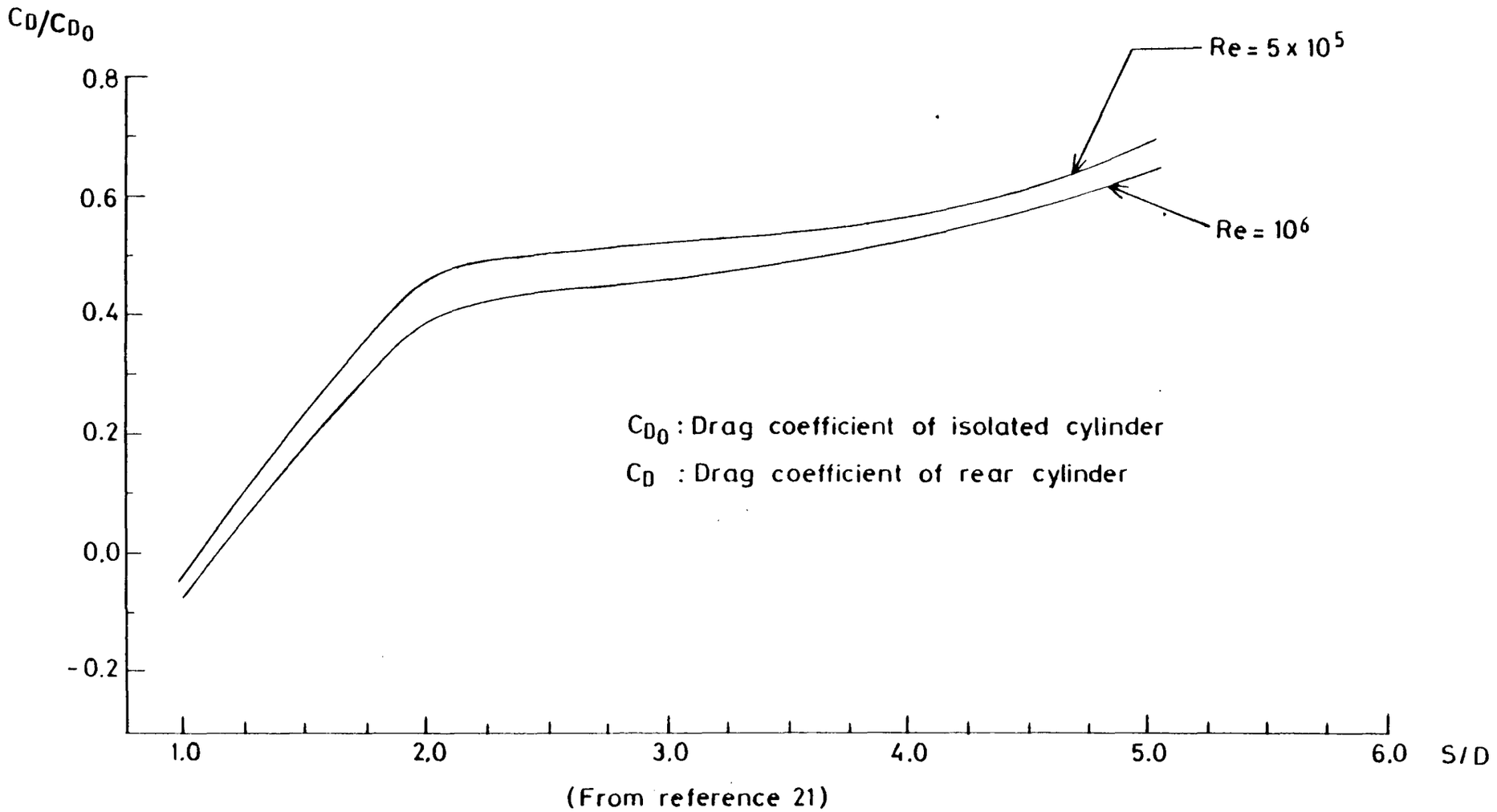

(From reference 21)

Fig. 22-A

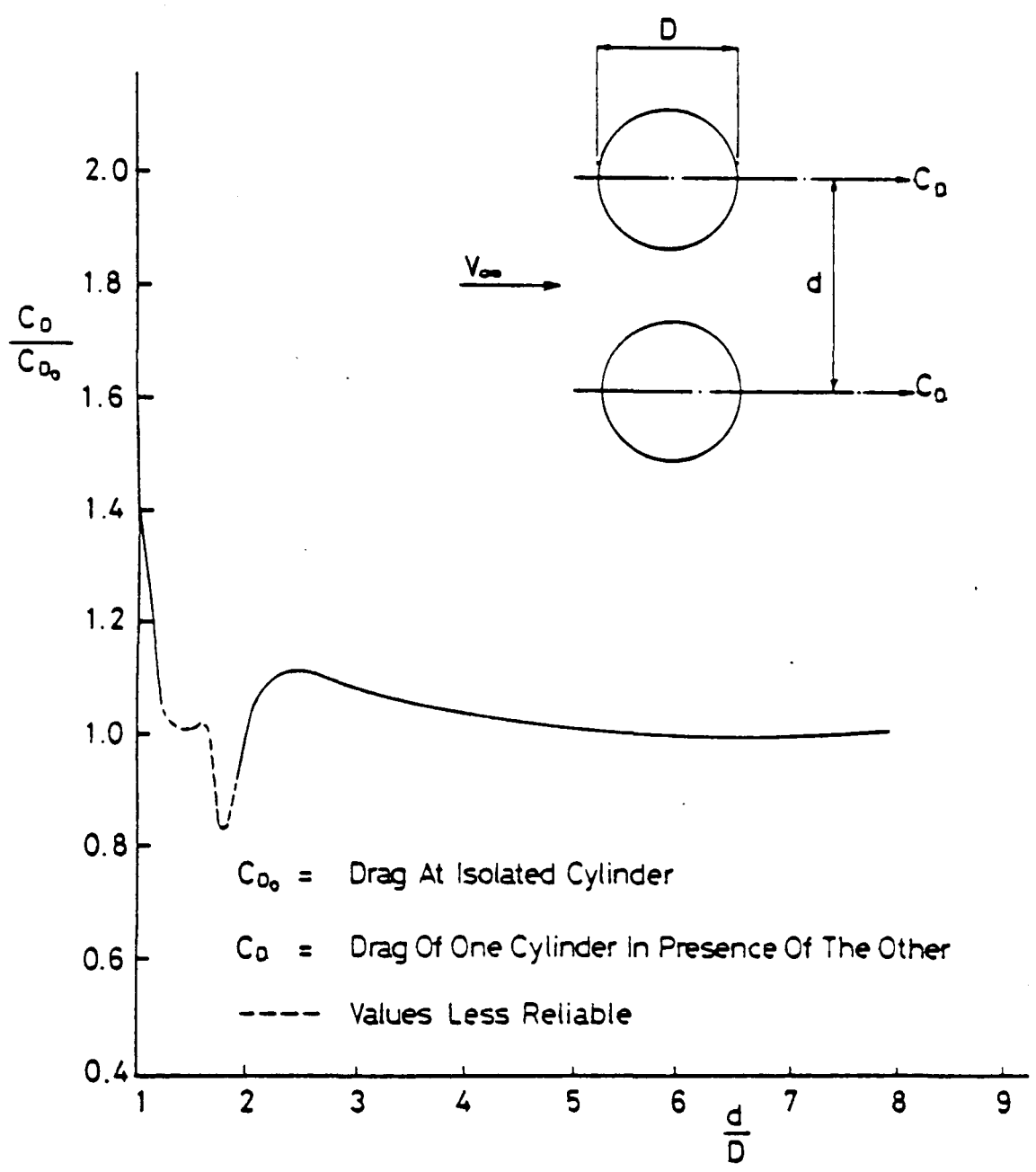

The Drag Coefficient Of Two Long Equal Plain Circular Cylinders Side By Side ($Re < Re_{crit.}$)
(From Reference 20)

Figure 23

The experiments mentioned above were carried out in the range of Reynolds Numbers smaller than 5×10^6. (See also Chapter 6).

2.1.8.2 *Drag force on two circular cylinders side by side:* According to reference [20], it was found from the tests in the sub-critical region in steady flow conditions that when the spacing between the cylinders is more than five diameters the interference is nil, when the spacing is reduced to about two diameters, the drag reduces because the separate vortex shedding system around each cylinder forms a single vortex system; when the spacing is reduced to one diameter the interference drag rapidly increases, Fig. 23. Since the experimental results were made non-dimensional by dividing the drag coefficient, including the interference effects by that for a single cylinder, these results have been used in this study during wave loading computations for the model scale. (See also Chapter 6).

In addition to the experimental work with cylinder arrays in steady flow [20,21], some experiments have also been carried out in oscillatory flow [22,23] and in waves [24]. In reference [23] it was reported that the blockage effect for cylinder arrays should be considered very carefully when the model test results are applied to the full scale which is in unconfined fluid. For groups of cylinders the blockage effect is quite different than that on a single cylinder, and the separation of blockage from interference impossible. In reference [24] wave tank tests were reported on three cylinders which were normal to the wave propagation direction and situated side by side. The results show that, in the sub-critical region, when the spacing between two cylinders is less than about one diameter, wave forces increase significantly. Certainly more tests in waves are needed for a better understanding of the problem.

2.1.9 Effect of inclination angle of cylindrical members on wave force calculations. Inclined cylindrical members are mainly used as support

bracing elements in the design of fixed offshore structures and are less common in floating structures. There are two main problems in doing wave force calculations on such members;

(i) The method to be used to apply the wave force equation (57) to an inclined member, and

(ii) The value of C_M and C_D to be used in the calculations.

In the literature [25,26,27] four different methods have been described for the application of equation (57) as summarised in the following.

1. In the first method inertia and drag forces are calculated as if they act on a vertical cylinder at any point along the inclined member and then normal components of those forces with respect to the inclined cylinder axes are taken into account. The method may be illustrated as follows:

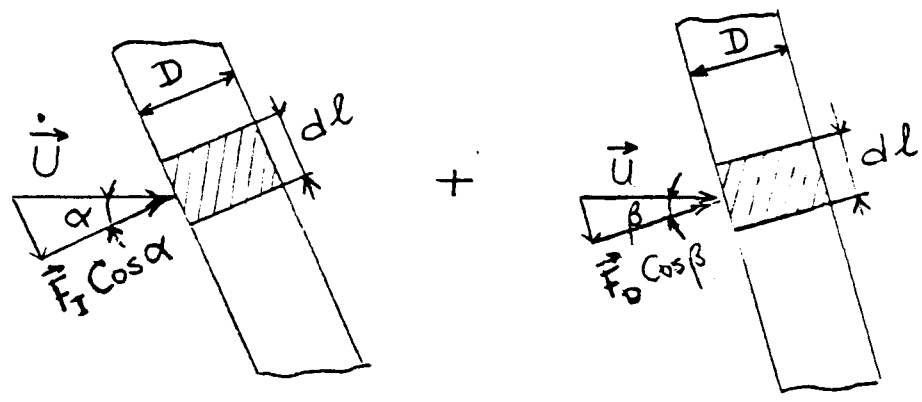

Fig. 24.

$$F_{T,1} = \rho \int_0^{\ell} [C_M A_s \dot{\vec{U}} \cos\alpha(\ell) + \frac{1}{2} C_D A_L \vec{U}|\vec{U}| \cos\beta(\ell)] \, d\ell \qquad (89)$$

where $A_s = \pi D^2/4$, $A_L = D$

C_M and C_D, inertia and drag coefficients for a circular section respectively.

2. The second method assumes that the acceleration and velocity vectors of the water particles always act normal to the inclined cylinder axis if the yaw angle is equal to or less than 60 degrees.

In comparison with the first method, the cosine factor is not used in this method. When the yaw angle is greater than 60 degrees a correction factor is applied. The method was found to be quite conservative. The principle of this method is illustrated as follows:

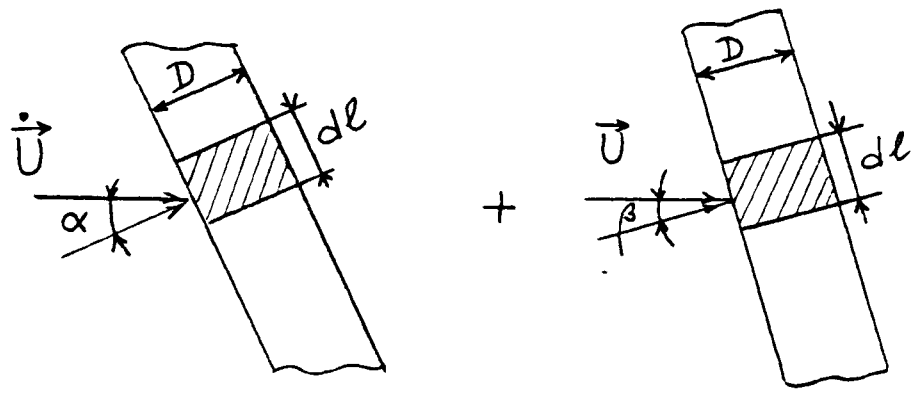

Fig. 25.

$$F_{T,2} = \rho \int_{o}^{\ell} [C_M A_s \dot{\vec{U}} k + \frac{1}{2} C_D A_L \vec{U}|\vec{U}|k] \, d\ell \qquad (90)$$

where $k = 1$ for $0° \leq \alpha$ (or β) $\leq 60°$

$$k = \frac{\tan(\frac{\pi}{2} - \alpha \text{ (or } \beta))}{\tan 30} \quad \text{for} \quad \alpha \text{ (or } \beta) \geq 60°$$

$A_s = \pi D^2/4$, $A_L = D$

C_M and C_D are the inertia and drag coefficients for a circular section respectively.

3. In the third method only the normal components of the acceleration and velocity of the water particles with respect to the inclined cylinder's axis are assumed to give rise to the wave loading. It can easily be seen that the difference between number (1) above and this method is that the drag force term in this method has a cosine squared term which gives less total force in the case of wave loading calculations where drag forces are significant, i.e. fixed and jacket types of offshore structures. This method was used by the author during his

development of generalised equations for wave force and moment calculations on circular cylinders [28] and by Chakrabarti et al, during their experimental investigations of the wave forces on randomly oriented tubes [27]. The method may be illustrated as follows:

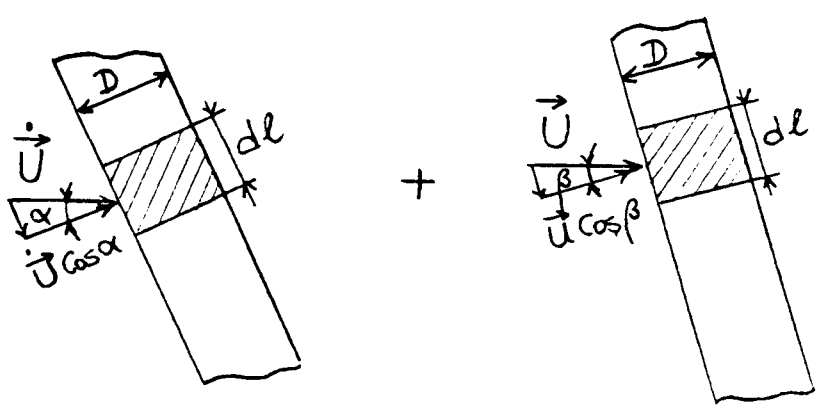

Fig. 26.

$$F_{T,3} = \rho \int_{o}^{\ell} [C_M A_s \dot{\vec{U}} \cos\alpha(\ell) + \frac{1}{2} C_D A_L \vec{U} \cos\beta(\ell) \left|\vec{U}\cos\beta(\ell)\right|] d\ell \quad (91)$$

where $A_s = \pi D^2/d$, $A_L = D$

C_M and C_D are the inertia and drag coefficients for a circular section.

4. The fourth method assumes that inertia and drag forces F_T and F_D act on the projected area of the inclined cylinder. This method, therefore, requires the C_M and C_D coefficients to be known for elliptical sections whose major axes are always parallel to the inertia and velocity vectors of the wave particles along the length of the inclined member. This method is not very practicable, for the determination of wave loading on the fixed or jacket type offshore platforms. The method may be illustrated with the following figure:

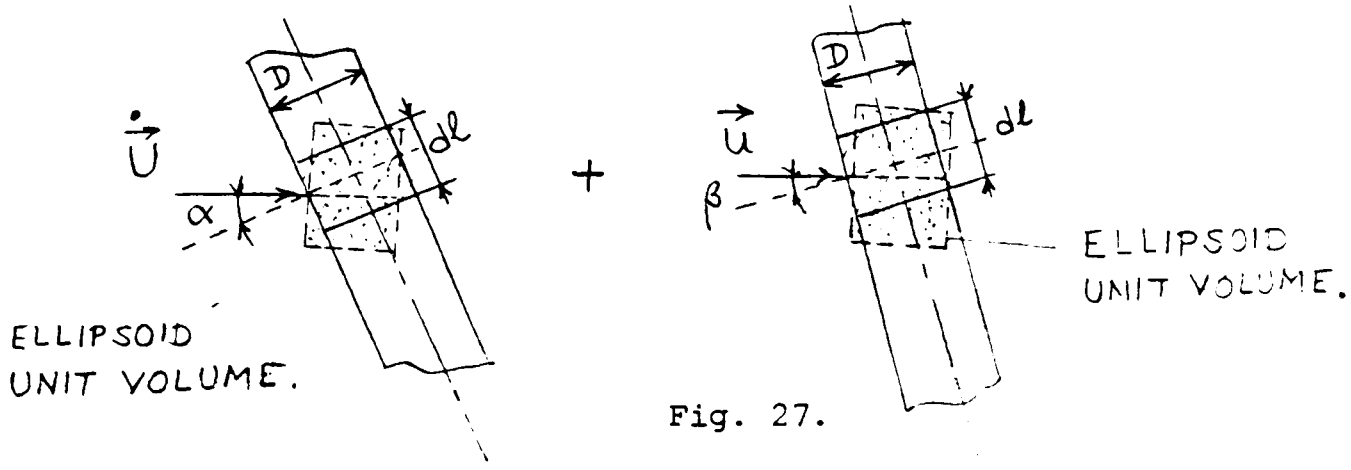

Fig. 27.

$$F_{T,4} = \rho \int_0^{\ell} \left| \overline{C}_M A_s \text{Cos}\alpha(\ell) \dot{\vec{U}} + \frac{1}{2} \overline{C}_D A_L \text{Cos}\beta(\ell) \vec{U} \right| d\ell \qquad (92)$$

where $\overline{C}_M$: inertia coefficient for elliptical section

$\overline{C}_D$: drag coefficient for elliptical section

$A_s = \pi D^2/4, \qquad A_L = D$

Regardless of which method is used to calculate the wave loading on the inclined cylindrical members of offshore structures, the C_M and C_D coefficients will be quite different from the values found from the experiments carried out with unyawed cylinders, simply because axial flow will occur.

Very few experimental results have been published on C_M and C_D coefficients of inclined cylinders in wavy or in steady flow.

The experimental investigation [29] done in steady flow conditions showed that the Reynolds Number at which the drag begins to decrease generally appears to decrease with increasing yaw angle, e.g. in reference [29] it is stated that the critical Reynolds Number decreased from 3.65×10^5 for an unyawed cylinder to 1.00×10^5 for a 60^0 yawed cylinder. Therefore it becomes clear that the drag characteristics of an inclined cylinder cannot be related solely to the Reynolds Number based on normal velocity components for Reynolds Numbers in and above the critical region. The results of the above mentioned work have been used in the wave loading computer programs develoepd by the author [30] for the comparison of theoretical calculations with model test results.

Recently some experimental work has been published [27] to report on the measurements of wave force coefficients on randomly oriented yawed cylinders in waves. The results have been presented for C_M and C_D values as a function of the Kuelegan-Carpenter Number. Although the results once again verify that variation in C_D and C_M coefficients is significant, as orientation and the yaw angle changes the test only

covers a very narrow sub-critical Reynolds Number and therefore further testing in the higher Reynolds Number range is vital so that the results can be used in the design of offshore structures.

2.1.10 The effect of roughness on the wave force coefficients of circular cylinders. All structures in the sea enviornment, either by marine fouling or by corrosion become roughed. The forces exerted by waves are, in general, increased by this roughness. When growths accumulate on the surface of a cylindrical member there is an increase in diameter which gives higher inertia and drag forces. Apart from this obvious effect, inertia and drag forces are also a function of relative roughness k/D as was mentioned in Section 2.1.3.

The experiments done in steady and oscillatory flow [31,32] indicate that drag coefficients decrease considerably as relative roughness increases for the Reynolds Numbers below the critical region. Above the critical region drag coefficients increase as relative roughness increases. The model test results both in waves [13] and in oscillating flow [14,15] show that the drag coefficients are a reverse function of inertia coefficients, hence, inertia coefficients increase as Reynolds Numbers increase below the critical region. Above the critical region, inertia coefficients decrease as relative roughness increases. In this study steady flow results are used to take the effect of roughness into account, even though very approximate. Full scale experiments in waves are needed so that appropriate constants can be used in wave loading calculations for offshore structures.

2.1.11 The non-linear effects on wave force calculations. Linearised free surface boundary conditions have been assumed in all equations concerned with wave particulars and wave loading.

The linearised free surface condition is the combination of the kinematic boundary condition, which states that normal velocities of the fluid and of the boundary surface must be equal, and the dynamic boundary condition which states that the pressure on the free surface must be atmospheric. If we assume that the vertical displacement of any point on the free surface may be defined by a function $y=\eta(x,z,t)$ (for two dimensional flow $y=\eta(x,t)$) then if we write the substantial derivative of $y-\eta$

$$\frac{D}{Dt}(y-\eta) = \frac{\partial y}{\partial t} - \frac{\partial \eta}{\partial t} - U_x \frac{\partial \eta}{\partial x} - U_z \frac{\partial \eta}{\partial z} \qquad (93)$$

Since on the free surface $y=\eta$, and

$$\frac{\partial y}{\partial t} = U_y = \frac{\partial \Phi}{\partial y} \quad , \quad U_x = \frac{\partial \Phi}{\partial x} \quad \text{and} \quad U_z = \frac{\partial \Phi}{\partial z}$$

equation (93) can also be written in the following form

$$\frac{\partial \Phi}{\partial y} - \frac{\partial \eta}{\partial t} - \frac{\partial \Phi}{\partial x}\frac{\partial \eta}{\partial x} - \frac{\partial \Phi}{\partial z}\frac{\partial \eta}{\partial z} = 0 \qquad (93\text{-A})$$

If the wave elevation is small $\frac{\partial \eta}{\partial x}$ and $\frac{\partial \eta}{\partial z}$ are small also.

Therefore the last two terms in equation (93-A) can be ignored and the kinematic boundary condition is as follows

$$\frac{\partial \Phi}{\partial y} = \frac{\partial \eta}{\partial t} \qquad (94)$$

Equation (94) verifies the kinematic boundary conditions as defined above.

The dynamic boundary condition can easily be obtained from Bernoulli's equation given in equation (23)

$$\eta = -\frac{1}{g}\left[\frac{\partial \phi}{\partial t} + \frac{1}{2}\nabla\Phi\nabla\Phi\right] \qquad (95)$$

By neglecting the last term we obtain a linearised equation for the free surface

$$\eta = -\frac{1}{g}\frac{\partial \Phi}{\partial t} \qquad (96)$$

Combining equations (94) and (96), the linear free surface boundary condition becomes,

$$\frac{\partial^2 \Phi}{\partial t^2} + g \frac{\partial \Phi}{\partial y} = 0 \quad \text{on} \quad y = 0 \tag{97}$$

or,

$$\frac{\partial \Phi}{\partial y} - \frac{\omega^2}{g} \Phi = 0 \quad \text{on} \quad y = 0 \tag{97-A}$$

(Since, $\Phi = c \, \text{Sin}\omega t$.)

To derive the non-linear free surface boundary condition exact solutions of equations (93) and (95) can be obtained or a combination of the kinematic and dynamic boundary conditions solved by defining the change of pressure on the moving free surface as constant, i.e.

$$\frac{Dp}{Dt} = \left(\frac{\partial}{\partial t} + \nabla\Phi\nabla\right) p = 0 \tag{98}$$

If we substitute Bernoulli's equation (23) into equation (98), the exact free surface boundary condition can be obtained

$$\frac{\partial^2 \Phi}{\partial t^2} + g \frac{\partial \Phi}{\partial y} + 2\nabla\Phi\nabla \frac{\partial \Phi}{\partial t} + \frac{1}{2} \nabla\Phi\nabla \, (\nabla\Phi\nabla\Phi) = 0 \tag{99}$$

A function f(x,y,z,t) can be expanded around y using Taylor's series expansion as follows

$$f(x,y,z,t) = f(x,o,z,t) + y\left(\frac{\partial f}{\partial y}\right)_{y=0} + \frac{1}{2} y^2 \left(\frac{\partial^2 f}{\partial y^2}\right)_{y=0} + \text{---} \tag{100}$$

If we apply equation (100) to equation (99) the following set of free surface boundary conditions are obtained

$$\frac{\partial^2 \Phi^{(1)}}{\partial t^2} + g \frac{\partial \Phi^{(1)}}{\partial y} = 0 \tag{101}$$

$$\frac{\partial^2 \Phi^{(2)}}{\partial t^2} + g \frac{\partial \Phi^{(2)}}{\partial y} = - 2\nabla\Phi^{(1)} \nabla \frac{\partial \Phi^{(1)}}{\partial t} + \frac{1}{g} \frac{\partial \Phi^{(1)}}{\partial t} \frac{\partial}{\partial y} \left(\frac{\partial^2 \Phi^{(1)}}{\partial t^2} + g \frac{\partial \Phi^{(1)}}{\partial y} \right) \tag{102}$$

If we substitute the first order velocity potential of the undisturbed waves

$$\Phi_o = Re \left[- i \frac{0.5g\ H_w}{\omega} e^{ky}\ e^{ikx}\ e^{-i\omega t} \right]$$

into equation (102) this potential also satisfies second order boundary conditions, and therefore, we can state that the first order potential is a solution of the second-order boundary value problem.

Equation (100) can also be applied to equation (95) to obtain the second-order correction for surface elevation

$$\eta = - \frac{1}{g} \left[\frac{\partial \Phi}{\partial t} + \frac{1}{2} \nabla\Phi\nabla\Phi\right]_{y=\eta} \qquad (103)$$

$$= - \frac{1}{g} \left[\frac{\partial \Phi}{\partial t} + \frac{1}{2} \nabla\Phi\nabla\Phi\right]_{y=0} + \eta \frac{\partial}{\partial y} \left\{ - \frac{1}{g} \left(\frac{\partial \Phi}{\partial t} + \frac{1}{2} \nabla\Phi\nabla\Phi\right) \right\}_{y=0}$$

$$= - \frac{1}{g} \left(\frac{\partial \Phi}{\partial t} + \frac{1}{2} \nabla\Phi\nabla\Phi - \frac{1}{g} \frac{\partial \Phi}{\partial t} \frac{\partial^2 \Phi}{\partial y \partial t}\right)_{y=0}$$

If we substitute the velocity potential for undisturbed waves

$$\Phi_o = Re \left[- i \frac{0.5g\ H_w}{\omega} e^{ky}\ e^{ikx}\ e^{-i\omega t} \right]$$

into equation (103) the surface elevation η takes the following form

$$\eta = 0.5\ H_w\ Cos(kx-\omega t) - \frac{1}{2} k(0.5\ H_w)^2 + k(0.5\ H_w)^2\ Cos\ (kx-\omega t) \qquad (104)$$

or

$$\eta = 0.5\ H_w\ Cos(kx-\omega t) + \frac{1}{2} k(0.5\ H_w)^2\ Cos2(kx-\omega t) \qquad (104\text{-}A)$$

2.1.11.1 *Second-order time dependent forces:* Lighthill shows in reference [9] that linearisation of the free surface boundary conditions requires a quadratic correction to the linear velocity potential, and this results in associated corrections to the wave forces. In addition to the correction due to the modified potential, the linear potential also gives rise to time varying second-order forces as was

shown in Section 2.1.1 equation (54). If we rewrite the second-order force part from equation (24) for a fixed member, it takes the following form

$$\vec{F}_{x,s,d} = - \iint_{S_M} \frac{1}{2} \rho \, (\nabla \Phi_F)^2 \, \vec{n}_x \, dS \qquad (105)$$

where

$$|\vec{n}_x| \, dS = - R \, \mathrm{Cos}\theta \, d\theta$$

Using undisturbed wave potential and doublet representation of a cylinder in waves from equation (72) the linear velocity potential may be written as

$$\Phi_{F,L} = U_x \left[X + \frac{R^2 X}{r^2} \right] = U_x \left[r + \frac{R^2}{r} \right] \mathrm{Cos}\theta \qquad (106)$$

where

$$U_x = 0.5 \, H_w \, \omega e^{ky} \, \mathrm{Cos}(kx - \omega t)$$

When $F_{x,s,d}$ is calculated by substituting equation (106) into equation (105) the result will be zero. But in reference [9] it was shown that $\Phi_{F,L}$ should also include a response to "fluctuating extensional motions". Extensional motion is defined as the horizontal gradient of horizontal velocity. Hence, second-order forces will result from the interaction between the member's response to the oncoming wave's velocity and its extension.

The velocity potential due to the response to the "extension" is given as follows (Fig. 28)

$$\Phi_{E,L} = \frac{1}{4} E \, (r^2 - 2R^2 \ell nr) + \frac{1}{4} E \, \left(r^2 + \frac{R^4}{r^2}\right) \mathrm{Cos}2\theta \qquad (107)$$

where E represents the extensional motions of fluid particles and can be expressed as

$$E(x,y,t) = \frac{\partial U_x}{\partial x} = - 0.5 \, H_w \, k\omega e^{ky} \, \mathrm{Sin}(kx - \omega t) \qquad (108)$$

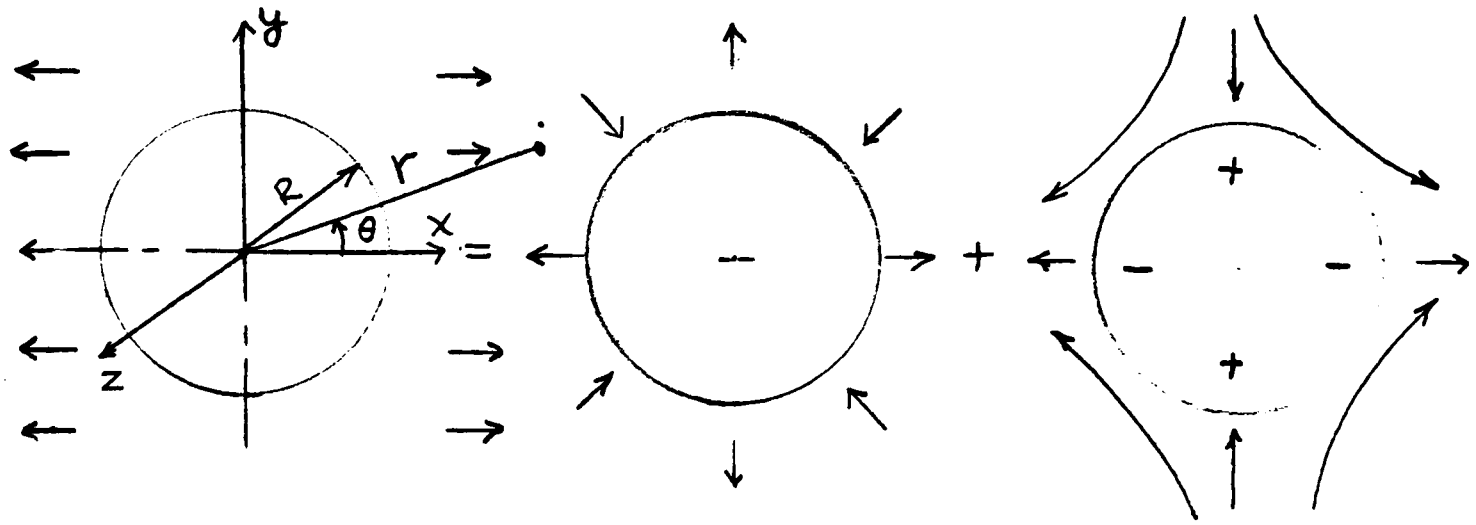

RESPONSE TO EXTENSION = MONOPOLE RESPONSE + QUADRUPOLE RESPONSE

$$\frac{1}{4}E\left(r^2 - 2R^2 \ell nr\right) \qquad \frac{1}{4}E\left(r^2 + \frac{R^4}{r^2}\right)\cos 2\theta$$

Fig. 28. (From reference [9].)

If we replace Φ_F with $\Phi_{F,L} + \Phi_{E,L}$ in equation (105)

$$F_{x,s,d} = -\int_{-d}^{0}\int_{o}^{2\pi} \frac{1}{2}\rho \left\{\nabla\left[U_x\left(r + \frac{R^2}{r}\right)\cos\theta + \frac{1}{4}E(r^2 - 2R^2 \ell nr)\right.\right.$$

$$\left.\left. + \frac{1}{4}E\left(r^2 + \frac{R^4}{r^2}\right)\cos 2\theta\right]_{r=R}\right\}^2 R\cos\theta\, d\theta\, dy \qquad (109)$$

$(\nabla\phi)^2$ in cylindrical co-ordinates can be written as follows

$$(\nabla\phi)^2 = \left(\frac{\partial\phi}{\partial r}\right)^2 + \left(\frac{1}{r}\frac{\partial\phi}{\partial\theta}\right)^2 + \left(\frac{\partial\phi}{\partial z}\right)^2 \qquad (110)$$

If we apply equation (110) to equation (109) $F_{x,s,d}$ can be determined in the following form

$$F_{x,s,d} = -\int_{-d}^{o}\int_{o}^{2\pi} \frac{1}{2}\rho \left[(2U_x \sin\theta + ER\sin 2\theta)^2 + (2U_x kR\cos\theta - k^{-1}E)^2\right]$$

$$R\cos\theta\, d\theta\, dy \qquad (111)$$

The second bracket in equation (111) is the vertical velocity which was derived from the velocity potential given in equation (106) and the velocity potential of the undisturbed wave field given in equation (6-A). Calculating the above integral with respect to θ,

$$F_{x,s,d} = \int_{-d}^{o} - \rho\, U_x E\pi R^2 dy = + \int_{-d}^{o} \rho g\pi (0.5\, H_w\, k)^2\, e^{2ky} R^2 \mathrm{Sin}(kx-\omega t)$$

$$\mathrm{Cos}(kx-\omega t)\ dy \qquad (112)$$

or

$$F_{x,s,d} = + 0.5\, \rho g\pi (0.5\, H_w)^2\, kR^2 [1-e^{-2kd}]\ \mathrm{Sin}(kx-\omega t)\ \mathrm{Cos}(kx-\omega t) \qquad (112\text{-A})$$

This force is called the second-order dynamic force and has half the value of the second-order correction force calculated in equation (54).

When a vertical cylindrical member penetrates the water surface, in the region between y=0 and y=η, an additional force will be exerted on the member. This force is the result of hydrostatic pressure and the dynamic pressure force, and can be written in the following form

$$F_{x,s,w} = F_{x,DYN} - F_{x,HIDR} \qquad (113)$$

where

$$F_{x,DYN} = - \int_{\theta=0}^{2\pi} \int_{y=0}^{\eta} \rho \frac{\partial \Phi_o}{\partial t} R\mathrm{Cos}\theta\ d\theta\ dy = \int_{\theta=0}^{2\pi} \int_{y=0}^{\eta} 0.5\rho g\, H_w\, R\mathrm{Cos}\theta$$

$$\mathrm{Cos}(kx-\omega t)\ d\theta\ dy$$

$$= \int_{o}^{2\pi} \rho g \eta^2\, R\mathrm{Cos}\theta\ d\theta \qquad (113\text{-A})$$

(It is assumed that dynamic pressure does not change between y=0 and y=η.)

$$F_{x,HIDR} = \int_{\theta=0}^{2\pi} \int_{y=0}^{\eta} \rho g y\, R\mathrm{Cos}\theta\ d\theta\ dy = \int_{o}^{2\pi} \frac{1}{2} \rho g \eta^2\, R\mathrm{Cos}\theta\ d\theta \qquad (113\text{-B})$$

If we substitute equation (96) in equations (113-A) and (113-B), equation (113) becomes

$$F_{x,s,w} = \frac{1}{2} \int_{o}^{2\pi} \frac{\rho}{g} \left(\frac{\partial \Phi}{\partial t}\right)^2 R\mathrm{Cos}\theta\ d\theta \qquad (114)$$

where

$$\frac{\partial \Phi}{\partial t} = \frac{\partial \Phi_{F,L}}{\partial t} + \frac{\partial \Phi_{o}}{\partial t}$$

Calculating the derivatives of $\Phi_{F,L}$ and Φ_{o} using equations (106) and (6-A) respectively, $F_{x,s,w}$ takes the following form

$$F_{x,s,w} = \frac{1}{2} \int_{o}^{2\pi} \frac{\rho}{g} [H_w \, kg \, Sin(kx-\omega t) \, RCos\theta - 0.5 \, H_w g \, Cos(kx-\omega t)]^2$$

$$R(-\, Cos\theta) \, d\theta \qquad (115)$$

or

$$F_{x,s,w} = 2.0 \, \rho g \pi \, (0.5 \, H_w)^2 \, kR^2 \, Sin(kx-\omega t) \, Cos(kx-\omega t) \qquad (115\text{-}A)$$

If we sum the second-order correction force given in equation (54), and the second-order dynamic and waterline forces given in equations (112-A) and (115-A) respectively, we may obtain a correction force to the wave force equation given in equation (57) as follows

$$\Delta F_{x,c} = F_{x,s,c} + F_{x,s,d} + F_{x,s,w} \qquad (116)$$

or

$$\Delta F_{x,c} = \rho g \pi \, (0.5 \, H_w)^2 \, kR^2 \, [2-0.5 \, (1-e^{-2kd})] \, Sin(kx-\omega t) \, Cos(kx-\omega t) \qquad (116\text{-}A)$$

The effect of second-order forces is shown in Figs 29 and 30 for varying values of kR and H_w/D.

The correction given in reference [9] only includes $F_{x,s,d}$ and $F_{x,s,w}$ terms and may written as follows

$$F'_{x,c} = \rho g \pi \, (0.5 \, H_w)^2 \, kR^2 \, [2+0.5 \, (1-e^{-2kd})] \, Sin(kx-\omega t) \, Cos(kx-\omega t) \qquad (117)$$

The results of equation (117) are also shown in Figs 31 and 32 for varying kR and H_w/D values.

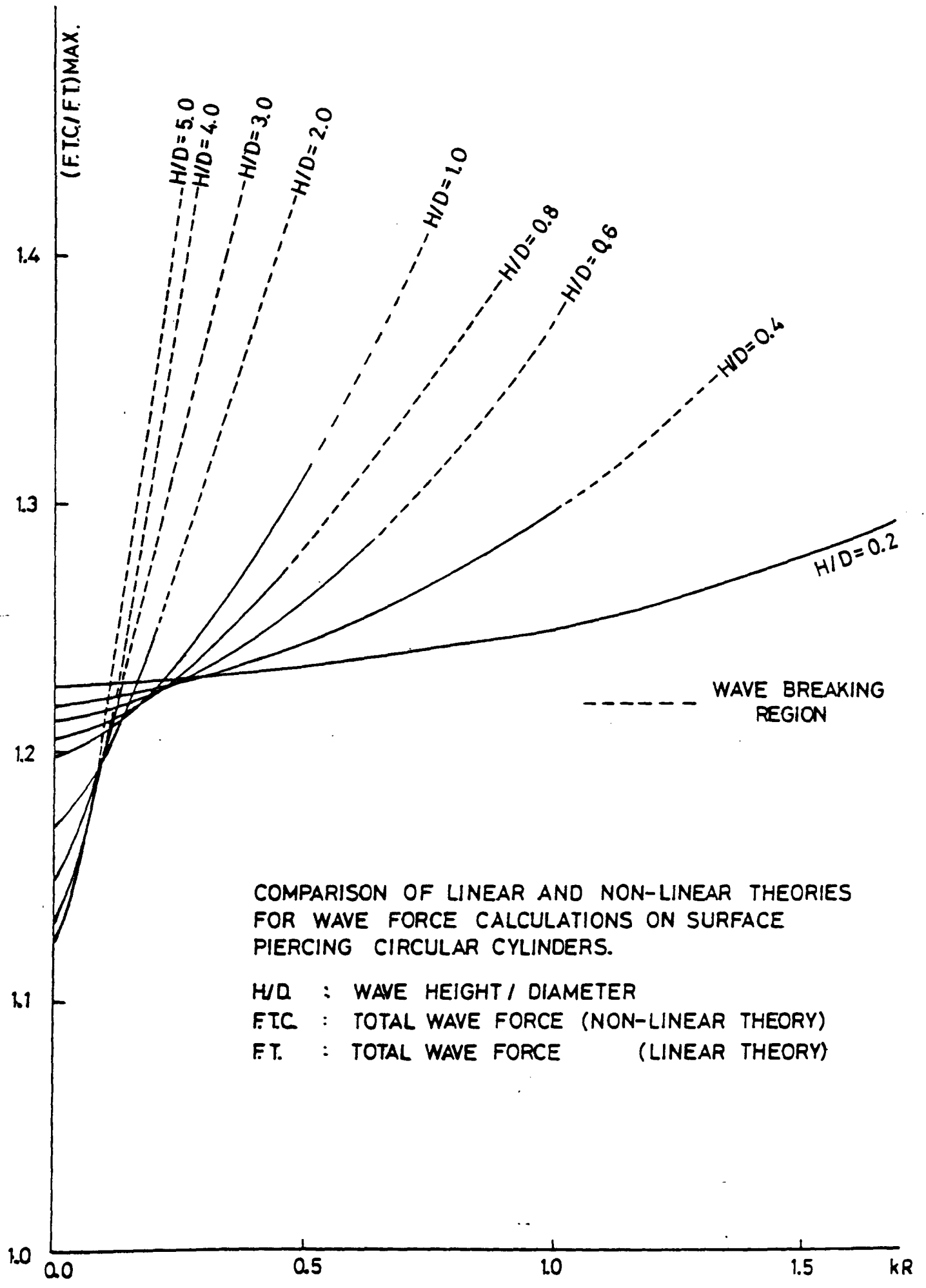
(F.T.C./F.T)MAX.
1.4
1.3
1.2
1.1
1.0
0.0
0.5
1.0
1.5
kR
H/D= 5.0
H/D= 4.0
H/D= 3.0
H/D= 2.0
H/D= 1.0
H/D= 0.8
H/D= 0.6
H/D= 0.4
H/D= 0.2
WAVE BREAKING REGION
COMPARISON OF LINEAR AND NON-LINEAR THEORIES FOR WAVE FORCE CALCULATIONS ON SURFACE PIERCING CIRCULAR CYLINDERS.
H/D : WAVE HEIGHT / DIAMETER
F.T.C. : TOTAL WAVE FORCE (NON-LINEAR THEORY)
F.T. : TOTAL WAVE FORCE (LINEAR THEORY)

Fig. 29

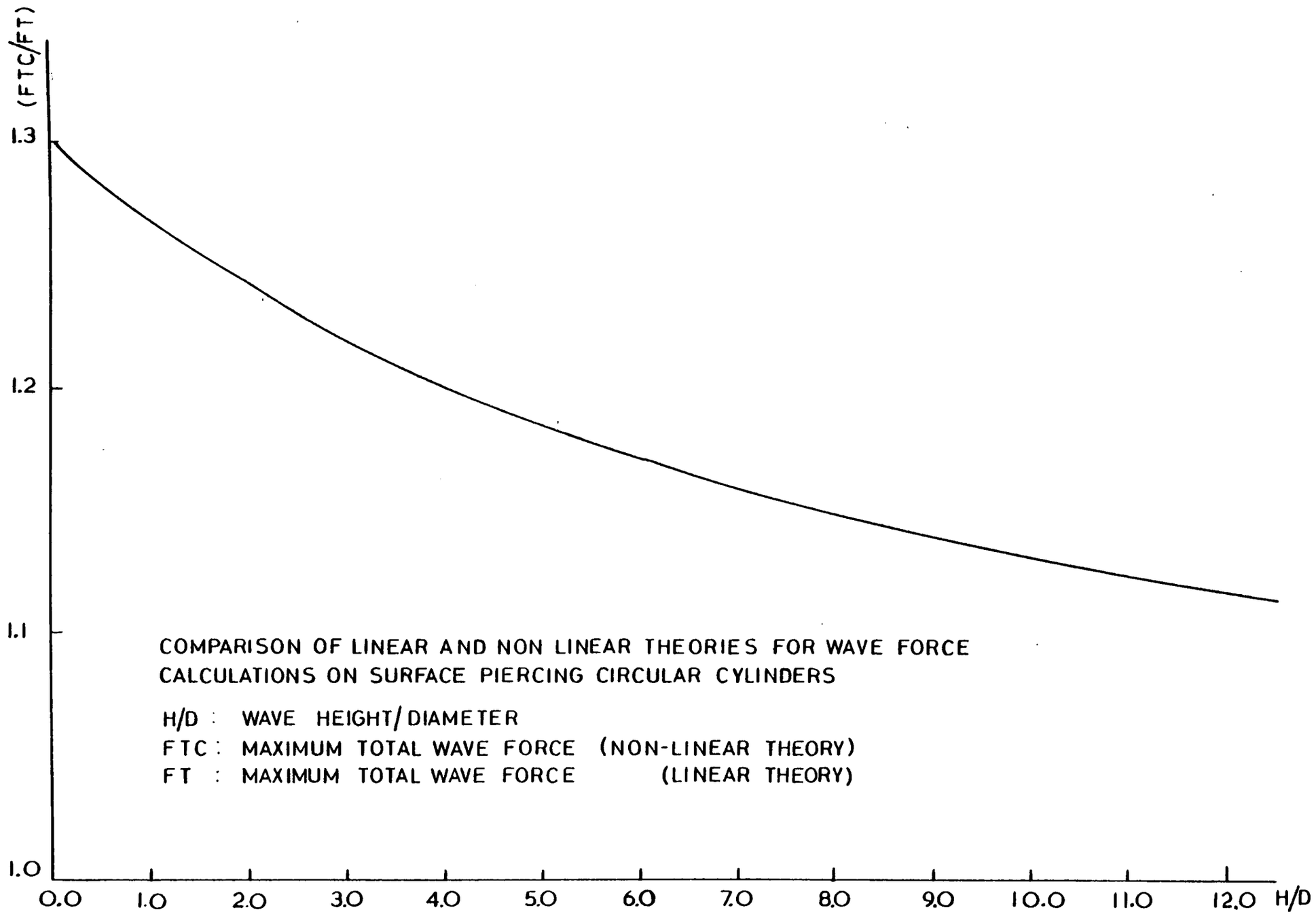
F/F (FTC/FT)
1.3
1.2
1.1
1.0
COMPARISON OF LINEAR AND NON LINEAR THEORIES FOR WAVE FORCE
CALCULATIONS ON SURFACE PIERCING CIRCULAR CYLINDERS
H/D : WAVE HEIGHT/DIAMETER
FTC : MAXIMUM TOTAL WAVE FORCE (NON-LINEAR THEORY)
FT : MAXIMUM TOTAL WAVE FORCE (LINEAR THEORY)
0.0
1.0
2.0
3.0
4.0
5.0
6.0
7.0
8.0
9.0
10.0
11.0
12.0
H/D

Fig. 30

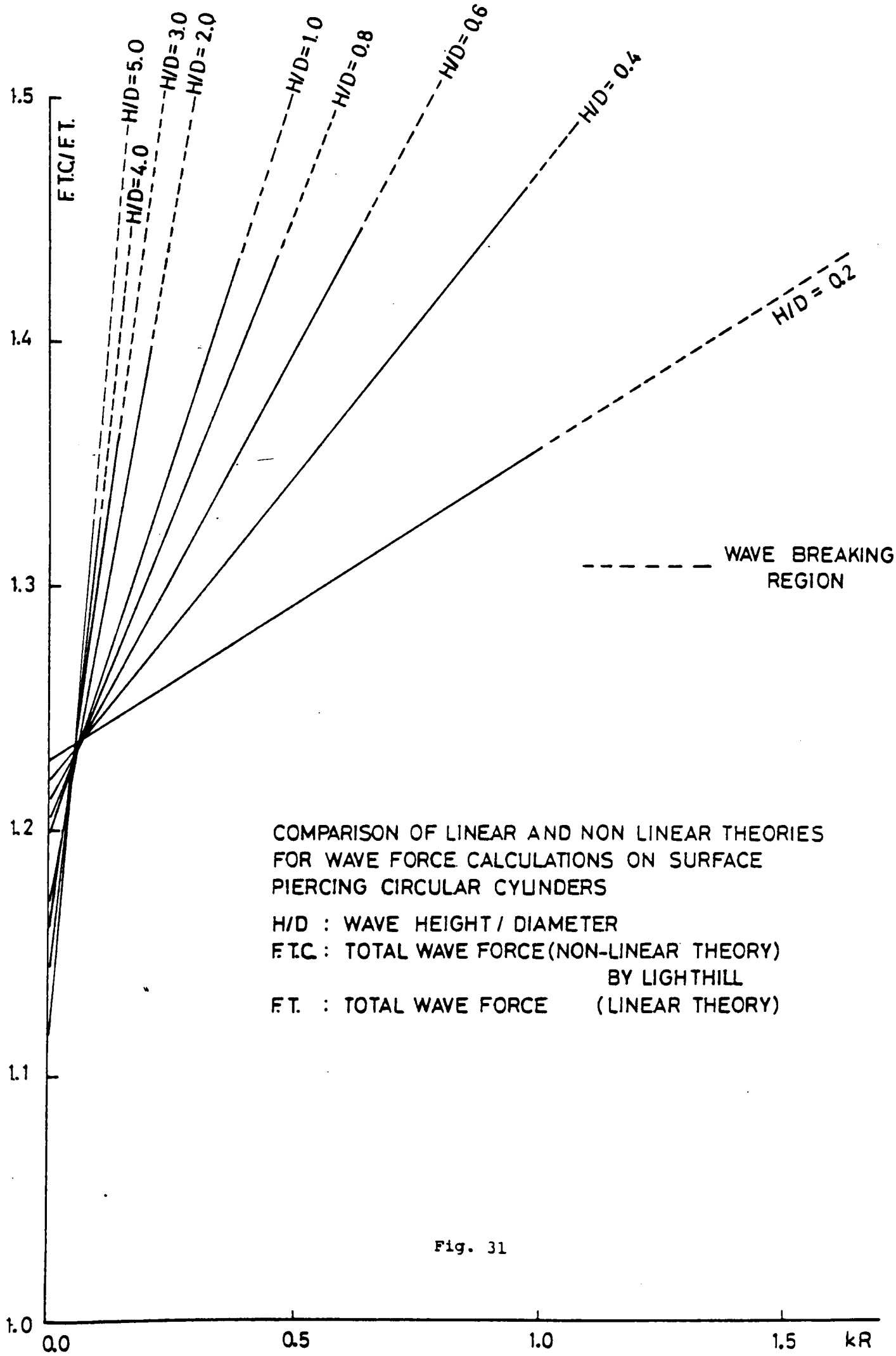
H/D=5.0
H/D=4.0
H/D=3.0
H/D=2.0
H/D=1.0
H/D=0.8
H/D=0.6
H/D=0.4
H/D=0.2
F.T.C./F.T.
1.5
1.4
1.3
1.2
1.1
1.0
0.0
0.5
1.0
1.5
kR
WAVE BREAKING REGION
COMPARISON OF LINEAR AND NON LINEAR THEORIES FOR WAVE FORCE CALCULATIONS ON SURFACE PIERCING CIRCULAR CYLINDERS
H/D : WAVE HEIGHT / DIAMETER
F.T.C. : TOTAL WAVE FORCE (NON-LINEAR THEORY) BY LIGHTHILL
F.T. : TOTAL WAVE FORCE (LINEAR THEORY)

Fig. 31

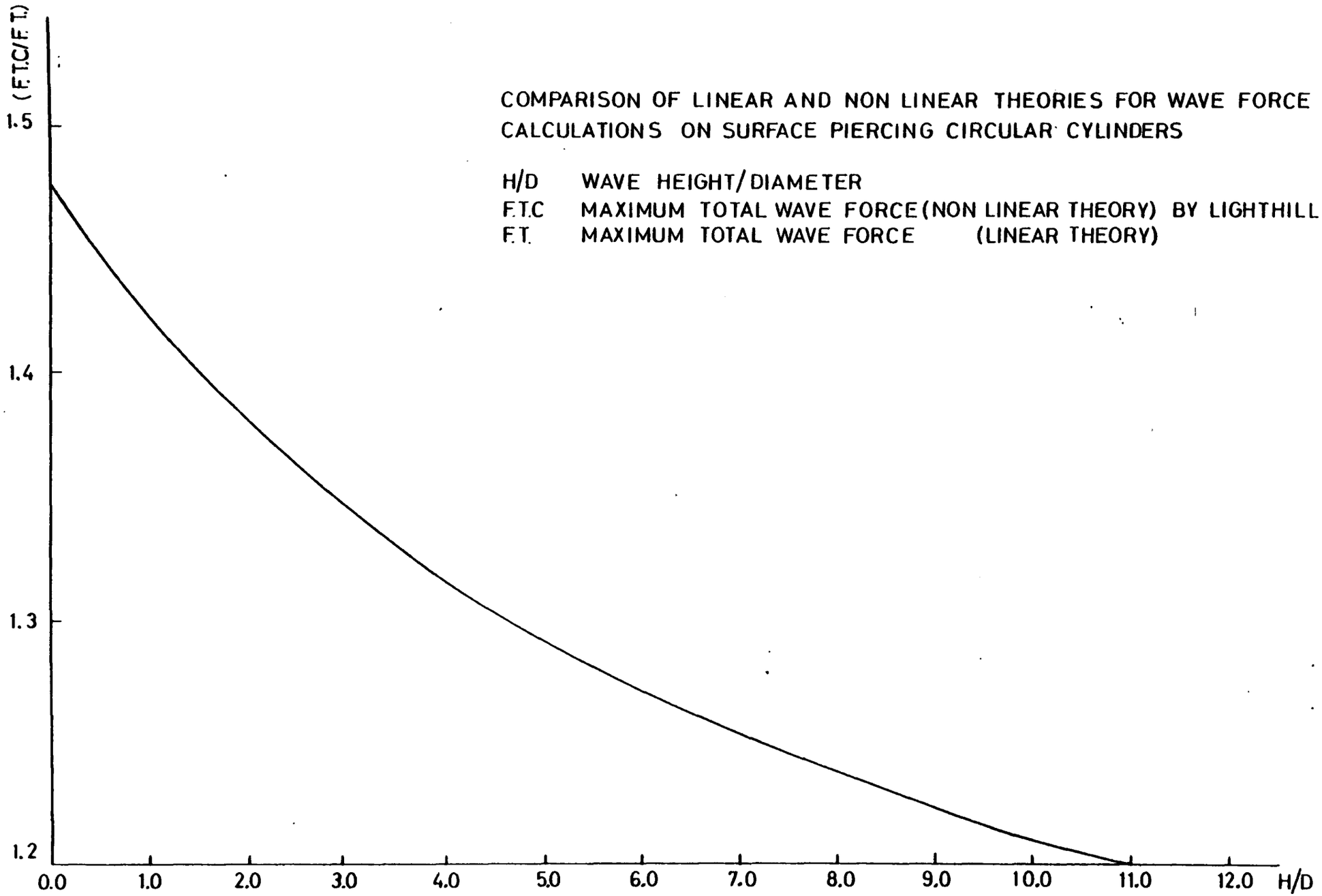

COMPARISON OF LINEAR AND NON LINEAR THEORIES FOR WAVE FORCE CALCULATIONS ON SURFACE PIERCING CIRCULAR CYLINDERS

H/D WAVE HEIGHT/DIAMETER
F.T.C MAXIMUM TOTAL WAVE FORCE (NON LINEAR THEORY) BY LIGHTHILL
F.T. MAXIMUM TOTAL WAVE FORCE (LINEAR THEORY)

Fig. 32

2.1.11.2 *Second-order time independent forces:* In addition to the time varying second-order forces, it can be shown that the velocity potential $\Phi_{F,L}$ given in equation (106) produces second-order steady forces. Since the velocity potential $\Phi_{F,L}$ is only valid for small diameter members, i.e. $D/\lambda<0.2$. The results given in this section are restricted to the members of offshore structures which are in inertia, intertia + drag or drag regimes.

The second-order steady forces in the diffraction regime will also be discussed in Section 2.2. Second-order steady forces may have an important contribution in explaining the tilt phenomena which occurs during the semi-submersible model tank experiments [33].

The complete solution for second-order vertical forces on a submerged circular cylinder was given first by Ogilvie in reference [34]. In the following, the approximate solution will be summarised using the velocity potential given in equation (106). If we substitute equation (106) into the second-order force part in equation (24), the vertical force can easily be written in the following form (Fig. 33)

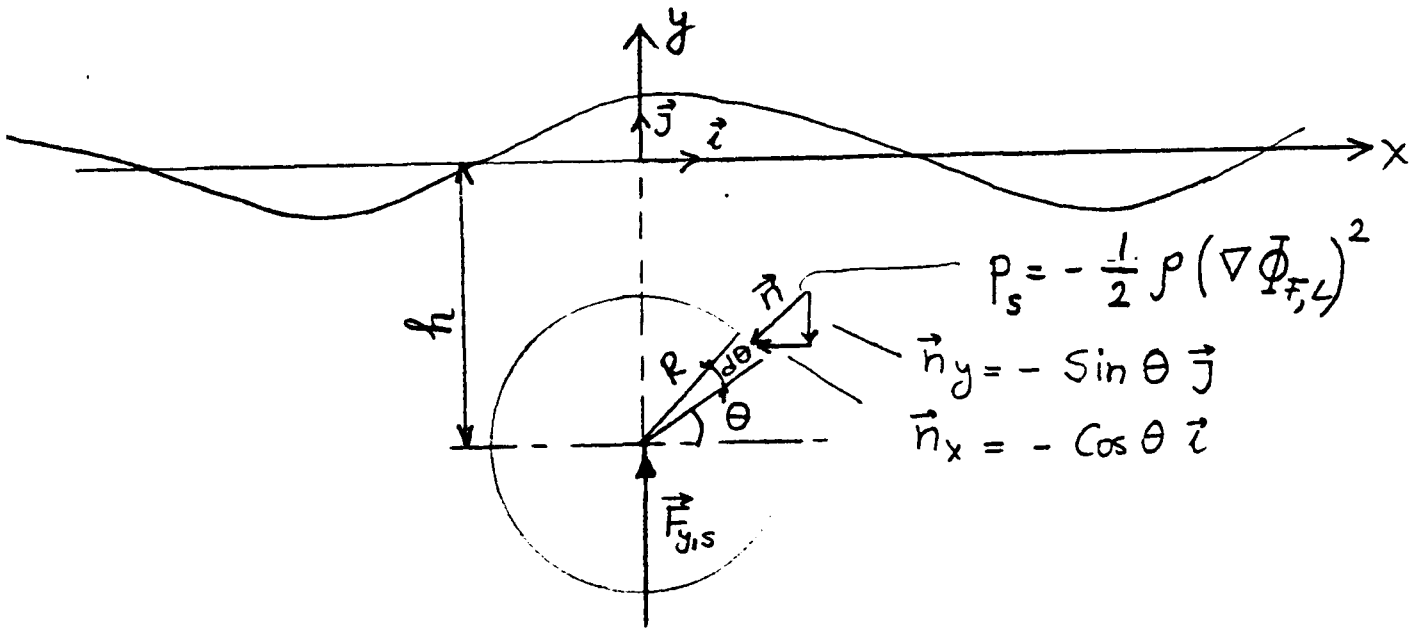

Fig. 33.

$$\vec{F}_{y,s} = -\frac{1}{2}\rho \iint_{S_M} [\nabla(H_w\, \omega e^{ky}\, \chi\, \mathrm{Cos}\omega t)]^2\, \vec{n}_y\, dS \qquad (118)$$

$$= \frac{1}{2}\rho \int_{z=0}^{\ell} \int_{\theta=0}^{2\pi} \rho[H_w^2\, \omega^2 e^{2ky}\, \mathrm{Cos}^2\omega t\, (1+k^2x^2)]\, R\mathrm{Sin}\theta\, d\theta\, dz\, \vec{j}$$

Replacing $y = -(h-R\mathrm{Sin}\theta)$, $\chi = R\mathrm{Cos}\theta$ and using the following relation given in reference [35]

$$e^{a\mathrm{Sin}\theta} = I_o(a) + 2\sum_{j=0}^{\infty} (-1)^j\, I_{2j+1}(a)\, \mathrm{Sin}\{(2j+1)\theta\}$$

$$+ 2\sum_{j=1}^{\infty} (-1)^j\, I_{2j}(a)\, \mathrm{Cos}(2j\theta) \qquad (119)$$

where $I_j(a)$ are the "Modified Bessel" Functions.

Equation (118) becomes

$$\vec{F}_{y,s} = \int_o^{\ell} \rho g \pi H_w^2\, kR\, e^{-2hR}\, \mathrm{Cos}^2\omega t\, I_1(2kR)\, dz\, \vec{j} \qquad (120)$$

The time average of a function can be written as

$$\mu = \lim_{T\to\infty} \frac{1}{2T} \int_{-T}^{T} \chi(t)\, dt \qquad (121)$$

If we apply equation (121) to equation (120)

$$\overrightarrow{\overrightarrow{F}}^{t}_{y,s} = \int_o^{\ell} 2\rho g\pi\, (0.5\, H_w)^2\, kR\, e^{-2hR}\, I_1(2kR)\, dz\, \vec{j} \qquad (122)$$

where I_1 is the first kind modified Bessel function.

The same equation can be obtained by replacing $\mathrm{Cos}^2\omega t = \frac{1}{2}(1-\mathrm{Cos}2\omega t)$ and only retaining the time independent part. The second-order time independent forces for horizontal circular cylinders beneath the free surface have been calculated and the results are shown in Fig. 34 for varying values of kR and Y/D. It was found from the comparison of steady tilt angle measurements with second-order steady force calculations that the maximum tilt angle occurs at about the same frequency at which the second-order steady forces reach a maximum value.

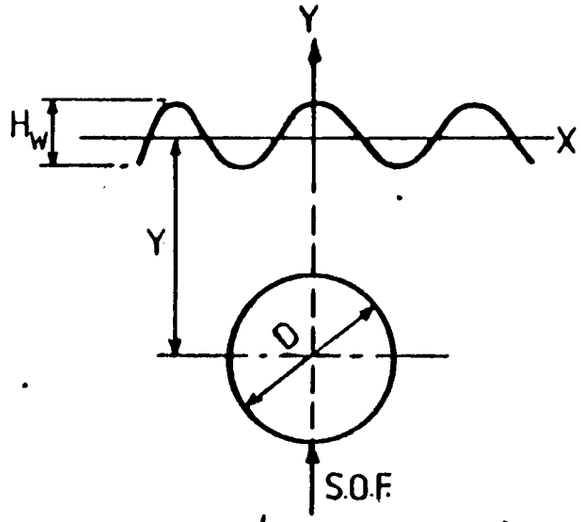

SECOND ORDER TIME INDEPENDENT FORCES (LINEAR THEORY)

Fig. 34.

The second type of steady-state force occurs due to the time independent components of horizontal wave particle velocity, and, therefore, can be significant in the drag regime where members of offshore structures have relatively small sectional dimensions. These forces, the so-called drift forces, which are in the same direction as wave propagation, can be important in the design of riser systems, mooring cables, etc.

We define the fluid particles' position with the position vector $\vec{r}_o(x_o,y_o,t)$. If particles are displaced by a small amount, the new position vector will be $\vec{r}(x,y,t)$. Similarly, velocity vectors of fluid particles can be written as $\vec{v}_o(x_o,y_o,t)$ and $\vec{v}(x,y,t)$ for first and second positions respectively.

$$\vec{v}_o = U_{x,o}\ (x_o,y_o,t)\ \vec{i} + U_{y,o}\ (x_o,y_o,t)\ \vec{j}$$
$$\vec{v} = U_x\ (x,y,t)\ \vec{i} + U_y\ (x,y,t)\ \vec{j} \qquad (123)$$

if we write Taylor's series expansions for $\{U_{x_o},U_x\}$ and $\{U_{y_o},U_y\}$ the following equations are obtained

$$U_{x,o} = U_x + (x_o-x)\ \frac{\partial U_x}{\partial x} + (y-y_o)\ \frac{\partial U_x}{\partial y} + \text{---} \qquad (124)$$

$$U_{y,o} = U_y + (x_o-x)\ \frac{\partial U_y}{\partial x} + (y-y_o)\ \frac{\partial U_y}{\partial y} + \text{---} \qquad (124\text{-A})$$

where

$$U_x = \frac{\partial \Phi_o}{\partial x} = 0.5\ H_w\ \omega\ e^{ky}\ \mathrm{Cos}(kx-\omega t) \qquad (125)$$

$$U_y = \frac{\partial \Phi_o}{\partial y} = 0.5\ H_w\ \omega\ e^{ky}\ \mathrm{Sin}(kx-\omega t) \qquad (125\text{-A})$$

If we integrate U_x and U_y with respect to time, the fluid particle trajectories can be determined as follows

$$x_o - x \simeq \int U_x\ dt = -\ 0.5\ H_w\ e^{ky}\ \mathrm{Sin}(kx-\omega t) \qquad (126)$$

$$y_o - y \simeq \int U_y \, dt = 0.5 \, H_w \, e^{ky} \, \mathrm{Cos}(kx-\omega t) \tag{126-A}$$

$$\frac{\partial U_x}{\partial x} = - 0.5 \, H_w \, \omega \, e^{ky} \, \mathrm{Sin}(kx-\omega t) \tag{126-B}$$

$$\frac{\partial U_x}{\partial y} = 0.5 \, H_w \, \omega \, k \, e^{ky} \, \mathrm{Cos}(kx-\omega t) \tag{126-C}$$

$$\frac{\partial U_y}{\partial x} = 0.5 \, H_w \, \omega \, k \, e^{ky} \, \mathrm{Cos}(kx-\omega t) \tag{126-D}$$

$$\frac{\partial U_y}{\partial y} = 0.5 \, H_w \, \omega \, k \, e^{ky} \, \mathrm{Sin}(kx-\omega t) \tag{126-E}$$

If the above equations (126-126-E) are substituted into equations (124) and (124-A) the following water particle velocity vector components can be obtained

$$U_{x,o} = U_x + (0.5 \, H_w)^2 \, \omega \, k \, e^{2ky} = 0.5 \, H_w \, \omega \, e^{ky} \, \mathrm{Cos}(kx-\omega t) + (0.5 \, H_w)^2 \, \omega \, k \, e^{2ky} \tag{127}$$

$$U_{y,o} = U_y = 0.5 \, H_w \, \omega \, e^{ky} \, \mathrm{Sin}(kx-\omega t) \tag{127-A}$$

The second term in equation (127) is calculated first by Stokes [7] and called after his name as "Stokes' Drift" in the literature.

By analogy to the drag forces given in Section 2.1.2 equation (56), the second-order steady horizontal forces (drift forces) may be written as follows

$$F_{x,s} = \int_o^{\ell} \frac{1}{2} \rho \, D \, U_{x_{o,s}} \, |U_{x_{o,s}}| \, C_D \, (Re) \, dz \tag{128}$$

where

$$U_{x_{o,s}} = (0.5 \, H_w)^2 \, \omega \, k \, e^{2ky}$$

In Fig. 35 values of $U_{x_{o,s}}$ versus ka and ω are shown, and Fig. 36 shows $F_{x,s}$ versus Y/D, kR and ω.

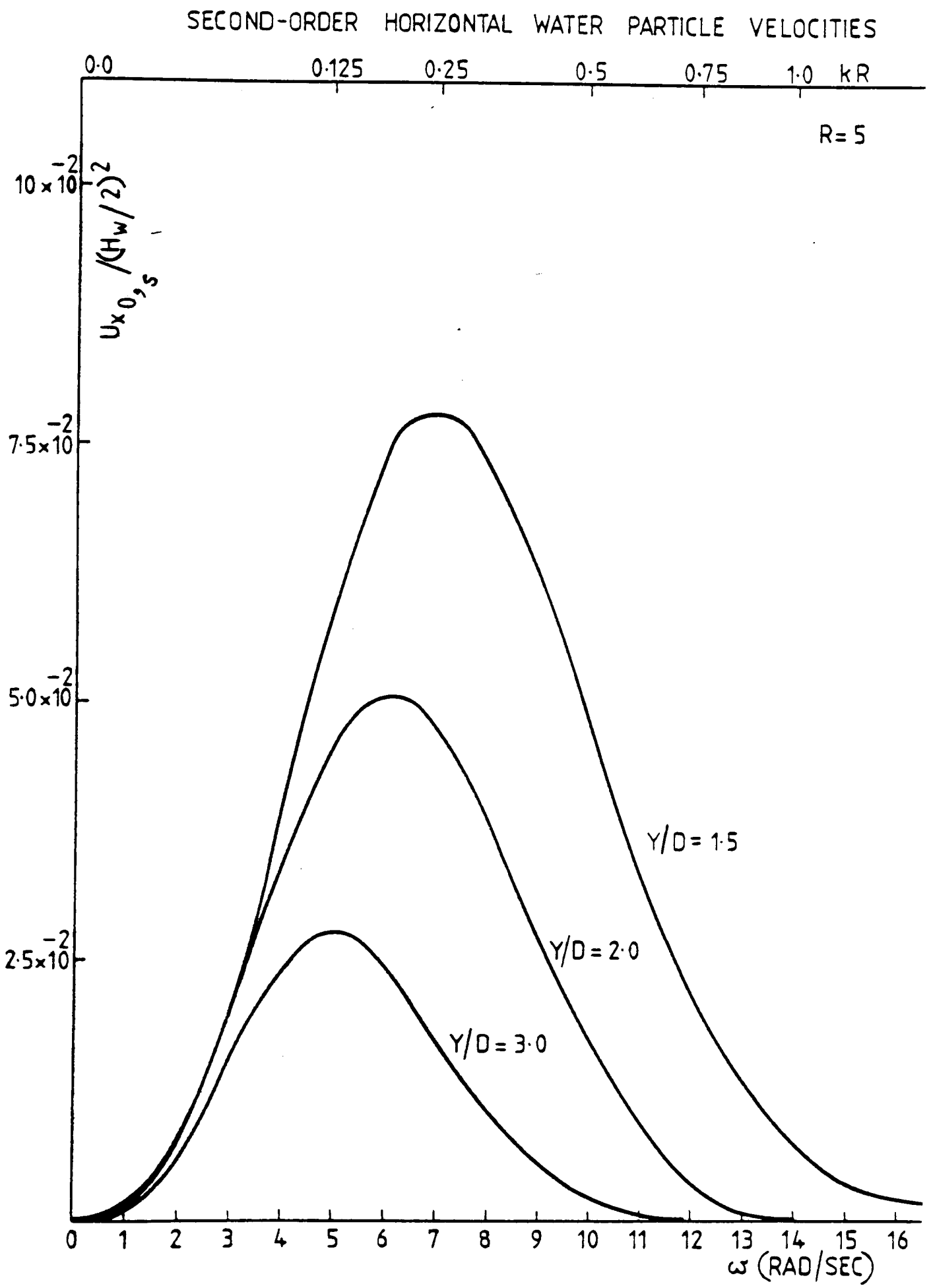
SECOND-ORDER HORIZONTAL WATER PARTICLE VELOCITIES
0·0
0·125
0·25
0·5
0·75
1·0
kR
R= 5
10×10^{-2}
$7{\cdot}5 \times 10^{-2}$
$5{\cdot}0 \times 10^{-2}$
$2{\cdot}5 \times 10^{-2}$
$U_{x\,0,s}/(H_w/2)^2$
Y/D = 1·5
Y/D = 2·0
Y/D = 3·0
0 1 2 3 4 5 6 7 8 9 10 11 12 13 14 15 16
ω (RAD/SEC)

Fig. 35.

SECOND-ORDER WAVE DRIFT FORCES

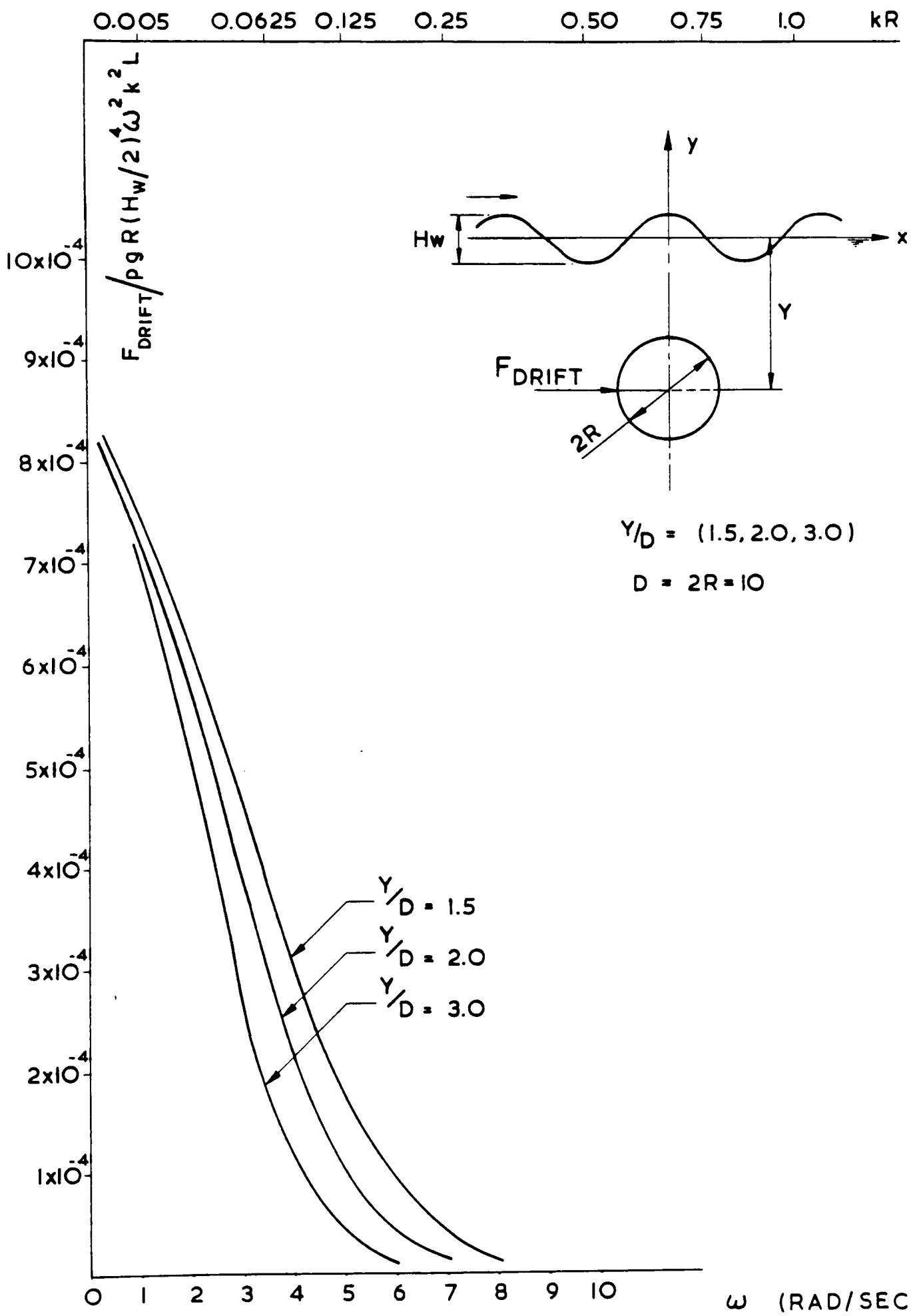

Figure 36

2.2 Wave Forces on Large Diameter Members

When the members of an offshore structure are subject to wave loading in the diffraction regime where $D/\lambda>0.2$ the velocity potential to take account of the interference between the structure and fluid particles cannot be represented by the relative flow between the member and the fluid as was given in equation (26). As the diameter of the cylindrical members increase, wave diffraction occurs. When the oncoming waves hit the cylinder, the resulting scattering potential flow field which satisfies the Laplace equation and the boundary and radiation conditions [equations (9-12) in Section 1] should be defined. The scattered waves must radiate in the direction of $r>0$ and since oncoming waves are periodic in x the scattered waves should also be periodic in θ with a period 2π (see Fig. 37).

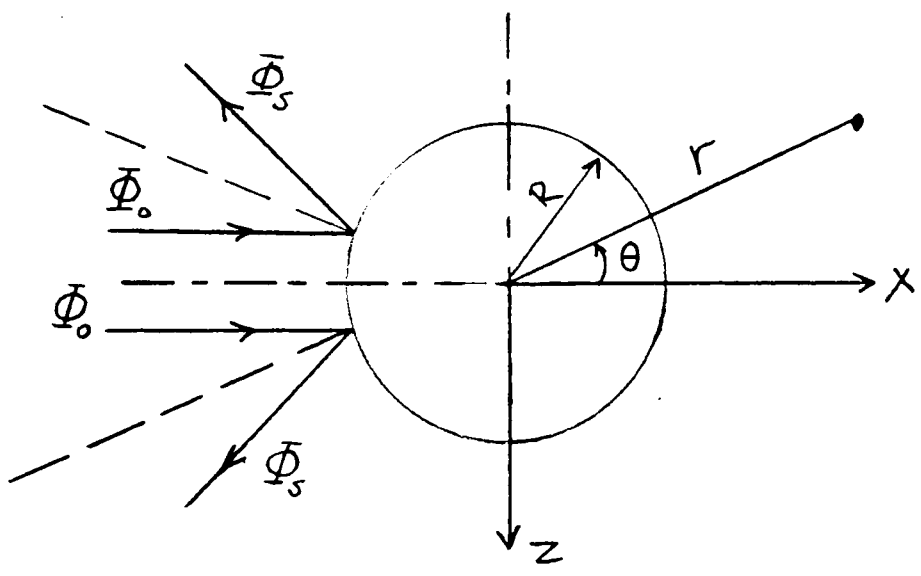

Fig. 37.

By analogy to the oncoming wave potential, the scattering wave potential may be written as follows

$$\Phi_s = \mathrm{Re}\ [-\, i\, R(r)\, e^{ky}\, e^{im\theta}\, e^{-i\omega t}] \qquad (129)$$

If we put y=0, i.e. assume that the scattering potential is constant along the y axis, equation (129) corresponds to the scattering potential of plane sound waves and must satisfy the following wave equation given in reference [36]

$$\frac{\partial^2 \Phi_s}{\partial t^2} - C_o^2 \nabla^2 \Phi_s = 0 \qquad (130)$$

where C_o : wave celerity $= \frac{\lambda}{T} = \frac{\omega}{k}$

$$\nabla^2 \Phi_s = \frac{\partial^2 \Phi_s}{\partial r^2} + \frac{1}{r}\frac{\partial \Phi_s}{\partial r} + \frac{1}{r^2}\frac{\partial^2 \Phi_s}{\partial \theta^2}$$

When equation (129) is substituted into equation (130), the following differential equation is obtained

$$\frac{\partial^2 R}{\partial r^2} + \frac{1}{r}\frac{\partial R}{\partial r} + (k^2 - \frac{m^2}{r^2})\, R = 0 \qquad (131)$$

Equation (131) is Bessel's equation. Its general solution is a linear combination of Bessel functions of the first and second kinds, $J_m(kr)$ and $Y_m(kr)$ of order m, and can be written as

$$R(r) = AJ_m(kr) + BY_m(kr) \qquad (132)$$

Having replaced R(r) in equation (129) with (132) it can be seen that Φ_s does not satisfy the Sommerfeld radiation condition which is given for two-dimensional cases [37] as follows

$$\lim_{r\to\infty} \sqrt{r}\,(\frac{\partial \Phi_s}{\partial r} - i\,k\,\Phi_s) = 0 \qquad (133)$$

For outgoing scattered waves it was shown in reference [38] that the first kind of Hankel function $[H_m^{(1)} = J_m(x) + iY_m(x)]$ satisfies equation (133) and R(r) can be written as follows

$$R(r) = \sum_{m=0}^{\infty} A_m H_m^{(1)}(kr) \qquad (134)$$

If we substitute equation (134) into equation (129) the following velocity potential for scattered waves is obtained

$$\Phi_s = \text{Re}\left[- i \sum_{m=0}^{\infty} A_m H_m^{(1)}(kr)\ e^{ky}\ e^{im\theta}\ e^{-i\omega t}\right] \qquad (135)$$

The total potential can be written by summing the velocity potentials of the oncoming waves and of the scattered waves as follows

$$\Phi(r,\theta,y,t) = \text{Re}\ [\phi_o(r,\theta,t) + \phi_s(r,\theta,t)]\ e^{-i\omega t} \qquad (136)$$

The oncoming wave potential which has been given in cortesion co-ordinates can be written in terms of cylindrical co-ordinates using the following relation given in reference [39]

$$e^{ikR\text{Cos}\theta} = J_o(kr) + 2 \sum_{m=1}^{\infty} i^m J_m(kr)\ \text{Cos}(m\theta) \qquad (137)$$

Now ϕ_o given in equation (6-A) can be expressed in polar co-ordinates using equation (137) as follows

$$\phi_o = - \frac{i\ 0.5g\ H_w\ e^{ky}}{\omega}\left[J_o(kr) + 2 \sum_{m=1}^{\infty} i^m J_m(kr)\ \text{Cos}(m\theta)\right] \qquad (138)$$

or

$$\phi_o = - \frac{i\ 0.5g\ H_w\ e^{ky}}{\omega}\left[\alpha_m\ i^m \sum_{m=0}^{\infty} J_m(kr)\ \text{Cos}(m\theta)\right] \qquad (138\text{-A})$$

and $\Phi_o = \text{Re}\ [\phi_o\ e^{-i\omega t}]$ (138-B)

where $J_m(kr)$ are Bessel functions of the first kind and $\alpha_m=1$ for $m=0$ and $\alpha_m=2$ for $m\geq 1$.

For the complete determination of equation (135) the A_m coefficients in that equation should be known. This can be achieved using the boundary condition given in equation (8)

$$\left.\frac{\partial \Phi_o}{\partial r}\right|_{r=R} = - \left.\frac{\partial \Phi_s}{\partial r}\right|_{r=R} \qquad (139)$$

or

$$\frac{0.5g\ H_w\ e^{ky}}{\omega}\ \alpha_m\ i^m\ \sum_{m=0}^{\infty} J_m'(kR)\ \mathrm{Cos}(m\theta)\ e^{-i\omega t} =$$

$$-\ \sum_{m=0}^{\infty} A_m\ H_m^{(1)'}(kR)\ e^{ky}\ e^{im\theta}\ e^{-i\omega t} \qquad (139\text{-A})$$

$$A_m = -\ \frac{0.5g\ H_w\ e^{ky}}{\omega}\ \alpha_m\ i^m\ \frac{J_m'(kR)\ \mathrm{Cos}(m\theta)}{H_m^{(1)'}(kR)\ e^{im\theta}} \qquad (139\text{-B})$$

where

$$H_m^{(1)'}(kR) = J_m'(kR) + i\ Y_m'(kR) \qquad (139\text{-C})$$

The following relations can also be written from reference [35]

$$Y_{m+1}(x) = \frac{2m}{x}\ Y_m(x) - Y_{m-1}(x) \qquad (140)$$

$$J_{m+1}(x) = \frac{2m}{x}\ J_m(x) - J_{m-1}(x) \qquad (140\text{-A})$$

$$2J_m'(x) = J_{m-1}(x) - J_{m+1}(x) \qquad (141)$$

$$2Y_m'(x) = Y_{m-1}(x) - Y_{m+1}(x) \qquad (141\text{-A})$$

If equation (139-B) is substituted into equation (135) the scattering potential becomes

$$\Phi_s = \mathrm{Re}\left[-\ i\ \frac{0.5g\ H_w}{\omega}\ e^{ky}\ \sum_{m=0}^{\infty} \alpha_m\ i^m\ \frac{J_m'(kR)}{H_m^{(1)'}(kR)}\ H_m^{(1)}(kr)\ \mathrm{Cos}(m\theta)\ e^{-i\omega t}\right] \qquad (142)$$

Finally, the total velocity potential given in equation (136) can be written as

$$\Phi(r,\theta,y,t) = \mathrm{Re}\left[-\ i\ \frac{0.5g\ H_w\ e^{ky}}{\omega}\ \sum_{m=0}^{\infty} \alpha_m\ i^m\ \left(J_m(kr) - \frac{J_m'(kR)}{H_m^{(1)'}(kR)}\right.\right.$$

$$\left.\left. H_m^{(1)}(kr)\right)\ \mathrm{Cos}(m\theta)\ e^{-i\omega t}\right] \qquad (143)$$

The total velocity potential of the flow field in waves in the above form was first given in the field of electromagnetic theory by Nicholson in reference [39] and of hydrodynamic theory by Havelock in reference [6]. It was first applied to the design of piles in waves by MacCamy and Fuchs in reference [40]. In the following, the wave elevation and pressure distribution around the circular cylinder will be given and the first and second-order wave forces will be calculated.

2.2.1 Pressure distribution, wave elevation and first-order time dependent forces on large diameter circular cylinders. The pressure distribution around the large diameter circular cylinder can be obtained by substituting equation (143) into Bernoulli's equation (23) (second-order terms are neglected in Bernoulli's equation).

$$p = \mathrm{Re}\left[\rho g\ 0.5\ H_w\ e^{ky} \sum_{m=0}^{\infty} \alpha_m \left(i^m\ J_m(kR) - \frac{J_m'(kR)}{H_m^{(1)'}(kR)}\ H_m^{(1)}(kR) \right) \right.$$
$$\left. \mathrm{Cos}(m\theta)\ e^{-i\omega t} \right] \qquad (144)$$

$\left(J_m(kR) - \dfrac{J_m'(kR)}{H_m^{(1)'}(kR)}\ H_m^{(1)}(kR) \right)$ can be shown to be equal

to $\dfrac{2i}{(\pi kR)\ H_m^{(1)'}(kR)}$ using equations (139-C) - (141-A), and

and 'Wronskians' theorem which can be represented by the following equation [35]

$$W\{J_m(x),\ Y_m(x)\} = J_{m+1}(x)\ Y_m(x) - J_m(x)\ Y_{m+1}(x) = \frac{2}{\pi x} \qquad (145)$$

equation (144) becomes

$$p = \mathrm{Re}\left[\frac{\rho g\ H_w\ e^{ky}}{\pi kR} \left(\sum_{m=0}^{\infty} \alpha_m\ i^{m+1}\ \frac{\mathrm{Cos}(m\theta)}{H_m^{(1)'}(kR)} \right) e^{-i\omega t} \right] \qquad (146)$$

Wave elevation around the circular cylinder can also be obtained from Bernoulli's equation and the result takes the following form

$$\eta = -\frac{1}{g}\frac{\partial \Phi}{\partial t}\bigg|_{y=0} = \mathrm{Re}\left[\frac{H_w}{\pi kR}\left(\sum_{m=0}^{\infty} \alpha_m\, i^{m+1}\, \frac{\mathrm{Cos}(m\theta)}{H_m^{(1)'}(kR)}\right) e^{-i\omega t}\right] \qquad (147)$$

The total horizontal time dependent force on the circular cylinder can be calculated by integrating the pressure given in equation (146) on the surface of the cylinder as follows

$$F_x = \int_{-d}^{o}\int_{o}^{2\pi} -pR\mathrm{Cos}\theta\, d\theta\, dy = \int_{-d}^{o} \mathrm{Re}\left[\frac{2\rho g\, H_w\, e^{ky}}{k}\, \frac{1}{H_1^{(1)'}(kR)}\right] e^{-i\omega t}\, dy \qquad (148)$$

The following relations from reference [35] will be used for the simplification of the above total force equation

$$N_m = \left|H_m^{(1)'}(x)\right| = \sqrt{J_m'^{2}(x) + Y_m'^{2}(x)} \qquad (149)$$

$$\theta_m = \arg H_m^{(1)'}(x) = \arctan\left(\frac{Y_m'(x)}{J_m'(x)}\right) \qquad (149\text{-A})$$

$$J_m'(x) = N_m\, \mathrm{Cos}\theta_m \qquad (149\text{-B})$$

$$Y_m'(x) = N_m\, \mathrm{Sin}\theta_m \qquad (149\text{-C})$$

Using equations (139-C), (149) - (149-C) the total horizontal force equation (148) becomes

$$F_x = \int_{-d}^{o} \frac{2\rho g\, H_w\, e^{ky}}{k}\, \frac{\mathrm{Cos}(\omega t-\theta)}{\sqrt{J_1'^{2}(kR) + Y_1'^{2}(kR)}}\, dy \qquad (150)$$

where

$$\theta = \arctan\left(\frac{Y_1'(kR)}{J_1'(kR)}\right)$$

and $$J_1'(kR) = J_o(kR) - \frac{1}{(kR)} J_1(kR)$$

$$Y_1'(kR) = Y_o(kR) - \frac{1}{(kR)} Y_1(kR)$$

The J_1' and Y_1' values are shown in Figs 38 and 39 respectively.

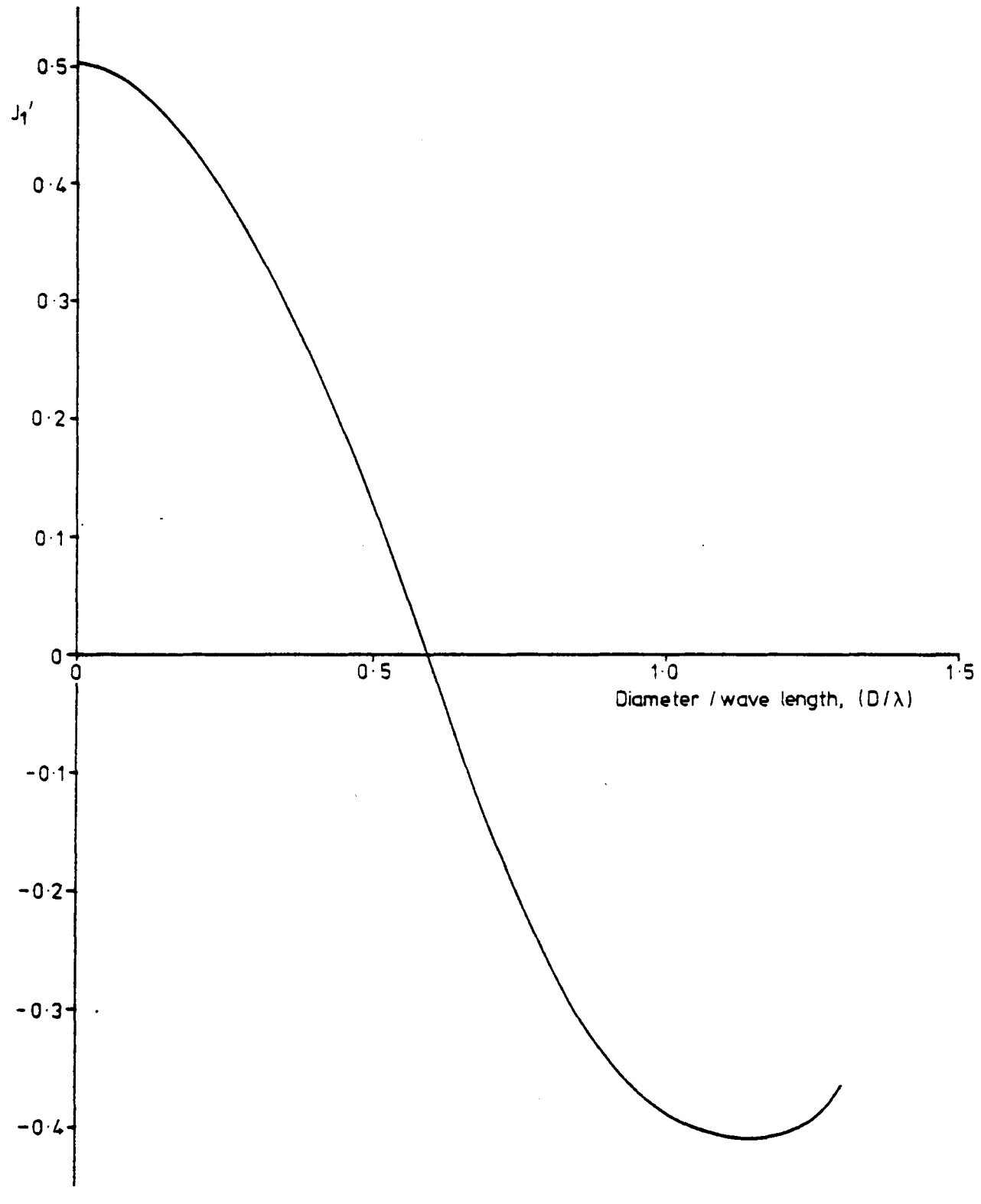

Fig. 38

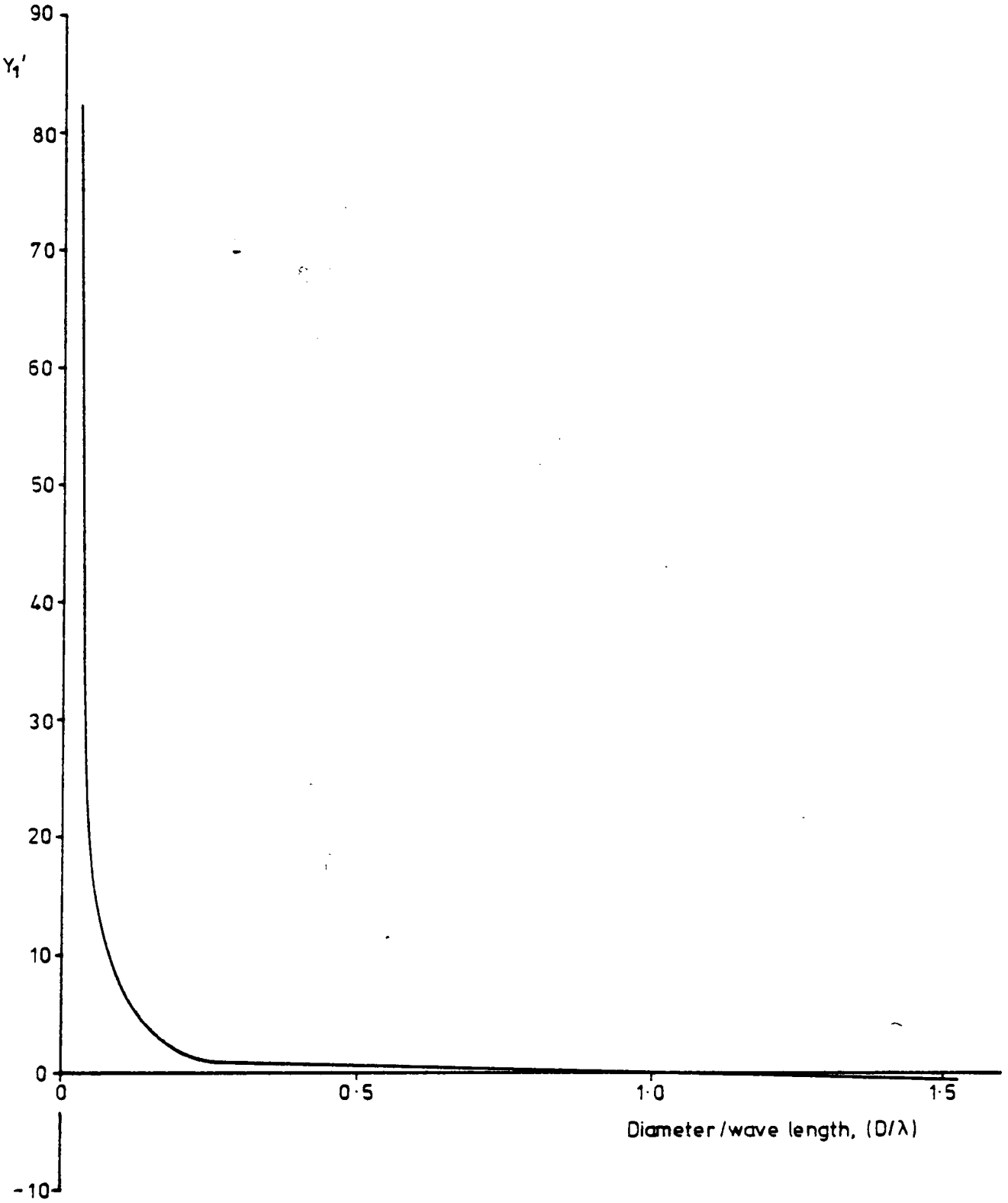
90
Y_1'
80
70
60
50
40
30
20
10
0
-10
0
0·5
1·0
1·5
Diameter / wave length, (D/λ)

Fig. 39

Equation (150) can also be generalised for the application to circular members both in the inertia and diffraction regimes. If we set equation (55-A) equal to equation (150) the following relation can be obtained

$$F_x = \int_{-d}^{o} \rho\pi R^2 C_m \omega^2 0.5 H_w e^{ky} \text{Sin}(kx-\omega t)\, dz = \int_{-d}^{o} \frac{2\rho g H_w e^{ky}}{k} f_D(kR) \text{Cos}(kx-\omega t+\theta)\, dz \qquad (151)$$

where

$$f_D(kR) = \frac{1}{\sqrt{J_1'^2(kR) + Y_1'^2(kR)}}$$

The right hand side of equation (151) can also be written as

$$\int_{-d}^{o} \frac{2\rho g H_w e^{ky}}{k} f_D(kR) \frac{0.5\ \pi R^2 \omega^2}{0.5\ \pi R^2 \omega^2} \frac{\text{Sin}(kx-\omega t)}{\text{Sin}(kx-\omega t)} \text{Cos}(kx-\omega t+\theta)\, dz \qquad (151\text{-A})$$

Comparing equation (151-A) and the left hand side of equation (151) it can be seen that C_M can be written as follows

$$C_M = \frac{4}{\pi} \frac{1}{(\pi D/\lambda)^2} \frac{\text{Cos}(kx-\omega t+\theta)}{\text{Sin}(kx-\omega t)} f_D(kR) \qquad (152)$$

or for the maximum value of C_M

$$C_M = \frac{4}{\pi} \frac{1}{(\pi D/\lambda)^2} f_D(kR) \qquad (152\text{-A})$$

Now the horizontal wave force on large diameter cylinders can also be written in the following form

$$F_x = \int_{-d}^{o} C_M \rho\, \pi\, D^2/4\, a_x \qquad (153)$$

where C_M will be calculated from equation (152-A)

and $a_x = 0.5 H_w \omega^2 e^{ky} \text{Sin}(kx-\omega t)$.

In Fig. 40 values of C_M versus D/λ are shown. Figure 41 shows wave forces on a vertical circular cylinder in the inertia and diffract-

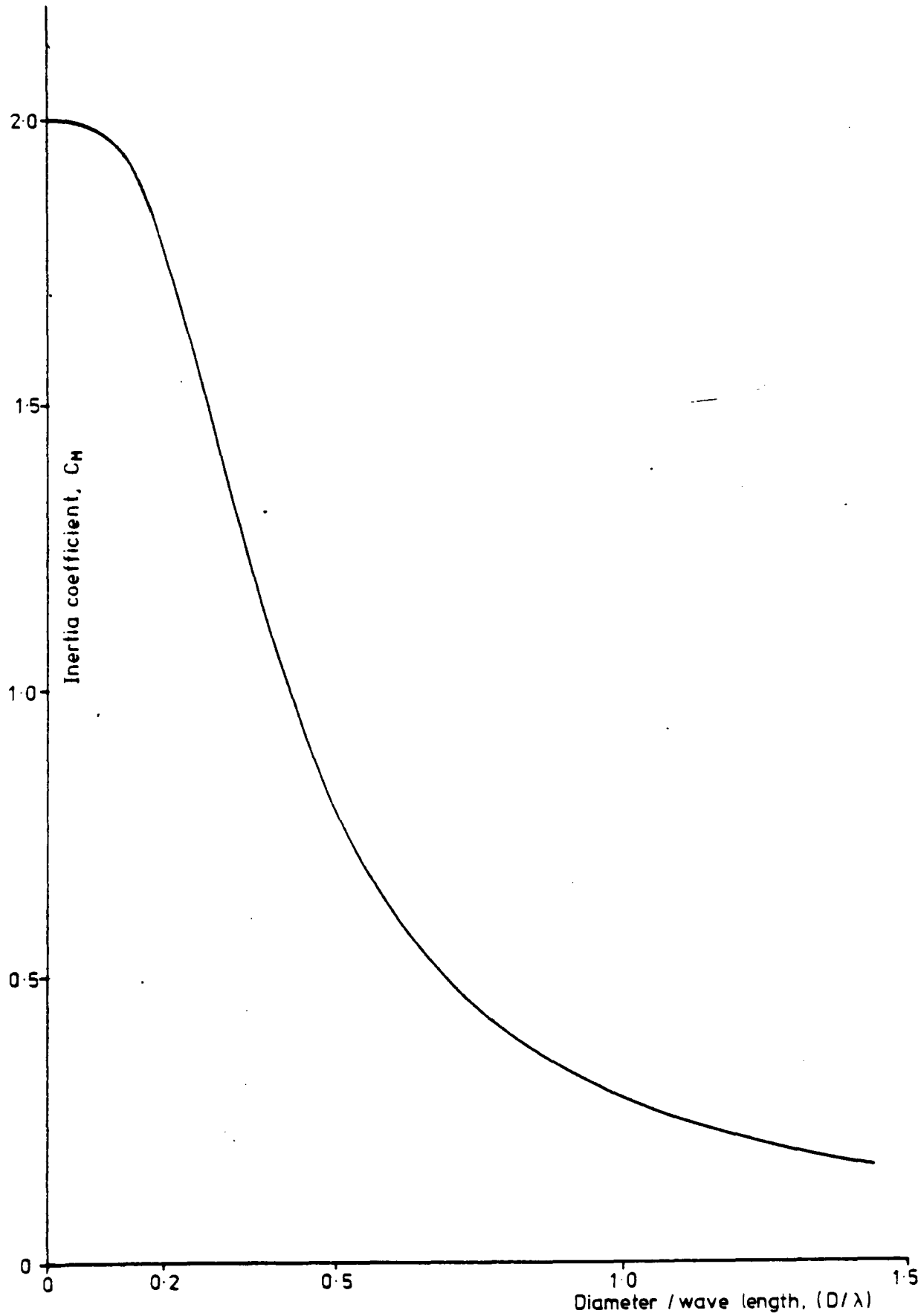
2·0
1·5
1·0
0·5
0
Inertia coefficient, C_M
0
0·2
0·5
1·0
1·5
Diameter / wave length, (D/λ)

Fig. 40

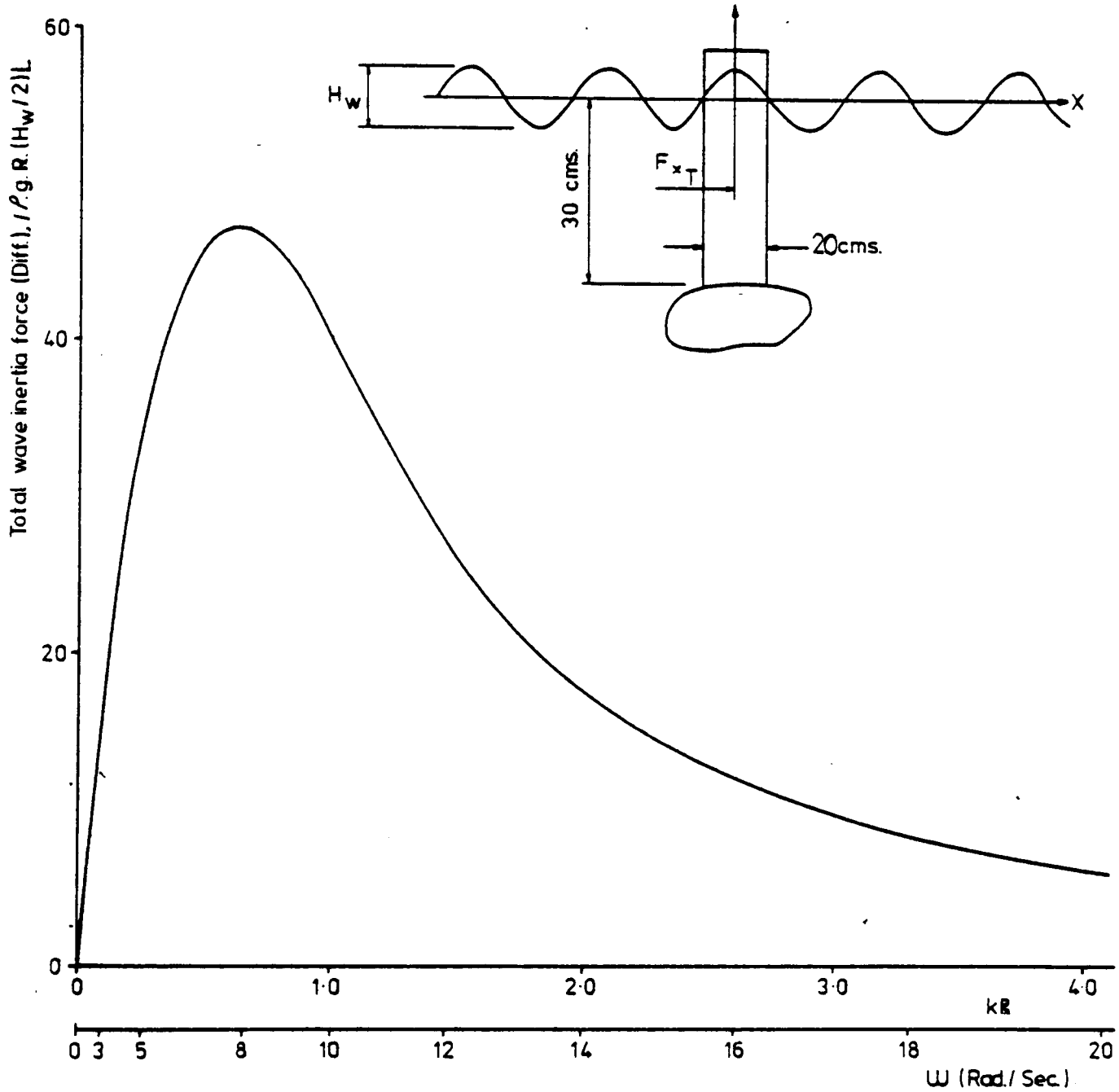
Total wave inertia force (Diff.), / ρ g R. (H_w / 2) L
60
40
20
0
0
1·0
2·0
3·0
4·0
kR
0 3 5 8 10 12 14 16 18 20
W (Rad./ Sec.)
H_w
Y
X
30 cms.
F_x_T
20cms.

Fig. 41

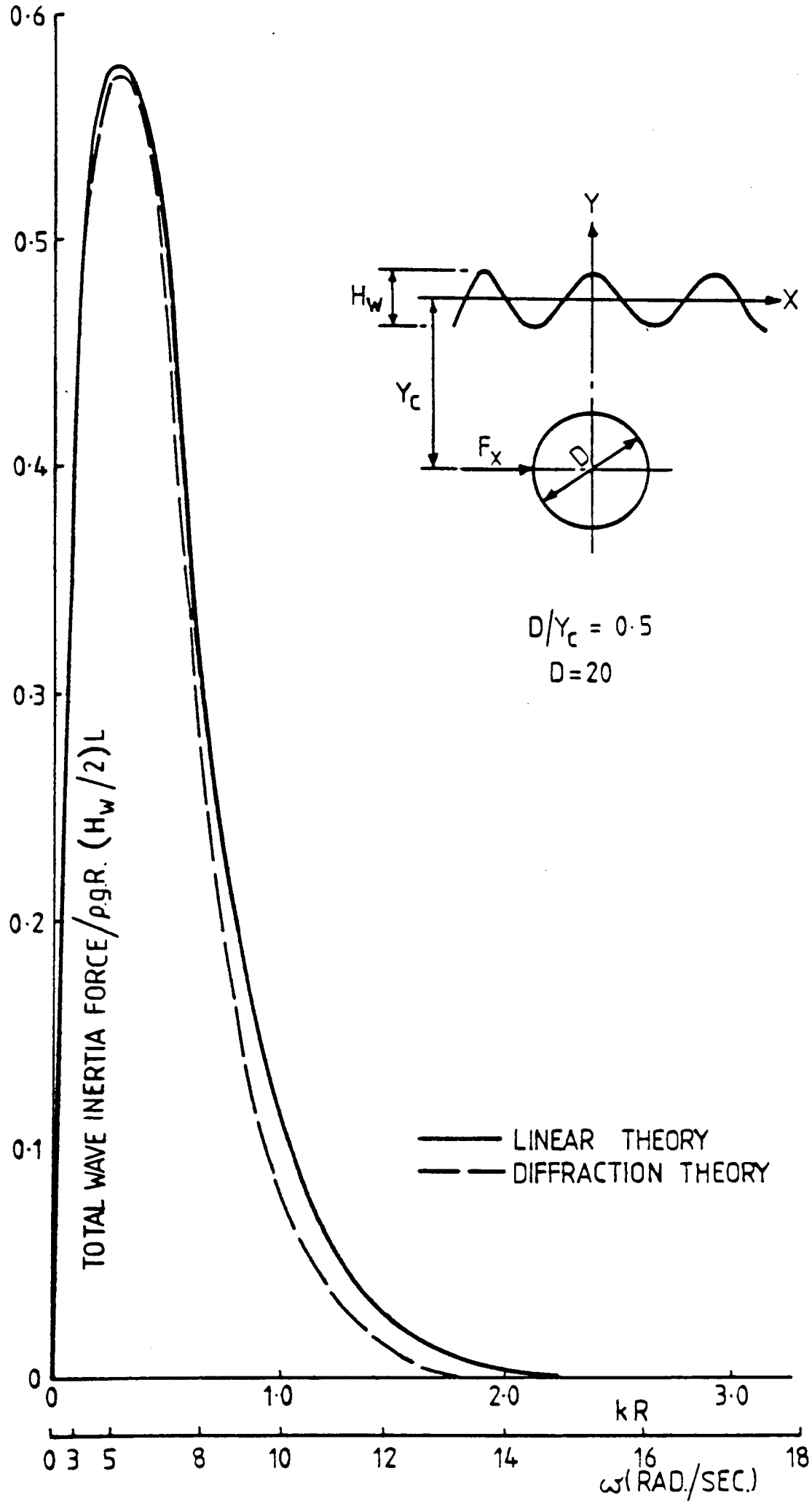
0·6
0·5
0·4
0·3
0·2
0·1
0
TOTAL WAVE INERTIA FORCE/ρ.g.R.(Hw/2)L
Y
X
Hw
Yc
Fx
D
D/Yc = 0·5
D=20
LINEAR THEORY
DIFFRACTION THEORY
0
1·0
2·0
3·0
kR
0 3 5 8 10 12 14 16 18
ω(RAD./SEC.)

Fig. 42.

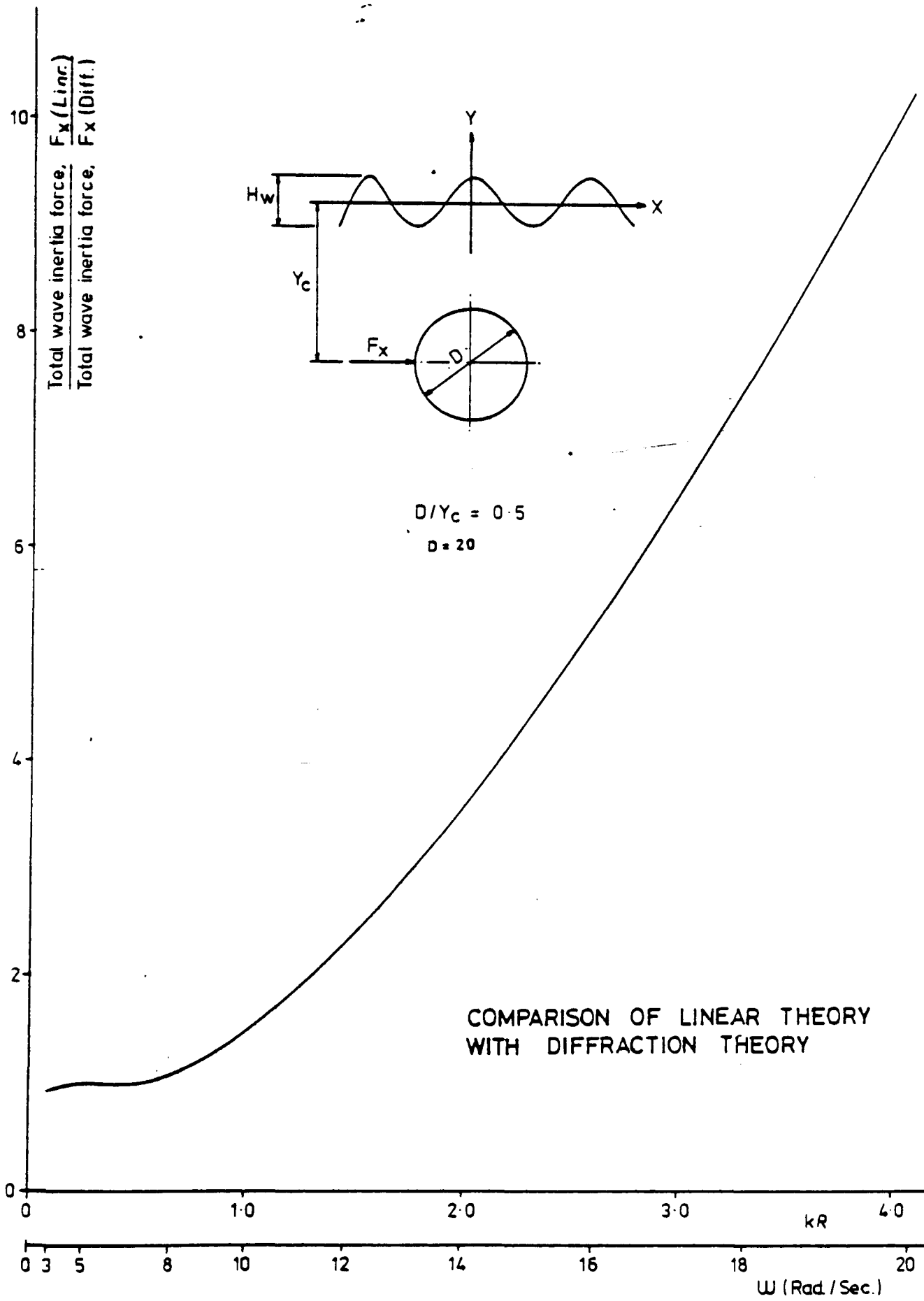
Total wave inertia force, Fx (Linr.) / Total wave inertia force, Fx (Diff.)
10
8
6
4
2
0
Y
X
Hw
Yc
Fx
D
D/Yc = 0·5
D = 20
COMPARISON OF LINEAR THEORY
WITH DIFFRACTION THEORY
0
1·0
2·0
3·0
4·0
kR
0 3 5 8 10 12 14 16 18 20
W (Rad. / Sec.)

Fig. 43

ion regimes. In Figs 42, 43, the wave forces on circular members which are working in the inertia or on the diffraction regimes, calculated using equations (55-A) and (150), are compared.

2.2.2 Application of Stokes' fifth-order wave theory to the wave loading calculations on large diameter cylinders. So far, the potential flow function for oncoming waves was assumed to satisfy linear-free surface boundaries, i.e. linear sinusoidal boundaries. This assumption is quite accurate in deep water where the ratio of wave height to wave length is small, except for short waves. The limiting value for that ratio is shown to be 0.14 in reference [3]. In shallow water the wave height/wave length ratio will increase (this can be proved using the principle of energy conservation) and in consequence the effect of a non-linear free surface will be significant. Non-linear solutions for incident waves were first given by Stokes in terms of a trigonometric series [7]. The coefficients in these series are lengthy and it is quite tedious to do the numerical calculations, unless computer programs are used. The convergence of this trigonometric series is restricted to certain values of H_w/λ_s and h/λ_s. (The subscript s used to discriminate values in shallow water from those in deep water.)

For the calculation of wave loading the potential function should first be defined.

The series form for the potential of oncoming fifth-order waves was given in reference [8] as follows

$$\begin{aligned}\phi_{o,s} = \frac{C_s}{k_s} [&(\delta A_{11} + \delta^3 A_{13} + \delta^5 A_{15}) \cosh(k_s y) \sin(k_s x - \omega t) \\ &+ (\delta^2 A_{22} + \delta^4 A_{24}) \cosh(2k_s y) \sin 2(k_s x - \omega t) \\ &+ (\delta^3 A_{33} + \delta^5 A_{35}) \cosh(3k_s y) \sin 3(k_s x - \omega t) \\ &+ \delta^4 A_{44} \cosh(4k_s y) \sin 4(k_s x - \omega t) \\ &+ \delta^5 A_{55} \cosh(5k_s y) \sin 5(k_s x - \omega t)]\end{aligned} \qquad (154)$$

and the wave profile is given by

$$\eta_s = \frac{1}{k_s}\left[\delta \cos(k_s x-\omega t) + (\delta^2 B_{22} + \delta^4 B_{24}) \cos 2(k_s x-\omega t) + (\delta^3 B_{33} + \delta^5 B_{35}) \cos 3(k_s x-\omega t) + \delta^4 B_{44} \cos 4(k_s x-\omega t) + \delta^5 B_{55} \cos 5(k_s \cdot \mathbf{x} -\omega t)\right] \quad (155)$$

where

$$C_s^2 = \frac{C_o^2}{k_s}(1 + \delta^2 C_1 + \delta^4 C_2) \quad (156)$$

$$C_o^2 = g \tanh(kh) = \left(\frac{\lambda}{T}\right)^2 \quad (157)$$

$$k_s = \frac{2\pi}{\lambda_s}$$

δ : Constant

λ : Wave length in deep water

λ_s : Wave length in shallow water

A_{ii}, B_{ii}, C_i values are tabulated in Table I.

For the given values of wave height H_w, water depth h, and wave period T, the coefficient δ and the wave length λ_s can be determined from the solutions of the following simultaneous equations

$$\frac{\pi H_w}{h} = \frac{1}{(h/\lambda_s)}\left[\delta + \delta^3 B_{33} + \delta^5 (B_{35} + B_{55})\right] \quad (158)$$

and $$\frac{h}{\lambda} = \frac{h}{\lambda_s} \tanh(k_s \cdot h)[1 + \delta^2 C_1 + \delta^4 C_2] \quad (159)$$

The complex velocity potential of oncoming waves will be

$$\Phi_{o,s} = \mathrm{Re}\left[-i \frac{C_s}{k_s} \sum_{n=1}^{5} \varepsilon_n \cosh(nk_s y)\, e^{ink_s x}\, e^{-i\omega t}\right] \quad (160)$$

where $\varepsilon_1 = \delta A_{11} + \delta^3 A_{13} + \delta^5 A_{15}$

$\varepsilon_2 = \delta^2 A_{22} + \delta^4 A_{24}$

$\varepsilon_3 = \delta^3 A_{33} + \delta^5 A_{35}$

$\varepsilon_4 = \delta^4 A_{44}$

$\varepsilon_5 = \delta^5 A_{55}$

Equation (160) can also be written in terms of cylindrical coordinates as follows

$$\Phi_{o,s} = Re\left[-i\frac{C_s}{k_s}\sum_{n=1}^{5}\varepsilon_n \cosh(nk_s y)\left(\alpha_m i^m \sum_{m=0}^{\infty} J_m(nk_s r)\cos(m\theta)\, e^{-i\omega t}\right)\right] \tag{161}$$

where $J_m(kr)$ are Bessel functions of the first kind and $\alpha_m=1$ for $m=0$ and $\alpha_m=2$ for $m\geq 1$.

Similar to equation (135) the potential function for scattering waves may be written as

$$\Phi_{s,s} = Re\left[-i\sum_{m=0}^{\infty} A_m H_m^{(1)}(nk_s r)\, e^{im\theta}\, e^{-i\omega t}\right] \tag{162}$$

The A_m coefficients in the above equation can be determined using the boundary condition given in equation (8)

$$\frac{C_s}{k_s}\sum_{n=1}^{5}\varepsilon_n \cosh(nk_s y)\left[\alpha_m i^m \sum_{m=0}^{\infty} J_m'(nk_s R)\cos(m\theta)\right] e^{-i\omega t} = -\sum_{m=0}^{\infty} A_m H_m^{(1)'}(nk_s R)\, e^{im\theta}\, e^{-i\omega t} \tag{163}$$

or

$$A_m = -\frac{C_s}{k_s}\sum_{n=1}^{5}\varepsilon_n \cosh(nk_s y)\,\alpha_m i^m \frac{J_m'(nk_s R)\cos(m\theta)}{H_m^{(1)'}(nk_s R)\, e^{im\theta}} \tag{164}$$

Finally, the total velocity potential for the Stokes' fifth-order waves becomes

$$\Phi_{T,S}(r,\theta,y,t) = Re\left\{-i\frac{C_s}{k_s}\sum_{n=1}^{5}\varepsilon_n \cosh(nk_s y)\left[\sum_{m=0}^{\infty}\alpha_m i^m \left(J_m(nk_s r) - \frac{J_m'(nk_s R)}{H_m^{(1)'}(nk_s R)} H^{(1)}(nk_s r)\cos(m\theta)\right] e^{-i\omega t}\right\} \tag{165}$$

The pressure distribution around the large diameter cylinder can be written by substituting equation (165) into Bernoulli's equation (23)

and neglecting the second-order terms as follows

$$p_s = \text{Re}\left[\rho \frac{C_s}{k_s} \omega \sum_{n=1}^{5} \varepsilon_n \text{Cosh}(nk_s y) \left[\sum_{m=0}^{\infty} \alpha_m i^m \left(J_m(nk_s R) - \frac{J_m'(nkR)}{H_m^{(1)'}(nkR)} H_m^{(1)}(nk_s R)\right) \text{Cos}(m\theta)\right] e^{-i\omega t}\right] \quad (166)$$

Similar to equation (146) the above equation can also be written in the following simplified form

$$p_s = \text{Re}\left[2\rho \frac{C_s \omega}{k_s R} \sum_{n=1}^{5} \varepsilon_n \text{Cosh}(nk_s y) \left(\sum_{m=0}^{\infty} \alpha_m i^{m+1} \frac{\text{Cos}(m\theta)}{H_m^{(1)'}(nk_s R)}\right) e^{-i\omega t}\right] \quad (167)$$

and the wave elevation around the circular cylinder becomes

$$\eta_s = \text{Re}\left[\frac{2C_s \omega}{k_s R} \sum_{n=1}^{5} \varepsilon_n \text{Cosh}(nk_s y) \left(\sum_{m=0}^{\infty} \alpha_m i^{m+1} \frac{\text{Cos}(m\theta)}{H_m^{(1)'}(nk_s R)}\right) e^{-i\omega t}\right] \quad (168)$$

The integration of the above equation around the circumference gives the total horizontal force on the cylinder as follows

$$F_{x(s)} = \int_{-d}^{o} \int_{o}^{2\pi} - p_s R \, \text{Cos}\theta \, d\theta \, dy = \int_{-d}^{o} \text{Re}\left[\frac{4\rho C_s \omega}{k_s} \frac{\sum_{n=1}^{5} \varepsilon_n \text{Cosh}(nk_s y)}{H_1^{(1)'}(nk_s R)} e^{-i\omega t}\right] dy \quad (169)$$

or, similar to equation (150)

$$F_{x(s)} = \int_{-d}^{o} \frac{4\rho C_s \omega}{k_s} \sum_{n=1}^{5} \varepsilon_n \text{Cosh}(nk_s y) \frac{\text{Cos}(kx - \omega t + \theta)}{\sqrt{J_1'^2(nk_s R) + Y_1'^2(nk_s R)}} \quad (169\text{-A})$$

2.2.3 Second-order forces on large diameter circular cylinders. The second-order forces on large diameter cylinders can be obtained by substituting the total velocity potential of the oncoming and scattered

waves given in equation (143) into the second-order force part in Bernoulli's equation (eq. 23).

The velocity potential given in equation (143) can be simplified as follows using the procedure followed to obtain equation (146)

$$\Phi(r,\theta y,t) = \mathrm{Re}\left[- i \frac{g H_w e^{ky}}{\pi k R \omega} \sum_{m=0}^{\infty} \frac{\alpha_m i^{m+1}}{H_m^{(1)'}(kR)} \mathrm{Cos}(m\theta)\ e^{-i\omega t}\right] \qquad (170)$$

or

$$\Phi(r,\theta,y,t) = \mathrm{Re}\left[- i A e^{ky} \sum_{m=0}^{\infty} \alpha_m i^{m+1} \frac{J_m'(kR) - i Y_m'(kR)}{J_m'^2(kR) + Y_m'^2(kR)} \mathrm{Cos}(m\theta)\ e^{-i\omega t}\right] \qquad (170\text{-A})$$

where

$$A = \frac{g H_w}{\pi k R \omega}$$

Similarly to equation (118) the second-order force on large diameter cylinders takes the following form (Fig. 46)

$$\vec{F}_{y,s} = -\frac{1}{2}\rho \iint_{S_M} \left\{\nabla\left[-iA e^{ky} \sum_{m=0}^{\infty} \alpha_m i^{m+1} \frac{J_m'(kR) - i Y_m'(kR)}{J_m'^2(kR) + Y_m'^2(kR)} \mathrm{Cos}(m\theta)\ e^{-i\omega t}\right]\right\}^2 \vec{n}y\, dS \qquad (171)$$

If we evaluate equation (171) using equations (110) and (119) and replacing y by - (h-R Sinθ) $F_{y,s}$ becomes

$$\vec{F}_{y,s} = \int_o^{\ell} \mathrm{Re}\left[\frac{A^2 e^{-2kh}}{R^2} I_1(2kR)\ \pi R\ \alpha_1^2 \frac{J_1'^2(kR) - 2i J_1'(kR) Y_1'(kR) - Y_1'^2(kR)}{(J_1'^2(kR) + Y_1'^2(kR))^2} e^{-2i\omega t}\right] dz\, \vec{j} \qquad (172)$$

where $\alpha_1 = 2$.

From equation (172) the time independent second-order forces on large diameter cylinders can be written as

$$\vec{F}_{y,s} = \int_o^{\ell} -\frac{4\rho g H_w^2 e^{-2kh}}{\pi k^3 R^3} I_1(2kR) \frac{J_1'^2(kR) - Y_1'^2(kR)}{(J_1'^2(kR) + Y_1'^2(kR))^2} dz\, \vec{j} \qquad (173)$$

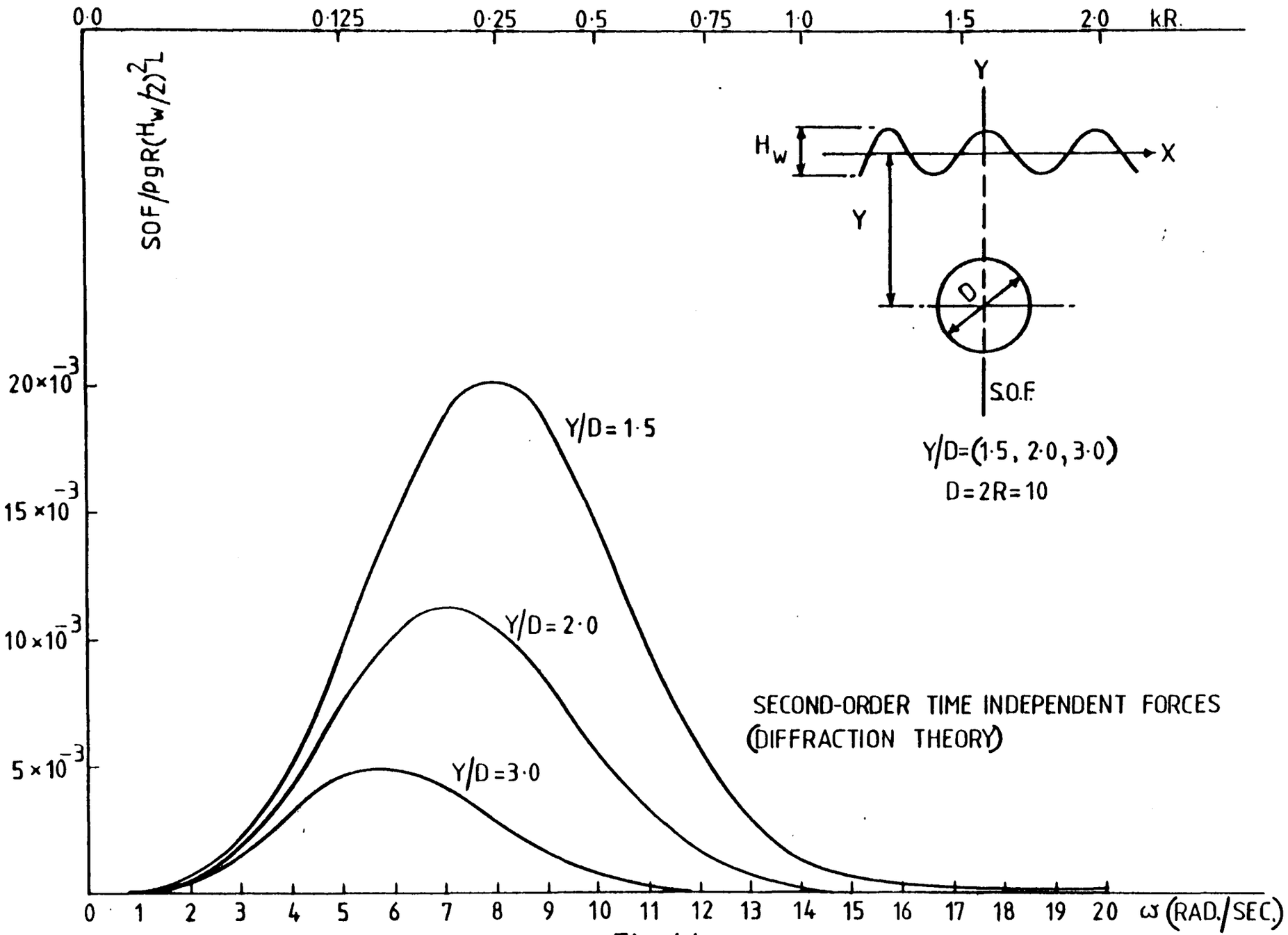
0·0
0·125
0·25
0·5
0·75
1·0
1·5
2·0
kR.
SOF/ρgR(Hw/2)²L
20×10⁻³
15×10⁻³
10×10⁻³
5×10⁻³
Y/D = 1·5
Y/D = 2·0
Y/D = 3·0
0 1 2 3 4 5 6 7 8 9 10 11 12 13 14 15 16 17 18 19 20 ω (RAD./SEC.)
Y
X
Hw
Y
D
S.O.F
Y/D=(1·5, 2·0, 3·0)
D=2R=10
SECOND-ORDER TIME INDEPENDENT FORCES
(DIFFRACTION THEORY)

Fig. 44.

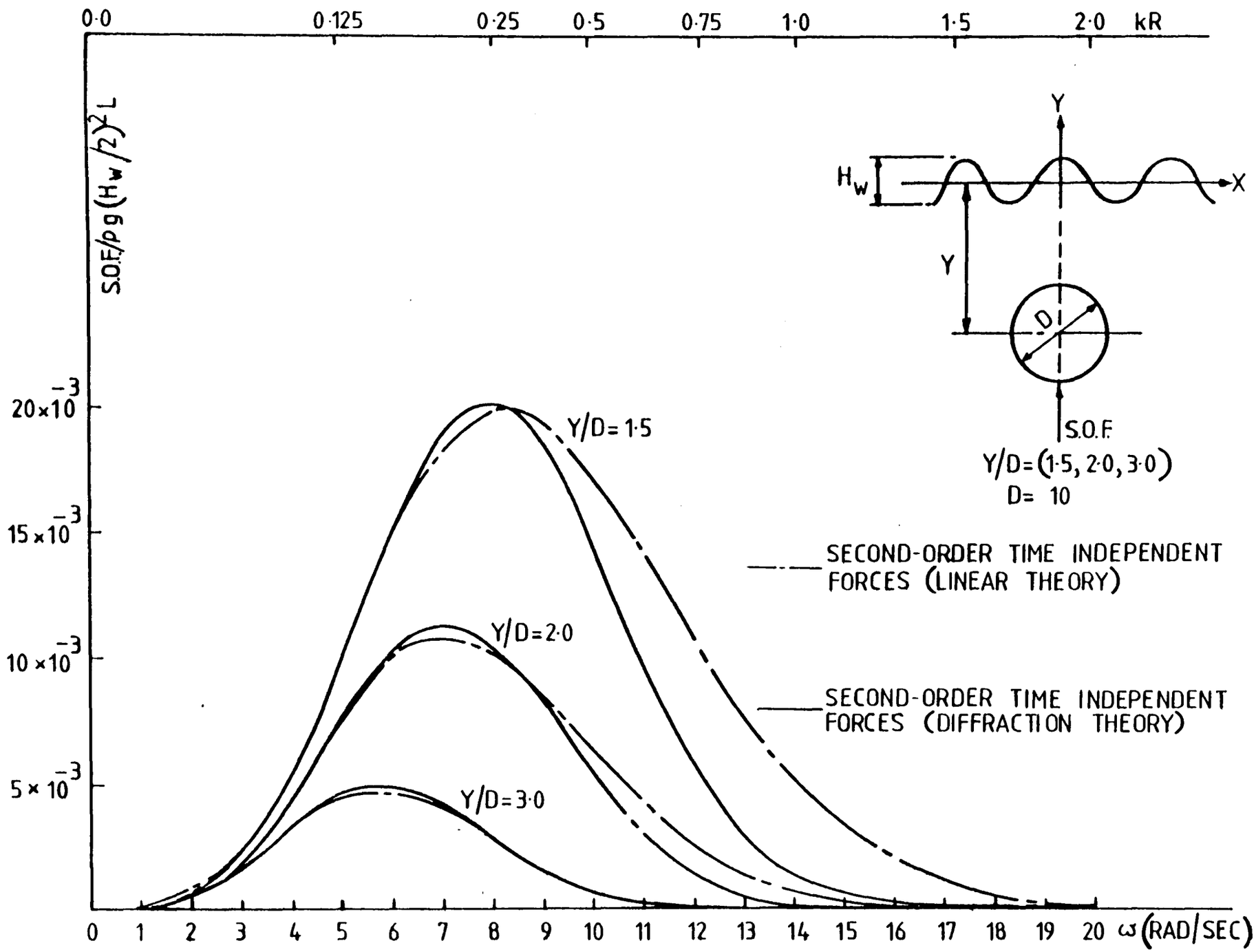
0·0
0·125
0·25
0·5
0·75
1·0
1·5
2·0
kR
S.O.F/ρg(Hw/2)²L
20×10⁻³
15×10⁻³
10×10⁻³
5×10⁻³
Y/D=1·5
Y/D=2·0
Y/D=3·0
0 1 2 3 4 5 6 7 8 9 10 11 12 13 14 15 16 17 18 19 20 ω(RAD/SEC)
Hw
Y
X
D
S.O.F
Y/D=(1·5, 2·0, 3·0)
D= 10
SECOND-ORDER TIME INDEPENDENT FORCES (LINEAR THEORY)
SECOND-ORDER TIME INDEPENDENT FORCES (DIFFRACTION THEORY)

Fig. 45.

The second-order time independent forces for horizontal circular cylinders beneath the free surface have been calculated and the results are shown in Fig. 44 for varying values of kR and Y/D.

In Fig. 45 second-order time independent forces given with equation (122) in drag or drag + inertia regimes compared with those given with equation (173) for diffraction regime. From the comparison it can be concluded that equation (173) can be valid for all regimes.

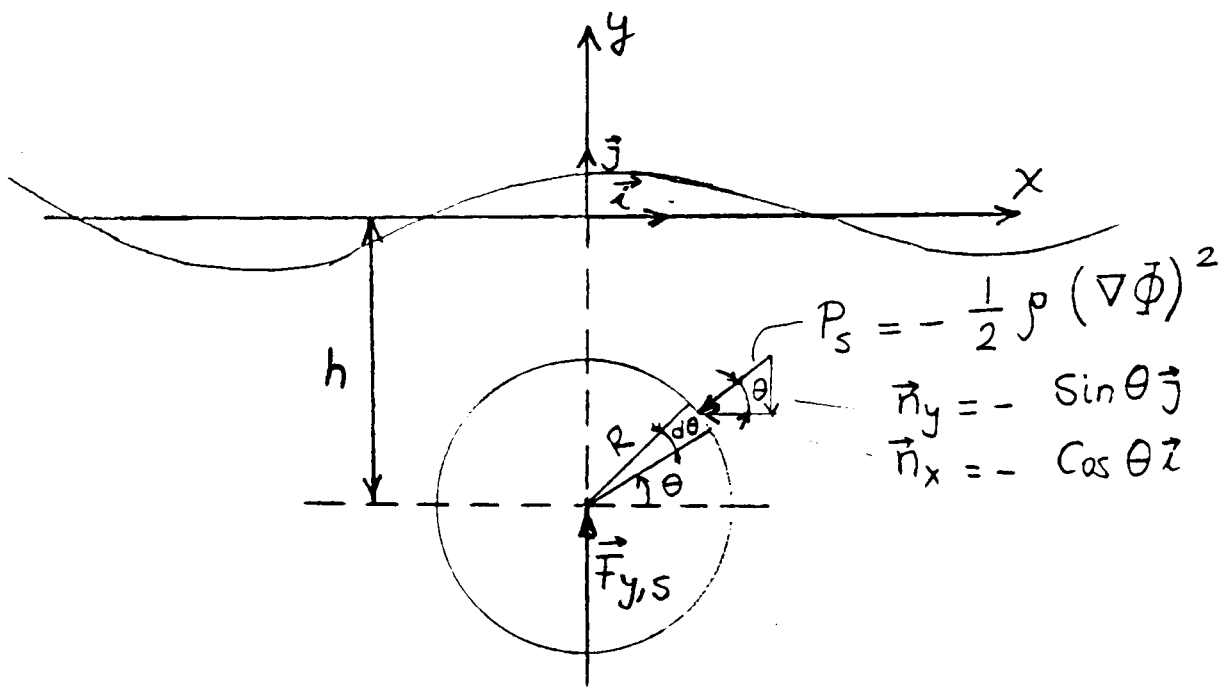

Fig. 46.

Similarly, second-order time dependent forces may be written as follows

$$\vec{F}_{Y,s} = -\int_0^{\ell} \frac{8\rho g H_w^2 e^{-2kh}}{\pi k^3 R^3} \frac{I_1(2kR)}{(J_1'^2(kR) + Y_1'^2(kR))} \Big(J_1'(kR)\, Y_1'(kR)\, \mathrm{Sin}2(kx+\omega t) - (J_1'^2(kR) - Y_1'^2(kR))\, \mathrm{Cos}2(kx-\omega t)\Big)\, dz\, \vec{j} \qquad (174)$$

The maximum values of second-order time dependent forces on large diameter cylinders are shown in Fig. 42 for varying values of kR and Y/D.

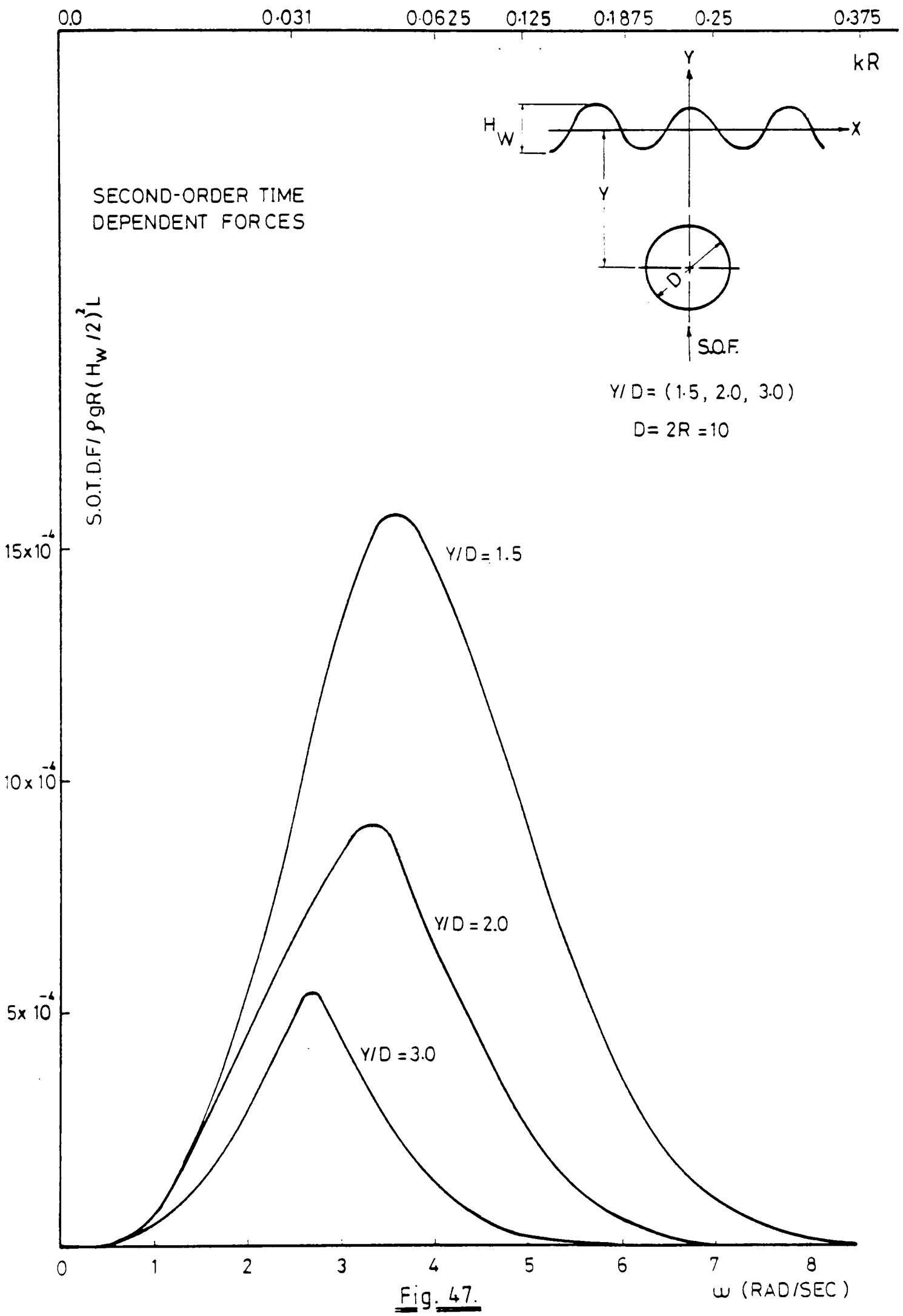
0.0
0·031
0·0625
0·125
0·1875
0·25
0·375
kR
Y
X
H_W
Y
D
S.O.F.
SECOND-ORDER TIME
DEPENDENT FORCES
Y/D = (1·5, 2·0, 3·0)
D= 2R =10
S.O.T.D.F/ ρgR $(H_W/2)^2$L
15×10^{-4}
10×10^{-4}
5×10^{-4}
Y/D = 1.5
Y/D = 2.0
Y/D = 3.0
0
1
2
3
4
5
6
7
8
ω (RAD/SEC)

Fig. 47.

$$A_{11} = 1/s$$

$$A_{13} = \frac{-c^2\ (5c^2+1)}{8s^5}$$

$$A_{15} = \frac{-(1184c^{10}-1440c^8-1992c^6+2641c^4-249c^2+18)}{1536s^{11}}$$

$$A_{22} = \frac{3}{8s^4}$$

$$A_{24} = \frac{(192c^8-424c^6-312c^4+480c^2-17)}{768s^{10}}$$

$$A_{33} = \frac{(13-4c^2)}{64s^7}$$

$$A_{35} = \frac{(512c^{12}+4224c^{10}-6800c^8-12,808c^6+16,704c^4-3154c^2+107)}{4096s^{13}\ (6c^2-1)}$$

$$A_{44} = \frac{(80c^6-816c^4+1338c^2-197)}{1536s^{10}\ (6c^2-1)}$$

$$A_{55} = \frac{-(2880c^{10}-72,480c^8+324,000c^6-432,000c^4+163,470c^2-16,245)}{61,440s^{11}\ (6c^2-1)(8c^4-11c^2+3)}$$

$$B_{22} = \frac{(2c^2+1)}{4s^3}\,c$$

$$B_{24} = \frac{c(272c^8-504c^6-192c^4+322c^2+21)}{384s^9}$$

$$B_{33} = \frac{3(8c^6+1)}{64s^6}$$

$$B_{35} = \frac{(88,128c^{14}-208,224c^{12}+70,848c^{10}+54,000c^8-21,816c^6+6264c^4-54c^2-81)}{12,288s^{12}\ (6c^2-1)}$$

$$B_{44} = \frac{c(768c^{10}-448c^8-48c^6+48c^4+106c^2-21)}{384s^9\ (6c^2-1)}$$

$$B_{55} = \frac{(192,000c^{16}-262,720c^{14}+83,680c^{12}+20,160c^{10}-7280c^8)}{12,288s^{10}\ (6c^2-1)(8c^4-11c^2+3)} +$$

$$+ \frac{(7160c^6-1800c^4-1050c^2+225)}{12,288s^{10}\ (6c^2-1)(8c^4-11c^2+3)}$$

contd. over ...

TABLE I

[From reference 8.]

TABLE I, contd:

$$C_1 = \frac{(8c^4-8c^2+9)}{8s^4}$$

$$C_2 = \frac{(3840c^{12}-4096c^{10}+2592c^8-1008c^6+5944c^4-1830c^2+147)}{512s^{10}\ (6c^2-1)}$$

$$C_3 = -\frac{1}{4sc}$$

$$C_4 = \frac{(12c^8+36c^6-162c^4+141c^2-27)}{192cs^9}$$

where

$$s = \mathrm{Sinh}(2\pi h/\lambda)$$

$$c = \mathrm{Cosh}(2\pi h/\lambda)$$

Chapter 3: A GENERAL METHOD AND A COMPUTER PROGRAM TO CALCULATE WAVE LOADING ON THE CIRCULAR CYLINDRICAL MEMBERS OF FIXED AND OF FLOATING STRUCTURES

INTRODUCTION

In this chapter a general method for calculating wave forces and moments on circular cylinders is derived. The wave loading on cylindrical members of fixed and of floating offshore structures oriented randomly in waves can be calculated using the method developed. The method uses the basic hydrodynamic theory and calculation procedures summarised in Chapter 2. A computer program, based on a general three dimensional method, has been developed to determine wave loading in terms of nodal loads distributed throughout the structure. This format of output provides a ready means of input for structural response analysis. The same output may also be used for dynamic response analysis. The computer program requires the start and the end co-ordinates of each member of an offshore structure and some information about intersecting members. All calculations for the geometrical details of the structure and the generation of nodal points are automatically performed and stored by the program. The three dimensional graphical representation of the geometry of the structure can also be produced on either screen or on a plotter using the same program so that the user can check the structure from different viewpoints to make sure that it is correctly defined. At the same time a summary list of the geometrical details of the structure, continuous and inter-costal members and the specifications for the corrections due to the inter-costal members are printed-out, so that the user can check that all the calculations to specify the geometry are correctly carried out by the program. Once the geometrical data has been verified the wave loading program which has automatic access to the data file can be run to obtain the wave loading distributed throughout the structure, and the required corrections due to the covered up areas between continuous and

inter-costal members, for varying angles of wave headings, draft, wave frequency and wave amplitude sets.

In the following derivation of the general method, the wave loading program and some examples on the usage of the program will be presented.

1. THE DERIVATION OF A GENERAL METHOD TO DETERMINE WAVE LOADING ON CIRCULAR CYLINDRICAL MEMBERS OF FIXED AND FLOATING OFFSHORE STRUCTURES

Circular cylindrical members are the basic support elements in the design of offshore structures. They resist external dynamic loads as well as internal static structural loads. In general, the wave loading on each member of the structure will be assumed to consist of the following force components. (See also Section 2 of Chapter 2.)

1. Dynamic Pressure Force: (= Froude-Krylov Force):

This force is due to the hydrodynamic pressure change below the surface of a wave while the wave is proceeding. It is assumed that the presence of the cylinder does not interfere with the flow field.

2. Acceleration Force:

The presence of the cylinder fixed relative to the waves gives rise to the acceleration force which is calculated by the product of the added virtual mass and the acceleration of the fluid particles. In order to calculate the wave acceleration forces on the ends of the cylinder, two different approaches can be found in the literature:

(i) Multiplying the acceleration of the water particles at the centre of top or bottom cross-sections of the cylinder by the added mass of a disk which has the same diameter as the cylinder in question. The method may be formulated as follows

$$F_y = (m_{22})_{disk}\ 0.5\ \dot{U}_y = \frac{4}{3}\ \rho\ R^3\ \dot{U}_y \qquad (1)$$

This method does not take into account the aspect ratio of the cylindrical member in the added mass determination. Present data shows that the effect of aspect ratio in different cylinder geometries such as rectangular, elliptical, etc., is significant and so for circular cylinders should be taken into account. This method has been used by Hooft in reference [1].

(ii) The method developed by Miller in reference [2] gives allowance for the aspect ratio of the circular cylinder as well as taking a correction due to the three dimensional form into account. In the method the cylinder is divided into strips lengthwise, say n number of strips and the added virtual mass of n rectangular strips and the acceleration force on those strips are calculated. The total acceleration force on the cylinder is obtained by summing the acceleration forces on each strip. The method, strictly speaking, requires the added mass coefficients to be known for each rectangular strip, but in reference [2] it was suggested that the average value for the aspect ratio of n strips can be defined and this can be used to determine the added mass values of all the strips. The method may be summarised as follows. (See Fig. 1.)

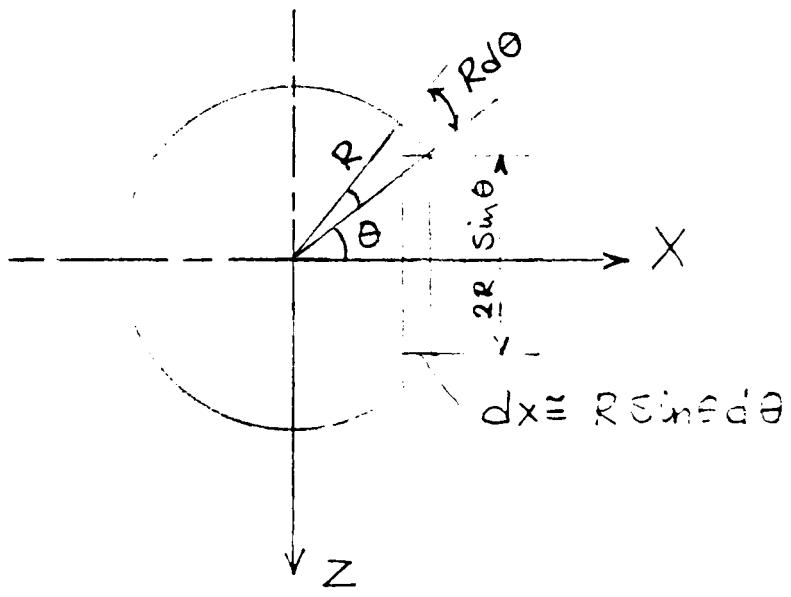

Fig. 1

Aspect ratio of i^{th} strip : $\frac{2R \sin\theta}{d}$

Mean aspect ratio of n strips : $\frac{\int_0^{\pi} (2R \sin\theta)\, dx}{2Rd}$

$$= \frac{\int_0^{\pi} 2R^2 \sin^2\theta \, d\theta}{2Rd} = \frac{R\pi}{2d}$$

The added mass of a fully submerged cylinder oscillating along the axis normal to its cross-sections is given as

$$m_{22} = \int_0^{\pi} (R \sin\theta)^2 \, k_{22} \, \rho \, \pi \, K_1 \, R \sin\theta \, d\theta$$

$$= \frac{4}{3} \rho \, \pi \, R^3 \, k_{22} \, K_1 \qquad (2)$$

where k_{22} is the added mass coefficient for the rectangular strip having an aspect ratio of $R\pi/2d$, and K_1 is the coefficient to take the effect of three dimensionality into account. As d decreases k_{22} approaches 1 and m_{22} can be calculated as the added mass of a disk, hence equation (2) becomes

$$m_{22} = \frac{4}{3} \rho \, \pi \, R^3 \, K_1 \doteq \frac{8}{3} \rho \, R^3 \qquad (3)$$

and $$K_1 = \frac{2}{\pi} = 0.636 \qquad (4)$$

Now the wave acceleration force on the top or bottom sides of a cylinder can be calculated using the following equation

$$F_y = (m_{22}) \; 0.5 \; \dot{U}_y = 0.424 \, \rho \, \pi \, R^3 \, k_{22} \, \dot{U}_y \qquad (5)$$

3. Drag Force:

The drag force mainly results from the turbulent flow downstream of the body due to the viscous effects which are significant when diameter/ wave height <0.125 for circular cylinders.

In this study, as discussed in Section 2.1.9.3 of Chapter II, in the case of an inclined cylindrical member, the normal components of the acceleration and velocity of the water particles with respect to the inclined cylinders' axes are assumed to give rise to the wave loading.

The following basic philosophy has been employed to derive the general three dimensional method for wave loading calculations:

(a) All the wave properties, i.e. dynamic pressure change, velocity and acceleration of water particles which are defined in the wave reference system are first transferred to the structure reference system and from the structure reference system to the member reference systems.

(b) All force and moment calculations are carried out in the member's reference system and distributed over the nodes of each member.

(c) The results of the force and moment calculations are transferred back to the structure reference system and summed up along the principle axes to obtain heave, surge and sway forces, as well as pitch, roll and yaw moments.

1.1 The Definition of Reference Systems

In the most general case, we may define the wave properties, i.e. pressure, velocity and acceleration of water particles in the wave reference system (x, y, z). (See Chapter II equations (50-51).)

The structural global reference system (X, Y, Z) is usually chosen in such a way that the origin of the system is at the centre of gravity for a floating or moored structure, but may be taken at any convenient point for a fixed structure. (u, v, w) are the reference axes for an individual member within the structure. (Fig. 2.)

To calculate the pressure acceleration and velocity forces the co-ordinates defined in the (x,y,z) system are transferred to the (X,Y,Z) system using the following transformation matrix.

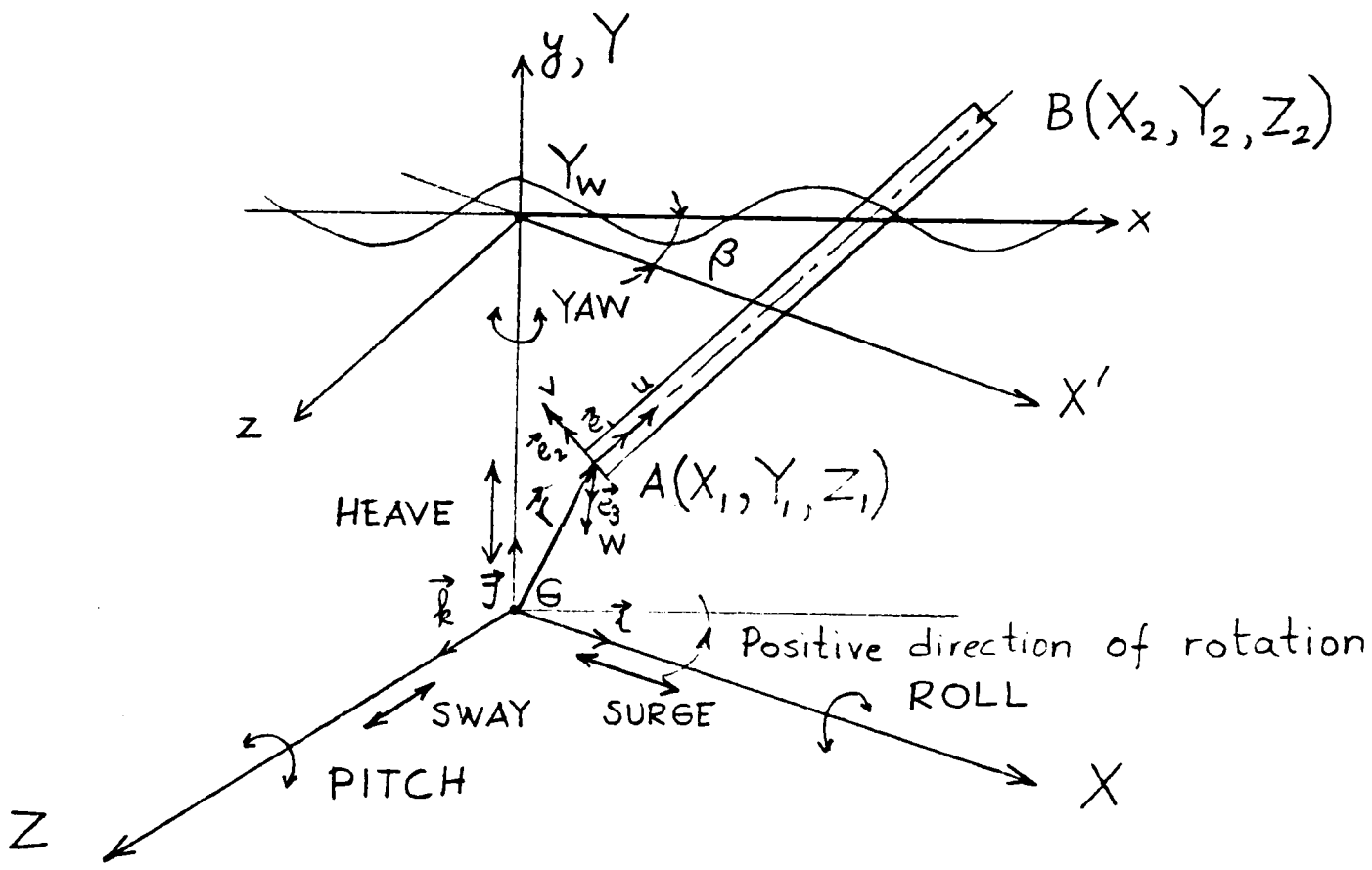

Fig. 2.

$$\begin{bmatrix} x \\ y \\ z \end{bmatrix} = \begin{bmatrix} \beta_{11} & \beta_{12} & \beta_{13} \\ \beta_{21} & \beta_{22} & \beta_{23} \\ \beta_{31} & \beta_{32} & \beta_{33} \end{bmatrix} \begin{bmatrix} X \\ Y \\ Z \end{bmatrix} + \begin{bmatrix} X_o \\ Y_o \\ Z_o \end{bmatrix} \qquad (6)$$

where, referring to Fig. 2:

$\beta_{11} = \cos\beta$: The Cosine of the angle between x and X axes.

$\beta_{12} = \cos(90) = 0$: The Cosine of the angle between x and Y axes.

$\beta_{13} = \cos(\frac{\pi}{2} + \beta)$: The Cosine of the angle between x and Z axes.

$\beta_{21} = \cos(90) = 0$: The Cosine of the angle between y and X axes.

$\beta_{22} = \cos(0) = 1$: The Cosine of the angle between y and Y axes.

$\beta_{23} = \cos(90) = 0$: The Cosine of the angle between y and Z axes.

$\beta_{31} = \text{Cos}(\frac{\pi}{2} - \beta)$: The Cosine of the angle between z and X axes.

$\beta_{32} = \text{Cos}(90) = 0$: The Cosine of the angle between z and Y axes.

$\beta_{33} = \text{Cos}(\beta)$: The Cosine of the angle between z and Z axes.

and $X_o = 0$, $Y_o = - Y_w$ and $Z_o = 0$.

Now equations (6) can be written in the following form

$$\begin{bmatrix} x \\ y \\ z \end{bmatrix} = \begin{bmatrix} \text{Cos}\beta & 0 & - \text{Sin}\beta \\ 0 & 1 & 0 \\ \text{Sin}\beta & 0 & \text{Cos}\beta \end{bmatrix} \begin{bmatrix} X \\ Y \\ Z \end{bmatrix} - \begin{bmatrix} 0 \\ Y_w \\ 0 \end{bmatrix} . \qquad (7)$$

Using the transformation equations given in (7), the velocity, acceleration and pressure equations of a water particle in the wave, by referring to the structural reference system, can be written as follows:

Horizontal velocity: $U_{x_{(s)}} = 0.5\ H_w\ \omega\ e^{k(Y-Y_w)}\ \text{Cos}[k(X\ \text{Cos}\beta - Z\text{Sin}\beta) - \omega t]$ (8-A)

Vertical velocity : $U_{y_{(s)}} = 0.5\ H_w\ \omega\ e^{k(Y-Y_w)}\ \text{Sin}[k(X\ \text{Cos}\beta - Z\text{Sin}\beta) - \omega t]$ (8-B)

Horizontal acceleration : $\dot{U}_{x_{(s)}} = 0.5\ H_w\ \omega^2\ e^{k(Y-Y_w)}\ \text{Sin}[k(X\text{Cos}\beta - Z\text{Sin}\beta) - \omega t]$ (8-C)

Vertical acceleration : $\dot{U}_{y_{(s)}} = - 0.5\ H_w\ \omega^2\ e^{k(Y-Y_w)}\ \text{Cos}[k(X\text{Cos}\beta - Z\text{Sin}\beta) - \omega t]$ (8-D)

Pressure : $p_{(s)} = - \rho\ g(Y-Y_w) + 0.5\ \rho\ g\ H_w\ e^{k(Y-Y_w)}\ \text{Cos}[k(X\text{Cos}\beta - Z\text{Sin}\beta) - \omega t]$ (8-E)

To be able to make force and moment calculations on an individual member of the structure we have to transfer these velocity, acceleration and pressure equations which have been written in the structure reference system to the member reference system with the following matrix equation:

$$\begin{bmatrix} X \\ Y \\ Z \end{bmatrix} = \begin{bmatrix} \alpha_{11} & \alpha_{12} & \alpha_{13} \\ \alpha_{21} & \alpha_{22} & \alpha_{23} \\ \alpha_{31} & \alpha_{32} & \alpha_{33} \end{bmatrix} \begin{bmatrix} u \\ v \\ w \end{bmatrix} + \begin{bmatrix} X_1 \\ Y_1 \\ Z_1 \end{bmatrix} \qquad (9)$$

where

α_{11} : The Cosine of the angle between X and u.

α_{12} : The Cosine of the angle between X and v.

α_{13} : The Cosine of the angle between X and w.

α_{21} : The Cosine of the angle between Y and u.

α_{22} : The Cosine of the angle between Y and v.

α_{23} : The Cosine of the angle between Y and w.

α_{31} : The Cosine of the angle between Z and u.

α_{32} : The Cosine of the angle between Z and v.

α_{33} : The Cosine of the angle between Z and w.

The method of obtaining the direction Cosines will be given in the next section.

1.2 The Determination of Direction Cosines

In order to determine the direction Cosines (α_{ij}, i=1,3, j=1,3) we have to define the unit vector $\vec{e}_1$ which lies along the u axis and $\vec{e}_2$ and $\vec{e}_3$ unit vectors which are perpendicular to each other as well as to the $\vec{e}_1$ vector. In other words, $\vec{e}_1$, $\vec{e}_2$ and $\vec{e}_3$ are the orthogonal vectors. (See Fig. 2.) At the start of the problem the co-ordinates of the points A and B in the structure reference system are known, so the $\vec{e}_1$ unit vector can easily be determined as follows [3]

$$\vec{e}_1 = \frac{\vec{AB}}{|\vec{AB}|} \qquad (10)$$

where

$$\vec{AB} = \vec{GB} - \vec{GA}$$

$$\vec{GB} = X_2\vec{i} + Y_2\vec{j} + Z_2\vec{k}$$

$$\vec{GA} = X_1\vec{i} + Y_1\vec{j} + Z_1\vec{k}$$

$$\vec{AB} = (X_2-X_1)\vec{i} + (Y_2-Y_1)\vec{j} + (Z_2-Z_1)\vec{k}$$

$$|\vec{AB}| = \sqrt{(X_2-X_1)^2 + (Y_2-Y_1)^2 + (Z_2-Z_1)^2}$$

To determine the $\vec{e}_2$ unit vector, the plane [Q] which passes through the point A and is perpendicular to the vector $\vec{AB}$ will be defined. It can be supposed that we have defined the equation of the plane [Q] and then chosen a point P(X,Y,Z) on this plane. We can write the equation of the vector $\vec{AP}$ as follows

$$\vec{AP} = (X-X_1)\vec{i} + (Y-Y_1)\vec{j} + (Z-Z_1)\vec{k} \qquad (11)$$

Since the vector $\vec{AB}$ is perpendicular to the [Q] plane the vector $\vec{AB}$ should also be perpendicular to the vector AP. This gives us the following equation to determine the equation of the [Q] plane

$$\vec{AP}\cdot\vec{AB} = 0 \qquad (12)$$

or

$$[Q] \equiv (X-X_1)(X_2-X_1) + (Y-Y_1)(Y_2-Y_1) + (Z-Z_1)(Z_2-Z_1) = 0 \qquad (13)$$

Now we have to define the $\vec{AP}$ vector in terms of known quantities. If we choose any arbitrary X_Q, Y_Q points in space and substitute them into equation (13), the Z_Q co-ordinate of point P can easily be obtained.

If we replace the arbitrary co-ordinates X,Y,Z with the co-ordinates X_Q, Y_Q and Z_Q in equation (11) we can obtain the vector $\vec{AP}$.

$$\vec{e}_2 = \frac{\vec{AP}}{|\vec{AP}|} \qquad (14)$$

From the orthogonality condition, $\vec{e}_3$ can also readily be obtained as follows

$$\vec{e}_3 = \vec{e}_1 \Lambda \vec{e}_2 \tag{15}$$

Having obtained the unit vectors in a member reference system the direction Cosines can be written in the following forms

$$\begin{aligned}
\alpha_{11} &= \vec{i}\cdot\vec{e}_1 \qquad \alpha_{12} = \vec{i}\cdot\vec{e}_2 \qquad \alpha_{13} = \vec{i}\cdot\vec{e}_3 \\
\alpha_{21} &= \vec{j}\cdot\vec{e}_1 \qquad \alpha_{22} = \vec{j}\cdot\vec{e}_2 \qquad \alpha_{23} = \vec{j}\cdot\vec{e}_3 \\
\alpha_{31} &= \vec{k}\cdot\vec{e}_1 \qquad \alpha_{32} = \vec{k}\cdot\vec{e}_2 \qquad \alpha_{33} = \vec{k}\cdot\vec{e}_3
\end{aligned} \tag{16}$$

1.3 Calculation of Wave Forces

1.3.1 Calculation of pressure force. The hydrodynamic pressure change with depth below the surface of a wave in the structural reference system is given in equation (8-E). Equation (8-E) can be transformed to the member reference system, using matrix equation (9) as follows

$$p_{(m)} = 0.5\ \rho\ g\ H_w\ e^{k(B+Y_1-Y_w)}\ \mathrm{Cos}\{k[A\ \mathrm{Cos}\beta - C\ \mathrm{Sin}\beta] - \omega t\} \tag{17}$$

where

$$A = \alpha_{11}\ u + \alpha_{12}\ v + \alpha_{13}\ w + X_1$$

$$B = \alpha_{21}\ u + \alpha_{22}\ v + \alpha_{23}\ w$$

$$C = \alpha_{31}\ u + \alpha_{32}\ v + \alpha_{33}\ w + Z_1$$

The total pressure force on a member in this member's reference system can be determined using the following integration equation

$$\vec{FP}_{i,(m)} = -\int_{u=0}^{\ell}\int_{\theta=0}^{2\pi} (p_{(m)}\ R\ \mathrm{Cos}\theta\ d\theta\ du\ \vec{e}_2 + p_{(m)}\ R\ \mathrm{Sin}\theta\ d\theta\ du\ \vec{e}_3) \tag{18}$$

Since

$$dS = R\ d\theta\ du$$

$\vec{n}$: unit normal vector to surface (positive outwards)

$$= \mathrm{Cos}\theta\ \vec{e}_2 + \mathrm{Sin}\theta\ \vec{e}_3$$

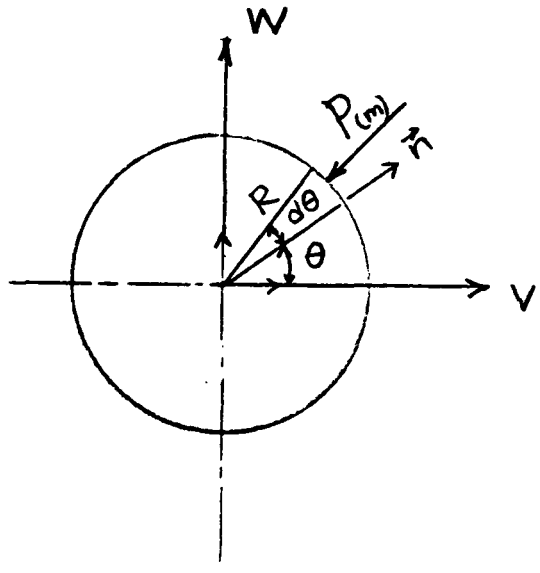

Fig. 3.

$\vec{FP}_{i,(m)}$ becomes

$$\vec{FP}_{i,(m)} = - \iint_S p_{(m)} \vec{n} \, dS \tag{19}$$

Using the divergence theorem of Gauss [3], the surface integral form of $\vec{FP}_{i,(m)}$ in equation (19) can be converted to the volume integral for the sake of simplicity. That is

$$\vec{FP}_{i,(m)} = - \iint_S p_{(m)} \vec{n} \, dS = - \iiint_V \nabla p_{(m)} \, dV \tag{20}$$

where V is the volume bounded by a closed surface S and

$$\nabla = \frac{\partial}{\partial u} \vec{e}_1 + \frac{\partial}{\partial v} \vec{e}_2 + \frac{\partial}{\partial w} \vec{e}_3$$

The pressure force components along the w and v axes can be written in the form of a volume integral as follows

$$\vec{FP}_{w_{i,(m)}} = - \iiint_V \frac{\partial}{\partial w} p_{(m)} \, dV \, \vec{e}_3 \tag{21}$$

or

$$FP_{w_{i,(m)}} = -\left(0.5\ \rho\ g\ H_w\ k \int_{u=0}^{\ell} \int_{r=0}^{R} \int_{\theta=0}^{2\pi} \alpha_{23}\ e^{k(B'+Y_1-Y_w)}\right.$$

$$\mathrm{Cos}\{k[A'\ \mathrm{Cos}\beta - C'\ \mathrm{Sin}\beta] - \omega t\}\ dV - \int_{u=0}^{\ell} \int_{r=0}^{R} \int_{\theta=0}^{2\pi} (\alpha_{13}\ \mathrm{Cos}\beta - \alpha_{33}\ \mathrm{Sin}\beta)$$

$$\left. e^{k(B'+Y_1-Y_w)}\ \mathrm{Sin}\{k[A'\ \mathrm{Cos}\beta - C'\ \mathrm{Sin}\beta] - \omega t\})\ dV\right) \qquad (21\text{-}1)$$

where

$$A' = \alpha_{11}\ u + \alpha_{12}\ r\ \mathrm{Cos}\theta + \alpha_{13}\ r\ \mathrm{Sin}\theta + X_1$$

$$B' = \alpha_{21}\ u + \alpha_{22}\ r\ \mathrm{Cos}\theta + \alpha_{23}\ r\ \mathrm{Sin}\theta$$

$$C' = \alpha_{31}\ u + \alpha_{32}\ r\ \mathrm{Cos}\theta + \alpha_{33}\ r\ \mathrm{Sin}\theta + Z_1$$

$$dV = r\ d\theta\ dr\ du$$

$$v = r\ \mathrm{Cos}\theta \quad \text{and} \quad w = r\ \mathrm{Sin}\theta$$

Since $kv \ll 1$ and $kw \ll 1$ in the case of small diameter cylinders ($D/\lambda < 0.2$) the terms involved with kv and kw can be neglected and therefore some more simplifications can be made in equation (21-1)

$$FP_{w_{i,(m)}} = -\left(0.5\ \rho\ g\ \pi\ R^2\ H_w\ k \int_{u=0}^{\ell} \alpha_{23}\ e^{k(\alpha_{21}u+Y_1-Y_w)}\right.$$

$$\mathrm{Cos}\{k[(\alpha_{11}\ \mathrm{Cos}\beta - \alpha_{31}\ \mathrm{Sin}\beta)\ u + X_1\ \mathrm{Cos}\beta - Z_1\ \mathrm{Sin}\beta] - \omega t\}\ du -$$

$$\int_{u=0}^{\ell} (\alpha_{13}\ \mathrm{Cos}\beta - \alpha_{33}\ \mathrm{Sin}\beta)\ e^{k(\alpha_{21}u+Y_1-Y_w)}\ \mathrm{Sin}\{k[(\alpha_{11}\ \mathrm{Cos}\beta - \alpha_{31}\ \mathrm{Sin}\beta)u$$

$$\left. + X_1\ \mathrm{Cos}\beta - Z_1\ \mathrm{Sin}\beta] - \omega t\}\ du)\right) \qquad (21\text{-}2)$$

Similarly, the pressure force along the v direction can be obtained as follows

$$\vec{FP}_{v_{i,(m)}} = -\iiint_V \frac{\partial p_{(m)}}{\partial v}\ dV\ \vec{e}_2 \qquad (22)$$

$$\vec{FP}_{v_{i,(m)}} = -\,(0.5\,\rho\,g\,\pi\,R^2\,H_w\,k \int_{u=0}^{\ell} \alpha_{22}\, e^{k(\alpha_{21}u+Y_1-Y_w)}$$

$$\mathrm{Cosk}[(\alpha_{11}\,\mathrm{Cos}\beta - \alpha_{31}\,\mathrm{Sin}\beta)\,u + X_1\,\mathrm{Cos}\beta - Y_1\,\mathrm{Sin}\beta] - \omega t)\,du$$

$$- \int_{u=0}^{\ell} (\alpha_{12}\,\mathrm{Cos}\beta - \alpha_{32}\,\mathrm{Sin}\beta)\, e^{k(\alpha_{21}u+Y_1-Y_w)}\,\mathrm{Sin}\{k[(\alpha_{11}\,\mathrm{Cos}\beta -$$

$$\alpha_{31}\,\mathrm{Sin}\beta)\,u + X_1\,\mathrm{Cos}\beta - Z_1\,\mathrm{Sin}\beta] - \omega t\}\,du)) \qquad (22\text{-}1)$$

The pressure forces at the bottom and at the top of the cylindrical member can be written as follows

$$FP_{u=0_{i,(m)}} = \int_{r=0}^{R} \int_{\theta=0}^{2\pi} p_{(m)}\; r\; dr\; d\theta \qquad (23)$$

Since the dynamic pressure change may be assumed to be constant across the diameter of the cylindrical member, equation (23) can take the following form

$$FP_{u=0_{i,(m)}} = 0.5\,\rho\,g\,H_w\,\pi\,R^2\,e^{k(Y_1-Y_w)}\,\mathrm{Cos}\{k[X_1\,\mathrm{Cos}\beta - Z_1\,\mathrm{Sin}\beta] - \omega t\} \qquad (24)$$

Similarly the pressure force at the top end of the cylindrical member will be

$$FP_{u=\ell_{i,(m)}} = 0.5\,\rho\,g\,H_w\,\pi\,R^2\,e^{k(\alpha_{21}\ell+Y_1-Y_w)}$$
$$\mathrm{Cos}\{k[(\alpha_{11}\ell + X_1)\,\mathrm{Cos}\beta - (\alpha_{31}\ell + Z_1)\,\mathrm{Sin}\beta] - \omega t\} \qquad (25)$$

If we write the total pressure force acting on a member in the member and structure reference systems, the following equations are obtained

$$\vec{FP}_{i,(m)} = FP_{w_{i,(m)}}\,\vec{e}_3 + FP_{v_{i,(m)}}\,\vec{e}_2 + (FP_{u=0_{i,(m)}} - FP_{u=\ell_{i,(m)}})\,\vec{e}_1 \qquad (26)$$

$$\vec{FP}_{i,(s)} = (\vec{FP}_{i,(m)} \cdot \vec{i})\cdot\vec{i} + (\vec{FP}_{i,(m)} \cdot \vec{j})\vec{j} + (\vec{FP}_{i,(m)} \cdot \vec{k})\vec{k} \qquad (27)$$

Using the direction Cosines, the pressure equation given above can also be written in the following form

$$\vec{FP}_{i,(s)} = [FP_{w_{i,(m)}} \alpha_{13} + FP_{v_{i,(m)}} \alpha_{12} + (FP_{u=0_{i,(m)}} - FP_{u=\ell_{i,(m)}})\alpha_{11}]\vec{i}$$

↓

surge force components

$$[FP_{w_{i,(m)}} \alpha_{23} + FP_{v_{i,(m)}} \alpha_{22} + (FP_{u=0_{i,(m)}} - FP_{u=\ell_{i,(m)}})\alpha_{21}]\vec{j}$$

↓

heave force components

$$[FP_{w_{i,(m)}} \alpha_{33} + FP_{v_{i,(m)}} \alpha_{32} + (FP_{u=0_{i,(m)}} - FP_{u=\ell_{i,(m)}})\alpha_{31}]\vec{k}$$

↓

sway force components

1.3.2 The calculation of acceleration force. The x and y components of acceleration of a water particle in the structure reference system have been given in equation (8-C) and (8-D). These components can be transferred into the member reference system as follows

$$\dot{U}_{x_{(m)}} = 0.5\ \omega^2\ H_w\ e^{k(B+Y_1-Y_w)}\ \mathrm{Sin}[k\{(A\ \mathrm{Cos}\beta - C\ \mathrm{Sin}\beta)\} - \omega t] \qquad (28)$$

$$\dot{U}_{y_{(m)}} = -\ 0.5\ \omega^2\ H_w\ e^{k(B+Y_1-Y_w)}\ \mathrm{Cos}[k\{(A\ \mathrm{Cos}\beta - C\ \mathrm{Sin}\beta)\} - \omega t] \qquad (28\text{-}1)$$

Assuming the change of acceleration with depth of cylinder can be neglected for small diameter cylinders the following simplifications can be made in equations (28) and (28-1)

$$\dot{U}_{x,(m)} = 0.5\ \omega^2\ H_w\ e^{k(\alpha_{21}u+Y_1-Y_w)}\ \mathrm{Sin}[k\{(\alpha_{11}u + X_1)\ \mathrm{Cos}\beta - (\alpha_{31}u + Z_1)\ \mathrm{Sin}\beta\} - \omega t] \qquad (29)$$

$$\dot{U}_{Y,(m)} = -\,0.5\;\omega^2\;H_w\;e^{k(\alpha_{21}u+Y_1-Y_w)}\;\mathrm{Cos}[k\{(\alpha_{11}u+X_1)\;\mathrm{Cos}\beta - (\alpha_{31}u+Z_1)\;\mathrm{Sin}\beta\} - \omega t] \qquad (29\text{-}1)$$

The above expressions for acceleration have been written in the member reference system but they are along lines which are parallel to the wave propagation. If we resolve them along the structure reference system's axes the following equations are obtained

$$\dot{U}_{X_{(m)}} = \dot{U}_{x_{(m)}}\;\mathrm{Cos}\beta \qquad (30)$$

$$\dot{U}_{Y_{(m)}} = \dot{U}_{Y_{(m)}} \qquad (30\text{-}1)$$

$$\dot{U}_{Z_{(m)}} = -\,\dot{U}_{x_{(m)}}\;\mathrm{Sin}\beta \qquad (30\text{-}2)$$

Now we can write the acceleration forces in the member reference system along the w and v axes

$$FA_{w_{i,(m)}} = k_{33}\;\rho\;\left(\int_{u=0}^{\ell}\dot{U}_{X_{(m)}}\;\mathrm{Cos}(w,X)\,dV + \int_{u=0}^{\ell}\dot{U}_{Y_{(m)}}\;\mathrm{Cos}(w,Y)\,dV + \int_{u=0}^{\ell}\dot{U}_{Z_{(m)}}\;\mathrm{Cos}(w,Z)\,dV\right) \qquad (31)$$

Substituting $k_{33}=1$ (since the acceleration force is calculated along the w axis on circular cylinders), and the values of $\dot{U}_{X_{(m)}}$, $\dot{U}_{Y_{(m)}}$, $\dot{U}_{Z_{(m)}}$ from equations (30), (30-1), (30-2) respectively and $dV=\pi R^2 du$ into equation (31) the acceleration force equation (31) becomes

$$FA_{w_{i,(m)}} = \rho\;\pi\;R^2\;\left[\int_{u=0}^{\ell}\dot{U}_{x_{(m)}}\;(\alpha_{13}\;\mathrm{Cos}\beta - \alpha_{33}\;\mathrm{Sin}\beta)\;du + \int_{u=0}^{\ell}\dot{U}_{Y_{(m)}}\;\alpha_{23}\;du\right] \qquad (32)$$

If we replace $\dot{U}_{x_{(m)}}$ and $\dot{U}_{Y_{(m)}}$ with the equations given at (29) and (29-1) respectively, equation (32) can be written as follows

$$FA_{w_{i,(m)}} = -(0.5\ \rho\ g\ \pi\ R^2\ H_w\ k(\int_{u=0}^{\ell} \alpha_{23}\ e^{k(\alpha_{21}u+Y_1-Y_w)}$$

$$\cos\{k[(\alpha_{11}\ \cos\beta - \alpha_{31}\ \sin\beta)u + X_1\ \cos\beta - Z_1\ \sin\beta] - \omega t\}\ du$$

$$-\int_{u=0}^{\ell} (\alpha_{21}\ \cos\beta - \alpha_{33}\ \sin\beta)\ e^{k(\alpha_{21}u+Y_1-Y_w)}$$

$$\sin\{k[(\alpha_{11}\ \cos\beta - \alpha_{31}\ \sin\beta)u + X_1\ \cos\beta - Z_1\ \sin\beta] - \omega t\}\ du)) \qquad (33)$$

If we compare equations (21-2) and (33) it can be seen that these two equations are identical, so it is proved that for circular cylinders, regardless of the direction of wave and position of cylinder, the pressure force is equal to the acceleration force along the direction which is normal to the cylinder's curved surface.

A similar expression to that in equation (31) can be written to obtain $FA_{v_{i,(m)}}$

$$FA_{v_{i,(m)}} = k_{22}\ \rho\ (\int_{o}^{\ell} \dot{U}_{X_{(m)}}\ \cos(v,X)\ dV + \int_{o}^{\ell} \dot{U}_{Y_{(m)}}\ \cos(v,Y)\ dV$$

$$+\int_{o}^{\ell} \dot{U}_{Z_{(m)}}\ \cos(v,Z)\ dV) \qquad (34)$$

or

$$FA_{v_{i,(m)}} = -(0.5\ \rho\ g\ \pi\ R^2\ H_w\ k\ (\int_{u=0}^{\ell} \alpha_{22}\ e^{k(\alpha_{31}u+Y_1-Y_w)}$$

$$\cos\{k[(\alpha_{11}\ \cos\beta - \alpha_{31}\ \sin\beta)u + X_1\ \cos\beta - Z_1\ \sin\beta] - \omega t\}\ du$$

$$-\int_{u=0}^{\ell} (\alpha_{12}\ \cos\beta - \alpha_{32}\ \sin\beta)\ e^{k(\alpha_{21}u+Y_1-Y_w)}$$

$$\sin\{k[(\alpha_{11}\ \cos\beta - \alpha_{31}\ \sin\beta)u + X_1\ \cos\beta - Z_1\ \sin\beta] - \omega t\}\ du)) \qquad (35)$$

Finally, the acceleration forces on the end surfaces of a cylindrical member can be calculated as follows

$$FA_{u=0_{i,(m)}} = m_{11} (\dot{U}_{X_{(m)}} \text{Cos}(u,X) + \dot{U}_{Y_{(m)}} \text{Cos}(u,Y) + \dot{U}_{Z_{(m)}} \text{Cos}(u,Z)) \quad (36)$$

By using equations (5), (29), (29-1), (30), (30-1), (30-2), equation (36) can also be written as

$$FA_{u=0_{i,(m)}} = - (0.5\ \rho\ g\ \pi\ H_w\ k\ 0.423\ R^3\ k_{11}\ (\alpha_{21}\ e^{k(Y_1-Y_w)} \text{Cos}[k(X_1\ \text{Cos}\beta - Z_1\ \text{Sin}\beta) - \omega t] - (\alpha_{11}\ \text{Cos}\beta - \alpha_{31}\ \text{Sin}\beta)\ e^{k(Y_1-Y_w)}\ \text{Sin}[k(X_1\ \text{Cos}\beta - Z_1\ \text{Sin}\beta) - \omega t])) \quad (36\text{-A})$$

where k_{11} is the added mass coefficient of a rectangle having an aspect ratio of $\pi R/2\ell$.

Similarly, the acceleration force on the bottom surface of a cylinder will be

$$FA_{u=\ell_{i,(m)}} = - (0.5\ \rho\ g\ \pi\ H_w\ k\ 0.423\ R^3\ k_{11}\ (\alpha_{21}\ e^{k(\alpha_{21}\ell+Y_1-Y_w)} \text{Cos}\{k[(\alpha_{11}\ell + X_1)\ \text{Cos}\beta - (\alpha_{31}\ell + Z_1)\ \text{Sin}\beta] - \omega t\} - (\alpha_{11}\ \text{Cos}\beta - \alpha_{31}\ \text{Sin}\beta)\ e^{k(\alpha_{21}\ell + Y_1-Y_w)} \text{Sin}\{k[(\alpha_{11}\ell + X_1)\ \text{Cos}\beta - (\alpha_{31}\ell + Z_1)\ \text{Sin}\beta] - \omega t\} \quad (37)$$

1.3.3 <u>The calculation of velocity force</u>. As with the acceleration force calculations, if we neglect the velocity variation along the depth of the cylinder, and assuming that water particles move with a velocity equal to that at the centre of the cylinder cross-section, the following results can be obtained to calculate the velocity force.

The x and y components of water particle velocity given in the structure reference system in equations (8-A) and (8-B) can be trans-

ferred into the member reference system as follows

$$U_{x_{(m)}} = 0.5\ \omega\ H_w\ e^{k(\alpha_{21}u+Y_1-Y_w)}\ \mathrm{Cos}[k\{(\alpha_{11}u + X_1)\ \mathrm{Cos}\beta - (\alpha_{31}u + Z_1)\ \mathrm{Sin}\beta\} - \omega t] \tag{38}$$

$$U_{Y_{(m)}} = 0.5\ \omega\ H_w\ e^{k(\alpha_{21}u+Y_1-Y_w)}\ \mathrm{Sin}[k\{(\alpha_{11}u + X_1)\ \mathrm{Cos}\beta - (\alpha_{31}u + Z_1)\ \mathrm{Sin}\beta\} - \omega t] \tag{38-1}$$

The above expressions for velocity are written in member reference system but they are parallel to the direction of wave propagation. If we resolve them along lines which are parallel to the structure reference system's axes the following equations are obtained

$$U_{X_{(m)}} = U_{x_{(m)}}\ \mathrm{Cos}\beta \tag{39}$$

$$U_{Y_{(m)}} = U_{y_{(m)}} \tag{39-1}$$

$$U_{Z_{(m)}} = -\ U_{x_{(m)}}\ \mathrm{Sin}\beta \tag{39-2}$$

Now we can obtain the velocity forces in member reference systems along the w and v axes

$$FV_{w,} = \tfrac{1}{2} C_D \rho D \left[\int_{u=0}^{\ell} \left(U_{X_{(m)}}\ \mathrm{Cos}(w,X) + U_{Y_{(m)}}\ \mathrm{Cos}(w,Y) + U_{Z_{(m)}}\ \mathrm{Cos}(w,Z)\right) \left| \left(U_{X_{(m)}}\ \mathrm{Cos}(w,X) + U_{Y_{(m)}}\ \mathrm{Cos}(w,Y) + U_{Z_{(m)}}\ \mathrm{Cos}(w,Z)\right) \right| \right] du \tag{40}$$

or, substituting equations (39), (39-1), (39-2) into equation (40) the drag force along w axes on each member may also be written as

$$FV_{w_{i,(m)}} = \tfrac{1}{2}C_D\rho D\left[\int_{u=0}^{\ell}\left(U_{x_{(m)}}(\alpha_{13}\,\mathrm{Cos}\beta - \alpha_{33}\,\mathrm{Sin}\beta) + U_{y_{(m)}}\alpha_{23}\right)\left|\left(U_{x_{(m)}}(\alpha_{13}\mathrm{Cos}\beta - \alpha_{33}\mathrm{Sin}\beta) + U_{y_{(m)}}\alpha_{23}\right)\right|\right]du \qquad (40\text{-}1)$$

Similarly, the velocity force along the v axis will be

$$FV_{v_{i,(m)}} = \tfrac{1}{2}C_D\rho D\left[\int_{u=0}^{\ell}\left(U_{x_{(m)}}(\alpha_{12}\mathrm{Cos}\beta - \alpha_{32}\mathrm{Sin}\beta) + U_{y_{(m)}}\alpha_{22}\right)\left|\left(U_{x_{(m)}}(\alpha_{12}\mathrm{Cos}\beta - \alpha_{32}\mathrm{Sin}\beta) + U_{y_{(m)}}\alpha_{22}\right)\right|\right]du \qquad (41)$$

The velocity forces on the end surfaces of a cylindrical member are neglected in wave loading calculations because of the uncertainties about both the viscous flow state and the appropriate drag coefficients. The error will not be large except for cases where the pressure and inertia terms cancel one another.

1.3.4 Calculation of the total wave force. The total wave force will consist of hydrodynamic pressure force, acceleration force and velocity force. If we write the total force acting on the structure in the structure's reference system, the following resultant force components are obtained..

$$FT_{(s)} = \sum_{i=1}^{m}\left[\left(FT_{w_{i,(m)}}\alpha_{13} + FT_{v_{i,(m)}}\alpha_{12} + FT_{u_{i,(m)}}\alpha_{11}\right)\right]\vec{i}$$

$$\downarrow$$

surge force

$$+\sum_{i=1}^{m}\left[\left(FT_{w_{i,(m)}}\alpha_{23} + FT_{v_{i,(m)}}\alpha_{22} + FT_{u_{i,(m)}}\alpha_{21}\right)\right]\vec{j}$$

$$\downarrow$$

heave force (42)

contd. over ...

$$+ \sum_{i=1}^{m} [(FT_{w_{i,(m)}} \alpha_{33} + FT_{v_{i,(m)}} \alpha_{32} + FT_{u_{i,(m)}} \alpha_{31})] \vec{k}$$

$$\downarrow$$

sway force (42)

where

$$FT_{w_{i,(m)}} = FP_{w_{i,(m)}} + FA_{w_{i,(m)}} + FV_{w_{i,(m)}}$$

$$FT_{v_{i,(m)}} = FP_{v_{i,(m)}} + FA_{v_{i,(m)}} + FV_{v_{i,(m)}}$$

$$FT_{u_{i,(m)}} = FP_{u=0_{i,(m)}} + FP_{u=\ell_{i,(m)}} + FA_{u=0_{i,(m)}} + FA_{u=\ell_{i,(m)}}$$

The terms in the last equation are to be determined according to the cylindrical members exposed ends to the wave loading, i.e. if the member is inter-costal these terms will vanish.

1.4 Calculation of Total Moment

If we consider an individual element in a member reference system, the moments due to the wave forces about the member reference system's origin, A, can be written as follows (see Fig. 2):

$$\vec{m}_{A_i} = \int_{u=0}^{\ell} [u\vec{e}_1 \Lambda \frac{d}{du} (FT_{w_{i,(m)}} \vec{e}_3 + FT_{v_{i,(m)}} \vec{e}_2)] \, du \quad (43)$$

or

$$m_{A_i} = -\int_{u=0}^{\ell} \frac{d}{du} (FT_{w_{i,(m)}}) \, u \, du \, \vec{e}_2 + \int_{u=0}^{\ell} \frac{d}{du} (FT_{v_{i,(m)}}) \, u \, du \, \vec{e}_3 \quad (43\text{-}1)$$

The total moment about the structure reference system's origin can easily be obtained using the moment transformation rule as follows

$$\vec{m}_{G_i} = \vec{m}_{A_i} + \vec{r} \Lambda (FT_{w_{i,(m)}} \vec{e}_3 + FT_{v_{i,(m)}} \vec{e}_2 + FT_{u_{i,(m)}} \vec{e}_1) \quad (44)$$

where

$$\vec{r} = \vec{GA} = X_1 \vec{i} + Y_1 \vec{j} + Z_1 \vec{k}$$

and

$\vec{e}_2$ and $\vec{e}_3$ should be replaced with the values which will be obtained from equations (14) and (15) respectively.

The total moment acting on the structure

$$\vec{M} = \sum_{i=1}^{m} \vec{m}_{G_{(i)}} \tag{45}$$

The total moment vector can also be analysed in terms of principal components as follows

$$\vec{M} = \underset{\text{(roll moment)}}{a\vec{i}} + \underset{\text{(yaw moment)}}{b\vec{j}} + \underset{\text{(pitch moment)}}{c\vec{k}} \tag{46}$$

where

$$a = \sum_{i=1}^{m} \left[\int_{u=0}^{\ell} \frac{d}{du} \left(\alpha_{13}\, FT_{v_{i,(m)}} - \alpha_{12}\, FT_{w_{i,(m)}}\right) u\, du \right.$$

$$+ FT_{w_{i,(m)}} (Y_1\, \alpha_{33} - Z_1\, \alpha_{23}) + FT_{v_{i,(m)}} (Y_1\, \alpha_{32} - Z_1\, \alpha_{22})$$

$$\left. + FT_{u_{i,(m)}} (Y_1\, \alpha_{31} - Z_1\, \alpha_{21}) \right]$$

$$b = \sum_{i=1}^{m} \left[\int_{u=0}^{\ell} \frac{d}{du} \left(\alpha_{23}\, FT_{v_{i,(m)}} - \alpha_{22}\, FT_{w_{i,(m)}}\right) u\, du \right.$$

$$+ FT_{w_{i,(m)}} (Z_1\, \alpha_{13} - X_1\, \alpha_{33}) + FT_{v_{i,(m)}} (Z_1\, \alpha_{12} - X_1\, \alpha_{32})$$

$$\left. + FT_{u_{i,(m)}} (Z_1\, \alpha_{11} - X_1\, \alpha_{31}) \right]$$

$$c = \sum_{i=1}^{m} \left[\int_{u=0}^{\ell} \frac{d}{du} \left(\alpha_{33}\, FT_{v_{i,(m)}} - \alpha_{32}\, FT_{w_{i,(m)}}\right) \right.$$

$$+ FT_{w_{i,(m)}} (X_1\, \alpha_{23} - Y_1\, \alpha_{13}) + FT_{v_{i,(m)}} (X_1\, \alpha_{22} - Y_1\, \alpha_{12})$$

$$\left. + FT_{u_{i,(m)}} (X_1\, \alpha_{21} - Y_1\, \alpha_{11}) \right]$$

In the following the computer program which enables a user to calculate the wave loading using the above summarised method will be described.

2. THE DESCRIPTION OF A GENERAL THREE DIMENSIONAL WAVE LOADING PROGRAM FOR CIRCULAR CYLINDRICAL MEMBERS OF FIXED AND OF FLOATING OFFSHORE STRUCTURES

Having developed the general method, the next task was to develop a computer program which could use the calculation procedure based on this method. This computer program determines wave loading on the structure with minimum input data, space and time as well as having enough options to provide high flexibility and reliability. The wave loading calculations on the structure are done using two main programs:

FILER: All the data regarding the geometry are fed into this program as input. A data file is generated with this information for use in the wave loading program. FILER also creates another data file which is used as input to the BONES program. BONES produces graphical representation of the geometry of the structure on screen or on plotter for visual check.

WAVLOVA: This program calls a data file created by FILER and calculates the wave loading at nodal points of all the members

2.1 The Description of FILER

The input data to the FILER program is the geometrical details of a structure which should be prepared as follows:

(a) The structure should be idealised as a space frame system and preliminary nodal points should be defined. This can be done by joining the start and end co-ordinates of each member with their centrelines. A nodal point (joint) can be either the free end of a member, e.g. the

end of a hull, caisson, leg, etc., or the intersection between two or more members, in which case, one member and only one member must be continuous (see (i) below), and up to 8 members may end at this joint. The co-ordinates of the joints which are requested as input data by FILER actually refer to the co-ordinates of intersections or ends of member axes. It is not permissible to have joints at which no members end. (See also Fig. 4.)

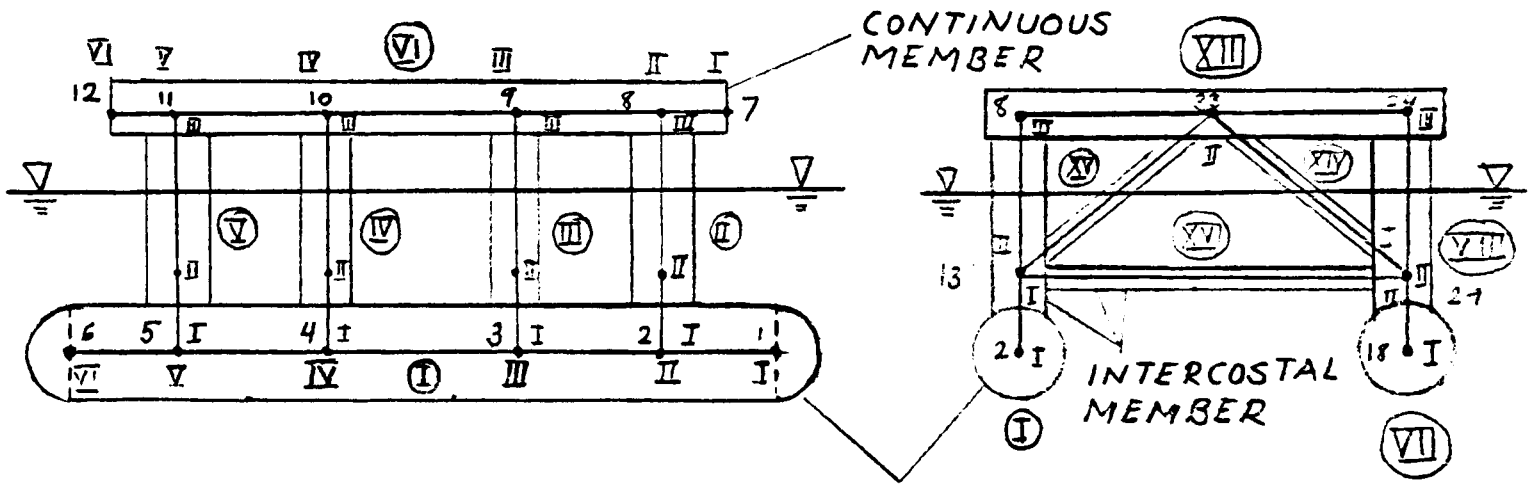

Fig. 4.

Two problems can arise in the identification of members and joints:

(i) If more than one continuous member passes through the same joint this case must be considered by dividing one of the continuous members into two, in other words making one member inter-costal while leaving the other one continuous. (See Fig. 5.)

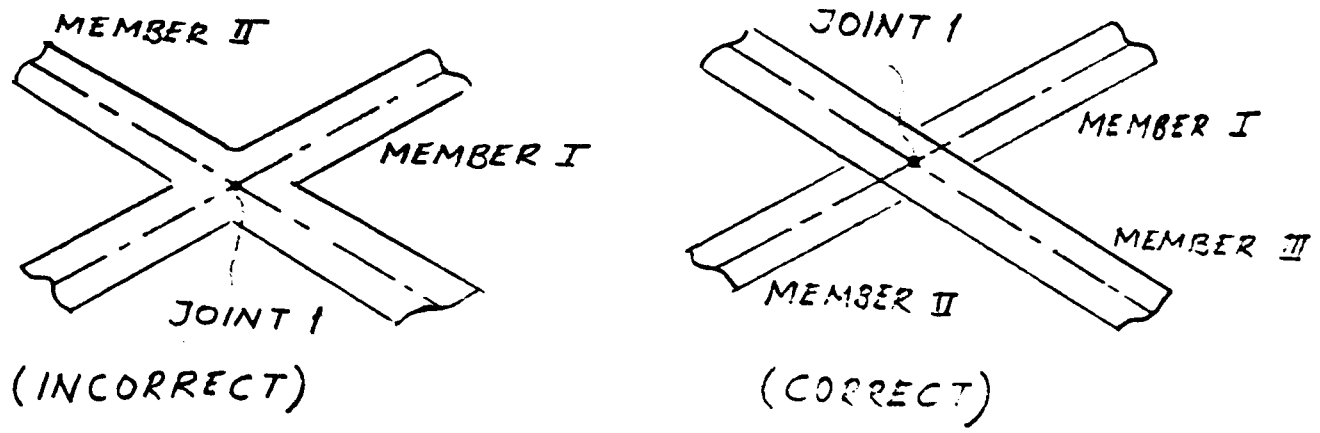

Fig. 5.

(ii) In the case of neither member being continuous at a particular joint, a new joint must be introduced such that member 1 is continuous at joint 1 and has a free end at joint 2 and member 2 ends at joint 1. (See Fig. 6.)

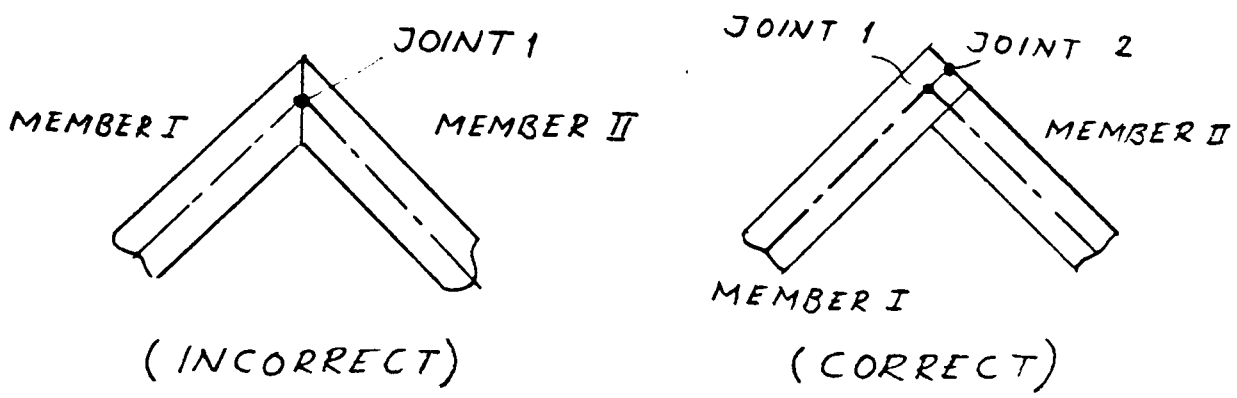

Fig. 6.

(b) Once the nodes are determined, every member and each joint throughout the structure must be given a unique number. The member node numbering system must also be devised so that all joints on each member can be numbered starting from 1 up to a maximum of 10. (This number can easily be increased by altering the neumber in the DIMENSION statement of FILER).

(c) Having defined the numbering system for nodes and members, the number of nodes on each member, the radius of the members and the co-ordinates of each node should be tabulated.

(d) The last part of the input data concerns end corrections. FILER determines at which joint members are continuous or inter-costal using the input information. At this stage the user may take account of the covered up areas at intersections. This procedure is explained by the following illustrative example.

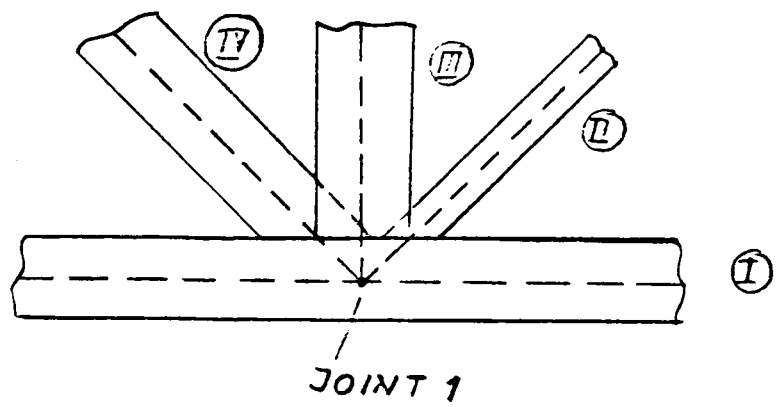

Fig. 7.

In Fig. 7 the corrections which are to deduct the wave loading due to the covered up areas are considered separately by FILER for intersections between I & IV, I & III, I & II.

If the user requires corrections for all of these three cases, since these three sets of corrections are performed independently of each other the total correction would be over-estimated. If only members II and IV are taken into consideration the total correction would be much closer to the true case. To obtain these corrections the end specification for member III at joint 1 should be entered as 'O' and for members II and IV should be 1.

When the final part of the data has been supplied regarding these end corrections FILER prints out the member and joint information as well as linking the geometrical data to the BONES program so that a three dimensional view of the structure can be represented on the plotter or on the screen. An example on the use of FILER is given in Section 3.

2.2 The Description of WAVLOA

WAVLOA was written to determine wave loading in terms of nodal loads distributed throughout the structure. Calculation procedures used

in the development of WAVLOA have been given in Section 1. WAVLOA uses geometrical information generated by FILER as input data as well as some additional data on wave particulars and draft of the structure which are to be supplied during each run.

As was described in Section 2.1 FILER generates information on joints only, i.e. the start and end points of members or intersections between the members. WAVLOA generates additional nodal points in between the joints at which wave forces are calculated. The number of nodes is determined according to the required spacing between the nodes and adjusted to make the total node number even on each member so that Simpson's rule can be applied for integrations. WAVLOA also determines surface piercing members and adjusts the last node at which wave forces are calculated to be on the calm water surface. Similarly, the first node is generated to be at the starting point of an inter-costal member at its intersection.

The following output is produced by WAVLOA:

(a) The transformation matrices for each member so that the direction of the u,v,w axes can be defined to determine the applied wave force in the correct sense.

(b) Wave loadings in the v and w directions at each node point of each member. These are given as force per unit length.

(c) At each joint, the end loads for each inter-costal member are uniformly spread over the appropriate length. (See Table VII, and Fig. 14.)

(d) Axial loads due to the exposed ends of members.

(e) The total forces on each member.

(f) The total forces on the structure.

An example on the use of WAVLOA is given in Section 3.

2.3 The Description of BONES

BONES was written to verify the co-ordinates of joints which are fed to the FILER program. It produces a graphical representation of a three dimensional structure. The structure may be viewed from any point in space to make sure that all members and nodes are registered into a data file as intended. BONES is linked to FILER and graphics are automatically produced after the data file regarding the geometry of a structure has been generated.

The method employed in the BONES program was developed to produce the two dimensional diagram from the three dimensional structure using the co-ordinate transformations described in Section 1.1. In the method all the nodal points of a structure defined in the structure reference system are transformed to a reference system (u,v,w) using the following equation

$$[B] = [T]^{-1} \{[A] - [C]\} \qquad (47)$$

where

$$[A] = \begin{bmatrix} X \\ Y \\ Z \end{bmatrix}, \quad [B] = \begin{bmatrix} u \\ v \\ w \end{bmatrix}, \quad [C] = \begin{bmatrix} X \\ Y \\ Z \end{bmatrix} \text{ (= View-point)}$$

$$[T]^{-1} = \frac{1}{|T|} \text{ adj } [T]$$

$$[T] = \begin{bmatrix} \alpha_{11} & \alpha_{12} & \alpha_{13} \\ \alpha_{21} & \alpha_{22} & \alpha_{23} \\ \alpha_{31} & \alpha_{32} & \alpha_{33} \end{bmatrix}$$

$$\text{adj}[T] = \begin{bmatrix} \alpha'_{11} & \alpha'_{21} & \alpha'_{31} \\ \alpha'_{12} & \alpha'_{22} & \alpha'_{32} \\ \alpha'_{13} & \alpha'_{23} & \alpha'_{33} \end{bmatrix}$$

α_{ij} - The cofactors of the elements of (T) matrix

The origin of the (u,v,w) reference system is the viewpoint and the w axis on the line which connects the origin of structure reference system to the viewpoint. (See Fig. 8.)

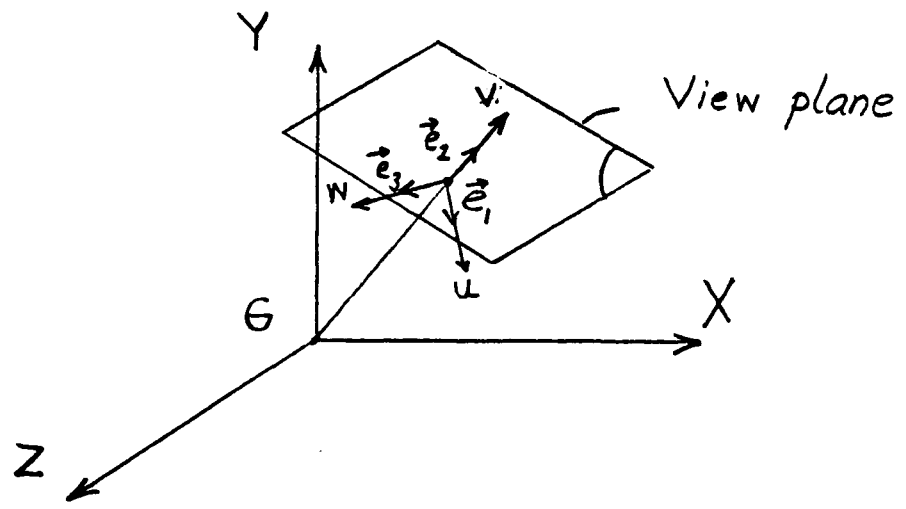

Fig. 8.

The (u,v,w) system and the $\vec{e}_1$, $\vec{e}_2$, $\vec{e}_3$ orthogonal unit vectors are determined using the procedure described in Section 1.2.

The graphics were drawn feeding only the (u,v) co-ordinates of each point into the "Graphic plotter Package" installed at the Hydrodynamic Laboratory's PDP 11/40 computer.

Examples on the use of BONES are given in Section 3.

3. AN EXAMPLE ON THE USE OF COMPUTER PROGRAMS

The use of FILER, BONES and WAVLOA computer programs are illustrated by calculating wave loading on the members of a twin circular hull semi-submersible with the following example. The geometry and the main dimensions of the platform are shown in Fig. 9.

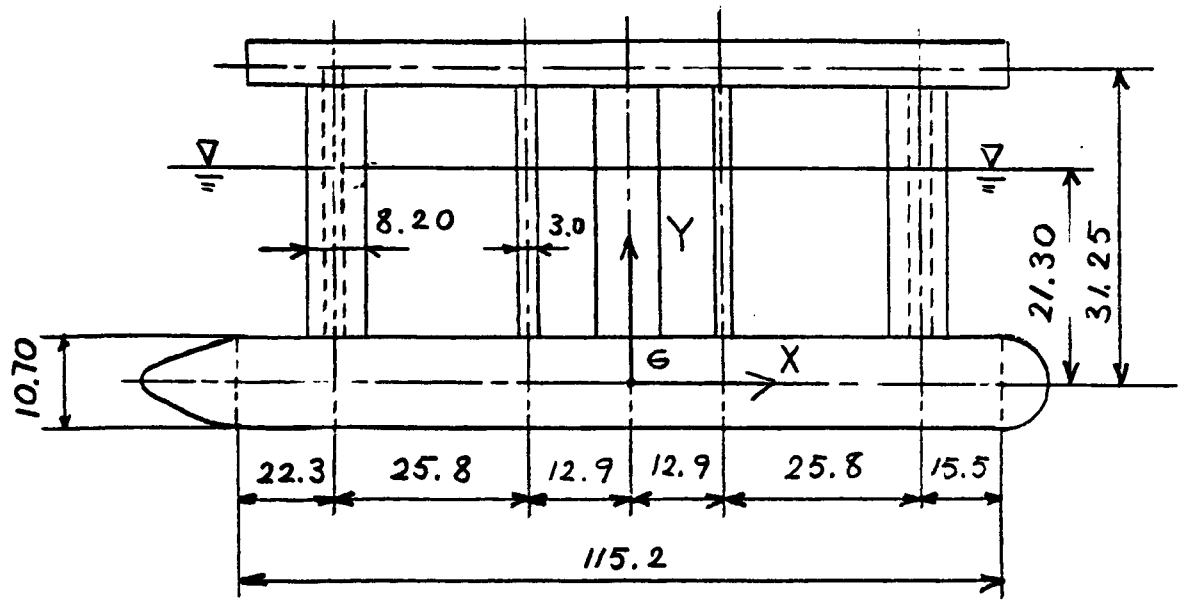
8.20
3.0
Y
G
X
10.70
21.30
31.25
22.3
25.8
12.9
12.9
25.8
15.5
115.2

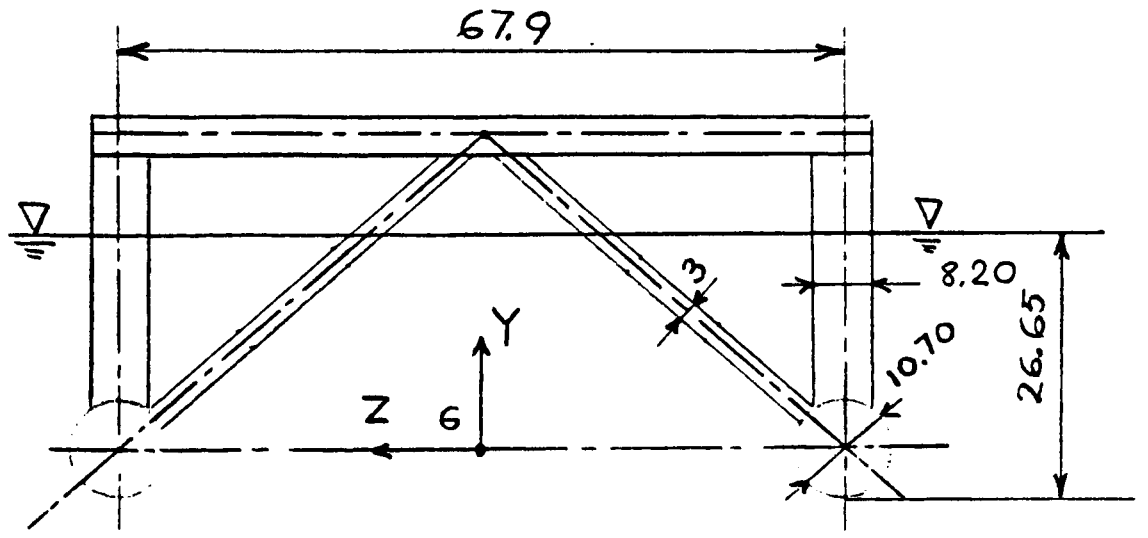
67.9
3
8.20
Y
Z
G
10.70
26.65

Fig. 9.

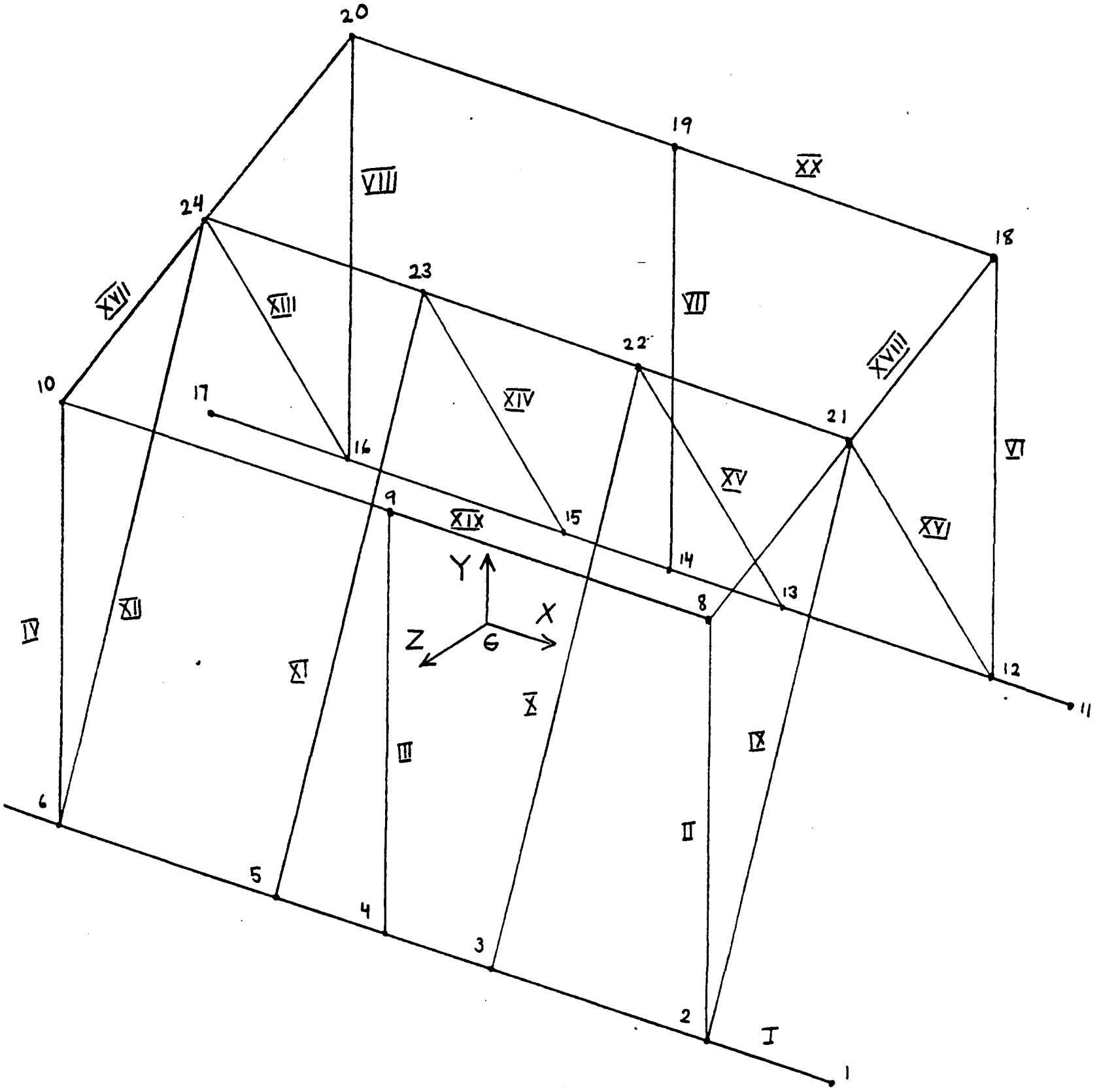

Fig. 10.

In Fig. 10 a space frame idealisation of the platform is shown. Members are designated with Roman numbers and Joints with decimal numbers. In Tables I and II member and joint data to the FILER program are illustrated respectively. These data tables were prepared using Figs 9 and 10.

MEMBER DATA TABLE (Total number of members = 21)

Member	Number of Nodes	Radius [meters]
I	7	5.35
II	2	4.10
III	2	4.10
IV	2	4.10
V	2	5.35
VI	7	4.10
VII	2	4.10
VIII	2	4.10
IX	2	1.5
X	2	1.5
XI	2	1.5
XII	2	1.5
XIII	2	1.5
XIV	2	1.5
XV	2	1.5
XVI	2	1.5
XVII	3	Dummy
XVIII	3	Dummy
XIX	3	Dummy
XX	3	Dummy
XI	4	Dummy

TABLE I.

JOINT DATA TABLE (Total number of joints = 24)

Joint	X	Y	Z
	Co-ordinates [meters]		
1	54.2	0.0	33.95
2	38.7	0.0	33.95
3	12.9	0.0	33.95
4	0.0	0.0	33.95
5	-12.9	0.0	33.95
6	-38.7	0.0	33.95
7	-61.0	0.0	33.95
8	38.7	31.25	33.95
9	0.0	31.25	33.95
10	-38.7	31.25	33.95
11	54.2	0.0	-33.95
12	38.7	0.0	-33.95
13	12.9	0.0	-33.95
14	0.0	0.0	-33.95
15	-12.9	0.0	-33.95
16	-38.7	0.0	-33.95
17	-61.0	0.0	-33.95
18	38.7	31.25	-33.95
19	0.0	31.25	-33.95
20	-38.7	31.25	-33.95
21	38.7	31.25	0.0
22	12.9	31.25	0.0
23	-12.9	31.25	0.0
24	-38.7	31.25	0.0

TABLE II.

3.1 Input to FILER

Geometrical information about the structure tabulated in Tables I and II is the main input to the FILER program. Since the programs prepared were of an interactive nature, to provide the data, a user only need answer the questions using Tables I and II. An example of the usage of the FILER program is illustrated in Table III. All information provided by a user is that typed after the asterisks. After all the geometrical data regarding the members and joints have been fed into FILER, the program automatically determines which member is continuous or inter-costal at each joint and asks if corrections due to the covered-up areas are required.

3.2 Output of FILER

When all the data for members and joints are completed FILER asks if those data are to be linked to the BONES program for graphical or for visual display and prints out a summary data table so that the user can check whether the geometry of the structure is understood and stored correctly by FILER. See Table IV.

3.3 Usage of BONES

Use of the BONES program is presented in Table V. The graphical displays from two different viewpoints are shown in Figs 11 and 12.

3.4 Input to WAVLOA

The wave loading calculations for the twin-circular hull type semi-submersible (Fig. 9) were carried out for different wave orientations. The procedure to run WAVLOA is presented in Table VI.

3.5 Output of WAVLOA

The output begins by printing out the transformation matrices so that a user who wishes to carry out the structural response calculations

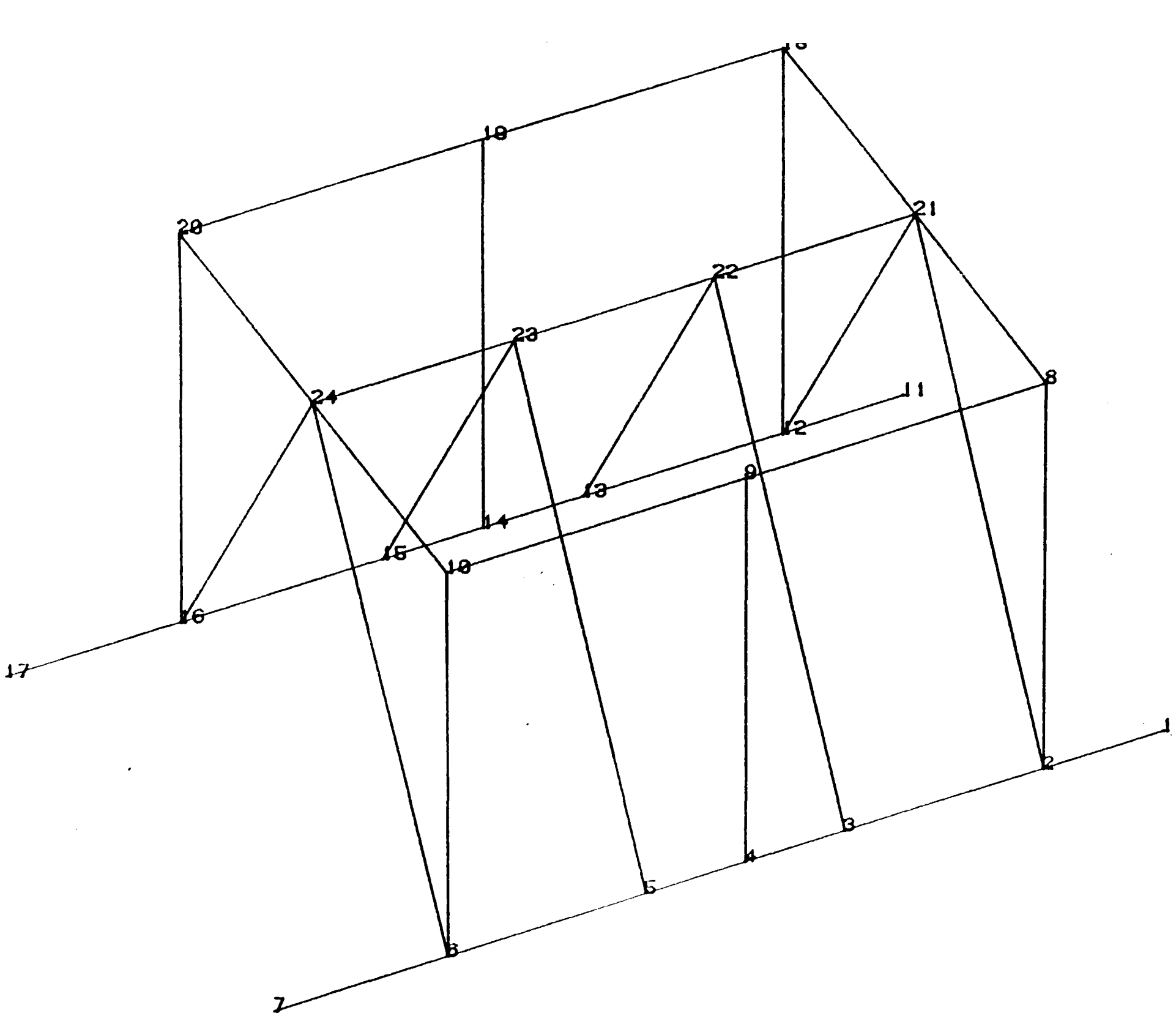

Viewing Co-ordinates:

X = 1.0
Y = 2.0
Z = 1.0

Fig. 11.

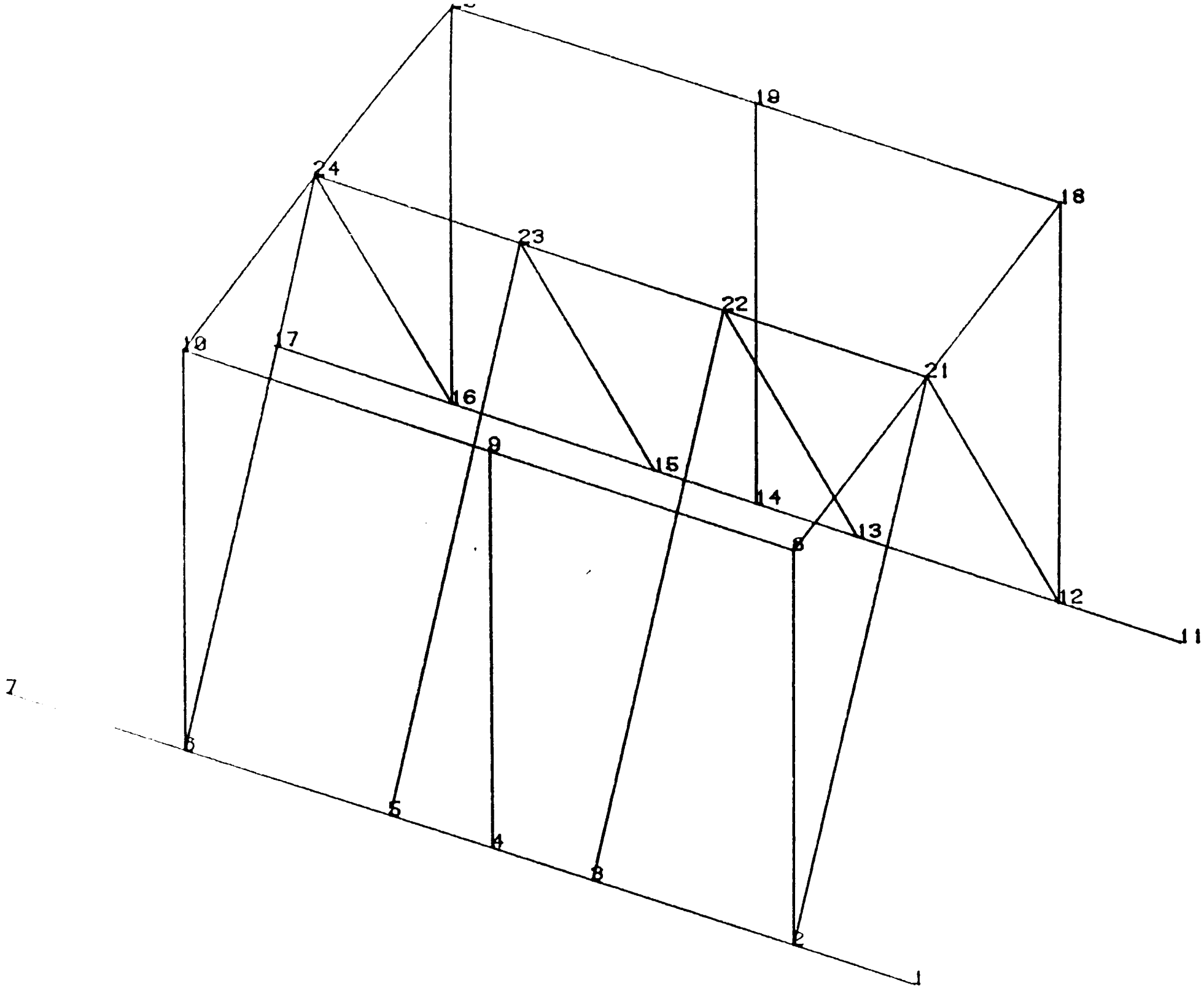

Viewing Co-ordinates:
X = -1
Y = 2.0
Z = 1.0

Fig. 12.

in the time domain can load the structure with the correct direction of wave forces and the corrections due to the intersecting members. In the output, member loads in their reference systems as well as total forces and moments on the structure in the structure reference system are given for t=0 and t=T/4 where T is the wave period. The output of WAVLOA is presented in Table VII.

In the following the use of transformation matrices is illustrated to determine the member reference systems with respect to the structural reference system.

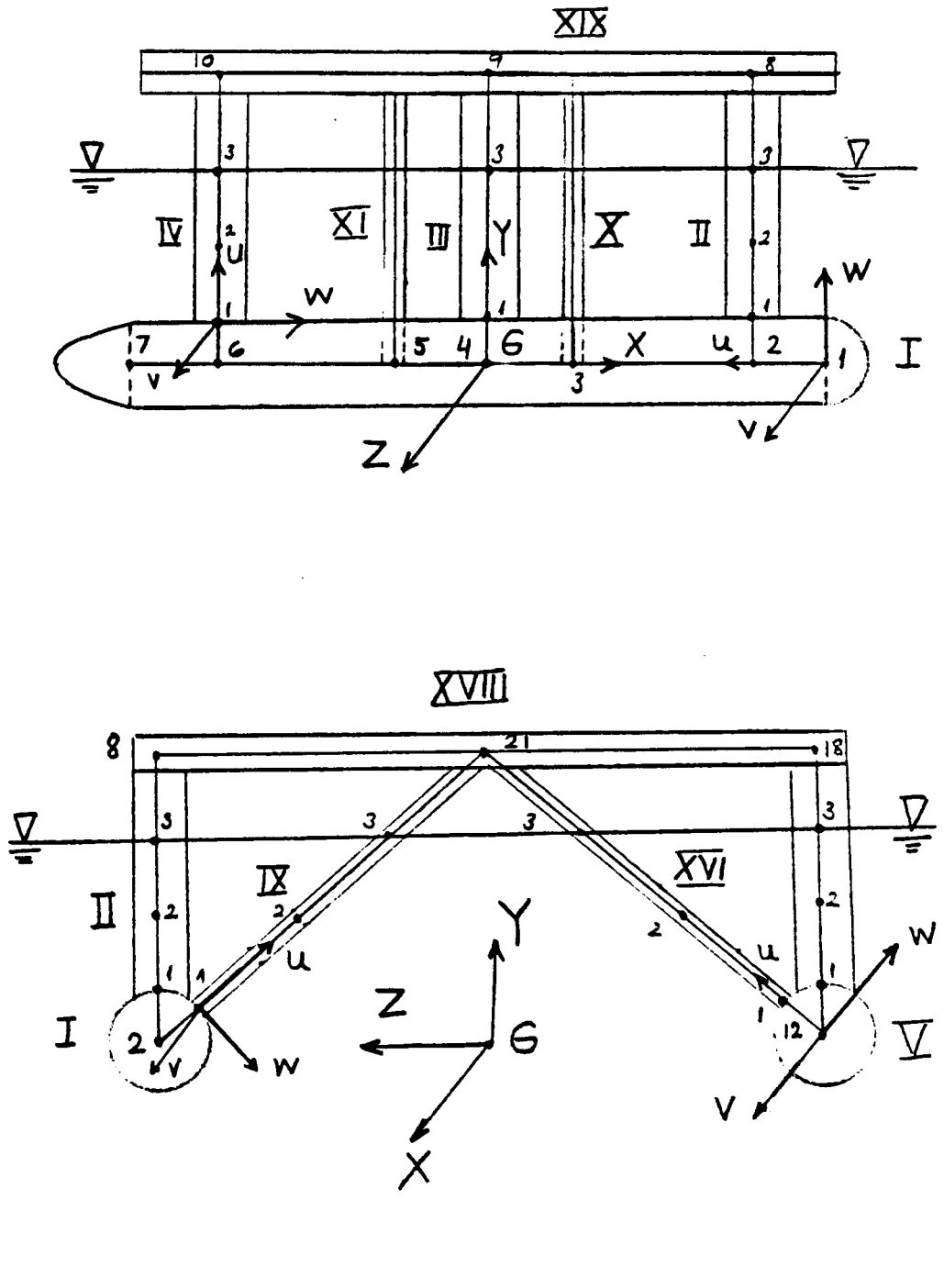

Fig. 13.

```
>RUN FILER
ENTER STRUCTURE NAME .DAT ( UPTO 13 CHARACTERS ) * CIRHULLWB.DAT
ENTER TOTAL NO OF MEMBERS AND JOINTS [INTEGERS] * 21,24


ENTER NO OF NODES [INTEGER] AND RADIUS (METRES) [REAL] FOR MEMBER   1 * 7,5.35
ENTER NO OF NODES [INTEGER] AND RADIUS (METRES) [REAL] FOR MEMBER   2 * 2,4.10
ENTER NO OF NODES [INTEGER] AND RADIUS (METRES) [REAL] FOR MEMBER   3 * 2,4.10
ENTER NO OF NODES [INTEGER] AND RADIUS (METRES) [REAL] FOR MEMBER   4 * 2,4.10
ENTER NO OF NODES [INTEGER] AND RADIUS (METRES) [REAL] FOR MEMBER   5 * 7,5.35
ENTER NO OF NODES [INTEGER] AND RADIUS (METRES) [REAL] FOR MEMBER   6 * 2,4.10
ENTER NO OF NODES [INTEGER] AND RADIUS (METRES) [REAL] FOR MEMBER   7 * 2,4.10
ENTER NO OF NODES [INTEGER] AND RADIUS (METRES) [REAL] FOR MEMBER   8 * 2,4.10
ENTER NO OF NODES [INTEGER] AND RADIUS (METRES) [REAL] FOR MEMBER   9 * 2,1.5
ENTER NO OF NODES [INTEGER] AND RADIUS (METRES) [REAL] FOR MEMBER  10 * 2,1.5
ENTER NO OF NODES [INTEGER] AND RADIUS (METRES) [REAL] FOR MEMBER  11 * 2,1.5
ENTER NO OF NODES [INTEGER] AND RADIUS (METRES) [REAL] FOR MEMBER  12 * 2,1.5
ENTER NO OF NODES [INTEGER] AND RADIUS (METRES) [REAL] FOR MEMBER  13 * 2,1.5
ENTER NO OF NODES [INTEGER] AND RADIUS (METRES) [REAL] FOR MEMBER  14 * 2,1.5
ENTER NO OF NODES [INTEGER] AND RADIUS (METRES) [REAL] FOR MEMBER  15 * 2,1.5
ENTER NO OF NODES [INTEGER] AND RADIUS (METRES) [REAL] FOR MEMBER  16 * 2,1.5
ENTER NO OF NODES [INTEGER] AND RADIUS (METRES) [REAL] FOR MEMBER  17 * 3,4.0
ENTER NO OF NODES [INTEGER] AND RADIUS (METRES) [REAL] FOR MEMBER  18 * 3,4.0
ENTER NO OF NODES [INTEGER] AND RADIUS (METRES) [REAL] FOR MEMBER  19 * 3,4.0
ENTER NO OF NODES [INTEGER] AND RADIUS (METRES) [REAL] FOR MEMBER  20 * 3,4.0
ENTER NO OF NODES [INTEGER] AND RADIUS (METRES) [REAL] FOR MEMBER  21 * 4,4.0
ENTER X , Y AND Z COORDINATES (METRES) [REAL] FOR JOINT   1 * 54.2,0.0,33.95
ENTER X , Y AND Z COORDINATES (METRES) [REAL] FOR JOINT   2 * 38.7,0.0,33.95
ENTER X , Y AND Z COORDINATES (METRES) [REAL] FOR JOINT   3 * 12.9,0.0,33.95
ENTER X , Y AND Z COORDINATES (METRES) [REAL] FOR JOINT   4 * 0.0,0.0,33.95
ENTER X , Y AND Z COORDINATES (METRES) [REAL] FOR JOINT   5 * -12.9,0.0,33.95
ENTER X , Y AND Z COORDINATES (METRES) [REAL] FOR JOINT   6 * -38.7,0.0,33.95
ENTER X , Y AND Z COORDINATES (METRES) [REAL] FOR JOINT   7 * -61.0,0.0,33.95
ENTER X , Y AND Z COORDINATES (METRES) [REAL] FOR JOINT   8 * 38.7,31.25,33.95
ENTER X , Y AND Z COORDINATES (METRES) [REAL] FOR JOINT   9 * 0.0,31.25,33.95
ENTER X , Y AND Z COORDINATES (METRES) [REAL] FOR JOINT  10 * -38.7,31.25,33.95
ENTER X , Y AND Z COORDINATES (METRES) [REAL] FOR JOINT  11 * 54.2,0.0,-33.95
ENTER X , Y AND Z COORDINATES (METRES) [REAL] FOR JOINT  12 * 38.7,0.0,-33.95
ENTER X , Y AND Z COORDINATES (METRES) [REAL] FOR JOINT  13 * 12.9,0.0,-33.95
ENTER X , Y AND Z COORDINATES (METRES) [REAL] FOR JOINT  14 * 0.0,0.0,-33.95
ENTER X , Y AND Z COORDINATES (METRES) [REAL] FOR JOINT  15 * -12.9,0.0,-33.95
ENTER X , Y AND Z COORDINATES (METRES) [REAL] FOR JOINT  16 * -38.7,0.0,-33.95
ENTER X , Y AND Z COORDINATES (METRES) [REAL] FOR JOINT  17 * -61.0,0.0,-33.95
ENTER X , Y AND Z COORDINATES (METRES) [REAL] FOR JOINT  18 * 38.7,31.25,-33.95
ENTER X , Y AND Z COORDINATES (METRES) [REAL] FOR JOINT  19 * 0.0,31.25,-33.95
ENTER X , Y AND Z COORDINATES (METRES) [REAL] FOR JOINT  20 * -38.7,31.25,-33.95
```

TABLE III.

(Contd. over ..

```
ENTER X , Y AND Z COORDINATES (METRES) [REAL] FOR JOINT 21 * 38.7,31.25,0.0
ENTER X , Y AND Z COORDINATES (METRES) [REAL] FOR JOINT 22 * 12.9,31.25,0.0
ENTER X , Y AND Z COORDINATES (METRES) [REAL] FOR JOINT 23 * -12.9,31.25,0.0
ENTER X , Y AND Z COORDINATES (METRES) [REAL] FOR JOINT 24 * -38.7,31.25,0.0
ENTER JOINT NUMBER OF NODE  1 ON MEMBER   1 [INTEGER] * 1
ENTER JOINT NUMBER OF NODE  2 ON MEMBER   1 [INTEGER] * 2
ENTER JOINT NUMBER OF NODE  3 ON MEMBER   1 [INTEGER] * 3
ENTER JOINT NUMBER OF NODE  4 ON MEMBER   1 [INTEGER] * 4
ENTER JOINT NUMBER OF NODE  5 ON MEMBER   1 [INTEGER] * 5
ENTER JOINT NUMBER OF NODE  6 ON MEMBER   1 [INTEGER] * 6
ENTER JOINT NUMBER OF NODE  7 ON MEMBER   1 [INTEGER] * 7
ENTER JOINT NUMBER OF NODE  1 ON MEMBER   2 [INTEGER] * 2
ENTER JOINT NUMBER OF NODE  2 ON MEMBER   2 [INTEGER] * 8
ENTER JOINT NUMBER OF NODE  1 ON MEMBER   3 [INTEGER] * 4
ENTER JOINT NUMBER OF NODE  2 ON MEMBER   3 [INTEGER] * 9
ENTER JOINT NUMBER OF NODE  1 ON MEMBER   4 [INTEGER] * 6
ENTER JOINT NUMBER OF NODE  2 ON MEMBER   4 [INTEGER] * 10
ENTER JOINT NUMBER OF NODE  1 ON MEMBER   5 [INTEGER] * 11
ENTER JOINT NUMBER OF NODE  2 ON MEMBER   5 [INTEGER] * 12
ENTER JOINT NUMBER OF NODE  3 ON MEMBER   5 [INTEGER] * 13
ENTER JOINT NUMBER OF NODE  4 ON MEMBER   5 [INTEGER] * 14
ENTER JOINT NUMBER OF NODE  5 ON MEMBER   5 [INTEGER] * 15
ENTER JOINT NUMBER OF NODE  6 ON MEMBER   5 [INTEGER] * 16
ENTER JOINT NUMBER OF NODE  7 ON MEMBER   5 [INTEGER] * 17
ENTER JOINT NUMBER OF NODE  1 ON MEMBER   6 [INTEGER] * 12
ENTER JOINT NUMBER OF NODE  2 ON MEMBER   6 [INTEGER] * 18
ENTER JOINT NUMBER OF NODE  1 ON MEMBER   7 [INTEGER] * 14
ENTER JOINT NUMBER OF NODE  2 ON MEMBER   7 [INTEGER] * 19
ENTER JOINT NUMBER OF NODE  1 ON MEMBER   8 [INTEGER] * 16
ENTER JOINT NUMBER OF NODE  2 ON MEMBER   8 [INTEGER] * 20
ENTER JOINT NUMBER OF NODE  1 ON MEMBER   9 [INTEGER] * 2
ENTER JOINT NUMBER OF NODE  2 ON MEMBER   9 [INTEGER] * 21
ENTER JOINT NUMBER OF NODE  1 ON MEMBER  10 [INTEGER] * 3
ENTER JOINT NUMBER OF NODE  2 ON MEMBER  10 [INTEGER] * 22
ENTER JOINT NUMBER OF NODE  1 ON MEMBER  11 [INTEGER] * 5
ENTER JOINT NUMBER OF NODE  2 ON MEMBER  11 [INTEGER] * 23
ENTER JOINT NUMBER OF NODE  1 ON MEMBER  12 [INTEGER] * 6
ENTER JOINT NUMBER OF NODE  2 ON MEMBER  12 [INTEGER] * 24
ENTER JOINT NUMBER OF NODE  1 ON MEMBER  13 [INTEGER] * 16
ENTER JOINT NUMBER OF NODE  2 ON MEMBER  13 [INTEGER] * 24
ENTER JOINT NUMBER OF NODE  1 ON MEMBER  14 [INTEGER] * 15
ENTER JOINT NUMBER OF NODE  2 ON MEMBER  14 [INTEGER] * 23
ENTER JOINT NUMBER OF NODE  1 ON MEMBER  15 [INTEGER] * 13
ENTER JOINT NUMBER OF NODE  2 ON MEMBER  15 [INTEGER] * 22
ENTER JOINT NUMBER OF NODE  1 ON MEMBER  16 [INTEGER] * 12
ENTER JOINT NUMBER OF NODE  2 ON MEMBER  16 [INTEGER] * 21
ENTER JOINT NUMBER OF NODE  1 ON MEMBER  17 [INTEGER] * 10
ENTER JOINT NUMBER OF NODE  2 ON MEMBER  17 [INTEGER] * 24
```

TABLE III.

(Contd. over ...)

```
ENTER JOINT NUMBER OF NODE  3 ON MEMBER  17 [INTEGER] * 20
ENTER JOINT NUMBER OF NODE  1 ON MEMBER  18 [INTEGER] * 8
ENTER JOINT NUMBER OF NODE  2 ON MEMBER  18 [INTEGER] * 21
ENTER JOINT NUMBER OF NODE  3 ON MEMBER  18 [INTEGER] * 18
ENTER JOINT NUMBER OF NODE  1 ON MEMBER  19 [INTEGER] * 8
ENTER JOINT NUMBER OF NODE  2 ON MEMBER  19 [INTEGER] * 9
ENTER JOINT NUMBER OF NODE  3 ON MEMBER  19 [INTEGER] * 10
ENTER JOINT NUMBER OF NODE  1 ON MEMBER  20 [INTEGER] * 18
ENTER JOINT NUMBER OF NODE  2 ON MEMBER  20 [INTEGER] * 19
ENTER JOINT NUMBER OF NODE  3 ON MEMBER  20 [INTEGER] * 20
ENTER JOINT NUMBER OF NODE  1 ON MEMBER  21 [INTEGER] * 21
ENTER JOINT NUMBER OF NODE  2 ON MEMBER  21 [INTEGER] * 22
ENTER JOINT NUMBER OF NODE  3 ON MEMBER  21 [INTEGER] * 23
ENTER JOINT NUMBER OF NODE  4 ON MEMBER  21 [INTEGER] * 24
AT JOINT  1 , CONTINUOUS MEMBER :  0 INTERCOSTAL :  1,
WHICH MEMBERS REQUIRE END CORRECTIONS(YES: 1 , NO: 0)
MEMBER  1 * 1
AT JOINT  2 , CONTINUOUS MEMBER :  1 INTERCOSTAL :  2,  9,
WHICH MEMBERS REQUIRE END CORRECTIONS(YES: 1 , NO: 0)
MEMBER  2 * 1
MEMBER  9 * 1
AT JOINT  3 , CONTINUOUS MEMBER :  1 INTERCOSTAL :  10,
WHICH MEMBERS REQUIRE END CORRECTIONS(YES: 1 , NO: 0)
MEMBER  10 * 1
AT JOINT  4 , CONTINUOUS MEMBER :  1 INTERCOSTAL :  3,
WHICH MEMBERS REQUIRE END CORRECTIONS(YES: 1 , NO: 0)
MEMBER  3 * 1
AT JOINT  5 , CONTINUOUS MEMBER :  1 INTERCOSTAL :  11,
WHICH MEMBERS REQUIRE END CORRECTIONS(YES: 1 , NO: 0)
MEMBER  11 * 1
AT JOINT  6 , CONTINUOUS MEMBER :  1 INTERCOSTAL :  4, 12,
WHICH MEMBERS REQUIRE END CORRECTIONS(YES: 1 , NO: 0)
MEMBER  4 * 1
MEMBER  12 * 1
AT JOINT  7 , CONTINUOUS MEMBER :  0 INTERCOSTAL :  1,
WHICH MEMBERS REQUIRE END CORRECTIONS(YES: 1 , NO: 0)
MEMBER  1 * 1
AT JOINT  8 , CONTINUOUS MEMBER :  0 INTERCOSTAL :  2, 18, 19,
WHICH MEMBERS REQUIRE END CORRECTIONS(YES: 1 , NO: 0)
MEMBER  2 * 0
MEMBER  18 * 0
MEMBER  19 * 0
AT JOINT  9 , CONTINUOUS MEMBER :  19 INTERCOSTAL :  3,
WHICH MEMBERS REQUIRE END CORRECTIONS(YES: 1 , NO: 0)
MEMBER  3 * 0
AT JOINT 10 , CONTINUOUS MEMBER :  0 INTERCOSTAL :  4, 17, 19,
WHICH MEMBERS REQUIRE END CORRECTIONS(YES: 1 , NO: 0)
MEMBER  4 * 0
```

TABLE III.

(Contd. over ...)

```
MEMBER  17 * Ø
MEMBER  19 * Ø
AT JOINT 11 , CONTINUOUS MEMBER :   Ø INTERCOSTAL :   5,
WHICH MEMBERS REQUIRE END CORRECTIONS(YES: 1 , NO: Ø)
MEMBER   5 * 1
AT JOINT 12 , CONTINUOUS MEMBER :   5 INTERCOSTAL :   6, 16,
WHICH MEMBERS REQUIRE END CORRECTIONS(YES: 1 , NO: Ø)
MEMBER   6 * 1
MEMBER  16 * 1
AT JOINT 13 , CONTINUOUS MEMBER :   5 INTERCOSTAL :  15,
WHICH MEMBERS REQUIRE END CORRECTIONS(YES: 1 , NO: Ø)
MEMBER  15 * 1
AT JOINT 14 , CONTINUOUS MEMBER :   5 INTERCOSTAL :   7,
WHICH MEMBERS REQUIRE END CORRECTIONS(YES: 1 , NO: Ø)
MEMBER   7 * 1
AT JOINT 15 , CONTINUOUS MEMBER :   5 INTERCOSTAL :  14,
WHICH MEMBERS REQUIRE END CORRECTIONS(YES: 1 , NO: Ø)
MEMBER  14 * 1
AT JOINT 16 , CONTINUOUS MEMBER :   5 INTERCOSTAL :   8, 13,
WHICH MEMBERS REQUIRE END CORRECTIONS(YES: 1 , NO: Ø)
MEMBER   8 * 1
MEMBER  13 * 1
AT JOINT 17 , CONTINUOUS MEMBER :   Ø INTERCOSTAL :   5,
WHICH MEMBERS REQUIRE END CORRECTIONS(YES: 1 , NO: Ø)
MEMBER   5 * 1
AT JOINT 18 , CONTINUOUS MEMBER :   Ø INTERCOSTAL :   6, 18, 2Ø,
WHICH MEMBERS REQUIRE END CORRECTIONS(YES: 1 , NO: Ø)
MEMBER   6 * Ø
MEMBER  18 * Ø
MEMBER  2Ø * Ø
AT JOINT 19 , CONTINUOUS MEMBER :  2Ø INTERCOSTAL :   7,
WHICH MEMBERS REQUIRE END CORRECTIONS(YES: 1 , NO: Ø)
MEMBER   7 * Ø
AT JOINT 2Ø , CONTINUOUS MEMBER :   Ø INTERCOSTAL :   8, 17, 2Ø,
WHICH MEMBERS REQUIRE END CORRECTIONS(YES: 1 , NO: Ø)
MEMBER   8 * Ø
MEMBER  17 * Ø
MEMBER  2Ø * Ø
AT JOINT 21 , CONTINUOUS MEMBER :  18 INTERCOSTAL :   9, 16, 21,
WHICH MEMBERS REQUIRE END CORRECTIONS(YES: 1 , NO: Ø)
MEMBER   9 * Ø
MEMBER  16 * Ø
MEMBER  21 * Ø
AT JOINT 22 , CONTINUOUS MEMBER :  21 INTERCOSTAL :  1Ø, 15,
WHICH MEMBERS REQUIRE END CORRECTIONS(YES: 1 , NO: Ø)
MEMBER  1Ø * Ø.Ø
MEMBER  15 * Ø.Ø
AT JOINT 23 , CONTINUOUS MEMBER :  21 INTERCOSTAL :  11, 14,
```

TABLE III.

(Contd. over ...)

```
HICH MEMBERS REQUIRE END CORRECTIONS(YES: 1 , NO: Ø)
EMBER  11 * Ø.Ø
EMBER  14 * Ø.Ø
T JOINT 24 , CONTINUES MEMBER : 17 INTERCOSTAL : 12, 13, 21,
HICH MEMBERS REQUIRE END CORRECTIONS(YES: 1 , NO: Ø)
EMBER  12 * Ø.Ø
EMBER  13 * Ø.Ø
EMBER  21 * Ø.Ø
RAPHICAL DISPLAY ? (Y/N) : Y
AME FOR NODE FILENAME : CIRHULLN.DAT
AME FOR MEMBER FILENAME : CIRHULLM.DAT

T6 -- STOP
```

TABLE III.

SUMMARY OF DATA FOR STRUCTURE : CIRHULLWB.DAT

MEMBER DATA

MEMBER NUMBER	START JOINT	END JOINT	NO OF JOINTS	RADIUS	LENGTH
1	1	7	7	5.350	115.200
2	2	8	2	4.100	31.250
3	4	9	2	4.100	31.250
4	6	10	2	4.100	31.250
5	11	17	7	5.350	115.200
6	12	18	2	4.100	31.250
7	14	19	2	4.100	31.250
8	16	20	2	4.100	31.250
9	2	21	2	1.500	46.143
10	3	22	2	1.500	46.143
11	5	23	2	1.500	46.143
12	6	24	2	1.500	46.143
13	16	24	2	1.500	46.143
14	15	23	2	1.500	46.143
15	13	22	2	1.500	46.152
16	12	21	2	1.500	46.143
17	10	20	3	4.000	67.900
18	8	18	3	4.000	67.900
19	8	10	3	4.000	77.400
20	18	20	3	4.000	77.400
21	21	24	4	4.000	77.400

TABLE IV.

(Contd. over ...)

JOINT DATA

JOINT NUMBER	X, Y, Z COORDINATES			CONTINUOUS MEMBER	INTERCOSTAL MEMBERS	MEMBERS REQUIRING END CORRECTIONS
1	54.200,	0.000,	33.950	–	1	1
2	38.700,	0.000,	33.950	1	2 9	2 9
3	12.900,	0.000,	33.950	1	10	10
4	0.000,	0.000,	33.950	1	3	3
5	-12.900,	0.000,	33.950	1	11	11
6	-38.700,	0.000,	33.950	1	4 12	4 12
7	-61.000,	0.000,	33.950	–	1	1
8	38.700,	31.250,	33.950	–	2 18 19	–
9	0.000,	31.250,	33.950	19	3	–
10	-38.700,	31.250,	33.950	–	4 17 19	–
11	54.200,	0.000,	-33.950	–	5	5
12	38.700,	0.000,	-33.950	5	6 16	6 16
13	12.900,	0.000,	-33.950	5	15	15
14	0.000,	0.000,	-33.950	5	7	7
15	-12.900,	0.000,	-33.950	5	14	14
16	-38.700,	0.000,	-33.950	5	8 13	8 13
17	-61.000,	0.000,	-33.950	–	5	5
18	38.700,	31.250,	-33.950	–	6 18 20	–
19	0.000,	31.250,	-33.950	20	7	–
20	-38.700,	31.250,	-33.950	–	8 17 20	–
21	38.700,	31.250,	0.000	18	9 16 21	–
22	12.900,	31.250,	0.000	21	10 15	–
23	-12.900,	31.250,	0.000	21	11 14	–
24	-38.700,	31.250,	0.000	17	12 13 21	–

TABLE IV.

```
.UN DK4:[6,1] BONES
PE Ø FOR SCREEN, 1 FOR PLOTTER : 1
ITER NODE FILE NAME : CIRHULLN.DAT
ITER MEMBER DATA FILE : CIRHULLM.DAT
ITER VIEWING COORDINATES (X,Y,Z) : 1.Ø,2.Ø,1.Ø
.OT =     1 PLOTTER SELECTED
BEL NODES ? (Y/N) : Y
ARACTER SIZE : Ø.5
OTHER VIEWPOINT ? Y
ITER VIEWING COORDINATES (X,Y,Z) : -1.Ø,2.Ø,1.Ø
.OT =     1 PLOTTER SELECTED
BEL NODES ? (Y/N) : Y
ARACTER SIZE : Ø.5
OTHER VIEWPOINT ? N
6  --  STOP
```

TABLE V.

```
RUN WAVLOA
NTER STRUCTURE NAME .DAT * CIRHULLWB.DAT
NTER ANGLE OF ORIENTATION (DEGREES) AND DRAFT (M) * Ø.Ø,21.3Ø
NTER WAVE FREQUENCY (HZ) AND WAVE AMPLITUDE (M) * Ø.Ø8,6.Ø
T6  --  STOP
RUN WAVLOA
NTER STRUCTURE NAME .DAT * CIRHULLWB.DAT
NTER ANGLE OF ORIENTATION (DEGREES) AND DRAFT (M) * 45.Ø,21.3Ø
NTER WAVE FREQUENCY (HZ) AND WAVE AMPLITUDE (M) * Ø.Ø8,6.Ø
T6  --  STOP
RUN WAVLOA
NTER STRUCTURE NAME .DAT * CIRHULLWB.DAT
NTER ANGLE OF ORIENTATION (DEGREES) AND DRAFT (M) * 9Ø.Ø,21.3Ø
NTER WAVE FREQUENCY (HZ) AND WAVE AMPLITUDE (M) * Ø.Ø8,6.Ø
T6  --  STOP
```

TABLE VI.

For member I the following direction cosines can be written for the angles between structural reference system's axes and the individual reference system's axes from the output shown in Table VII.

α_{11}: The Cosine of the angle between X and u = -1 → A_{11} = 180°

α_{12}: The Cosine of the angle between X and v = 0 → A_{12} = 90°

α_{13}: The Cosine of the angle between X and w = 0 → A_{13} = 90°

α_{21}: The Cosine of the angle between Y and u = 0 → A_{21} = 90°

α_{22}: The Cosine of the angle between Y and v = 0 → A_{22} = 90°

α_{23}: The Cosine of the angle between Y and w = 1 → A_{23} = 0°

α_{31}: The Cosine of the angle between Z and u = 0 → A_{31} = 90°

α_{32}: The Cosine of the angle between Z and v = 1 → A_{32} = 0°

α_{33}: The Cosine of the angle between Z and w = 0 → A_{33} = 90°

Since all the angles between the structure and the individual reference systems' axes are known the individual member reference system can be drawn using this information. (See Fig. 13.)

The same procedure can be repeated to find all individual reference systems' axes. Some of the members' reference systems are shown in Fig. 13.

In Fig. 14 the distribution of wave loading on the nodal points throughout the structure is presented. Figs 15 - 20 show the principal forces and moments on the structure in the frequency domain for different wave headings.

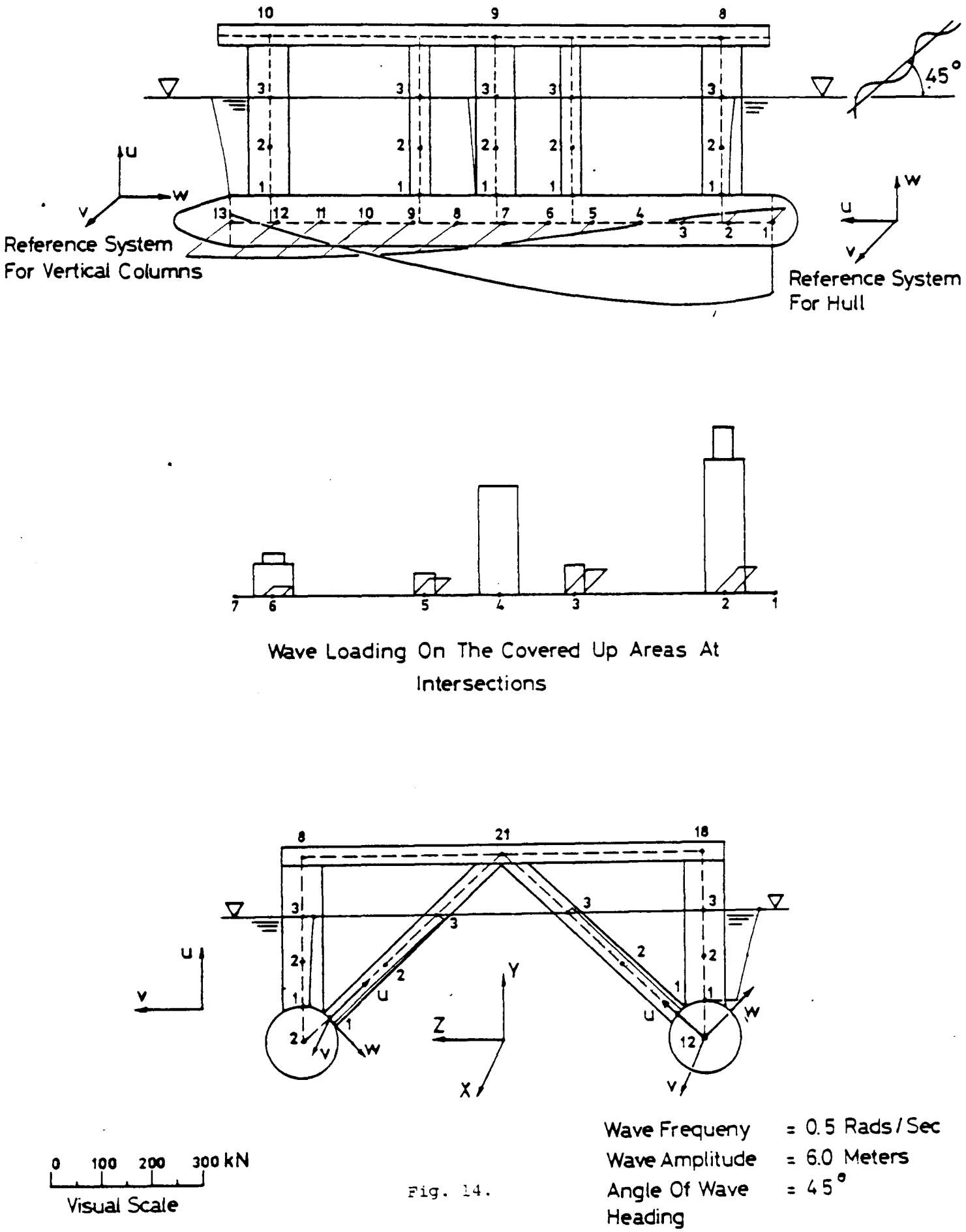

Fig. 14.

Distribution Of Wave Loading On The Nodal Points Of A Twin Circular Hull Design Semi Submersible

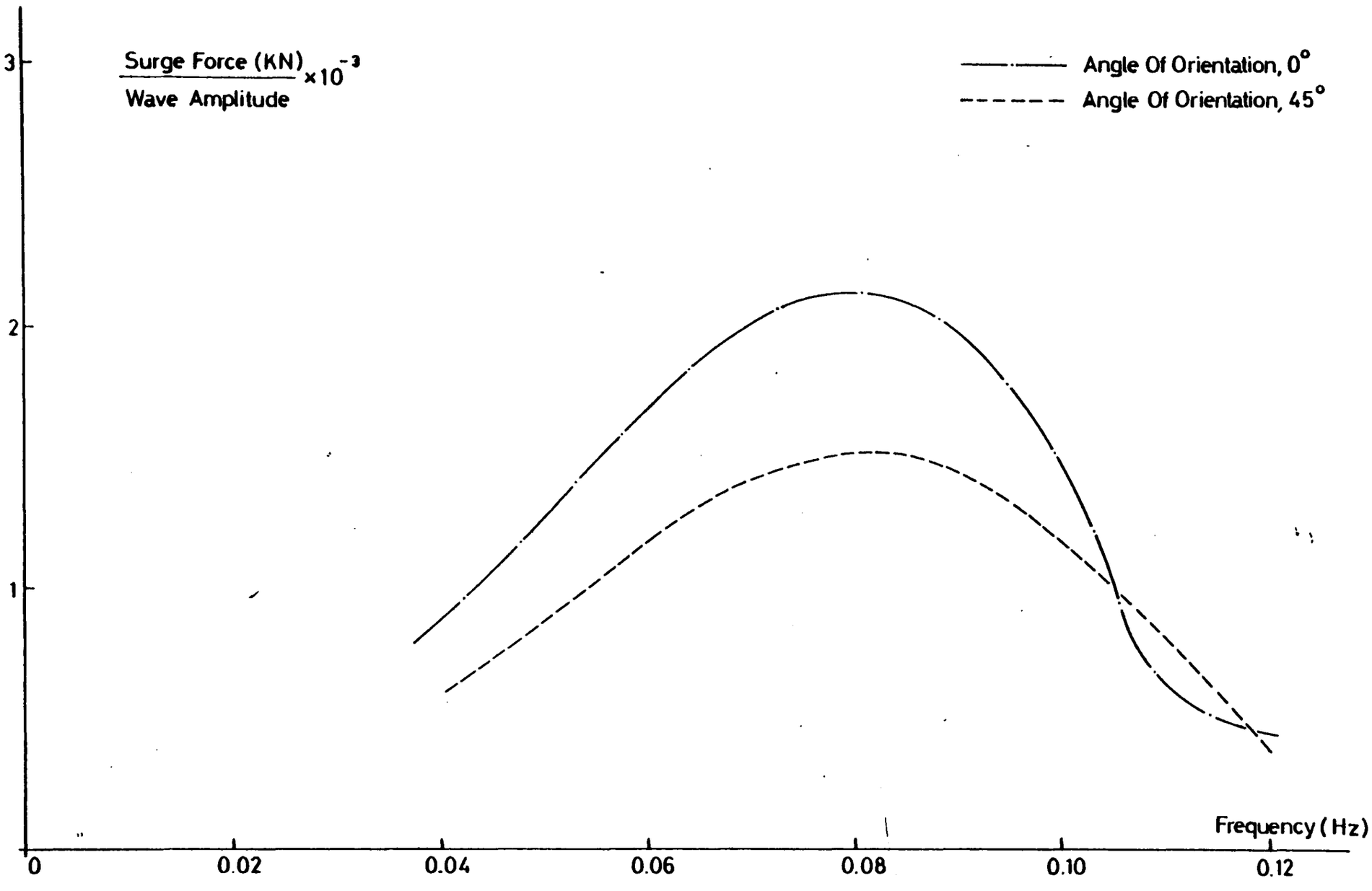
Surge Force (KN) / Wave Amplitude ×10⁻³
Angle Of Orientation, 0°
Angle Of Orientation, 45°
3
2
1
0
0.02
0.04
0.06
0.08
0.10
0.12
Frequency (Hz)

Fig. 15.

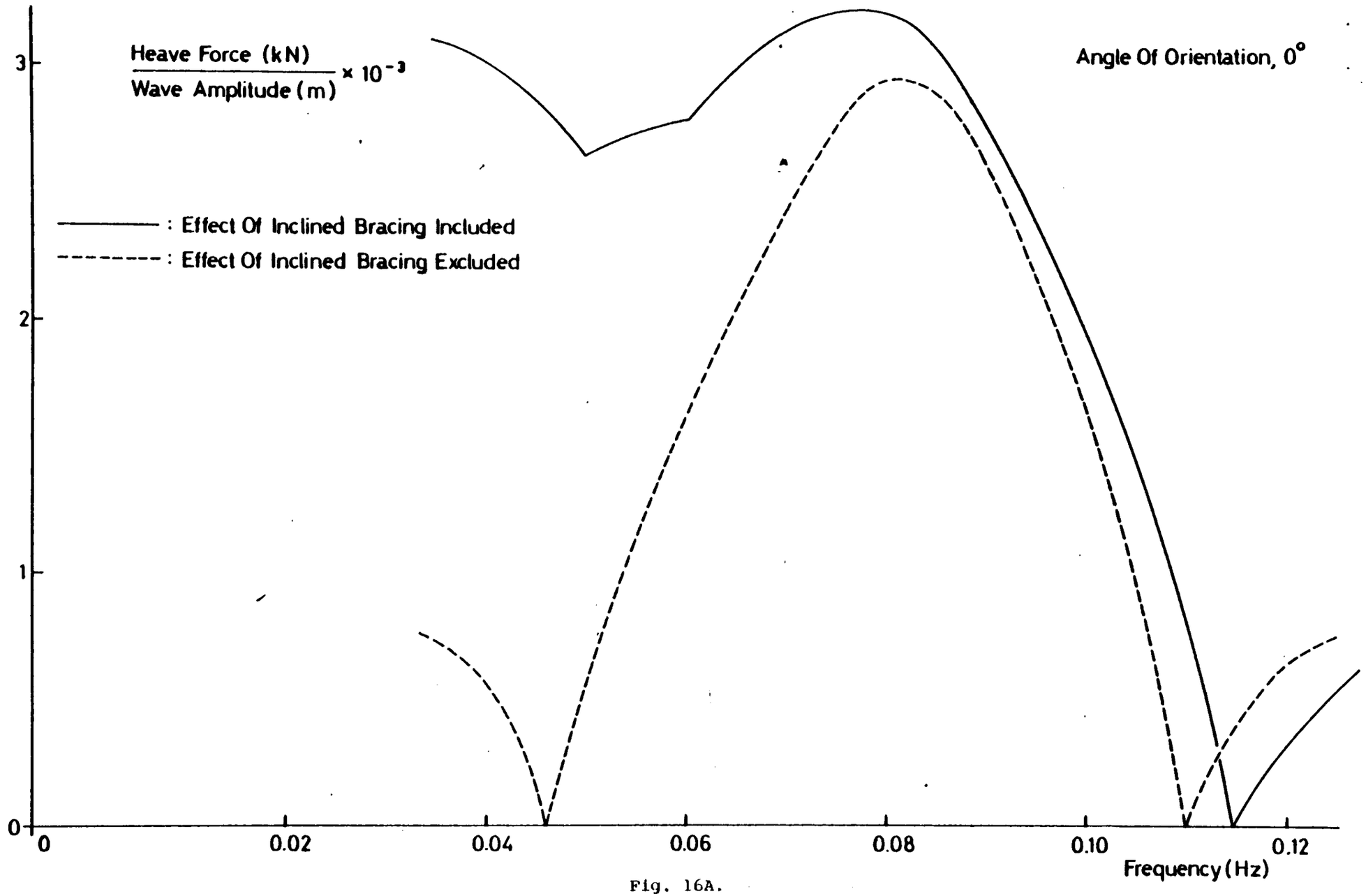
Heave Force (kN) / Wave Amplitude (m) × 10⁻³
Angle Of Orientation, 0°
: Effect Of Inclined Bracing Included
: Effect Of Inclined Bracing Excluded
3
2
1
0
0
0.02
0.04
0.06
0.08
0.10
0.12
Frequency (Hz)

Fig. 16A.

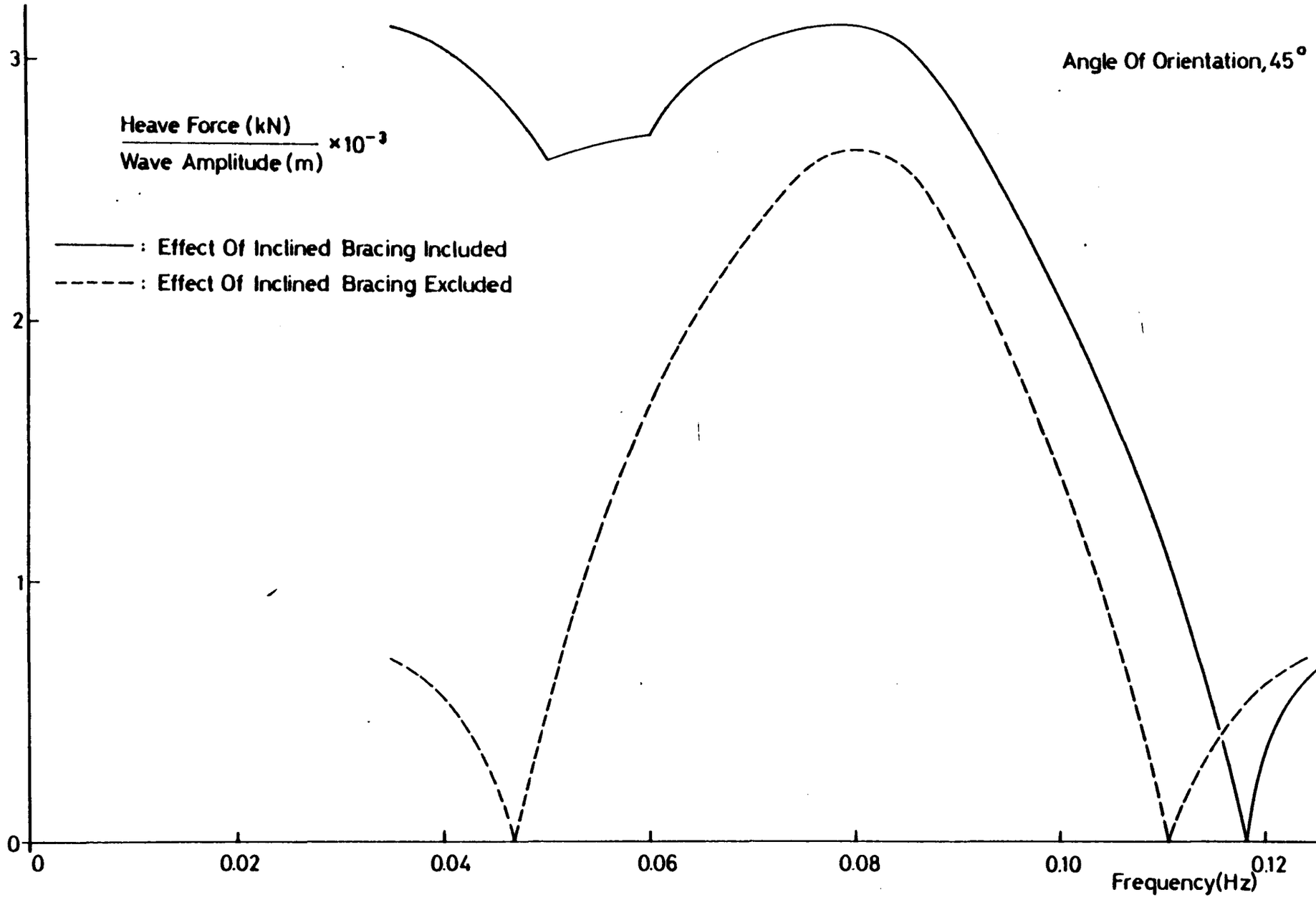
Angle Of Orientation, 45°
Heave Force (kN) / Wave Amplitude (m) ×10⁻³
——— : Effect Of Inclined Bracing Included
- - - - - : Effect Of Inclined Bracing Excluded
3
2
1
0
0
0.02
0.04
0.06
0.08
0.10
0.12
Frequency(Hz)

Fig. 16B.

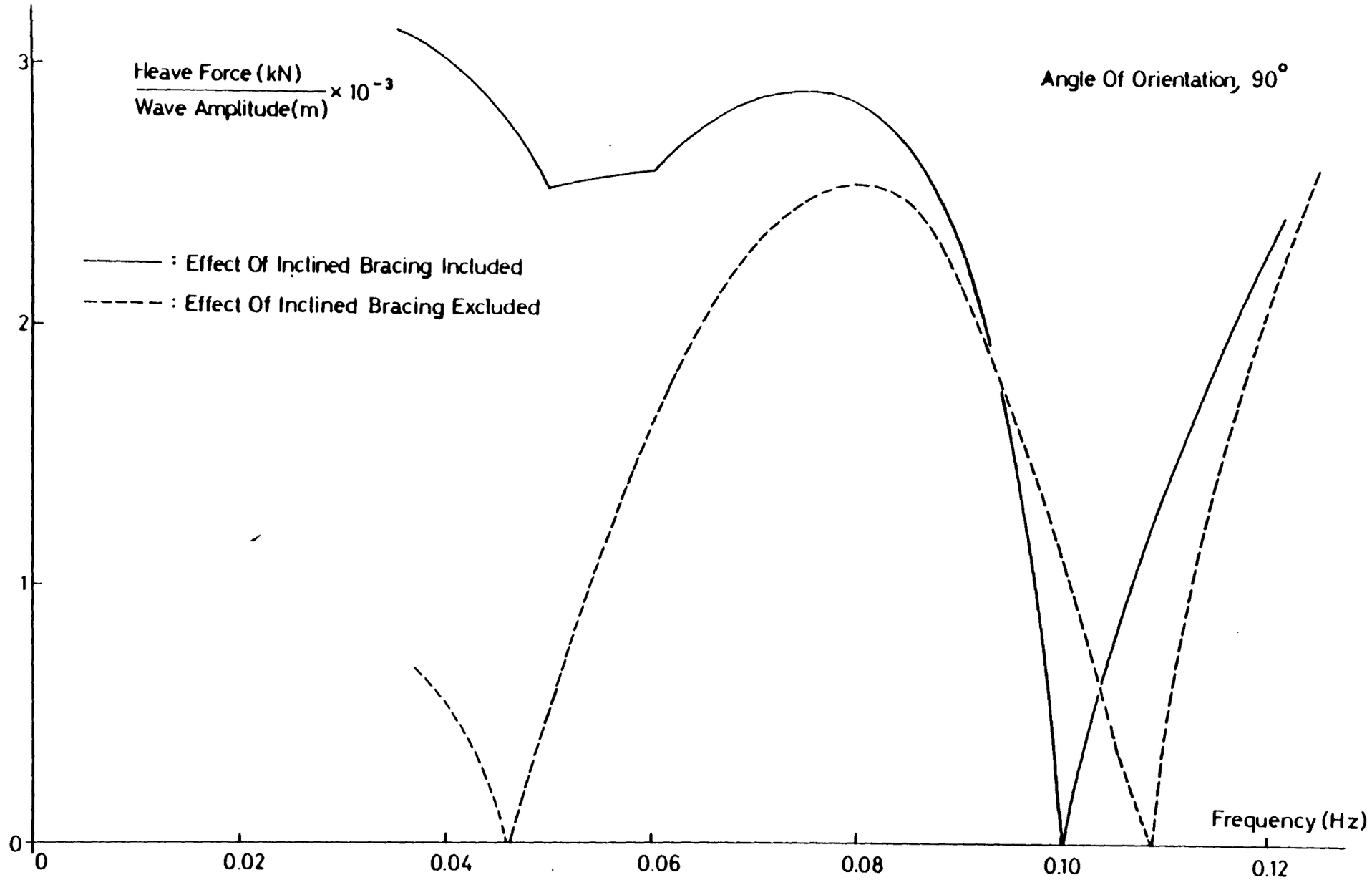
Heave Force (kN) / Wave Amplitude(m) × 10⁻³
Angle Of Orientation, 90°
——— : Effect Of Inclined Bracing Included
- - - - - : Effect Of Inclined Bracing Excluded
3
2
1
0
0
0.02
0.04
0.06
0.08
0.10
0.12
Frequency (Hz)

Fig. 16C.

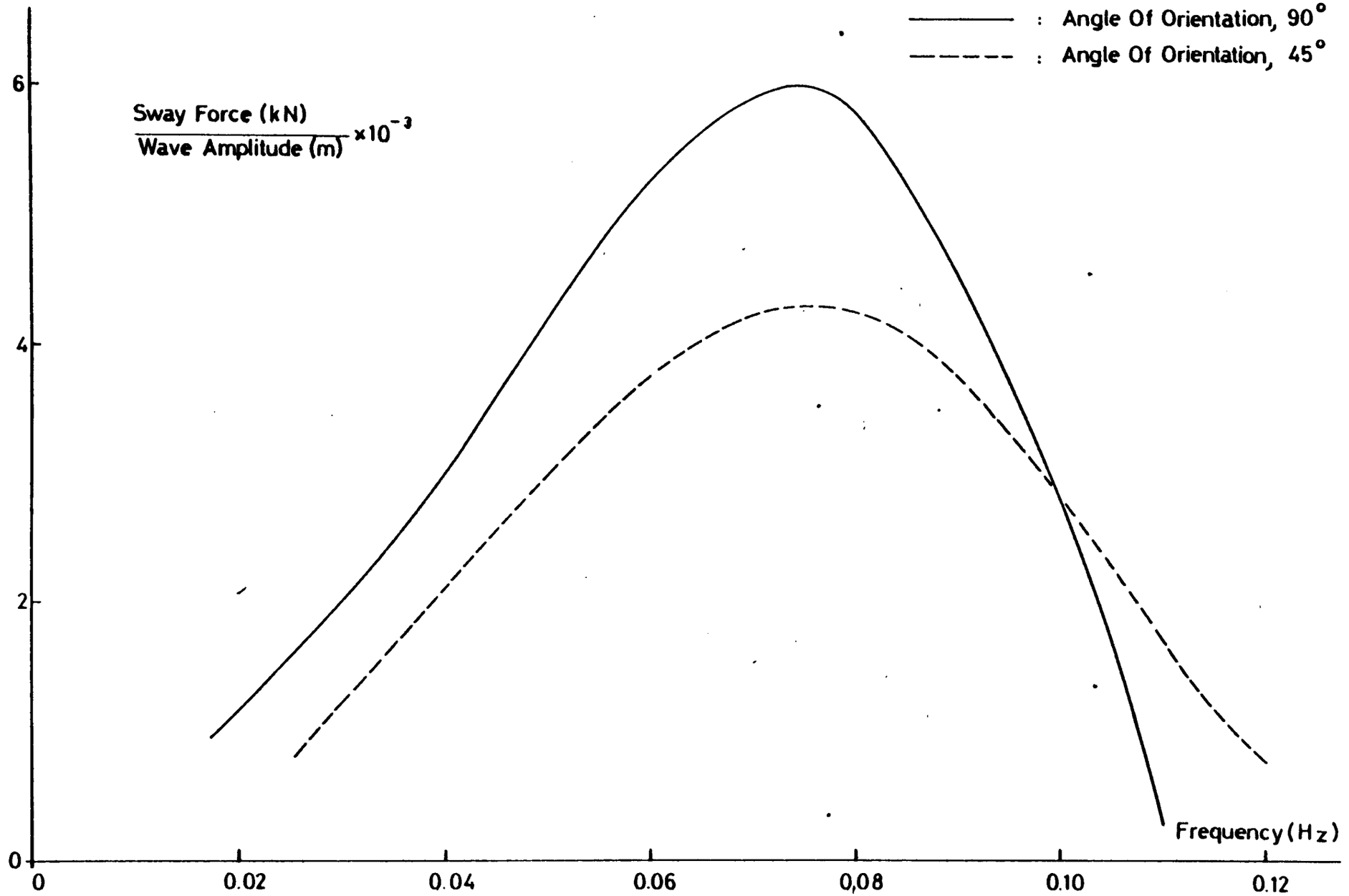
Angle Of Orientation, 90°
Angle Of Orientation, 45°
Sway Force (kN) / Wave Amplitude (m) ×10⁻³
6
4
2
0
0
0.02
0.04
0.06
0,08
0.10
0.12
Frequency (Hz)

Fig. 17.

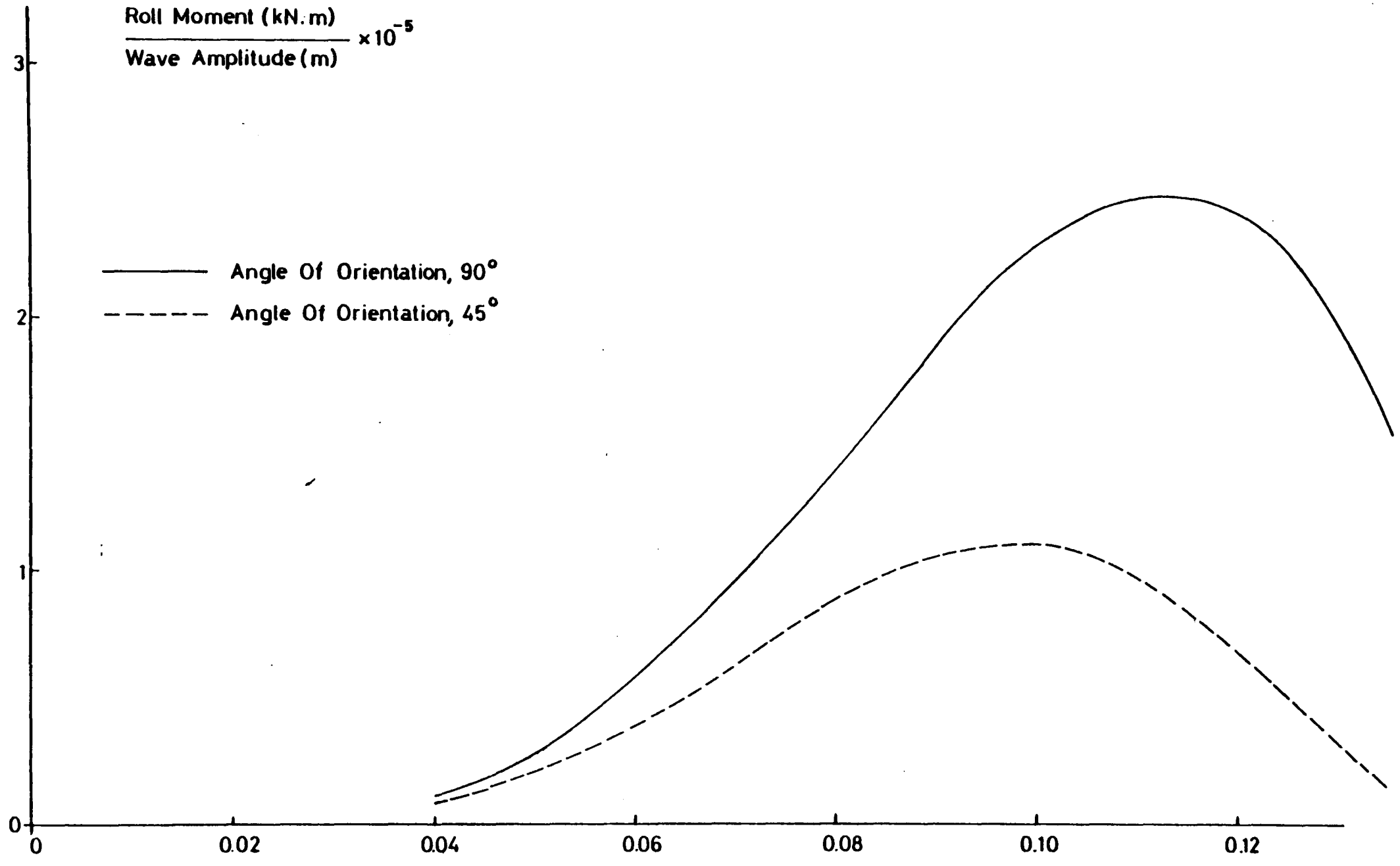
Roll Moment (kN.m)
Wave Amplitude (m)
$\times 10^{-5}$
3
2
1
0
Angle Of Orientation, 90°
Angle Of Orientation, 45°
0
0.02
0.04
0.06
0.08
0.10
0.12

Fig. 18.

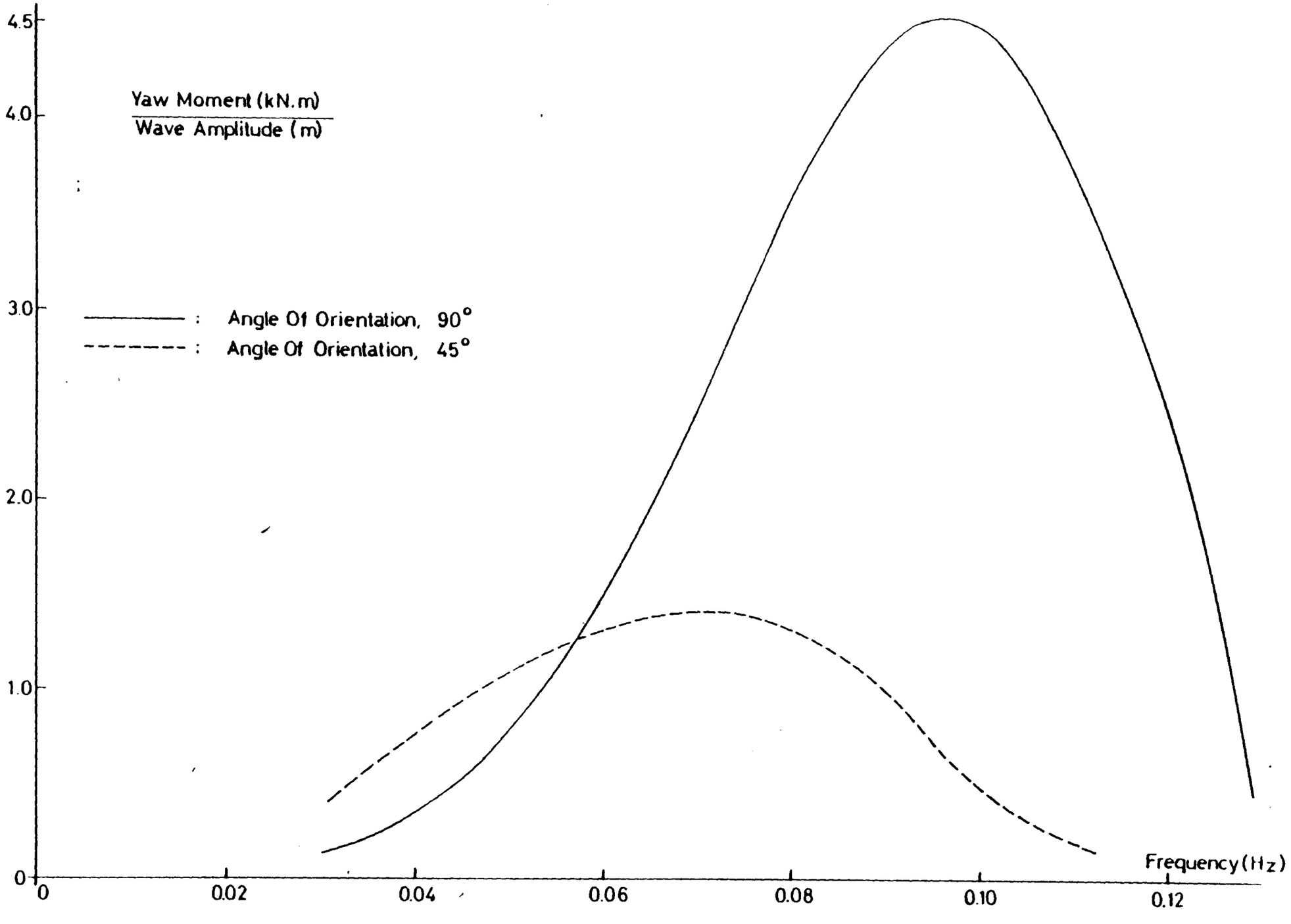
4.5
4.0
3.0
2.0
1.0
0
Yaw Moment (kN.m)
Wave Amplitude (m)
: Angle Of Orientation, 90°
: Angle Of Orientation, 45°
0
0.02
0.04
0.06
0.08
0.10
0.12
Frequency (Hz)

Fig. 19.

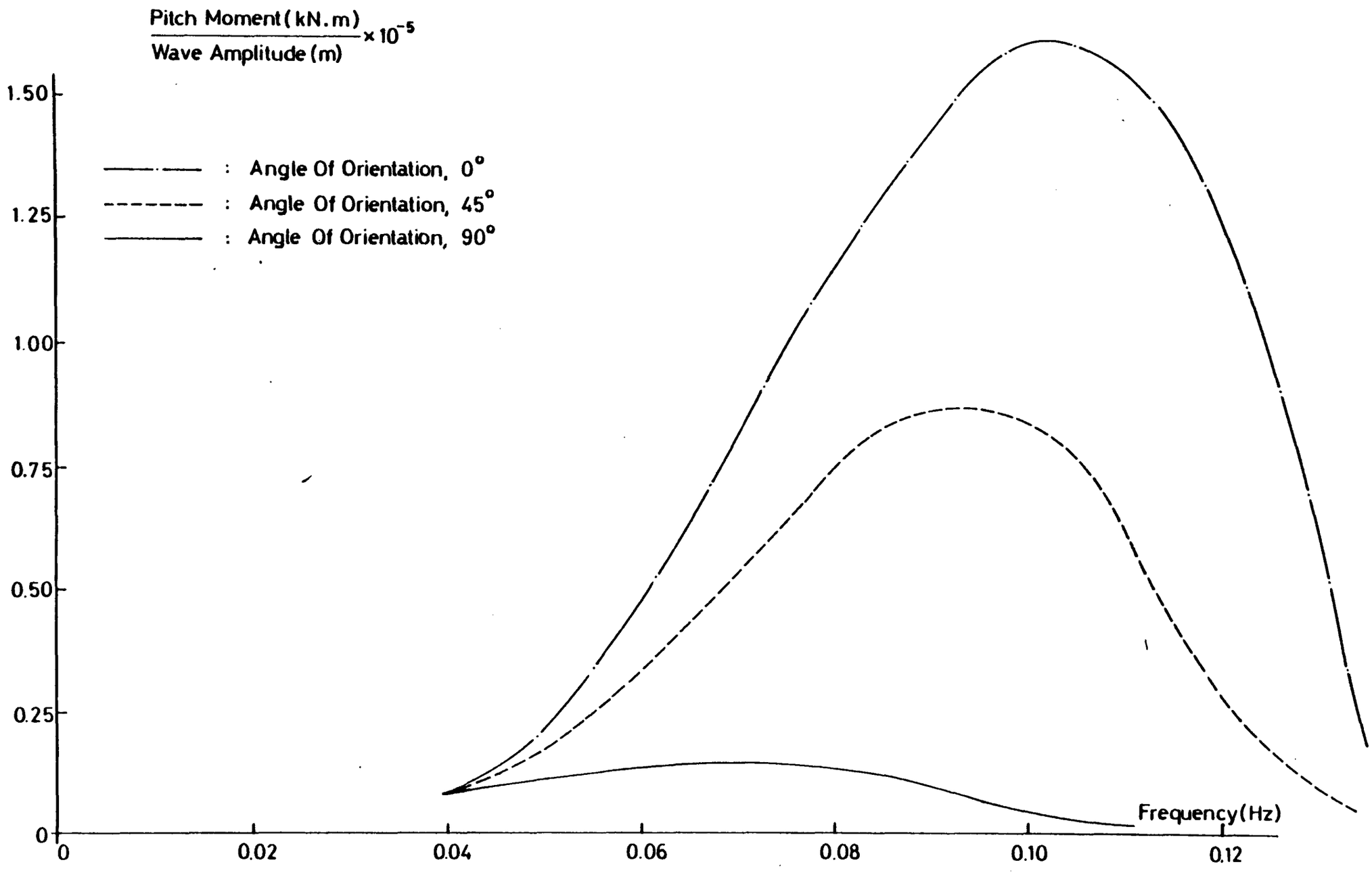
Pitch Moment (kN.m) / Wave Amplitude (m) × 10⁻⁵
1.50
1.25
1.00
0.75
0.50
0.25
0
: Angle Of Orientation, 0°
: Angle Of Orientation, 45°
: Angle Of Orientation, 90°
0
0.02
0.04
0.06
0.08
0.10
0.12
Frequency (Hz)

Fig. 20.

STRUCTURE CIRHULLW8.DAT

DRAFT 21.300 (M) ANGLE OF ORIENTATION 45.000 (DEGREES)

WAVE LENGTH 243.955 (M) WAVE FREQUENCY 0.000 (HZ) WAVE AMPLITUDE 6.000 (M)

==========

TABLE VII.

(Contd. over ...)

TRANSFORMATION MATRICES FOR EACH MEMBER

MEMBER NO 1

X		-1.00	0.00	0.00	U
Y	=	0.00	0.00	1.00	V
Z		0.00	1.00	0.00	W

MEMBER NO 2

X		0.00	0.00	1.00	U
Y	=	1.00	0.00	0.00	V
Z		0.00	1.00	0.00	W

MEMBER NO 3

X		0.00	0.00	1.00	U
Y	=	1.00	0.00	0.00	V
Z		0.00	1.00	0.00	W

MEMBER NO 4

X		0.00	0.00	1.00	U
Y	=	1.00	0.00	0.00	V
Z		0.00	1.00	0.00	W

MEMBER NO 5

X		-1.00	0.00	0.00	U
Y	=	0.00	0.00	1.00	V
Z		0.00	1.00	0.00	W

MEMBER NO 6

X		0.00	0.00	1.00	U
Y	=	1.00	0.00	0.00	V
Z		0.00	1.00	0.00	W

MEMBER NO 7

X		0.00	0.00	1.00	U
Y	=	1.00	0.00	0.00	V
Z		0.00	1.00	0.00	W

MEMBER NO 8

X		0.00	0.00	1.00	U
Y	=	1.00	0.00	0.00	V
Z		0.00	1.00	0.00	W

MEMBER NO 9

X		0.00	1.00	0.00	U
Y	=	0.68	0.00	-0.74	V
Z		-0.74	0.00	-0.68	W

MEMBER NO 10

X		0.00	1.00	0.00	U
Y	=	0.68	0.00	-0.74	V
Z		-0.74	0.00	-0.68	W

MEMBER NO 11

X		0.00	1.00	0.00	U
Y	=	0.68	0.00	-0.74	V
Z		-0.74	0.00	-0.68	W

MEMBER NO 12

X		0.00	1.00	0.00	U
Y	=	0.68	0.00	-0.74	V
Z		-0.74	0.00	-0.68	W

MEMBER NO 13

X		0.00	1.00	0.00	U
Y	=	0.68	0.00	0.74	V
Z		0.74	0.00	-0.68	W

MEMBER NO 14

X		0.00	1.00	0.00	U
Y	=	0.68	0.00	0.74	V
Z		0.74	0.00	-0.68	W

MEMBER NO 15

X		0.00	1.00	0.00	U
Y	=	0.68	0.00	0.74	V
Z		0.74	0.00	-0.68	W

MEMBER NO 16

X		0.00	1.00	0.00	U
Y	=	0.68	0.00	0.74	V
Z		0.74	0.00	-0.68	W

MEMBER NO 17

X		0.00	1.00	0.00	U
Y	=	0.00	0.00	-1.00	V
Z		-1.00	0.00	0.00	W

MEMBER NO 18

X		0.00	1.00	0.00	U
Y	=	0.00	0.00	-1.00	V
Z		-1.00	0.00	0.00	W

MEMBER NO 19

X		-1.00	0.00	0.00	U
Y	=	0.00	0.00	1.00	V
Z		0.00	1.00	0.00	W

MEMBER NO 20

X		-1.00	0.00	0.00	U
Y	=	0.00	0.00	1.00	V
Z		0.00	1.00	0.00	W

MEMBER NO 21

X		-1.00	0.00	0.00	U
Y	=	0.00	0.00	1.00	V
Z		0.00	1.00	0.00	W

TABLE VII.

MEMBER LOAD DISTRIBUTIONS

T1/T= 0.00

MEMBER NO 1

DISTRIBUTION OF LATERAL LOADS ALONG THE U AXIS

NODE NO	AXIAL DISTANCE FROM FIRST JOINT ON MEMBER (METRES)	V DIRECTION LOAD (KN/M)	W DIRECTION LOAD (KN/M)
1	0.000	-45.501	-149.301
2	9.600	-26.814	-158.056
3	19.200	-7.176	-161.421
4	28.800	12.830	-159.742
5	38.400	32.585	-153.767
6	48.000	51.448	-143.613
7	57.600	68.786	-129.473
8	67.200	83.999	-111.632
9	76.800	96.543	-90.478
10	86.400	105.961	-66.504
11	96.000	111.904	-40.319
12	105.600	114.149	-12.637
13	115.200	112.860	15.730
TOTAL MEMBER FORCE:		6524.583	-12458.317
TOTAL MEMBER MOMENT: (ABOUT FIRST JOINT ON MEMBER)		567068.812	-521994.969

CORRECTIONS FOR INTERSECTING MEMBERS

JOINT NO	INTERSECTING MEMBER	AXIAL DIST FROM START PT OF MEMBER TO START PT OF LOADING (M)	END PT OF LOADING (M)	V DIRECTION LOAD (KN/M)	W DIRECTION LOAD (KN/M)
2	2	11.400	19.600	0.000	268.196
4	3	50.100	58.300	0.000	219.365
6	4	88.800	97.000	0.000	66.002
2	9	14.000	17.000	-66.327	61.052
3	10	39.800	42.800	-63.670	58.607
5	11	65.600	68.600	-47.214	43.459
6	12	91.400	94.400	-20.524	18.891
TOTAL MEMBER COR. FORCE:				-593.203	5085.248
TOTAL MEMBER COR. MOMENT: (ABOUT FIRST JOINT OF MEMBER)				-26196.965	205975.187

TABLE VII.

AXIAL FORCE AT END 1 (U DIRECTION) 2876.905(KN)

AXIAL FORCE AT END 2 (U DIRECTION) 622.472(KN)

MEMBER NO 2

DISTRIBUTION OF LATERAL LOADS ALONG THE U AXIS

NODE NO	AXIAL DISTANCE FROM FIRST JOINT ON MEMBER (METRES)	V DIRECTION LOAD (KN/M)	W DIRECTION LOAD (KN/M)
1	5.350	-11.654	11.654
2	13.325	-15.713	15.713
3	21.300	-21.409	21.409
TOTAL MEMBER FORCE:		-254.967	254.968
TOTAL MEMBER MOMENT: (ABOUT FIRST JOINT ON MEMBER)		-3604.243	3604.249

CORRECTIONS FOR INTERSECTING MEMBERS

JOINT NO	INTERSECTING MEMBER	AXIAL DIST FROM START PT OF MEMBER TO START PT OF LOADING (M)	END PT OF LOADING (M)	V DIRECTION LOAD (KN/M)	W DIRECTION LOAD (KN/M)
TOTAL MEMBER COR. FORCE:				0.000	0.000
TOTAL MEMBER COR. MOMENT: (ABOUT FIRST JOINT OF MEMBER)				0.000	0.000

TABLE VII.

MEMBER NO 3

DISTRIBUTION OF LATERAL LOADS ALONG THE U AXIS

NODE NO	AXIAL DISTANCE FROM FIRST JOINT ON MEMBER (METRES)	V DIRECTION LOAD (KN/M)	W DIRECTION LOAD (KN/M)
1	5.350	41.258	-41.258
2	13.325	49.728	-49.728
3	21.300	59.653	-59.653
TOTAL MEMBER FORCE:		797.036	-797.036
TOTAL MEMBER MOMENT: (ABOUT FIRST JOINT ON MEMBER)		11010.478	-11010.489

CORRECTIONS FOR INTERSECTING MEMBERS

JOINT NO	INTERSECTING MEMBER	AXIAL DIST FROM START PT OF MEMBER TO START PT OF LOADING (M)	END PT OF LOADING (M)	V DIRECTION LOAD (KN/M)	W DIRECTION LOAD (KN/M)
TOTAL MEMBER COR. FORCE:				0.000	0.000
TOTAL MEMBER COR. MOMENT: (ABOUT FIRST JOINT OF MEMBER)				0.000	0.000

MEMBER NO 4

DISTRIBUTION OF LATERAL LOADS ALONG THE U AXIS

NODE NO	AXIAL DISTANCE FROM FIRST JOINT ON MEMBER (METRES)	V DIRECTION LOAD (KN/M)	W DIRECTION LOAD (KN/M)
1	5.350	74.303	-74.303
2	13.325	91.161	-91.161
3	21.300	111.819	-111.819
TOTAL MEMBER FORCE:		1464.117	-1464.118
TOTAL MEMBER MOMENT: (ABOUT FIRST JOINT ON MEMBER)		20304.695	-20304.717

CORRECTIONS FOR INTERSECTING MEMBERS

JOINT NO	INTERSECTING MEMBER	AXIAL DIST FROM START PT OF MEMBER TO START PT OF LOADING (M)	END PT OF LOADING (M)	V DIRECTION LOAD (KN/M)	W DIRECTION LOAD (KN/M)
TOTAL MEMBER COR. FORCE:				0.000	0.000
TOTAL MEMBER COR. MOMENT: (ABOUT FIRST JOINT OF MEMBER)				0.000	0.000

TABLE VII.

MEMBER NO 16

DISTRIBUTION OF LATERAL LOADS ALONG THE U AXIS

NODE NO	AXIAL DISTANCE FROM FIRST JOINT ON MEMBER (METRES)	V DIRECTION LOAD (KN/M)	W DIRECTION LOAD (KN/M)
1	5.350	9.520	5.549
2	18.400	11.489	5.343
3	31.451	13.798	4.637
TOTAL MEMBER FORCE:		301.358	137.278
TOTAL MEMBER MOMENT: (ABOUT FIRST JOINT ON MEMBER)		5787.974	2474.248

CORRECTIONS FOR INTERSECTING MEMBERS

JOINT NO	INTERSECTING MEMBER	AXIAL DIST FROM START PT OF MEMBER TO START PT OF LOADING (M)	END PT OF LOADING (M)	V DIRECTION LOAD (KN/M)	W DIRECTION LOAD (KN/M)
TOTAL MEMBER COR. FORCE:				0.000	0.000
TOTAL MEMBER COR. MOMENT: (ABOUT FIRST JOINT OF MEMBER)				0.000	0.000

SUMMARY OF TOTAL FORCES AND MOMENTS ON THE STRUCTURE

(MOMENTS ABOUT ORIGIN OF THE STRUCTURE REF. SYSTEM) (T1/T= 0.00)

TOTAL SURGE FORCE=	269.084	(KN)
TOTAL HEAVE FORCE=	-16130.583	(KN)
TOTAL SWAY FORCE =	-325.922	(KN)
TOTAL ROLL MOMENT=	-9150.138	(KN.M)
TOTAL YAW MOMENT=	161979.125	(KN.M)
TOTAL PITCH MOMENT=	76615.508	(KN.M)

TABLE VII.

MEMBER NO 1

DISTRIBUTION OF LATERAL LOADS ALONG THE U AXIS

NODE NO	AXIAL DISTANCE FROM FIRST JOINT ON MEMBER (METRES)	V DIRECTION LOAD (KN/M)	W DIRECTION LOAD (KN/M)
1	0.000	105.840	-66.895
2	9.600	111.839	-40.739
3	19.200	114.143	-13.074
4	28.800	112.905	15.289
5	38.400	108.512	43.464
6	48.000	101.065	70.518
7	57.600	90.733	95.510
8	67.200	77.758	117.532
9	76.800	62.457	135.756
10	86.400	45.222	149.476
11	96.000	26.516	158.150
12	105.600	6.867	161.430
13	115.200	-13.140	159.681
TOTAL MEMBER FORCE:		8704.139	9044.571
TOTAL MEMBER MOMENT: (ABOUT FIRST JOINT ON MEMBER)		359924.031	795607.500

CORRECTIONS FOR INTERSECTING MEMBERS

JOINT NO	INTERSECTING MEMBER	AXIAL DIST FROM START PT OF MEMBER TO START PT OF LOADING (M)	END PT OF LOADING (M)	V DIRECTION LOAD (KN/M)	W DIRECTION LOAD (KN/M)
2	2	11.400	19.600	0.000	257.690
4	3	50.100	58.300	0.000	203.262
6	4	88.800	97.000	0.000	51.976
2	9	14.000	17.000	-65.068	59.893
3	10	39.800	42.800	-62.378	57.417
5	11	65.600	68.600	-46.169	42.497
6	12	91.400	94.400	-19.952	18.366
TOTAL MEMBER COR. FORCE:				-580.701	4740.529
TOTAL MEMBER COR. MOMENT: (ABOUT FIRST JOINT OF MEMBER)				-25608.807	186256.875

AXIAL FORCE AT END 1 (U DIRECTION) 3044.527(KN)

AXIAL FORCE AT END 2 (U DIRECTION) 474.034(KN)

TABLE VII.

MEMBER NO 2

DISTRIBUTION OF LATERAL LOADS ALONG THE U AXIS

NODE NO	AXIAL DISTANCE FROM FIRST JOINT ON MEMBER (METRES)	V DIRECTION LOAD (KN/M)	W DIRECTION LOAD (KN/M)
1	5.350	76.630	-76.630
2	13.325	94.092	-94.092
3	21.300	115.531	-115.531
TOTAL MEMBER FORCE:		1511.338	-1511.340
TOTAL MEMBER MOMENT: (ABOUT FIRST JOINT ON MEMBER)		20963.291	-20963.316

CORRECTIONS FOR INTERSECTING MEMBERS

JOINT NO	INTERSECTING MEMBER	AXIAL DIST FROM START PT OF MEMBER TO START PT OF LOADING (M)	END PT OF LOADING (M)	V DIRECTION LOAD (KN/M)	W DIRECTION LOAD (KN/M)
TOTAL MEMBER COR. FORCE:				0.000	0.000
TOTAL MEMBER COR. MOMENT: (ABOUT FIRST JOINT OF MEMBER)				0.000	0.000

MEMBER NO 3

DISTRIBUTION OF LATERAL LOADS ALONG THE U AXIS

NODE NO	AXIAL DISTANCE FROM FIRST JOINT ON MEMBER (METRES)	V DIRECTION LOAD (KN/M)	W DIRECTION LOAD (KN/M)
1	5.350	64.403	-64.403
2	13.325	79.562	-79.562
3	21.300	98.419	-98.419
TOTAL MEMBER FORCE:		1278.842	-1278.844
TOTAL MEMBER MOMENT: (ABOUT FIRST JOINT ON MEMBER)		17761.721	-17761.744

CORRECTIONS FOR INTERSECTING MEMBERS

JOINT NO	INTERSECTING MEMBER	AXIAL DIST FROM START PT OF MEMBER TO START PT OF LOADING (M)	END PT OF LOADING (M)	V DIRECTION LOAD (KN/M)	W DIRECTION LOAD (KN/M)
TOTAL MEMBER COR. FORCE:				0.000	0.000
TOTAL MEMBER COR. MOMENT: (ABOUT FIRST JOINT OF MEMBER)				0.000	0.000

TABLE VII.

SUMMARY OF TOTAL FORCES AND MOMENTS ON THE STRUCTURE

(MOMENTS ABOUT ORIGIN OF THE STRUCTURE REF. SYSTEM) (T1/T= 0.25)

TOTAL SURGE FORCE=	-9105.962	(KN)
TOTAL HEAVE FORCE=	9744.171	(KN)
TOTAL SWAY FORCE =	25501.559	(KN)
TOTAL ROLL MOMENT=	-523004.375	(KN.M)
TOTAL YAW MOMENT=	-148119.453	(KN.M)
TOTAL PITCH MOMENT=	-444192.219	(KN.M)

SUMMARY OF MAXIMUM FORCES AND MOMENTS ON THE STRUCTURE

MAX. SURGE FORCE=	9109.937	(KN)
MAX. HEAVE FORCE=	18845.279	(KN)
MAX. SWAY FORCE =	25503.641	(KN)
MAX. ROLL MOMENT=	523084.406	(KN.M)
MAX. YAW MOMENT=	219491.719	(KN.M)
MAX. PITCH MOMENT=	450751.219	(KN.M)

TABLE VII.

Chapter 4: MOTION RESPONSE OF FLOATING OFFSHORE PLATFORMS UNDER WAVE EXCITATION

INTRODUCTION

In this chapter, the hydrodynamic loading due to the motion of floating structures which are composed of circular cylinders, the structural loading due to the acceleration and the velocity of the structure, and the restoring forces and moments will be discussed. The motion equations will be obtained by combining the wave and hydrodynamic loading with the restoring forces using Newton's second law. The effect of the free surface and that of the interference between closely spaced circular members on hydrodynamic coefficients are also discussed.

1. HYDRODYNAMIC LOADING DUE TO RIGID BODY MOTION OF FLOATING STRUCTURES

The wave excitation on floating stable platforms will result in small amplitude rigid body motions which can be resolved into heave, surge, sway, roll, pitch and yaw. In this section the calculation procedure will be presented to determine the hydrodynamic loading and the resulting motions of such structures.

When we consider a rigid body oscillating arbitrarily in an unbounded fluid the forces and the moments acting on this body can be written as follows. (Fig. 1.)

$$\vec{F} = - \rho \frac{d}{dt} \iint_{S_M} \Phi \, \vec{n} \, dS \tag{1}$$

$$\vec{M} = - \rho \frac{d}{dt} \iint_{S_M} \Phi \, (\vec{r} \wedge \vec{n}) \, dS \tag{2}$$

where $\Phi(X,Y,Z,t) = R_e[\sum_{j=1}^{6} X_j \, \phi_j(X,Y,Z) e^{-i\omega t}]$

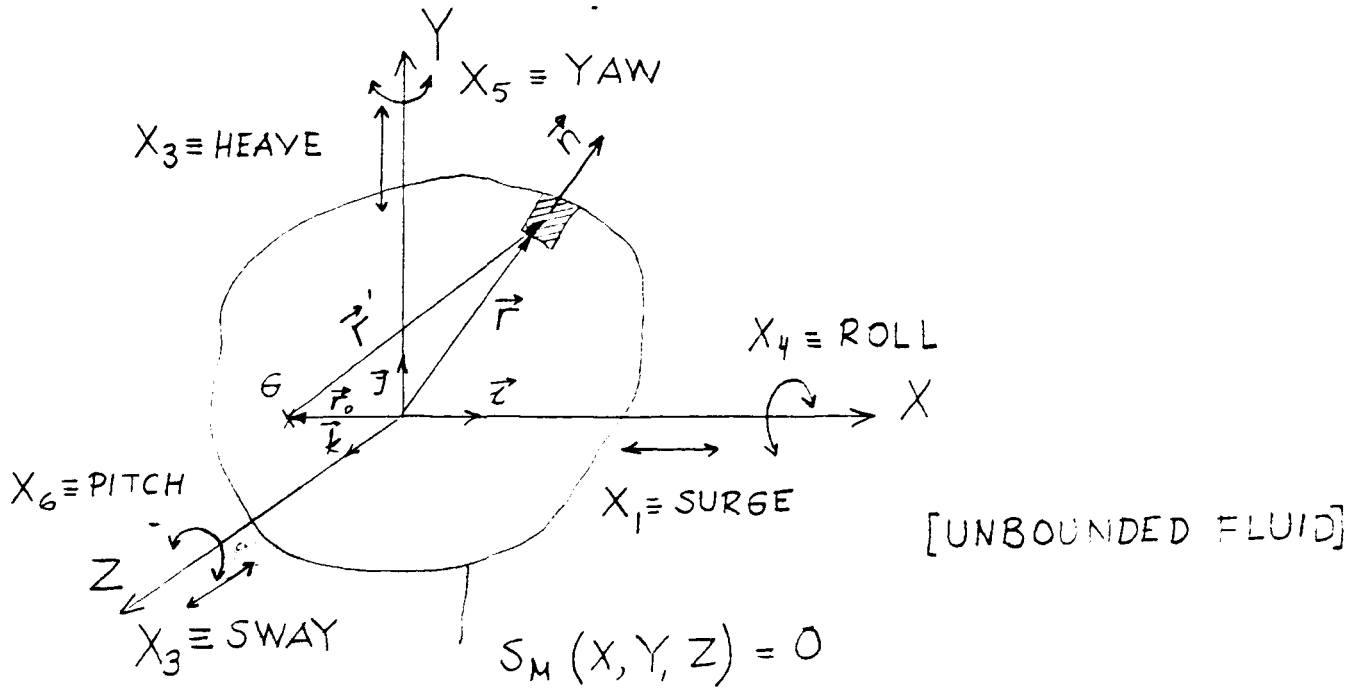

Fig. 1.

Here $\phi_j(X,Y,Z)$ represents the velocity potential of a rigid body motion with unit amplitude and $\Phi(X,Y,Z,t)$ should satisfy the appropriate boundary conditions on the surface of a body. That is,

$$\frac{\partial \phi}{\partial n} = \vec{U} \cdot \vec{n} + \vec{\Omega} \cdot (\vec{r}' \wedge \vec{n}) \tag{3}$$

where $\phi = X_j \phi_j$

$$\vec{U} = U_1 \vec{i} + U_2 \vec{j} + U_3 \vec{k}$$

$$\vec{\Omega} = U_4 \vec{i} + U_5 \vec{j} + U_6 \vec{k}$$

Since $U_j = \mathrm{Re}[-i\omega X_j e^{-i\omega t}]$ $j=1,2, \ldots 6$, Φ can satisfy the boundary condition given in equation (3) provided that ϕ_j satisfies the following conditions:

$$\frac{\partial \phi_j}{\partial n} = - i\omega n_j \qquad j=1,2,3 \tag{4}$$

$$\frac{\partial \phi_j}{\partial n} = - i\omega (\vec{r}' \wedge \vec{n})_{j-3} \qquad j=4,5,6 \tag{5}$$

Equations (1) and (2) can also be written in the following form:

$$\vec{F} = - \rho \, Re[\frac{d}{dt} (\sum_{j=1}^{6} \iint_{S_M} (X_j \phi_j \, e^{-i\omega t}) \, \vec{n} dS)] \tag{6}$$

or

$$\vec{F} = \rho \, Re[\sum_{j=1}^{3} \iint_{S_M} (i\omega X_j \phi_j \, e^{-i\omega t}) \, \vec{n} dS] \tag{6-A}$$

Similarly,

$$\vec{M} = \rho \, Re[\sum_{j=4}^{6} \iint_{S_M} (i\omega X_j \phi_j \, e^{-i\omega t}) (\vec{r} \wedge \vec{n})_{j-3} \, dS] \tag{7}$$

If we replace r with r' by assuming that the centre of rotation coincides with the centre of the space fixed reference system, equation (7) becomes:

$$\vec{M} = \rho \, Re[\sum_{j=4}^{6} \iint_{S_M} (i\omega X_j \phi_j \, e^{-i\omega t}) (\vec{r}' \wedge \vec{n})_{j-3} \, dS] \tag{7-A}$$

Equations (6-A) and (7-A) can be combined, using the boundary conditions given in (4) and (5), in the following equation:

$$F_i = - \rho \, Re[\sum_{j=1}^{6} \iint_{S_M} \frac{\partial \phi_i}{\partial n} \phi_j X_j \, e^{-i\omega t} \, dS] \qquad i=1,2, \ldots 6 \tag{8}$$

By analogy to Newton's second law, equation (8) can be expressed in the following form:

$$F_i = Re[\sum_{j=1}^{6} (C_{ij} X_j \, e^{-i\omega t})] \qquad i=1,2, \ldots 6 \tag{9}$$

where $C_{ij} = - \rho \iint_{S_M} \frac{\partial \phi_i}{\partial n} \phi_j \, dS$

Initially it is assumed that the body is arbitrarily oscillating in an unbounded fluid, in which case C_{ij} becomes:

$$C_{ij} = m_{ij}\ \omega^2 \qquad (10)$$

and equation (9) becomes:

$$F_i = - \mathrm{Re}\left[\sum_{j=1}^{6} (m_{ij}\ \omega^2\ X_j\ e^{-i\omega t}) \right] \qquad i=1,2, \ldots 6 \qquad (11)$$

or

$$F_i = - \sum_{j=1}^{6} m_{ij}\ \dot{U}_j \qquad i=1,2, \ldots 6 \qquad (11\text{-}A)$$

The hydrodynamic forces due to the motions of a circular cylinder are shown with the following matrix. (Fig. 2.)

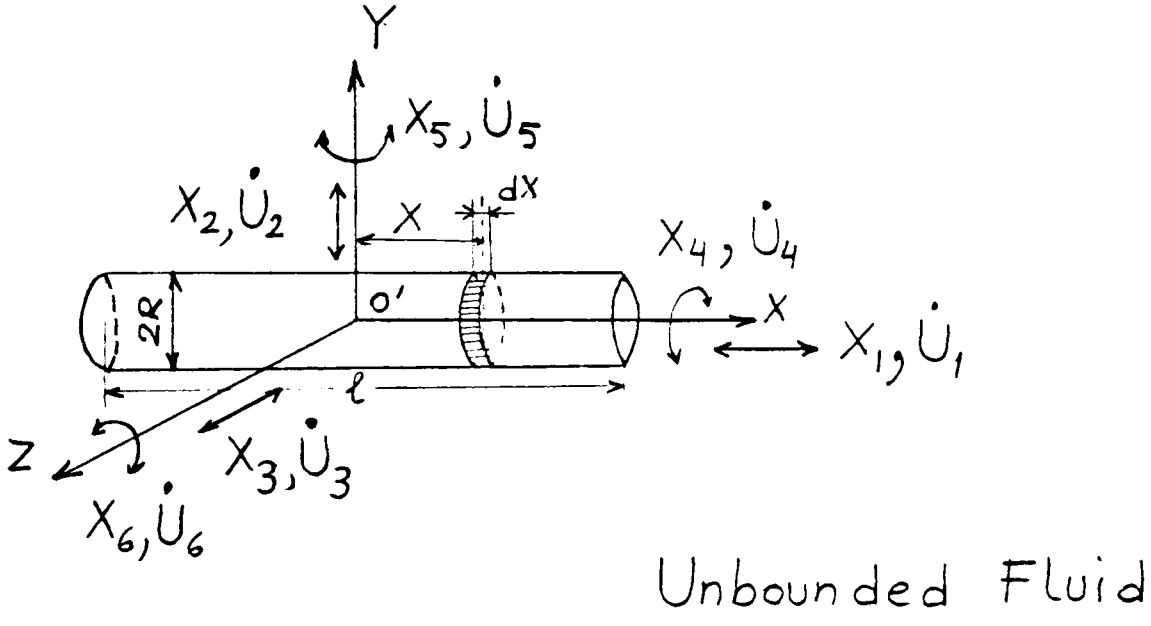

Fig. 2.

$$\begin{bmatrix} F_1 \\ F_2 \\ F_3 \\ F_4 \\ F_5 \\ F_6 \end{bmatrix} = - \begin{bmatrix} 0.424\rho\pi R^3 k_{11} & 0 & 0 & 0 & 0 & 0 \\ 0 & \rho\pi R^2 \ell & 0 & 0 & 0 & \rho\pi R^2 \int_{-\ell/2}^{+\ell/2} X dX \\ 0 & 0 & \rho\pi R^2 \ell & 0 & \rho\pi R^2 \int_{-\ell/2}^{+\ell/2} X dX & 0 \\ 0 & 0 & 0 & 0 & 0 & 0 \\ 0 & 0 & \rho\pi R^2 \int_{-\ell/2}^{+\ell/2} X dX & 0 & \rho\pi R^2 \int_{-\ell/2}^{+\ell/2} X^2 dX & 0 \\ 0 & \rho\pi R^2 \int_{-\ell/2}^{+\ell/2} X dX & 0 & 0 & 0 & \rho\pi R^2 \int_{-\ell/2}^{+\ell/2} X^2 dX \end{bmatrix} \begin{bmatrix} \dot{U}_1 \\ \dot{U}_2 \\ \dot{U}_3 \\ \dot{U}_4 \\ \dot{U}_5 \\ \dot{U}_6 \end{bmatrix} \tag{12}$$

where k_{11} is the added mass coefficient for a rectangular strip,

F_1: Surge Force, F_2: Heave Force, F_3: Sway Force, F_4: Roll Moment,

F_5: Yaw Moment, F_6: Pitch Moment.

m_{ij} matrix is assembled according to the geometry of the circular cylinder, and $m_{ij}=m_{ji}$ because of the symmetry of the circular cylinder geometry with respect to X,Y,Z axes.

When we consider a body oscillating in or near the free surface C_{ij} becomes complex as a result of the free surface. That is,

$$C_{ij} = \omega^2 a_{ij} - i\omega b_{ij} \tag{13}$$

and equation (9) becomes,

$$F_i = \mathrm{Re}\left[\sum_{j=1}^{6} (\omega^2 a_{ij} - i\omega b_{ij}) X_j e^{-i\omega t} \right] \tag{14}$$

or

$$F_i = - \sum_{j=1}^{6} (a_{ij} \dot{U}_j + b_{ij} U_j) \tag{14-A}$$

The added mass tensor m_{ij} in the unbounded fluid differs from the added mass tensor a_{ij} in the fluid domain with a free surface. Since elements of the b_{ij} tensor give forces proportinal to the body velocity they are called damping coefficients. a_{ij} and b_{ij} tensors can be obtained by determining the $\phi_j(X,Y,Z)$ velocity potential. It can easily be shown that the a_{ij} and b_{ij} values are frequency dependent. As stated in Section 1 of Chapter 2 ϕ_j should satisfy Laplace's equation (2.9), the free surface equation (2.11), the radiation condition (2.12) and the kinematic boundary conditions (4) and (5).

If we write the linear free surface boundary conditions as $\omega \to 0$ and $\omega \to \infty$ the following conditions are obtained:

$$\frac{\partial \phi_j}{\partial y} = 0 \qquad \text{on} \quad y=0 \qquad \text{for} \quad \omega \to 0 \tag{15}$$

$$\phi_j = 0 \qquad \text{on} \quad y=0 \qquad \text{for} \quad \omega \to \infty$$

Equations (15) and (16) show that ϕ_j will be frequency dependent hence the C_{ij} values will also be dependent on the frequency. Theoretical and experimental investigations were carried out by several authors [1-5] for the determination of hydrodynamic coefficients of swaying, heaving and rolling cylinders in a free surface. These investigations show that as oscillation frequencies approach zero a_{ij} values in surge, sway and yaw modes approach the corresponding m_{ij} values in an unbounded fluid. On the other hand as oscillation frequencies approach infinity a_{ij} values in heave, roll and pitch modes approach corresponding m_{ij} values in an unbounded fluid. The elements of the damping tensor approach zero as oscillation frequencies approach either zero or infinity. Similarly, as the depth of an oscillating body below the free surface increases, a_{ij} values for all modes approach the corresponding m_{ij} values in an unbounded fluid.

Since the principal parts of all members of offshore structures are deeply submerged in their operational mode, the unbounded added-mass tensor will be used to calculate the hydrodynamic forces on floating offshore structures. However, in Section 3 a simple approach will be given to take into account the free surface effect in added-mass calculations for circular cylinders oscillating close to the free surface.

2. DERIVATION OF A GENERAL METHOD TO CALCULATE HYDRODYNAMIC LOADING ON THE CIRCULAR CYLINDRICAL MEMBERS OF OFFSHORE STRUCTURES

In order to determine the hydrodynamic loading due to the rigid body motion of the floating platform, the hydrodynamic loading on each individual member will be estimated in terms of the velocities and accelerations of the structure in its translational and rotational modes. The total hydrodynamic loading will be obtained by summing these forces along the principal axes of the structure reference system (X,Y,Z). The velocities and the accelerations of the structure can be determined from the solutions of the motion equations which will be discussed in Section 7.

If we choose the origin of the structure reference system to be at the centre of rotation which is generally assumed to be the centre of gravity of the floating platform, the translational velocity and acceleration of any point on an individual member can be defined in terms of the structure's velocities and accelerations in translational and in rotational modes as follows (see Fig. 3).

The velocity and the acceleration of a point on an individual member in this member's reference system will be:

$$\vec{U}_{M,T,S} = \vec{U}_{S,T} + \vec{U}_{S,R} \wedge \vec{R} = \vec{U}_{S,T} + \vec{U}_{S,R} \wedge (\vec{r} + \vec{AC}) \qquad (17)$$

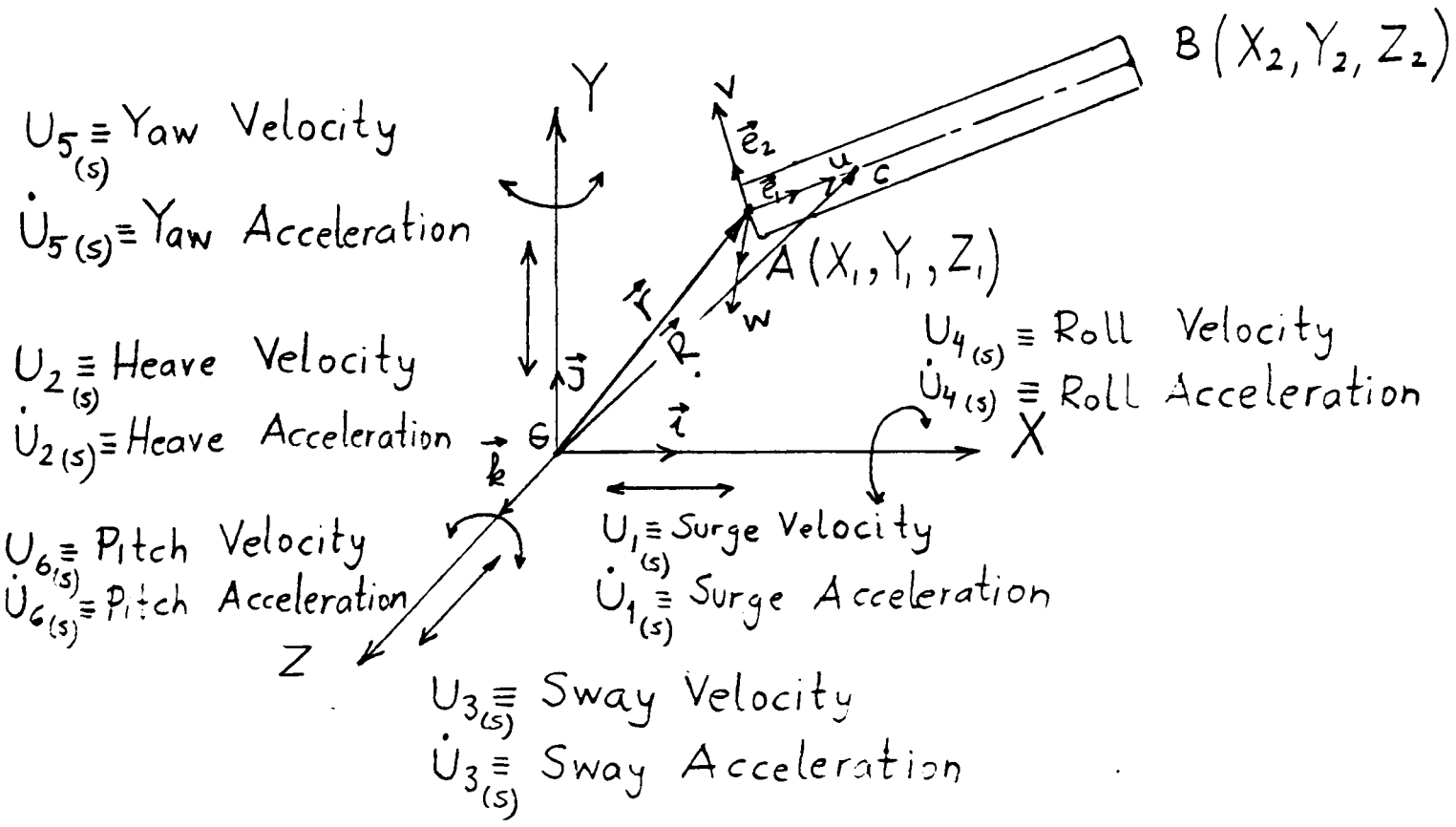

Fig. 3.

$$\dot{\vec{U}}_{M,T,S} = \dot{\vec{U}}_{S,T} + \vec{U}_{S,R} \wedge (\vec{U}_{S,R} \wedge \vec{R}) + \dot{\vec{U}}_{S,R} \wedge \vec{R} \qquad (18)$$

or

$$\dot{\vec{U}}_{M,T,S} = \dot{\vec{U}}_{S,T} + \vec{U}_{S,R} \wedge [\vec{U}_{S,R} \wedge (\vec{r} + \vec{AC})] + \dot{\vec{U}}_{S,R} \wedge (\vec{r} + \vec{AC}) \qquad (18\text{-A})$$

where $\vec{U}_{S,T} = U_{1(S)}\,\vec{i} + U_{2(S)}\,\vec{j} + U_{3(S)}\,\vec{k}$

$\vec{U}_{S,R} = U_{4(S)}\,\vec{i} + U_{5(S)}\,\vec{j} + U_{6(S)}\,\vec{k}$

$\dot{\vec{U}}_{S,T} = \dot{U}_{1(S)}\,\vec{i} + \dot{U}_{2(S)}\,\vec{j} + \dot{U}_{3(S)}\,\vec{k}$

$\dot{\vec{U}}_{S,R} = \dot{U}_{4(S)}\,\vec{i} + \dot{U}_{5(S)}\,\vec{j} + \dot{U}_{6(S)}\,\vec{k}$

$$\vec{AC} = u(\alpha_{11}\vec{i} + \alpha_{12}\vec{j} + \alpha_{13}\vec{k})$$

α_{ij}: Transformation matrix for the (X,Y,Z) and (u,v,w) systems.

The second term in equations (18) and (18-A) can be omitted since the rigid body motion of the floating structure will be of a small amplitude.

The equations (17), (18) and (18-A) written in the member reference system are along lines parallel to the structure's reference system. These velocity and acceleration vectors can also be written with reference to lines parallel to the member reference system's axes using the following transformation matrix:

$$\vec{U}_{M,T,M} = [T]^T \vec{U}_{M,T,S} \tag{19}$$

$$\dot{\vec{U}}_{M,T,M} : [T]^T \dot{\vec{U}}_{M,T,S} \tag{20}$$

where

$$[T]^T = \begin{bmatrix} \alpha_{11} & \alpha_{21} & \alpha_{31} \\ \alpha_{12} & \alpha_{22} & \alpha_{32} \\ \alpha_{13} & \alpha_{23} & \alpha_{33} \end{bmatrix}$$

The $\vec{U}_{M,T,S}$, $\dot{\vec{U}}_{M,T,S}$, $\vec{U}_{M,T,M}$, $\dot{\vec{U}}_{M,T,M}$, vectors can also be written explicitly with reference to the chosen axes system of a member, the rigid body velocities of the structure and the member co-ordinate u as follows:

$$\begin{aligned} \vec{U}_{M,T,S} = {} & [U_1 + U_5 (Z_1 + u\alpha_{13}) - U_6 (Y_1 + u\alpha_{12})]\,\vec{i} \\ & + [U_2 + U_6 (X_1 + u\alpha_{11}) - U_4 (Z_1 + u\alpha_{13})]\,\vec{j} \\ & + [U_3 + U_4 (Y_1 + u\alpha_{12}) - U_5 (X_1 + u\alpha_{11})]\,\vec{k} \end{aligned} \tag{21}$$

$$\dot{\vec{U}}_{M,T,S} = [\dot{U}_1 + \dot{U}_5 (Z_1 + u\alpha_{13}) - \dot{U}_6 (Y_1 + u\alpha_{12})] \vec{i}$$
$$+ [\dot{U}_2 + \dot{U}_6 (X_1 + u\alpha_{11}) - \dot{U}_4 (Z_1 + u\alpha_{13})] \vec{j} \quad (22)$$
$$+ [\dot{U}_3 + \dot{U}_4 (Y_1 + u\alpha_{12}) - \dot{U}_5 (X_1 + u\alpha_{11})] \vec{k}$$

$$\vec{U}_{M,T,M} = A(u) \vec{e}_1 + B(u) \vec{e}_2 + C(u) \vec{e}_3 \quad (23)$$

where

$$A(u) = A1(u)\alpha_{11} + B1(u)\alpha_{21} + C1(u)\alpha_{31}$$
$$B(u) = A1(u)\alpha_{12} + B1(u)\alpha_{22} + C1(u)\alpha_{32}$$
$$C(u) = A1(u)\alpha_{13} + B1(u)\alpha_{23} + C1(u)\alpha_{33}$$

and,

$$A1(u) = U_1 + U_5 (Z_1 + u\alpha_{13}) - U_6 (Y_1 + u\alpha_{12})$$
$$B1(u) = U_2 + U_6 (X_1 + u\alpha_{11}) - U_4 (Z_1 + u\alpha_{13})$$
$$C1(u) = U_3 + U_4 (Y_1 + u\alpha_{12}) - U_5 (X_1 + u\alpha_{11})$$

Similarly,

$$\dot{\vec{U}}_{M,T,M} = \dot{A}(u) \vec{e}_1 + \dot{B}(u) \vec{e}_2 + \dot{C}(u) \vec{e}_3 \quad (24)$$

where

$$\dot{A}(u) = \dot{A}1(u)\alpha_{11} + \dot{B}1(u)\alpha_{21} + \dot{C}1(u)\alpha_{31}$$
$$\dot{B}(u) = \dot{A}1(u)\alpha_{12} + \dot{B}1(u)\alpha_{22} + \dot{C}1(u)\alpha_{32}$$
$$\dot{C}(u) = \dot{A}1(u)\alpha_{13} + \dot{B}1(u)\alpha_{23} + \dot{C}1(u)\alpha_{33}$$

and,

$$\dot{A}1(u) = \dot{U}_1 + \dot{U}_5 (Z_1 + u\alpha_{13}) - \dot{U}_6 (Y_1 + u\alpha_{12})$$
$$\dot{B}1(u) = \dot{U}_2 + \dot{U}_6 (X_1 + u\alpha_{11}) - \dot{U}_4 (Z_1 + u\alpha_{13})$$
$$\dot{C}1(u) = \dot{U}_3 + \dot{U}_4 (Y_1 + u\alpha_{12}) - \dot{U}_5 (X_1 + u\alpha_{11})$$

The total hydrodynamic loads and moments on an individual member can be written in this member's reference system as follows:

$$\vec{F}_{i,M} = \{[a_{11}\dot{A}(u) + b_{11}A(u)]_{u=0} + [a_{11}\dot{A}(u) + b_{11}A(u)]_{u=\ell}\}\ \vec{e}_1 + \int_{u=0}^{\ell} (a_{22}\dot{B}(u) + b_{22}B(u))\ du\ \vec{e}_2 + \int_{u=0}^{\ell} (a_{33}\dot{C}(u) + b_{33}C(u))\ du\ \vec{e}_3 \quad (25)$$

$$\vec{M}_{i,M} = \int_{u=0}^{\ell} [\vec{e}_1 \wedge [(a_{22}\dot{B}(u) + b_{22}B(u))\ \vec{e}_2 + (a_{33}\dot{C}(u) + b_{33}C(u))\ \vec{e}_3]\ udu \quad (26)$$

The first component of the force vector given in equation (25) is to be determined according to the cylindrical members' exposed ends to the wave loading, i.e. if the member is inter-costal this component will vanish.

The moment due to hydrodynamic loading about the origin of the structure's reference system can be written as follows:

$$\vec{M}_{i,S} = \vec{M}_{i,M} + \vec{r} \wedge \vec{F}_{i,M} \quad (27)$$

The total hydrodynamic forces and moments are calculated to obtain the principal components as follows:

$$\vec{F} = -\ (a\vec{i} + b\vec{j} + c\vec{k}) \quad (28)$$

(surge force) (heave force) (sway force)

$$\vec{M} = -\ (d\vec{i} + e\vec{j} + f\vec{k}) \quad (28\text{-A})$$

(roll moment) (yaw moment) (pitch moment)

where

$$a = \sum_{i=1}^{m} [\alpha_{11} F_{1,i(m)} + \alpha_{12} F_{2,i(m)} + \alpha_{13} F_{3,i(m)}]$$

$$b = \sum_{i=1}^{m} [\alpha_{21} F_{1,i(m)} + \alpha_{22} F_{2,i(m)} + \alpha_{23} F_{3,i(m)}]$$

$$c = \sum_{i=1}^{m} [\alpha_{31} F_{1,i(m)} + \alpha_{32} \dot{F}_{2,i(m)} + \alpha_{33} F_{3,i(m)}]$$

$$F_{1,i(m)} = [a_{11}\dot{A}(u) + b_{11}A(u)]_{u=0} + [a_{11}\dot{A}(u) + b_{11}A(u)]_{u=\ell}$$

$$F_{2,i(m)} = \int_{u=0}^{\ell} (a_{22}\dot{B}(u) + b_{22}B(u))\, du$$

$$F_{3,i(m)} = \int_{u=0}^{\ell} (a_{33}\dot{C}(u) + b_{33}C(u))\, du$$

Using equations (26) and (27) the principal components of the hydrodynamic moment vector can be written as follows:

$$d = \sum_{i=1}^{m} [\alpha_{13} M_{2,i(m)} - \alpha_{12} M_{3,i(m)} + Y_1 c_i' - Z_1 b_i']$$

$$e = \sum_{i=1}^{m} [\alpha_{23} M_{2,i(m)} - \alpha_{22} M_{3,i(m)} + Z_1 a_i - X_1 c_i]$$

$$f = \sum_{i=1}^{m} [\alpha_{33} M_{2,i(m)} - \alpha_{32} M_{3,i(m)} + X_1 b_i' - Y_1 a_i']$$

where

$$a_i' = \alpha_{11} F_{1,i(m)} + \alpha_{12} F_{2,i(m)} + \alpha_{13} F_{3,i(m)}$$

$$b_i' = \alpha_{21} F_{1,i(m)} + \alpha_{22} F_{2,i(m)} + \alpha_{23} F_{3,i(m)}$$

$$c_i' = \alpha_{31} F_{1,i(m)} + \alpha_{32} F_{2,i(m)} + \alpha_{33} F_{3,i(m)}$$

$$M_{2,i(m)} = \int_{u=0}^{\ell} (a_{22}\dot{B}(u) + b_{22}B(u))\, udu$$

$$M_{3,i(m)} = \int_{u=0}^{\ell} (a_{33}\dot{C}(u) + b_{33}C(u))\, udu$$

The general method derived above can also be summarised with matrix notations which may be found suitable for the numerical applications. The hydrodynamic force can be written as,

$$[F] = -\{[T]([AM][AT][A1F][\dot{U}] + [DM][AT][A1F][U])\} \qquad (29)$$

where

$$[F] = \begin{bmatrix} F_1 \\ F_2 \\ F_3 \end{bmatrix}$$

$$[T] = \begin{bmatrix} \alpha_{11} & \alpha_{12} & \alpha_{13} \\ \alpha_{21} & \alpha_{22} & \alpha_{23} \\ \alpha_{31} & \alpha_{32} & \alpha_{33} \end{bmatrix} \qquad [AM] = \begin{bmatrix} a_{11} & 0 & 0 \\ 0 & a_{22} & 0 \\ 0 & 0 & a_{33} \end{bmatrix}$$

a_{11} in [AM] matrix will be determined according to both ends of the cylindrical member, i.e. if the member is inter-costal a_{11} takes the negative sign

$$[AT] = \begin{bmatrix} \alpha_{11}\, Q_1 & \alpha_{21}\, Q_1 & \alpha_{31}\, Q_1 \\ \alpha_{12}\, Q_2 & \alpha_{22}\, Q_2 & \alpha_{32}\, Q_2 \\ \alpha_{13}\, Q_2 & \alpha_{23}\, Q_2 & \alpha_{33}\, Q_2 \end{bmatrix}$$

Where Q_1 and Q_2 are the operators according to which A1F matrix will be calculated.

A. When Q_1 is in use A1F matrix takes the following forms:

(a) Both ends of the member are submerged

$$[A1F]_{Q_1} = \begin{bmatrix} 2 & 0 & 0 & 0 & (2Z_1 + \ell\alpha_{13}) & -(2Y_1 + \ell\alpha_{12}) \\ 0 & 2 & 0 & -(2Z_1 + \ell\alpha_{13}) & 0 & (2X_1 + \ell\alpha_{11}) \\ 0 & 0 & 2 & (2Y_1 + \ell\alpha_{12}) & -(2X_1 + \ell\alpha_{11}) & 0 \end{bmatrix}$$

(b) The end of the member is submerged where U = O

$$[AlF]_{Q_1} = \begin{bmatrix} 1 & O & O & O & Z_1 & -Y_1 \\ O & 1 & O & -Z_1 & O & X_1 \\ O & O & 1 & (Y_1 + \ell\alpha_{12}) & -(X_1 + \ell\alpha_{11}) & O \end{bmatrix}$$

(c) One end of the member is submerged where U = ℓ

$$[AlF]_{Q_1} = \begin{bmatrix} 1 & O & O & O & (Z_1 + \ell\alpha_{13}) & -(Y_1 + \ell\alpha_{12}) \\ O & 1 & O & -(Z_1 + \ell\alpha_{13}) & O & X_1 + \ell\alpha_{11}) \\ O & O & 1 & (Y_1 + \ell\alpha_{12}) & -(X_1 + \ell\alpha_{11}) & \end{bmatrix}$$

B. When Q_2 is in use [AlF] matrix takes the following form:

$$[AlF]_{Q_2} = \begin{bmatrix} \ell & O & O & O & (Z_1\ell + \tfrac{1}{2}\ell^2\alpha_{13}) & -(Y_1\ell + \tfrac{1}{2}\ell^2\alpha_{12}) \\ O & \ell & O & -(Z_1\ell + \tfrac{1}{2}\ell^2\alpha_{13}) & O & (X_1\ell + \tfrac{1}{2}\ell^2\alpha_{11}) \\ O & O & \ell & (Y_1\ell + \tfrac{1}{2}\ell^2\alpha_{12}) & -(X_1\ell + \tfrac{1}{2}\ell^2\alpha_{11}) & O \end{bmatrix}$$

$$[DM] = \begin{bmatrix} b_{11} & 0 & 0 \\ 0 & b_{22} & 0 \\ 0 & 0 & b_{33} \end{bmatrix}$$

$$[\dot{U}] = \begin{bmatrix} \dot{U}_1 \\ U_2 \\ U_3 \\ U_4 \\ U_5 \\ U_6 \end{bmatrix} \quad , \qquad [U] = \begin{bmatrix} U_1 \\ U_2 \\ U_3 \\ U_4 \\ U_5 \\ U_6 \end{bmatrix}$$

Similarly, the hydrodynamic moment can be written as,

$$[M] = -([TM][M1] + [G][F]) \tag{30}$$

where

$$[M] = \begin{bmatrix} F_4 \\ F_5 \\ F_6 \end{bmatrix}$$

$$[TM] = \begin{bmatrix} 0 & \alpha_{13} & -\alpha_{12} \\ 0 & \alpha_{23} & -\alpha_{22} \\ 0 & \alpha_{33} & -\alpha_{32} \end{bmatrix}$$

$$[M1] = [AM][BT][A1M][\dot{U}] + [DM][BT][A1M][U]$$

and

$$[A1M] = \begin{bmatrix} \frac{1}{2}\ell^2 & 0 & 0 & 0 & (Z_{12}\frac{\ell^2}{2} + \frac{1}{3}\ell^3\alpha_{13}) & -(Y_{12}\frac{\ell^2}{2} + \frac{1}{3}\ell^3\alpha_{12}) \\ 0 & \frac{1}{2}\ell^2 & 0 & -(Z_{12}\frac{\ell^2}{2} + \frac{1}{3}\ell^3\alpha_{13}) & 0 & (X_{12}\frac{\ell^2}{2} + \frac{1}{3}\ell^3\alpha_{11}) \\ 0 & 0 & \frac{1}{2}\ell^2 & (Y_{12}\frac{\ell^2}{2} + \frac{1}{3}\ell^3\alpha_{12}) & -(X_{12}\frac{\ell^2}{2} + \frac{1}{3}\ell^3\alpha_{11}) & 0 \end{bmatrix}$$

$$[G] = \begin{bmatrix} 0 & -Z_1 & Y_1 \\ Z_1 & 0 & -X_1 \\ -Y_1 & X_1 & 0 \end{bmatrix}$$

In the following an example is given to determine the hydrodynamic forces on a horizontal circular cylinder member of a floating structure oscillating under the free surface using the calculation procedure developed above. (See Fig. 4.)

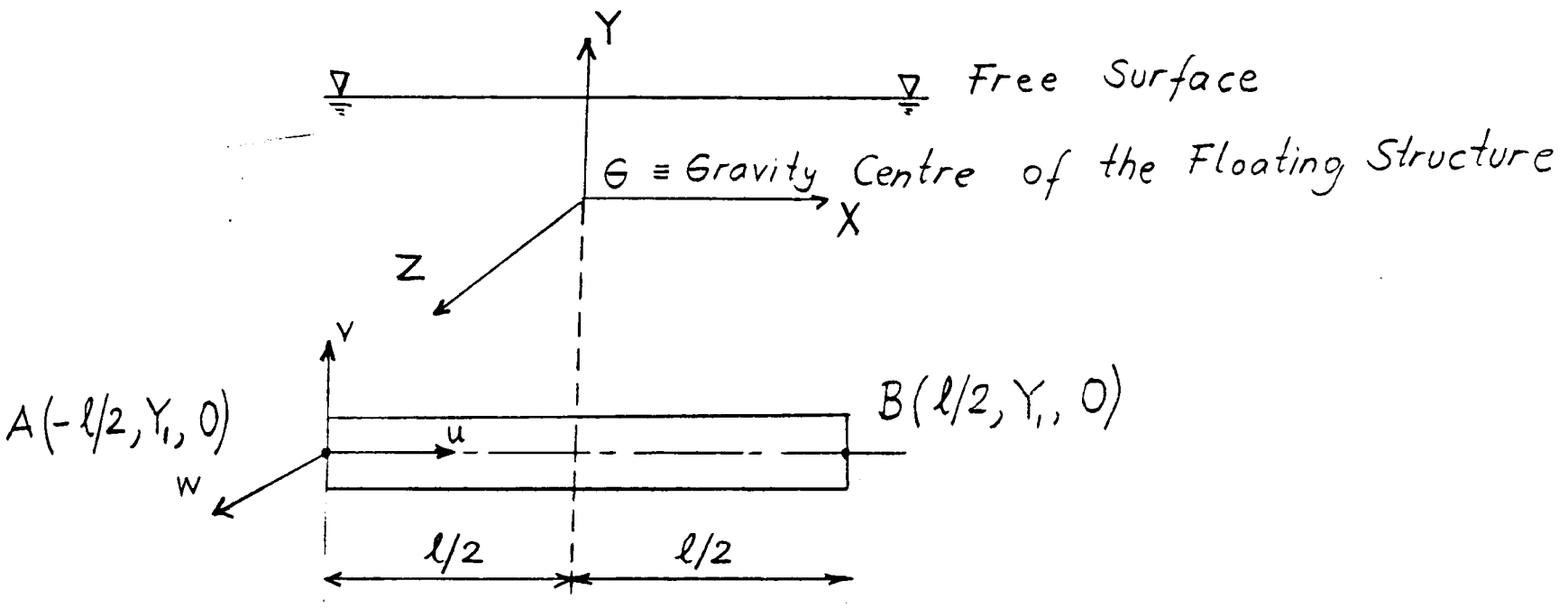

Fig. 4.

The Hydrodynamic forces can easily be calculated by determining the matrices given in equation (29).

$$[T] = \begin{bmatrix} 1 & 0 & 0 \\ 0 & 1 & 0 \\ 0 & 0 & 1 \end{bmatrix} \qquad (31)$$

$$[AM] = \begin{bmatrix} 0.424\rho\pi R^3 k_{11} & 0 & 0 \\ 0 & \rho\pi R^2 & 0 \\ 0 & 0 & \rho\pi R^2 \end{bmatrix} \tag{32}$$

$$[AT] = \begin{bmatrix} 1\ Q_1 & 0 & 0 \\ 0 & 1\ Q_2 & 0 \\ 0 & 0 & 1\ Q_2 \end{bmatrix} \tag{33}$$

$$[AlF]_{Q_1} = \begin{bmatrix} 2 & 0 & 0 & 0 & 0 & -2Y_1 \\ 0 & 2 & 0 & 0 & 0 & -\ell \\ 0 & 0 & 2 & 2Y_1 & 0 & 0 \end{bmatrix} \tag{34-A}$$

$$[AlF]_{Q_2} = \begin{bmatrix} \ell & 0 & 0 & 0 & 0 & -Y_1\ell \\ 0 & \ell & 0 & 0 & 0 & 0 \\ 0 & 0 & \ell & Y_1\ell & 0 & 0 \end{bmatrix} \tag{34-B}$$

If equations (31), (32), (33) and (34) are substituted in equation (29) and neglecting the damping terms, the following matrix equation is obtained:

$$\begin{bmatrix} F_1 \\ F_2 \\ F_3 \end{bmatrix} = -\begin{bmatrix} 0.848\rho\pi R^3 k_{11} & 0 & 0 & 0 & 0 & -Y_1 0.848\rho\pi R^3 k_{11} \\ 0 & \rho\pi R^2 \ell & 0 & 0 & 0 & 0 \\ 0 & 0 & \rho\pi R^2 \ell & Y_1 \ell \rho\pi R^2 & 0 & 0 \end{bmatrix} \begin{bmatrix} \dot{U}_1 \,|\, u=0 \\ \dot{U}_1 \,|\, u=\ell \\ \dot{U}_2 \\ \dot{U}_3 \\ \dot{U}_4 \\ \dot{U}_5 \\ \dot{U}_6 \end{bmatrix} \qquad (35)$$

If we transfer the centre of rotation of the cylinder to the centre of rotation of the structure by setting $Y_1=0$ equation (35) becomes identical to equation (12).

Similarly, the hydrodynamic moments can be obtained using equation (30) as follows. (See Fig. 4.)

$$[TM] = \begin{bmatrix} 0 & 0 & 0 \\ 0 & 0 & -1 \\ 0 & 1 & 0 \end{bmatrix} \quad (36), \qquad [G] = \begin{bmatrix} 0 & 0 & Y_1 \\ 0 & 0 & \ell/2 \\ -Y_1 & -\ell/2 & 0 \end{bmatrix} \quad (37)$$

$$[AM] = \begin{bmatrix} a_{11}R^2 & 0 & 0 \\ 0 & \rho\pi R^2 & 0 \\ 0 & 0 & \rho\pi R^2 \end{bmatrix} \quad (38), \qquad [BT] = \begin{bmatrix} 1 & 0 & 0 \\ 0 & 1 & 0 \\ 0 & 0 & 1 \end{bmatrix} \quad (39)$$

$$a_{11} = 0.424\ \rho\pi R^3 k_{11}$$

$$[A1M] = \begin{bmatrix} 0 & 0 & 0 & 0 & 0 & 0 \\ 0 & \frac{1}{2}\ell^2 & 0 & 0 & 0 & \frac{1}{12}\ell^3 \\ 0 & 0 & \frac{1}{2}\ell^2 & \frac{Y_1\ell^2}{2} & -\frac{1}{12}\ell^3 & 0 \end{bmatrix} \quad (40)$$

If we substitute equations (35) - (40) into equation (30) the hydrodynamic moment equation becomes,

$$\begin{bmatrix} F_4 \\ F_5 \\ F_6 \end{bmatrix} = \begin{bmatrix} 0 & 0 & Y_1\rho\pi R^2\ell & Y_1^2\rho\pi R^2\ell & 0 & 0 \\ 0 & 0 & 0 & 0 & \frac{\ell^3}{12}\rho\pi R^2 & 0 \\ -Y_1 0.848\rho\pi R^3 k_{11} & 0 & 0 & 0 & 0 & Y_1^2 0.848\rho\pi R^3 k_{11} + \frac{1}{12}\ell^3\rho\pi R^2 \end{bmatrix} \begin{bmatrix} \dot{U}_1 \\ \dot{U}_2 \\ \dot{U}_3 \\ \dot{U}_4 \\ \dot{U}_5 \\ \dot{U}_6 \end{bmatrix} \quad (41)$$

If we transfer the centre of rotation of the cylinder to the centre of rotation of the structure by setting $Y_1=0$, then matrix equation (41) becomes identical to equation (12).

The total hydrodynamic forces and moments on the structure can be calculated by summing the forces and moments on each individual member as follows:

$$[FT] = \sum_{i=1}^{m} [F]_i \tag{42}$$

$$[MT] = \sum_{i=1}^{m} [M]_i \tag{43}$$

3. CORRECTIONS TO THE ADDED MASS VALUE IN UNBOUNDED FLUID DUE TO THE FREE SURFACE AND INTERFERENCE EFFECT OF CLOSELY SPACED MEMBERS

As mentioned in Section 1 one may obtain added mass and damping coefficients including free surface effects, i.e. the frequency dependence of the added mass and the damping coefficients, by finding the velocity potential ϕ_i. In the literature basically two approaches have been used to determine ϕ_i values due to the harmonic rigid-body motion of floating structures. The first approach was initiated by Ursell whose work may be considered the beginning of the modern history of theoretical work on forced-oscillation problems [1,2].

Ursell derived the velocity potential for a circular cylinder oscillating on the free-surface by an infinite series of non-orthogonal polynomials (multipoles) and then adding to this a suitable wave source at the origin of the cylinder. This superposition satisfies the physical phenomena since the oscillating cylinder produces standing waves in its vicinity and propagating waves at a large distance from the cylinder.

Multipole and source potentials satisfy the Laplace equation and linear free surface conditions. The source potential also satisfies

the radiation condition. The only unknowns in the multipole potential which are source strengths can be determined from the boundary conditions on the body surface. In this section Ursell's results will be used in the suggested procedure to correct added mass values when the circular cylindrical members of offshore structures are working near to the free surface.

An alternative approach to Ursell's solution is the method of integral equations following the application of Green's theorem.

The potential function due to the rigid body motion may be obtained in a manner similar to that in which the scattering wave potential has been obtained in equation 2.17. The Fredholm integral equation in this case takes the following form:

$$- f_j(x,y,z) + \frac{1}{2\pi} \iint_S f_j(\xi,\eta,\zeta) \frac{\partial G}{\partial n}(x,y,z,\xi,\eta,\zeta)\, dS = i\omega X_j N \quad (44)$$

where $N = n_j$ for $j = 1,2,3$

$N = (\vec{r} \wedge \vec{n})_{j-3}$ for $j=4,5,6.$

Equation (44) can only be solved numerically to find f_j values and this requires a considerable amount of computer space and time. Since in this study unbounded added-mass values have been used, a correction procedure will be suggested to take the free surface effect into account. In Section 2.1.7 of Chapter 2 the effect of fixed boundaries on the wave intertia coefficients has been calculated. The same calculation procedure may be applied to take into account the interference effect between the free surface and the body as follows:

$$a_{22} = a_{33} = 1 + \frac{\int_0^{2\pi} \frac{\sin^2\theta}{1+2\alpha\cos\theta+\alpha^2}\, d\theta}{\pi} \rho\pi R^2 \quad (45)$$

where $\alpha = \frac{2h}{R}$

h: The distance between the free surface and the centre of cylinder.

Initially equation (45) was derived in Section 2.1.7 of Chapter 2 to take the wall effect into account for the fluid or body motion parallel to the wall. However, Yamamoto, in reference [7], shows that the added mass coefficient given with the following expression to take the effect of wall proximity into account is independent of direction of oscillation:

$$a_{22} = a_{33} = (1 + \frac{2}{\alpha^2})\ \rho\pi R^2 \qquad (46)$$

Since equations (45) and (46) are similar, the result of independence of direction of motion with respect to the free surface in equation (46) may be applied to equation (45). See also Fig. 21 of chapter 2.

To correct the frequency dependence of the added mass coefficients Ursell's results will be used to correct the unbounded added mass values in heave oscillation [1,2]. The added mass values of a heaving circular cylinder on the free-surface given by Ursell can be represented by the following approximation:

$$k_{22}(kR) = 0.6348(kR)^{-0.26035} \qquad \text{for } kR > 0 \qquad (47)$$

Either equation (45) or (46) may be combined with equation (47) to correct unbounded added mass values for the free surface effect with the following steps. The free surface effect vanishes as the ratio of submergence/diameter approaches 2.5.

(a) Calculate the increase, say a, in the unbounded added mass as a percentage due to the fixed free surface from either equation (45) or (46). If the increase is 2.0% or less it is not necessary to correct the added mass values for frequency dependence.

(b) If the increase in (a) is 2.0% or more obtain an increase or decrease of the unbounded added mass values, say b, due to the frequency dependence from equation (47).

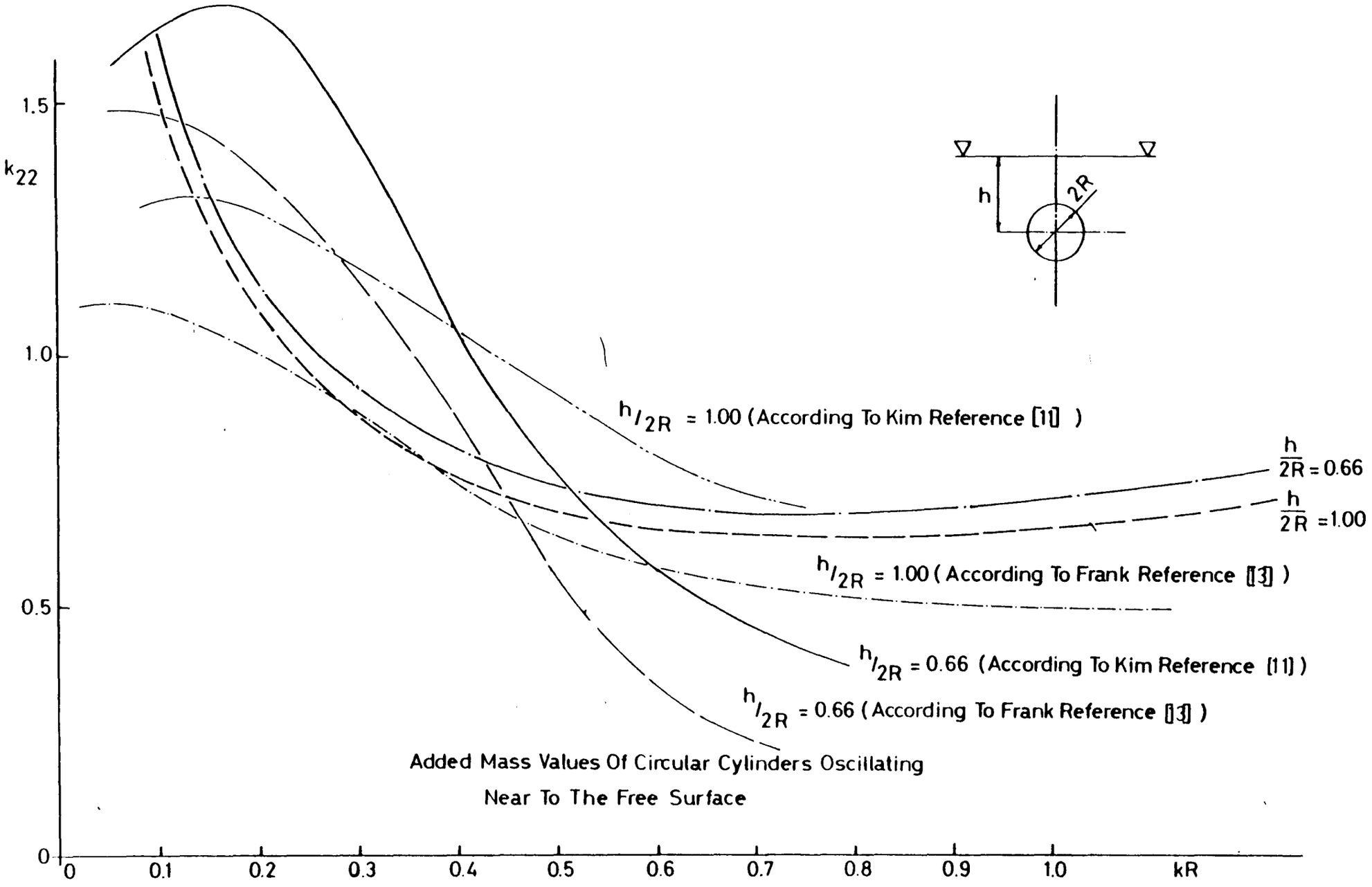
1.5
1.0
0.5
0
k_{22}
h
2R
$h/_{2R}$ = 1.00 (According To Kim Reference [11])
$\frac{h}{2R}$ = 0.66
$\frac{h}{2R}$ = 1.00
$h/_{2R}$ = 1.00 (According To Frank Reference [13])
$h/_{2R}$ = 0.66 (According To Kim Reference [11])
$h/_{2R}$ = 0.66 (According To Frank Reference [13])
Added Mass Values Of Circular Cylinders Oscillating
Near To The Free Surface
0
0.1
0.2
0.3
0.4
0.5
0.6
0.7
0.8
0.9
1.0
kR

Fig. 5

Combination of (a) and (b) takes the following form:

$$a_{22} = m_{22}(1+a)(1+b) \tag{48}$$

where

$$a = \frac{\int_0^{2\pi} \frac{\sin^2\theta}{1+2\alpha\cos\theta+\alpha^2}\, d\theta}{\pi} \quad \text{or} \quad a = \frac{2}{\alpha^2}$$

$$b = 0.6343(kR)^{-0.26035} - 1$$

Added mass values calculated using this approximate method are compared with those obtained from the complete solutions based on Green's theorem [11,13] in Figure 5.

Similarly, added mass values in sway motion may be corrected for the free surface with the following approximation:

$$a_{33} = m_{33}(1+a) \tag{49}$$

The correction in the added mass values due to the circular cylindrical members' close proximity may be obtained by using the equations (2.77-A), 2.79), 2.84) and (2.86) given in Chapter 2.

4. DETERMINATION OF DAMPING COEFFICIENTS

Damping coefficients relate the floating structures rigid body velocities to the hydrodynamic damping (or drag) forces as was defined in Section 1. Two types of damping forces may be experienced on the floating structures which oscillate near or on the free surface.

(a) Wave damping forces due to the dissipation of energy in the form of surface waves which are generated as a result of rigid body motion of floating structures.

(b) The viscous damping forces which are due to the turbulent flow in the lee of a body.

4.1 Wave Damping Forces

As was mentioned in Section 1, wave damping forces can be obtained with procedures similar to the determination of the hydrodynamic added mass forces, by calculating the velocity potential $\phi_j(X,Y,Z)$ [1,2,3].

Newman [8] shows a relation between the wave exciting forces and the wave damping forces using the energy radiation of the oscillating structure at infinity. In the three dimensional case the relation between the damping coefficient and exciting force was given in reference [8] as:

$$b_{ii} = \frac{\omega k}{4\pi\rho g^2 (0.5\ H_w)^2} \int_0^{2\pi} [F_i(\beta)]^2\ d\beta \qquad (50)$$

where β: Angle of oncoming wave propagation.

In reference 9 the relation between damping coefficients and the exciting wave forces for a body which is symmetrical about X=0 plane was given as:

$$b_{ii} = \frac{\omega}{\rho g^2 (0.5\ H_w)^2} F_i^2 \qquad (51)$$

The wave damping forces associated with the free surface approaches zero as the depth of the submergence/diameter ratio approaches 2.5. Since generally the principal parts of all members of semi-submersible type floating platforms are deeply submerged in their operational modes the wave damping is of little significance. However, the free surface effect in added-mass and damping coefficients may be of importance for some of the floating offshore structures such as crane or pipe laying barges.

Experimental values of added virtual mass and damping coefficients for the geometries of cylinder, rectangle and sphere oscillating near

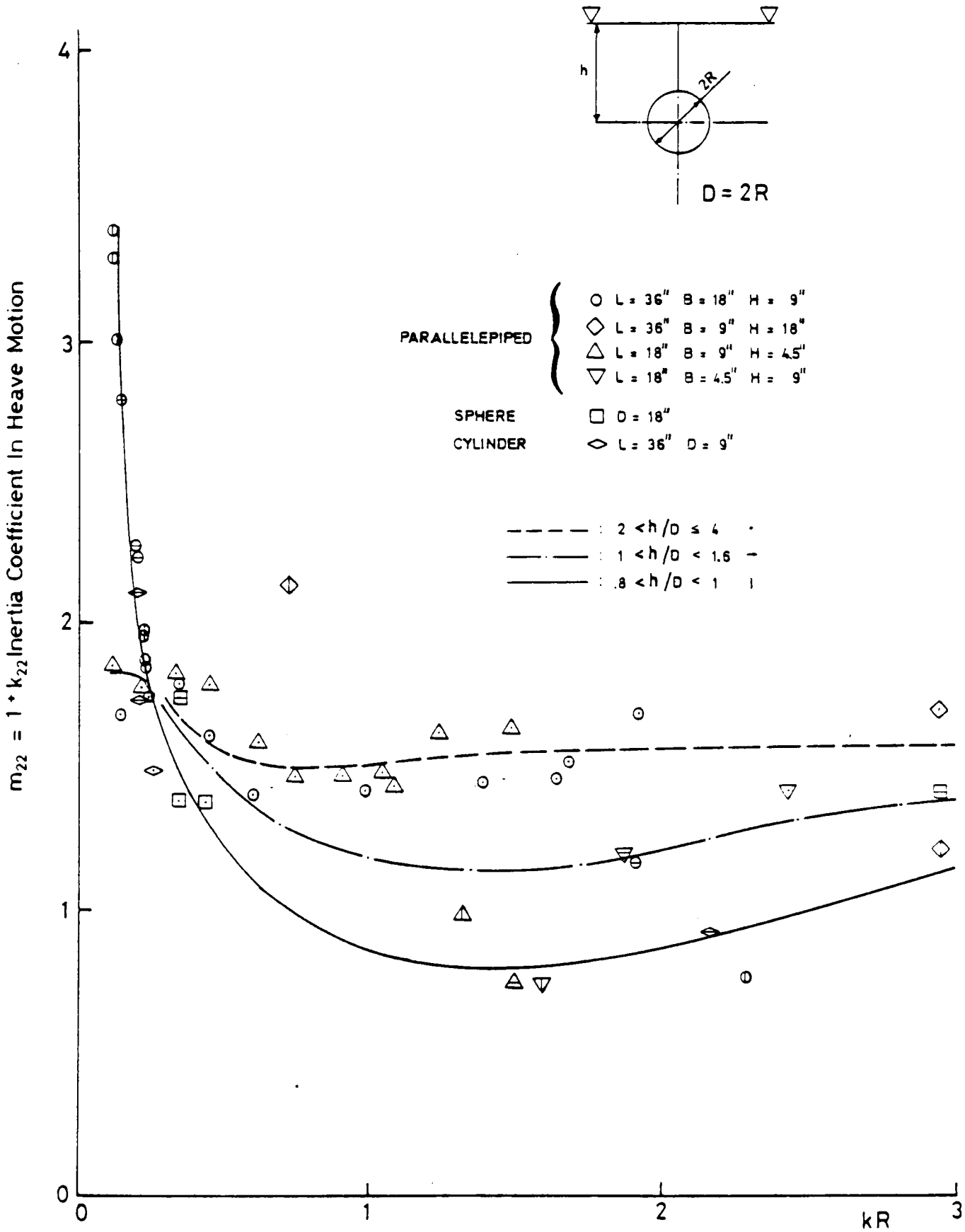

Measured Values Of Inertia Coefficient Vs kR
(From Reference [12])

Fig. 6

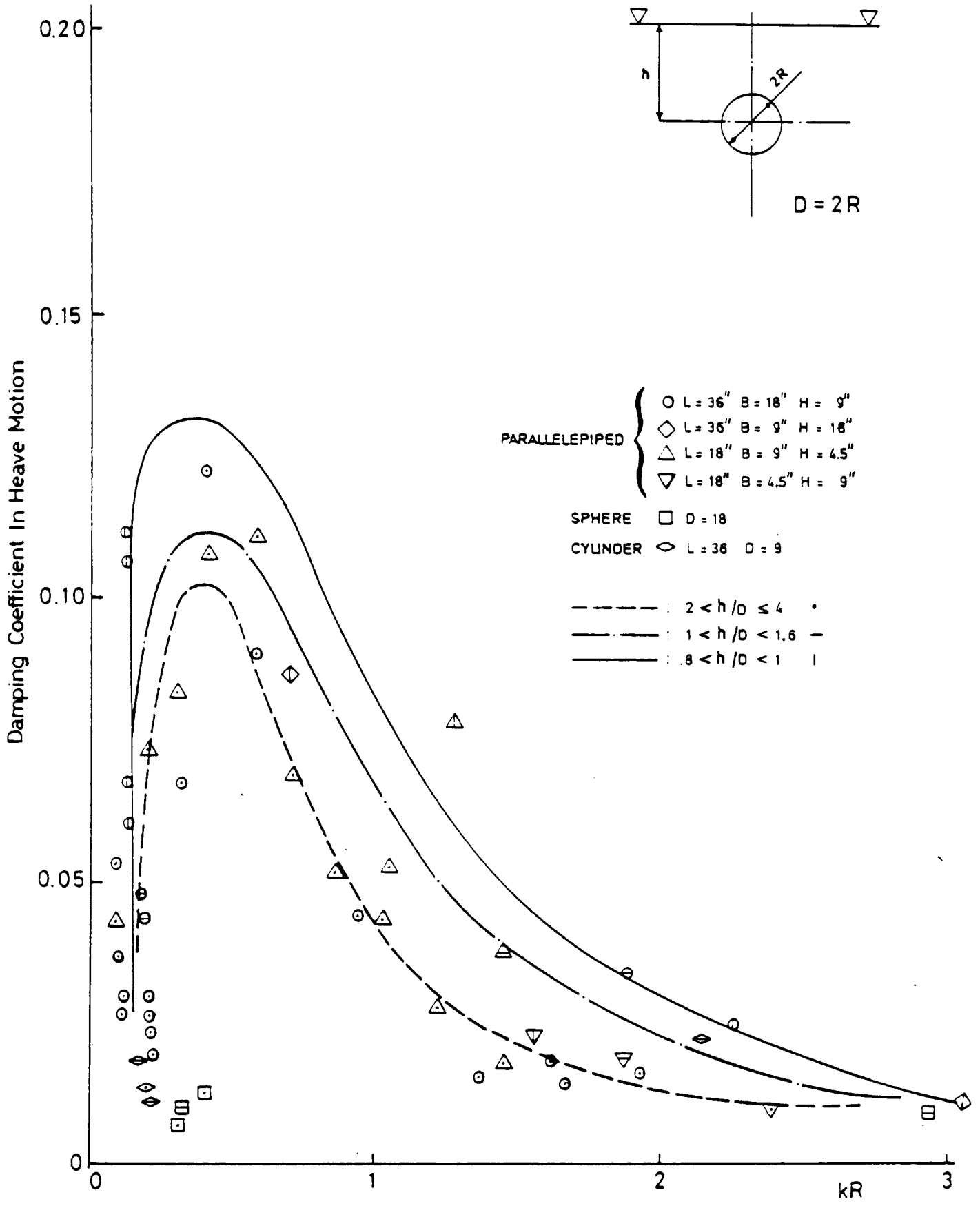

Measured Values Of Damping Coefficient Vs kR

(From Reference [12])

Fig. 7

the free surface are presented in reference [12]. They are also presented in Figs. 6,7.

It may be of interest to point out the similarity between the added mass coefficients given in Figs 6 and 7 and the added mass values for circular cylinders given in Fig. 5, which were produced according to the suggested method in Section 3. -

4.2 Viscous Damping Forces

The viscous damping forces occur due to a deviation of the pressure distribution from its ideal fluid value. Similar to the wave drag force calculations, viscous damping forces may be expressed as a quadratic function of the structure's rigid body velocity and the drag coefficient will be determined for the appropriate Reynolds number However, when viscous damping forces are calculated as a quadratic function of the velocity, the motion equation (68) cannot be linear any longer and this adds complications to the solution of the differential motion equations.

Blagoveschchensky [10] suggest a method of calculating non-linear viscous damping forces using equivalent linear viscous damping coefficients and the linear velocity terms. The linear drag coefficient is obtained by setting the energy dissipation due to the linear viscous forces equal to the energy dissipation of non-linear viscous forces. That is,

$$b_{ii} \int_0^{\frac{T}{4}} U_i^2 \, dt = C_D \int_0^{\frac{T}{4}} U_i^3 \, dt \qquad (52)$$

replacing U_i with $U_{i,M}$ Sinωt in equation (52) b_{ii} becomes

$$b_{ii} = \frac{8U_{i,M}}{3\pi} C_D \qquad (53)$$

or

$$b_{ii} = \frac{8\omega X_i}{3\pi} C_D \qquad (53\text{-A})$$

To determine b_{ii} values $U_{i,M} = \omega X_i$ should be known and this can only be achieved by assuming an amplitude of motion.

Assuming an amplitude of motion linear damping coefficients are calculated and then the motion equations are solved. Motion amplitudes obtained from these equations can now be used to determine new linear damping coefficients and the motion equations again solved. This iteration procedure continues until two successive linear damping coefficients are close enough to each other.

5. CALCULATION OF RESTORING FORCES

In this section the restoring forces and moments which are due to the displacement of a floating structure from its equilibrium state will be discussed. The restoring forces and moments can be hydrostatic or elastic. The total force and moments due to the mass of the body plus the external forces such as mooring forces, must be in equilibrium at rest. When the floating structure's under water displacement changes by movements in translational or in rotational modes, restoring forces and moments occur to satisfy the static equilibrium.

For floating structures the hydrostatic restoring forces and moments can be related to the translational or rotational displacements with the following matrix equation by making use of standard naval architectural formulae [6].

$$\begin{bmatrix} F_1 \\ F_2 \\ F_3 \\ F_4 \\ F_5 \\ F_6 \end{bmatrix}_{HIDR} = - \begin{bmatrix} 0 & 0 & 0 & 0 & 0 & 0 \\ 0 & \rho g A_W & 0 & 0 & 0 & 0 \\ 0 & 0 & 0 & 0 & 0 & 0 \\ 0 & 0 & 0 & \rho g \nabla GM_T & 0 & 0 \\ 0 & 0 & 0 & 0 & 0 & 0 \\ 0 & 0 & 0 & 0 & 0 & \rho g \nabla GM_L \end{bmatrix} \begin{bmatrix} X_1 \\ X_2 \\ X_3 \\ X_4 \\ X_5 \\ X_6 \end{bmatrix} \tag{54}$$

where

A_W: Total water plane area of surface piercing members.

∇ : Displacement of the floating structure.

GM_T, GM_L: Transverse and the longitudinal metacentric heights respectively and given as

$$GM_{T,L} = KB + BM_{T,L} - KG$$

where

KB: Centre of immersed volume

$$BM_{T,L} = \frac{I_{T,L}}{\nabla}$$

I_T = Total moment of inertia of the water plane area of surface piercing members about X axis.

I_L = Total moment of inertia of the water plane area of surface piercing members about Z axis.

K_G = Centre of gravity of the floating structure.

In this study the effects of catenary mooring systems in motion response calculations are neglected. The mooring forces have to be calculated as a function of the displacements of the floating structure and the catenary and the elastic properties of the mooring lines and their hydrodynamic interactions with the waves and the currents. No attempt has been made to solve this problem here.

6. CALCULATION OF BODY FORCES

In this section inertia forces and moments defined from Newton's second law as the multiplication of actual mass of a cylinder element $\rho_M dV$ and the absolute body acceleration of the structure will be calculated.

$$\vec{F} = M\dot{\vec{U}}_G \tag{55}$$

$$\vec{M} = \rho_M \iiint_V \vec{r}_A \wedge \dot{\vec{U}}_i \, dV \tag{56}$$

where M : Total mass of the floating structure

$\dot{\vec{U}}_G$: Acceleration vector at the gravity centre of the platform

$\vec{r}_A = \vec{r}_G + \vec{r}_i$

$\vec{r}_G$: Position vector of centre of rotation from the centre of gravity

ρ_M: Mass density

$\dot{\vec{U}}_i$: Acceleration vector at the centre of the mass element i.

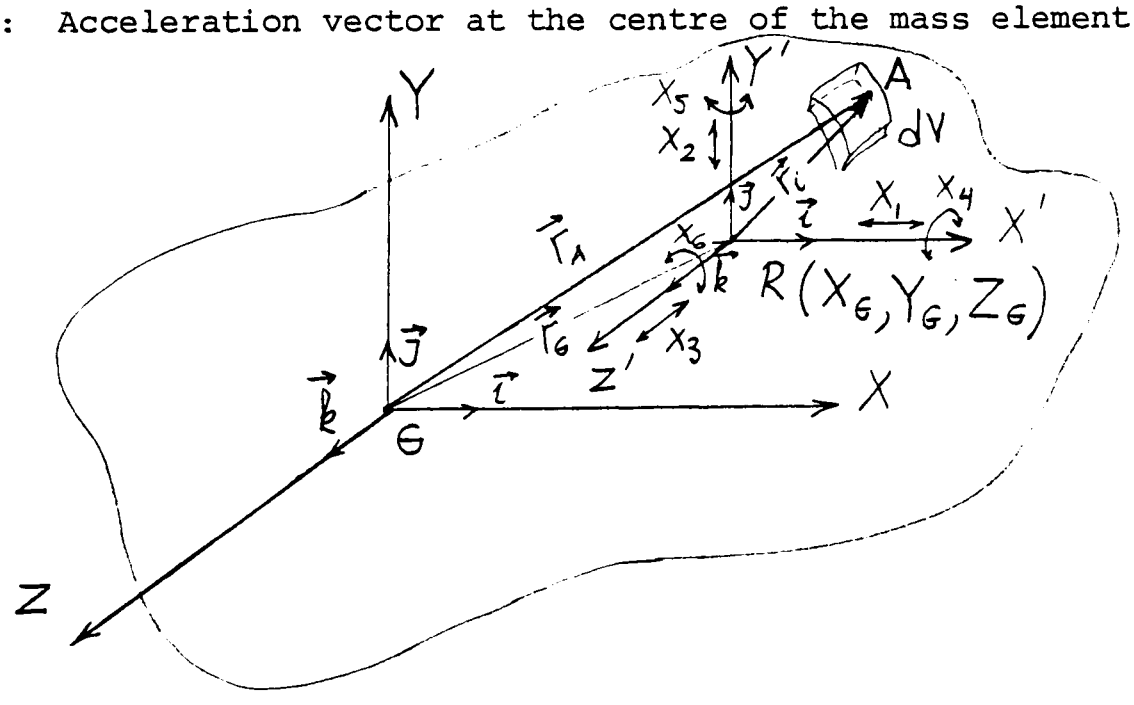

Fig. 8

$\vec{r}_i$ = Position vector of the mass element (i) from the centre of rotation.

The total force vector can be calculated in terms of translational and rotational acceleration and the total mass as follows.

Since

$$\dot{\vec{U}}_G = \dot{\vec{U}}_{S,T} + \dot{\vec{U}}_{S,R} \wedge \vec{r}_G \tag{57}$$

where

$$\dot{\vec{U}}_{S,T} = \dot{U}_1\vec{i} + \dot{U}_2\vec{j} + \dot{U}_3\vec{k}$$

$$\dot{\vec{U}}_{S,R} = \dot{U}_4\vec{i} + \dot{U}_5\vec{j} + \dot{U}_6\vec{k}$$

$$\vec{r}_G = X_G\vec{i} + Y_G\vec{j} + Z_G\vec{k}$$

If equation (57) is substituted in equation (55) the total force vector becomes:

$$\vec{F} = M(\dot{U}_1 + \dot{U}_5Z_G - \dot{U}_6Y_G)\vec{i} + M(\dot{U}_2 + \dot{U}_6X_G - \dot{U}_4Z_G)\vec{j} + M(\dot{U}_3 + \dot{U}_4Y_G - \dot{U}_5X_G)\vec{k} \tag{58}$$

If we replace $\vec{r}_A$ with $\vec{r}_G+\vec{r}_i$ and $\dot{\vec{U}}_i$ with $\dot{\vec{U}}_{S,T}+\dot{\vec{U}}_{S,R}\wedge\vec{r}_G$ in equation (56), the following equation is obtained to calculate moments due to the structure's rigid body acceleration:

$$\vec{M} = \rho_M \iiint_V \{[- Z_G\dot{U}_2 + Y_G\dot{U}_3 + \dot{U}_4(Y_i^2+Z_i^2) - X_iY_i\dot{U}_5 - X_iZ_i\dot{U}_6]\vec{i} + [Z_G\dot{U}_1 - X_G\dot{U}_3 - \dot{U}_4Y_iX_i + \dot{U}_5(X_i^2+Z_i^2) - \dot{U}_6Y_iZ_i]\vec{j} + [- Y_G\dot{U}_1 + X_G\dot{U}_2 - Z_iX_i\dot{U}_4 - Z_iY_i\dot{U}_5 + \dot{U}_6(X_i^2+Y_i^2)]\vec{k}\} \, dV \tag{59}$$

The basic definitions to find the mass and mass moments of inertia can be written as follows:

$$M = \rho_M \iiint_V dV \tag{60}$$

$$I_{XX} = \rho_M \iiint_V (Y_i^2+Z_i^2) \, dV \tag{61-A}$$

$$I_{YY} = \rho_M \iiint_V (X_i^2+Z_i^2) \, dV \tag{61-B}$$

$$I_{ZZ} = \rho_M \iiint_V (X_i^2+Y_i^2) \, dV \tag{61-C}$$

$$I_{XY} = I_{YX} = - \rho_M \iiint_V X_i Y_i \, dV \tag{61-D}$$

$$I_{XZ} = I_{ZX} = - \rho_M \iiint_V X_i Z_i \, dV \tag{61-E}$$

$$I_{YZ} = I_{ZY} = - \rho_M \iiint_V Y_i Z_i \, dV \tag{61-F}$$

Equations (58) and (59) can be summarised with the following matrix equation using equations (60) - (61-F):

$$\begin{bmatrix} F_1 \\ F_2 \\ F_3 \\ F_4 \\ F_5 \\ F_6 \end{bmatrix} = \begin{bmatrix} M & 0 & 0 & 0 & MZ_G & -MY_G \\ 0 & M & 0 & -MZ_G & 0 & MX_G \\ 0 & 0 & M & MY_G & -MX_G & 0 \\ 0 & -MZ_G & MY_G & I_{XX} & I_{XY} & I_{XZ} \\ MZ_G & 0 & -MX_G & I_{YX} & I_{YY} & I_{YZ} \\ -MY_G & MX_G & 0 & I_{ZX} & I_{ZY} & I_{ZZ} \end{bmatrix} \begin{bmatrix} \dot{U}_1 \\ \dot{U}_2 \\ \dot{U}_3 \\ \dot{U}_4 \\ \dot{U}_5 \\ \dot{U}_6 \end{bmatrix} \tag{62}$$

For structures having cylindrical members, the mass moment of inertia values can be generalised in terms of the mass distribution and reference system for each member. It will be assumed that the mass of each volume element can be concentrated at the centre of this volume. Since the diameter over length ratio is generally small this assumption may be acceptable and can be formulated as follows:

$$\rho_M \iiint_V dV = \rho_M \int_{u=0}^{\ell} \pi R^2 \, dU \tag{63}$$

Following the above statement the X_i, Y_i, Z_i co-ordinates can be written in the individual member's reference system as:

$$X_i = u\alpha_{11} + X_1 \tag{64-A}$$

$$Y_i = u\alpha_{21} + Y_1 \tag{64-B}$$

$$Z_i = u\alpha_{31} + Z_1 \tag{64-C}$$

If we substitute equations (64-A) - (64-C) into equations (61-A) - (61-F) the following mass moment of inertia values are obtained for an individual member:

$$i_{XX_i} = m_i \left[\frac{1}{3}\ell^2(\alpha_{21}^2 + \alpha_{31}^2) + \ell(Y_1\alpha_{21} + Z_1\alpha_{31}) + Y_1^2 + Z_1^2\right] \quad (65\text{-A})$$

$$i_{YY_i} = m_i \left[\frac{1}{3}\ell^2(\alpha_{11}^2 + \alpha_{31}^2) + \ell(X_1\alpha_{11} + Z_1\alpha_{31}) + X_1^2 + Z_1^2\right] \quad (65\text{-B})$$

$$i_{ZZ_i} = m_i \left[\frac{1}{3}\ell^2(\alpha_{11}^2 + \alpha_{21}^2) + \ell(X_1\alpha_{11} + Y_1\alpha_{21}) + X_1^2 + Y_1^2\right] \quad (65\text{-C})$$

$$i_{XY_i} = m_i \left[\frac{1}{3}\ell^2\alpha_{11}\alpha_{21} + \frac{\ell}{2}(Y_1\alpha_{11} + X_1\alpha_{21}) + X_1Y_1\right] \quad (65\text{-D})$$

$$i_{XZ_i} = m_i \left[\frac{1}{3}\ell^2\alpha_{11}\alpha_{31} + \frac{\ell}{2}(Z_1\alpha_{11} + X_1\alpha_{31}) + X_1Z_1\right] \quad (65\text{-E})$$

$$i_{YZ_i} = m_i \left[\frac{1}{3}\ell^2\alpha_{21}\alpha_{31} + \frac{\ell}{2}(Z_1\alpha_{21} + Y_1\alpha_{31}) + Y_1Z_1\right] \quad (65\text{-F})$$

The total moment of inertia of mass can be calculated by summing equations (65-A) - (65-F) as follows:

$$I_{XX} = \sum_{i=1}^{m} i_{XX_i} \quad (66\text{-A})$$

$$I_{YY} = \sum_{i=1}^{m} i_{YY_i} \quad (66\text{-B})$$

$$I_{ZZ} = \sum_{i=1}^{m} i_{ZZ_i} \quad (66\text{-C})$$

$$I_{XY} = \sum_{i=1}^{m} i_{XY_i} \quad (66\text{-D})$$

$$I_{XZ} = \sum_{i=1}^{m} i_{XZ_i} \quad (66\text{-E})$$

$$I_{YZ} = \sum_{i=1}^{m} i_{YZ_i} \quad (66\text{-F})$$

7. DERIVATION AND SOLUTION OF MOTION RESPONSE EQUATIONS

Calculation procedures have been developed to determine the wave forces due to the absolute fluid particle motion (Chapter 3), and the hydrodynamic and body-inertia forces due to the absolute platform motion in this chapter. Since these forces should be in balance at any instant the following equilibrium equation can be written as the motion response equation:

$$-\vec{F}_W + \vec{F}_H + \vec{F}_{HIDR} + \vec{F}_I = 0 \qquad (67)$$

where

$\vec{F}_W$ = Wave excited force and moment vector given in equations (3.42) and (3.46),

$\vec{F}_H$ = Hydrodynamic force and moment vector given in equations (28) and (28-A),

$\vec{F}_{HIDR}$ = Restoring force vector given in Section 5.

$\vec{F}_I$ = The body-inertia force and moment vector given in equations (55) and (56).

Equation (67) can be rearranged as motion dependent terms on the left hand side and time dependent forcing terms on the right hand side to obtain the following form of six linear simultaneous, second-order differential equations:

$$[M][\ddot{X}] + [C][\dot{X}] + [K][X] = [F_W] \qquad (68)$$

where

$$[M] = [BM] + \left[\frac{[T][AM][AT][A1F]}{[MH1] + [MH2]}\right]$$

[BM]: Body-mass matrix derived in equation (62)

[MH1] = [TM][AM][BT][A1M]

[MH2] = [G][T][AM][AT][A1F]

$$[C] = \left[\frac{[T][DM][AT][A1F]}{[CH1] + [CH2]}\right]$$

$[CH1] = [TM][DM][BT][A1M]$

$[CH2] = [G][T][DM][AT][A1F]$

$[K]$: The restoring force matrix defined in equation (22)

$[\ddot{X}] = [\dot{U}]$: Column matrix of acceleration of the structure

$[\dot{X}] = [U]$: Column matrix of velocity of the structure

$[X]$: Column matrix of translational and rotational displacement of the structure

$[TM], [AM], [AT], [A1F], [DM]$: Defined in equation (29)

$[G], [A1M], [BT]$: Defined in equation (30).

The six simultaneous second-order linear differential equations given above which take the coupling effects between the different motion modes into account can be solved using standard computer library programs. One may also reduce the motion equations to a set of single degree of freedom equations for the corresponding principal motion modes by omitting the coupling terms. For example, the following single degree of freedom equation can be written for the heave motion of a floating structure.

$$(M + M'_{22})\ddot{X}_2 + C_{22}\dot{X}_2 + K_{22}X_2 = F_{w,HV} \qquad (69)$$

where

M'_{22} : Added mass of the structure in heave motion

C_{22} : Damping coefficient of the structure in heave motion

$K_{22} = \rho g A_w$

A_w : Total water plane area of surface piercing members

$F_{w,HV}$: Total heave force on the structure.

Although $F_{w,HV}$ in equation (69) is not a constant harmonic type function due to its variation with motion, it will be regarded as

constant at each discrete frequency and the standard solution for a single degree of freedom system will be applied to solve equation (69) as follows:

$$X_2 = X_{2_O} \cos\omega t \tag{70}$$

$$\text{where } X_{2_O} = \frac{F_{w,HV}}{\sqrt{(K_{22} - (M + M''_{22})\omega^2)^2 + C_{22}^2\omega^2}} \tag{70-A}$$

The phase angle between the applied force and the motion is given by:

$$\alpha = \tan^{-1} \frac{C_{22}\omega}{K_{22} - (M + M'')\omega^2} \tag{70-B}$$

It is usually convenient to write equation (70-A) in terms of frequency ratio and damping ratio as follows:

$$X_{2_O} = \frac{F_{w,HV}}{K_{22}\sqrt{(1-r^2)^2 + (2rd)^2}} \tag{71}$$

and phase angle

$$\alpha = \tan^{-1} \frac{2rd}{1-r^2} \tag{71-A}$$

where

$$r = \frac{\omega}{\omega_n} = \frac{\text{forcing frequency}}{\text{natural frequency}} \tag{71-B}$$

$$\omega_n = \sqrt{\frac{K_{22}}{M + M'_{22}}} \tag{71-C}$$

$$d = \frac{C_{22}}{2\sqrt{(M + M'_{22})K_{22}}} = \frac{\text{damping value}}{\text{critical damping value}} \tag{71-D}$$

The amplitude of response can also be represented in dimensionless form by defining the magnification factor, Q as follows:

$$Q = \frac{\text{motion amplitude}}{\text{equivalent static displacement}} \tag{72}$$

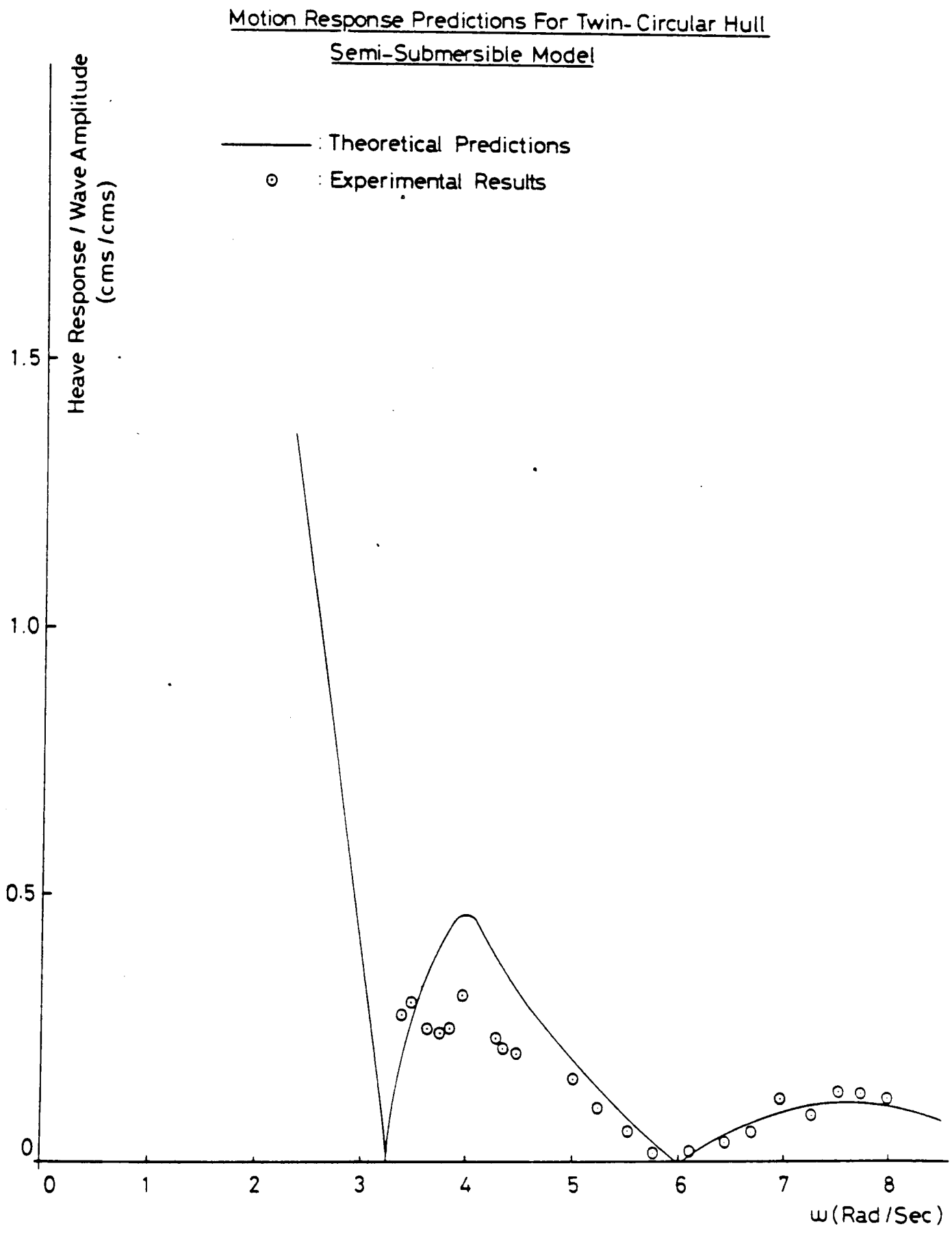
Motion Response Predictions For Twin-Circular Hull
Semi-Submersible Model
: Theoretical Predictions
: Experimental Results
Heave Response / Wave Amplitude
(cms / cms)
1.5
1.0
0.5
0
0
1
2
3
4
5
6
7
8
ω (Rad / Sec)

Fig. 9

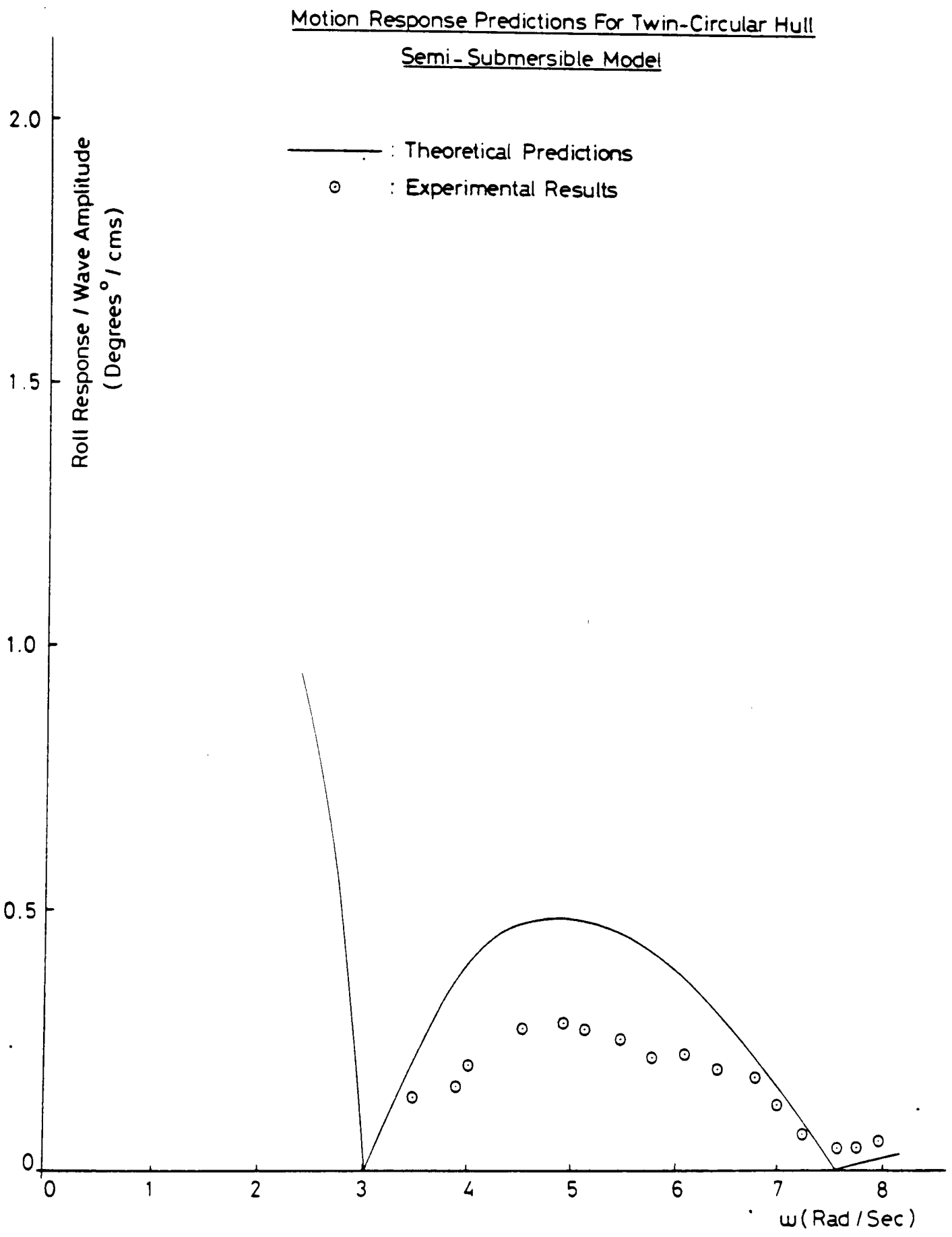
Motion Response Predictions For Twin-Circular Hull
Semi-Submersible Model
: Theoretical Predictions
: Experimental Results
Roll Response / Wave Amplitude
(Degrees ° / cms)
2.0
1.5
1.0
0.5
0
0
1
2
3
4
5
6
7
8
ω (Rad / Sec)

Fig. 10

$$Q = \frac{X_{2,O}}{F_{w,HV}/K_{22}} = \frac{1}{\sqrt{(1-r^2)^2 + (2rd)^2}} \qquad (72\text{-A})$$

An analysis of equation (72-A) reveals that if the forcing frequency is less than the natural frequency, the motion response is controlled by restoring forces and the mass of the structure and damping would have very little effect in controlling the response. If the forcing frequency is near, or equal to the natural frequency, the motion response will be very much larger than the static displacement, particularly when the damping is low. In the design of stable floating platforms this resonance region must be avoided, in the region of higher frequencies the response is reduced and controlled by the mass of structure and damping is not significant.

The single degree of freedom equations of heave and roll motion are applied to the semi-submersible model structure shown in figure 29 of Chapter 5 (details of the model are given in Chapter 7). The heave and the roll motion response predictions are compared with the experimental results in figures 9 and 10 respectively. Agreement between the predictions and the experimental results for heave is reasonably good. The over prediction of the heave results around the second peak may be explained by the changes in the heave forces due to roll motion. In addition, the harnesses which hold the model against drift forces may also effect the heave motion. These effects only become significant when heave magnitudes are large. The roll motion predictions do not agree with the experimental results as well as the heave motion predictions do. Possible reasons for this are:

a) The assumed centre of rotation may not be close to the actual centre of rotation while the structure is oscillating in heave and roll modes.

PHASE ANGLE PREDICTIONS, BETWEEN HEAVING FORCE AND HEAVING DISPLACEMENT, OF TWIN CIRCULAR HULL SEMI-SUBMERSIBLE MODEL

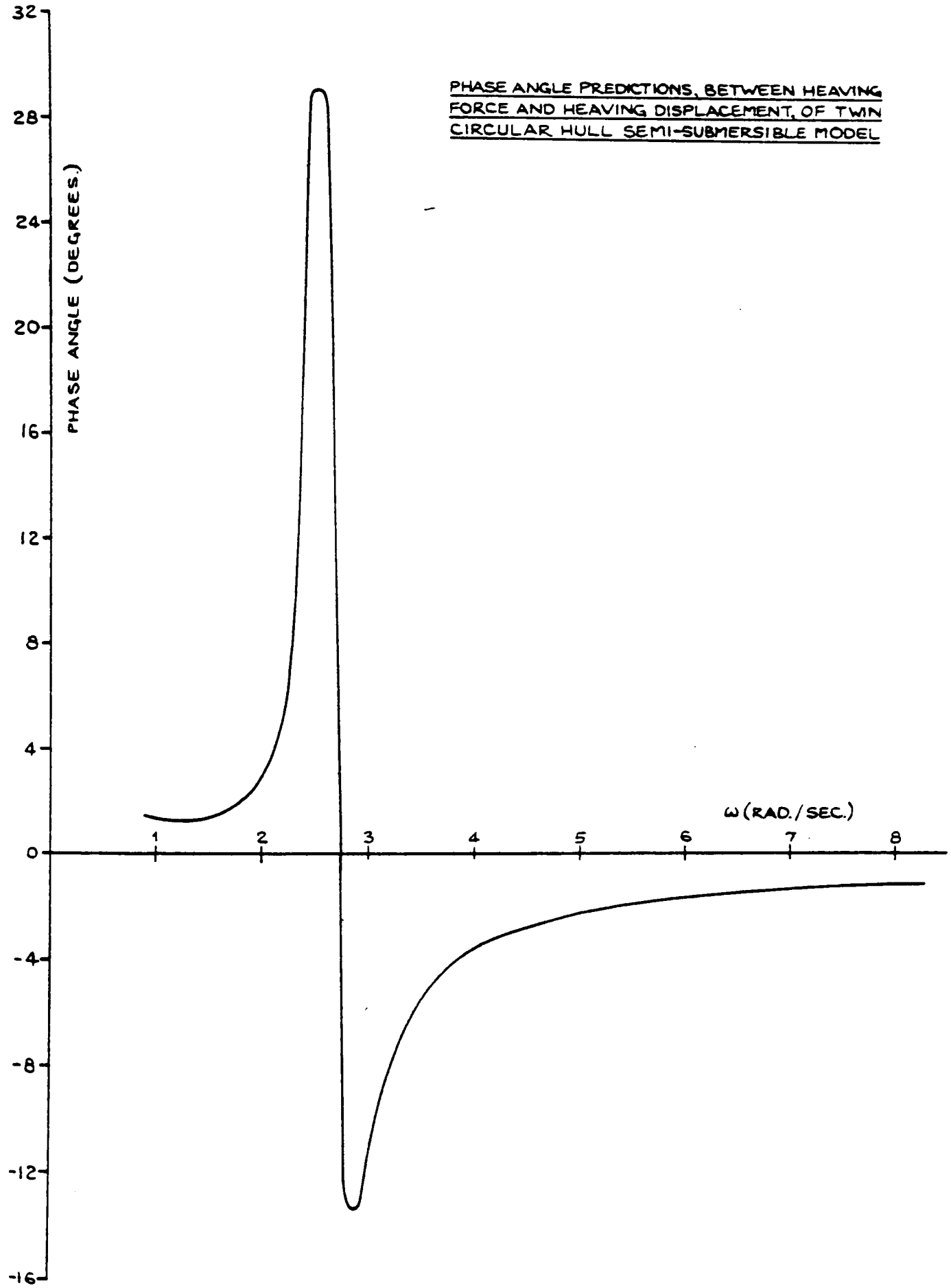

Fig. 11

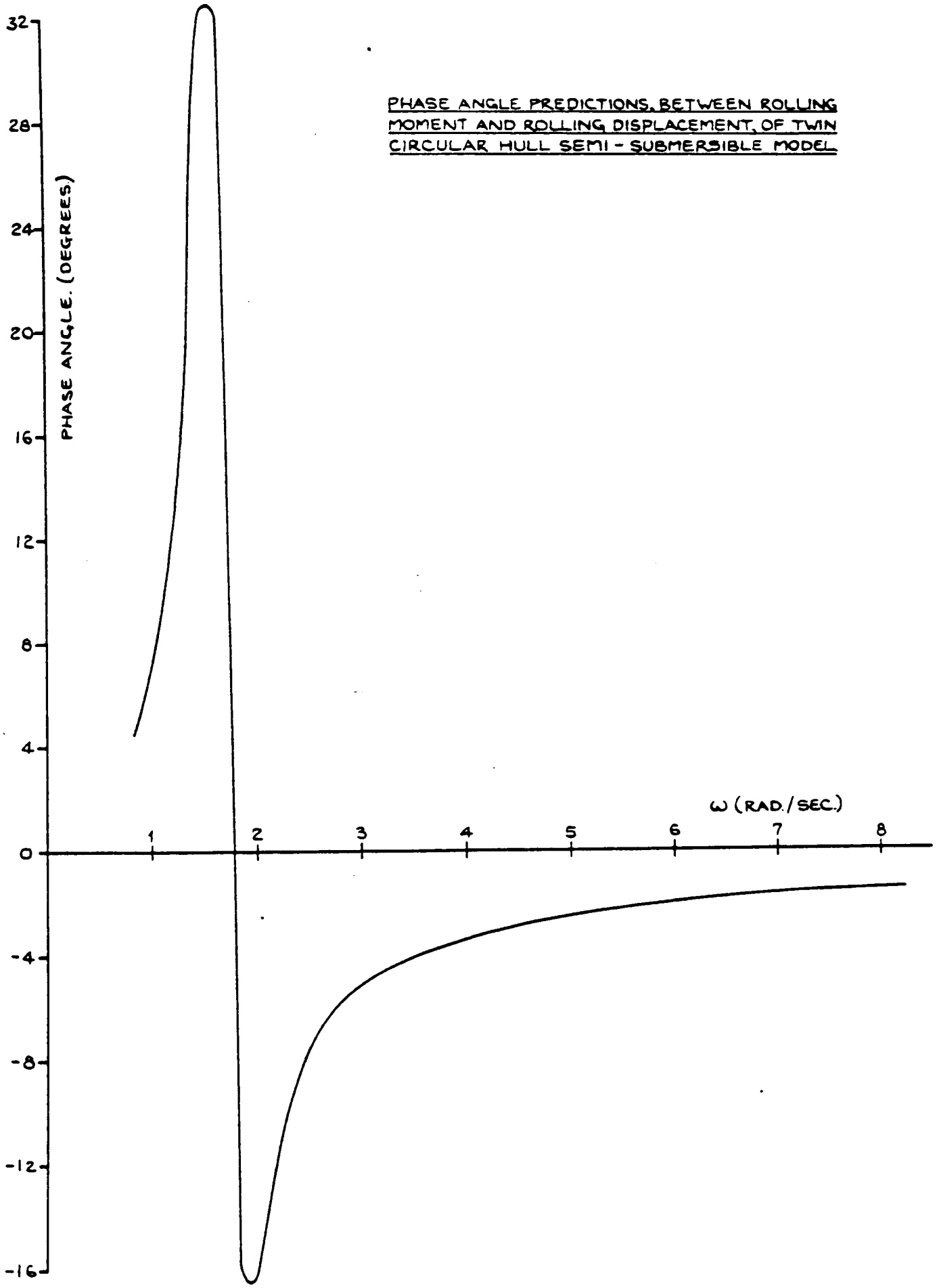

PHASE ANGLE PREDICTIONS, BETWEEN ROLLING MOMENT AND ROLLING DISPLACEMENT, OF TWIN CIRCULAR HULL SEMI - SUBMERSIBLE MODEL

Fig. 12

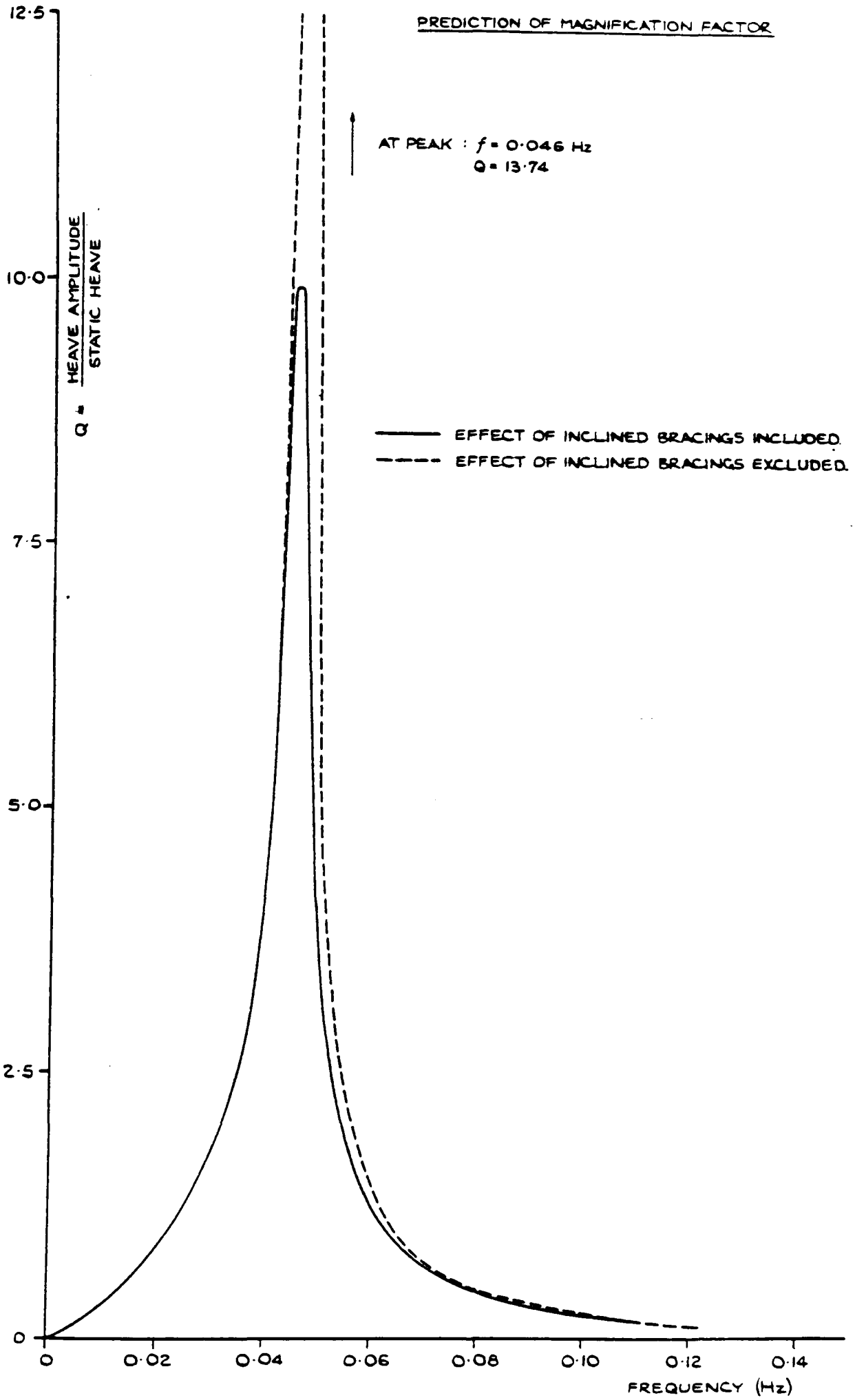
PREDICTION OF MAGNIFICATION FACTOR
AT PEAK : f = 0·046 Hz
Q = 13·74
EFFECT OF INCLINED BRACINGS INCLUDED
EFFECT OF INCLINED BRACINGS EXCLUDED
Q = HEAVE AMPLITUDE / STATIC HEAVE
12·5
10·0
7·5
5·0
2·5
0
0
0·02
0·04
0·06
0·08
0·10
0·12
0·14
FREQUENCY (Hz)

Fig. 13

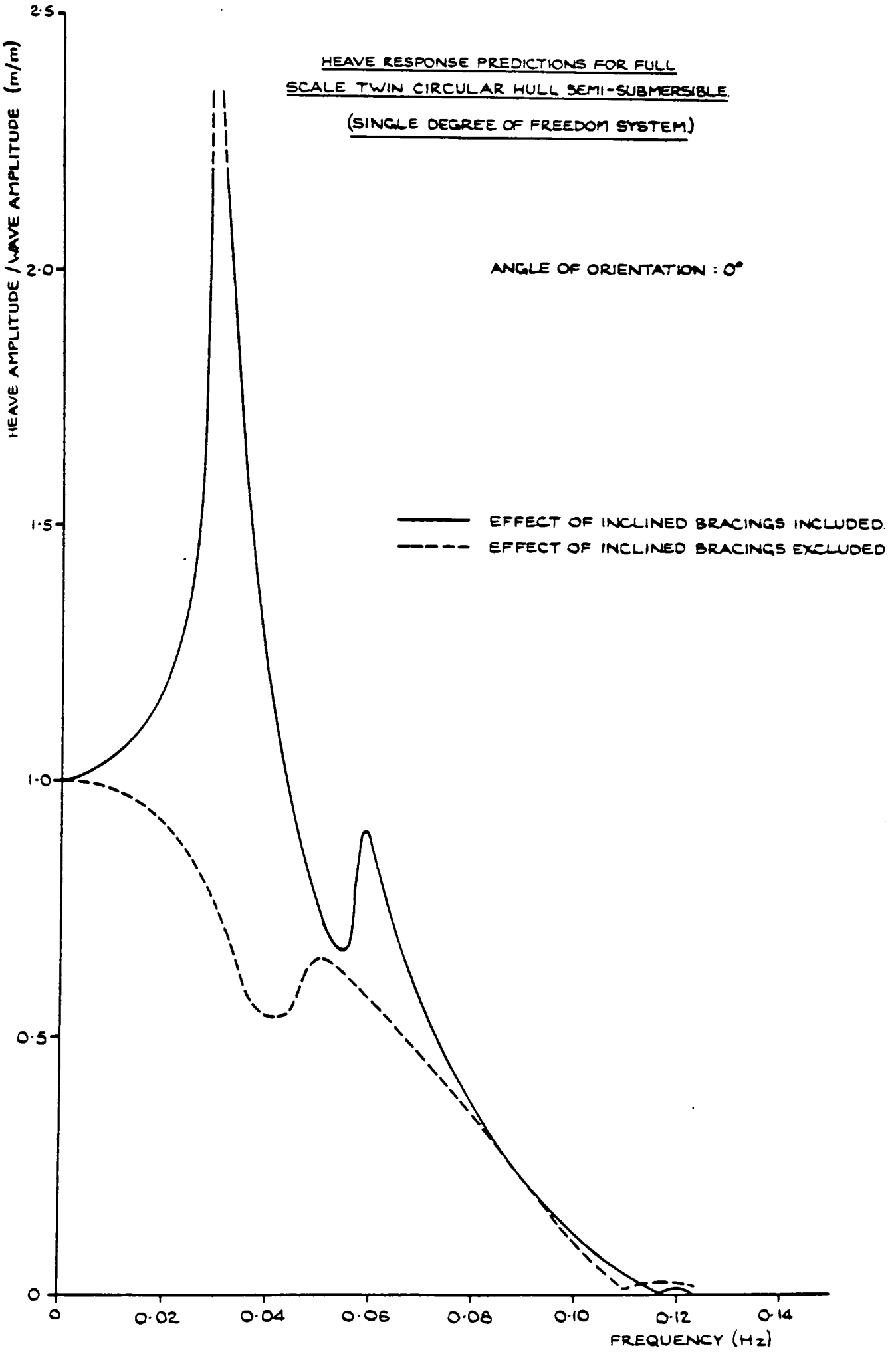
HEAVE RESPONSE PREDICTIONS FOR FULL
SCALE TWIN CIRCULAR HULL SEMI-SUBMERSIBLE.
(SINGLE DEGREE OF FREEDOM SYSTEM)
ANGLE OF ORIENTATION : 0°
EFFECT OF INCLINED BRACINGS INCLUDED.
EFFECT OF INCLINED BRACINGS EXCLUDED.
HEAVE AMPLITUDE / WAVE AMPLITUDE (m/m)
2·5
2·0
1·5
1·0
0·5
0
0
0·02
0·04
0·06
0·08
0·10
0·12
0·14
FREQUENCY (Hz)

Fig. 14

HEAVE RESPONSE PREDICTIONS FOR FULL SCALE TWIN CIRCULAR HULL SEMI-SUBMERSIBLE.

(SINGLE DEGREE OF FREEDOM)

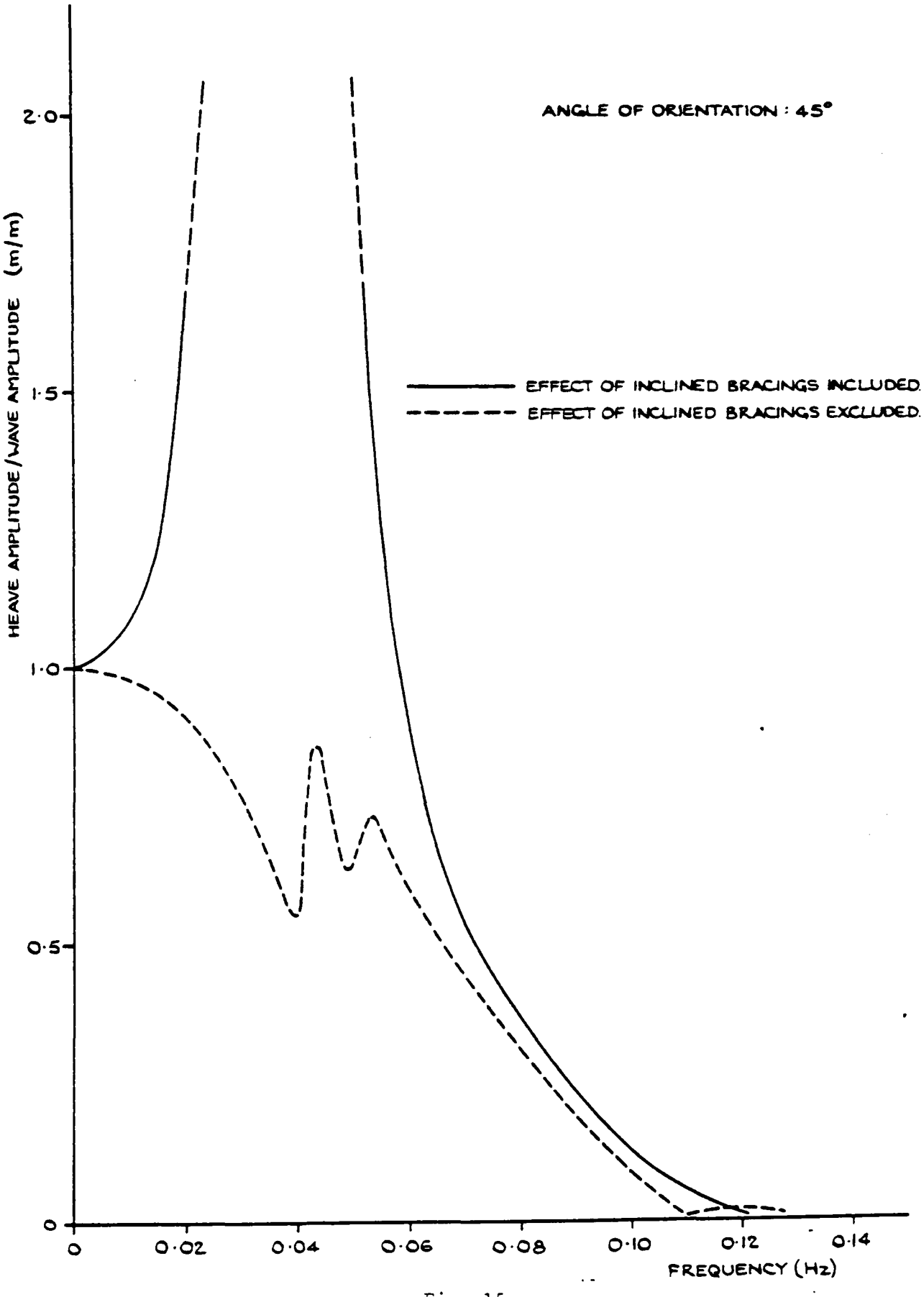

Fig. 15

HEAVE RESPONSE PREDICTIONS FOR FULL SCALE TWIN CIRCULAR HULL SEMI-SUBMERSIBLE.

(SINGLE DEGREE OF FREEDOM SYSTEM)

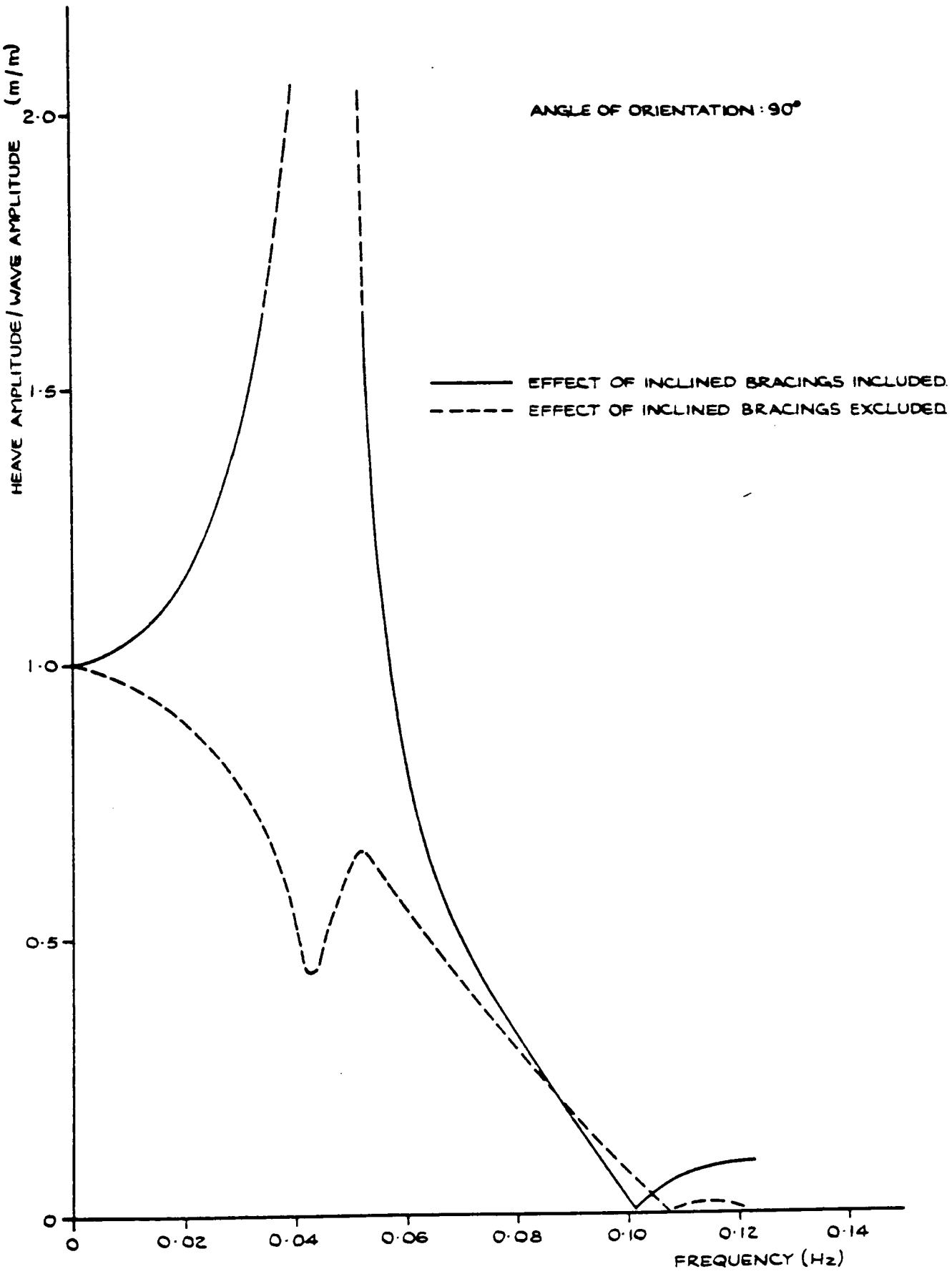

Fig. 16

ROLL RESPONSE PREDICTIONS FOR FULL SCALE TWIN CIRCULAR HULL SEMI-SUBMERSIBLE

(SINGLE DEGREE OF FREEDOM SYSTEM, EFFECT OF INCLINED BRACINGS INCLUDED)

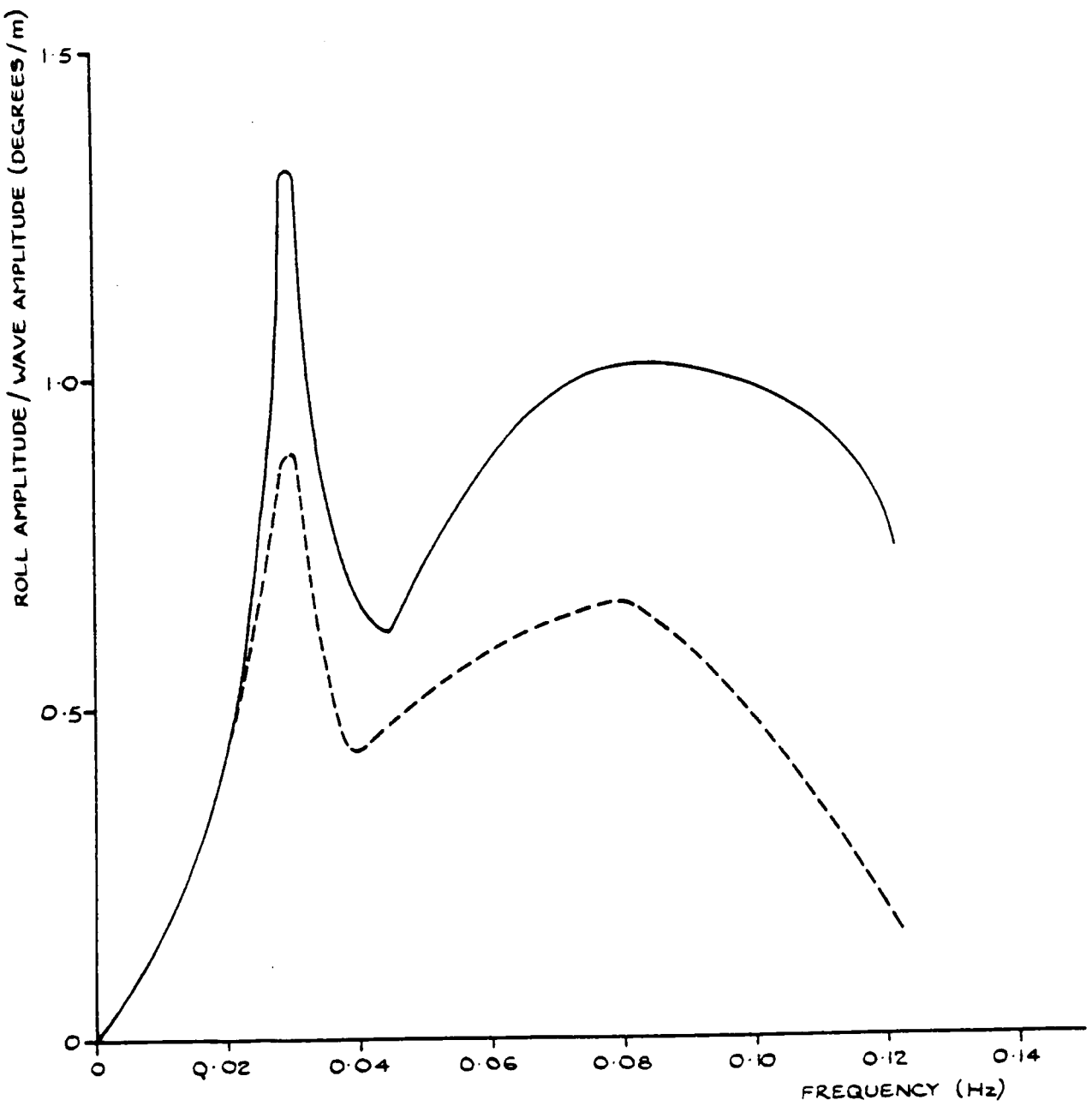

Fig. 17

PITCH RESPONSE PREDICTIONS FOR FULL SCALE TWIN CIRCULAR HULL SEMI-SUBMERSIBLE

(SINGLE DEGREE OF FREEDOM SYSTEM, EFFECT OF INCLINED BRACINGS INCLUDED)

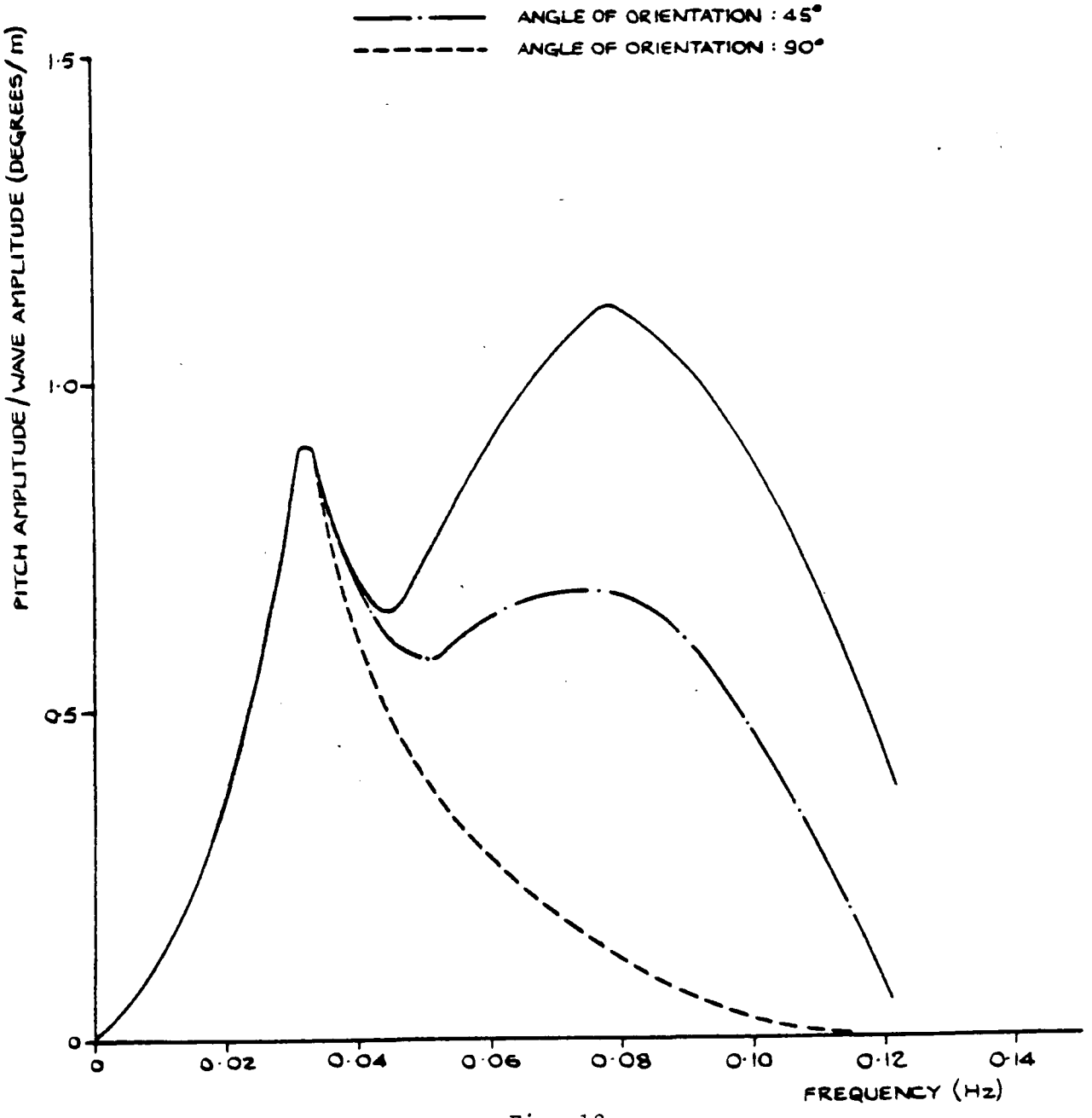

Fig. 18

b) Changes in the restoring and forcing moments due to heave motion are not taken into account. Some suggestions to improve heave and roll motion predictions will also be discussed in Section 8.

Figure 11 shows phase angle between the heaving force and the heaving displacement, and figure 12 shows the angle between the rolling moment and the rolling motion. These values will be used for finding the motion induced structural loading, as will be described in Chapter 5.

The method of motion prediction summarised in the above sections was also applied to the full scale semi-submersible design shown in figure 43 of Chapter 5.

Figure 13 shows the effect of the bracing members on the magnification factor. This shows that the effect of bracings becomes important around the resonance region only.

In figures 14, 15 and 16 the heave responses were plotted for head, quarter and beam seas with and without bracing members being included. When the wave loading variations on this semi-submersible (see figures 15-20 of Chapter 3) are studied along with figures 13, 14, 15 and 16 it becomes clear that the optimisation of this particular geometry of the semi-submersible to obtain minimum vertical force around the natural frequencies was carried out without the bracing members by the designer who determined this particular geometry. When the bracing members are included in the calculation, motion response significantly changes due to the wave loading on the bracing members.

Figures 17 and 18 show the variations in roll and pitch motion of the structure for various wave heading angles.

8. DERIVATION AND SOLUTION OF NON-LINEAR COUPLED MOTION RESPONSE EQUATIONS

During the derivation of the motion equations given in (68) and (69) it was assumed that the motion amplitudes of the floating structure would be small, thus wave and hydrodynamic force formulations were carried out which neglected the space variation of the structural members during a wave cycle. In other words, wave and hydrodynamic forces were calculated at the mean draft level of the structure. As shown in figures 8 and 9, this linearisation gives reasonable predictions of motion response for small amplitude motions.

In the previous sections, motion equations, including the coupling effects between the different motion modes due to the geometry of the structure, were formulated (see equations 29, 30 and 62). When a floating offshore structure moves with large amplitude rotational motions, coupling between the various modes of the rotational motions should also be included in the motion response equations.

Coupled velocity and acceleration vectors fixed in the X, Y, Z structure reference system can be shown with the following motion sequences:

1. The structure is rotated by positive amount X_4 about the X_o axis. Let the rotational velocity and the acceleration about the X_o axis be $U_{4(s)}$ and $\dot{U}_{4(s)}$ respectively (Figure 19).

1. (Cont'd)

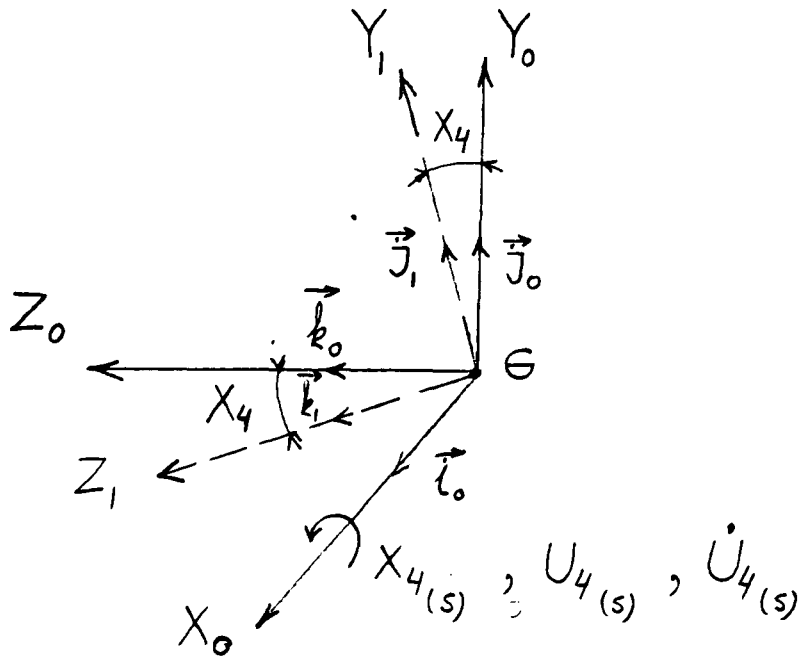

Fig. 19

The total rotational velocity and acceleration vector can be written as:

$$\vec{U}^{(1)}_{S,R} = U_{4(s)} \cdot \vec{i}_o \qquad (73)$$

$$\dot{\vec{U}}^{(I)}_{S,R} = \dot{U}_{4(s)} \cdot \vec{i}_o \qquad (73\text{-A})$$

2. The structure is now rotated by positive amount X_5 about the Y_1 axis. Let the rotational velocity and the acceleration about the Y_1 axis be $U_{5(s)}$ and $\dot{U}_{5(s)}$ respectively (Fig. 20).

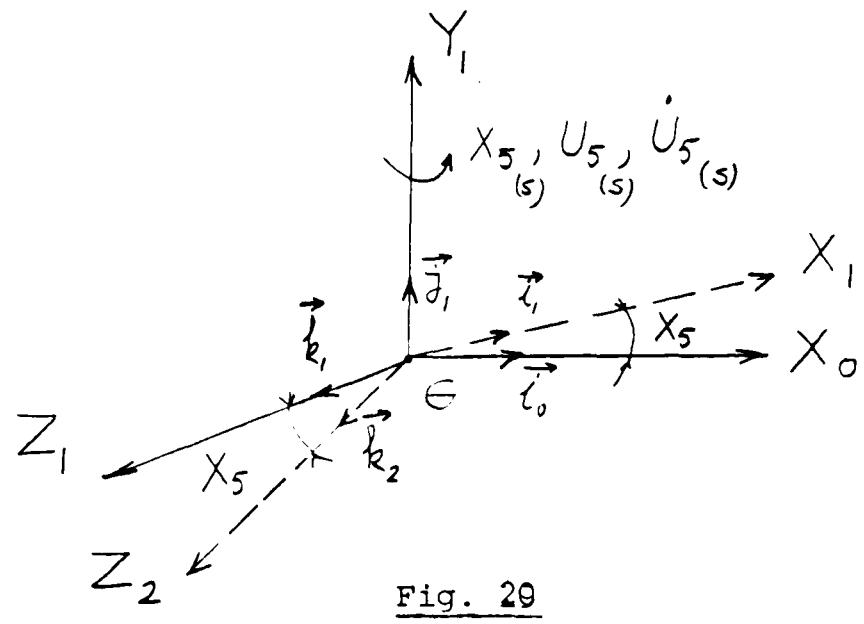

Fig. 20

2. (Cont'd)

The total velocity and acceleration vectors from equations (73) and (73-A) and figure 20 can be written as:

$$\vec{U}^{(2)}_{S,R} = U_4 \cos(X_5)\,\vec{i}_1 + U_5\,\vec{j}_1 + U_4 \sin(X_5)\,\vec{k}_1 \qquad (74)$$

$$\dot{\vec{U}}^{(2)}_{S,R} = \dot{U}_4 \cos(X_5)\,\vec{i}_1 + \dot{U}_5\,\vec{j}_1 + \dot{U}_4 \sin(X_5)\,\vec{k}_2 \qquad (74\text{-}A)$$

3. Finally, the structure is rotated by positive amount X_6 about the Z_2 axis. Let the rotational velocity and the acceleration about the Z_2 axis be $U_{6_{(s)}}$ and $\dot{U}_{6_{(s)}}$ respectively (Fig. 21).

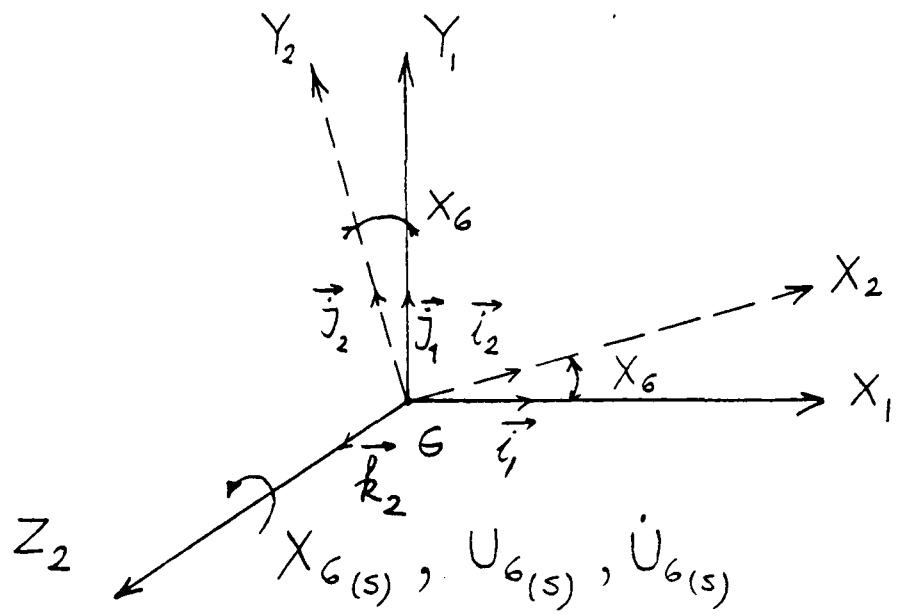

Fig. 21

The total velocity and acceleration vectors from equations (74) and (74-A) and from figure 20 can be written as:

3. (Cont'd)

$$\vec{U}^{(3)}_{S,R} = [U_4 \cos(X_5) \cos(X_6) + U_5 \sin(A_6)]\vec{i}_2 + [U_5 \cos(X_6) - U_4 \cos(X_5) \sin(X_6)]\vec{j}_2 + [U_6 + U_4 \sin(X_5)]\vec{k}_2 \quad (75)$$

$$\dot{\vec{U}}^{(3)}_{S,R} = [\dot{U}_4 \cos(X_5) \cos(X_6) + \dot{U}_5 \sin(X_6)]\vec{i}_2 + [\dot{U}_5 \cos(X_6) - \dot{U}_4 \cos(X_5) \sin(X_6)]\vec{j}_2 + [\dot{U}_6 + \dot{U}_4 \sin(X_5)]\vec{k}_2 \quad (75\text{-A})$$

X_2, Y_2 , Z_2 reference system forms the fixed structure reference system and the rotational velocity and acceleration vectors given in equations (17) and (18) should be replaced with equations (75) and (75-A) to take into account the coupling effects between the rotational motion modes.

Now the change in the wave force and moment vector due to the large amplitude of motion of the floating platform will be determined. In Chapter 3, wave loading was formulated for cylindrical members of fixed and of floating structures oriented randomly in waves. The main variables in the formulation are the end co-ordinates of each member, the draft of the structure and the wave heading angle. As the floating structure moves the new values of each of those variables can be sub-

stituted/

substituted into the wave loading equations given in Chapter 3. Let us assume a point A(a, b, c) on the structure in the fixed X, Y, Z structure co-ordinate system and study the variation of these co-ordinates a, b, c in terms of motion response values as the platform moves. The aim is to determine the new co-ordinates of A in the original X, Y, Z fixed structure reference system after the platform has undergone translational and rotational movements.

Let us assume that the floating structure will be displaced in the rotational and the translational modes with the following motion sequences:

a) The floating structure will be rotated about the X axis by a positive amount X_4 (Fig. 22). The co-ordinates of point A in the fixed reference system (X, Y, Z) can be written in terms of the same point's co-ordinates in the new reference system (X, Y_1, Z_1) and the rotation angle X_4 as:

$$b_Y = b_{Y_1} \text{Cos}(X_4) - c_{Z_1} \text{Sin}(X_4) \tag{76}$$

$$c_Z = b_{Y_1} \text{Sin}(X_4) + c_{Z_1} \text{Cos}(X_4) \tag{76-A}$$

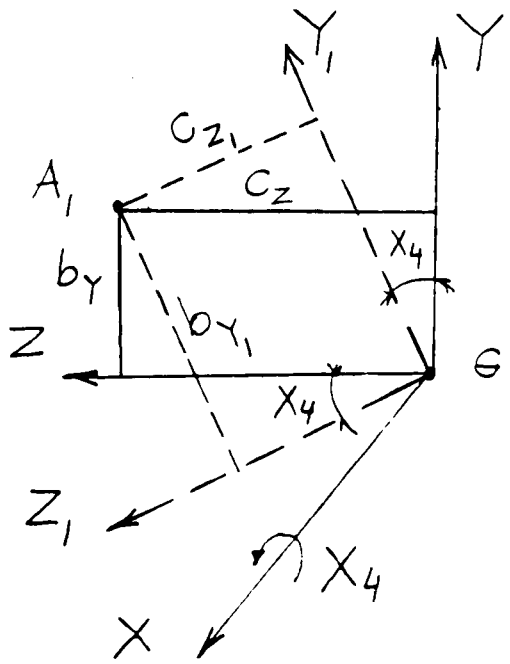

Fig. 22

b) The floating structure will now be rotated by a positive amount X_5 about the Y_1 axis. The co-ordinates of point A in the (X, Y_1, Z_1) reference system can be written in terms of the same point's co-ordinates in the new reference system (X_1, Y_1, Z_2) and the rotation angle X_5 as (Fig. 23):

$$a_X = a_{X_1} \cdot \text{Cos}(X_5) + c_{Z_2} \text{Sin}(X_5) \tag{77}$$

$$c_{Z_1} = -a_{X_1} \text{Sin}(X_5) + c_{Z_2} \text{Cos}(X_5) \tag{77-A}$$

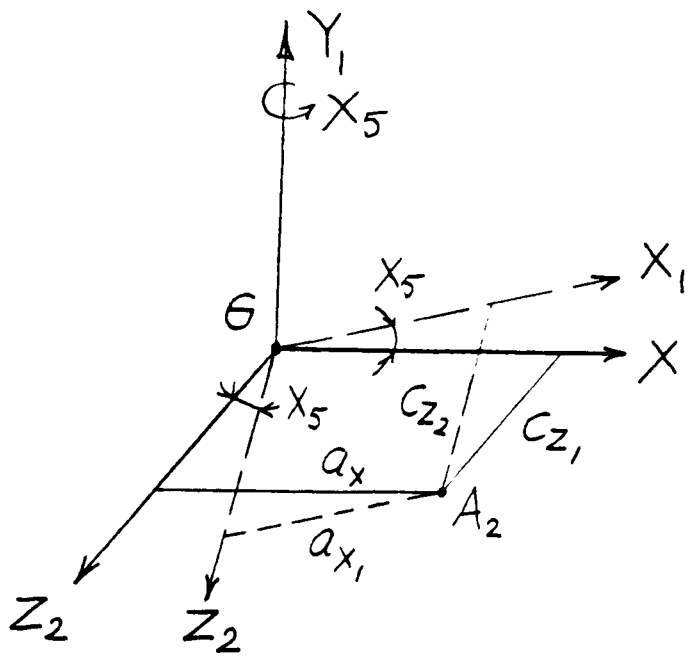

Fig. 23

c) Finally, the floating structure is rotated by a positive amount X_6 about the Z_2 axis. The co-ordinates of point A in the (X_1, Y_1, Z_2) reference system can be written in terms of the same point's co-ordinates in the new reference system (X_2, Y_2, Z_2) and the rotation angle X_6 as follows (Fig. 24):

c) (Cont'd)

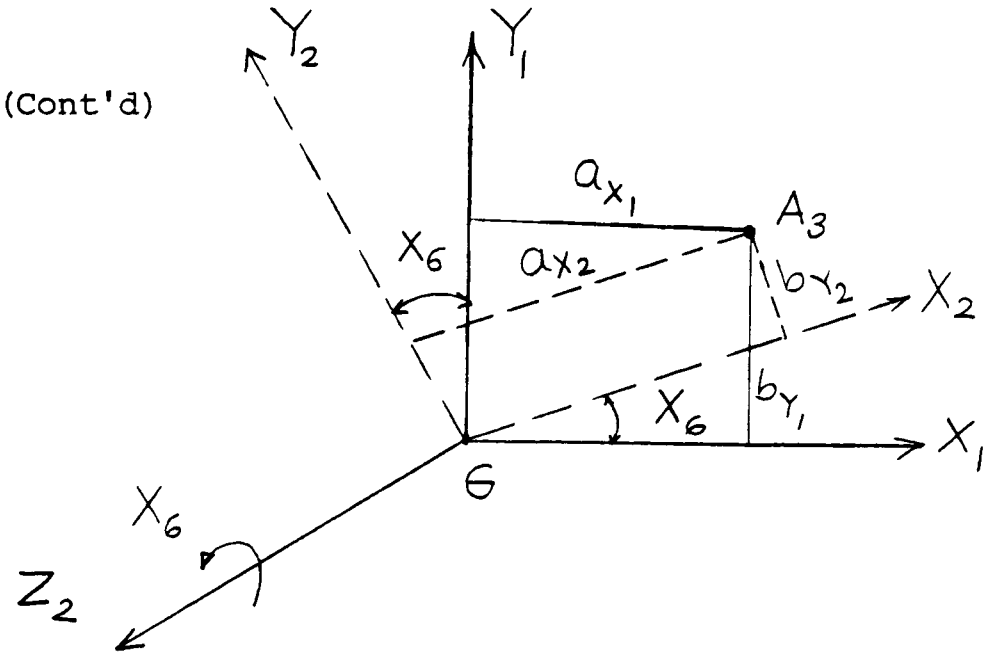

Fig. 24

$$a_{X_1} = a_{X_2} \text{Cos}(X_6) - b_{Y_2} \text{Sin}(X_6) \tag{78}$$

$$b_{Y_1} = a_{X_2} \text{Sin}(X_6) + b_{Y_2} \text{Cos}(X_6) \tag{78-A}$$

Since (X_2, Y_2, Z_2) reference system is the rotated form of the structure reference system (X, Y, Z), and point A is fixed in the structure reference system, the following equations will be valid:

$$a = a_{X_2} \tag{79}$$

$$b = b_{Y_2} \tag{79-A}$$

$$c = c_{Z_2} \tag{79-B}$$

Equations (76), (76-A) and (77) can be written to obtain co-ordinates of a point A in the original reference system (X , Y, Z), after the fixed structure reference system has undergone X_4, X_5, and X_6 rotational displacements, using (78-(79-B)) as follows:

(c) (Cont'd)

$$\begin{bmatrix} a_X \\ b_Y \\ c_Z \end{bmatrix} = \begin{bmatrix} \cos(X_5)\cos(X_6) & -\cos(X_5)\sin(X_6) & \sin(X_5) \\ \cos(X_4)\sin(X_6) + \sin(X_5)\cos(X_6)\sin(X_4) & \cos(X_6)\cos(X_4) - \sin(X_4)\sin(X_5)\sin(X_6) & -\sin(X_4)\cos(X_5) \\ \sin(X_4)\sin(X_6) - \cos(X_4)\sin(X_5)\cos(X_6) & \sin(X_4)\cos(X_6) + \cos(X_4)\sin(X_5)\sin(X_6) & \cos(X_4)\cos(X_5) \end{bmatrix} \begin{bmatrix} a \\ b \\ c \end{bmatrix} \quad (80)$$

$[a]_{(X,Y,Z)}$ $\qquad$ $[R]$ $\qquad$ $[a]_{(X_2,Y_2,Z_2)}$

or

$$[a]_{(X,Y,Z)} = [R]\,[a]_{(X_o,Y_o,Z_o)} \quad (80\text{-A})$$

(d) Now, the floating structure is displaced in surge (X_1), heave (X_2) and sway (X_3) modes successively. The co-ordinates of point A in the original reference system after the translational motion has taken place become (Fig.25) :

$$[a]_{(X,Y,Z)} = [R]\,[a]_{(X_2,Y_2,Z_2)} + [T] = [R]\,[a]_{(X_o,Y_o,Z_o)} + [T] \quad (81)$$

where, $[T] = \begin{bmatrix} X_1 \\ X_2 \\ X_3 \end{bmatrix}$

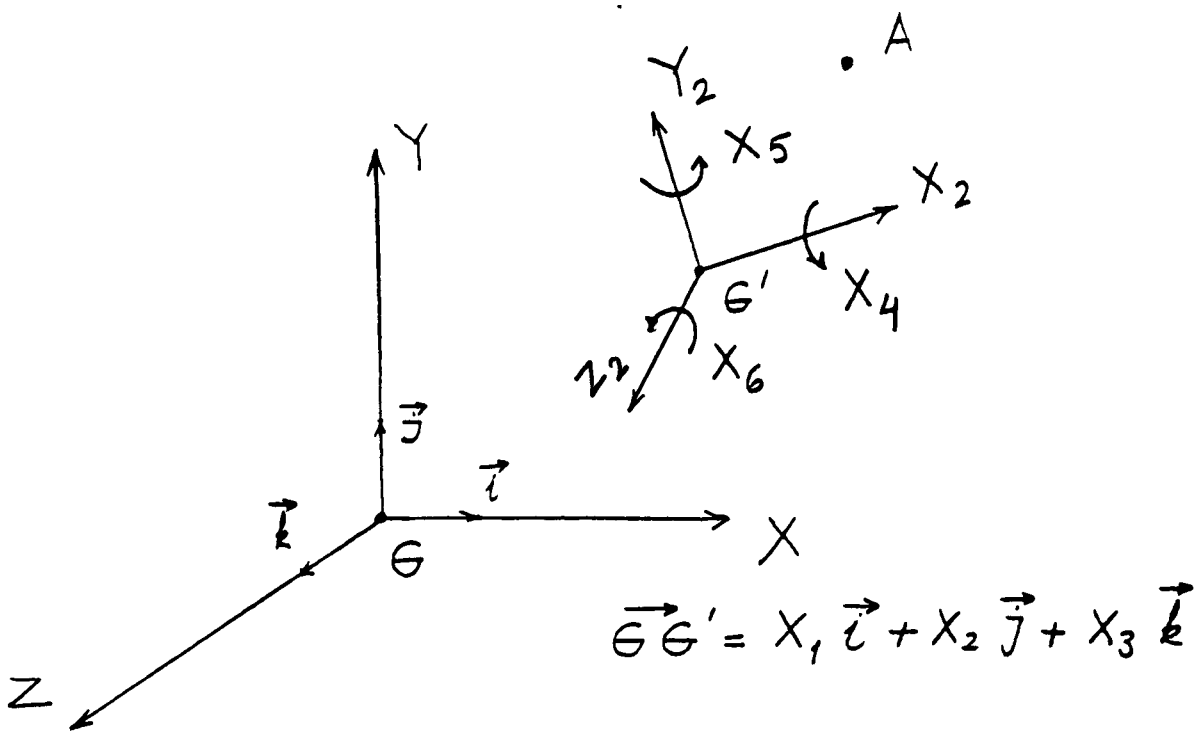

Fig. 25

When the large amplitude of motion is considered, the restoring force and moment matrix expression given in equation (54) becomes:

$$\begin{bmatrix} F_1 \\ F_2 \\ F_3 \\ F_4 \\ F_5 \\ F_6 \end{bmatrix}_{HIDR} = - \begin{bmatrix} 0 & 0 & 0 & 0 & 0 & 0 \\ 0 & \rho g A_w(X) & 0 & 0 & 0 & 0 \\ 0 & 0 & 0 & 0 & 0 & 0 \\ 0 & 0 & 0 & \rho g \nabla GM_T(X) & 0 & 0 \\ 0 & 0 & 0 & 0 & 0 & 0 \\ 0 & 0 & 0 & 0 & 0 & \rho g \nabla GM_L(X) \end{bmatrix} \begin{bmatrix} X_1 \\ X_2 \\ X_3 \\ \mathrm{Sin}(X_4) \\ X_5 \\ \mathrm{Sin}(X_6) \end{bmatrix} \tag{82}$$

The motion response equation given in (68) can be rewritten, taking into account the large amplitude of motion, as:

$$[M(X,t)][RC(X,t][\ddot{X}] + [C(X,t)][RC(X,t)][\dot{X}] + [K(X)][X]^* = [F_w(X,t)] \tag{83}$$

or

$$[MC(X,t)][\ddot{X}] + [CC(X,t)][\dot{X}] + [K(X)][X]^* = [F_w(X,t)] \tag{83-A}$$

where

$$[MC(X,t)] = [M(X,t)][RC(x,t)]$$

$$[CC(X,t)] = [C(X,t)][RC(X,t)]$$

$$[RC(X)] = \begin{bmatrix} 1 & 0 & 0 & 0 & 0 & 0 \\ 0 & 1 & 0 & 0 & 0 & 0 \\ 0 & 0 & 1 & 0 & 0 & 0 \\ 0 & 0 & 0 & \text{Cos}(X_5)\text{Cos}(X_6) & \text{Sin}(X_6) & 0 \\ 0 & 0 & 0 & -\text{Cos}(X_5)\text{Sin}(X_6) & \text{Cos}(X_6) & 0 \\ 0 & 0 & 0 & \text{Sin}(X_5) & 0 & 1 \end{bmatrix}$$

$$[X]^* = \begin{bmatrix} X_1 \\ X_2 \\ X_3 \\ \text{Sin}(X_4) \\ X_5 \\ \text{Sin}(X_6) \end{bmatrix}$$

[M(X)], [C(X)], [K(X)] can be determined as described in equation (68) using the displaced co-ordinates of each member. Similarly, $F_W(X)$ can be calculated with the displaced co-ordinates at each time increment from equations (3.42) and (3.46).

In order to complete the analysis a solution method for the non-linear coupled motion equations given in (83-A) will be discussed. The same method applies to the solution of the equations given in (68). Since the right and left hand sides of these equations are completely arbitrary in respect to time and position in space, solution is only possible if numerical integration procedures are used. There are various numerical integration procedures available in the literature and these are discussed in detail in references [14,15,16,17]. Computer library programs are also available for the direct usage of these numerical methods [18]. Amongst the various step-by-step integration procedures the linear acceleration method has been found to be the most suitable one for the solution of the motion equations given in (83-A). This method will be summarised as follows (see also ref. 4 of Chapter 5):

The period of a wave cycle will first be divided into an equal number of spaces. Starting from $t_1 = 0$, at each time increment, the variables in the motion equations will be calculated using the formulations described previously and acceleration, velocity, and the displacement values will be determined from the equilibrium of the system.

Solutions can be obtained using the initial values of the system. In the rigid body motion problem the initial conditions will be initial displacement and the velocity values of the rigid body.

When $t = t_1$, the equations of the motion given in (83-A) can be written as:

$$[MC(X,t_1)][\ddot{X}(t_1)] + [CC(X,t_1)][\dot{X}(t_1)] + [K(X)][X(t_1)] = [F_w(X,t_1)] \tag{84}$$

A small Δt time later equations (84) become:

$$[MC(X+\Delta X,t_1+\Delta t)][\ddot{X}(t_1+\Delta t)] + [CC(X+\Delta X,t_1+\Delta t)][\dot{X}(t_1+\Delta t)] + [K(X+\Delta X)][X(t_1+\Delta t)] = [F_w(X+\Delta X,t_1+\Delta t)] \tag{85}$$

When equation (85) is subtracted from equation (84), the incremental form of equations of motion becomes:

$$[\Delta f_1(X,t)] + [\Delta f_2(X,t)] + [\Delta f_3(X,t)] = [\Delta F_w(X,t)] \tag{86}$$

where

$$[\Delta f_1(X,t)] = [MC(X+\Delta X,t_1+\Delta t)][\ddot{X}(t_1+\Delta t)] - [MC(X,t_1)][\ddot{X}(t_1)]$$

$$[\Delta f_2(X,t)] = [CC(X+\Delta X,t_1+\Delta t)][\dot{X}(t_1+\Delta t)] - [CC(X,t_1)][\dot{X}(t_1)]$$

$$[\Delta f_3(X,t)] = [K(X+\Delta X)][X(t_1+\Delta t)] - [K(X)][X(t_1)]$$

$$[\Delta F_w(X,t)] = [F_w(X+\Delta X,t_1+\Delta t)] - [F_w(X,t_1)]$$

The equations given in (86) can also be written, from the equilibrium of the system, as:

$$[MC(X,t_1)][\Delta\ddot{X}(t)] + [CC(X,t_1)][\Delta\dot{X}(t)] + [K(X)][\Delta X(t)] = [\Delta F_w(X,t_1)] \tag{87}$$

When we assume that acceleration varies linearly, velocity varies quadratically, and displacement varies cubically during the time increment, the following relations can also be written using Taylor's expansion series:

Acceleration:

$$\ddot{X}(\tau) = \ddot{X}(t_1) + \frac{\Delta\ddot{X}(t)}{\Delta t} \cdot \tau \tag{88}$$

Velocity:

$$\dot{X}(\tau) = \dot{X}(t_1) + \ddot{X}(t_1)\cdot\tau + \frac{\Delta\ddot{X}(t)}{\Delta t} \cdot \frac{\tau^2}{2} \tag{89}$$

Displacement:

$$X(\tau) = X(t_1) + \dot{X}(t_1)\cdot\tau + \ddot{X}(t_1)\ \frac{\tau^2}{2} + \frac{\Delta\ddot{X}(t)}{\Delta t} \cdot \frac{\tau^3}{6} \tag{90}$$

Equations (89) and (90) can also be written in the following form by setting τ equal to Δt:

$$\Delta\dot{X}(t) = \ddot{X}(t_1)\Delta t + \Delta\ddot{X}(t)\ \frac{\Delta t}{2} \tag{91}$$

$$\Delta X(t) = \dot{X}(t_1)\Delta t + \ddot{X}(t_1)\ \frac{(\Delta t)^2}{2} + \Delta\ddot{X}(t)\ \frac{(\Delta t)^2}{6} \tag{92}$$

Equation (92) can be rearranged to obtain $\Delta\ddot{X}(t)$ as follows:

$$\Delta\ddot{X}(t) = 6\ \frac{\Delta X(t)}{(\Delta t)^2} - 6\ \frac{\dot{X}(t_1)}{\Delta t} - 3\ddot{X}(t_1) \tag{93}$$

When equation (93) is substituted into equation (92) $\Delta\dot{X}(t)$ can be obtained as:

$$\Delta\dot{X}(t) = \frac{3}{\Delta t}\ \Delta X(t) - 3\dot{X}(t_1) - \frac{\Delta t}{2}\ \ddot{X}(t_1) \tag{94}$$

The following equations can be written by using equations (93) and (94) to redefine the incremental form of motion equations given in (87):

$$[MC(X,t_1)]\left(\frac{6}{(\Delta t)^2}[\Delta X(t)] - \frac{6}{\Delta t}[\dot{X}(t_1)] - 3[\ddot{X}(t_1)]\right)$$

$$+ [CC(X,t_1)]\left(\frac{3}{\Delta t}[\Delta X(t)] - 3[\dot{X}(t_1)] - \frac{\Delta t}{2}[\ddot{X}(t_1)]\right) \qquad (95)$$

$$+ [K(X)][\Delta X(t)] = [\Delta F_w(X,t_1)]$$

Equation (95) can also be written as:

$$\overline{[K(X)]}[\Delta X(t)] = [\Delta P_w(X,t_1)] \qquad (96)$$

where

$$\overline{[K(X)]} = [K(X)] + \frac{6}{(\Delta t)^2}[MC(X,t_1)] + \frac{3}{\Delta t}[CC(X,t_1)]$$

$$[\Delta P(X,t_1)] = [\Delta F_w(X,t_1)] + [MC(X,t_1)]\left(\frac{6}{\Delta t}[\dot{X}(t_1)] + 3[\ddot{X}(t_1)]\right)$$

$$+ [CC(X,t_1)]\left(3[\dot{X}(t_1)] + \frac{\Delta t}{2}[\ddot{X}(t_1)]\right)$$

The step-by-step integration procedure, which is based on the linear acceleration method, can be summarised to solve non-linear coupled motion equations with the following steps:

1. Define the initial velocity and displacement values. Let us say $[\dot{X}] = [X] = 0$ when $t_1 = 0$.

2. Solve equation (84) to obtain $[\ddot{X}(t_1)]$ values as follows:

$$[\ddot{X}(t_1)] = [MC(X,t_1)]^{-1}\left([F_w(X,t_1)] - [CC(X,t_1)][\dot{X}(t_1)] - [K(X)][X(t_1)]\right)$$

3. Obtain load increments from equation (96)

$$[\Delta P(X,t_1)] = [\Delta F_w(X,t_1)]$$

$$+ [MC(X,t_1)]\left(\frac{6}{\Delta t}[\dot{X}(t_1)] + 3[\ddot{X}(t_1)]\right)$$

$$+ [CC(X,t_1)]\left(3[\dot{X}(t_1)] + \frac{\Delta t}{2}[\ddot{X}(t_1)]\right)$$

4. Determine the stiffness increments from equation (96)

$$\overline{[K(X)]} = [K(X)] + \frac{6}{(\Delta t)^2}[MC(X,t_1)] + \frac{3}{\Delta t}[CC(X,t_1)]$$

5. Calculate $[\Delta X(t)]$ from equation (96)

$$[\Delta X(t)] = \overline{[K(X)]}^{-1}\ [\Delta P(X,t_1)]$$

6. Calculate velocity increments from equation (94)

$$[\Delta \dot{X}(t)] = \frac{3}{\Delta t}[\Delta X(t)] - 3[\dot{X}(t_1)] - \frac{\Delta t}{2}[\ddot{X}(t_1)]$$

7. Calculate new displacement and the velocity factors

$$[X(t_1) + \Delta t)] = [X(t_1)] + [\Delta X(t)]$$

$$[\dot{X}(t_1 + \Delta t)] = [\dot{X}(t_1)] + [\Delta \dot{X}(t)]$$

8. Using the new displacement and the time values calculate:

$[MC(X + \Delta X, t_1 + \Delta t)]$, $[CC(X + \Delta X, t_1 + \Delta t)]$, $[K(X + \Delta X)]$ and $[F_w(X + \Delta X, t_1 + \Delta t)]$ matrices.

9. Repeat the procedure again starting from step 2.

The accuracy of the step-by-step integration procedure summarised above will be based on the following points:

(a) Correct choice of the time increment Δt which will be dependent on:

(i) The rate of variation of applied load;

(ii) Variation in the damping and the stiffness functions;

(iii) Natural frequencies of the system.

(b) Correct knowledge of the damping function.

Chapter 5: STRUCTURAL RESPONSE OF FLOATING OFFSHORE PLATFORMS UNDER WAVE EXCITATION

INTRODUCTION

In this chapter, the calculation procedure to determine the structural response values, i.e. axial force, shear force and bending moment on the members of a floating structure, will be discussed. The floating platform subject to dynamic loading, i.e. wave, hydrodynamic and platform mass-inertia loads, was divided into beam elements and analysed as a space frame to yield internal joint reactions in the frequency domain.

Firstly, determinate floating structures will be discussed to establish the calculation procedure for structural response under quasi-static and dynamic loading. (Here, the term quasi-static implies that loading on the floating structure will be assumed to be static at any instant over a wave cycle, i.e. local vibrations of the structural members will not be taken into account for the structural response calculations.)

Secondly, indeterminate floating structures will be analysed using the classical rigid frame analysis procedure based on the stiffness method. The plane frame analysis procedure and the associated computer programs will also be summarised in this chapter.

The theoretical structural response calculations were verified by testing a semi-submersible model in regular waves. (See also Chapter 7.)

1. CALCULATION OF STRUCTURAL RESPONSE FOR DETERMINATE FLOATING STRUCTURES UNDER WAVE LOADING

In Naval Architecture applications, structural response values are calculated by assuming a whole ship structure to be a single free-free beam of varying cross-section loaded with wave force (due to pressure, acceleration and velocity of water particles), hydrodynamic force (fluid force induced by rigid-body motion), restoring force (hydrostatic force) and ship mass-inertia force (due to the rigid body acceleration of the

structure) distributions [1-3]. Since these applied forces on the structure are in balance at every instant, the equilibrium equations can be written between external and internal forces to determine the structural response values. To obtain these values a portion of the structure is isolated by cutting it at the points where the structural analysis is desired. Since numerical integrations are involved in the structural response calculations, the absolute value of a calculated axial force, shear force or bending moment may differ depending on the side of a structure which is taken to be the free end in writing the equilibrium equations between external and internal forces. This problem may be overcome by averaging with sign the structural response values obtained for both sides of the cut.

The structural loading and response calculations for a ship (= a single beam) will be summarised to indicate the calculation procedure as an introduction to the analysis of floating structures with more complex geometry.

At the start of the structural response analysis, it will be assumed that mass distribution of the ship, ship cross-sectional areas, rigid body motion responses and phase angles of these responses, as well as wave and hydrodynamic loading distributions along the ship length are known. These loading distributions can be represented by the following diagrams.

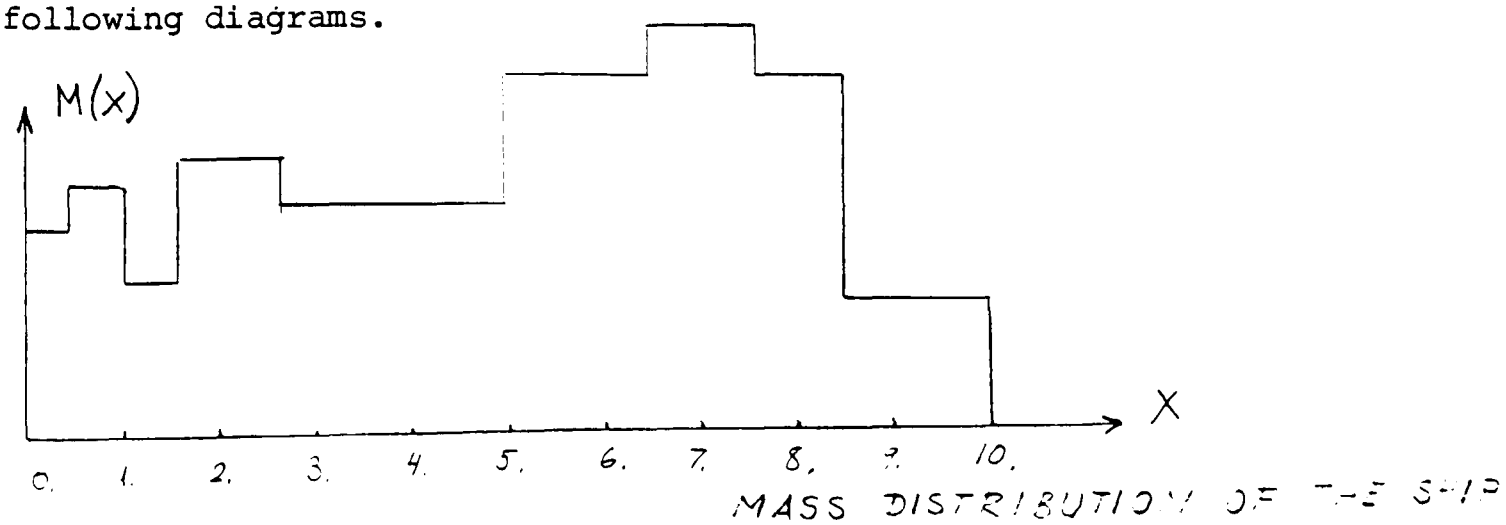

MASS DISTRIBUTION OF THE SHIP

Fig. 1-A

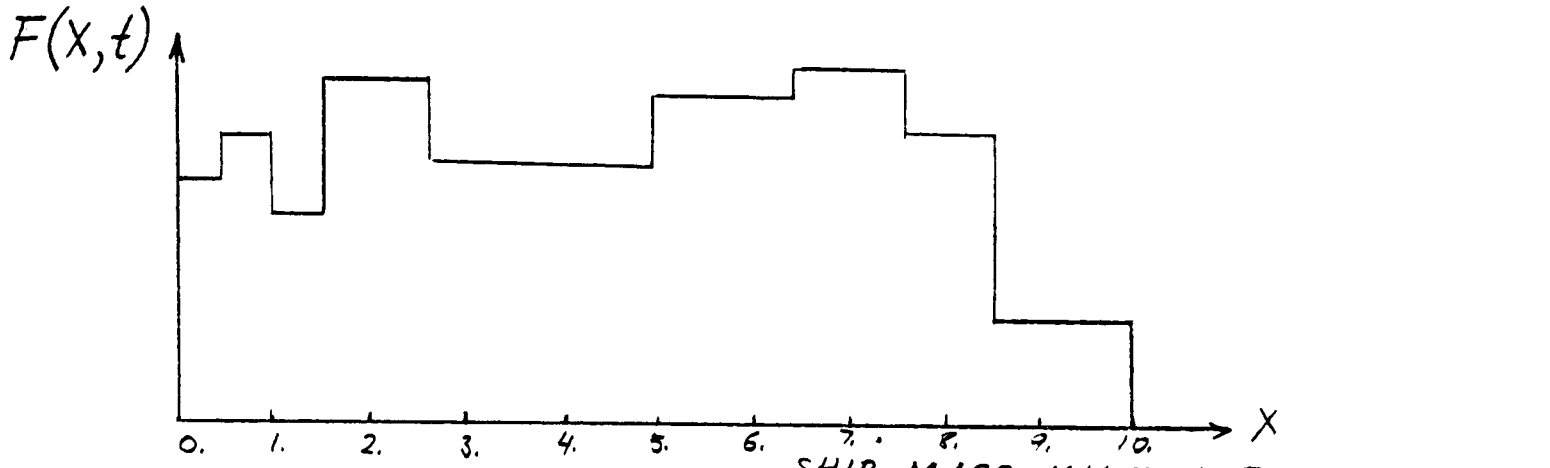

Fig. 1-B

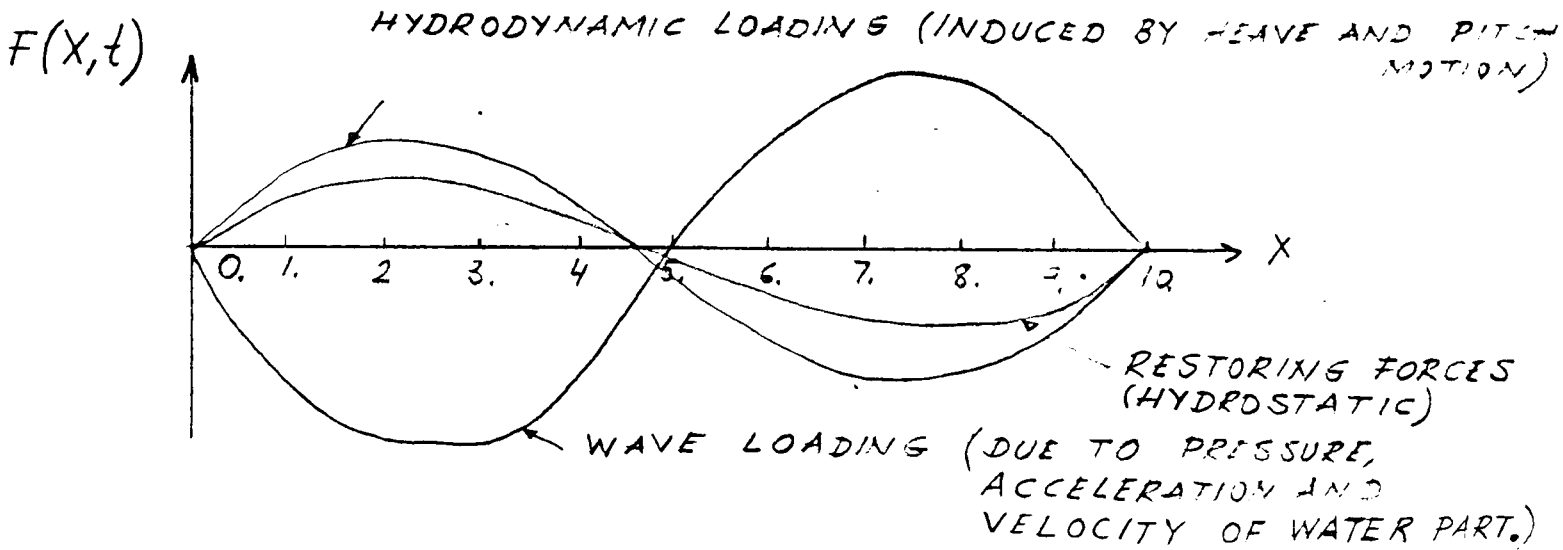

Fig. 1-C

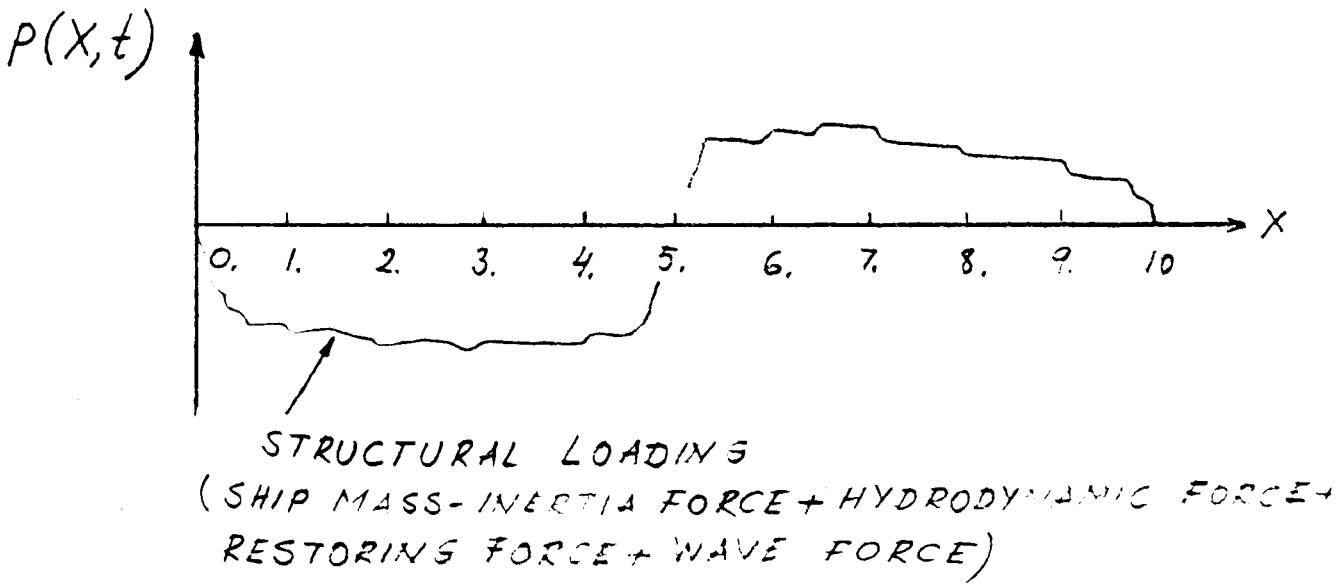

Fig. 1-D

Since the complete system of forces on the structure are in balance at every instant, the area under the structural loading curve given in Fig. 1-D should be zero, i.e. the shear forces should be zero at both ends of the ship. This can be expressed in the following equations:

$$\int_{X=0}^{\ell} p(X,t)\, dX = 0 \tag{1}$$

or

$$SF(0,t) = 0 \quad \text{and} \quad SF(\ell,t) = 0 \tag{1-A}$$

As with equation (1) or (1-A) the following equations should also be satisfied from the equilibrium of external forces acting on the ship, i.e. the total external moment acting on the ship beam should be zero.

$$\int_{X=0}^{\ell} SF(X,t)\, dX = 0 \tag{2}$$

or

$$BM(0,t) = 0 \quad \text{and} \quad BM(\ell,t) = 0 \tag{2-A}$$

Shear forces and bending moments may be calculated at any point along the ship length by averaging the shear forces and bending moments computed separately for the two ends of the ship as follows (taking due account of sign convention used).

$$SF(X_A,t) = \frac{1}{2}\left[\int_{X=0}^{X_A} p(X,t)\, dX + \int_{X=\ell}^{X_A} p(X,t)\right] dX \tag{3}$$

$$BM(X_A,t) = \frac{1}{2}\left[\int_{X=0}^{X_A}\int_{X=0}^{X_A} p(X,t)\, dX\, dX + \int_{X=\ell}^{X_A}\int_{X=\ell}^{X_A} p(X,t)\right] dX\, dX \tag{4}$$

or

$$BM(X_A,t) = \frac{1}{2}\left[\int_{X=0}^{X_A} SF(X,t)\, dX + \int_{X=\ell}^{X_A} SF(X,t)\right] dX \tag{4-A}$$

The calculation of the structural loading function $p(X,t)$ requires an accurate knowledge of the following parameters.

(a) Wave loading distribution along the ship length, which is a function of ship geometry and the sea state.

(b) Motion responses and their phase angles which are functions of wave loading, ship geometry, and ship mass.

(c) Hydrodynamic load distribution, which is a function of motion responses, their phase angles and ship geometry.

(d) Restoring force distributions which are a function of motion responses, their phase angles and ship geometry.

(e) Ship mass-inertia force distribution, which is a function of motion responses and their phase angles as well as ship mass distribution.

The structural loading function can be broken down into two categories as follows:

(a) Input forces = Wave loading.

(b) Output forces = Hydrodynamic, restoring, mass-inertia forces.

The total input forces will be equal in magnitude and opposite in sign to the total output forces as written in equation (1). As was shown in Fig. 1-D, the structural loading along the ship length will be the algebraic sum of the input and output force distributions. Since, as summarised earlier, a high number of variables are involved in the calculation of output force distributions, some errors due to various uncertainties, for example in mass distribution, added mass or damping coefficients, will generally be unavoidable. These errors in output force distribution will generally cause a reduction in the structural loading distribution and consequently an underestimation of maximum structural response values along the ship length. One point of importance is that the final form of structural loading is obtained as the algebraic summation of a number of very large magnitudes and a small percentage of errors in any one of them can produce a serious error in the final answer, e.g. the answer may be of the order 10^6 but be obtained as the difference of numbers of the order 10^8. This statement is supported by the experiments carried out in reference [2] and by the present author's own calculations (Sect. 1.4). Therefore, the author suggests that a consideration only of wave loading and the assumption

that the ship is somehow restrained in waves may avoid the under-estimation of the structural response values for preliminary design purposes.

The shear force and the bending moment values written in equations (3) and (4) do not reflect the full dynamic phenomena. When we consider the problem in dynamic terms the elastic deflections of the beam which represent the ship deformations in waves may be described with the following equation using elastic deflection-load relation (Euler-Bernoulli equation) [4]

$$E \frac{\partial^2}{\partial X^2} \left(I(X) \frac{\partial^2 y}{\partial X^2} \right) = p(X,t) \tag{5}$$

(Shear deformations and rotary inertia terms are neglected.)

where $p(X,t) = f_w(X,t) - \left[(M(X) + M'_{22}(X)) \frac{\partial^2 y}{\partial t^2} + C_{22}(X) \frac{\partial y}{\partial t} + K_{22}(X) \cdot y \right]$ (5-A)

or equation (5) becomes

$$E \frac{\partial^2}{\partial X^2} \left(I(X) \frac{\partial^2 y}{\partial t^2} \right) + (M(X) + M'_{22}(X)) \frac{\partial^2 y}{\partial t^2} + C_{22}(X) \frac{\partial y}{\partial t} + K_{22}(X)\, y = f_w(X,t) \tag{6}$$

If we consider the undamped free vibration of the ship, equation (6) becomes

$$E \frac{\partial^2}{\partial X^2} \left(I(X) \frac{\partial^2 y}{\partial x^2} \right) + (M(X) + M'_{22}(X)) \frac{\partial^2 y}{\partial t^2} + K_{22}(X)\, y = 0 \tag{7}$$

Since the total mass of a ship is distributed non-uniformly over the ship length, the ship in waves represents a multi-degree-of-freedom system and, therefore, there will be an infinite number of discrete natural frequencies.

A solution of equation (7) can be obtained by separation of variables assuming that the solution has the following form

$$y_d(X,t) = \phi(X)\, T(t) \tag{8}$$

where $\phi(X)$ represents a shape of the free vibrating beam and $T(t)$ represents the variation of the amplitude of this vibrating beam with time. The following equation is obtained by substituting

equation (8) into equation (7)

$$E\frac{\partial^2}{\partial X^2}\left(I(X)\ \frac{\partial^2\phi}{\partial x^2}\right)T(t)+\left[M(X)+M'_{22}(X)\right]\frac{\partial^2 T}{\partial t^2}\,\phi(X)+K_{22}(X)\ \phi(X)\,T(t)=0 \qquad (9)$$

When both sides of equation (9) are divided by $\left[M(X)+M'_{22}(X)\right]\phi(X)\,T(t)$ the following form is obtained

$$\frac{\partial^2}{\partial X^2}\left(I(X)\ \frac{\partial^2\phi}{\partial x^2}\right)\frac{E}{M(X)+M'_{22}(X)}\ \frac{1}{\phi(X)}+\frac{K_{22}(X)}{M(X)+M'_{22}(X)}+\frac{\partial^2 T}{\partial t^2}\ \frac{1}{T}=0 \qquad (10)$$

Since the first two terms are only a function of X and the third term is only a function of T, equation (10) can only be satisfied for abritrary X and t values if the following equation holds

$$\frac{\partial^2}{\partial X^2}\left(I(X)\frac{\partial^2\phi}{\partial x^2}\right)\frac{E}{M(X)+M'_{22}(X)}\ \frac{1}{\phi(X)}+\frac{K_{22}(X)}{M(X)+M'_{22}(X)}=C=-\frac{\partial^2 T}{\partial t^2}\ \frac{1}{T} \qquad (10\text{-}A)$$

Equation (10-A) generates two differential equations which can be solved as follows

$$\frac{\partial^2 T}{\partial t^2}+C\,T(t)=0 \qquad (11)$$

If we set $C=\omega^2$ the following form of solution for an ordinary differential equation is obtained

$$T(t)=A\cos(\omega t-\alpha) \qquad (11\text{-}A)$$

where A and α can be obtained from the systems initial conditions.

The second differential equation from equation (10-A) takes the following form

$$\frac{\partial^2}{\partial X^2}\left(I(X)\ \frac{\partial^2\phi}{\partial x^2}\right)\frac{E}{M(X)+M'_{22}(X)}\ \frac{1}{\phi(X)}+\frac{K_{22}(X)}{M(X)+M'_{22}(X)}=\omega^2 \qquad (12)$$

When both sides of equation (12) are divided by $\dfrac{E}{M(X)+M'_{22}(X)}$

and rearrangement of equation (12) gives

$$\frac{\partial^2}{\partial X^2}\left(I(X)\ \frac{\partial^2\phi}{\partial X^2}\right)\frac{1}{\phi(X)}=\frac{\omega^2\left[M(X)+M'_{22}(X)\right]}{E}-\frac{K_{22}(X)}{E} \qquad (13)$$

$$\text{or} \quad \frac{\partial^2}{\partial X^2}\left(I(X)\,\frac{\partial^2 \phi}{\partial X^2}\right) - \alpha(X)\;\phi(X) = 0 \tag{13-A}$$

$$\text{where} \quad \alpha(X) = \frac{\omega^2\,(M(X) + M'_{2\,2}(X)) - K_{2\,2}(X)}{E}$$

when $\alpha(X) = 0$ in equation (13-A) this case corresponds to the rigid body vibration of the ship with the following frequency

$$\omega^2 = \frac{\int_0^{\ell} K_{2\,2}(X)\,dX}{\int_0^{\ell} (M(X) + M'_{2\,2}(X))\,dX}$$

The solution of the ordinary differential equation given in (13-A), which represents undamped free vibration of a beam, should be in the following form

$$\phi(X) = A_1\phi_1(X) + A_2\phi_2(X) + A_3\phi_3(X) + A_4\phi_4(X) \tag{14}$$

The following relations can also be written from the boundary conditions of the free-free beam

$$EI(X)\left.\frac{\partial^2 \phi}{\partial X^2}\right|_{X\,=\,o,\ell} = EI(X)\;\phi''(X)\Big|_{X\,=\,o,\ell} \tag{15}$$

$$EI(X)\left.\frac{\partial^3 \phi}{\partial X^3}\right|_{X\,=\,o,\ell} = EI(X)\phi'''(X)\Big|_{X\,=\,o,\ell} \tag{15-A}$$

When equation (14) is substituted into equations (15) and (15-A) the following simultaneous equations are obtained

$$A_1\phi_1''(o) + A_2\phi_2''(o) + A_3\phi_3''(o) + A_4\phi_4''(o) = 0 \tag{16}$$

$$A_1\phi_1'''(o) + A_2\phi_2'''(o) + A_3\phi_3'''(o) + A_4\phi_4'''(o) = 0 \tag{16-A}$$

$$A_1\phi_1''(\ell) + A_2\phi_2''(\ell) + A_3\phi_3''(\ell) + A_4\phi_4''(\ell) = 0 \tag{16-B}$$

$$A_1\phi_1'''(\ell) + A_2\phi_2'''(\ell) + A_3\phi_3'''(\ell) + A_4\phi_4'''(\ell) = 0 \tag{16-C}$$

A_1, A_2, A_3 and A_4 can only exist if the following determinant vanishes

$$\begin{vmatrix} \phi_1''(o) & \phi_2''(o) & \phi_3''(o) & \phi_4''(o) \\ \phi_1'''(o) & \phi_2'''(o) & \phi_3'''(o) & \phi_4'''(o) \\ \phi_1''(\ell) & \phi_2''(\ell) & \phi_3''(\ell) & \phi_4''(\ell) \\ \phi_1'''(\ell) & \phi_2'''(\ell) & \phi_3'''(\ell) & \phi_4'''(\ell) \end{vmatrix} = 0 \qquad (16\text{-D})$$

The above determinant provides an equation which will be in ω and its roots will be the natural frequencies of free-free beam. For each ω_i value the A_1, A_2, A_3 and A_4 values and the corresponding shape function $\phi_i(X)$ can be found.

The forced vibration of the beam given in equation (6) may be solved using the mode superposition analysis. Details of the mode superposition analysis are given in reference [4] and the application of the forced vibration for the ship case were discussed in references [5,6].

Once $y_d(X,t)$ values are obtained the dynamic structural response values can be determined directly as follows

$$BM(X,t) = - \sum_{i=1}^{n} EI(X) \frac{\partial^2 y_d}{\partial X^2} \qquad (17)$$

$$SF(X,t) = - \sum_{i=1}^{n} EI(X) \frac{\partial^2 y_d}{\partial X^2} \qquad (17\text{-A})$$

It should also be noted that for most types of loadings the contributions of the various modes generally are greatest for the lowest frequencies and tend to decrease for the higher frequencies. Consequently, it is not usually necessary to include all the higher modes of vibration in the superposition process (in equations (17) and (17-A)). The summation can provide enough accuracy with the first few terms.

When floating offshore structures are considered, theoretical predictions for the structural response become more difficult simply because the above summarised procedures for a beam which represents the ship should be applied for an array of beams which comprise the floating structure. Therefore, a high number of equations will be involved in quasi-static or in dynamic analysis. Solutions of these equations require extensive use of computers.

In this study, the structural response analysis for floating offshore platforms is carried out to find the shear forces, bending moments and axial forces along the structural members of the platform by analysing the entire structure as a space frame. Having obtained wave loading, hydrodynamic loading, restoring forces and platform mass inertia distributions along the members of the floating structure, a frame analysis can be carried out. (The procedures to determine wave loading were described in Chapter 3, and the hydrodynamic loading, restoring forces and platform-mass inertia forces were derived in Chapter 4.)

In this section a structural analysis procedure will be summarised for a determinate floating structure for the following cases:

(a) Structure is restrained in waves, loading is quasi-static.

(b) Structure is free-floating, loading is quasi-static.

(c) Structure is restrained in waves, loading is dynamic.

(d) Structure is free-floating, loading is dynamic.

Here the term quasi-static implies that the deformations of the members under the time varying loading are the same magnitude as would have occurred if the loading were static. The term of dynamic loading implies that structural response values are calculated by taking the dynamic deformations of the members into account.

An analysis of these four different loading conditions will be made to study the effects of rigid-body and local vibrations on the structural response evaluations.

1.1 Floating Structure is Restrained in Waves, Loading is Quasi-Static

At the first stage of analysis, let us assume that the floating structure comprises two vertical cylinders and a horizontal beam as shown in Fig. 2. It will also be assumed that the structure is somehow prevented from all rigid body motions. However, no physical boundaries

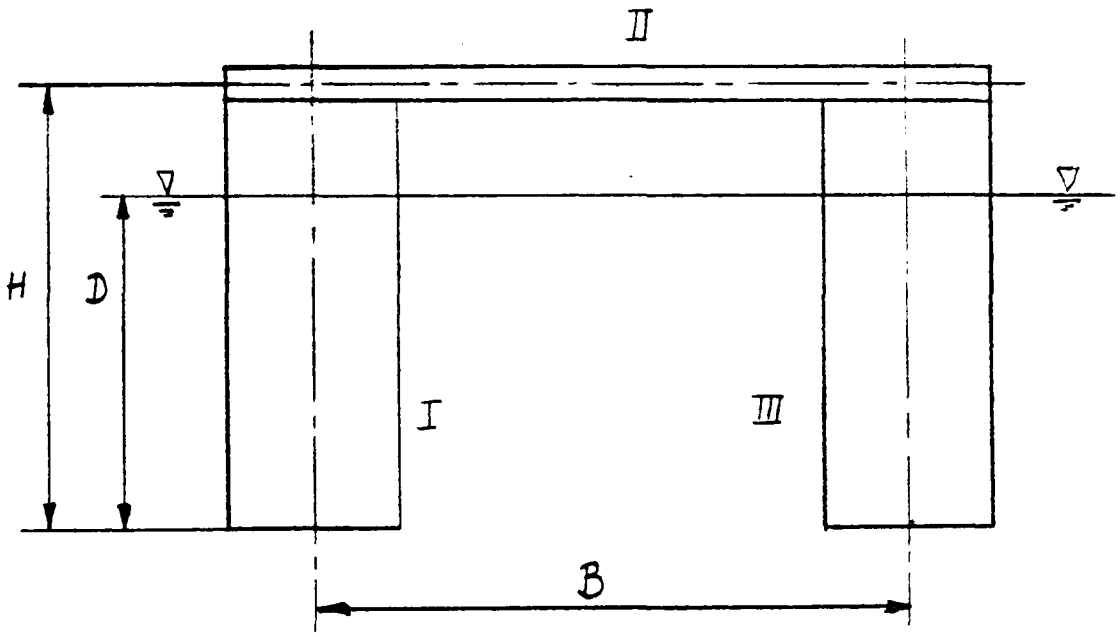

Fig. 2

are introduced for the structural response analysis at this stage since response values depend on the boundary conditions. Therefore, the analysis will be carried out as if the floating structure is in quasi-equilibrium at each instant over the given wave period and axial force, bending moment and shear forces at any point throughout the structure are calculated by writing the equilibrium equation between the external and the internal forces at that particular point. The structural response analysis procedure for the floating structure shown in Fig. 2 may be summarised as follows.

(a) Representation of the structure as a frame system and the division of each member into a finite number of beam elements. The number of beam elements is chosen arbitrarily depending on the size of the global elements.

(b) Calculation of wave loading on each node (Fig. 3). At each wave frequency the corresponding period is divided into 20 steps and calculations are carried out at each time step throughout the full cycle. The calculation procedure is discussed in detail in Chapter 3. When wave loading computations are done using the "WAVLOA" program the generation of the nodal points and the distribution of wave loading over the nodal points are performed simultaneously by the computer routine.

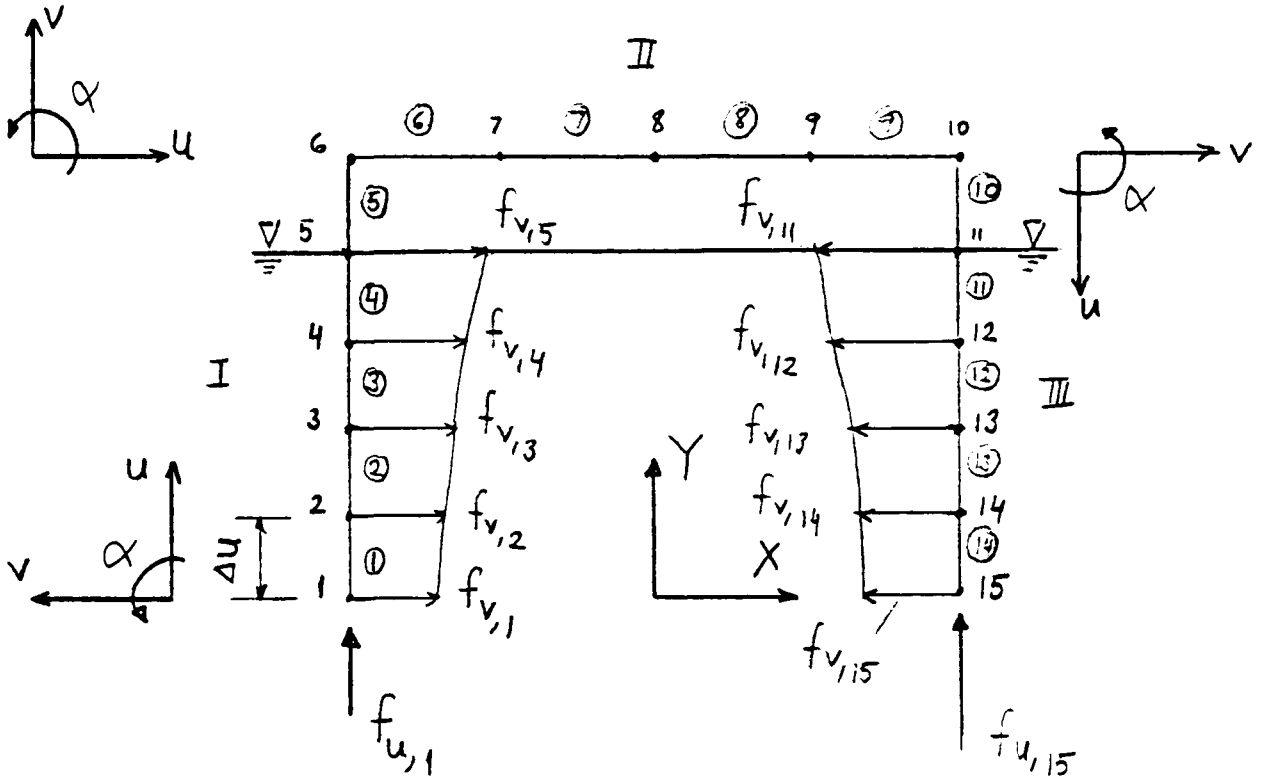

Fig. 3

(c) Determination of the structural response to the wave loading at each time step. A calculation procedure to obtain shear forces, bending moments and the axial forces due to wave loading for the structure shown in Fig. 3 is given in the following.

Global Member: I:

$$\text{Shear Forces: } SF_i(u,t) = \left[2f_{v,i} + \left(\frac{f_{v,i+1} - f_{v,i}}{\Delta u}\right)(u - i\Delta u)\right]\frac{\Delta u}{2} \cdot \varepsilon_i + SF_{i-1}(u,t)\Big|_{u=(i-1)\Delta u} \tag{18}$$

where

$SF_i(u,t)$: Shear force variation along the member i. (u,v) is the local co-ordinate system for each member.

$f_{w,i}, f_{u,i}$: Wave force magnitude on the node i. $f_{w,i}, f_{u,i}$ values are functions of time and the structure's orientation in waves.

$\varepsilon_i = 1$ for $i < 5$

$\varepsilon_i = 0$ for $i = 5$

Δu: The distance between the two nodes, if this distance differs on each member, equation (18) can be written as:

$$SF_i(u,t) = \left[2f_{v,i} + \frac{f_{v,i+1} - f_{v,i}}{\Delta u_i}\left(u - \sum_{n=1}^{i} n\Delta u\right)\right]\frac{\Delta u_i}{2} \cdot \varepsilon_i + SF_{i-1}(u,t)\Big|_{u=\sum_{n=1}^{i} n\Delta u} \tag{18-A}$$

where

Δu_i: The distance between the two nodes of member i.

Similarly bending moments may be written as,

$$BM_i(u,t) = -\left\{\left[3f_{v,i} + \frac{f_{v,i+1} - f_{v,i}}{u}(u - i\Delta u)\right]\frac{(\Delta u)^2}{6}\varepsilon_i + BM_{i-1}(u,t)\Big|_{u=(i-1)\Delta u}\right\} \tag{19}$$

where

$BM_i(u,t)$: Bending moment variation along the member i.

$\varepsilon_i = 1$ for $i < 5$

$\varepsilon_1 = 0$ for $i = 5$

Axial forces on Global Member I may be written as,

$$AF_i(u,t) = - f_{u,1} \tag{20}$$

Global Member: II:

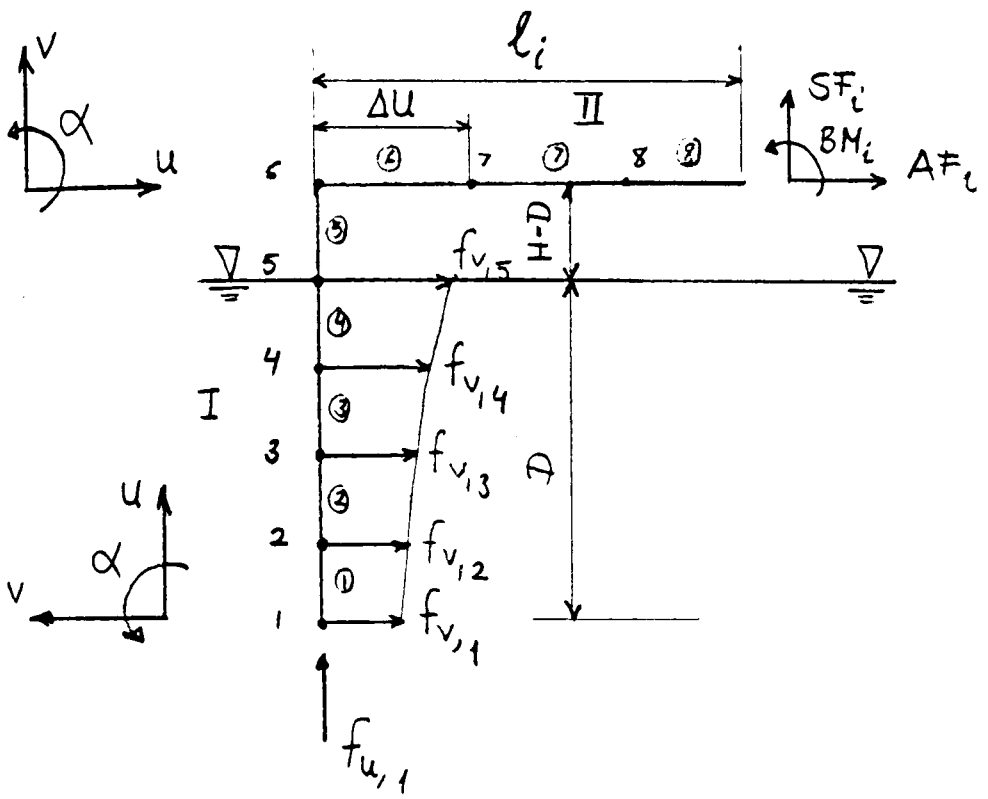

Fig. 4

$$\text{Shear Forces} \quad : \quad SF_i(u,t) = - f_{u,1} \tag{21}$$

$$\text{Bending Moments:} \quad BM_i(u,t) = - \left\{ BM_4(u,t)\Big|_{u_1=4\Delta u} + SF_4(u,t)\Big|_{u_1=4\Delta u} (H-D) - f_{u,1}\,\ell_i \right\} \tag{22}$$

$$\text{Axial Forces} \quad : \quad AF_i(u,t) = - SF_4(u,t)\Big|_{u_1=4u} \tag{23}$$

where u_1 shows the distance on global member I.

Global Member: III:

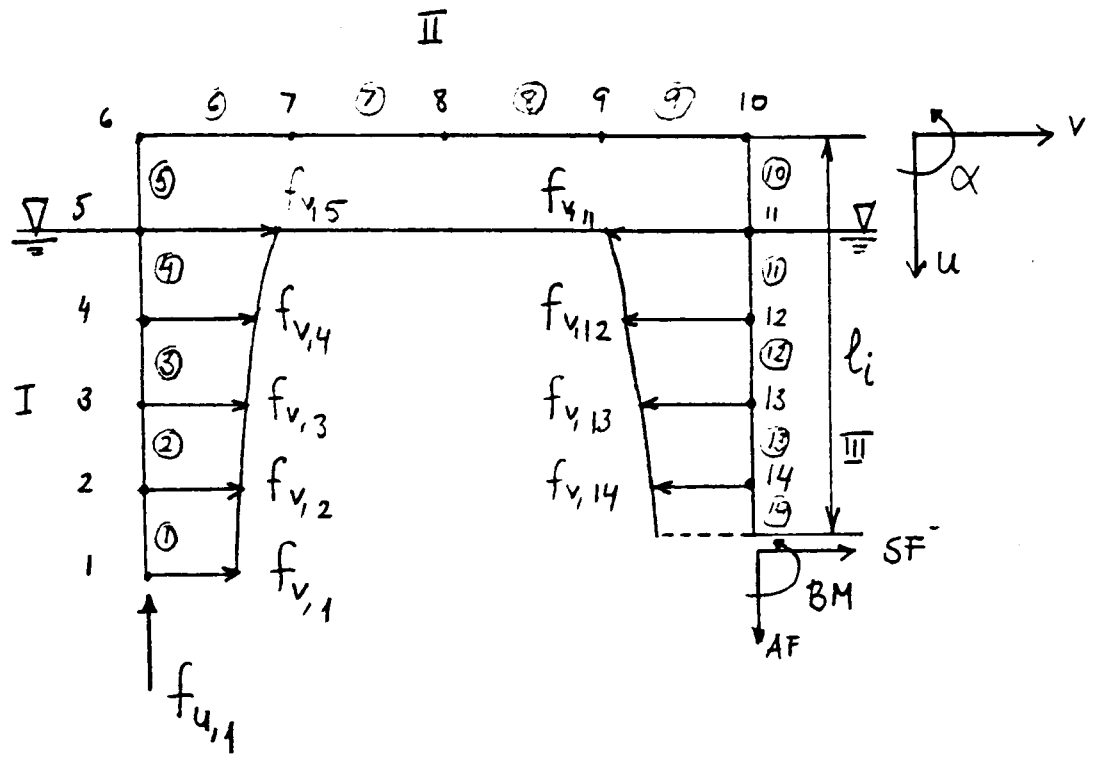

Fig. 5

Shear Forces:

$$SF_i(u,t) = SF_4(u,t) - \left\{\left[2f_{v,i} - \left(\frac{f_{v,i} - f_{v,i+1}}{\Delta u}\right)(u - (i-10)\Delta u)\right]\right.$$

$$\left.\frac{\Delta u}{2} \cdot \varepsilon_i + SF_{i-1}(u,t)\Big|_{u=(i-10)\Delta u} \cdot \varepsilon_{i-1} \cdot \varepsilon_i\right\} \qquad (24)$$

where $\varepsilon_i = 0$ for $i = 10$

$\varepsilon_1 = 1$ for $i > 10$

Bending Moments:

$$BM_i(u,t) = BM_4(u,t) + SF_4(u,t)\,[H - D - \ell_i]$$

$$- \left\{\left[3f_{v,i} - \left(\frac{f_{v,i} - f_{v,i+1}}{\Delta u}\right)(u - (i-10)\Delta u)\right]\right.$$

$$\left.\frac{(\Delta u)^2}{6} \cdot \varepsilon_i + BM_{i-1}(u,t)\Big|_{u=(i-10)\Delta u} \varepsilon_{i-1}\, \varepsilon_i\right\} \qquad (25)$$

where $\varepsilon_i = 0$ for $i = 10$

$\varepsilon_1 = 1$ for $i > 10$

Axial Forces: $AF_i(u,t) = f_{u,1}$ (26)

So far, structural response values have been obtained by writing the equilibrium equations between external and internal forces in the form of an integration which is calculated starting from the left hand side of the structure. The same procedure may also be followed starting from the right hand side of the structure. The response values of a point on the structure should be independent of the integration route. However, this may not hold in the case of the calculation procedure given above because external forces acting on the structure may not be in balance at every instant over a given wave cycle. The structural non-compatibility problem can be overcome by introducing fictitious supports on the frame representation of the floating platform. These support points should be chosen in such a way that their influences on the response values will be minimal. (This aspect will be discussed later.) For the present case it is suggested that structural response predictions should be made by averaging the shear force, bending moment, and axial force values obtained from the equilibrium equations integrated from both the left and the right hand sides of the structure.

This may be formulated as,

$$\text{Shear Forces} : \bar{SF}_i(u,t) = \tfrac{1}{2}[SF_i(u,t)_{LEFT} + SF_i(u,t)_{RIGHT}] \quad (27)$$

$$\text{Bending Moments}: \bar{BM}_i(u,t) = \tfrac{1}{2}[BM_i(u,t)_{LEFT} + BM_i(u,t)_{RIGHT}] \quad (28)$$

$$\text{Axial Forces} : \bar{AF}_i(u,t) = \tfrac{1}{2}[AF_i(u,t)_{LEFT} + AF_i(u,t)_{RIGHT}] \quad (29)$$

where, $\bar{SF}_i(u,t)$, $\bar{BM}_i(u,t)$, $\bar{AF}_i(u,t)$ are the average shear force, bending moment and axial force values of a point on the structure respectively.

To find out the maximum structural response values at a particular wave frequency, calculations should be repeated throughout the corresponding wave period. In this study calculations are repeated 21 times throughout one wave cycle. However, if symmetry exists in the wave loading, depending on geometry and orientation of the structure in waves, it may be sufficient to consider only a quarter of a wave cycle.

The structural response to the wave loading will be determined by introducing successively two fictitious fixed supports at convenient points on the right and left hand sides of the floating structure. Response calculations will be carried out for both cases and then the required response values will be the average of these two results. In this procedure response values on the supports should not be taken into account, i.e. the actual values on the supports will be zero. The procedure may be illustrated as follows.

(a) Introduction of the fixed end support on the last node at the right hand side of the structure, Fig. 6.

(b) Calculation of the structural response values when the last node at the right hand side is fixed for translational and rotational movements.

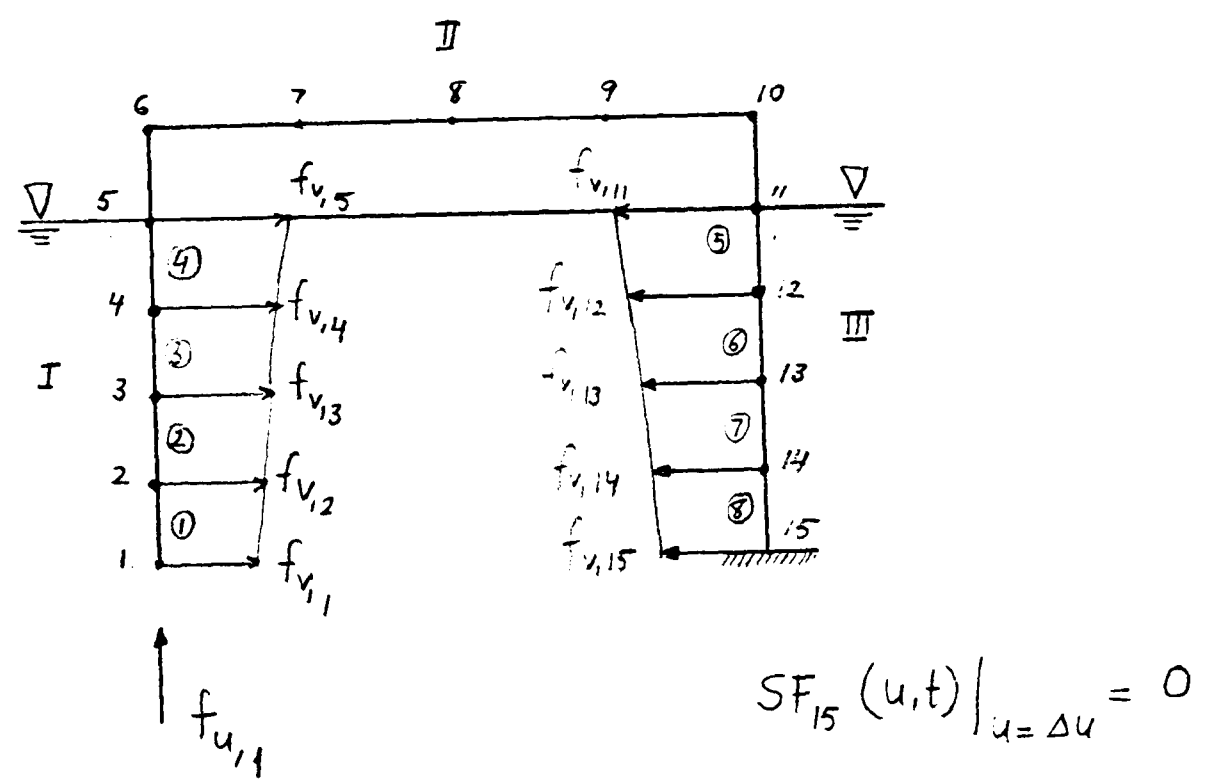

Fig. 6

(c) Introduction of the fixed end support on the last node at the left hand side of the structure, Fig. 7.

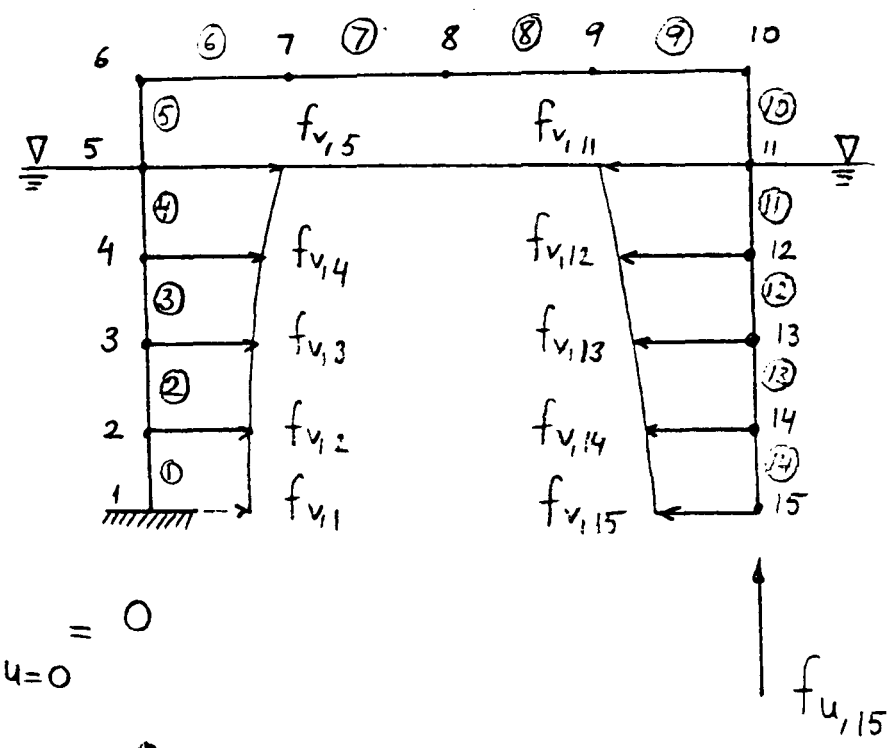

$$SF_1(u,t)\Big|_{u=0} = 0$$

$$BM_1(u,t)\Big|_{u=0} = 0$$

$$AF_1(u,t)\Big|_{u=0} = 0$$

Fig. 7

(d) Calculation of the structural response values when the last node at the left hand side is fixed for translational and rotational movements.

(e) The structural response values at any point on the structure may be obtained as follows:

$$\overline{SF}_i(u,t) = \frac{1}{2}\left\{SF_i(u,t)\right\}_{\substack{\text{RIGHT HAND}\\ \text{SIDE FIXED}}} + \left\{SF_i(u,t)\right\}_{\substack{\text{LEFT HAND}\\ \text{SIDE FIXED}}} \qquad (30)$$

$$\overline{BM}_i(u,t) = \frac{1}{2}\left\{BM_i(u,t)\right\}_{\substack{\text{RIGHT HAND}\\ \text{SIDE FIXED}}} + \left\{BM_i(u,t)\right\}_{\substack{\text{LEFT HAND}\\ \text{SIDE FIXED}}} \qquad (31)$$

$$\overline{AF}_i(u,t) = \frac{1}{2}\left\{AF_i(u,t)\right\}_{\substack{\text{RIGHT HAND}\\ \text{SIDE FIXED}}} + \left\{AF_i(u,t)\right\}_{\substack{\text{LEFT HAND}\\ \text{SIDE FIXED}}} \qquad (32)$$

Equations (30-32) are identical to the equations given in (27-29). This can also be shown with the following calculations. If single horizontal and vertical point loads are assumed to be applied on the first and the last members of a floating structure shown in Fig. 2 (this loading case is chosen for the sake of simplicity) the following

structural response values can be obtained for the unsupported structure case shown in Fig. 8.

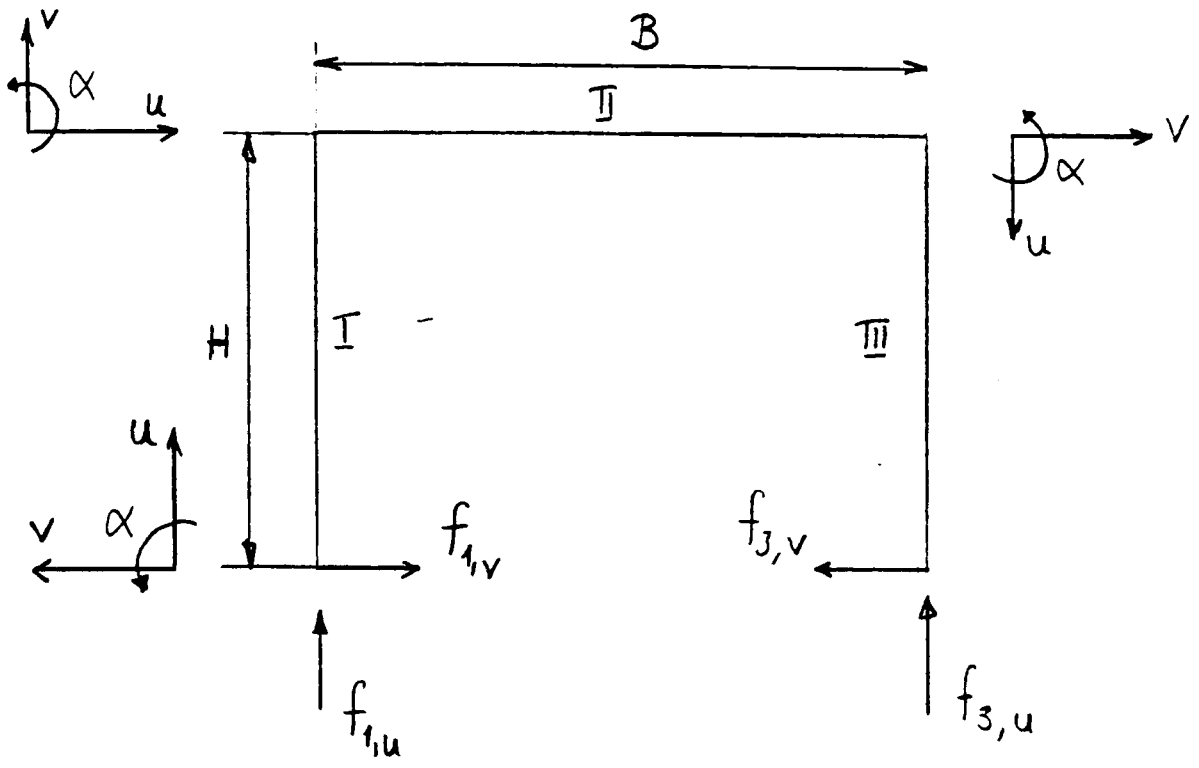

Fig. 8

(a) Integration from the left hand side:

Global Member: I:

$$\text{Shear Forces} : SF_1(u,t) = f_{1,v} \tag{33-A}$$

$$\text{Bending Moments}: BM_1(u,t) = - f_{1,v} \cdot u \tag{33-B}$$

$$\text{Axial Forces} : AF_1(u,t) = - f_{1,u} \tag{33-C}$$

Global Member: II:

$$\text{Shear Forces} : SF_2(u,t) = - f_{1,u} \tag{34-A}$$

$$\text{Bending Moments}: BM_2(u,t) = - f_{1,v} \cdot H + f_{1,u} \cdot u \tag{34-B}$$

$$\text{Axial Forces} : AF_2(u,t) = - f_{1,v} \tag{34-C}$$

Global Member: III:

$$\text{Shear Forces} : SF_3(u,t) = - f_{1,v} \tag{35-A}$$

$$\text{Bending Moments}: BM_3(u,t) = - f_{1,v} (H-u) + f_{1,u} \cdot B \tag{35-B}$$

$$\text{Axial Forces} : AF_3(u,t) = f_{1,u} \tag{35-C}$$

(b) Integration from the right hand side:

Global Member: I:

Shear Forces : $SF_1(u,t) = f_{3,v}$ (36-A)

Bending Moments: $BM_1(u,t) = - f_{3,v} u + f_{3,u} \cdot B$ (36-B)

Axial Forces : $AF_1(u,t) = + f_{3,u}$ (36-C)

Global Member: II:

Shear Forces : $SF_2(u,t) = f_{3,u}$ (37-A)

Bending Moments: $BM_2(u,t) = - f_{3,v} \cdot H + f_{3,u} \cdot (B-u)$ (37-B)

Axial Forces : $AF_2(u,t) = - f_{3,v}$ (37-C)

Global Member: III:

Shear Forces : $SF_3(u,t) = - f_{3,v}$ (38-A)

Bending Moments: $BM_3(u,t) = - f_{3,v} (H-u)$ (38-B)

Axial Forces : $AF_3(u,t) = - f_{3,u}$ (38-C)

(c) The structural response values along the members:

Global Member: I:

Shear Forces : $\overline{SF}_1(u,t) = \frac{1}{2}[f_{1,v} + f_{3,v}]$ (39-A)

Bending Moments: $\overline{BM}_1(u,t) = \frac{1}{2}[Bf_{3,u} - (f_{1,v} + f_{3,v})u]$ (39-B)

Axial Forces : $\overline{AF}_1(u,t) = \frac{1}{2}[- f_{1,u} + f_{3,u}]$ (39-C)

Response values for Member I will be valid if $u>0$; for $u=0$;

$\overline{SF}_1(0,t)=0$; $\overline{BM}_1(0,t)=0$; $\overline{AF}_1(0,t)=0$.

Global Member: II:

Shear Forces : $\overline{SF}_2(u,t) = \frac{1}{2}[- f_{1,u} + f_{3,u}]$ (40-A)

Bending Moments: $\overline{BM}_2(u,t) = \frac{1}{2}[u(f_{1,u} + f_{3,u}) - H(f_{1,v} + f_{3,v}) + Bf_{3,u}]$ (40-B)

Axial Forces : $\overline{AF}_2(u,t) = \frac{1}{2}[- f_{1,v} - f_{3,v}]$ (40-C)

Global Member: III:

$$\text{Shear Forces} : \bar{SF}_3(u,t) = \tfrac{1}{2}[-f_{1,v} - f_{3,v}] \quad (41\text{-A})$$

$$\text{Bending Moments}: \bar{BM}_3(u,t) = \tfrac{1}{2}[Bf_{1,u} - (H-u)(f_{1,v} + f_{3,v})] \quad (41\text{-B})$$

$$\text{Axial Forces} : \bar{AF}_3(u,t) = \tfrac{1}{2}[f_{1,u} - f_{3,u}] \quad (41\text{-C})$$

Response values for Member III will be valid if $u<H$; for $u=H$; $\bar{SF}_3(H,t)=0$; $\bar{BM}_3(H,t)=0$; $\bar{AF}_3(H,t)=0$.

The structural response values given by equations (33-A - 41-C) were calculated using the formulations written in equations (18-29).

The same results as were given in equations (33-A), (35-C) can be obtained by introducing a fixed support at the end of Member III (Fig. 9-B). Similarly, when the fixed support condition is applied at the beginning of the first member, response values calculated for this loading case (Fig. 9-C) will be identical to the values given in (36-A - 38-C). The average of these two cases will give the total response values as identical to the ones given in equations (39-A - 41-C).

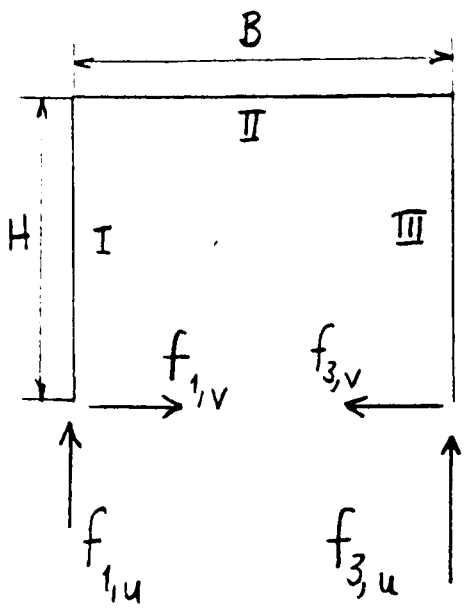

Fig. 9-A

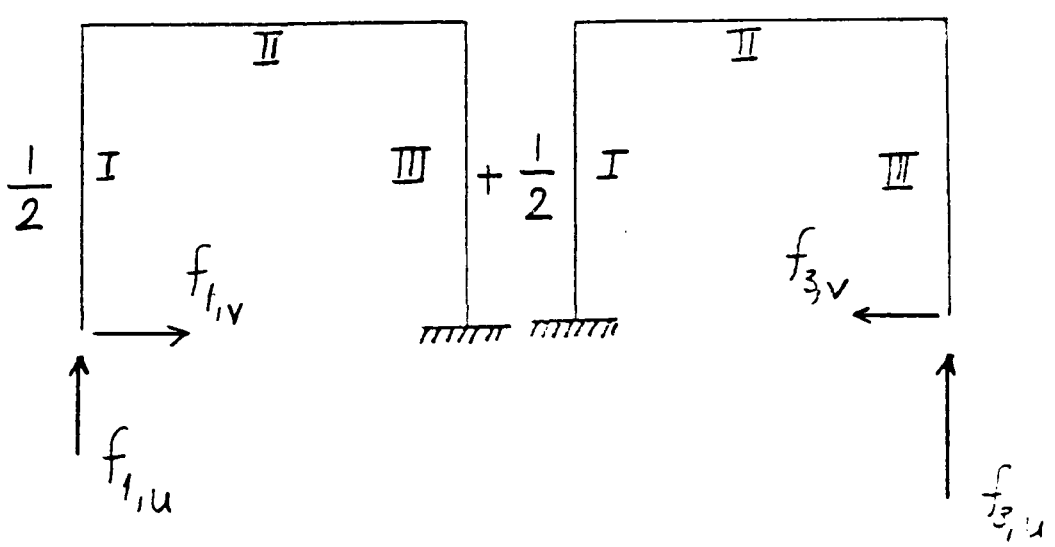

Fig. 9-B

Fig. 9-C

The introduction of the fixed support conditions and the application of the calculation procedure suggested above for the determination

of structural response values solves the non-compatibility problem and provides a suitable form of analysis for general structural analysis procedures which require some kind of physical boundaries to exist on the structure. A general analysis procedure will be important in the case of indeterminate frame analysis problems as will be discussed in Section 2.

Now, the response values of the structure shown in Fig. 8 will be re-calculated for different support conditions, (Fig. 10).

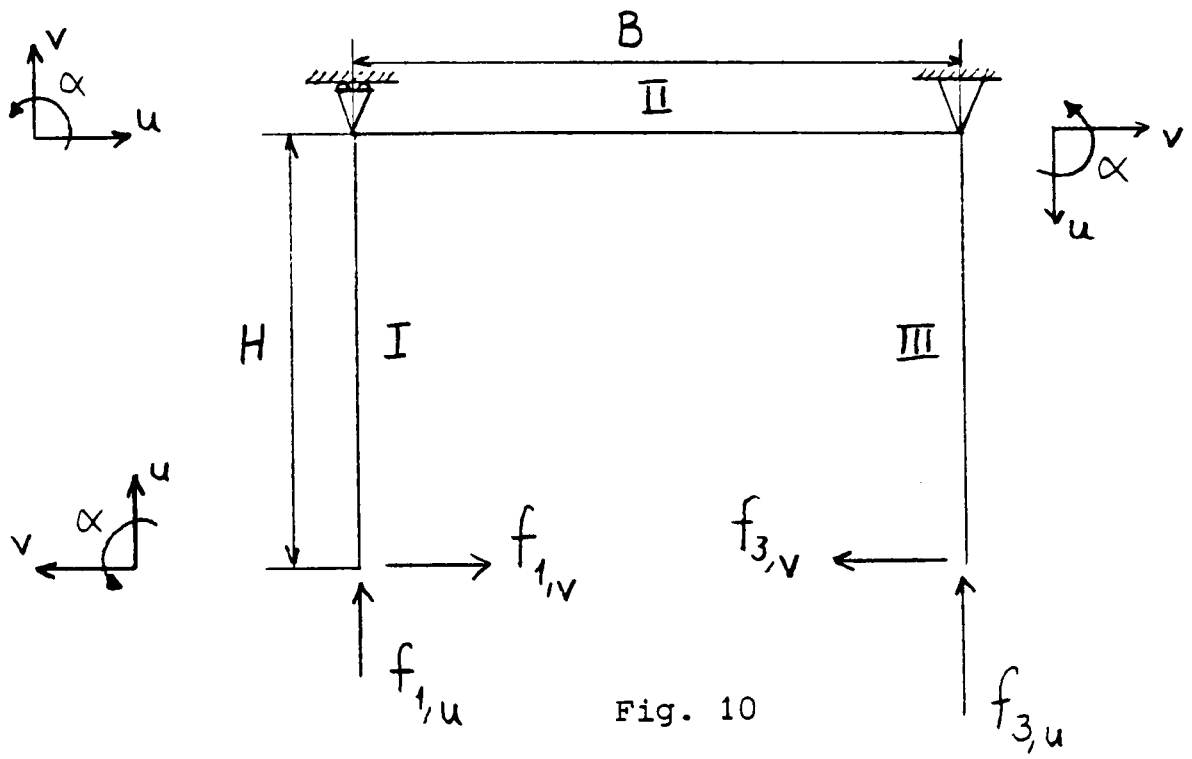

Fig. 10

Global Member: I:

$$\text{Shear Forces} : \overline{SF}_1(u,t) = f_{1,v} \tag{42-A}$$

$$\text{Bending Moments}: \overline{BM}_1(u,t) = - f_{1,v} \cdot u \tag{42-B}$$

$$\text{Axial Forces} : \overline{AF}_1(u,t) = - f_{1,u} \tag{42-C}$$

Global Member: II:

$$\text{Shear Forces} : \overline{SF}_2(u,t) = \frac{H}{B}(f_{1,v} - f_{3,v}) \tag{43-A0}$$

$$\text{Bending Moments}: \overline{BM}_2(u,t) = H[f_{1,v} - \frac{u}{B}(f_{1,v} - f_{3,v})] \tag{43-B}$$

$$\text{Axial Forces} : \overline{AF}_2(u,t) = - f_{1,v} \tag{43-C}$$

Global Member: III:

$$\text{Shear Forces} : \bar{SF}_3(u,t) = - f_{3,v} \tag{44-A}$$

$$\text{Bending Moments}: \bar{BM}_3(u,t) = - f_{3,v}(H-u) \tag{44-B}$$

$$\text{Axial Forces} : \bar{AF}_3(u,t) = - f_{3,u} \tag{44-C}$$

The comparison between equations (39-A - 41-C) and (42-A - 44-C) shows that two different support conditions give completely different response values. (Under some special loading cases, some of the response values can be identical in both cases.) This comparison also reveals that the structural analysis of floating offshore structures will be sensitive to the distribution of the output forces (distribution of hydrodynamic, restoring and mass-inertia forces) which replaces the physical support forces of the examples given above. Thus very precise knowledge of mass distribution, added mass and damping coefficients, motion response values, phase angles, hydrostatic parameters and the kinematic body velocity and acceleration distributions will be essential. If some of the output force distributions cannot be predicted with any certainty the author suggests that a structural response analysis should be carried out under the input force distributions alone (wave loading) using the most pessimistic fictitious support conditions.

1.2 Floating Structure is Free in Waves, Loading is Quasi-Static

When a structure is free floating, applied input wave forces will be balanced by the external output forces at any instant over a wave cycle.

As long as the output force distributions are determined correctly, a structural analysis can be carried out either using the procedure described for a determinate structure by equations (18-26) in which case integrations from either the left or the right hand side will be sufficient, or using any other structural analysis procedures. Since support forces will be zero, as the applied external forces are in balance at any

instant, any support conditions can be applied arbitrarily for a chosen analysis procedure whenever necessary.

In the following, the effects of the output forces will be analysed using the simple loading case shown in Fig. 11. It will be assumed that weight of Member II will be neglected and that the geometry and the weight distributions are identical for Members I and III.

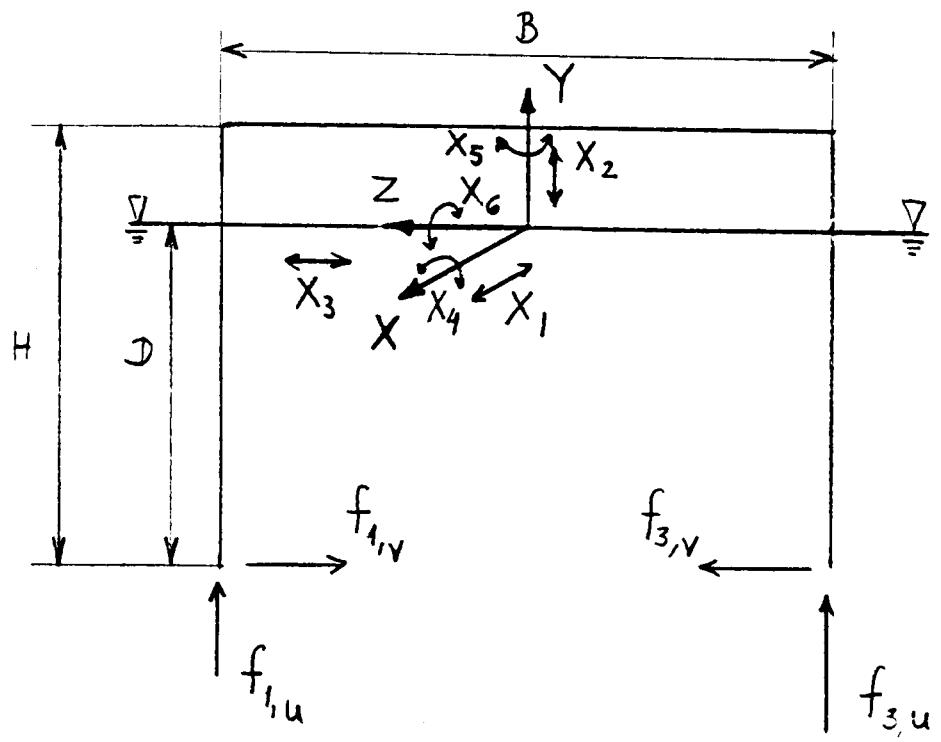

Fig. 11

Case (a) $f_{1,u} = f_{3,u}$ and $f_{3,v} = -f_{1,v}$

When horizontal forces are equal in magnitude and opposite in sign to each other, there will be no output forces due to sway. Similarly, since vertical forces $f_{1,u}$ and $f_{3,u}$ are equal to each other in sign and in magnitude, there will be no rolling induced output forces. The only output forces will be due to the heave motion. The relation between input wave forces and the output forces can be written using the equation given in (69) of Chapter IV.

$$(M+M'_{22})\ddot{X}_2 + C_{22}\dot{X}_2 + K_{22}X_2 = f_{1,u} + f_{3,u} \qquad (43)$$

where

$M\ddot{X}_{22}$: Body-mass inertia force.

$M'_{22}\ddot{X}_{22}$, $C_{22}\dot{X}_2$: Hydrodynamic force induced due to heave acceleration and heave velocity respectively.

$K_{22}X_2$: Hydrostatic force.

The distribution of the input and the output forces is shown in the following diagram. (It is assumed that input wave force frequency ω is greater than natural frequency of rigid body motion ω_n.)

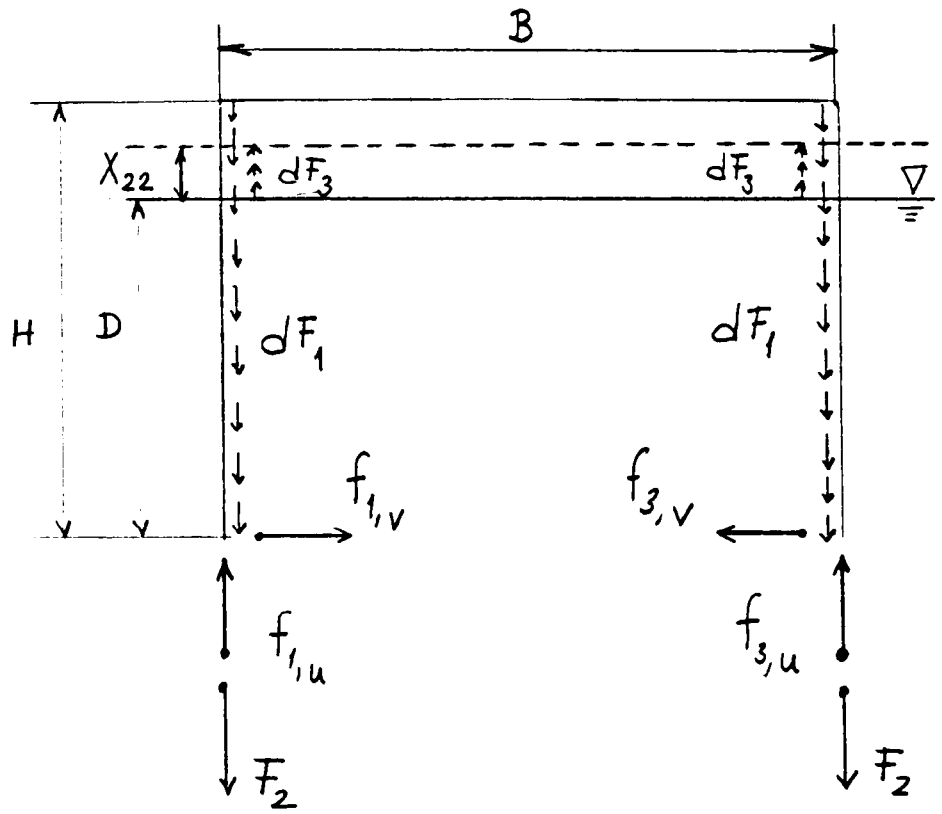

$$dF_1 = \frac{M}{2H}\ddot{X}_2\,du \tag{44}$$

$$F_1 = \int_{u=0}^{H} dF_1\,du \tag{44-A}$$

$$F_2 = \frac{M'_{22}\ddot{X}_{22} + C_{22}\dot{X}_2}{2} \tag{44-B}$$

$$dF_3 = \frac{K_{22}X_2}{2X_2} = \frac{K_{22}}{2}\,du \tag{44-C}$$

$$F_3 = \int_{u=D-X_{22}}^{D} dF_3\,du \tag{44-D}$$

$$2(F_1+F_2-F_3) = f_{1,u} + f_{3,u} \tag{44-E}$$

or $$F_1+F_2-F_3 = f_{1,u} = f_{3,u} \tag{44-F}$$

The structural response values can be determined by writing the equilibrium equations between externally applied loads and internal response loads at points where structural analysis is sought.

Global Member: I:

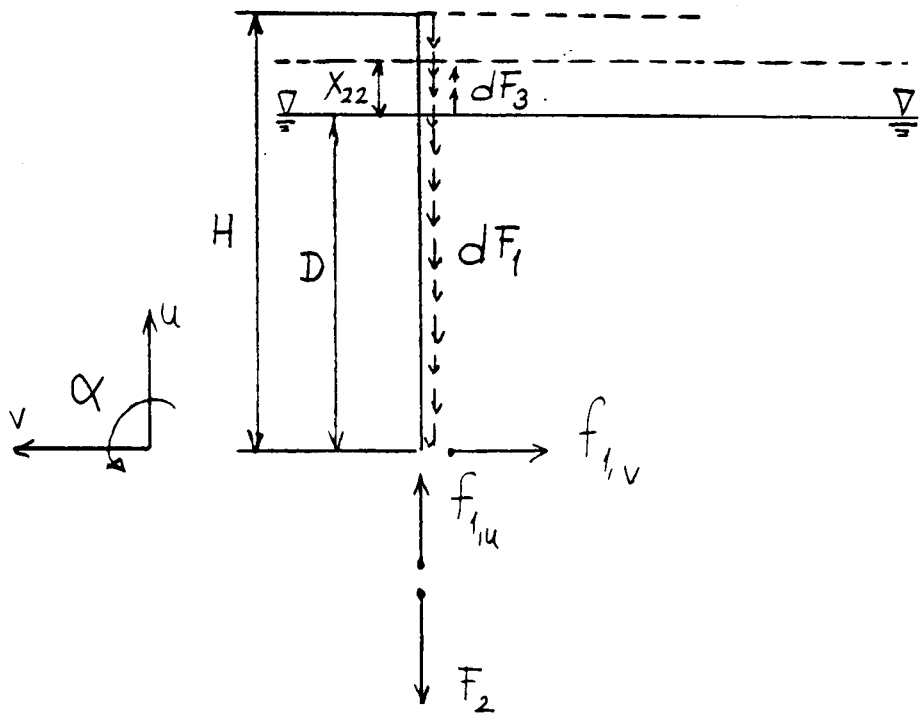

Fig. 12

$$\text{Shear Forces} \quad : \quad SF_1(u,t) = f_{1,v} \tag{45-A}$$

$$\text{Bending Moments:} \quad BM_1(u,t) = - f_{1,v} \cdot u \tag{45-B}$$

$$\text{Axial Forces} \quad : \quad AF_1(u,t) = \int_{u=0}^{u} dF_1 + F_2 - \int_{u=D}^{D+X_{22}} dF_3 - f_{1,u} \tag{45-C}$$

If we compare equations (45-A - 45-C) and (39-A - 39-C) for the present loading case it will be found that shear forces will be the same for both cases. On the other hand, bending moments will be under-predicted by equation (39-B) and axial forces will be overpredicted by equation (39-C).

Global Member: II:

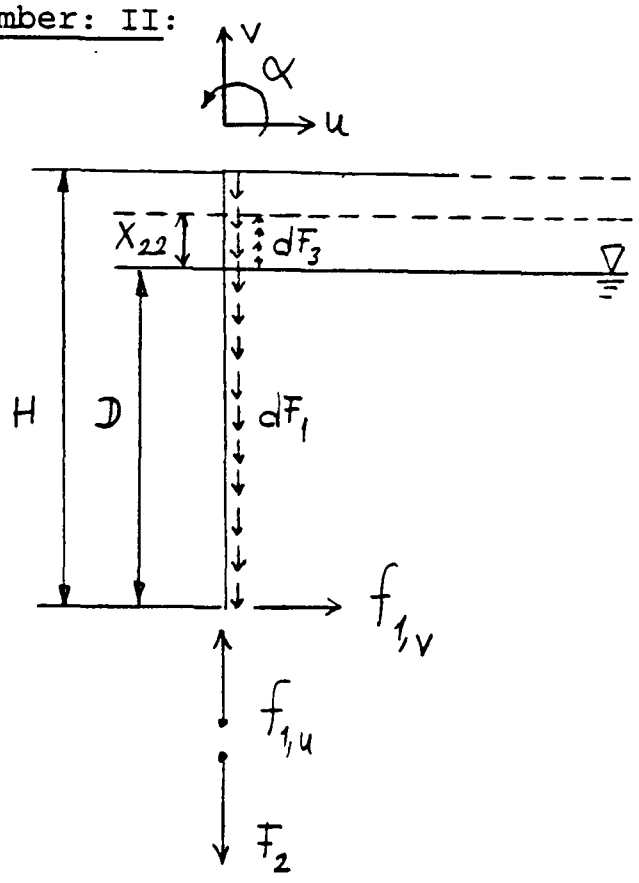

Fig. 13

$$\text{Shear Force} \quad : \quad SF_2(u,t) = \int_{u=0}^{H} dF_1 + F_2 - \int_{u=D}^{D+X_{22}} dF_3 - f_{1,u} = 0 \qquad (46\text{-A})$$

$$\text{Bending Moments:} \quad BM_2(u,t) = (F_1 + F_2 - F_3 - f_{1,u})u - f_{1,v} \cdot H = -f_{1,v} \cdot H \qquad (46\text{-B})$$

$$\text{Axial Forces} \quad : \quad AF_3(u,t) = -f_{1,v} \qquad (46\text{-C})$$

A comparison of equations (40-A - 40-C) with equations (46-A - 46-C) reveals that axial and shear forces are identical in both cases and bending moments are underpredicted by equation (40-B).

Global Member: III:

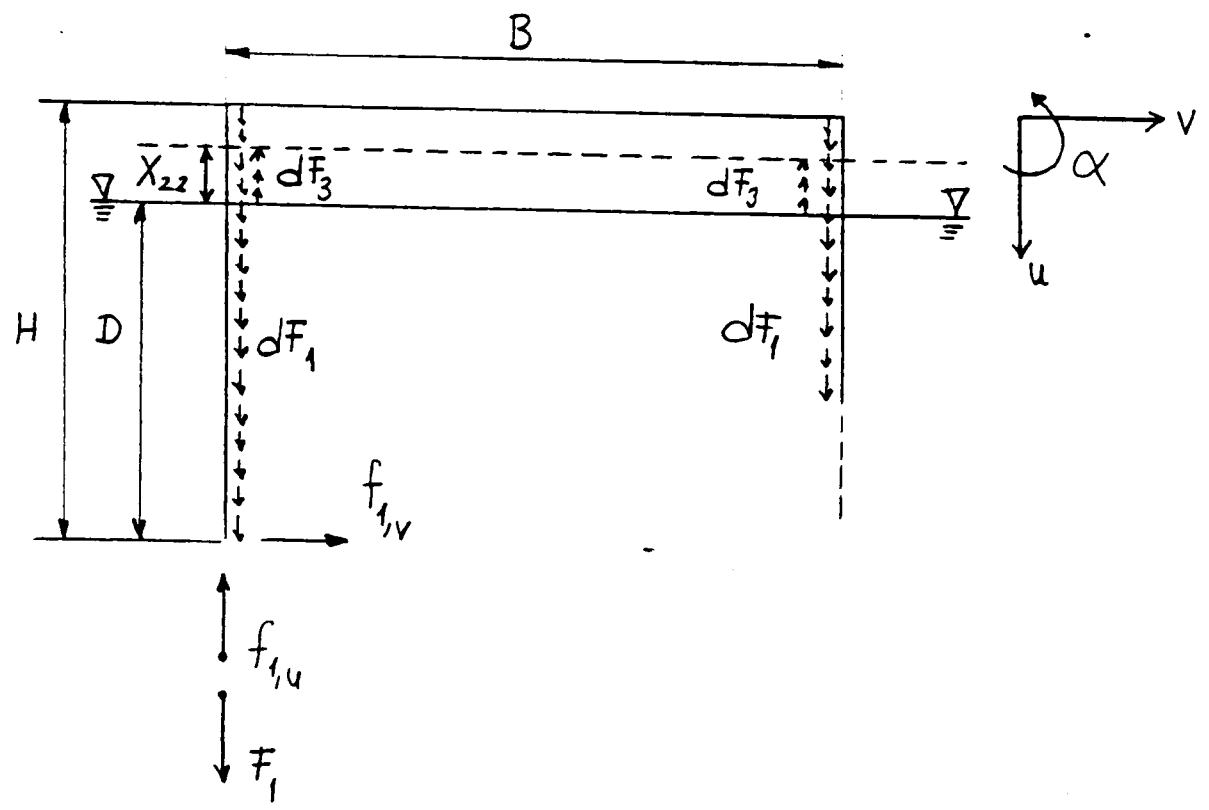

Fig. 14

Shear Forces : $SF_3(u,t) = - f_{1,v}$ (47-A)

Bending Moments: $BM_3(u,t) = (F_1 + F_2 - F_3 - f_{1,u})B - f_{1,v}(H-u)$

$= - f_{1,v}(H-u)$ (47-B)

Axial Forces : $AF_3(u,t) = F_1 + F_2 - F_3 - f_{1,u} = 0$ (47-C)

The comparison between equations (47-A - 47-C) and (41-A - 41-C) shows that shear and axial forces in both cases are the same, and bending moments on Member III are underpredicted by equation (41-B).

Case (b) $f_{3,u} = - f_{1,u}$ and $f_{3,v} = - f_{1,v}$

In this case the output forces will be induced due to roll motion only.

As with equation (43) the relation between input wave forces and the output forces can be written as follows:

$$(I_{XX} + I'_{XX})\ \ddot{X}_4 + C_{44}\dot{X}_4 + K_{44}X_4 = \tfrac{1}{2}B(f_{3,u} + f_{1,u}) = Bf_{3,u} = Bf_{1,u} \qquad (48)$$

where

$I_{XX}\ddot{X}_{44}$: Body mass inertia moment

$I'_{XX}\ddot{X}_4$, $C_{44}\dot{X}_4$: Hydrodynamic moment induced due to roll acceleration and roll velocity respectively

$K_{44}X_4$: Hydrostatic moment.

The distribution of the input and the output forces are shown in the following diagrams.

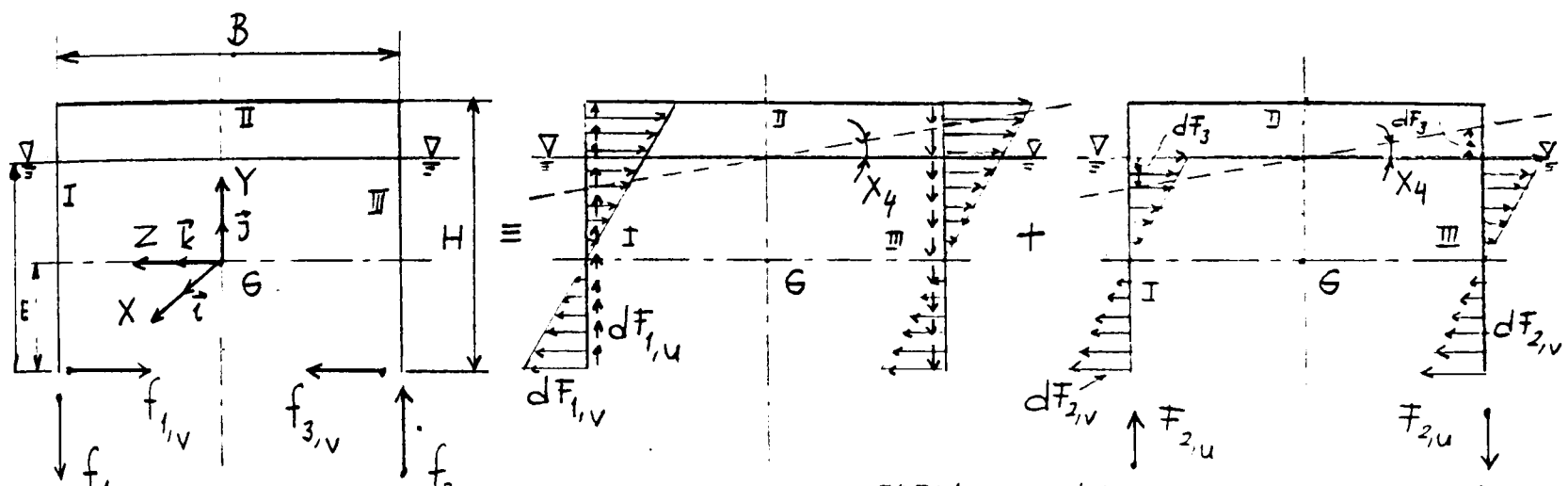

Fig. 15

The velocity and the acceleration of any point along Members I and III can be written for roll motion using equations (17) and (18) of Chapter IV.

$$u_i = \dot{X}_4 \vec{i} \wedge \vec{r}_i = \dot{X}_4 \vec{i} \wedge (Y_i \vec{j} + Z_i \vec{k}) \tag{49}$$

or

$$u_i = \dot{X}_4 (Y_i \vec{k} - Z_i \vec{j}) \tag{49-A}$$

Similarly

$$\dot{u}_i = \ddot{X}_4 \vec{i} \wedge \vec{r}_i = \ddot{X} (Y_i \vec{k} - Z_i \vec{j}) \tag{50}$$

Using the acceleration relation given in equation (50) the body inertia force distribution can be determined as follows:

$$dF_{1,u} = - \ddot{X}_4 Z_i \, dm \tag{51-A}$$

$$dF_{1,v} = + \ddot{X}_4 Y_i \, dm \tag{51-B}$$

where

$$dm = \frac{M}{2H} du$$

The moment vector due to body inertia force can also be written as follows:

$$\vec{M}_1 = 2\vec{r}_i \wedge \int_{u=0}^{H} (dF_{1,u} \vec{j} + dF_{1,v} \vec{k}) \frac{M}{2H} du \tag{52-A}$$

or

$$\vec{M}_1 = 2\ddot{X}_4 \int_{u=0}^{H} (Z_i^2 + Y_i^2) \frac{M}{H} du\vec{i} = I_{XX}\ddot{X}_4 \vec{i} \tag{52-B}$$

Similarly, hydrodynamic force distribution along the structure can be determined as follows:

$$F_{2,u} = - (\ddot{X}_4 Z_i M'_u + \dot{X}_4 Z_i b_{22}) \tag{53-A}$$

$$dF_{2,v} = (\ddot{X}_4 Y_i \, dM'_v + \dot{X}_4 Y_i b_{33} du) \tag{53-B}$$

where

$$M'_u = 0.424 \, \rho \, \pi R^3 \, k_{22}$$

$$dM'_v = \pi \, \rho \, R^2 \, a_{33} \, du = \pi \, \rho \, R^2 \, du$$

The moment due to hydrodynamic forces takes the following form:

$$\vec{M}_2 = 2\vec{r}_i \wedge (F_{2,u} \vec{j} + \int_{u=0}^{D} dF_{2,v} du \, \vec{k}) \tag{54}$$

or

$$\vec{M} = 2\left[\ddot{X}_4 \left(\frac{B}{2}\right)^2 M'_u + \ddot{X}_4 \pi \rho R^2 \int_{u=0}^{R} Y_i^2 \, du + \dot{X} \left(\frac{B}{2}\right)^2 b_{22} + \dot{X}_4 \int_{u=0}^{D} Y_i^2 \, b_{33} \, du\right] \vec{i} \tag{54-A}$$

Equation (54-A) can also be written as

$$M = I'_{XX}\ddot{X}_4 + C_{44}\dot{X}_4 \tag{54-B}$$

where

$$I'_{XX} = 2\left[M'_u \left(\frac{B}{2}\right)^2 + \pi \, \rho \, R^2 \int_{u=0}^{D} Y_i^2 \, du\right]$$

$$C_{44} = 2\left[\left(\frac{B}{2}\right)^2 b_{22} + \int_{u=0}^{D} Y_i^2 \, b_{33} \, du\right]$$

The hydrostatic force distribution due to roll motion can be obtained as follows:

$$dF_3 \simeq \frac{\rho g \nabla GM_T}{B^2 X_4} du \tag{55}$$

and

$$F_3 = \int_{u=D}^{D+BX_4/2} dF_3 \tag{55-A}$$

Having obtained the output force distributions for the loading case shown in Fig. 15 the structural response values can be determined as follows.

Global Member: I:

$$\text{Shear Forces} \quad : \quad SF_1(u,t) = f_{1,v} - \int_{u=0}^{u} (dF_{1,v} + dF_{2,v}) \tag{56-A}$$

$$\text{Bending Moments:} \quad BM_1(u,t) = -f_{1,v} \cdot u + \int_{u=0}^{u} \left(\frac{dF_{1,v}}{du} + \frac{dF_{2,v}}{du} \right) u \, du \tag{56-B}$$

$$\text{Axial Forces} \quad : \quad AF_1(u,t) = f_{1,u} - \int_{u=0}^{u} (dF_{1,u} - \varepsilon \cdot dF_3) - F_{1,u} \tag{56-C}$$

where

$\varepsilon = 0$ if $u \leq D$

$\varepsilon = 1$ if $u > D$

A comparison of equations (39-A - 39-C) with equations (56-A - 56-C) reveals that shear forces and axial forces are overpredicted by equations (39-A) and (39-C), and bending moments are underpredicted by equation (39-B).

Global Member: II:

$$\text{Shear Forces} \quad : \quad SF_2(u,t) = f_{1,u} - \int_{u_1=0}^{H} dF_{1,u} + \int_{u_1=D}^{H} dF_3 - F_{2,u} \tag{57-A}$$

Bending Moments: $$BM_2(u,t) = \int_{u_1=0}^{H} dF_{1,u}\ u - \left(\int_{u_1=D}^{D+BX_4/2} dF_3 \right) u$$

$$+ F_{2,u} \cdot u + \int_{u_1=0}^{H} dF_{1,v}\ u_1 + \int_{u_1=0}^{D} dF_{2,v}\ u_1 - (f_{1,u} \cdot u + f_{1,v} \cdot H) \quad (57\text{-B})$$

Axial Forces : $$AF_2(u,t) = \int_{u_1=0}^{H} dF_{1,v} + \int_{u_1=0}^{D} dF_{2,v} - f_{,v} \quad (57\text{-C})$$

(Note: u_1 implies that integration will be carried out along the Member I.)

The comparison between equations (40-A - 40-C) and (57-A - 57-C) shows that shear and axial forces are overpredicted by equations (40-A) and (40-C). Bending moment predictions vary depending on the position of the centre of rotation. If $E/(H-E) > 1$, the bending moment value at the centre of Member II will be overpredicted by equation (40-B) and for $E/(H-E) < 1$ the bending moment value at the same point will be underpredicted by equation (40-B). When $E/(H-E) = 1$ the bending moment value at the centre obtained by equation (40-B) will be the same as that obtained from equation (57-B).

Global Member: III:

Shear Forces : $$SF_3(u,t) = - f_{3,v} - \int_{u=H}^{H-u} (dF_{1,v} + dF_{2,v}) \quad (58\text{-A})$$

Bending Moments: $$BM_3(u,t) = -f_{3,v}(H-u) - \int_{u=H}^{H-u} \left(\frac{dF_{1,v}}{du} + \frac{dF_{2,v}}{du} \right) u\ du \quad (58\text{-B})$$

Axial Forces : $$AF_3(u,t) = -f_{3,u} + \int_{u=H}^{H-u} (dF_{1,u} + dF_{2,u} - \varepsilon dF_{3,u}) + F_{1,u} \quad (58\text{-C})$$

where

$\varepsilon = 0$ if $H-u \leq D - X_4 \cdot B$ and

$\varepsilon = 1$ if $H-u > D - X_4 \cdot B$

It can be concluded from a comparison of equations (58-A - 58-C) and (56-A - 56-C) that shear forces and axial forces are overpredicted by equations (41-A) and (41-C), bending moments are underpredicted by equation (58-B).

Case (c) $f_{1,v} = f_{3,v}$ and $f_{3,u} = f_{1,u} = 0$

In this case, the output forces will be due to sway motion as well as roll motion. The input and output force relations can be written as follows:

$$(M+M')\ddot{X}_3 + C_{33}\dot{X}_3 = -f_{1,v} - f_{3,v} = -2f_{1,v} = -2f_{3,v} \tag{59}$$

$$(I_{XX}+I'_{XX})\ddot{X}_4 + C_{44}\dot{X}_4 + K_{44}X_4 = 2f_{1,v}\cdot E = 2f_{3,v}\cdot E \tag{60}$$

where

$M\ddot{X}_3$: Body mass inertia force

$I_{XX}\ddot{X}_4$: Body mass inertia moment

$M'\ddot{X}_3$, $C_{33}\dot{X}_3$: Hydrodynamic force induced due to sway acceleration and sway velocity respectively

$I_{XX}\ddot{X}_4$, $C_{44}\dot{X}_4$: Hydrodynamic moment induced due to roll acceleration and roll velocity respectively

$K_{44}X_4$: Hydrostatic moment.

The distributions of the input and the output forces are shown in the following diagrams.

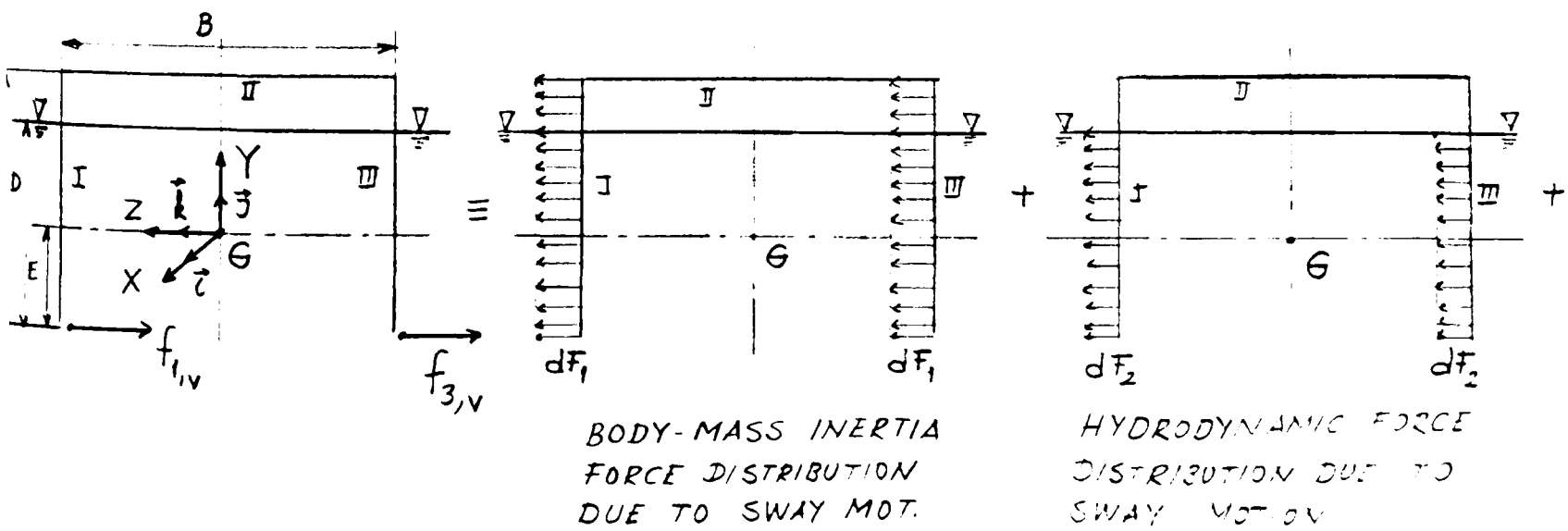

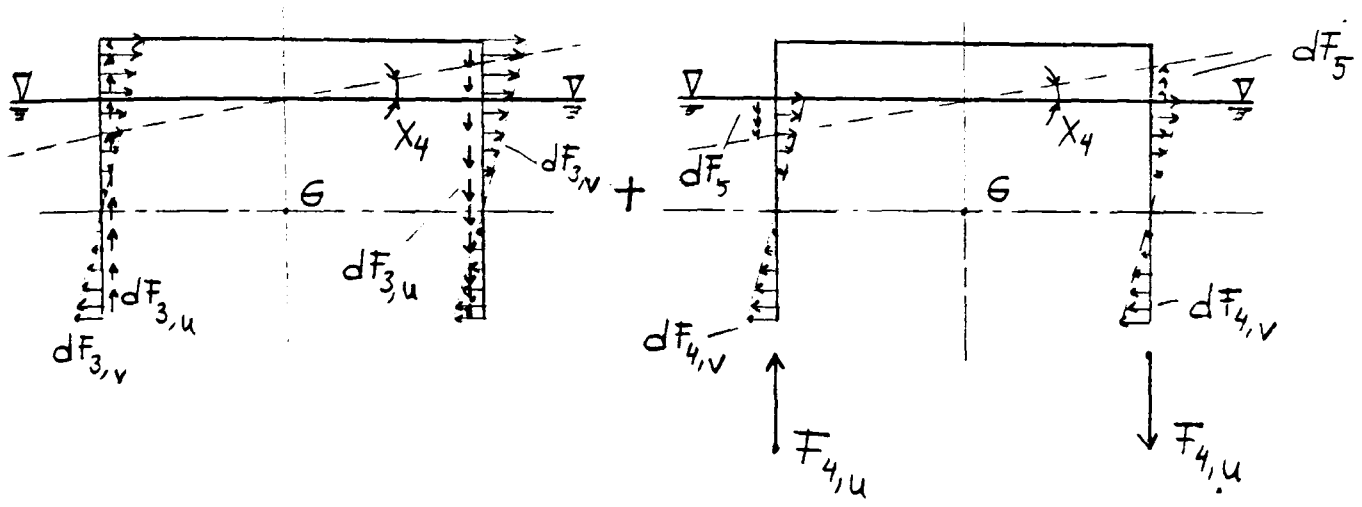

BODY-MASS INERTIA FORCE DISTRIBUTION DUE TO ROLL MOTION,

HYDRODYNAMIC AND HYDROSTATIC FORCE DISTRIBUTION DUE TO ROLL MOTION

Fig. 16

$$dF_1 = \frac{M}{2H} \ddot{X}_3 \, du \tag{61}$$

$$dF_2 = \left(\pi\rho R^2 \, a_{33} \ddot{X}_3 + b_{33} \dot{X}_3\right) du \tag{61-A}$$

$$= \left(\pi\rho R^2 \ddot{X}_3 + b_{33} \dot{X}_3\right) du$$

$$dF_{3,u} = -\frac{M}{2H} \ddot{X}_4 \, Z_i \, du \tag{61-B}$$

$$dF_{3,v} = \frac{M}{2H} \ddot{X}_4 \, Y_i \, du \tag{61-C}$$

$$F_{4,u} = -\left(M'_u \, Z_i \, \ddot{X}_4 + Z_i \, b_{22} \dot{X}_4\right) \tag{61-D}$$

$$F_{4,v} = \left(\ddot{X}_4 \, Y_i \, dM'_v + \dot{X}_4 \, Y_i \, b_{33}\right) \tag{61-E}$$

where

$$M'_u = 0.424 \, \rho\pi R^3 \, k_{22}$$

$$dM'_v = \pi\rho R^2 \, a_{33} \, du = \pi\rho R^2 \, du$$

$$dF_5 \simeq \frac{\rho g \nabla GM_T}{B^2 X_4} \, du \tag{61-F}$$

Having obtained the output force distributions for the loading case shown in Fig. 16 the structural response analysis may be carried out as follows.

Global Member: I:

$$\text{Shear Forces} \quad : \quad SF_1(u,t) = f_{1,v} - \int_{u=0}^{u_Q} (dF_1 + dF_2 + dF_{3,v} + dF_{4,v}) \tag{62-A}$$

$$\text{Bending Moments:} \quad BM(u,t) = - f_{1,v} \cdot u \int_{u=0}^{u_Q} \left(\frac{dF_1}{du} + \frac{dF_2}{du} + \frac{dF_{3,v}}{du} + \frac{dF_{4,v}}{du} \right) u \, du \tag{62-B}$$

$$\text{Axial Forces} \quad : \quad AF_1(u,t) = - \int_{u=0}^{u_Q} dF_{3,u} - \int_{u=D}^{u_Q} \varepsilon dF_5 - F_{4,u} \tag{62-C}$$

where $\varepsilon = 0$ if $u \leq D$

$\varepsilon = 1$ if $u > D$

The structural response equations given in equations (39-A - 41-C) are not valid for this asymmetrical loading case. However, a comparison can be made between the set of equations given in (33-A - 35-C) and (36-A - 38-C).

A comparison between equations (62-A - 62-C) and (33-A - 33-C) shows that, the structural response values for shear forces and bending moments will generally be overpredicted by equations (33-A - 33-B) unless roll induced output forces are dominant. On the other hand axial forces can only be predicted by equation (62-C).

Global Member: II:

$$\text{Shear Forces} \quad : \quad SF_2(u,t) = - \int_{u=0}^{H} dF_{3,u} - \int_{u=D}^{D+\frac{BX_4}{2}} dF_5 - F_{4,u} \tag{63-A}$$

$$\text{Bending Moments:} \quad BM_2(u,t) = - f_{1,v} \cdot H + \int_{u_1=0}^{H} \left(\frac{dF_1}{du} + \frac{dF_2}{du} + \frac{dF_{3,v}}{du} + \frac{dF_{4,v}}{du} \right) u \, du$$

$$+ \left(\int_{u_1=0}^{H} dF_{3,u} \right) u + \left(\int_{u_1=D}^{H} dF_5 \right) u + F_{4,u} \cdot u \tag{63-B}$$

Axial Forces: $$AF_2(u,t) = -f_{1,v} + \int_{u_1=0}^{H} dF_1 + \int_{u_1=0}^{D} dF_2 + \int_{u_1=0}^{H} dF_{3,v} + \int_{u_1=o}^{D} dF_{4,v} = O \quad (63\text{-}C)$$

The conclusion for Member II is similar to that given for Member I. The bending moments and the axial forces will generally be overpredicted by equations (34-B - 34-C), unless roll induced output forces are dominant. On the other hand shear forces can only be predicted by equation (63-A).

Global Member: III:

Shear Forces : $$SF_3(u,t) = +f_{3,v} - \int_{u=u_Q}^{H} \left(dF_1 + dF_2 + dF_{3,v} + dF_{4,v}\right) \quad (64\text{-}A)$$

Bending Moments: $$BM_3(u,t) = f_{3,v} \cdot (H-u_Q) \int_{u=u_Q}^{H} \left(\frac{dF_1}{du} + \frac{dF_2}{du} + \frac{dF_{3,v}}{du} + \frac{dF_{4,v}}{du}\right) (u-u_Q)\, du \quad (64\text{-}B)$$

Axial Forces : $$AF_3(u,t) = \int_{u=u_Q}^{H} dF_{3,u} + \int_{u=u_Q}^{H-D} \varepsilon dF_5 \quad (64\text{-}C)$$

If $u_G > (H-D)$ $\varepsilon - 1$

If $u_G \leq (H-D)$ $\varepsilon = 0$

The conclusion for Member III will be the same as that given for Global Member I.

The loading conditions discussed above had equal input loading in magnitude in each case. If loading on the first and third members is not equal, the superposition of the above given cases can be employed. The following diagram illustrates this (Fig. 17).

Although the mass of the second member was not included in the structural response analysis for the purpose of a simple comparison between the fixed and the floating cases given above, the same procedure

as was given for Members I and III may be applied to Member II for structural response analysis.

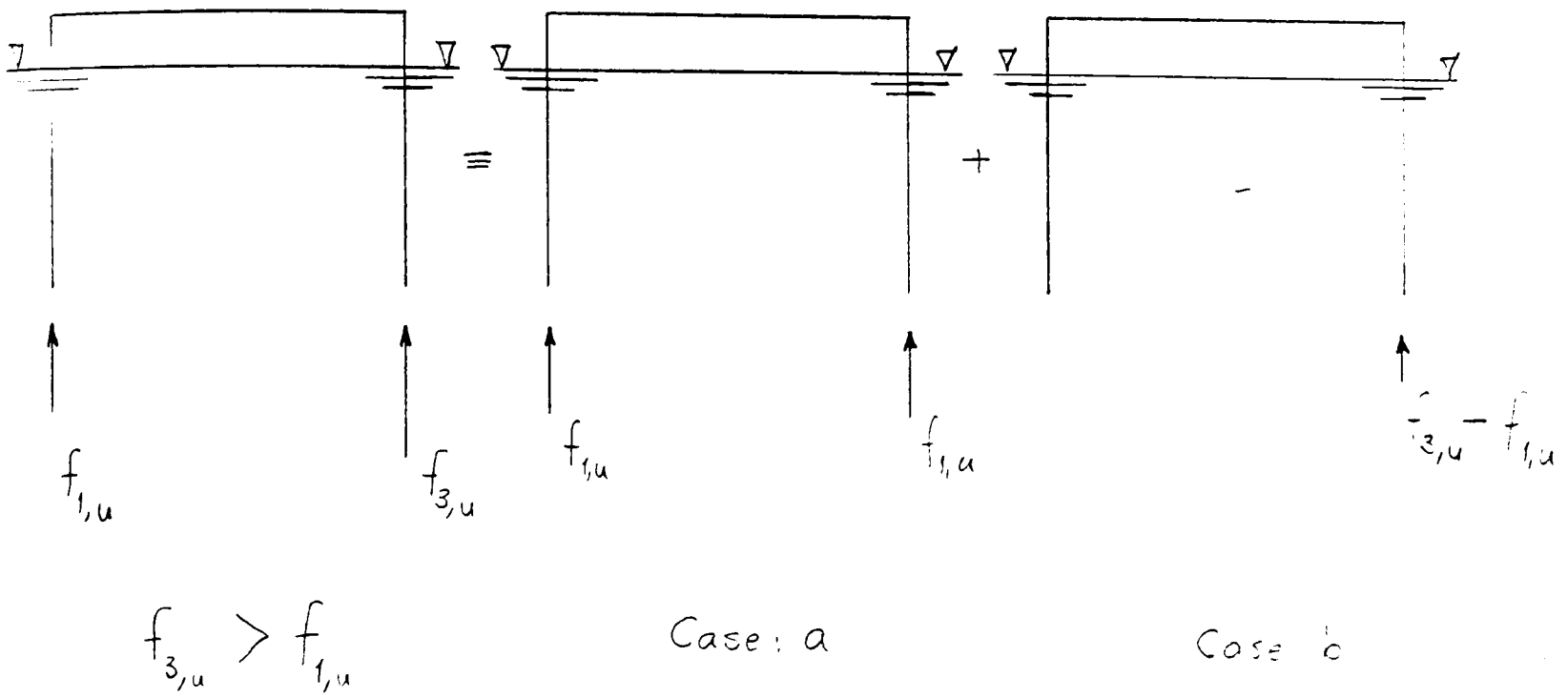

Fig. 17

1.3 Structure is Restrained or Free in Waves, Loading is Dynamic

In sections 1.1 and 1.2, the input and the output loadings on the structure were determined at any instant over a wave cycle and the structure was loaded with those quasi-static loads, i.e. time varying load is assumed to be static at any particular instant and structural response calculations were carried out under that static equivalency of the time varying load. Consequently, structural response values only correspond to the static deflections of the individual members.

Here a simplified procedure for calculating the structural response values for floating platforms which take dynamic deformations of the individual members into account will be discussed.

The structural response analysis of offshore platforms under dynamic loading require a larger amount of computational effort due to the high number of elements. If the offshore structure under consideration is a floating one, the size of the problem becomes much larger, simply because a floating platform is an unconstrained and generally indeterminate structure. In this study, no attempt has been made to bring a unified solution to the problem, and only a general description of the problem has been made. Some simplified dynamic loading calculations were carried out for the twin circular hull model semi-submersible on which the rigid body motions and the bending moment values on the deck were measured. The main aim of this simplified approach may be summarised as follows:

(a) To determine whether the fundamental frequency of the member deformations is near to the forcing frequencies which correspond to the maximum structural response values.

(b) To obtain the structural response values under the dynamic loading when the forcing frequencies which correspond to the maximum structural response values are near to the fundamental frequency.

When the fundamental frequency of the structure and the frequencies which correspond to the maximum structural response values, as well as the frequencies which correspond to the maximum energy of the sea where the platform is operated, are in the same region, a more detailed dynamic analysis is needed.

A unified dynamic analysis procedure for fixed and floating platforms is summarised in reference [7]. Reference [8] gives an analysis procedure for the dynamic response of fixed gravity platforms.

The dynamic loading concept for floating structures will be demonstrated with the following examples.

Consider a rigid floating object and a mass attached with a cantilever beam onto this floating body, the forces on that structure are shown in the following figure.

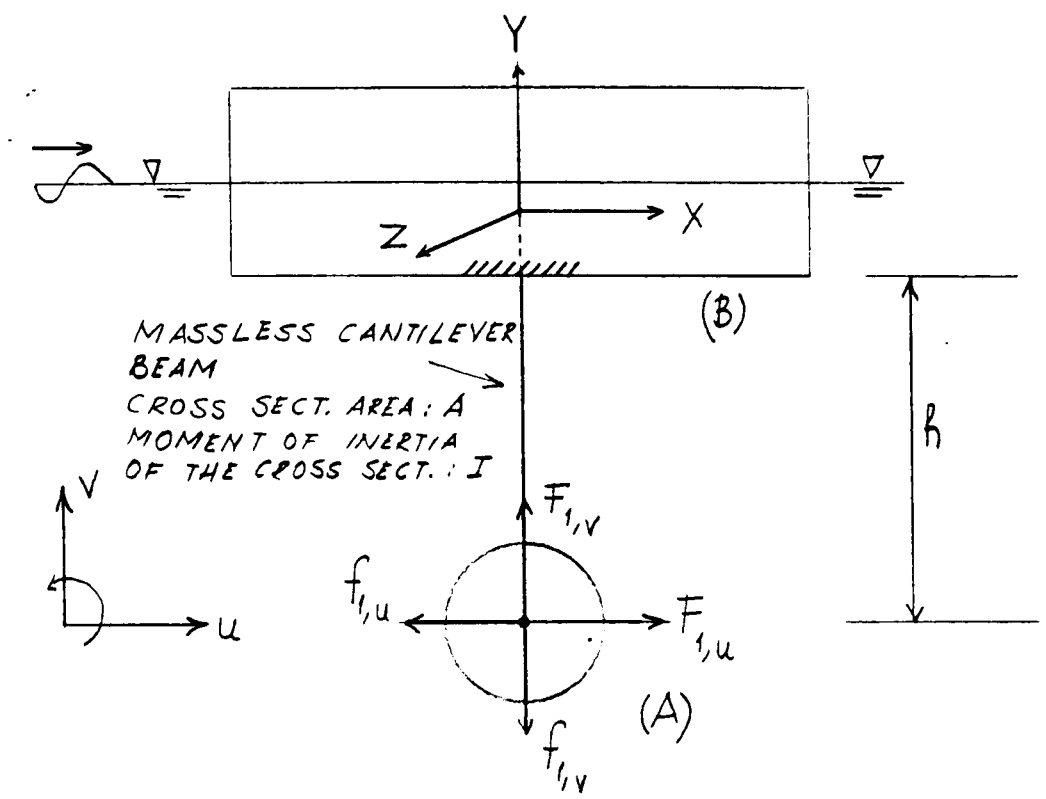

Fig. 18

The total force on the mass (A) may be written as follows

$$F_{T,u} = F_{1,u} - f_{1,u} \tag{65}$$

$$F_{T,v} = F_{1,v} - f_{1,v} \tag{65-A}$$

If the floating object is assumed to be restrained in waves, equations (65) and (65-A) become

$$F_{T,u} = - f_{1,u} \tag{65-B}$$

$$F_{T,v} = - f_{1,v} \tag{65-C}$$

where $f_{1,u}, f_{1,v}$: Wave induced forces on mass (A) in u and in v directions respectively.

$F_{1,u}, F_{1,u}$: Rigid body motion induced forces on mass (A) in u and in v directions respectively.

$f_{1,u}, f_{1,v}, F_{1,u}, F_{1,v}$ can also be written in the following form

$$f_{1,u} = f_{o,1,u} \cos(\omega t) \tag{66-A}$$

$$f_{1,v} = f_{o,1,v} \cos(\omega t - \alpha) \tag{66-B}$$

$$F_{1,u} = F_{1,1,u} \cos(\omega t - \beta) \tag{66-C}$$

$$F_{2,v} = F_{o,2,v} \cos(\omega t - \gamma) \tag{66-D}$$

where ω: Input wave force frequency

α: Phase angle between $f_{1,u}$ and $f_{1,v}$

β: Phase angle between $f_{1,u}$ and $F_{1,u}$

γ: Phase angle between $f_{1,u}$ and $F_{2,u}$

The structural response values for the cantilever beam under quasi-static loading become

$$\text{Shear Forces} : SF_s(v,t) = - F_{T,u} \tag{67-A}$$

$$\text{Bending Moments:} \quad BM_s(v,t) = - F_{T,u} \cdot v \tag{67-B}$$

$$\text{Axial Forces} : AF_s(v,t) = - F_{T,v} \tag{67-C}$$

A structural response analysis of the cantilever beam and mass system under dynamic loading may be carried out as follows:

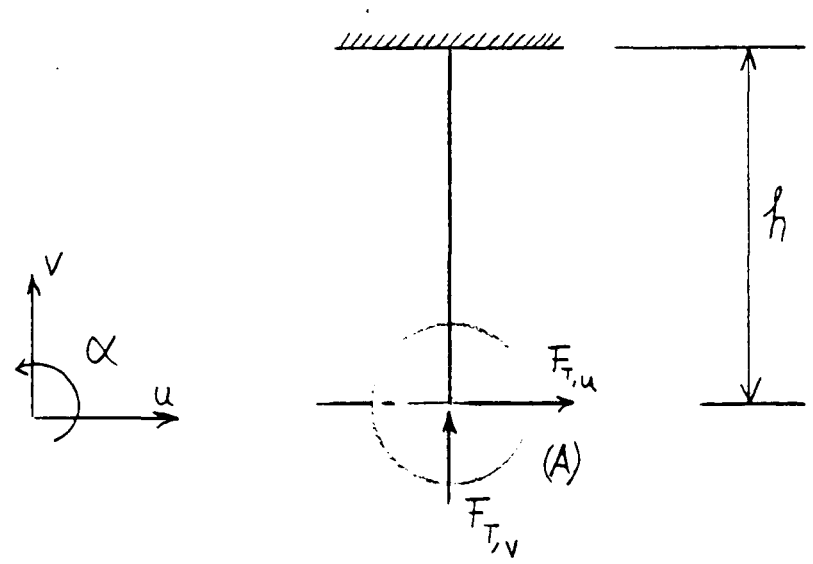

Fig. 19

If we assume that the cantilever beam is massless and that its geometrical and material properties A,E,I are known, the following differential equations can be written to determine the local deformations of the cantilever beam and mass system due to mass (A) and time varying $F_{T,u}$ and $F_{T,v}$ loads on the mass.

$$(m+m'_{11})\ddot{u} + k_{22}u = F_{T,u} \tag{68-A}$$

$$(m+m'_{22})\ddot{v} + k_{33}v = F_{T,v} \tag{68-B}$$

where m'_{22}: Added mass of object A in u direction

m'_{11}: Added mass of object A in v direction

k_{11}: Stiffness of the beam in u direction

k_{22}: Stiffness of the beam in v direction

$\ddot{u},\ddot{v}$: Acceleration of mass A due to elastic deformations of the cantilever beam in u and v directions respectively

u,v: Displacement of mass A due to elastic deformations of the cantilever beam under time varying loads in u and v directions respectively.

The solutions of equations (68-A) and (68-B) can be written as follows

$$\bar{u}_o = \frac{F_{o,T,u} \Big/ k_{11}}{\sqrt{\left[1 - \left(\frac{\omega}{\omega_{n,11}}\right)^2\right]^2}} \tag{69-A}$$

and

$$\bar{v}_o = \frac{F_{o,T,v} \Big/ k_{22}}{\sqrt{\left[1 - \left(\frac{\omega}{\omega_{n,22}}\right)^2\right]^2}} \tag{69-B}$$

where $\bar{u}_o,\bar{v}_o$: Maximum displacements of mass A due to elastic deformations of the cantilever beam, in u and v directions respectively.

$F_{o,T,u}, F_{o,T,v}$: Maximum total loads applied in u and v directions respectively.

$\omega_{n,_{11}}$: Natural frequency of beam and mass system in horizontal vibration mode

$$= \sqrt{\frac{k_{11}}{m+m'_{22}}}$$

$\omega_{n,_{22}}$: Natural frequency of beam and mass system in vertical vibration mode

$$= \sqrt{\frac{k_{22}}{m+m'_{33}}}$$

The following relations between the applied forces, static displacement and the stiffness can be written using beam theory as

$$\bar{u}_{o,_s} = \frac{F_{o,_{T,u}} \; h^3}{3E} \tag{70}$$

or $$\bar{u}_{o,_s} = \frac{F_{o,_{T,u}}}{k_{11}} \tag{70-A}$$

where $k_{11} = \frac{3EI}{h^3}$

and $$\bar{v}_{o,_s} = \frac{F_{o,_{T,v}} \cdot h}{AE} \tag{71}$$

or $$\bar{v}_{o,_s} = \frac{F_{o,_{T,v}}}{k_{22}} \tag{71-A}$$

where $k_{22} = \frac{AE}{h}$

The maximum dynamic displacements u_o, v_o can also be defined in terms of static displacements $u_{o,_s}$ and $v_{o,_s}$ as follows

$$\bar{u}_o = \bar{u}_{o,_s} \, Q_{n,_{11}} \tag{72}$$

$$\bar{v}_o = \bar{v}_{o,_s} \, Q_{n,_{22}} \tag{72-A}$$

where $Q_{n,_{11}}$: Magnification factor for the horizontal mode of vibration

$$Q_{n,_{11}} : = \frac{1}{\sqrt{\left[1 - \left(\frac{\omega}{\omega_{n,_{11}}}\right)^2\right]^2}}$$

$Q_{n,22}$: Magnification factor for the vertical mode of vibration

$$Q_{n,22} : = \frac{1}{\sqrt{\left[\left(1 - \frac{\omega}{\omega_{n,22}}\right)^2\right]^2}}$$

The elastic curve for the cantilever beam can easily be determined using the relations between applied load and the translational and the rotational displacements of the beam.

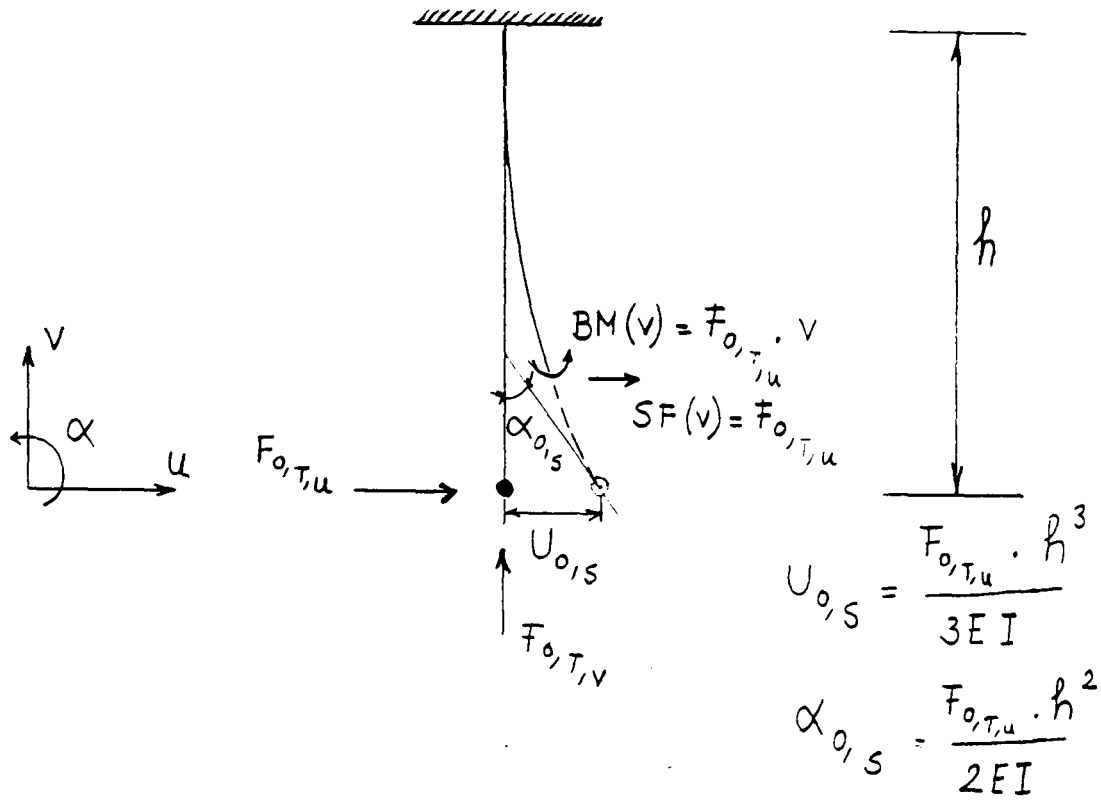

Fig. 20

If we consider a cross-section of the beam at distance v from the origin, the following static displacements occur in the u direction at that section due to the bending moment and the shear force.

$$\bar{u}(v,t)_{static} = \frac{BM(v)\,(h-v)^2}{2EI} + \frac{SF(v)\,(h-v)^3}{3EI} \qquad (73)$$

or

$$\bar{u}(v,t)_{static} = \frac{F_{o,T,u} \cdot v \cdot (h-v)^2}{2EI} + \frac{F_{o,T,u}\,(h-v)^3}{3EI} \qquad (73\text{-A})$$

The first term on the right hand side of equation (73) or (73-A) gives the translational displacement of the cantilever beam due to the bending moment, the second term on the right hand side of equation (73) or (73-A) gives the translational displacement of the cantilever beam

due to the shear force. (It is assumed that $F_{o,T,v}$ does not induce any horizontal displacement.)

As with equation (73-A), the maximum dynamic displacements of the cantilever beam can be written using equation (72) as follows

$$\bar{u}(v,t)_{dynamic} = \bar{u}(v,t)_{static} \cdot Q_{n,11}$$

$$= \left[\frac{F_{o,T,u}\, v(h-v)^2}{2EI} + \frac{F_{o,T,u}\,(h-v)^3}{3EI} \right] Q_{n,11} \qquad (74)$$

The horizontal displacements of the beam over a complete wave cycle can be expressed as follows

$$u(v,t) = \left[\frac{v(h-v)^2}{2EI} + \frac{(h-v)^3}{3EI} \right] F_{o,T,u} \cos(\omega t-\delta) \cdot Q_{n,11} \qquad (75)$$

where δ: Phase angle between $F_{T,u}$ and $f_{1,u}$

u(v,t) can also be expressed in terms of static displacements as follows

$$u(v,t) = u(v,t)_{static} \cdot Q_{n,11} \qquad (75\text{-A})$$

Similarly, dynamic axial displacements of the cantilever beam take the following form

$$\bar{v}(u)_{dynamic} = \bar{v}(t)_{static} \cdot Q_{n,22}$$

$$= \frac{F_{o,T,v}\, h}{AE} \cdot Q_{n,22} \qquad (76)$$

and $$v(t) = \frac{h}{AE} F_{o,T,v} \cdot Q_{n,22} \cos(\omega t-\psi) \qquad (77)$$

where ψ: Phase angle between $F_{T,v}$ and $f_{1,u}$

v(t) can also be expressed in terms of static displacements as follows

$$v(t) = v(t)_{static} \cdot Q_{n,22} \qquad (78)$$

The structural response values can be determined in terms of the dynamic displacements as follows

$$\text{Shear Forces: } [SF(v,t)]_{dynamic} = - EI \frac{\partial^3 u}{\partial v^3} \qquad (79)$$

If we substitute equation (75-A) into equation (79) the following relation is obtained

$$[SF(v,t)]_{dynamic} = [SF(v,t)]_{static} \cdot Q_{n,_{11}} \tag{79-A}$$

$$\text{Bending Moments:} \quad [BM(v,t)]_{dynamic} = - EI \frac{\partial^2 u}{\partial v^2} \tag{80}$$

$$\text{or} \quad [BM(v,t)]_{dynamic} = [BM(v,t)]_{static} \cdot Q_{n,_{11}} \tag{80-A}$$

$$\text{Axial Forces:} \quad [AF(t)]_{dynamic} = \frac{F_{o,_{T,v}}}{AE} \cos(\omega t - \psi) \cdot h \cdot Q_{n,_{22}} \tag{81}$$

$$[AF(t)]_{dynamic} = [AF(t)]_{static} \cdot Q_{n,_{11}} \tag{81-A}$$

The beam mass vibration problem for an n degrees-of-freedom system may be summarised as follows. Consider two submerged objects attached to the cantilever beam to represent a two degrees-of-freedom system. If the mass and the added mass of the first object are m_1 and m_1' respectively, and the time varying applied force on this object is $F^{(1)}_{T,u}$, and if the mass and the added mass of the second object are m_2, m_2' respectively, and the time varying applied force is $F^{(2)}_{T,u}$ (for simplicity only horizontal applied forces are considered) then

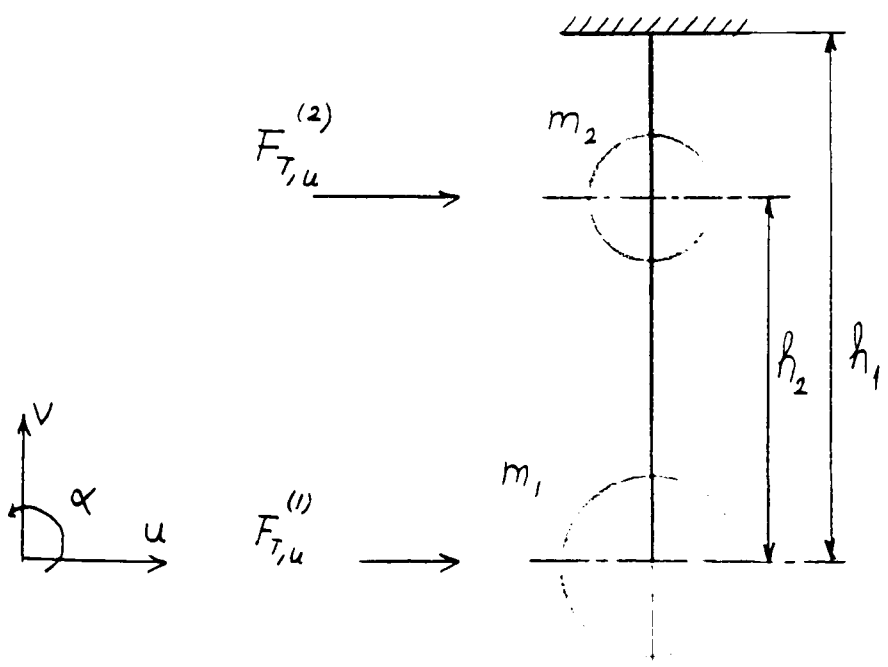

Fig. 21

The equilibrium equations for the beam and two masses system shown in Fig. 21 may be written as follows

$$(m_1+m'_{1,22})\ddot{u}_1 + k_{11}u_1 + k_{12}u_2 = F^{(1)}_{T,u} \tag{82}$$

$$(m_2+m'_{2,22})\ddot{u}_2 + k_{21}u_1 + k_{22}u_2 = F^{(2)}_{T,u} \tag{82-A}$$

where u_1, u_2: Horizontal displacements of the first and the second mass respectively.

k_{ij} : Stiffness coefficients which may be defined as the force at point (i) due to a unit displacement at point (j).

Since $F^{(1)}_{T,u}$ and $F^{(2)}_{T,u}$ are sinusoidally varying forces, u_1 and u_2 will also vary sinusoidally, and therefore the following relations between acceleration and velocity can be written as

$$\ddot{u}_1 = -\omega^2 u_1 \tag{83}$$

$$\ddot{u}_2 = -\omega^2 u_2 \tag{83-A}$$

If equations (83) and (83-A) are substituted in equations (82) and (82-A) the following equations are obtained

$$[k_{11} - (m_1+m'_{1,22})\omega^2]u_1 + k_{12}u_2 = F^{(1)}_{T,u} \tag{84}$$

$$k_{21}u_1 + [k_{22} - (m_2+m'_{2,22})\omega^2]u_2 = F^{(2)}_{T,u} \tag{84-A}$$

Equations (84) and (84-A) may also be converted into matrix form as follows

$$\begin{bmatrix} (k_{11} - (m_1+m'_{1,22})\omega^2) & k_{12} \\ k_{21} & (k_{22} - (m_2+m'_{2,22})\omega^2) \end{bmatrix} \begin{bmatrix} u_1 \\ u_2 \end{bmatrix} = \begin{bmatrix} F^{(1)}_{T,u} \\ F^{(2)}_{T,u} \end{bmatrix} \tag{85}$$

Equation (85) can also be written as follows

$$\left[\begin{bmatrix} k_{11} & k_{12} \\ k_{21} & k_{22} \end{bmatrix} - \omega^2 \begin{bmatrix} m_1+m'_{1,22} & 0 \\ 0 & m_2+m'_{2,22} \end{bmatrix} \right] \begin{bmatrix} u_1 \\ u_2 \end{bmatrix} = \begin{bmatrix} F^{(1)}_{T,u} \\ F^{(2)}_{T,u} \end{bmatrix} \tag{86}$$

$[K]_{ij}$ $[M]_{ij}$ $[F]_i$

$$\{[K]_{ij} - \omega^2[M]_{ij}\}\ [U]_i = [F_{T,u}]_i \qquad (86\text{-A})$$

where $[K]_{ij}$: Stiffness matrix of the beam two mass system

$[M]_{ij}$: Mass matrix

$[F_{T,u}]_i$: Force matrix.

In order to find the natural frequencies of the system shown in Fig. 21 the right hand side of equation (86-A) can be set to zero

$$\{[K]_{ij} - \omega^2[M]_{ij}\}\ [U]_i = 0 \qquad (87)$$

$[U]_i$ values can only exist if the following determinant is zero

$$||\{[K]_{ij} - \omega^2[M]_{ij}\}|| = 0 \qquad (88)$$

Equation (88) is called the frequency equation of the system. The N roots of this equation (ω_1^2, ω_2^2, ... ω_n^2) represent the natural frequencies of the N modes of the vibration which are possible in the system. The roots of the following equation give the natural frequencies of the system shown in Fig. 21.

$$\omega^4 M_1 M_2 - (M_1\omega^2 k_{22} + M_2\omega^2 k_{11}) - (k_{12} k_{21} + k_{11} k_{22}) = 0 \qquad (89)$$

where $M_1 = m_1 + m'_{1,22}$

$M_2 = m_2 + m'_{2,22}$

It is also possible to define the equations of motion in terms of the flexibility influence coefficients δ_{ij} which are defined as the displacement at i due to a unit force at j. For the system shown in Fig. 21 the displacements can be written using flexibility coefficients as

$$u_1 = \delta_{11} F_1 + \delta_{12} F_2 \qquad (90)$$

$$u_2 = \delta_{21} F_1 + \delta_{22} F_2 \qquad (90\text{-A})$$

For the forced vibration problem F_1 and F_2 become

$$F_1 = F_{T,u}^{(1)} - M_1\ddot{u}_1$$

$$F_2 = F_{T,u}^{(2)} - M_2\ddot{u}_2$$

and for the free vibration problem

$$F_1 = - M_1\ddot{u}_1 = M_1\omega^2 u_1$$

$$F_2 = - M_2\ddot{u}_2 = M_2\omega^2 u_2$$

For the free vibration problem equations (90) and (90-A) can also be written as

$$u_1 = M_1\omega^2 u_1\delta_{11} + M_2\omega^2 u_2\delta_{12} \tag{91}$$

$$u_2 = M_1\omega^2 u_1\delta_{21} + M_2\omega^2 u_2\delta_{22} \tag{91-A}$$

Equations (91) and (91-A) can be expressed in matrix form as

$$\begin{bmatrix} u_1 \\ u_2 \end{bmatrix} = \omega^2 \begin{bmatrix} \delta_{11} M_1 & \delta_{12} M_2 \\ \delta_{21} M_1 & \delta_{22} M_2 \end{bmatrix} \begin{bmatrix} u_1 \\ u_2 \end{bmatrix} \tag{92}$$

u_1 and u_2 can only exist if the following determinant vanishes

$$\begin{vmatrix} \delta_{11} M_1 - \frac{1}{\omega^2} & \delta_{12} M_2 \\ \delta_{21} M_1 & \delta_{22} M_2 - \frac{1}{\omega^2} \end{vmatrix} = 0 \tag{93}$$

When the determinant given in equation (93) is calculated the following equation can be obtained

$$\frac{1}{\omega^4} - \frac{1}{\omega^2}(\delta_{11}M_1 + \delta_{22}M_2) + (\delta_{11}\delta_{22} - \delta_{12}\delta_{21})\, M_1 \cdot M_2 = 0 \tag{94}$$

If it is assumed that the roots of equation (94) are $\frac{1}{\omega_1}$ and $\frac{1}{\omega_2}$, the following polynomial equation may be written

$$\left(\frac{1}{\omega^2} - \frac{1}{\omega_1^2}\right)\left(\frac{1}{\omega^2} - \frac{1}{\omega_2^2}\right) = \frac{1}{\omega^4} - \left(\frac{1}{\omega^2}\right)\left(\frac{1}{\omega_1^2} + \frac{1}{\omega_2^2}\right) + \frac{1}{\omega_1^2}\frac{1}{\omega_2^2} = 0 \tag{95}$$

A comparison between equations (94) and (95) leads to the following equation

$$\frac{1}{\omega_1^2} + \frac{1}{\omega_2^2} = \delta_{11}M_1 + \delta_{22}M_2 = \frac{M_1}{k_{11}} + \frac{M_2}{k_{22}} = \frac{1}{\omega_{11}^2} + \frac{1}{\omega_{22}^2} \tag{96}$$

where ω_1 : Natural frequency of the system which corresponds to the first mode. It is also called fundamental frequency.

ω_2 : Natural frequency of the system which corresponds to the second mode.

ω_{11}: The natural frequency of the system when only the first mass is present.

ω_{22}: The natural frequency of the system when only the second mass is present.

Since the natural frequency of the second mode will be higher than the fundamental frequency the following form of equation (96) can be written

$$\frac{1}{\omega_1^2} \simeq \frac{1}{\omega_{11}^2} + \frac{1}{\omega_{22}^2} \tag{97}$$

Equation (97) can be extended to any number of degrees-of-freedom to obtain fundamental frequency as follows

$$\frac{1}{\omega_1^2} \simeq \frac{1}{\omega_{11}^2} + \frac{1}{\omega_{22}^2} + \frac{1}{\omega_{33}^2} + \text{---} \frac{1}{\omega_{nn}^2} \tag{97-A}$$

Equation (97-A) is known as Dunkerly's equation [9]. Various applications of this equation can be found in references [10,11].

The natural frequencies of the beam-mass system shown in Fig. 21 may be written from equation (94)

$$\left(\frac{1}{\omega^2}\right)_{1,2} = \frac{1}{2}\left(M_1\delta_{11} + M_2\delta_{22}\right) \pm \sqrt{\frac{1}{4}\left(M_1\delta_{11} - M_2\delta_{22}\right)^2 + M_1M_2\delta_{12}^2} \tag{98}$$

where $\delta_{11} = \frac{h}{3EI}$

$$\delta_{21} = \delta_{12} = \frac{h_2(h_1-h_2)^2}{2EI} + \frac{(h_1-h_2)^3}{3EI}$$

$$\delta_{22} = \frac{(h_1-h_2)^3}{3EI}$$

The two roots of equation (98) correspond to natural frequencies for the first and the second modes of vibration.

It is also possible to determine the natural frequency for the first mode (= fundamental frequency) of the same system using Dunkerley's equation as given in (97) using equation (96)

$$\left(\frac{1}{\omega_1^2}\right)_1 = \frac{M_1 h^3}{3EI} + \frac{M_2 (h_1 - h_2)^3}{3EI} \qquad (98\text{-A})$$

Structural response values for two or higher degrees-of-freedom systems can only be found by solving the motion equations given in (86-A). Since the structure was analysed as a two mass system, dynamic structural response values can be obtained as

$$\text{Shear Forces} \quad : \quad [SF(v,t)]_d = [SF(v,t)]_{static} \cdot Q_1 \quad \text{for} \quad 0 < v < h_2 \qquad (99)$$

$$\text{Bending Moments:} \quad [BM(v,t)]_d = [BM(v,t)]_{static} \cdot Q_1 \quad \text{for} \quad 0 < v < h_2 \qquad (99\text{-A})$$

$$\text{where } Q_1 = \frac{[u(h_1,t)]_{dynamic}}{[u(h_1,t)]_{static}}$$

Similarly,

$$\text{Shear Forces} \quad : \quad [SF(v,t)]_d = [SF(v,t)]_{static} \cdot Q_2 \quad \text{for} \quad h_2 \leq v < h_1 \qquad (100)$$

$$\text{Bending Moments:} \quad [BM(v,t)]_d = [BM(v,t)]_{static} \cdot Q_2 \quad \text{for} \quad h_2 \leq v < h_1 \qquad (100\text{-A})$$

$$\text{where } Q_2 = \frac{[u(h_2,t)]_{dynamic}}{[u(h_2,t)]_{static}}$$

The examples given above can be extended to include N degrees-of-freedom systems following the same procedure.

As a second group of examples, the floating structure shown in Fig. 22 will be analysed under dynamic loading with the following assumptions:

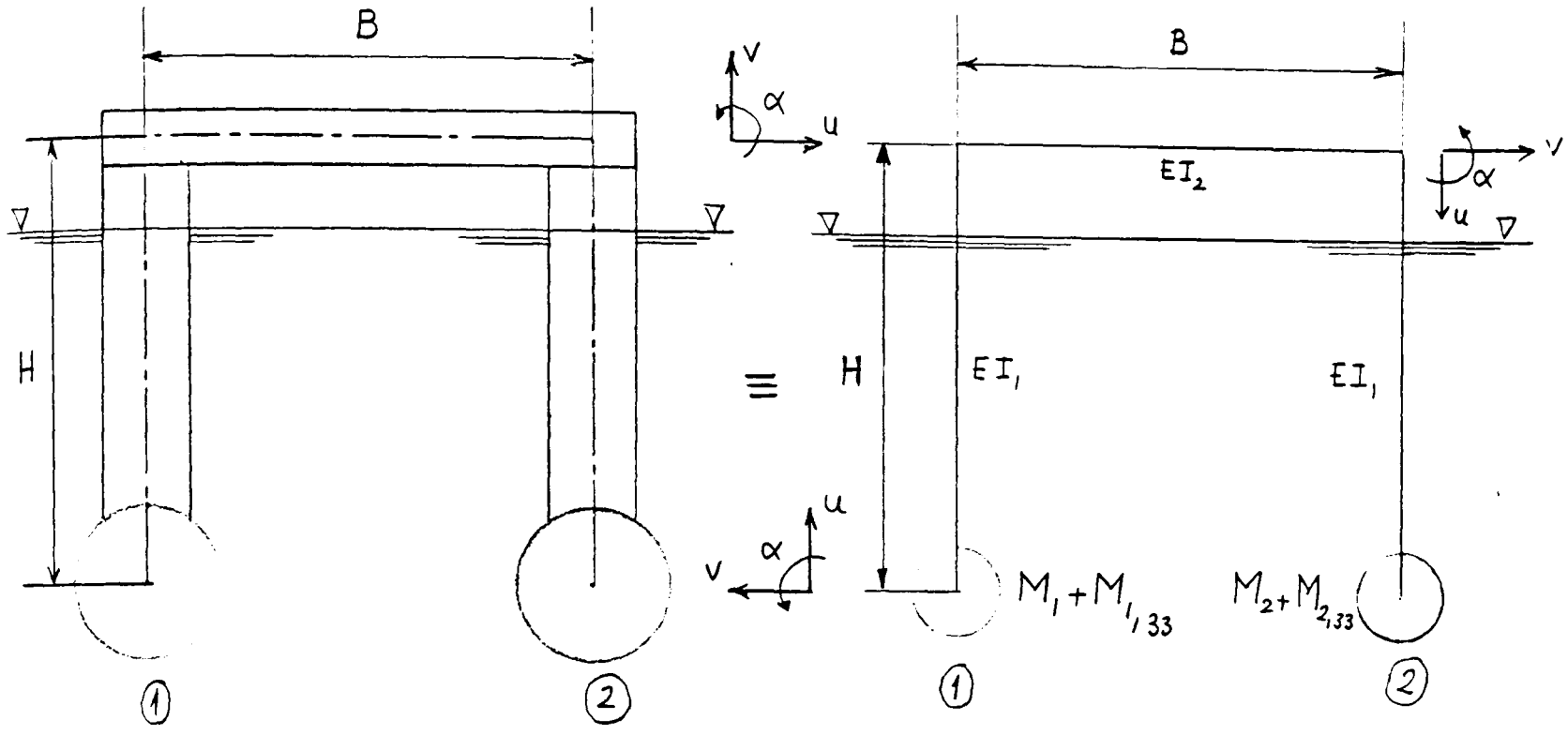

Fig. 22

(a) The weight of the vertical columns and the horizontal beam are neglected.

(b) The input wave forces as well as output forces on the columns are neglected.

(c) The mass of the circular volumes is concentrated in the centre of those volumes.

(d) The geometrical and the structural properties for both columns are identical.

(e) The masses and the geometrical properties for both circular volumes are identical.

The dynamic loading analysis of the floating structure shown in Fig. 22 will be carried out for the restrained and the free floating cases.

(i) Structure is restrained in waves

In this case basically two different types of loading and the corresponding support conditions may be chosen. The loading on the structure

at any instant over a given wave cycle can be found as the superposition of those two systems.

(i-1) Horizontally applied wave loading is symmetrical about the vertical centre-line: Since two horizontal forces which are equal in magnitude and opposite in sign to each other act on the system, the structure will be supported with the simple supports at the horizontal beam, as shown in Fig. 23.

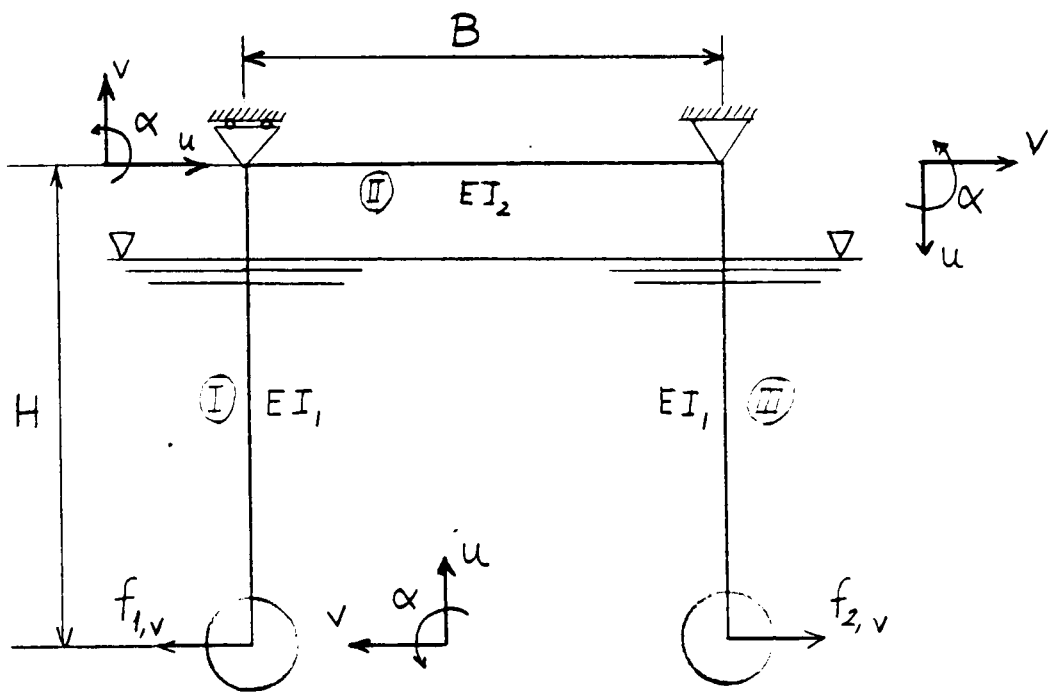

Fig. 23

The differential equations describing the displacements of mass (1) and mass (2) can be written as

$$(M_1+M_{1,33})\ddot{V}_1 + k_v V_1 = f_{1,v} \tag{101}$$

$$(M_2+M_{2,33})\ddot{V}_2 + k_v V_2 = f_{2,v} \tag{101-A}$$

Because of the symmetry in the structural and the geometrical properties, as well as in wave loading, equations (101) and (101-A) will be identical and therefore these two equations can be represented by a single equation as follows

$$(M_1+M_{1,33})\ddot{V}_1 + k_v \cdot V_1 = f_{1,v} \tag{102}$$

where M_1 : Mass of the first circular volume

$M_{1,33}$: Added mass of the first circular volume in the horizontal mode of translation

k_v : Stiffness of the system against the horizontal displacement of mass M_1

$f_{1,v}$: Horizontal wave input force.

Stiffness of the system against the horizontal displacement can be determined as follows.

The lateral displacements of mass (1) and mass (2) under quasi-static loading can be determined using Castigliono's theorem [12]

$$v_1 + v_2 = \frac{\partial u}{\partial \bar{f}_{1,v}} = \frac{\partial}{\partial \bar{f}_{1,v}} \left(\int_{u=0}^{H} \frac{M_1^2\, du}{2EI_1} + \int_{u=0}^{B} \frac{M_2^2\, du}{2EI_2} + \int_{u=0}^{H} \frac{M_3^2\, du}{2EI_1} \right) \tag{103}$$

where u : Total strain energy of the system

$\bar{f}_{1,v}$: Quasi-static wave force

$$M_1 = \bar{f}_{1,v} \cdot u \tag{103-A}$$

$$M_2 = \bar{f}_{1,v} \cdot H \tag{103-B}$$

$$M_3 = \bar{f}_{1,v} \cdot (H-u) \tag{103-C}$$

When equation (103) is determined using equations (103-A - 103-C), the lateral displacements of mass (1) and (2) become

$$v_1 + v_2 = 2v_1 = 2v_2 = \frac{\bar{f}_{1,v} H^2}{3} \left(\frac{2H}{EI_1} + \frac{3B}{EI_2} \right) \tag{104}$$

Now k_v value can easily be obtained from equation (104) as follows

$$k_v = \frac{6}{H^2} \left(\frac{1}{\frac{2H}{EI_1} + \frac{3B}{EI_2}} \right) \tag{105}$$

The differential equation which represents the free vibration of the system becomes

$$(M_1+M_{1,_{33}})\ddot{v}_1 + k_v \cdot v_1 = 0 \tag{106}$$

and the natural frequency of the system in symmetrical horizontally vibrating mode

$$\omega_{s,h} = \frac{1}{H}\sqrt{\frac{6}{(M_1+M_{1,_{33}})\left(\frac{2H}{EI_1}+\frac{3B}{EI_2}\right)}} \tag{107}$$

The displacement values of masses (1) and (2) can be obtained from equation (102) as follows

$$v_1(t) = v_2(t) = f_{1,v}\sqrt{k_v} \cdot Q_{s,h} \tag{108}$$

where $Q_{s,h} = \dfrac{1}{\sqrt{\left[1-\left(\dfrac{\omega}{\omega_{s,h}}\right)^2\right]^2}}$

(i-2) Vertically applied arbitrary load or horizontally applied arbitrary load: In this case, the structure will be supported by the fictitious supports on the right and left hand sides of the structure successively, and a similar calculation procedure to that carried out in the previous case will be used to obtain the natural frequencies, and the horizontal and the vertical displacements of masses (1) and (2) under the wave loading. The procedure may be illustrated as follows.

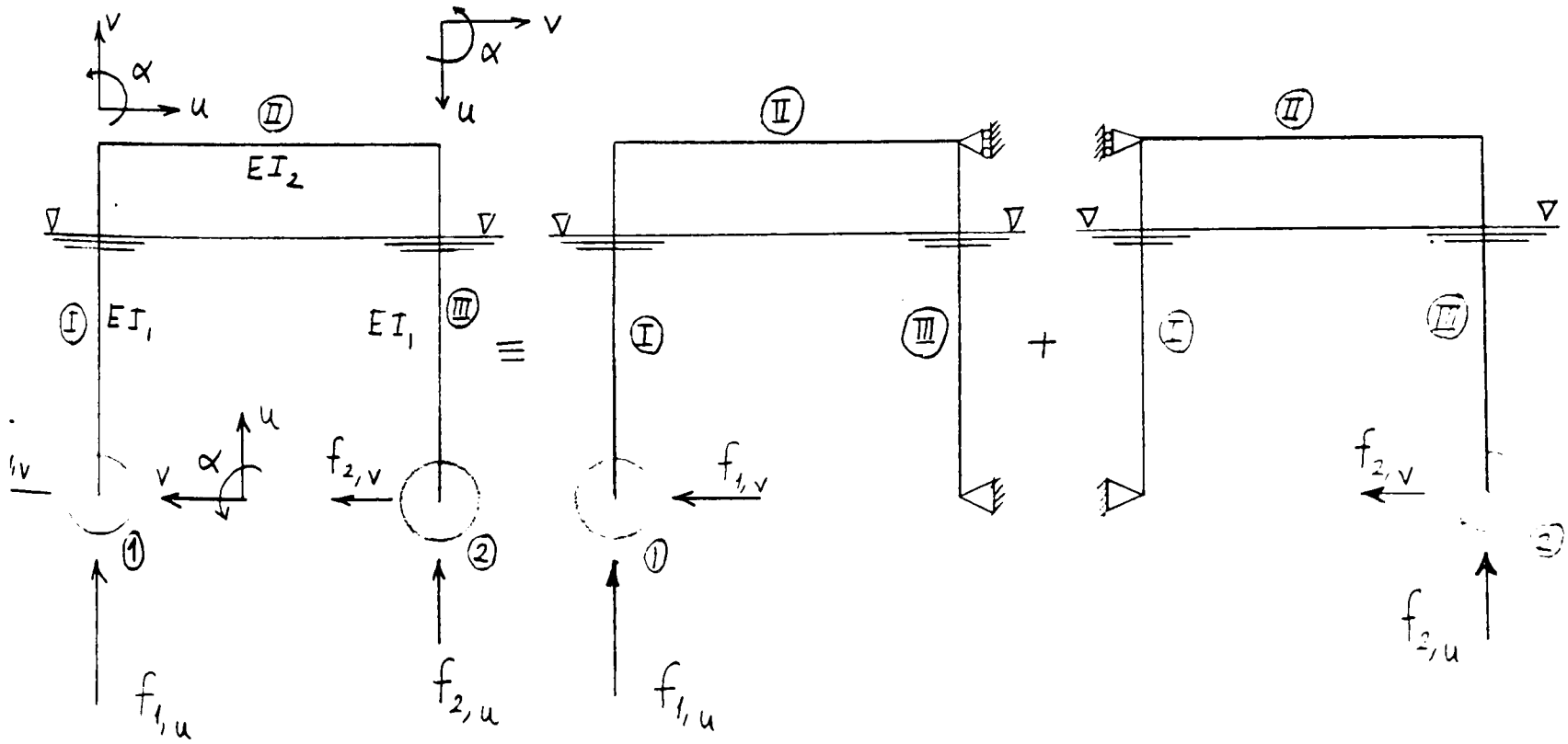

Fig. 24

The displacement of mass (1) in the horizontal and vertical modes may be described with the following uncoupled differential equations

$$(M_1+M_{1,33})\ddot{v}_1 + k_v \cdot v_1 = f_{1,v} \tag{109}$$

$$(M_1+M_{1,22})\ddot{u}_1 + k_u \cdot u_1 = f_{1,u} \tag{109-A}$$

where M_1: Mass of the first circular volume

$M_{1,33}, M_{1,22}$: Added mass of the first circular volume in the horizontal and the vertical mode of translation respectively

k_v, k_u : Stiffness of the system against the horizontal and the vertical mode of translation respectively

$f_{1,v}, f_{1,u}$: Wave forces in the horizontal and the vertical directions respectively.

Stiffness values in the horizontal and the vertical modes can be determined using Castigliano's theorem as was done in the previous case. k_v and k_u values are found as follows

$$k_v = \frac{3}{H^2}\left[\frac{1}{\frac{2H}{EI_1}+\frac{3B}{EI_2}}\right] \tag{110}$$

$$k_u = \frac{3}{B^2}\left[\frac{1}{\frac{B}{EI_1}+\frac{H}{EI_2}}\right] \tag{110-A}$$

Strictly, k_u should also include the stiffness due to hydrostatic restoring forces giving

$$k_u = \frac{3}{B^2}\left[\frac{1}{\frac{B}{EI_1}+\frac{H}{EI_2}}\right] + \rho g\, A_w \tag{110-B}$$

where A_w: Waterplane area of Member I.

Since generally the hydrostatic stiffness of floating platforms is very small compared to elastic stiffness, in this study hydrostatic stiffness is neglected in the dynamic structural response calculations.

The natural frequency of the system in the horizontal vibrating mode becomes

$$\omega_{as,h} = \frac{1}{H}\sqrt{\frac{3}{(M_1+M_{1,33})\left(\frac{2H}{EI_1}+\frac{3B}{EI_2}\right)}} \tag{111}$$

The natural frequency of the system in the vertical vibrating mode takes the following form

$$\omega_{as,v} = \frac{1}{B}\sqrt{\frac{3}{(M_1+M_{1,22})\left(\frac{B}{EI_1}+\frac{H}{EI_2}\right)}} \tag{111-A}$$

The displacement of mass (1) in the vertical and the horizontal directions becomes

$$v_1(t) = f_{1,v}/k_v \cdot Q_{as,h} \tag{112}$$

$$u_1(t) = f_{1,u}/k_u \cdot Q_{as,v} \tag{112-A}$$

where

$$Q_{as,h} = \frac{1}{\sqrt{\left[\left(1-\frac{\omega}{\omega_{as,h}}\right)^2\right]^2}}$$

$$Q_{as,v} = \frac{1}{\sqrt{\left[\left(1-\frac{\omega}{\omega_{as,v}}\right)^2\right]^2}}$$

Similarly, displacement of mass (2) in the vertical and horizontal modes becomes

$$v_2(t) = f_{2,v}/k_v \cdot Q_{as,h} \tag{113}$$

$$u_2(t) = f_{1,u}/k_u \cdot Q_{as,v} \tag{113-A}$$

The procedures for finding dynamic displacements, given above, will be used to obtain the structural response of a floating structure shown in Fig. 25 as follows.

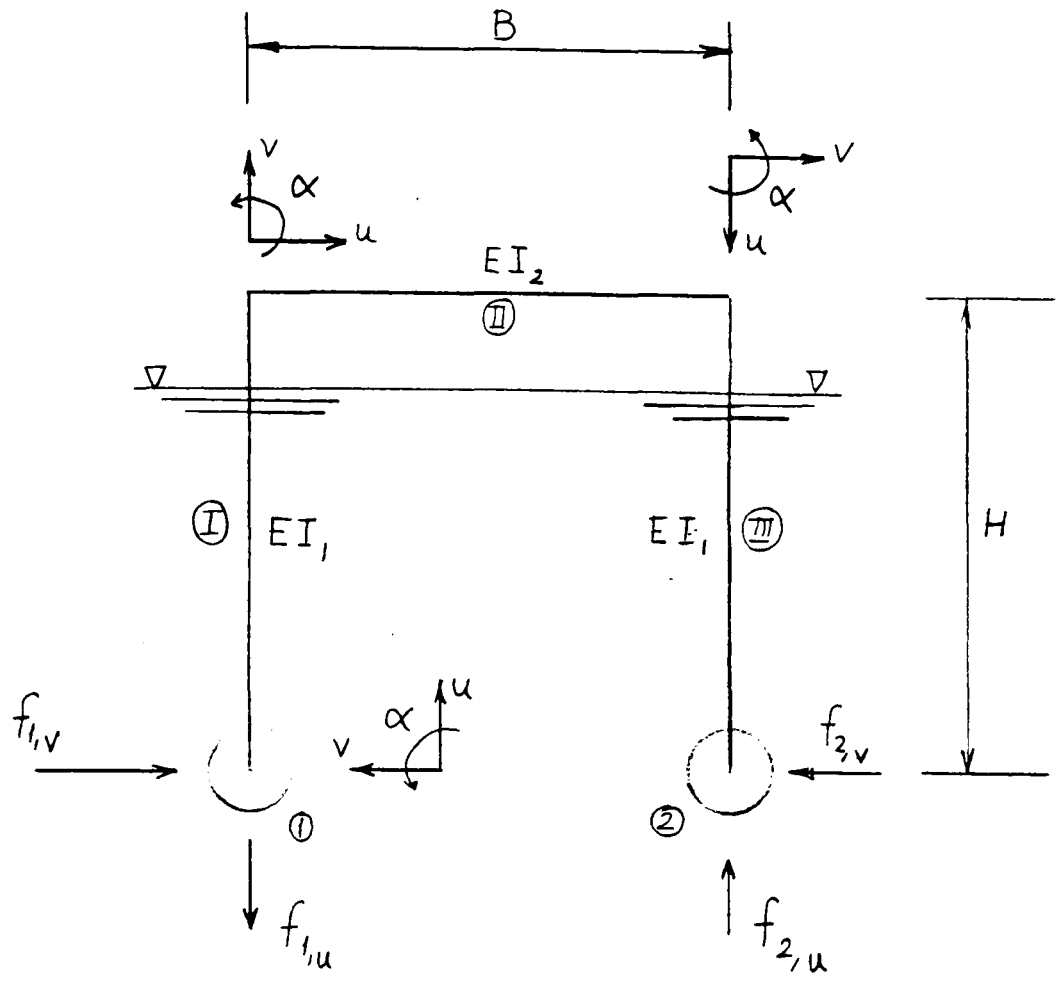

Fig. 25

The wave forces on this floating structure will be broken down as the symmetrical and the asymmetrical forces as shown in Fig. 26. The dynamic structural response values will be determined following the procedure used earlier to obtain equations (79-A),(80-A),81-A) in conjunction with equations (108),(112),(112-A),(113),(113-A).

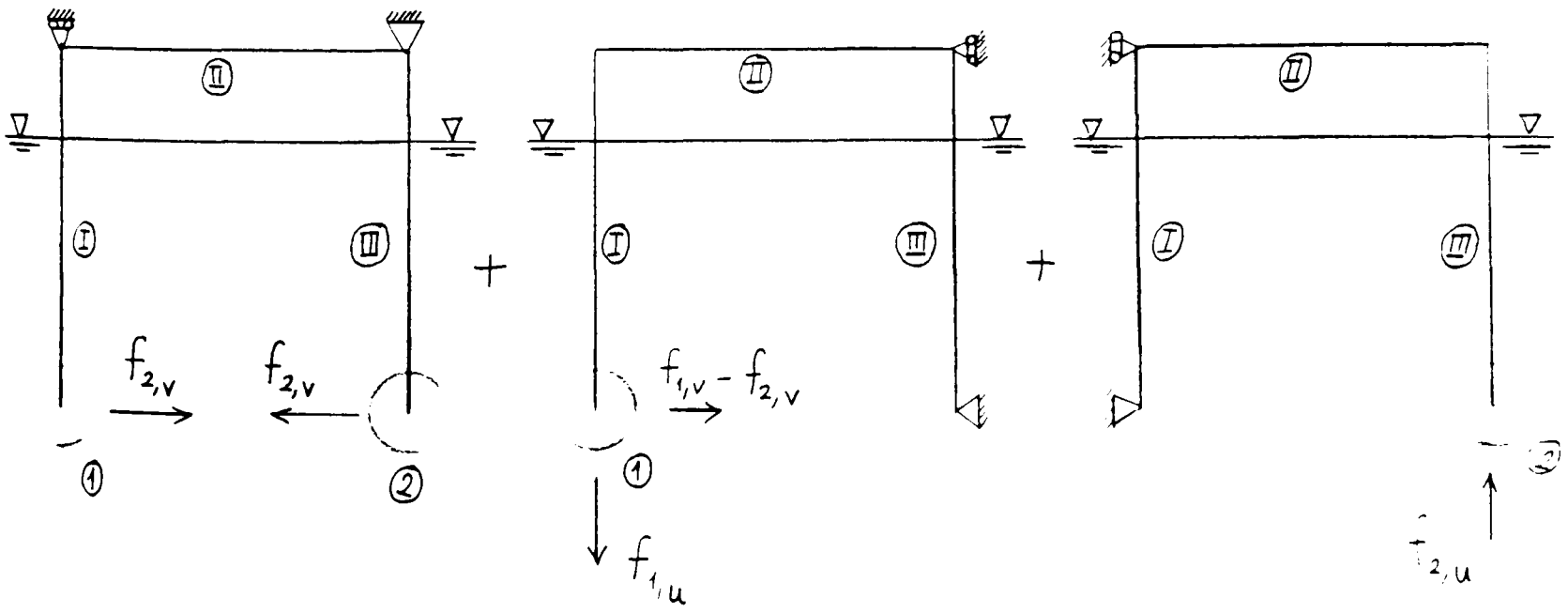

Fig. 26

Global Member: I:

Shear Forces : $$SF_1(u,t) = f_{2,v} \cdot Q_{s,h} + \frac{1}{2}\left[(f_{1,v}-f_{2,v})\, Q_{as,h} - f_{2,u}\,\frac{B}{H}\cdot Q_{as,v}\right] \quad (114\text{-A})$$

Bending Moments: $$BM_1(u,t) = -f_{2,v}\cdot u\cdot Q_{s,h} + \frac{1}{2}\left[-(f_{1,v}-f_{2,v})\cdot u\cdot Q_{as,h} + f_{2,u}\cdot\frac{B}{H}\cdot u\, Q_{as,v}\right] \quad (114\text{-B})$$

Axial Forces : $$AF_1(u,t) = \tfrac{1}{2}[f_{1,u}+f_{2,u}] \quad (114\text{-C})$$

Global Member: II:

Shear Forces : $$SF_2(u,t) = \tfrac{1}{2}[f_{1,u}+f_{2,u}]\, Q_{as,v} \quad (115\text{-A})$$

Bending Moments: $$BM_2(u,t) = -f_{2,v}\cdot H\cdot Q_{s,h} + \frac{1}{2}\left[-(f_{1,v}-f_{2,v})\cdot H\cdot Q_{as,h} + f_{2,u}\cdot B\cdot Q_{as,h} - (f_{1,u}-f_{2,u})\cdot u\cdot Q_{as,v}\right] \quad (115\text{-B})$$

Axial Forces : $$AF_2(u,t) = -f_{2,v} + \tfrac{1}{2}[-(f_{1,v}-f_{2,v}) = \tfrac{1}{2}[-f_{1,v}-f_{2,v}] \quad (115\text{-C})$$

It should be noticed that equations (115-A - 115-C) become identical to equations (40-A - 40-C) when $Q_{s,h} = Q_{as,h} = Q_{as,v} = 1$.

Global Member: III:

Shear Forces : $$SF_3(u,t) = -f_{2,v}\cdot Q_{s,h} + \frac{1}{2}\left[-(f_{1,v}-f_{2,v})\cdot Q_{as,h} - f_{1,u}\cdot\frac{B}{H}\cdot Q_{as,v}\right] \quad (116\text{-A})$$

Bending Moments: $$BM_3(u,t) = -f_{2,v}\,(H-u)\cdot Q_{s,h} + \frac{1}{2}\left[-(f_{1,v}-f_{2,v})(H-u)\cdot Q_{as,h} - \frac{f_{1,u}\cdot B}{H}\cdot u\cdot Q_{as,v}\right] \quad (116\text{-B})$$

Axial Forces : $$AF_3(u,t) = +\tfrac{1}{2}[-f_{1,u}-f_{2,u}] \quad (116\text{-C})$$

where $Q_{s,h}$, $Q_{as,h}$, $Q_{as,v}$ values were defined in equations (108), (112) and respectively.

(ii) Structure is free-floating in waves

In this case the output forces (= hydrodynamic, restoring and mass-inertia forces) on the circular volumes should be calculated.

The structural response values can be obtained using equations (114-A - 116-C) after the force terms have been replaced with the sum of the wave input and output forces.

The approximate method summarised above was applied to predict the bending moment values at the deck of a twin circular hull model semi-submersible. Since the deck structure of the model was built to be flexible in order to obtain higher and stable strain output from the strain gauges, the method of dynamic analysis was applied for the more reliable comparison between the experimental and the theoretical results. The results will be discussed in the next section.

Here it should be mentioned that in general most of the existing semi-submersible type floating structures have sufficiently rigid overall structural integrity between the members, so that the local mode of member deformations can be neglected in their analysis and therefore quasi-static analysis will be sufficient. However, the particular type of floating platform shown in Fig. 27 should also have been checked for dynamic loading. For this type of geometry, approximate analysis can easily be done using the model shown in Fig. 19. The Author was unable to obtain the structural particulars of this rig for the dynamic loading calculations, but the accident involving the breaking of the leg suggests that the actual loading may have been higher than expected.

Another type of semi-submersible design, shown in Fig. 28, also has flexible connections between the rigid deck structure and the main legs. Structural response calculations of those flexible connections under dynamic loading could have been important to the structural design. The

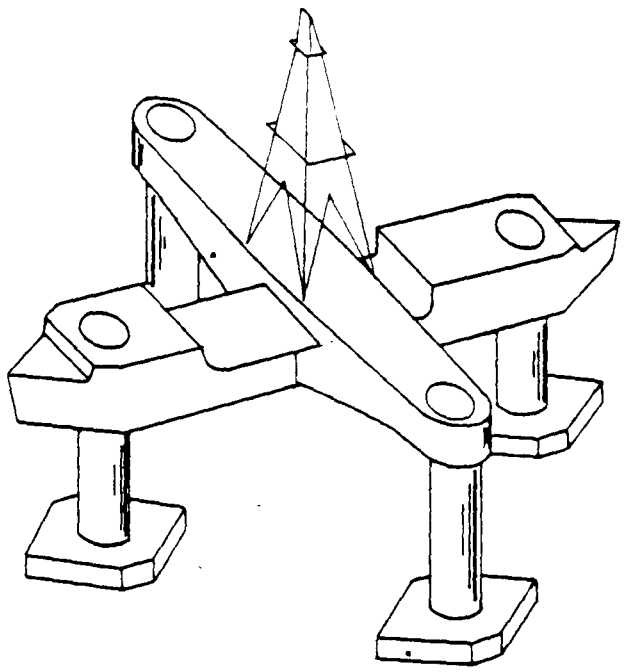

Figure 27 (From Reference 20)

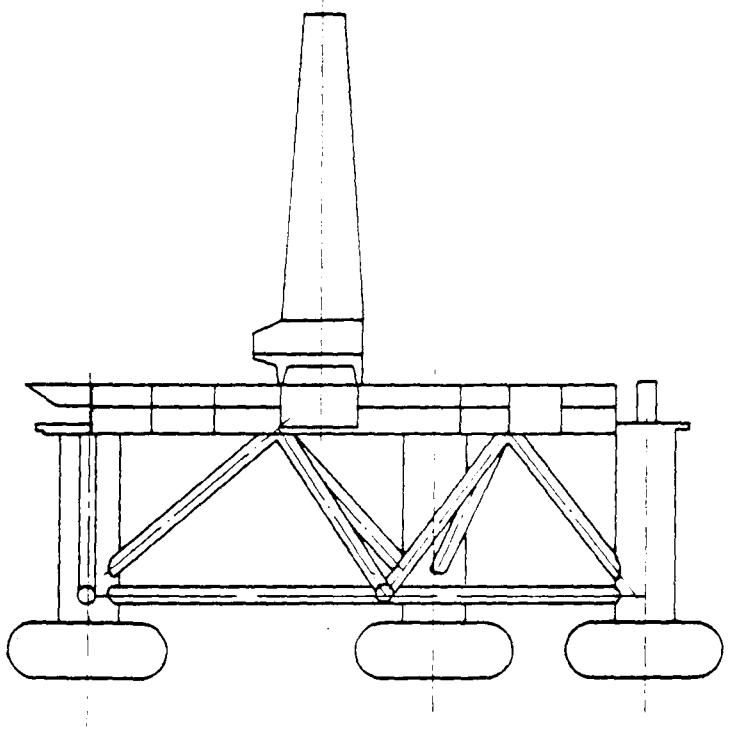

Figure 28

UPPER BRACINGS AND DECK ARRANGEMENT

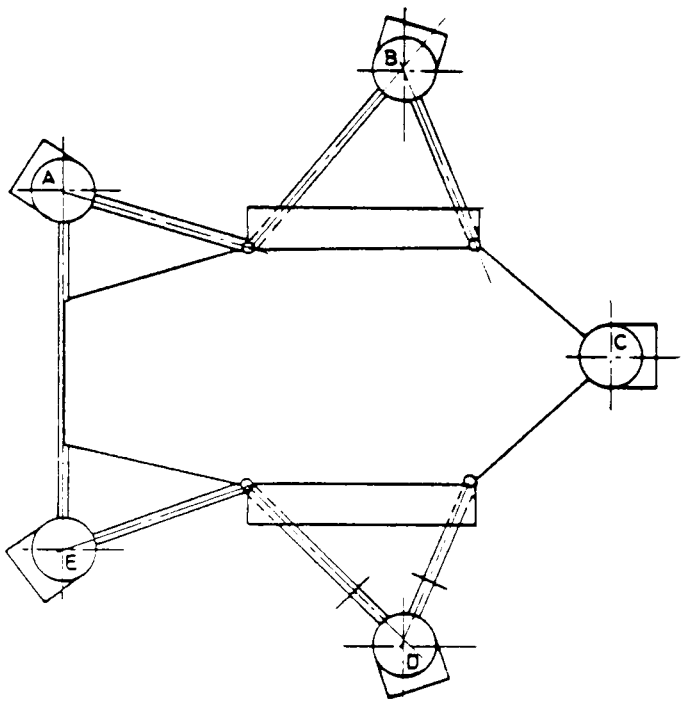

LOWER BRACINGS AND PONTOONS ARRANGEMENT

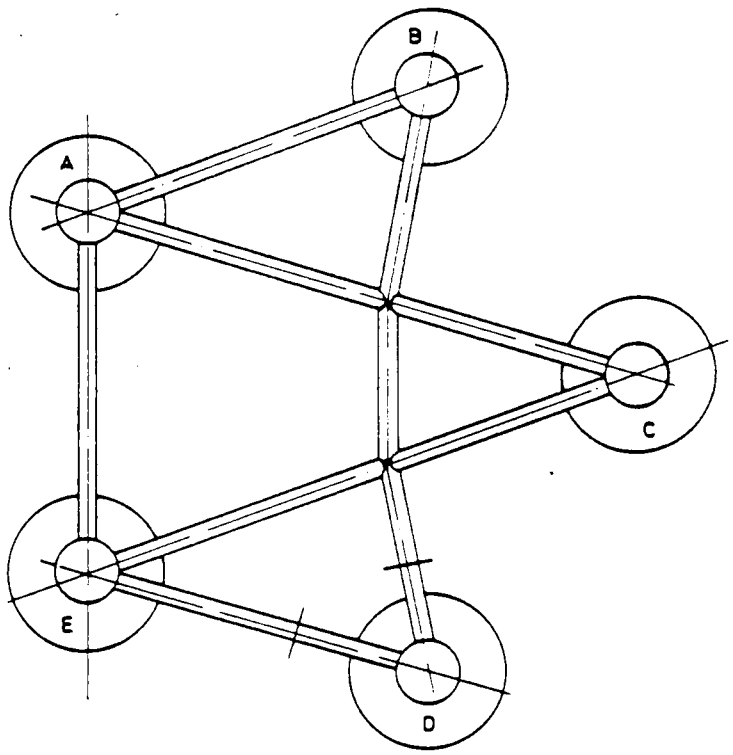

NOTE, LEG 'D' WAS BROKEN

Figure 28 (From Reference 21)

troubles experienced by those two types of design suggests that greater attention should be paid to those cases when the structural arrangements are such as to bring the natural frequencies down towards the wave frequencies.

The dynamic structural response analysis also becomes important and necessary in the following cases:

(a) In the design of structural members of a floating rig when they extend into deeper draught, i.e. riser cables, tension leg cables, cooling pipes of OTEC platforms, etc.

(b) Structural response of floating structures under impact loading. Impact loading may occur during vessel-platform collision or wave breaking between the members of a floating structure.

(c) Damage assessment of the whole structure after the damage has occurred.

1.4 Calculation of Structural Response Values for Twin Circular Hulled Semi-Submersible Model

The calculation procedures described in sections 1.1 - 1.3 (see also section 2.2) to obtain the structural response values were applied to a twin circular hulled semi-submersible model, shown in Fig. 29. (The full characteristics of the model are given in Appendix 1. In Fig. 30, the structural response analysis results for maximum bending moment at the centre of the deck in beam sea conditions are shown. In this case, the structure was assumed to be restrained and the results represent the linear quasi-static loading, non-linear quasi-static loading and non-linear dynamic loading. Input wave loading and the output force calculations were carried out using the computer program FLUID4A which is a wave loading, motion and structural response analysis program for twin circular hull multi-column type semi-submersibles. (FLUID4A is described in detail

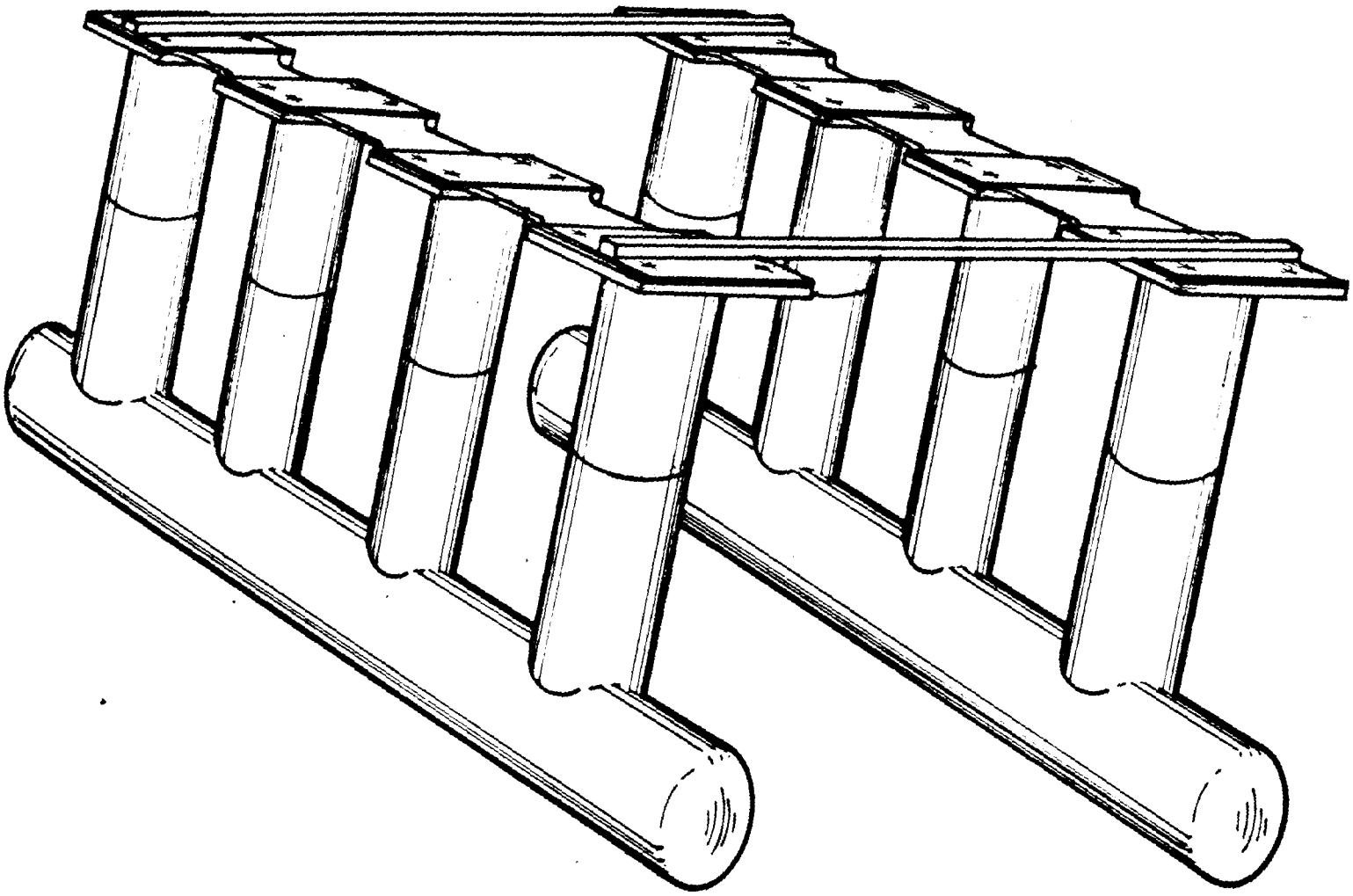

GENERAL VIEW OF THE SEMI-SUBMERSIBLE MODEL FOR STRUCTURAL RESPONSE EXPERIMENT

Fig. 29

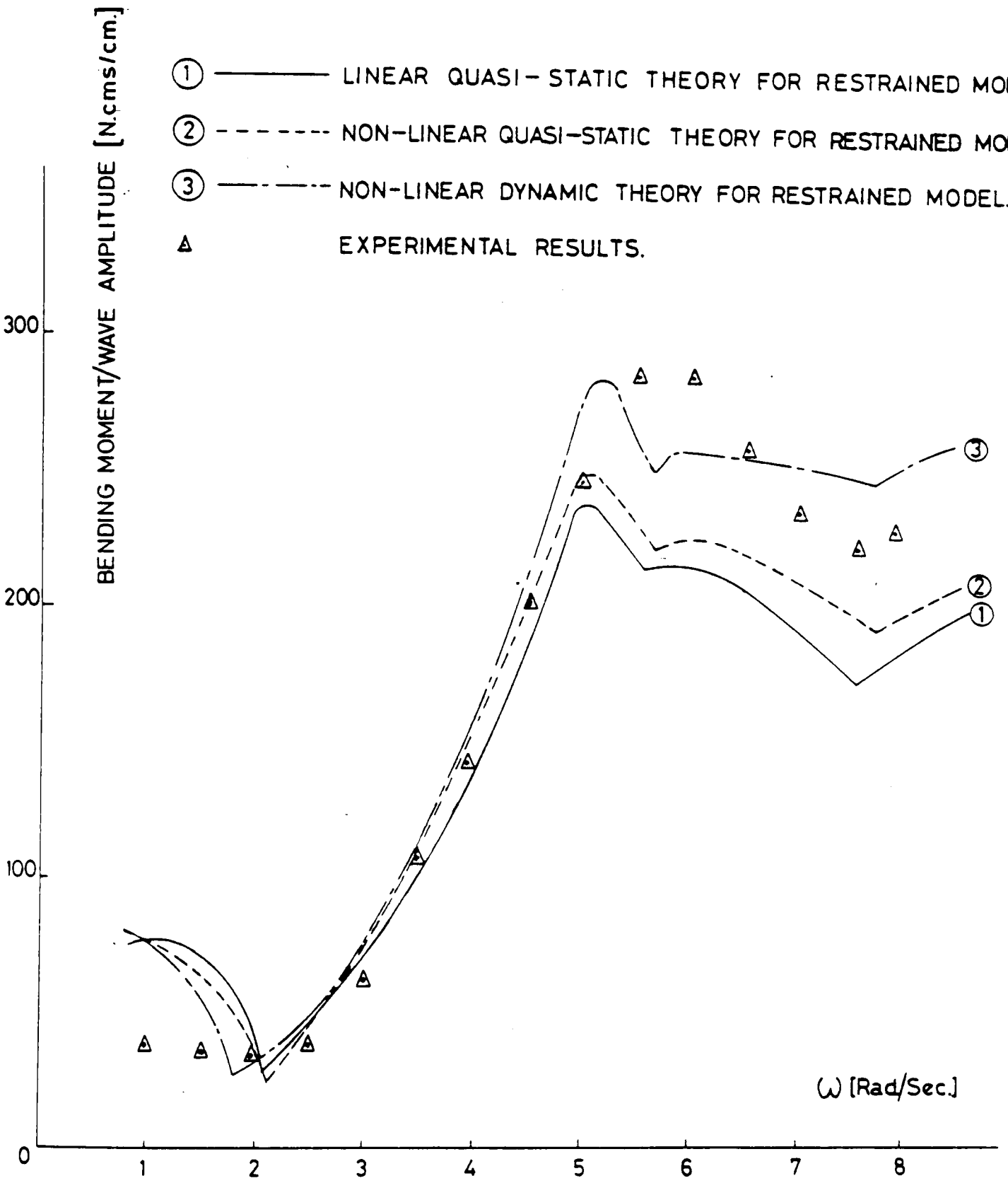

STRUCTURAL RESPONSE PREDICTIONS FOR
TWIN-CIRCULAR HULL SEMI-SUBMERSIBLE MODEL
(BENDING MOMENT ON THE DECK)

Fig. 30

in Chapter 6.) Non-linear loading calculations take into account non-linear free surface boundary conditions, as well as the effect of the second-order forces.

In Fig. 31, the bending moment values at the centre of the deck for the free floating model were presented. Loading conditions were taken to be the same as in the previous case.

In Fig. 32, a comparison is made between the bending moments at the centre of the deck for the restrained and the free floating model cases. In the case of the restrained model, the support conditions were chosen in the theoretical model such that the structural response values would be maximum. (See equations (40-A - 40-C) and (115-A - 115-C).) Figure 32 shows that the bending moments are generally overpredicted in the restrained model case. However, in the region where excitation frequencies approach the natural frequencies for the rigid body oscillation modes, the bending moment predictions for the free floating model are greater than the restrained model case. This may be due to the high output force distributions. The experimental results are generally in good agreement with the theoretical predictions. Some differences between the theoretical predictions and the experimental results may be due to the approximations involved in the motion response equations (see also Chapter 4), and in the prediction of dynamic structural response values. Some effects of the harnesses which hold the model in position in the waves may also be expected in the region where excitation frequencies approach the natural frequencies of the rigid body oscillations.

Although the theoretical predictions compare reasonably well with the experimental results in the case of a restrained mathematical model, one might have expected the theoretical predictions of the bending moments at the deck to be higher than the experimental results. This combined with the fact that the underestimation of the bending moment values for

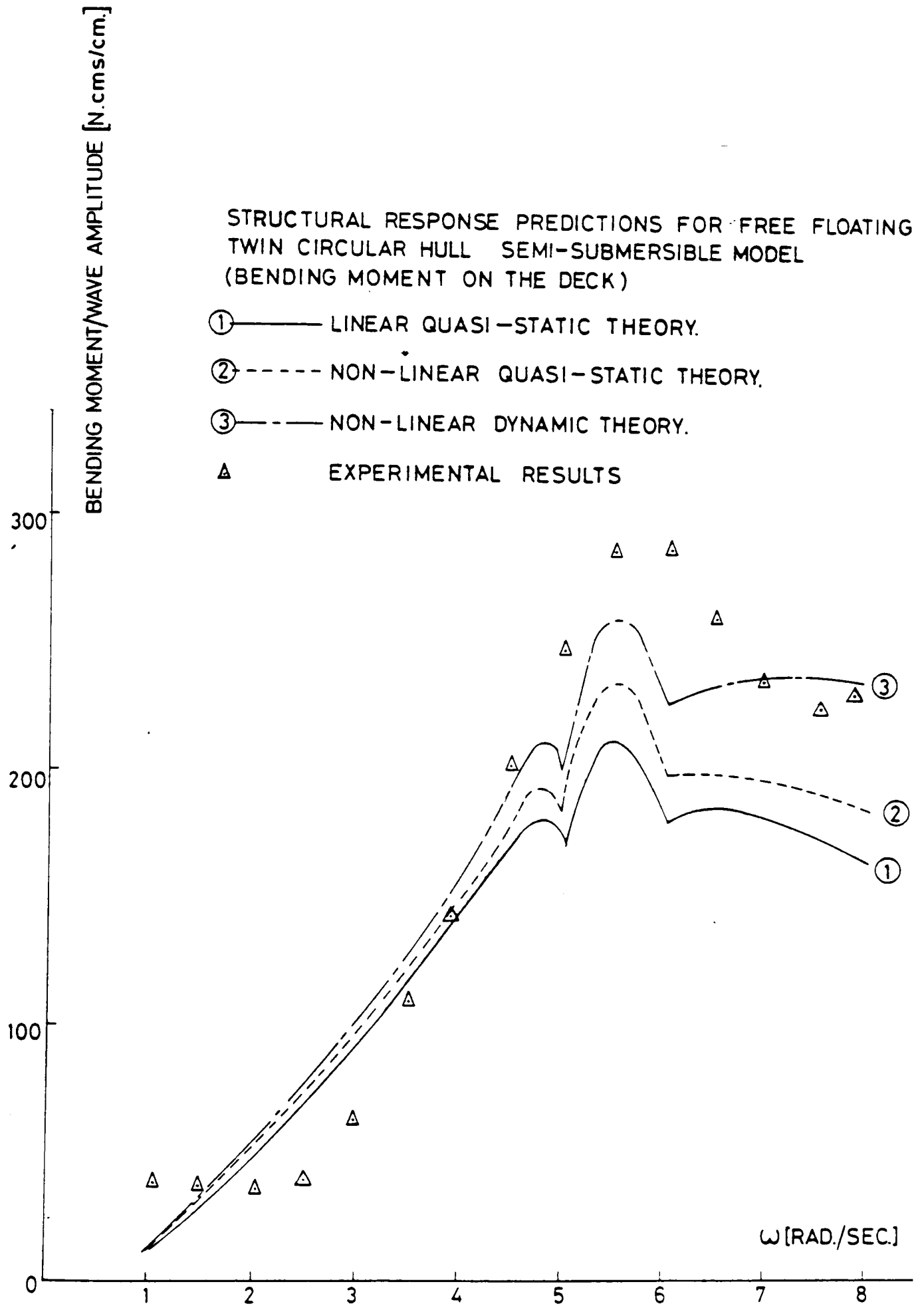
STRUCTURAL RESPONSE PREDICTIONS FOR FREE FLOATING TWIN CIRCULAR HULL SEMI-SUBMERSIBLE MODEL (BENDING MOMENT ON THE DECK)
① LINEAR QUASI-STATIC THEORY.
② NON-LINEAR QUASI-STATIC THEORY.
③ NON-LINEAR DYNAMIC THEORY.
EXPERIMENTAL RESULTS
BENDING MOMENT/WAVE AMPLITUDE [N.cms/cm.]
300
200
100
0
1
2
3
4
5
6
7
8
ω [RAD./SEC.]

Fig. 31

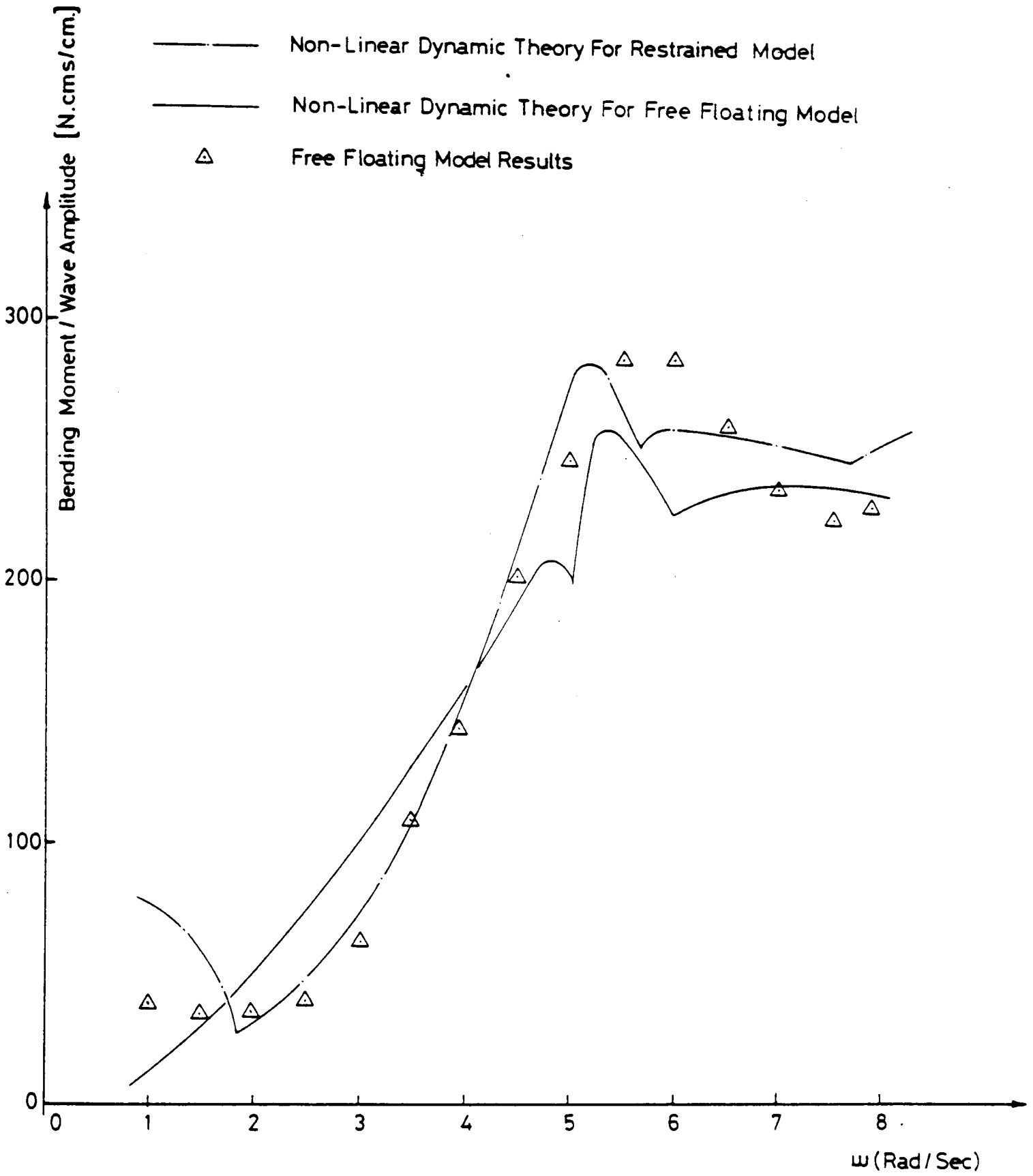

Bending Moment On The Deck Of A Twin Circular Hulled Semi-Submersible

Fig. 32

the free floating model case suggest that wave inertia coefficients should be higher than the values used in these predictions. In general, to determine the structural response values using the restrained mathematical structural model should give safer results. However, a designer who is going to use a structural analysis computer routine for the restrained model, must also choose support conditions which will give maximum structural response values under the particular wave loading.

In Fig. 33, various components of the bending moment values in the restrained model case under quasi-static loading were plotted against excitation frequency. This shows that the bending moment values on the deck are highly dominated by the wave loading on the hulls over a large range of excitation frequencies.

2. CALCULATION OF THE STRUCTURAL RESPONSE FOR INDETERMINATE STRUCTURES UNDER WAVE LOADING

In this section a structural analysis procedure to obtain shear force, bending moment and axial force values for an indeterminate floating structure will be discussed. In the case of an indeterminate structure the calculation procedure in terms of loading calculations and the selection of boundary conditions will be similar to the case of determinate structures.

In order to perform the structural response analysis of a floating offshore rig, the use of a computer routine will be necessary. One may either write a structural analysis program for a certain geometry, boundary conditions and the type of loading, using classical engineering methods [13] [14] or use general purpose frame analysis routines [15] [16].

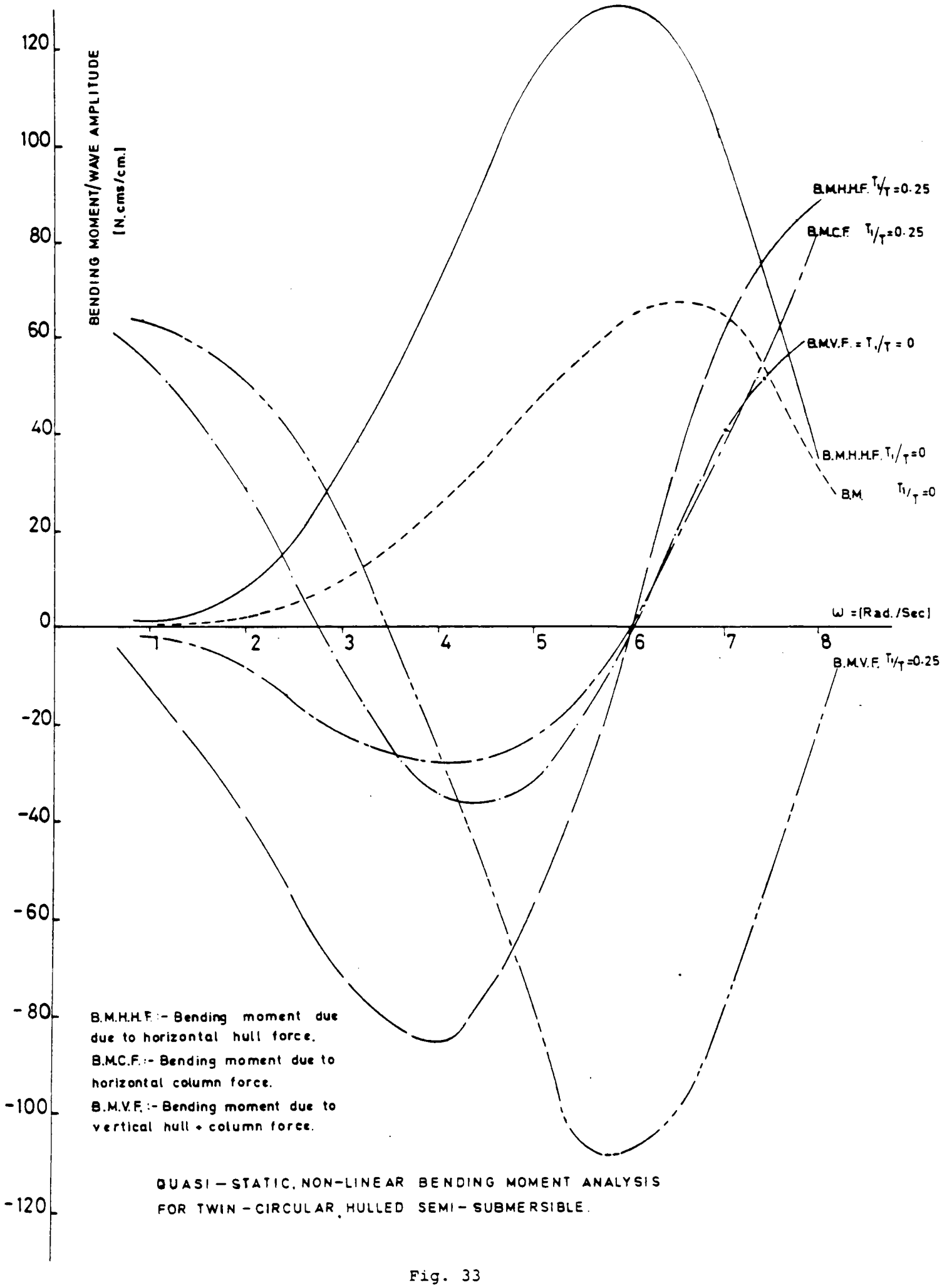
BENDING MOMENT/WAVE AMPLITUDE
[N.cms/cm.]
120
100
80
60
40
20
0
-20
-40
-60
-80
-100
-120
1
2
3
4
5
6
7
8
ω =[Rad./Sec]
B.M.H.H.F. T1/T =0.25
B.M.C.F. T1/T=0.25
B.M.V.F. = T1/T = 0
B.M.H.H.F. T1/T=0
B.M. T1/T =0
B.M.V.F. T1/T=0.25
B.M.H.H.F :- Bending moment due due to horizontal hull force.
B.M.C.F :- Bending moment due to horizontal column force.
B.M.V.F :- Bending moment due to vertical hull + column force.
QUASI - STATIC, NON-LINEAR BENDING MOMENT ANALYSIS
FOR TWIN - CIRCULAR HULLED SEMI - SUBMERSIBLE.

Fig. 33

In this study a general purpose two-dimensional frame analysis program FRAN2 was used. FRAN2 was originally written in BASIC language by I. Smith of the Civil Engineering Department, Glasgow University and converted to FORTRAN language and modified to include frame and load definition files by the author and C. Bradley, Computer Software Assistant, of the Naval Architecture and Ocean Engineering Department.

In this study, structural analysis calculations were carried out for symmetrical geometries, therefore a two-dimensional frame analysis computer routine was sufficient, following the procedure explained in section 2.2. In the case of asymmetric geometries, or when there are no limitations in terms of time, cost and the storage capability of the computer, general purpose three-dimensional space frame computer routines are more appropriate.

2.1 Analysis of Rigid Plane Frames

2.1.1 Loading is static or quasi-static. In this section the method which was used in FRAN2 will be summarised. The method was first devised by Livesley of Manchester University [17,18] and is known as the Stiffness Method in the literature.

When a single loaded member whose section area is A, second moment of inertia I and Young's modulus E, is taken from a frame system, the following relations between the forces and the deflections can be written.

For simplicity, the general form of a deflected member can be replaced with the superposition of the six cases as shown in Fig. 34.

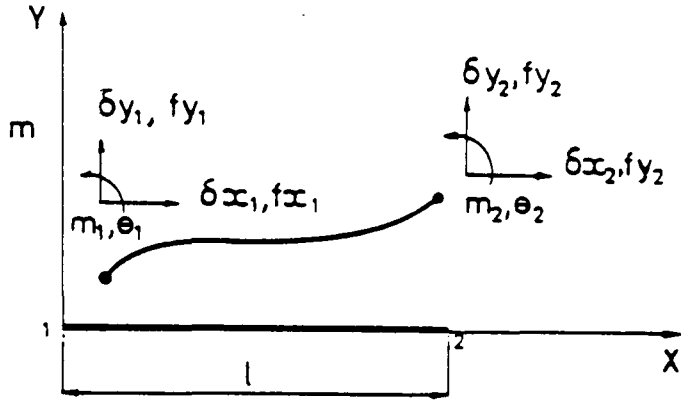
Y
m
δy1, fy1
δx1,fx1
m1,θ1
δy2,fy2
δx2,fy2
m2,θ2
1
2
l
X

(a)

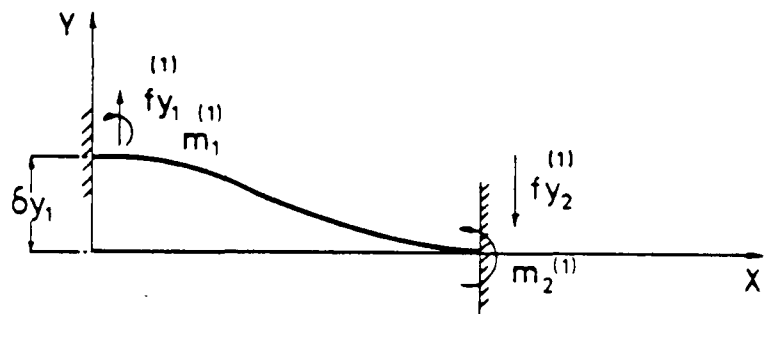
Y
(1)
fy1
(1)
m1
δy1
(1)
fy2
m2(1)
X

+ (b)

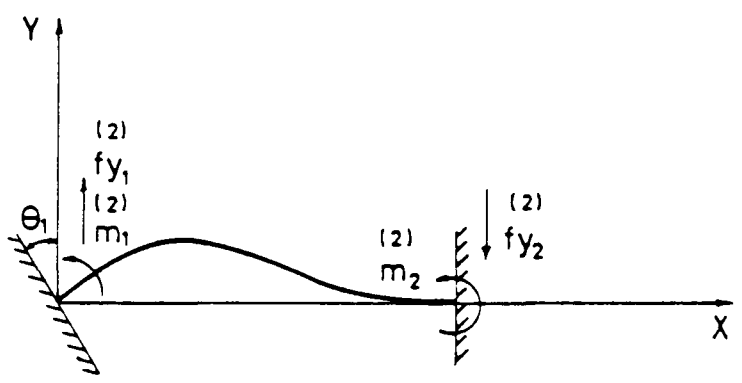
Y
(2)
fy1
(2)
m1
θ1
(2)
m2
(2)
fy2
X

(c)

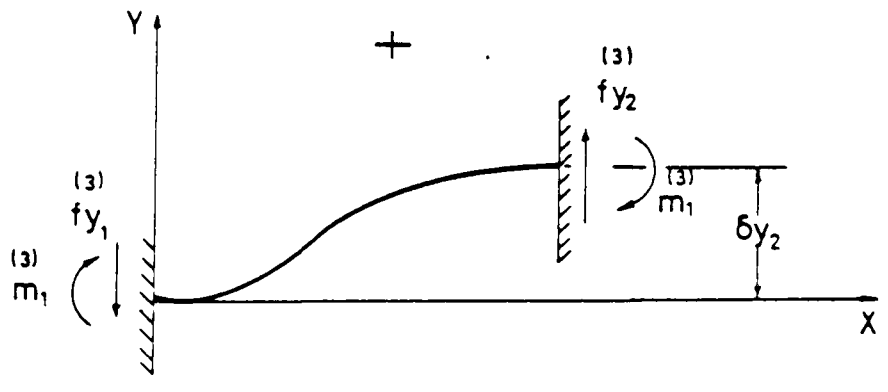
Y
(3)
fy1
(3)
m1
(3)
fy2
(3)
m1
δy2
X

+ (d)

Fig. 34

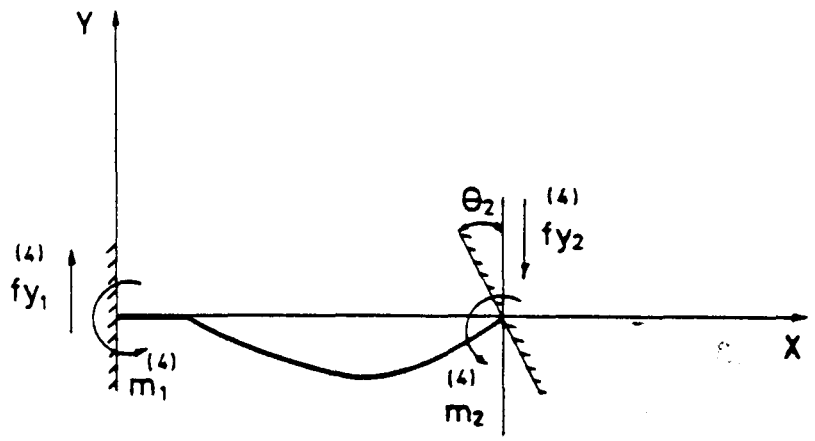

(e)

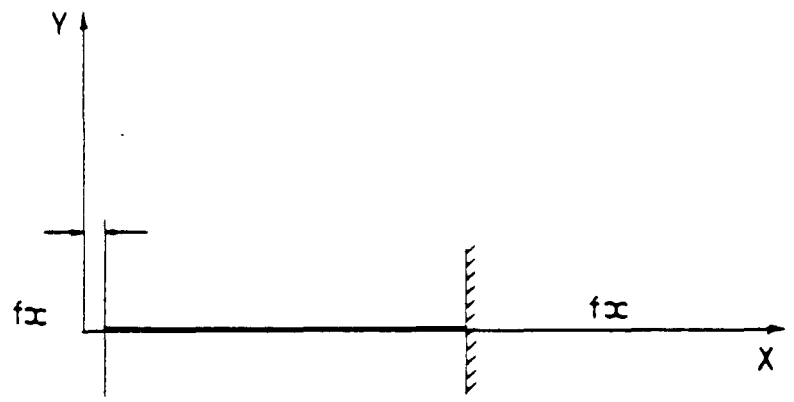

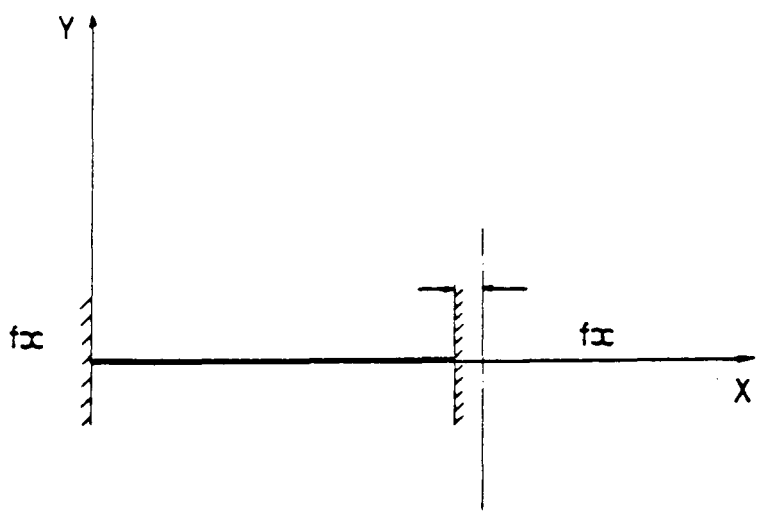

Fig. 34

For each case, the well-known relations between the forces and the displacements for a cantilever beam can be written [13]. Superposition of these cases gives the relations between the end forces and the end displacements of a member. This can be expressed with the following equations.

$$[f_1] = [k_{11}][d_1] + [k_{12}][d_2] \tag{117}$$

$$[f_2] = [k_{21}][d_1] + [k_{22}][d_2] \tag{117-A}$$

where

$$[f_1] = \begin{bmatrix} f_{x_1} \\ f_{y_1} \\ m_1 \end{bmatrix}, \qquad [f_2] = \begin{bmatrix} f_{x_2} \\ f_{y_2} \\ m_2 \end{bmatrix}$$

$$[k_{11}] = \begin{bmatrix} \frac{EA}{\ell} & 0 & 0 \\ 0 & \frac{12EI}{\ell^3} & \frac{6EI}{\ell^2} \\ 0 & \frac{6EI}{\ell^2} & \frac{4EI}{\ell} \end{bmatrix}$$

$$[k_{12}] = \begin{bmatrix} -\frac{EA}{\ell} & 0 & 0 \\ 0 & -\frac{12EI}{\ell} & \frac{6EI}{\ell^2} \\ 0 & -\frac{6EI}{\ell^2} & \frac{2EI}{\ell} \end{bmatrix}$$

$$[k_{21}] = \begin{bmatrix} -\frac{EA}{\ell} & 0 & 0 \\ 0 & -\frac{12EI}{\ell} & -\frac{6EI}{\ell} \\ 0 & \frac{6EI}{\ell^2} & \frac{2EI}{\ell} \end{bmatrix}$$

$$[k_{22}] = \begin{bmatrix} \frac{EA}{\ell} & 0 & 0 \\ 0 & \frac{12EI}{\ell} & -\frac{6EI}{\ell} \\ 0 & -\frac{6EI}{\ell^2} & \frac{4EI}{\ell} \end{bmatrix}$$

$$[d_1] = \begin{bmatrix} \delta x_1 \\ \delta y_1 \\ \theta_1 \end{bmatrix}, \qquad [d_2] = \begin{bmatrix} \delta x_2 \\ \delta y_2 \\ \theta_2 \end{bmatrix}$$

The relations between the end forces and the displacements of a member can also be expressed in a general form

$$\begin{bmatrix} f_{x_1} \\ f_{y_1} \\ m_1 \\ f_{x_2} \\ f_{y_2} \\ m_2 \end{bmatrix} = \begin{bmatrix} \frac{EA}{\ell} & 0 & 0 & -\frac{EA}{\ell} & 0 & 0 \\ 0 & \frac{12EI}{\ell^3} & \frac{6EI}{\ell^2} & 0 & -\frac{12EI}{\ell^3} & \frac{6EI}{\ell^2} \\ 0 & \frac{6EI}{\ell^2} & \frac{4EI}{\ell} & 0 & -\frac{6EI}{\ell^2} & \frac{2EI}{\ell} \\ -\frac{EA}{\ell} & 0 & 0 & \frac{EA}{\ell} & 0 & 0 \\ 0 & -\frac{12EI}{\ell^3} & -\frac{6EI}{\ell^2} & 0 & \frac{12EI}{\ell^3} & -\frac{6EI}{\ell^2} \\ 0 & \frac{6EI}{\ell^2} & \frac{2EI}{\ell} & 0 & -\frac{6EI}{\ell^2} & \frac{4EI}{\ell} \end{bmatrix} \cdot \begin{bmatrix} \delta x_1 \\ \delta y_1 \\ \theta_1 \\ \delta x_2 \\ \delta y_2 \\ \theta_2 \end{bmatrix} \qquad (118)$$

↓ Force Matrix of a member

↓ Stiffness Matrix of a member

↓ Displacement Matrix of a member

The stiffness equations written in equations (117) and (117-A) are related to the local axes of a member. However, in the case of frame systems some members may be inclined at different angles to any direction. Therefore it is necessary to choose an overall reference system for a given general system. In Fig. 35, the forces and displacement vectors on a member are shown with respect to the local and overall axes.

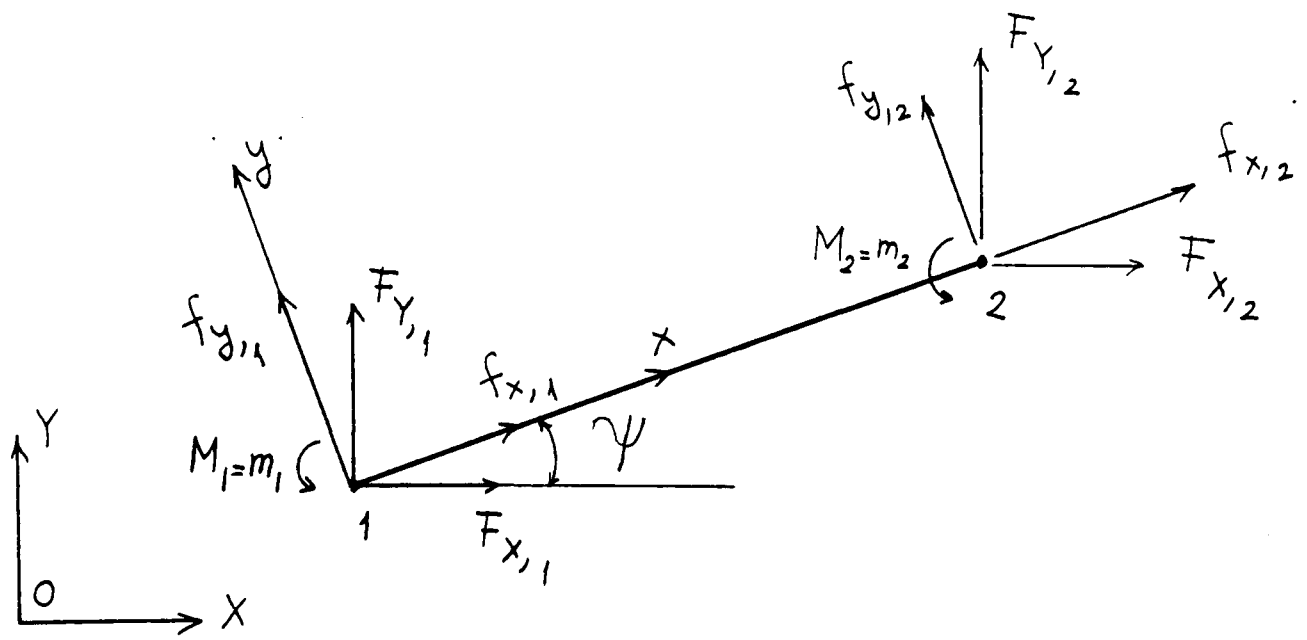

Fig. 35

The relation between end forces and displacements of a member in local axes and in overall axes can be shown as follows

$$F_{x,1} = f_{x,1} \cos\psi - f_{y,1} \sin\psi \qquad (118\text{-A})$$

$$F_{y,1} = f_{x,1} \sin\psi + f_{y,1} \cos\psi \qquad (118\text{-B})$$

$$M_1 = m_1 \qquad (118\text{-C})$$

and displacements

$$\Delta X_1 = \delta X_1 \cos\psi - \delta X_2 \sin\psi \qquad (119\text{-A})$$

$$\Delta Y_1 = \delta X_1 \sin\psi + \delta X_2 \cos\psi \qquad (119\text{-B})$$

$$\theta_1 = \theta_1 \qquad (119\text{-C})$$

or, in matrix form

$$\begin{bmatrix} F_{x,1} \\ F_{y,1} \\ M_1 \end{bmatrix} = \begin{bmatrix} \cos\psi & -\sin\psi & 0 \\ \sin\psi & \cos\psi & 0 \\ 0 & 0 & 1 \end{bmatrix} \begin{bmatrix} f_{x_1} \\ f_{y_1} \\ m_1 \end{bmatrix} \qquad (120\text{-A})$$

$$[F_1] = [T] \cdot [f_1]$$

and

$$\begin{bmatrix} \Delta X_1 \\ \Delta Y_1 \\ \theta_1 \end{bmatrix} = \begin{bmatrix} \cos\psi & -\sin\psi & 0 \\ \sin\psi & \cos\psi & 0 \\ 0 & 0 & 1 \end{bmatrix} \begin{bmatrix} \delta x_1 \\ \delta x_2 \\ \theta_1 \end{bmatrix} \qquad (120\text{-B})$$

$$[\Delta_1] = [T] \cdot [d_1]$$

Similarly it can be shown that

$$[F_2] = [T] \cdot [f_2] \qquad (121\text{-A})$$

$$[\Delta_2] = [T] \cdot [d_2] \qquad (121\text{-B})$$

If we substitute equation (117) into equation (120-A)

$$[F_1] = [T] \cdot ([k_{11}\ [d_1] + [k_{12}][d_2]) \qquad (122)$$

The following relations can also be written from equations (120-B) and (121-B)

$$[d_1] = [T]^{-1}\ [\Delta_1] \qquad (123)$$

$$[d_2] = [T]^{-1}\ [\Delta_2] \qquad (123\text{-A})$$

When equations (123) and (123-A) are substituted into equation (122) the following relation is obtained

$$[F_1] = [T][k_{11}][T]^{-1}\ [\Delta_1] + [T][k_{12}][T]^{-1}\ [\Delta_2] \qquad (124)$$

or

$$[F_1] = [S_{11}][\Delta_1] + [S_{12}][\Delta_2] \qquad (124\text{-A})$$

Similarly

$$[F_2] = [S_{21}][\Delta_1] + [S_{22}][\Delta_2] \qquad (124\text{-B})$$

where $[S_{11}] = [T][k_{11}][T^{-1}]$, $[S_{12}] = [T][k_{12}][T^{-1}]$

$[S_{21}] = [T][k_{21}][T^{-1}]$, $[S_{22}] = [T][k_{22}][T^{-1}]$

Equations (135-A) and (135-B) are the stiffness equations for any individual member of the frame system with respect to the overall axes.

After having obtained stiffness equations for a member of the frame system, the procedure which was followed in the FRAN2 computer program to

obtain the ends' reactions as well as the joint forces of the frame systems can be summarised as follows:

1. An overall axes system for the frame is chosen and ends 1 and 2 for all members are specified.
2. The frame system is replaced by two cases. In case 1, joints of loaded members are fixed and end reactions are calculated. In case 2, the response of the system to fixed end moments and joint loads is calculated using the stiffness method as follows:

2.1 Stiffness matrices are formed for each individual member.

2.2 At each joint the equilibrium equation is written taking into account external and internal loads. This process is repeated for all joints.

2.3 Internal force values are replaced in the equilibrium equations, then all the external load values and known displacements are inserted. In this way a set of equations can be obtained in which the joints' displacements are unknown.

2.4 The appropriate equations are solved to obtain displacement values.

2.5 Displacement values are inserted into the stiffness equations to obtain the forces and displacement values with respect to overall axes for each member.

2.6 Using the transformation matrices the forces are also obtained at the member reference system.

3. Each members' end forces are obtained from case 2, and superposition of case 1 and case 2 gives the structural response values of loaded members throughout their spans.

In the following, the application of the stiffness method will be illustrated by calculating the member forces of the frame shown in Fig. 36.

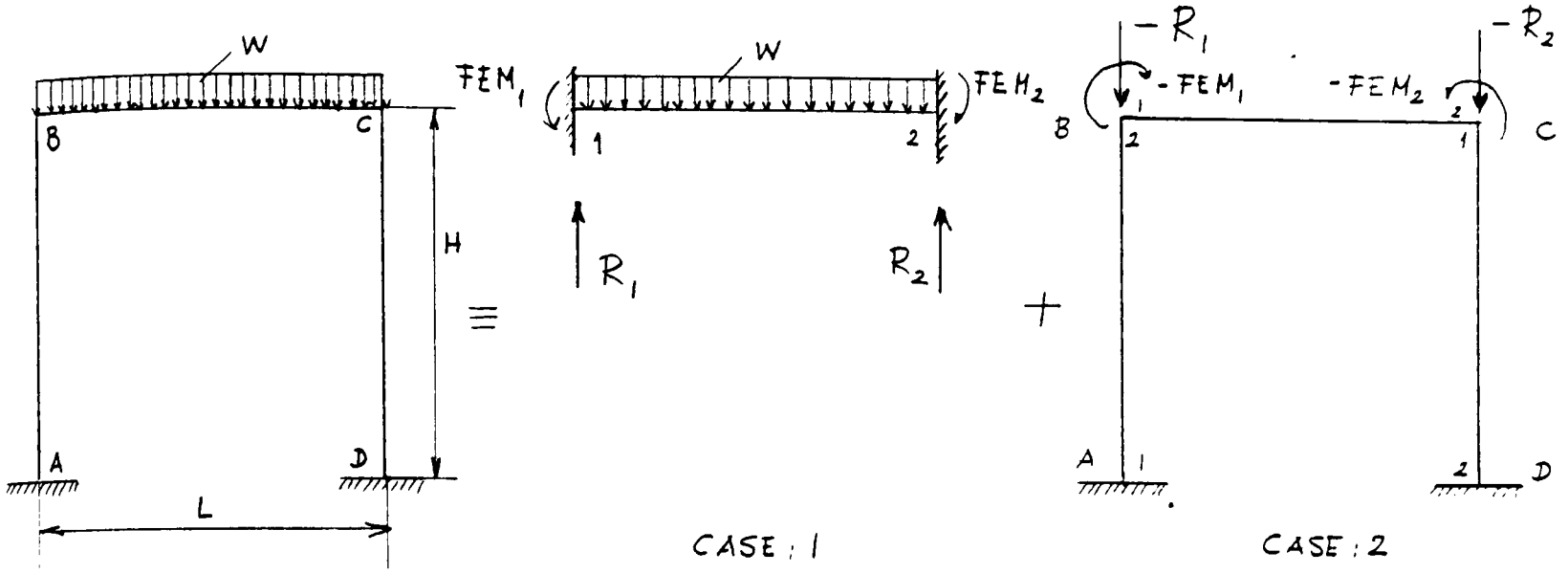

Fig. 36

Case 1: Fixed end moments for ends 1 and 2 will be

$$FEM_{1,B} = -FEM_{2,B} = \frac{WL^2}{12} \tag{125}$$

Similarly, vertical end reactions take the following form

$$R_1 = R_2 = \frac{WL}{2} \tag{125-A}$$

Case 2: There are two internal forces and one external force at both points B and C. If we write the equilibrium equations at these points

$$[L_B] = [F_{2,B}] + [F_{1,B}] \tag{126}$$

$$[L_C] = [F_{2,C}] + [F_{1,C}] \tag{126-A}$$

The following force equations can be written using equations (135-A) and (135-B)

$$[F_{2,B}] = [S_{21,AB}][\Delta_A] + [S_{22,AB}][\Delta_B] \tag{127}$$

$$[F_{1,B}] = [S_{11,B}][\Delta_B] + [S_{12,BC}][\Delta_C] \tag{127-A}$$

$$[F_{2,C}] = [S_{21,BC}][\Delta_B] + [S_{22,BC}][\Delta_C] \tag{128-B}$$

$$[F_{1,C}] = [S_{11,CD}][\Delta_C] + [S_{12,CD}][\Delta_D] \tag{128-C}$$

Since ends A and B are fixed

$$[\Delta_A] = 0 \tag{129}$$

$$[\Delta_D] = 0 \tag{129-A}$$

When equations (128 - 128-A) are substituted into equation (127) and equations (128-B - 128-C) are substituted into equation (127-A) and also making use of equations (129) and (129-A), the following simultaneous equations are obtained

$$[L_B] = [S_{22,AB}] \cdot [\Delta_B] + [S_{11,BC}] \cdot [\Delta_B] + [S_{12,BC}][\Delta_C] \tag{130}$$

$$[L_C] = [S_{21,BC}] \cdot [\Delta_B] + [S_{22,BC}] \cdot [\Delta_C] + [S_{11,CD}][\Delta_C] \tag{130-A}$$

In equations (130) and (130-A) the external loads $[L_B]$ and $[L_C]$ are known, as are the $[S_{ij}]$ matrices. The only unknowns Δ_B and Δ_C can be obtained from these two simultaneous equations as follows

$$\begin{bmatrix} [\Delta_B] \\ [\Delta_C] \end{bmatrix} = \begin{bmatrix} [S_{22,AB}] + [S_{11,BC}] & [S_{12,BC}] \\ [S_{21,BC}] & [S_{22,BC}] + [S_{11,CD}] \end{bmatrix}^{-1} \begin{bmatrix} [L_B] \\ [L_C] \end{bmatrix} \tag{131}$$

The forces at the ends of the members with respect to the local axes are as follows

Member AB, End 1: $[EF_1] = [T_{AB}]^{-1} [S_{12,AB}][\Delta_B]$ (132-A)

End 2: $[EF_2] = [T_{AB}]^{-1} [S_{22,AB}][\Delta_B]$ (132-B)

Member BC, End 1: $[EF_1] = [T_{BC}]^{-1} \{[S_{11,BC}][\Delta_B] + [S_{12,BC}][\Delta_C]\}$ (132-C)

End 2: $[EF_2] = [T_{BC}]^{-1} \{[S_{21,BC}][\Delta_B] + [S_{22,BC}][\Delta_C]\}$ (132-D)

Member CD, End 1: $[EF_1] = [T_{CD}]^{-1} \{[S_{11}, _{CD}][\Delta_C]\}$ (132-E)

End 2: $[EF_2] = [T_{CD}]^{-1} [S_{21}, _{CD}][\Delta_C]$ (132-F)

2.1.2 Example of the use of FRAN2. The two-dimensional frame analysis program FRAN2 is used with the two subsidiary programs DEFRAME and DELOAD.

DEFRAME was written to store the details of the frame geometry in a file. Similarly, DELOAD stores a particular loading case in a file so that the effect of changing the structure's geometry and boundary conditions, while retaining the original loading case, can easily be studied.

The use of DEFRAME, DELOAD and FRAN2 is illustrated with the following example.

In the example, the member forces of the frame shown in Fig. 37 will be determined by means of computer input and output.

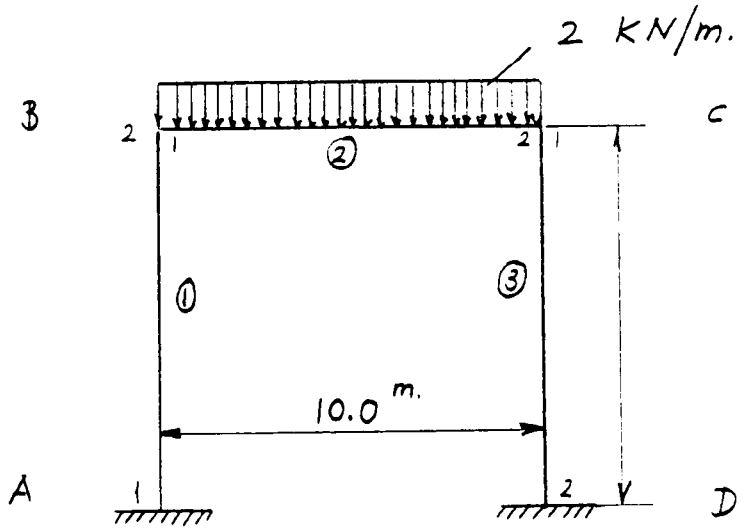

Fig. 37

Geometrical Properties of the frame shown in Fig. 37:

Member No.	Area of Cross-Section (mm^2)	Second Moment of Area (mm^4)
1	30×10^3	150×10^7
2	30×10^3	150×10^7
3	30×10^3	150×10^7

Young's Modulus = 210 KN/mm^2.

```
>RUN DK0:DEFRAME
ENTER NAME FOR FRAME DEFINITION FILE : BEAM3.FRM


 DO YOU WANT FULL DIAGNOSTICS ? (Y/N) * Y
 NUMBER OF MEMBERS IN FRAME (MAX=40) * 3
 NUMBER OF SUPPORTS (MAX=TOT MEMBERS - 1) * 2
 SUPPORT NUMBER    1 IS NODE NO * 1
 SUPPORT NUMBER    2 IS NODE NO * 4
DATA ENTERED SO FAR :

FULL DIAGNOSTICS    :   Y
TOTAL MEMBERS       :    3
TOTAL SUPPORTS      :    2
SUPPORT NODES       :    1   4
DO YOU WISH TO RETYPE ANY DATA ? (Y/N) : N
 NUMBER OF SECTION TYPES * 1

 SECTION TYPE    1
      AREA * 30000.0
      I-VALUE *150.0E07
DATA ENTERED :

NUMBER OF SECTION TYPES  :    1

   I       AREA          I-VALUE


   1   0.300000E+05   0.150000E+10
DO YOU WISH TO RETYPE ANY SECTION DATA ? * N
```

```
***** MEMBER NUMBER    1 *****
   START NODE NUMBER (MAX = TOT MEMBERS) * 1
IS THE NODE A PIN ? : N
IS THE NODE FIXED IN X,Y,M ? (3*A1) : YYY
     END NODE NUMBER (MAX = TOT MEMBERS) * 2
IS THE NODE A PIN ? : N
 X PROJECTION FOR CURRENT MEMBER * 0.0
 Y PROJECTION FOR CURRENT MEMBER * 20.0
 SECTION TYPE OF CURRENT MEMBER * 1
DATA READ FOR CURRENT MEMBER :


   START NODE NUMBER =    1
  FIXED IN X,Y,M ? :      Y  Y  Y
     END NODE NUMBER =    2
XPROJECTION =   0.000000E+00   Y PROJECTION =   0.200000E+02
SECTION TYPE =    1

DO YOU WISH TO RETYPE ANY DATA ? (Y/N) * N



***** MEMBER NUMBER    2 *****
   START NODE NUMBER (MAX = TOT MEMBERS) * 2
IS THE NODE A PIN ? : N
     END NODE NUMBER (MAX = TOT MEMBERS) * 3
IS THE NODE A PIN ? : N
 X PROJECTION FOR CURRENT MEMBER * 10.0
 Y PROJECTION FOR CURRENT MEMBER * 0.0
 SECTION TYPE OF CURRENT MEMBER * 1
DATA READ FOR CURRENT MEMBER :
```

```
   START NODE NUMBER =     2
     END NODE NUMBER =     3
XPROJECTION =    0.100000E+02    Y PROJECTION =    0.000000E+00
SECTION TYPE =     1

DO YOU WISH TO RETYPE ANY DATA ? (Y/N) * N



***** MEMBER NUMBER     3 *****
   START NODE NUMBER (MAX = TOT MEMBERS) * 3
IS THE NODE A PIN ? : N
     END NODE NUMBER (MAX = TOT MEMBERS) * 4
IS THE NODE A PIN ? : N
IS THE NODE FIXED IN X,Y,M ? (3*A1) : YYY
 X PROJECTION FOR CURRENT MEMBER * 0.0
 Y PROJECTION FOR CURRENT MEMBER * -20.0
 SECTION TYPE OF CURRENT MEMBER * 1
DATA READ FOR CURRENT MEMBER :


   START NODE NUMBER =     3
     END NODE NUMBER =     4
  FIXED IN X,Y,M ? :       Y   Y   Y
XPROJECTION =    0.000000E+00    Y PROJECTION =   -0.200000E+02
SECTION TYPE =     1

DO YOU WISH TO RETYPE ANY DATA ? (Y/N) * N
```

```
 YOUNG'S MODULUS * 210.0
IS VALUE    0.210000E+03 O.K. ? (Y/N) * Y
TT6  --  STOP
>
```

```
>RUN DKØ:DELOAD
ENTER LOADING CASE FILENAME : BEAM3.LOA
LOADED MEMBER NO * 2
NUMBER OF POINTS ON SPAN WHERE YOU WANT MOMENT AND SHEAR * 3
POINT NUMBER   1 FRACTION OF SPAN * Ø.Ø
POINT NUMBER   2 FRACTION OF SPAN * Ø.5
POINT NUMBER   3 FRACTION OF SPAN * 1.Ø
VALUE OF JOINT LOAD (ZERO ENDS LIST) * Ø.Ø
VALUE OF JOINT MOMENT (ZERO ENDS LIST) * Ø.Ø
VALUE OF POINT LOAD (ZERO ENDS LIST) * Ø.Ø
VALUE OF RECTANGULAR LOAD (ZERO ENDS LIST) * -2.Ø
LOAD DIRECTION- V,H,N- RET FOR DIRN COS'S * V
START OF LOAD - FRACTION OF SPAN * Ø.Ø
END OF LOAD - FRACTION OF SPAN * 1.Ø
VALUE OF RECTANGULAR LOAD (ZERO ENDS LIST) * Ø.Ø
VALUE OF TRIANGULAR LOAD (ZERO ENDS LIST) * Ø.Ø
MOMENT ON SPAN (CLOCKWISE +VE, ZERO ENDS LOADS ) * Ø.Ø
ARE THERE ANY MORE LOADED MEMBERS ? (Y/N) * N
TT6  --  STOP
>
```

```
>RUN DKØ:FRAN2
 LISTING DEVICE : BEAM3.RES
IS THERE A FRAME DEFINITION FILE ? (Y/N) * Y
ENTER NAME OF FRAME DEFINITION FILE : BEAM3.FRM
IS THERE A LOADING CASE FILE ? (Y/N) * Y
ENTER LOADING CASE FILENAME : BEAM3.LOA
 SAME FRAME WITH NEW LOAD CASE ? (Y/N) * N
TT6  --  STOP
>PIP BEAM3.RES/SP
>
```

FRAME ANALYSIS PROGRAM FRAN2

```
MEMBER     1 FREEDOMS     0    0    0    1    2    3

MEMBER     2 FREEDOMS     1    2    3    4    5    6

MEMBER     3 FREEDOMS     4    5    6    0    0    0

TOTAL NUMBER OF FREEDOMS =     6
NUMBER OF MEMBERS        =     3
YOUNG'S MODULUS          =    0.2100E+03

MEMBER   XPROJ      YPROJ       AREA         I

   1      0.000     20.000      30000.000    0.15000E+10
   2     10.000      0.000      30000.000    0.15000E+10
   3      0.000    -20.000      30000.000    0.15000E+10

    ***** START OF LOADING CASE *****

 ******** MEMBER NUMBER ********   2
INTENSITY OF DISTRIBUTED LOAD =        -2.000
W COMPONENT IN X DIRN =      0.000000
W COMPONENT IN Y DIRN =     -2.000000
LOAD STARTS AT         0.000000 ENDS AT        10.000000
LOAD INTENSITY        -2.000000
END  1
IN LOCAL COORDS
AXIAL FORCE          0.000000
REACTION            10.000000
MOMENT             -16.666666

 IN GLOBAL COORDS
FORCE IN X DIRECTION =          0.000000
FORCE IN Y DIRECTION =         10.000000
END  2
IN LOCAL COORDS
AXIAL FORCE          0.000000
REACTION            10.000000
MOMENT              16.666666

 IN GLOBAL COORDS
FORCE IN X DIRECTION =          0.000000
FORCE IN Y DIRECTION =         10.000000
TOTAL HOLDING FORCES
                      X                Y                M

  END    1            0.000           10.000       -16666.666
  END    2            0.000           10.000        16666.666

FREEDOM   ACT FORCES  CALC FORCES (BEFORE CORRECTS)
   1         0.000000        -0.000006
   2       -10.000000        -9.999999
   3     16666.666016     16666.666016
   4         0.000000         0.000006
   5       -10.000000        -9.999999
   6    -16666.666016    -16666.667769
```

DEFLECTIONS		X	Y	ROTATION
MEMBER 1	- END 1	0.000000E+00	0.000000E+00	0.000000E+00
	- END 2	0.495964E-03	-0.317460E-01	0.132294E-03
MEMBER 2	- END 1	0.495964E-03	-0.317460E-01	0.132294E-03
	- END 2	-0.495867E-03	-0.317460E-01	-0.132294E-03
MEMBER 3	- END 1	-0.495867E-03	-0.317460E-01	-0.132294E-03
	- END 2	0.000000E+00	0.000000E+00	0.000000E+00

FREEDOM	ACT FORCES	CALC FORCES (AFTER CORRECTS)
1	0.000000	0.000000
2	-10.000000	-10.000002
3	16666.666016	16666.667969
4	0.000000	0.000000
5	-10.000000	-10.000001
6	-16666.666016	-16666.664062

MEMBER FORCES
AXIAL TENS +VE
MOM SHEAR +VE IF +VE V WRT MEMBER DIRECTION U

	START	END
MEMBER NUMBER	1	
AXIAL	-10.000001	-10.000001
MOMENT	-4.164909	8.332161
SHEAR	0.624853	0.624853
MEMBER NUMBER	2	
AXIAL	-0.624854	-0.624854
MOMENT	8.332160	8.332163
SHEAR	-10.000000	10.000000

AT SPAN LENGTH 0.000000 MOMENT = 0.8332160E+01 SHEAR = -0.1000000E+02

AT SPAN LENGTH 5.000000 MOMENT = -0.1666784E+02 SHEAR = 0.0000000E+00

AT SPAN LENGTH 10.000000 MOMENT = 0.8332163E+01 SHEAR = 0.1000000E+02

MEMBER NUMBER	3	
AXIAL	-10.000001	-10.000001
MOMENT	8.332161	-4.164909
SHEAR	-0.624853	-0.624853

2.2 Calculation of Structural Response Values for Twin Circular Hulled Semi-Submersible Model with Bracings

The twin circular hulled semi-submersible model whose space frame representation is shown in Fig. 38, will be analysed in order to obtain the structural response values using FRAN2 with the procedure described in the following.

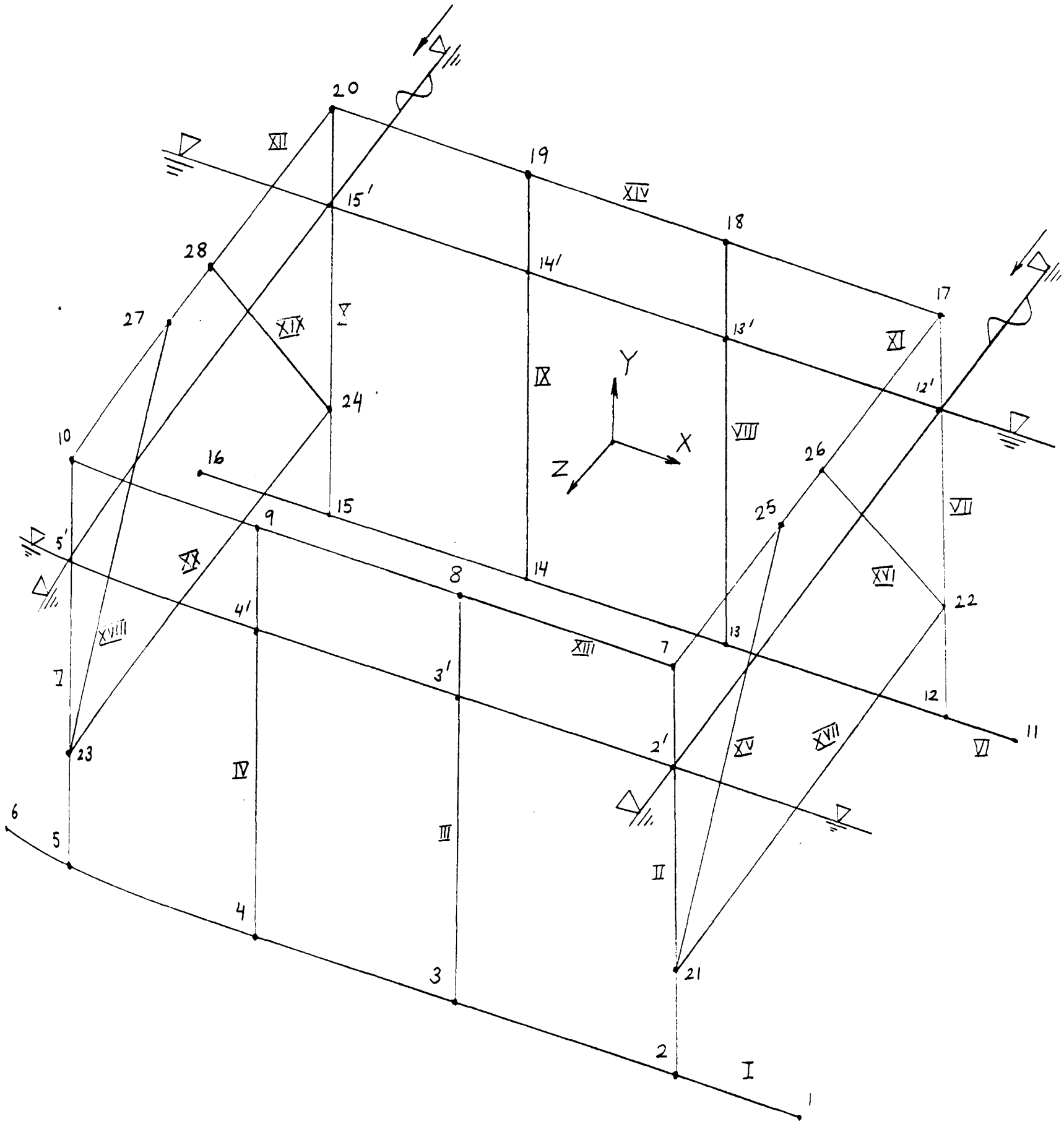

Fig. 38

When the platform is considered to be restrained in beam seas, the structural loading may be represented as the superposition of the following cases in order to analyse a three-dimensional structure with a series of two-dimensional frame representations.

Case (a):

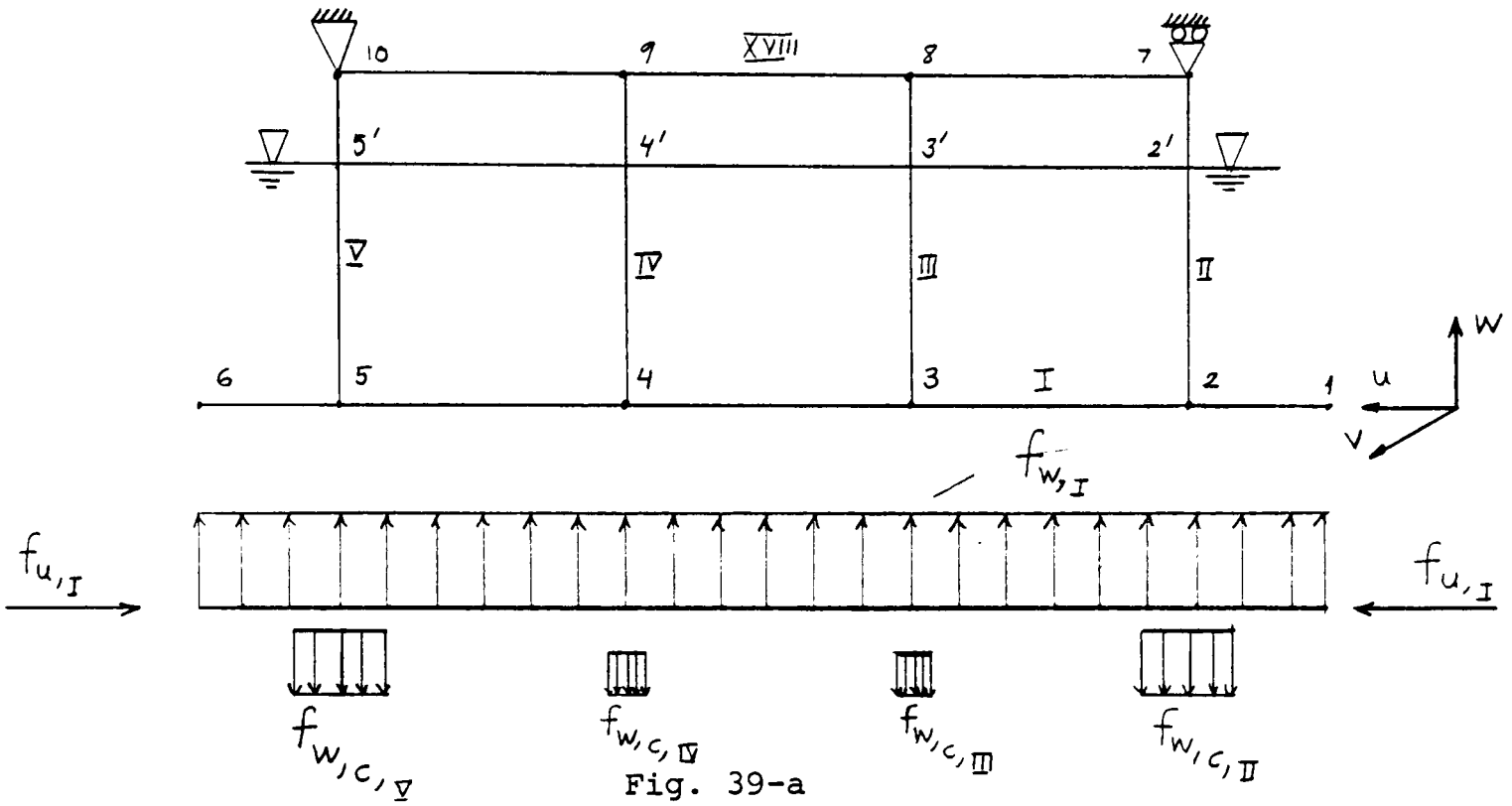

Fig. 39-a

Case (b):

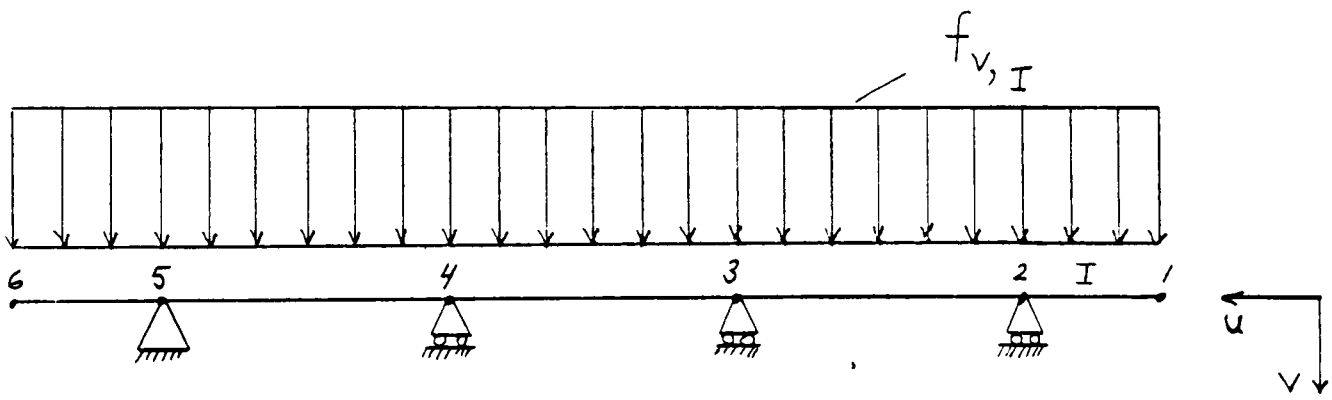

Fig. 39-b

Case (c):

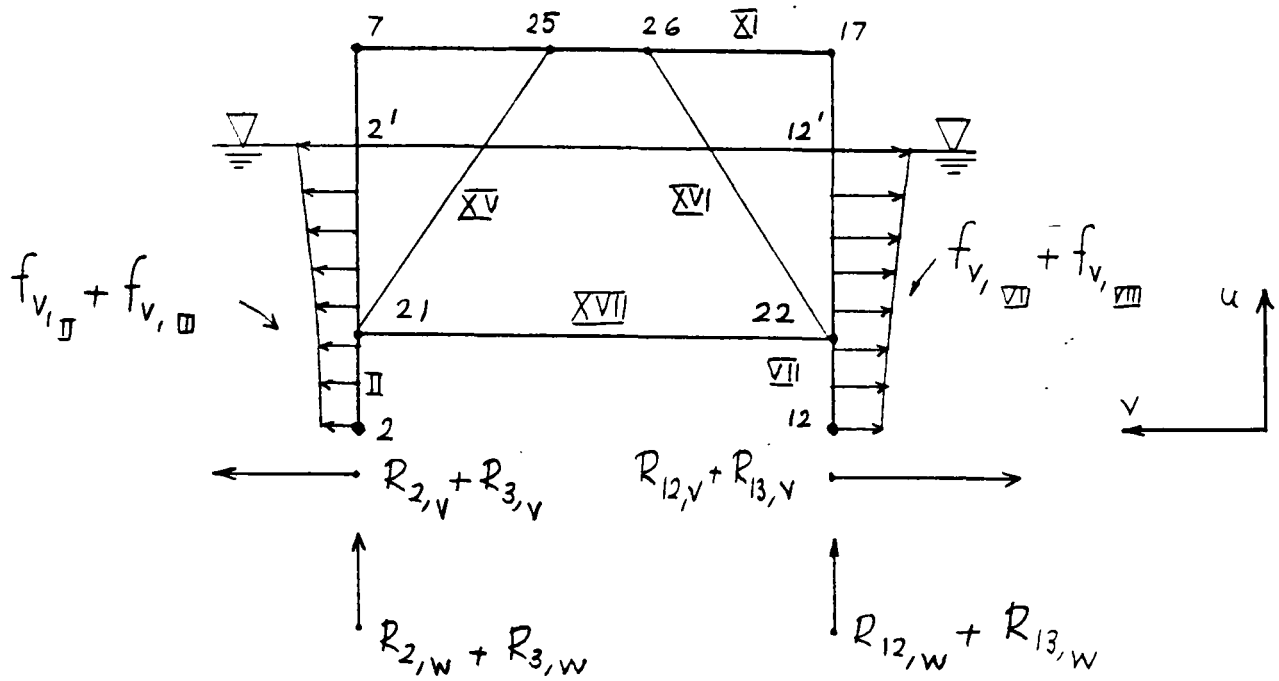

Fig. 39-c

Case (a): It is assumed that the hull (Member I) columns (Members II,III, IV,V) and longitudinal deck girder (Member XIII) can be isolated from the structure and loaded in u-w plane with wave loading (Fig. 39-a). The frame is constrained from nodes 7,10 with simple supports. Structural analysis under this loading yields axial forces on the hull, on the columns and on the longitudinal deck girder, as well as shear forces and bending moment values for the longitudinal deck girder. The analysis also yields shear forces and bending moment values for the hull in u-w plane. A similar analysis is carried out for the right hand side of the structure, i.e. Members VI,VII,VIII,IX and X.

Case (b): The hull is constrained with simple supports (which are assumed to be provided by the extended column ends in the hull) and loaded in the u-v plane with wave loading (Fig. 39-b). This case yields the shear force and bending moment values in u-v plane. The total shear force and bending moment values on the hull will be the vectorial summation of the two groups of results obtained in Cases (a) and (b). The same procedure is repeated for the second hull (Member VI).

Case (c): The loading case shown in Fig. 39-c was chosen to determine the structural response values on the transverse deck girder as well as on the horizontal and inclined bracings. $R_{i,_W}$ and $R_{i,_V}$ values are column reactions obtained from Cases (a) and (b) respectively.

The structural response analysis of the frame shown in Fig. 39-c is carried out by breaking the wave loading down as symmetrical and asymmetrical forces and choosing the constraints of the structure as illustrated in Fig. 39-c-1.

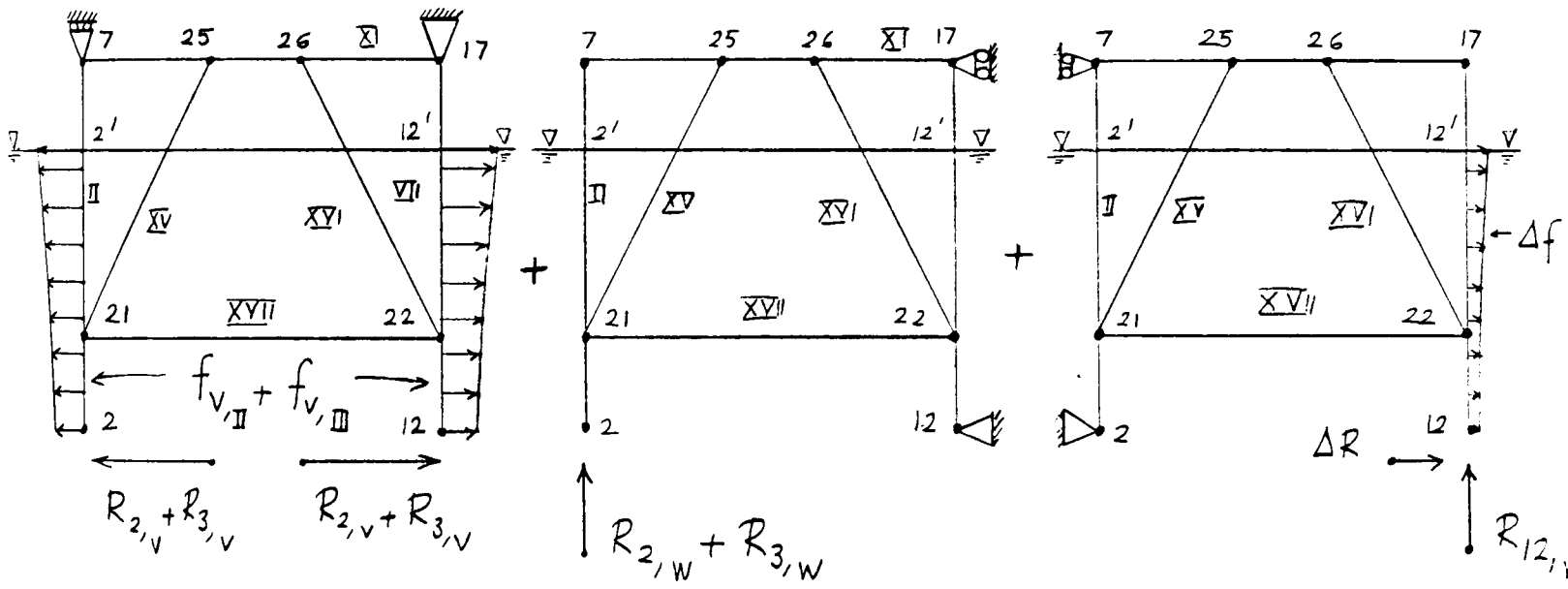

$$\Delta R = (R_{12,_V} + R_{13,_V}) - (R_{2,_V} + R_{3,_V})$$

$$\Delta f = (f_{V,VII} + f_{V,VIII}) - (f_{V,II} + f_{V,III})$$

Fig. 39-c-1

Finally, structural response values for columns can be determined from the following loading cases as illustrated in Fig. 39-d and 39-e.

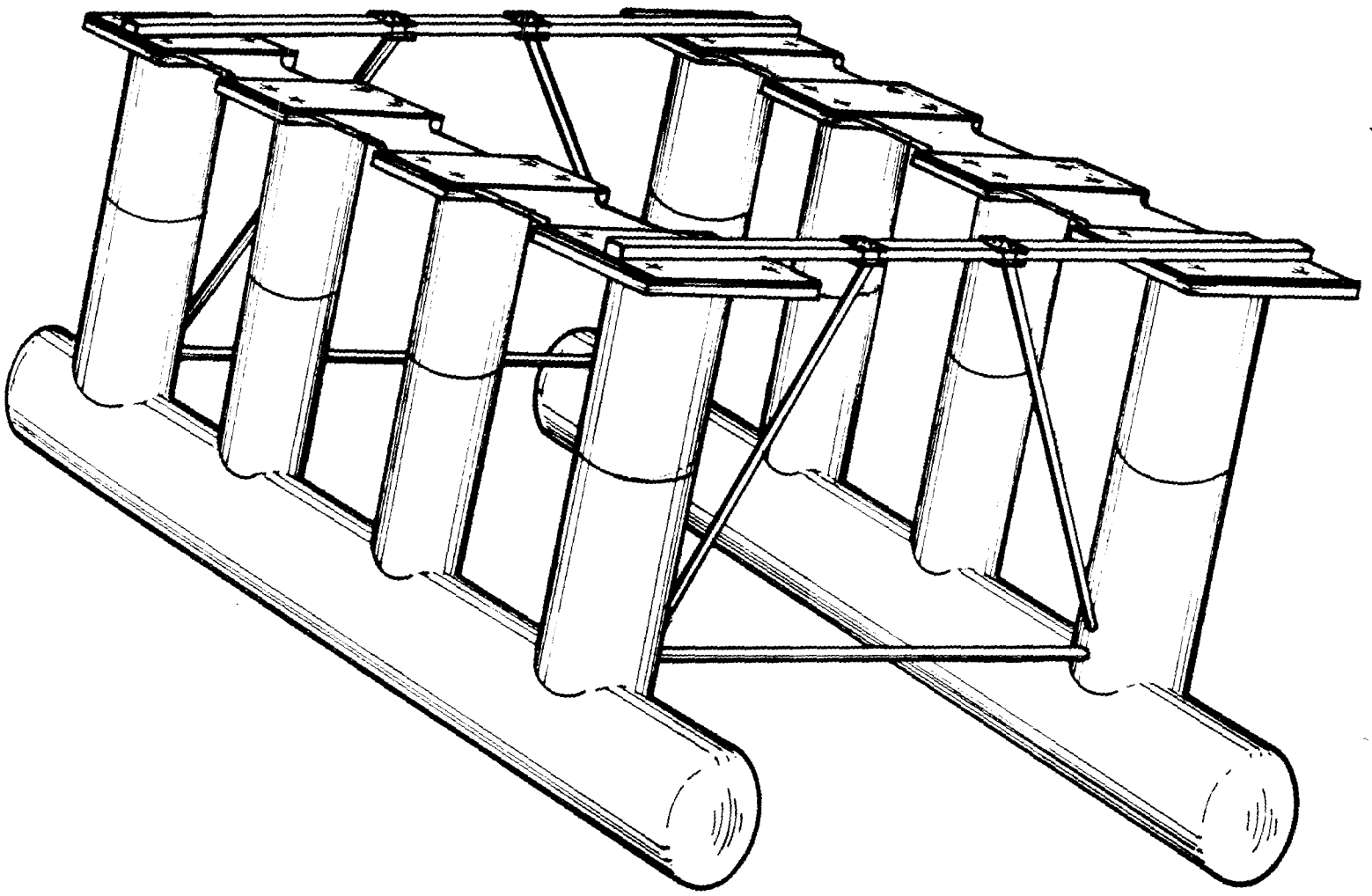

GENERAL VIEW OF THE SEMI-SUBMERSIBLE MODEL WITH BRACING ARRANGEMENTS

Fig. 40

Case (d):

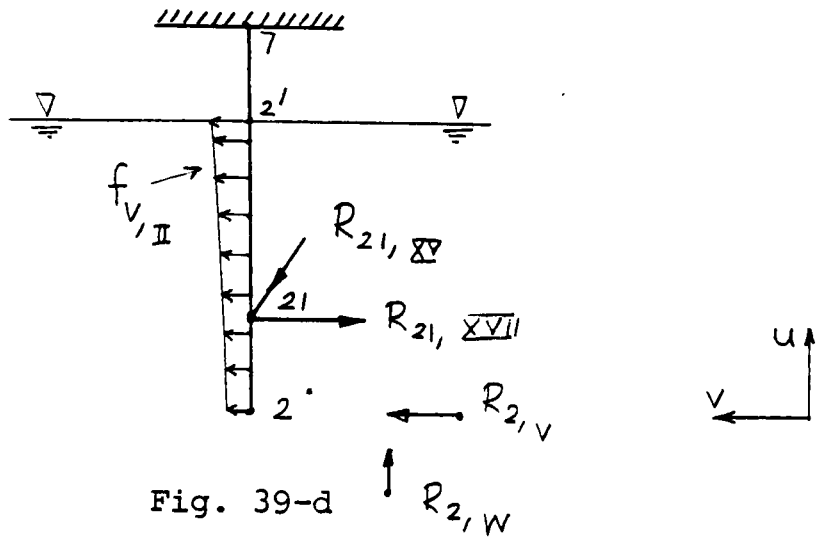

Fig. 39-d

Case (e):

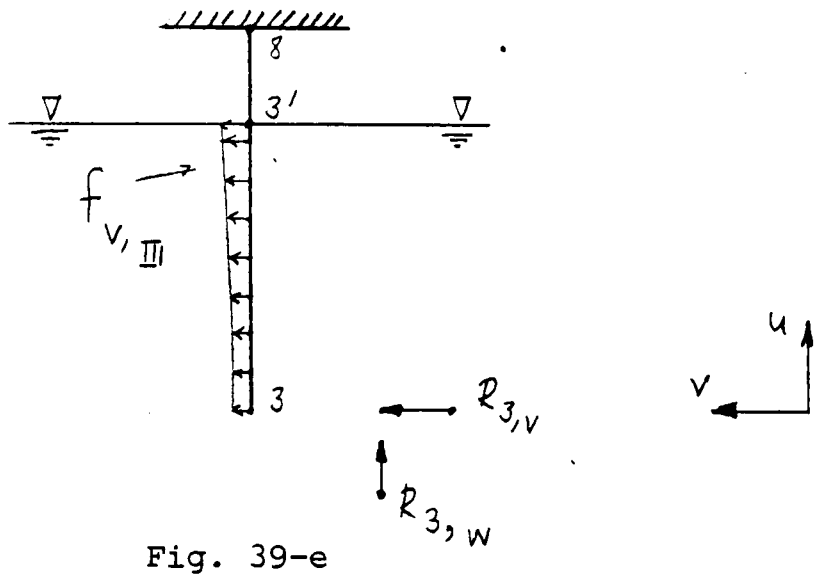

Fig. 39-e

Structural response values for Members III - V and VII - X can be obtained with similar representations.

Maximum shear force and bending values on the columns will be the vectorial summation of the two groups of results obtained in Cases (a), (d) and (e).

The analysis procedure summarised above was applied to the twin circular hull semi-submersible model shown in Fig. 40. (Structural details of the model are given in Appendix 1 and frame representation of the model shown in Fig. 38.) The bending moment values at the

centre of the transverse deck beam were calculated and results are shown in Fig. 41. The results of the experimental measurements for the same model were also plotted in the same figure. The theoretical predictions and the experimental measurements of axial forces on an inclined bracing of the same structure are shown in Fig. 42.

Fig. 41 and Fig. 42 show that the theoretical predictions compare reasonably well with the experimental predictions. However, as was the case where the model had no bracings, the theoretical predictions for the restrained mathematical model should have been found higher than the measured values of the free floating model. This may also indicate that the inertia coefficients used in the predictions should be higher than the estimated values. The increase in the wave inertia coefficients may be due to a hull-column interference effect which has not been studied in this research. The study reported in reference [19] also shows that measured wave inertia coefficients in sway mode for a semi-submersible model which was held fixed in waves are 20 - 50% higher than the calculated wave inertia coefficients.

The nature of the increase may be studied more in detail by measuring the wave forces on the elements of the structure individually and on the complete assembly of the structure.

2.3 Calculation of Structural Response Values for Full Scale Twin Circular Hull Semi-Submersible

The structural response calculation procedure for a restrained mathematical model summarised in this chapter was applied for a twin circular hull semi-submersible design with bracing arrangements. The geometrical and the structural details of the semi-submersible are given in Fig. 43 and the space frame representation of the structure is shown in Fig. 44.

Structural Response Predictions For Twin-Circular Hull Semi-Submersible Model With Bracing Arrangements (Bending Moment On The Deck)

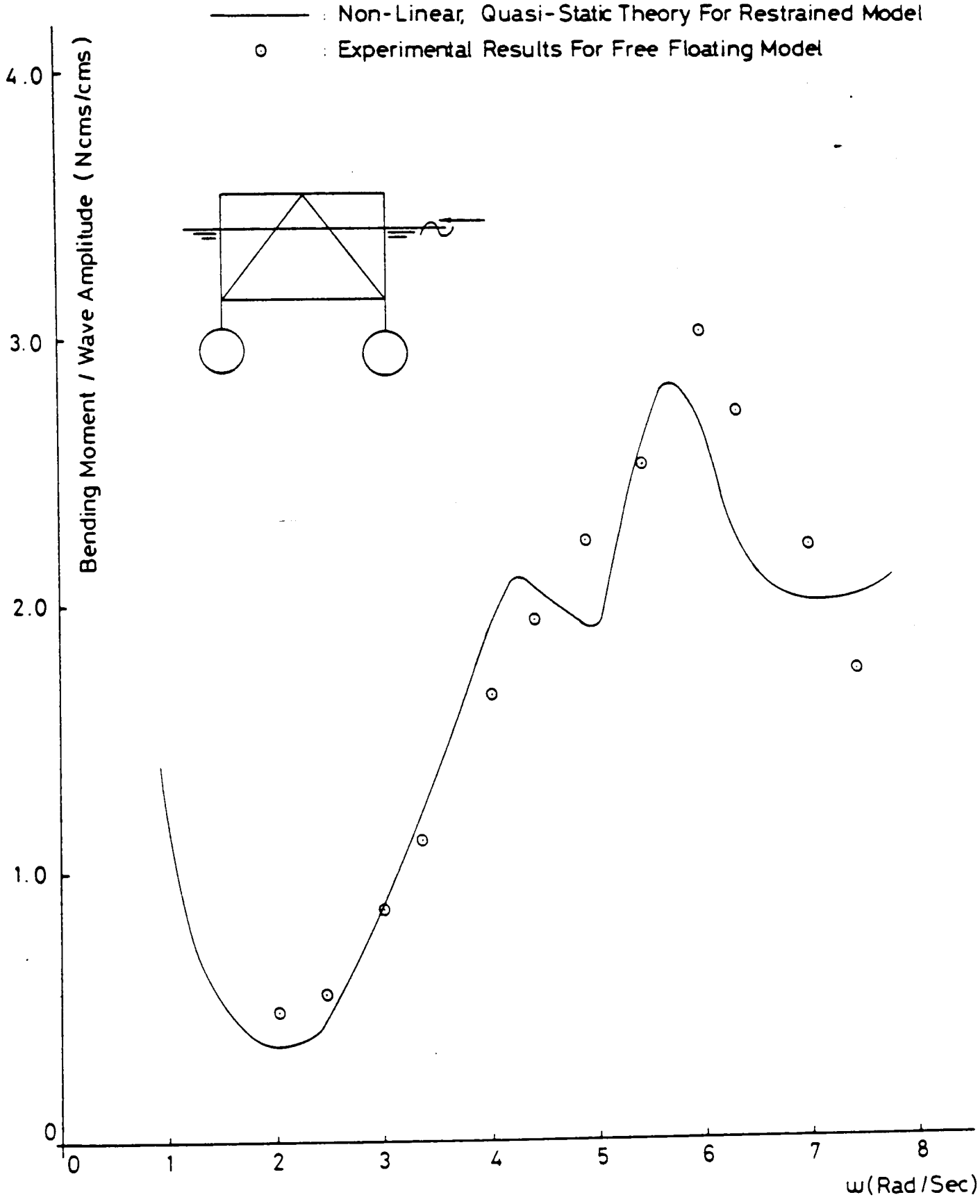

Fig. 41

Structural Response Predictions For Twin-Circular Hull Semi-Submersible Model With Bracing Arrangements (Axial Force On The Inclined Bracing A.)

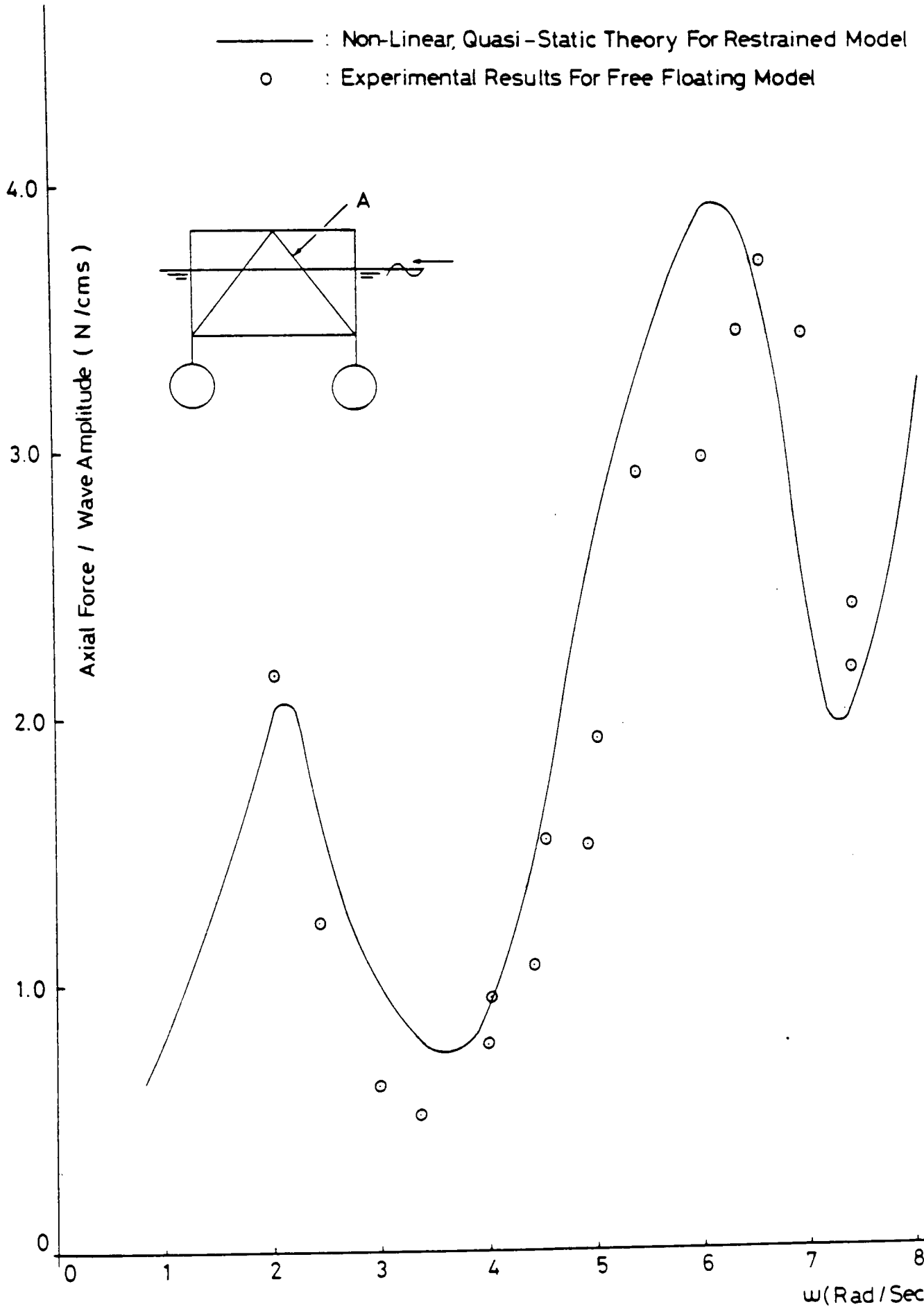

Fig. 42

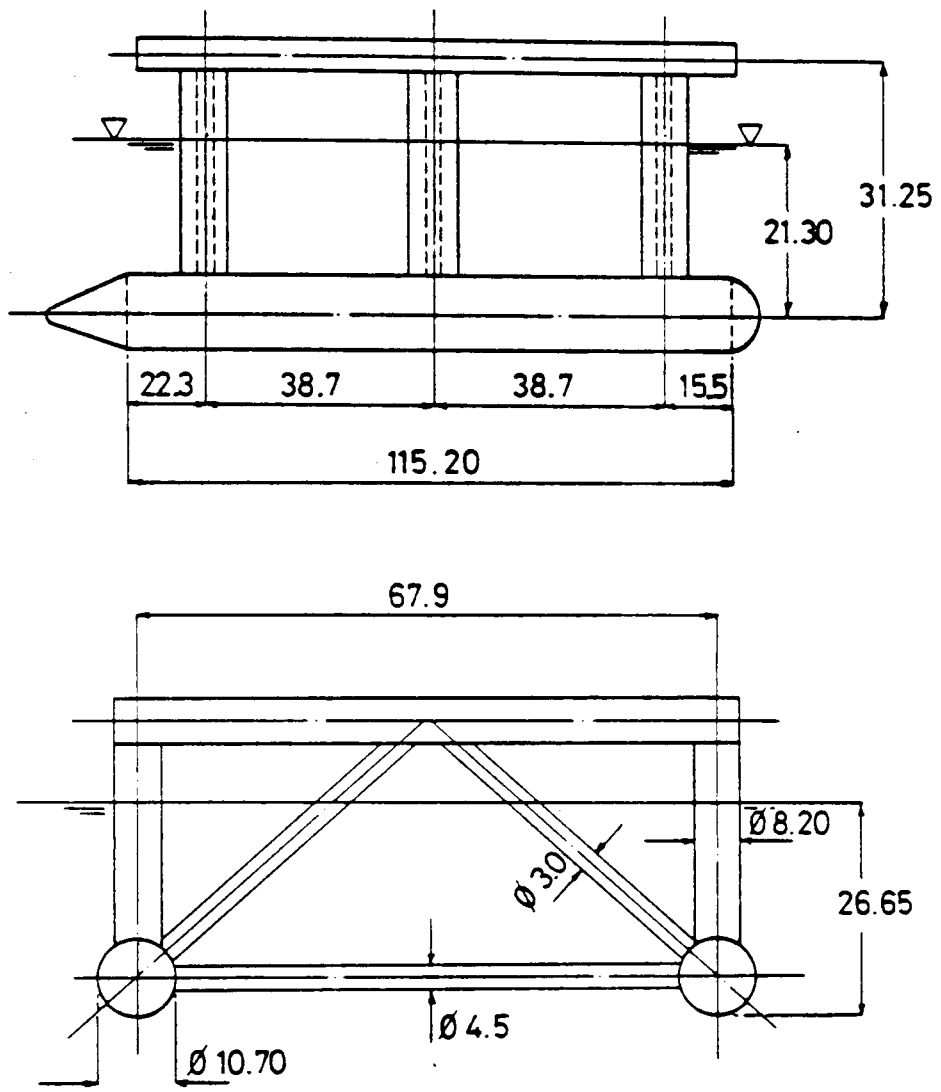

Element	Cross Sectional Area (m^2)	Second Moment Of Area (m^4)
Hull	1.8260	26.132
Vertical Columns	1.5359	12.288
Inclined Bracings	0.22081	0.24841
Long^T & Transverse Deck Girders	1.7958	7.7123

Displacement Of Structure Δ = 252800 kN

Fig. 43

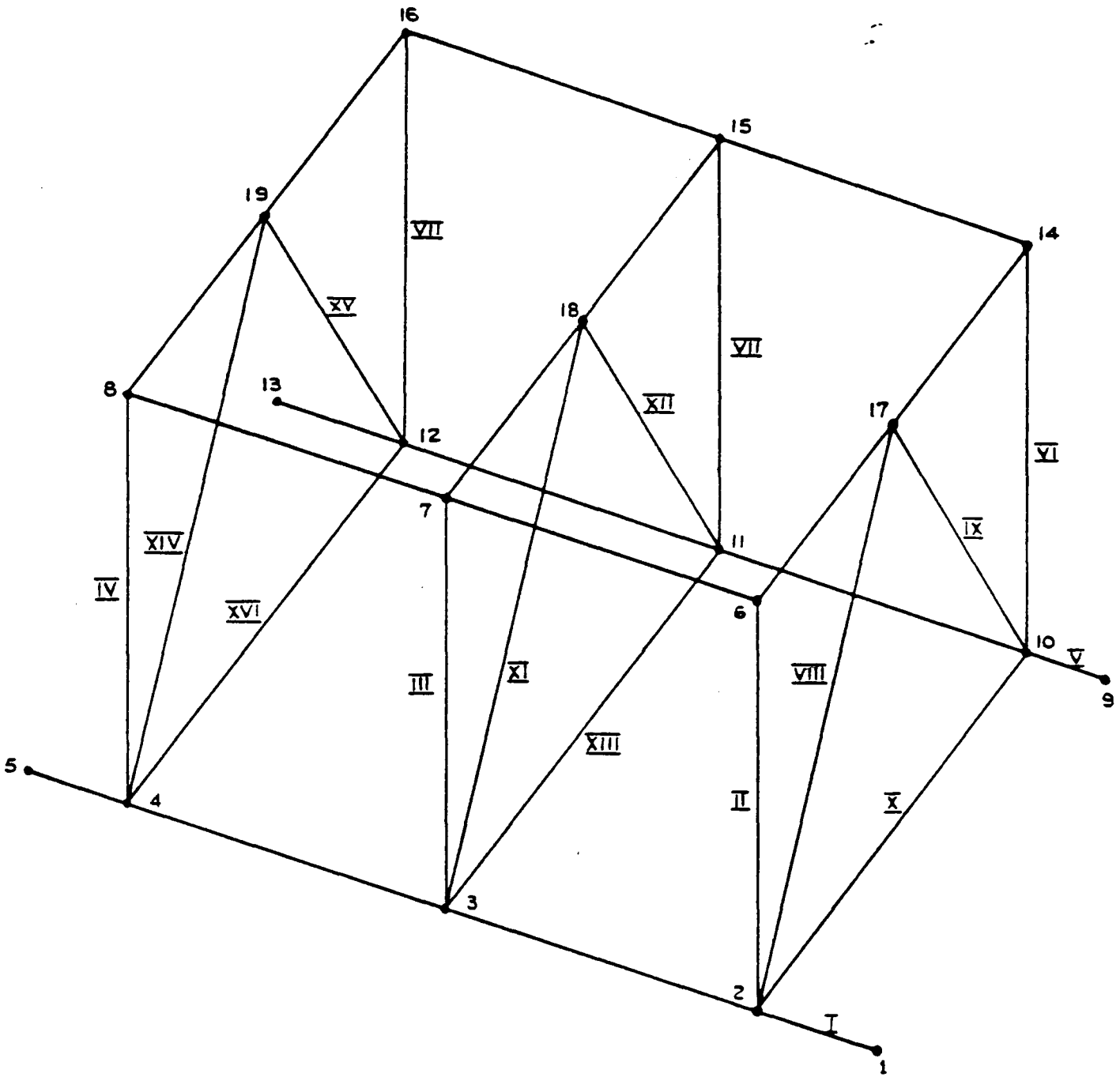

SPACE FRAME REPRESENTATION OF FULL SCALE TWIN CIRCULAR HULLED SEMI-SUBMERSIBE

Fig. 44

The structural response calculations were carried out for the head and beam sea conditions under the non-linear wave loading. Results have been presented to indicate maximum response values on each structural element versus excitation frequency.

Comparisons between Figs. [(45-a) - (45-c)] and [(46-a) - (46-c)] indicate that since the maximum structural response values on the hull and on the longitudinal deck girder occurred in beam seas, it may be suggested that the beam seas case should dictate the structural design of longitudinal strength members. Comparisons of structural response values on the columns [Figs. (45-a) - (45-c), (46-a) - (46-c) and (47-c)] show that beam seas should also dictate the structural design of columns.

Figures [(47-a) - (47-c)], [(48-a) - (48-e)] and [(49-a) - (49-c)] show the structural response values of the transverse strength members. These figures show that the effect of bracing elements on the structural response of the transverse deck girder is considerable. The addition of the horizontal bracing also significantly reduces the structural response values on the columns and on the inclined bracing elements.

If lower horizontal bracings had existed between legs D and C as well as on C and B on the structure shown in Fig. 28, the Alexander Kielland accident, due to failure of the lower horizontal bracing between legs E and D would possibly have been avoided.

The result presented in Figs. (45) - (47) can be readily incorporated into the spectral analysis to determine the statistical values for a detailed structural analysis.

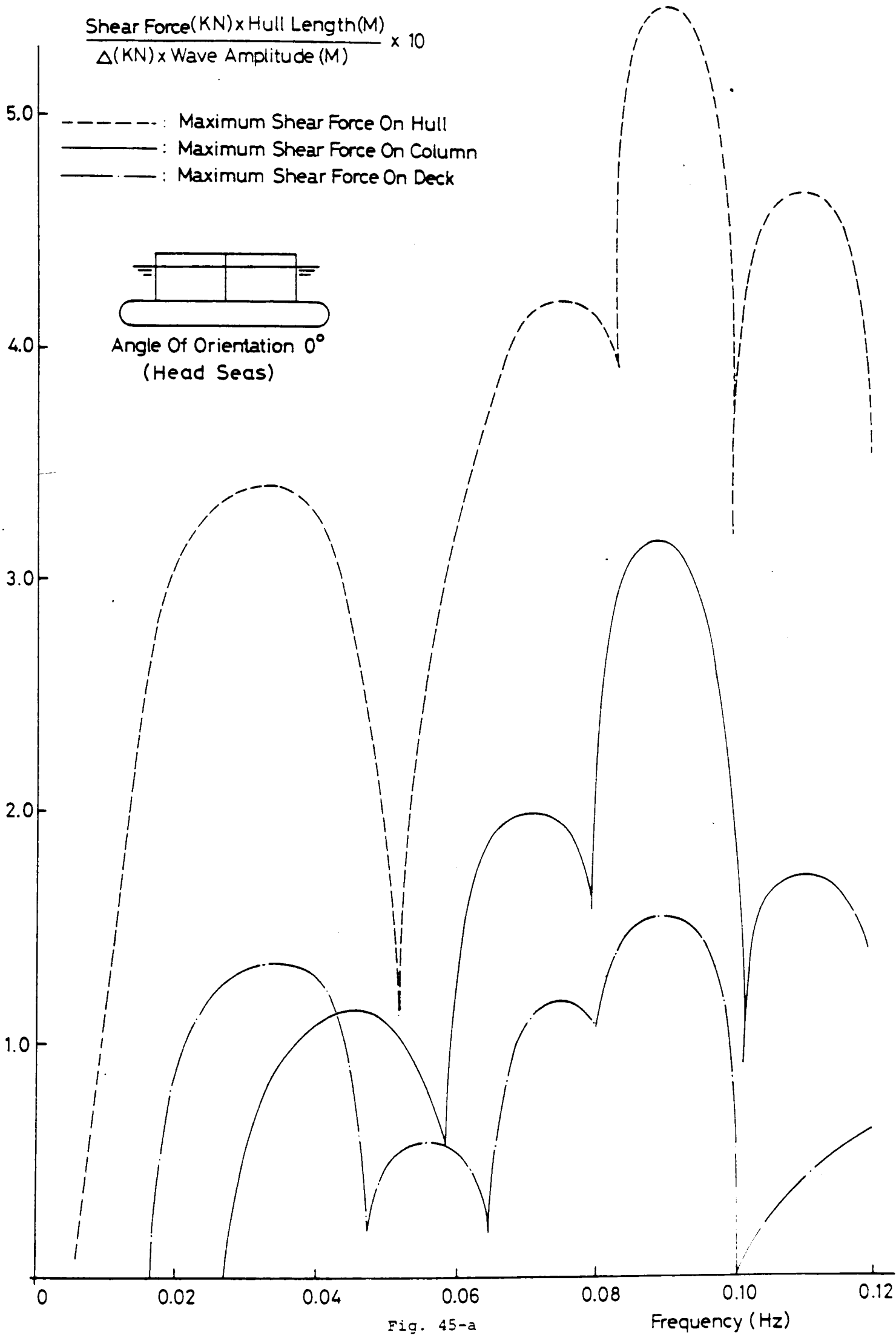
Shear Force(KN) x Hull Length(M) / Δ(KN) x Wave Amplitude (M) x 10
5.0
4.0
3.0
2.0
1.0
: Maximum Shear Force On Hull
: Maximum Shear Force On Column
: Maximum Shear Force On Deck
Angle Of Orientation 0°
(Head Seas)
0
0.02
0.04
0.06
0.08
0.10
0.12
Frequency (Hz)

Fig. 45-a

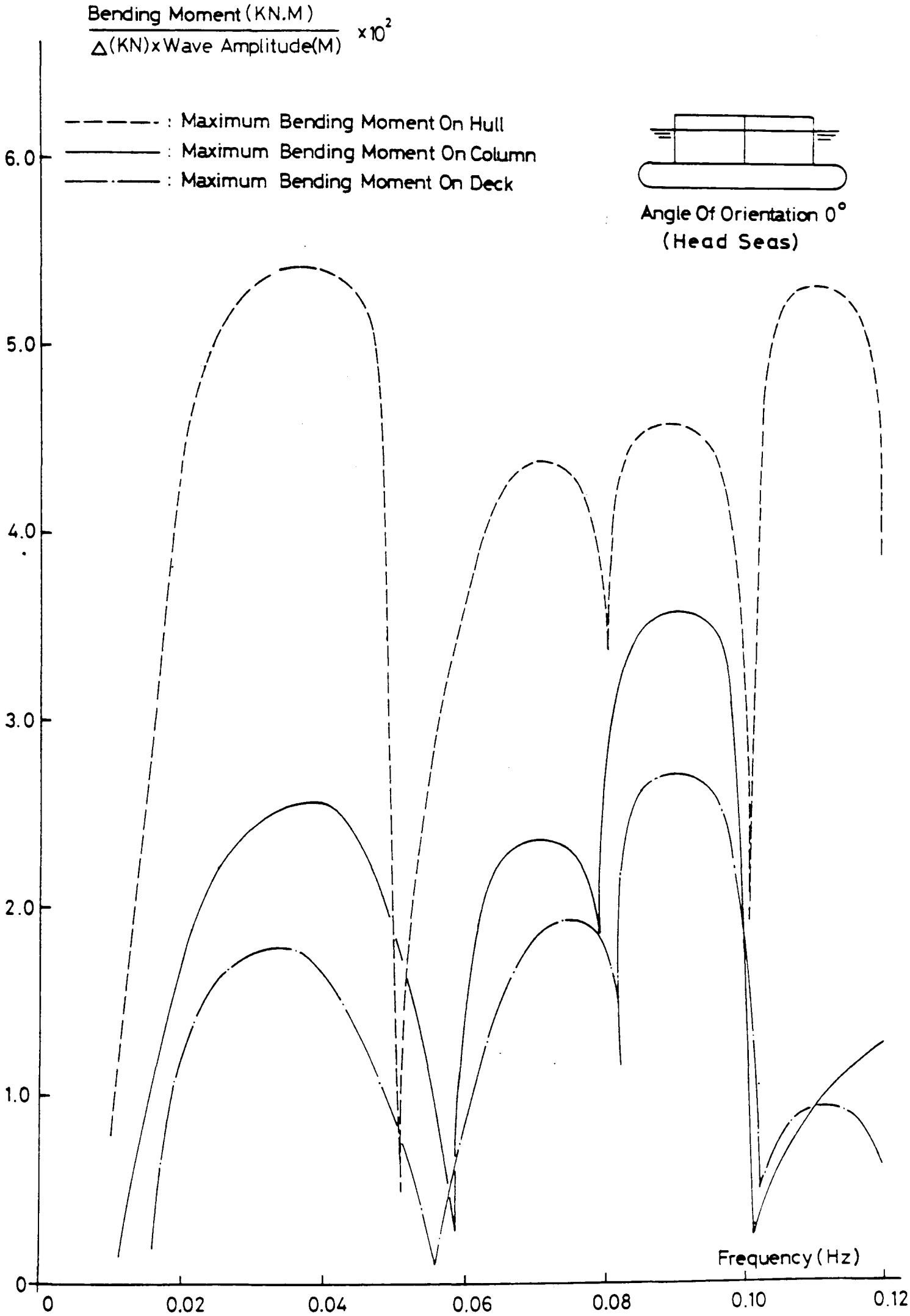
Bending Moment (KN.M) / △(KN) x Wave Amplitude(M) x10²
: Maximum Bending Moment On Hull
: Maximum Bending Moment On Column
: Maximum Bending Moment On Deck
Angle Of Orientation 0°
(Head Seas)
6.0
5.0
4.0
3.0
2.0
1.0
0
0
0.02
0.04
0.06
0.08
0.10
0.12
Frequency (Hz)

Fig. 45-b

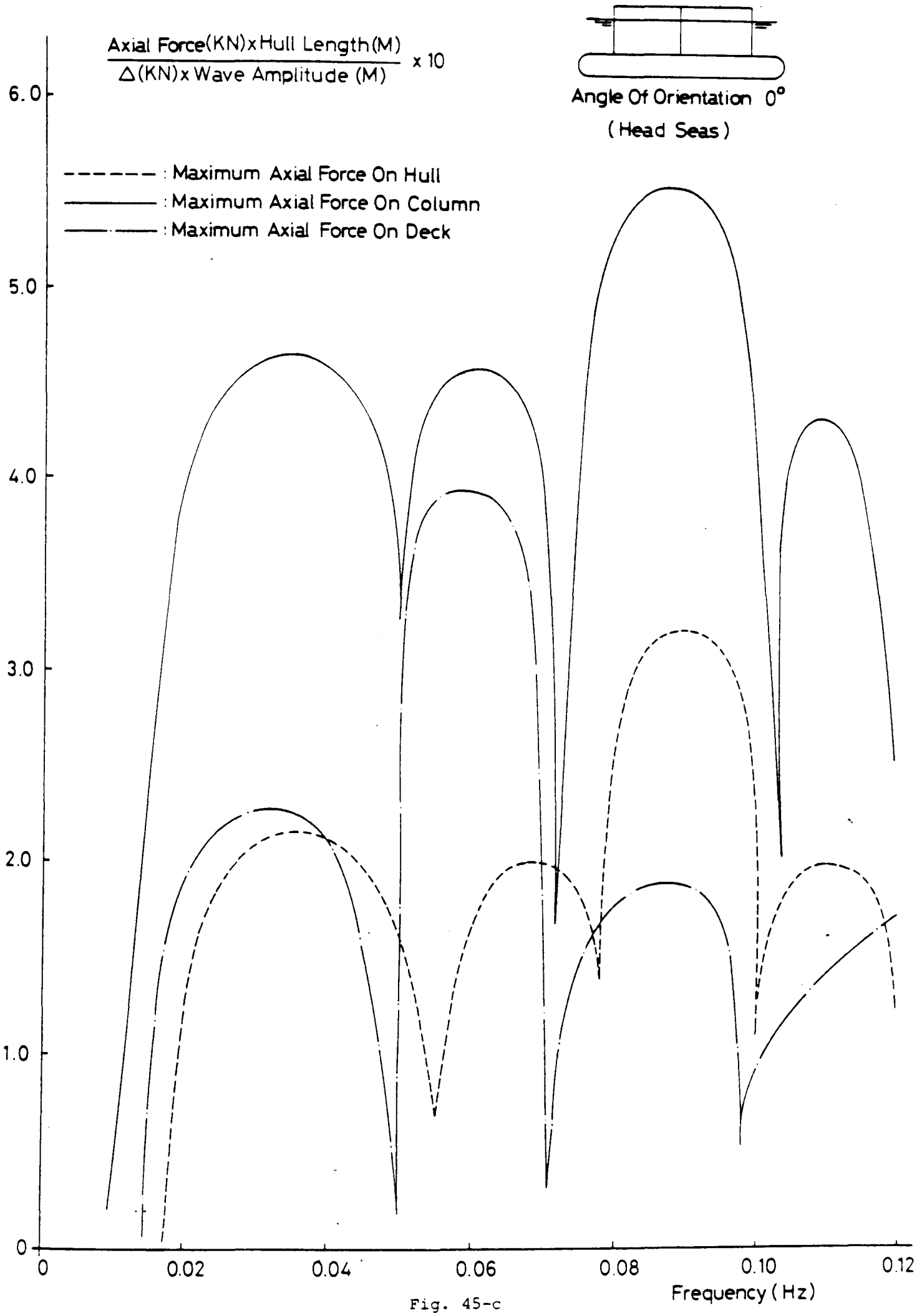
Axial Force(KN)x Hull Length(M) / Δ(KN)x Wave Amplitude (M) x 10
Angle Of Orientation 0°
(Head Seas)
------ : Maximum Axial Force On Hull
——— : Maximum Axial Force On Column
——·—— : Maximum Axial Force On Deck
6.0
5.0
4.0
3.0
2.0
1.0
0
0
0.02
0.04
0.06
0.08
0.10
0.12
Frequency (Hz)

Fig. 45-c

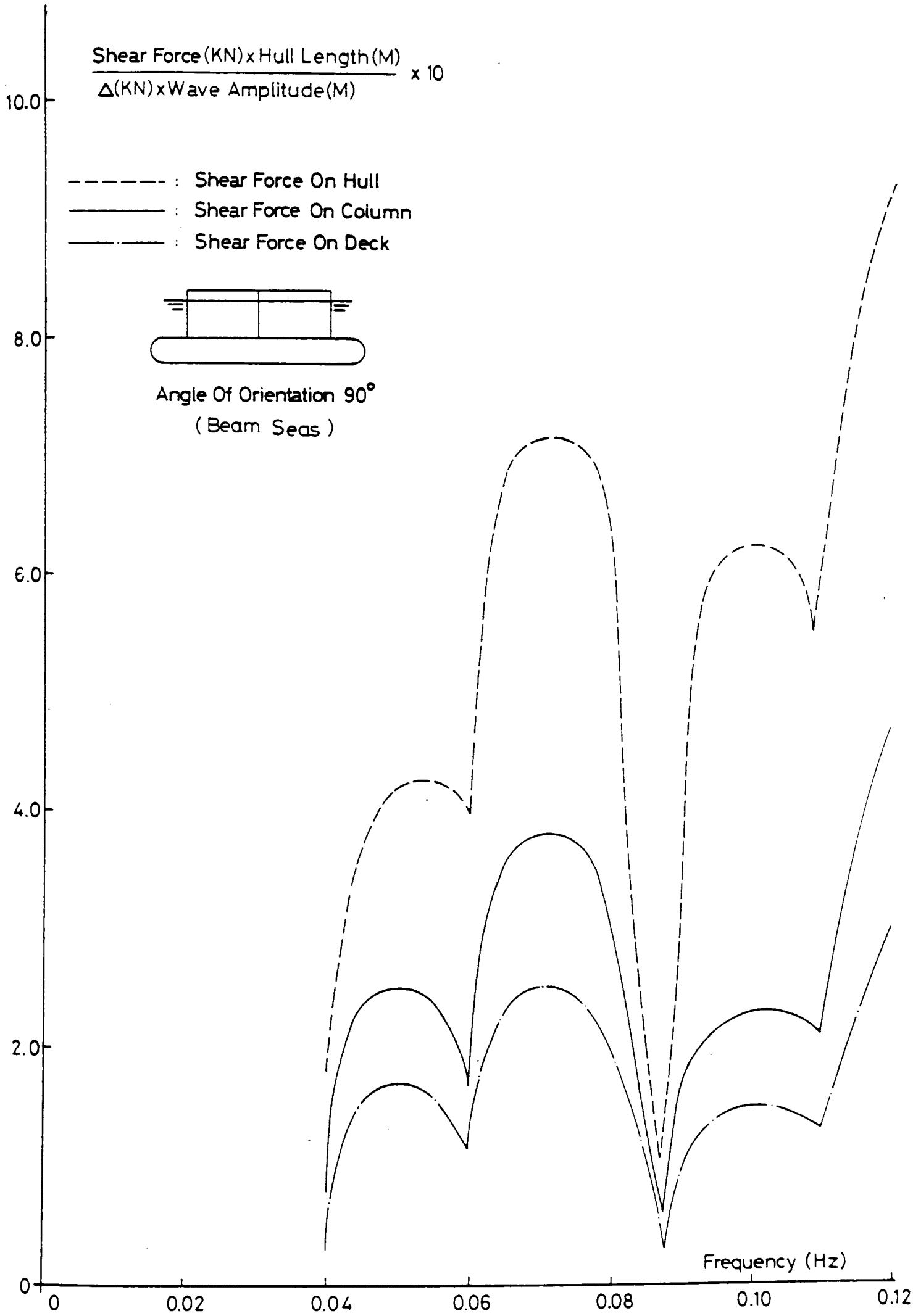
Shear Force (KN) x Hull Length (M) / Δ (KN) x Wave Amplitude (M) x 10
10.0
8.0
6.0
4.0
2.0
0
: Shear Force On Hull
: Shear Force On Column
: Shear Force On Deck
Angle Of Orientation 90°
(Beam Seas)
Frequency (Hz)
0
0.02
0.04
0.06
0.08
0.10
0.12

Fig. 46-a

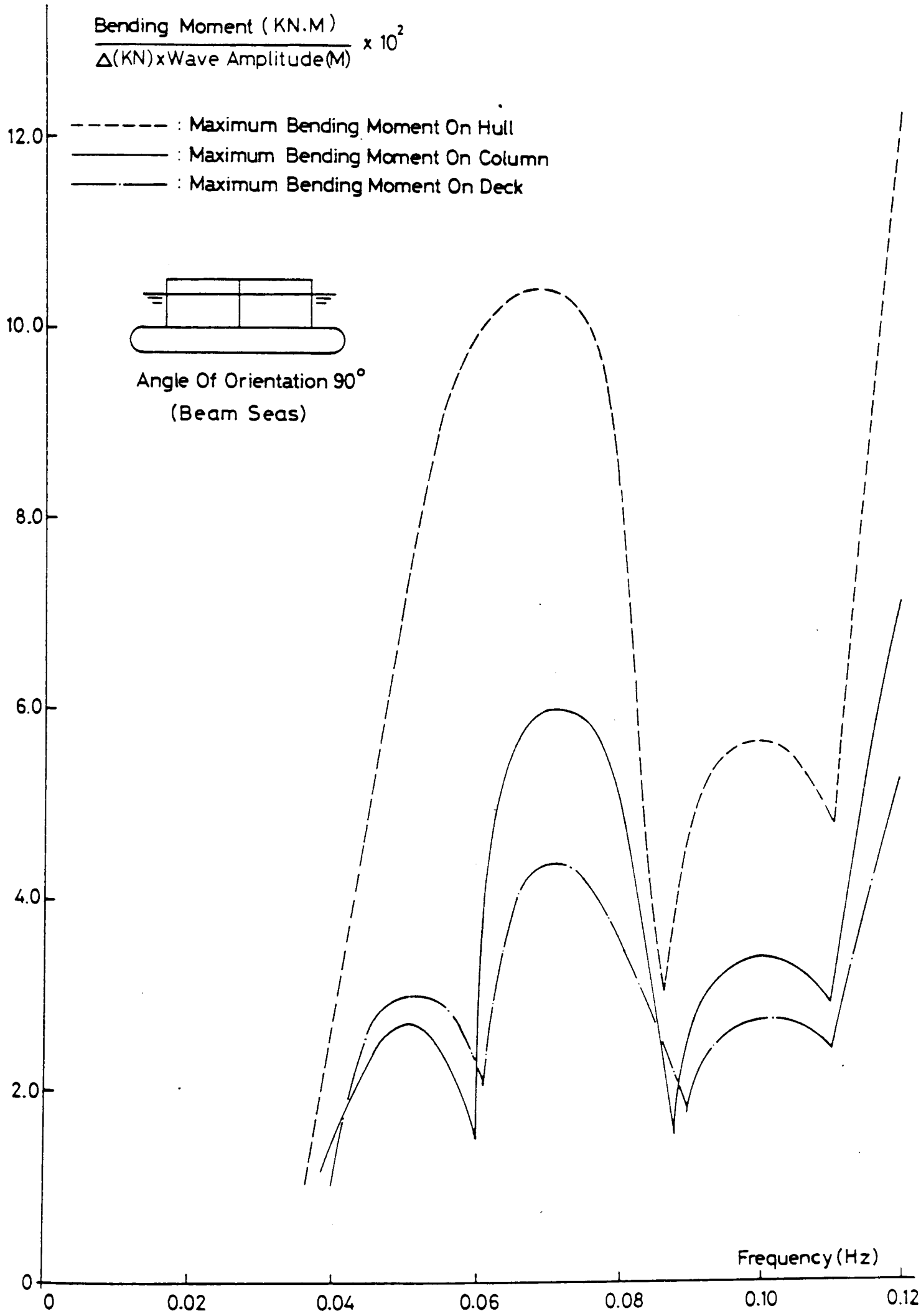
Bending Moment (KN.M)
Δ(KN) x Wave Amplitude(M) x 10²
: Maximum Bending Moment On Hull
: Maximum Bending Moment On Column
: Maximum Bending Moment On Deck
Angle Of Orientation 90°
(Beam Seas)
12.0
10.0
8.0
6.0
4.0
2.0
0
0
0.02
0.04
0.06
0.08
0.10
0.12
Frequency (Hz)

Fig. 46-b

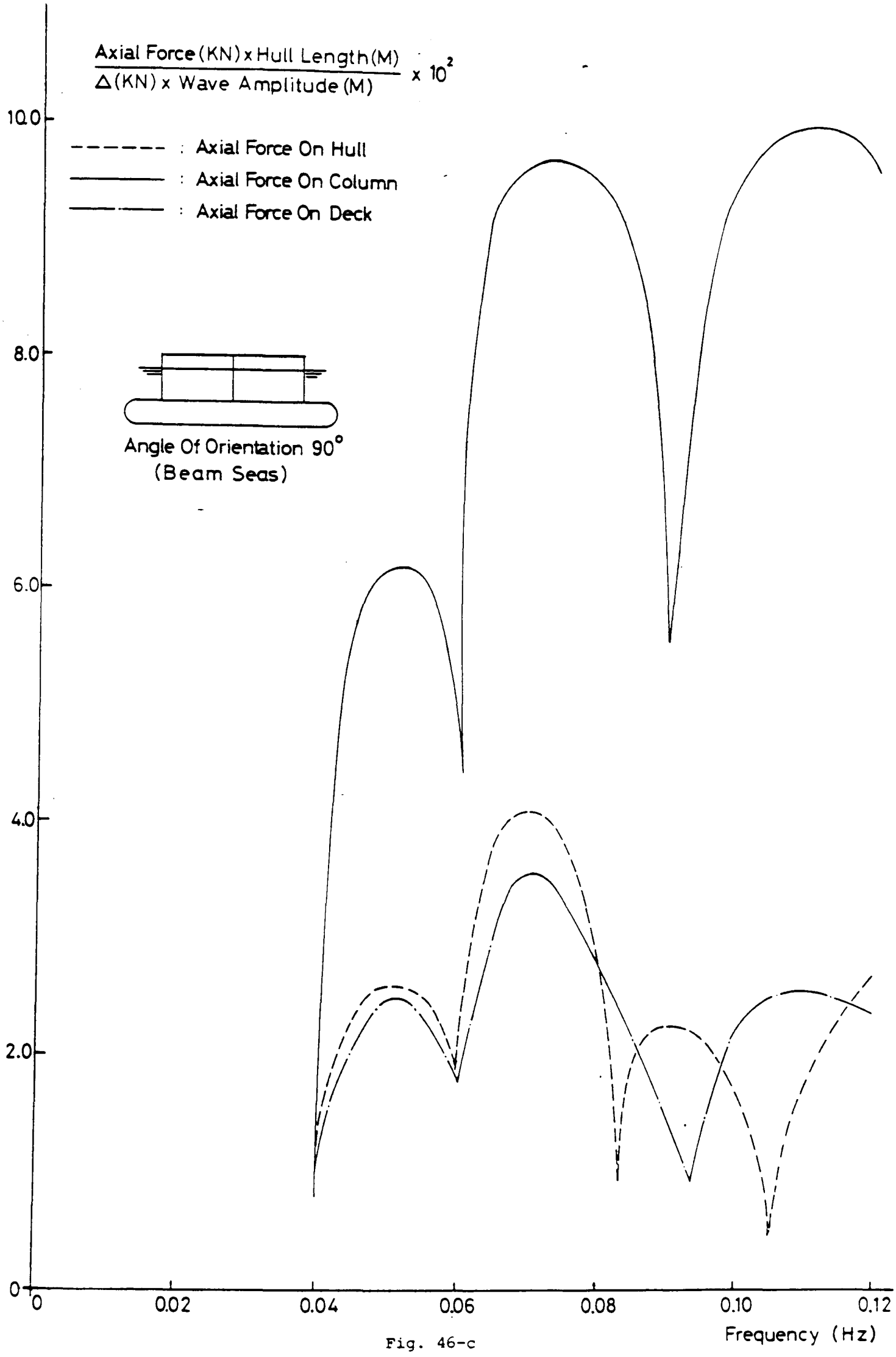
Axial Force (KN) x Hull Length (M) / Δ (KN) x Wave Amplitude (M) x 10²
: Axial Force On Hull
: Axial Force On Column
: Axial Force On Deck
Angle Of Orientation 90°
(Beam Seas)
10.0
8.0
6.0
4.0
2.0
0
0
0.02
0.04
0.06
0.08
0.10
0.12
Frequency (Hz)

Fig. 46-c

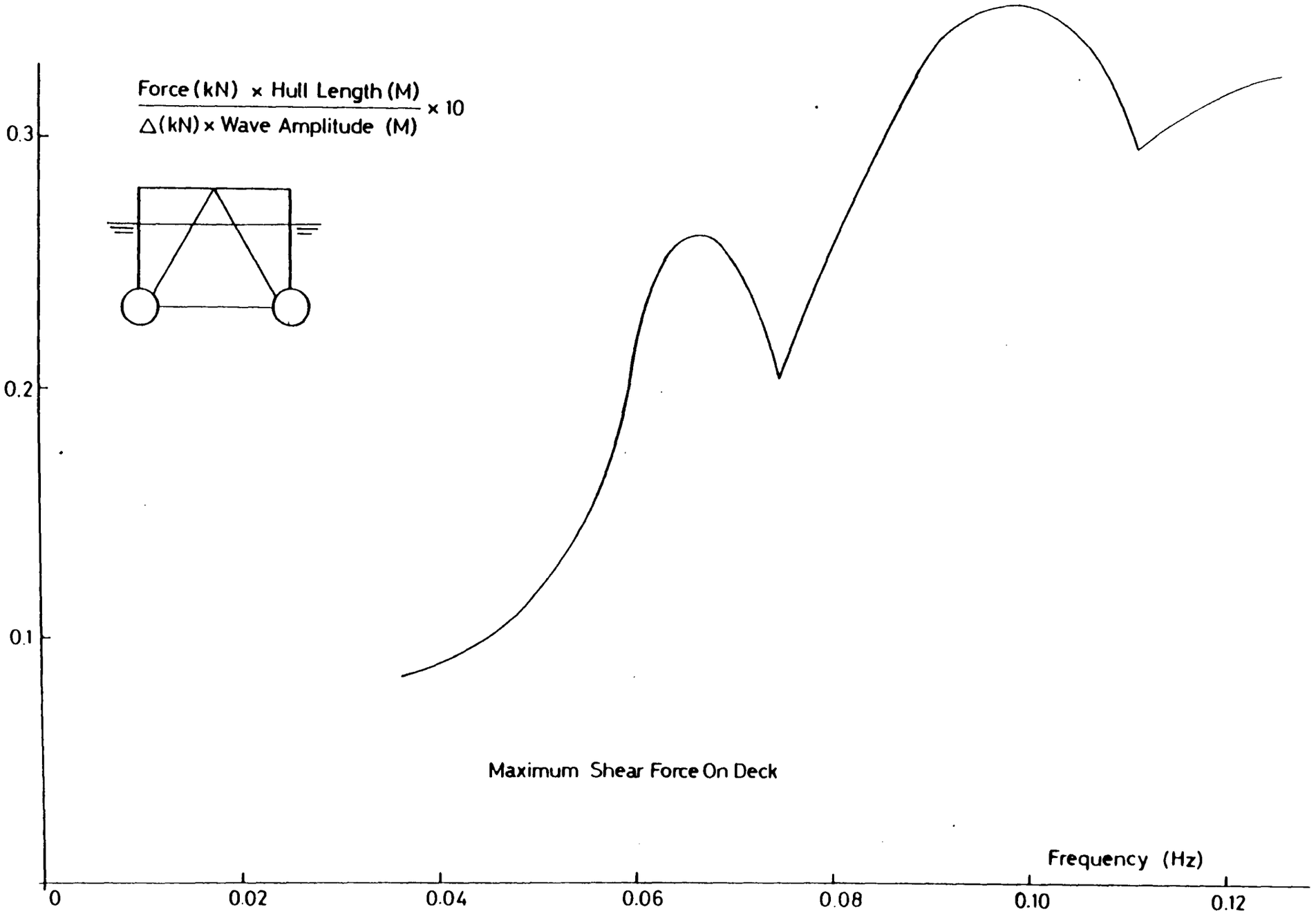
Force (kN) × Hull Length (M) / Δ (kN) × Wave Amplitude (M) × 10
0.3
0.2
0.1
Maximum Shear Force On Deck
Frequency (Hz)
0
0.02
0.04
0.06
0.08
0.10
0.12

Fig. 47-a

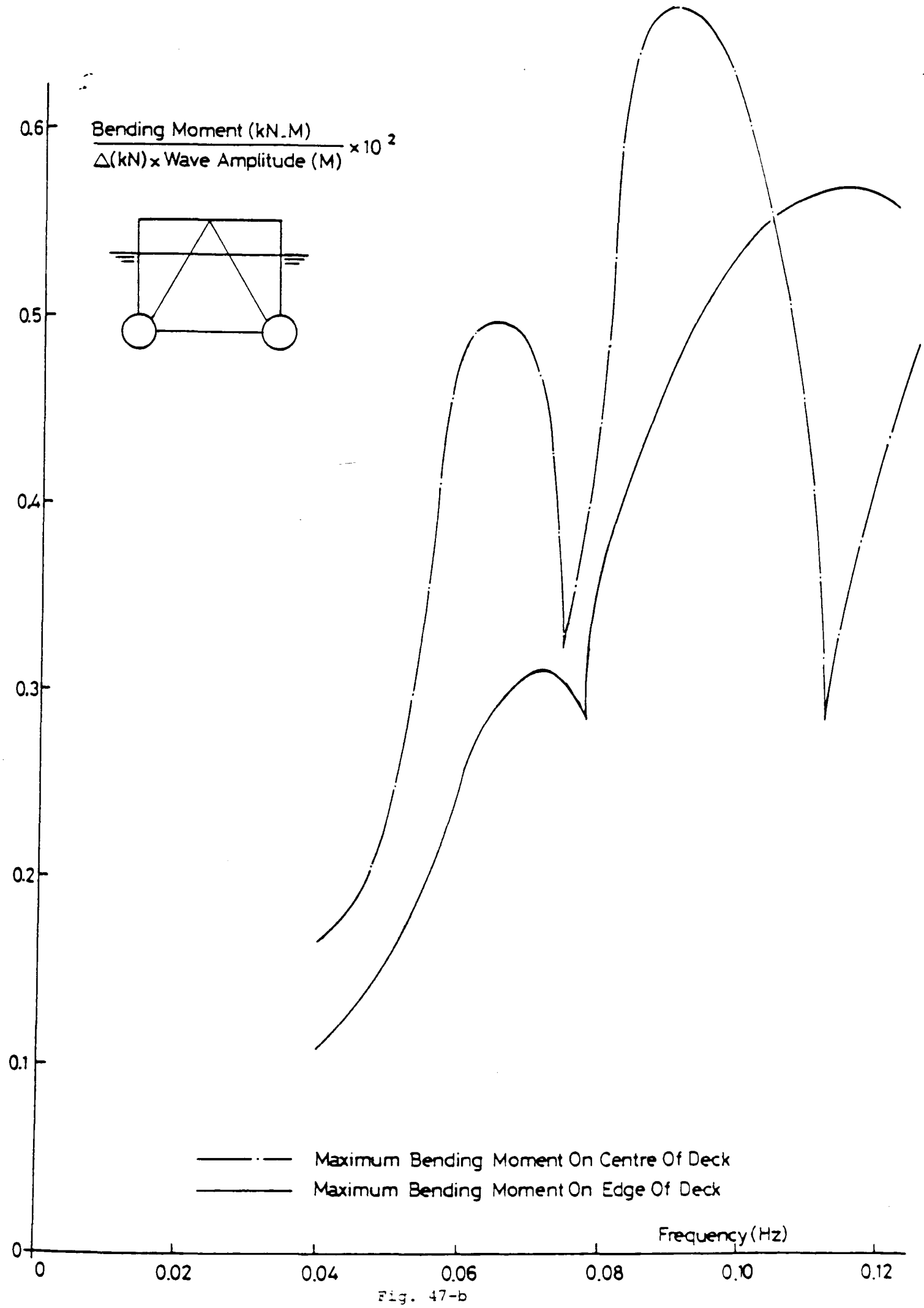
Bending Moment (kN.M) / △(kN) x Wave Amplitude (M) x 10 2
0.6
0.5
0.4
0.3
0.2
0.1
0
0
0.02
0.04
0.06
0.08
0.10
0.12
Frequency (Hz)
Maximum Bending Moment On Centre Of Deck
Maximum Bending Moment On Edge Of Deck

Fig. 47-b

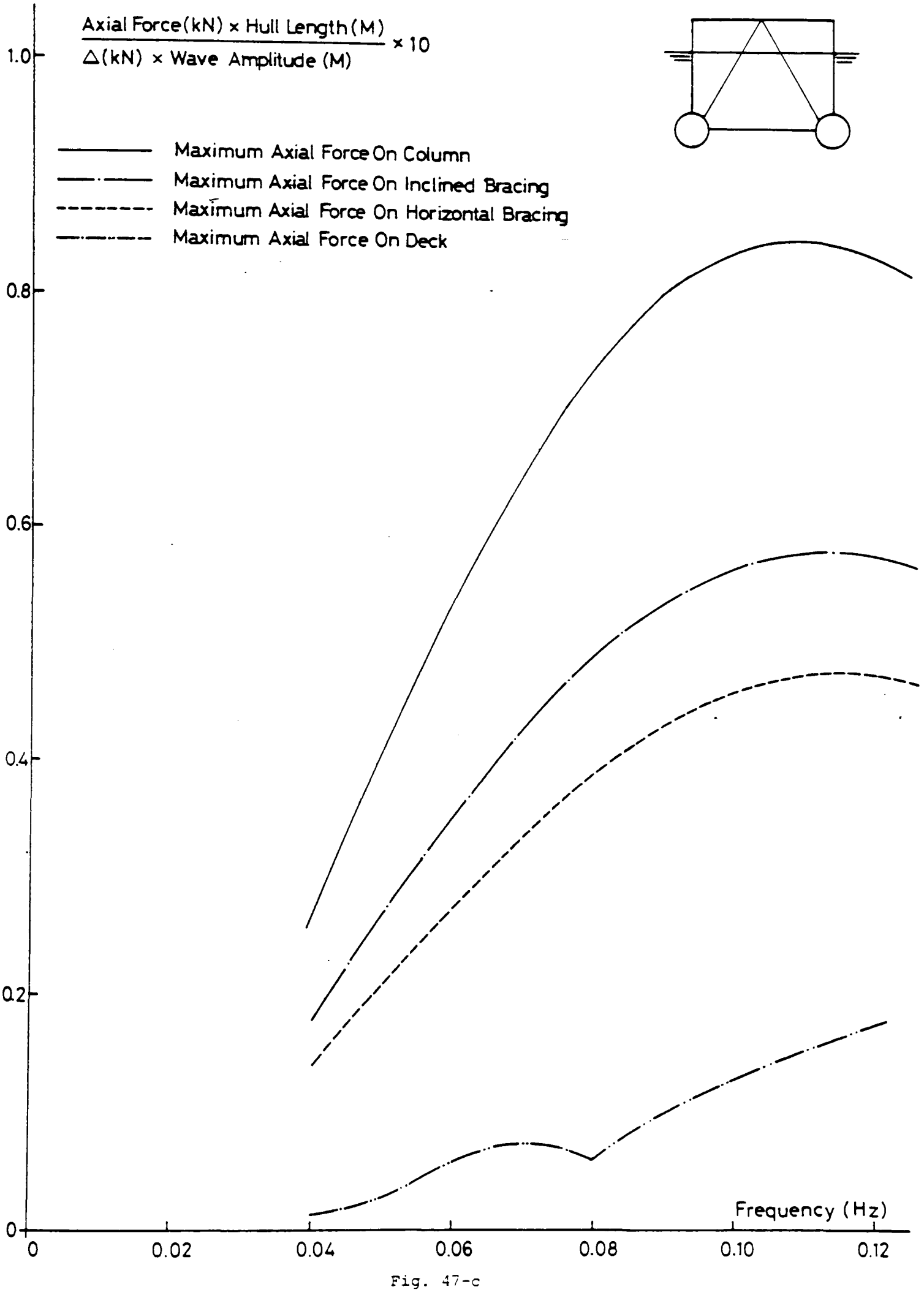
Axial Force(kN) × Hull Length(M) / △(kN) × Wave Amplitude (M) × 10
Maximum Axial Force On Column
Maximum Axial Force On Inclined Bracing
Maximum Axial Force On Horizontal Bracing
Maximum Axial Force On Deck
1.0
0.8
0.6
0.4
0.2
0
0
0.02
0.04
0.06
0.08
0.10
0.12
Frequency (Hz)

Fig. 47-c

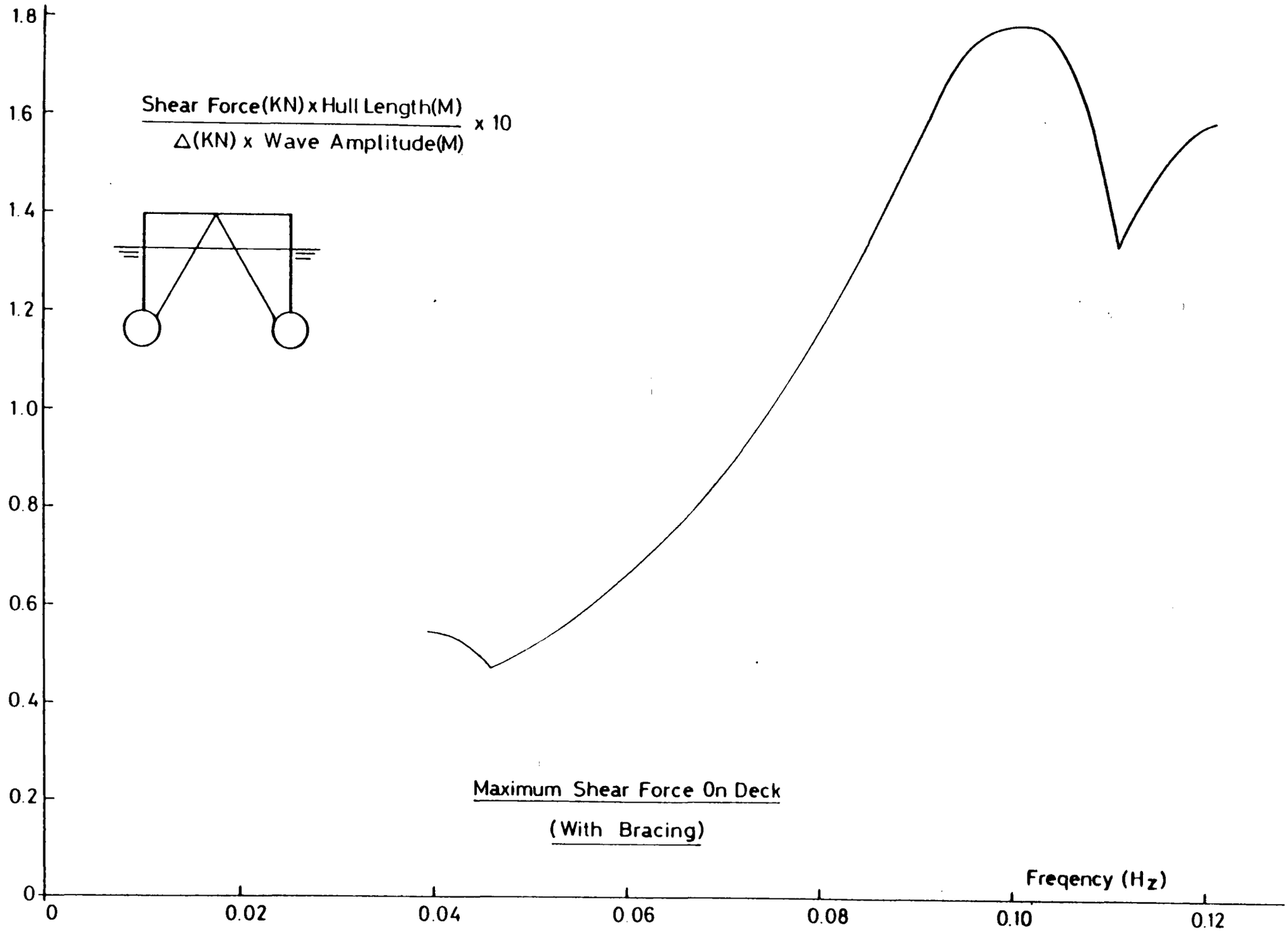
Shear Force(KN) x Hull Length(M) / Δ(KN) x Wave Amplitude(M) x 10
1.8
1.6
1.4
1.2
1.0
0.8
0.6
0.4
0.2
0
0
0.02
0.04
0.06
0.08
0.10
0.12
Freqency (Hz)
Maximum Shear Force On Deck
(With Bracing)

Fig. 48-a

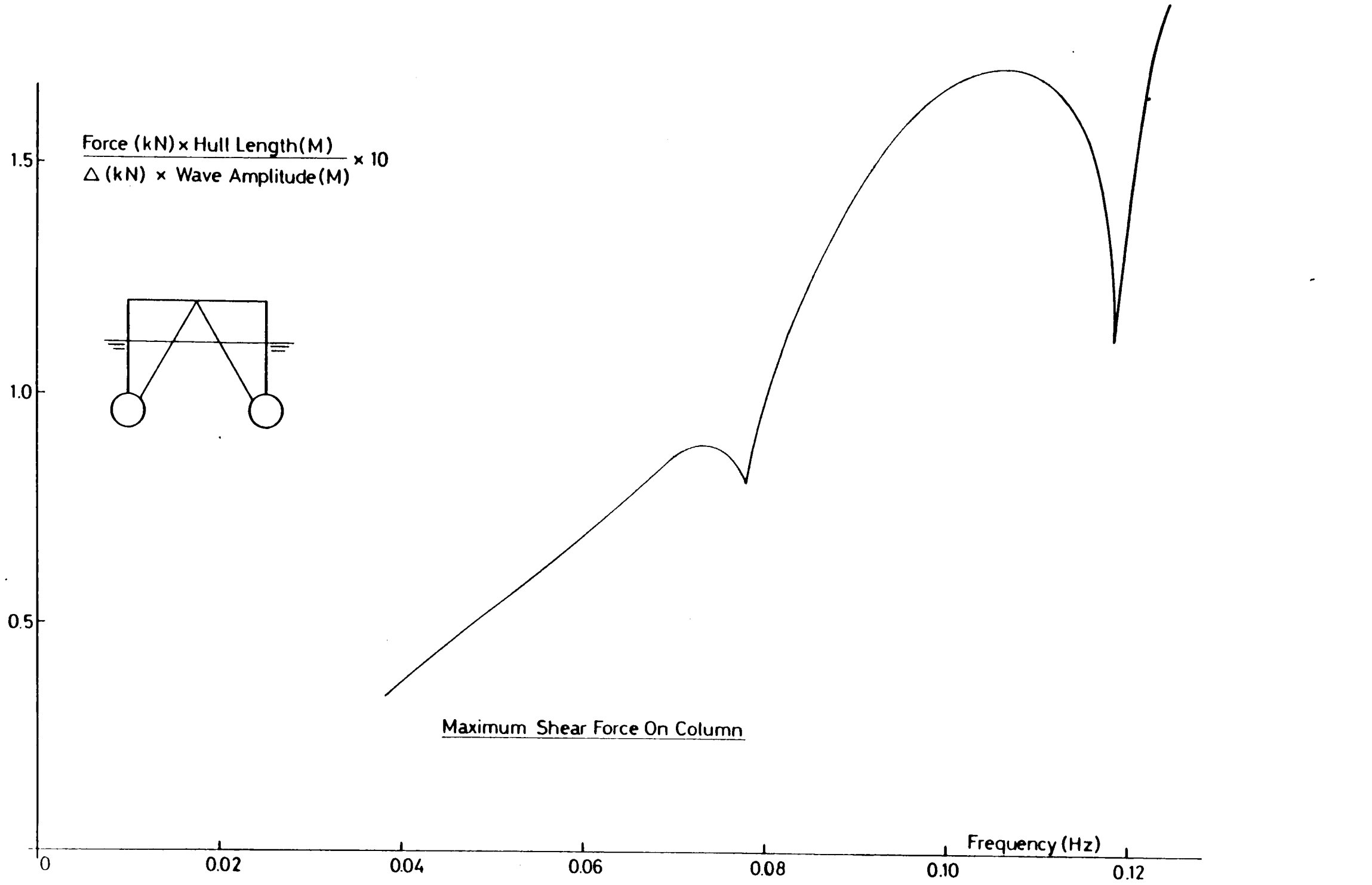
Force (kN) x Hull Length(M) / Δ (kN) x Wave Amplitude(M) x 10
1.5
1.0
0.5
Maximum Shear Force On Column
0
0.02
0.04
0.06
0.08
0.10
0.12
Frequency (Hz)

Fig. 48-b

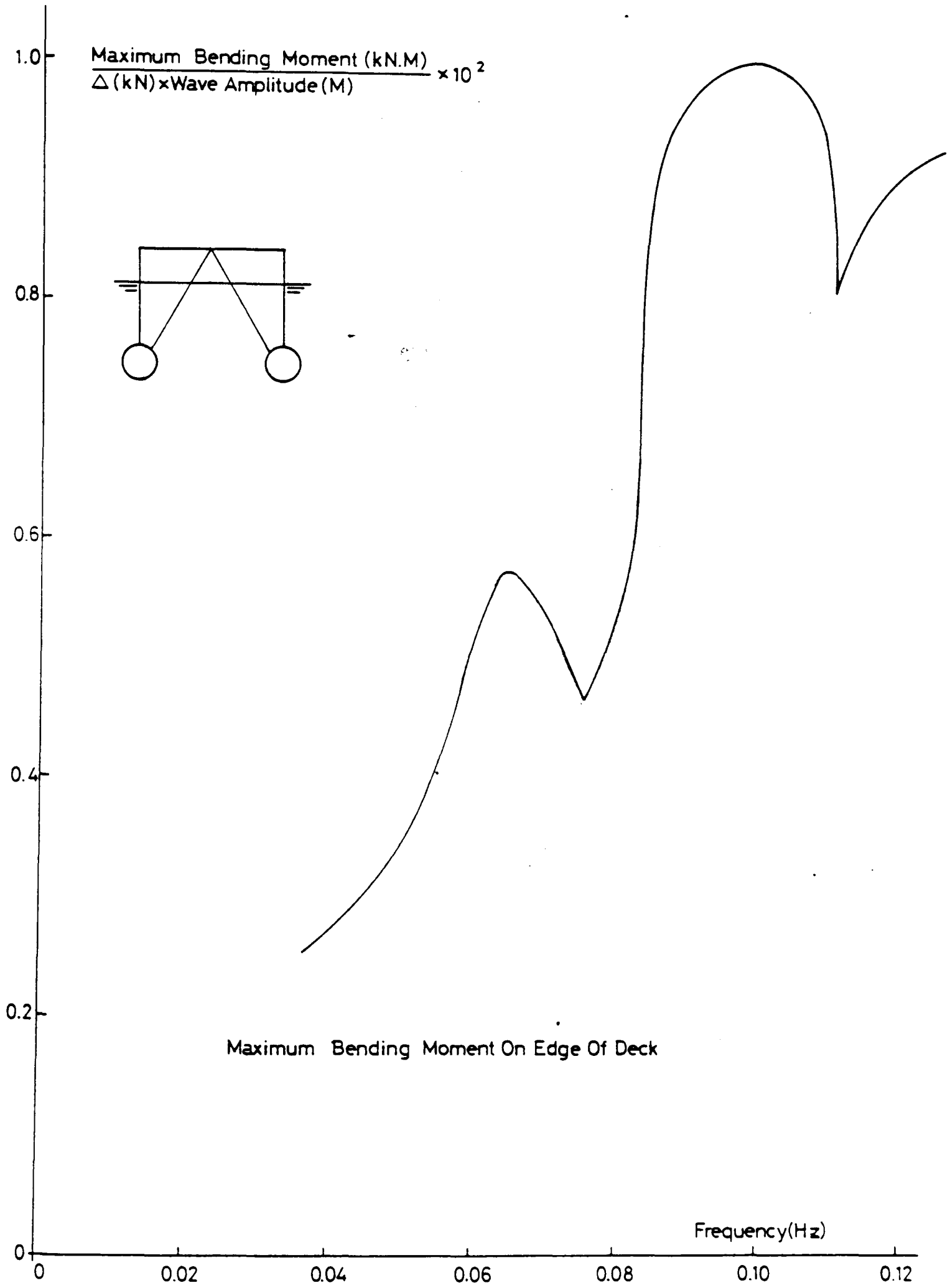
Maximum Bending Moment (kN.M) / Δ(kN)×Wave Amplitude(M) ×10²
1.0
0.8
0.6
0.4
0.2
0
Maximum Bending Moment On Edge Of Deck
Frequency(Hz)
0
0.02
0.04
0.06
0.08
0.10
0.12

Fig. 48-c

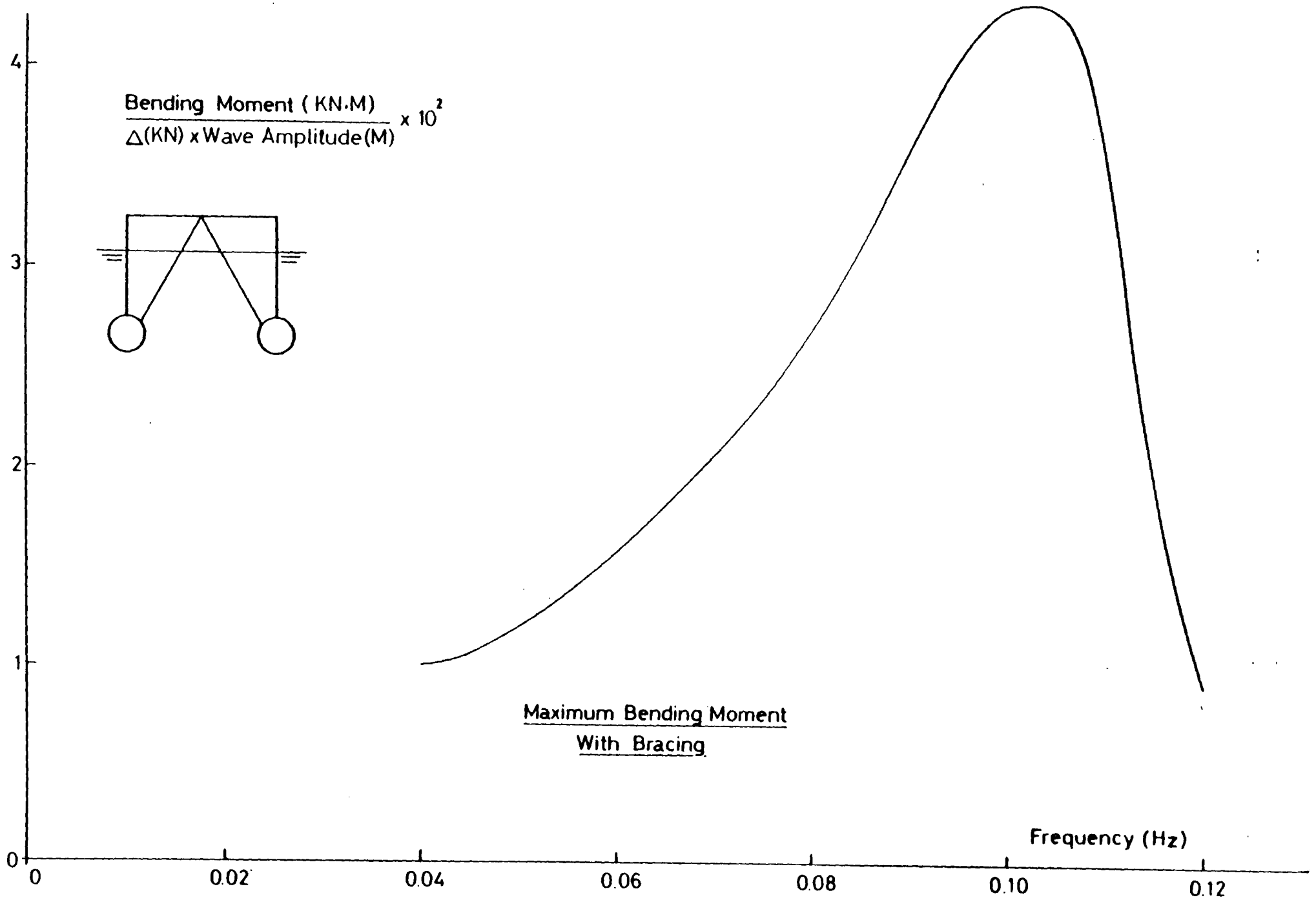
Bending Moment (KN.M)
Δ(KN) x Wave Amplitude(M) x 10²
4
3
2
1
0
0
0.02
0.04
0.06
0.08
0.10
0.12
Frequency (Hz)
Maximum Bending Moment
With Bracing

Fig. 48-d

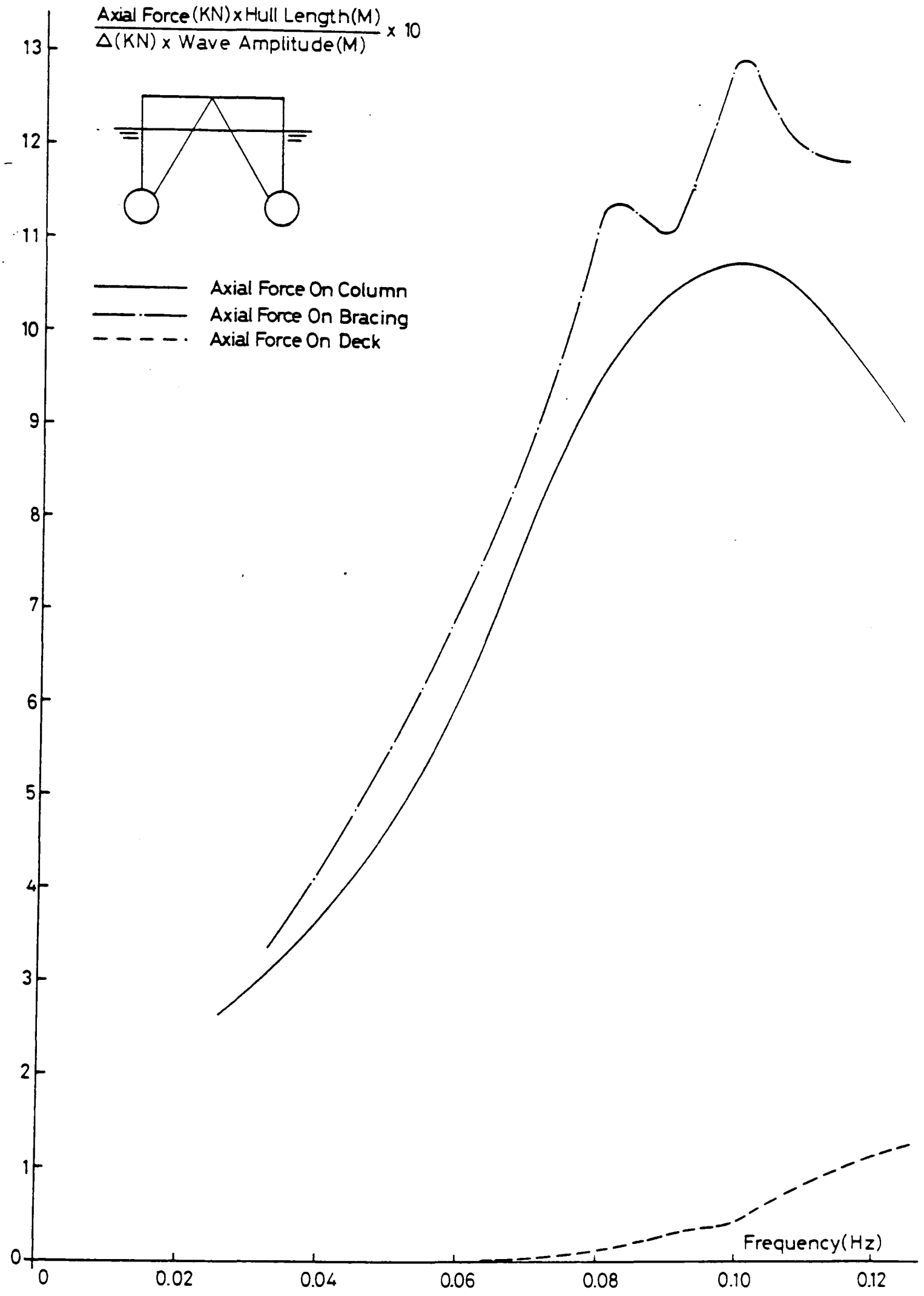
Axial Force (KN) x Hull Length (M) / Δ (KN) x Wave Amplitude (M) x 10
Axial Force On Column
Axial Force On Bracing
Axial Force On Deck
13
12
11
10
9
8
7
6
5
4
3
2
1
0
0
0.02
0.04
0.06
0.08
0.10
0.12
Frequency (Hz)

Fig. 48-e

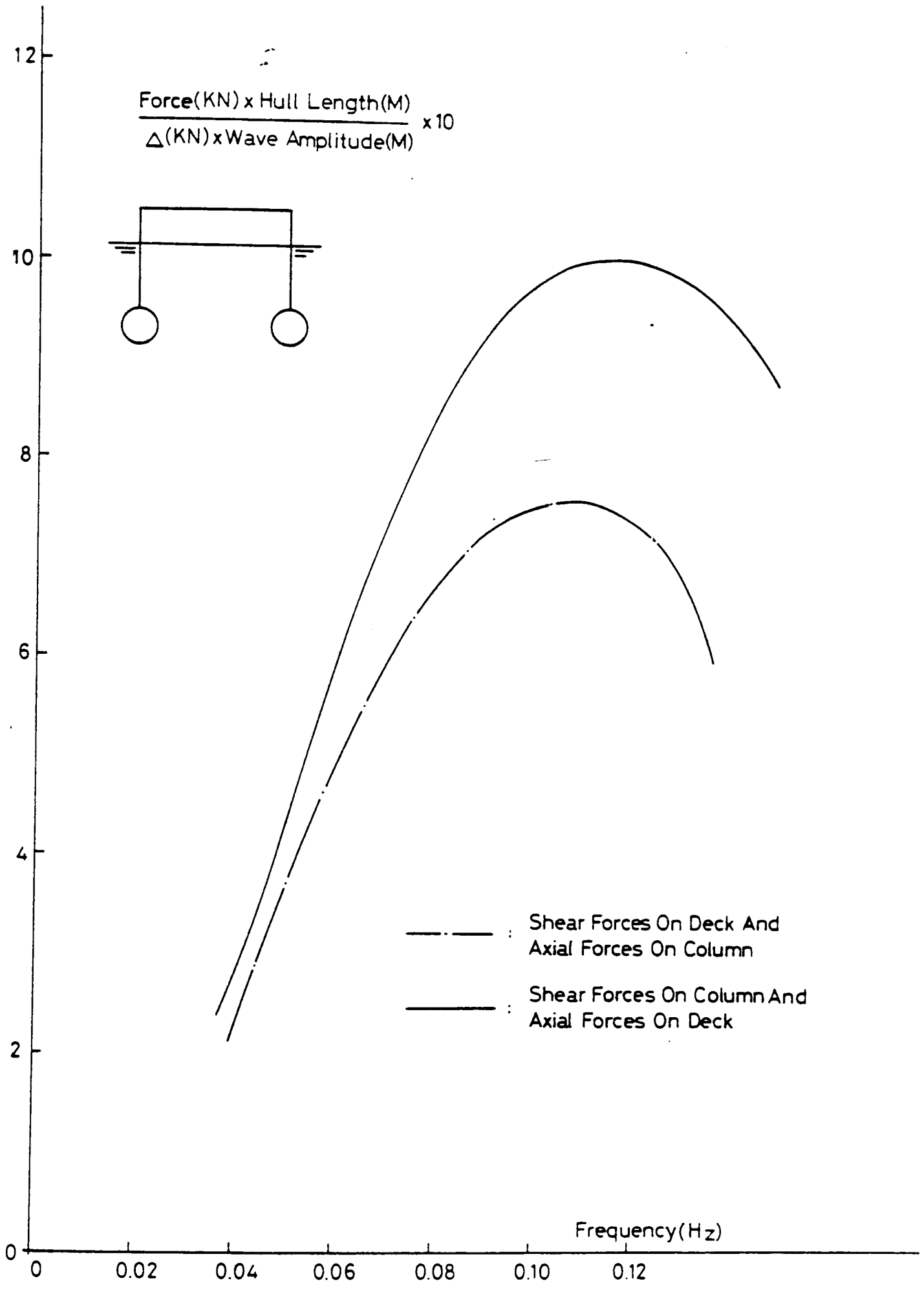
12
10
8
6
4
2
0
Force(KN) x Hull Length(M) / △(KN) x Wave Amplitude(M) x 10
0
0.02
0.04
0.06
0.08
0.10
0.12
Frequency(Hz)
Shear Forces On Deck And Axial Forces On Column
Shear Forces On Column And Axial Forces On Deck

Fig. 49-a

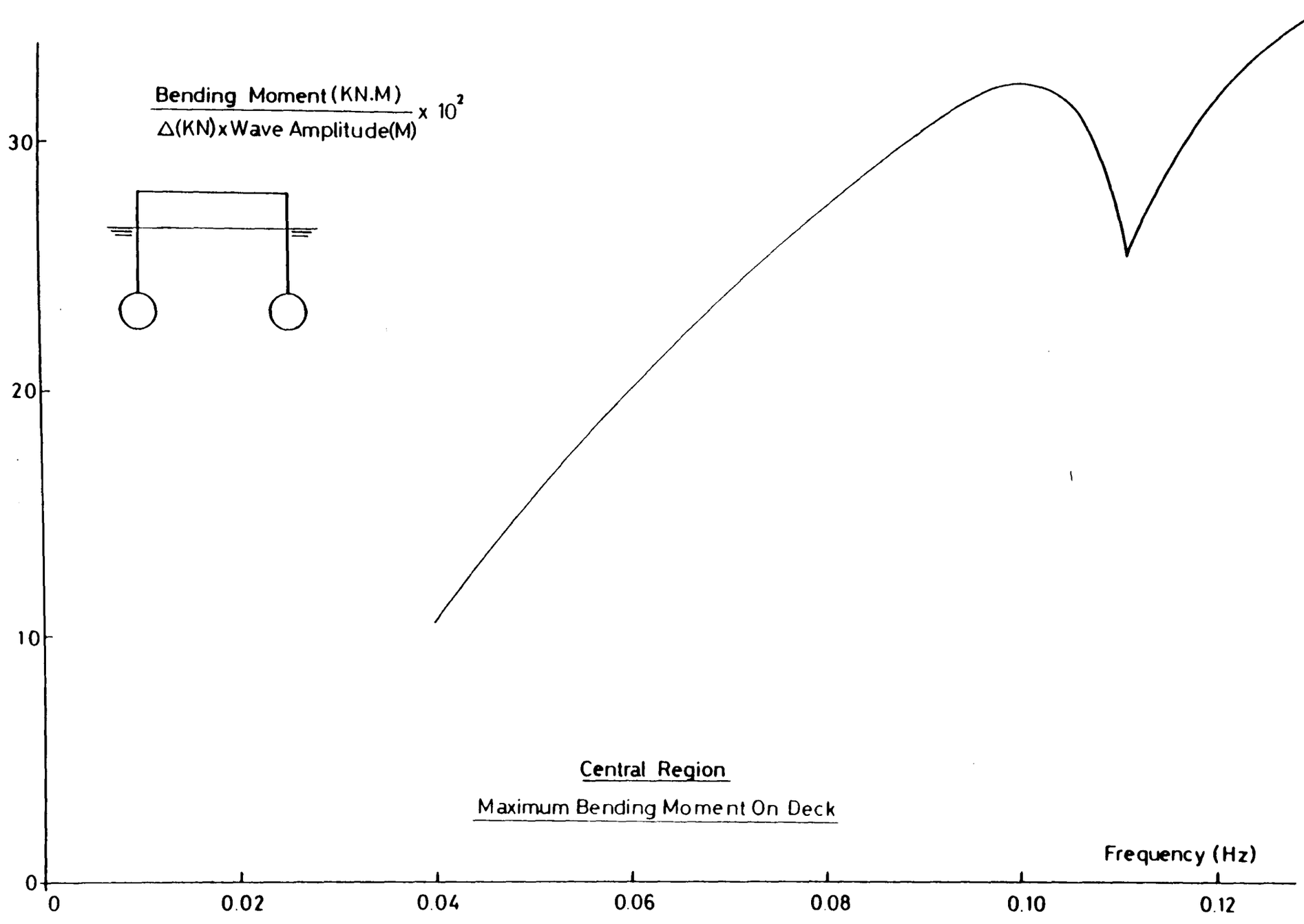
Bending Moment (KN.M) / Δ(KN) x Wave Amplitude(M) x 10²
30
20
10
0
0
0.02
0.04
0.06
0.08
0.10
0.12
Frequency (Hz)
Central Region
Maximum Bending Moment On Deck

Fig. 49-b

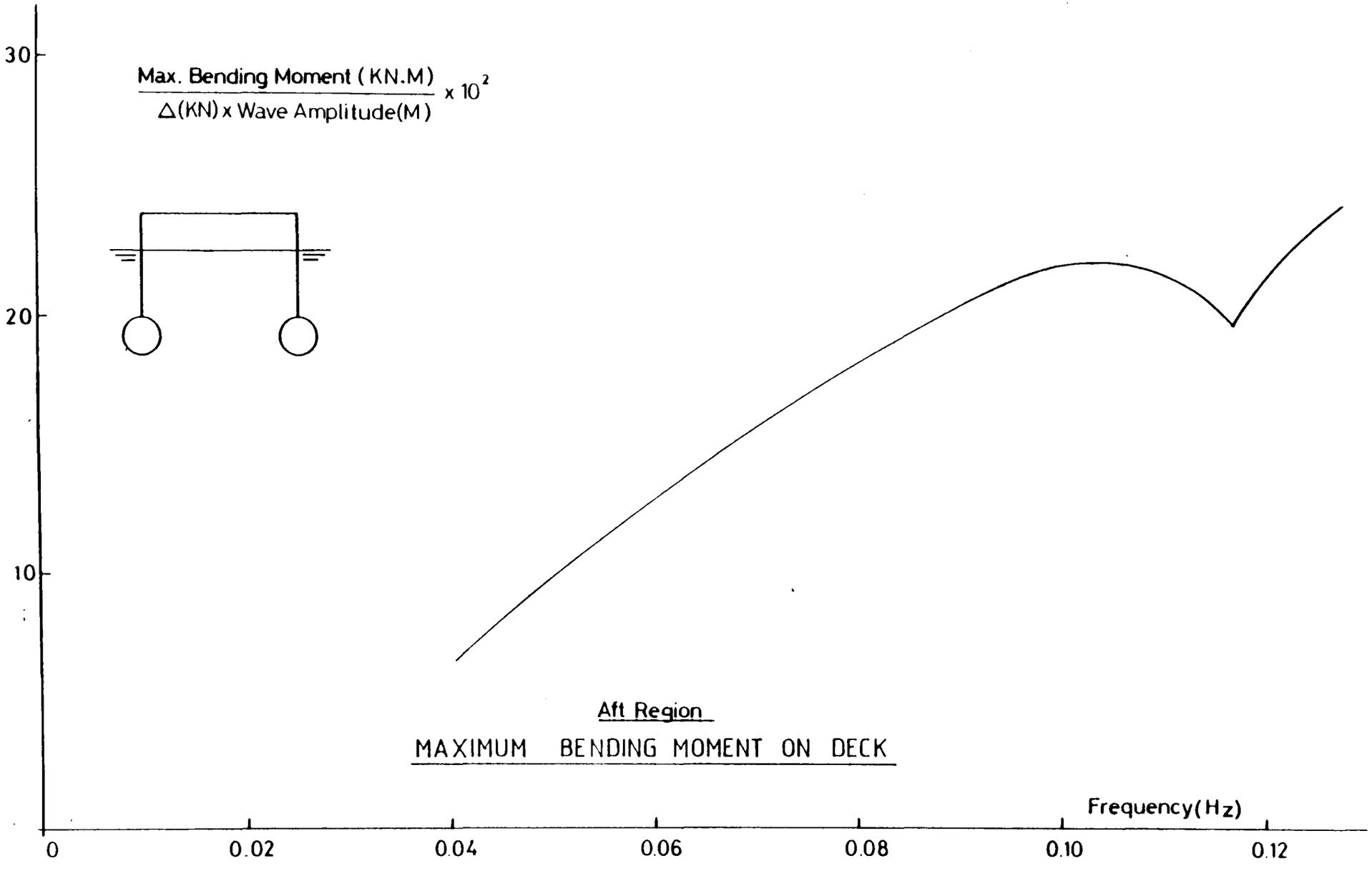
30
20
10
Max. Bending Moment (KN.M) / Δ(KN) x Wave Amplitude(M) x 10²
Aft Region
MAXIMUM BENDING MOMENT ON DECK
Frequency(Hz)
0
0.02
0.04
0.06
0.08
0.10
0.12

Fig. 49-c

Chapter 6: DESCRIPTION OF THE COMPUTER PROGRAM FLUID4A

INTRODUCTION

In this chapter the FLUID4A computer program will be described. FLUID4A is a special purpose program which has been written for a semi-submersible geometry of twin circular hulls with four columns in order to compare theoretical calculations with the experimental results.

FLUID4A consists of several subroutines which calculate the wave loading distributions on the members of the above mentioned geometry, as well as the motion and structural responses under the calculated wave loading.

FLUID4A has been written in FORTRAN programming language and runs on the Hydrodynamic Laboratory's PDP 11/40 computer at the University of Glasgow. FLUID4A requires about 30K words of storage space.

1. DESCRIPTION OF SUBROUTINES

1.1 Subroutine FLUID4A

This subroutine reads the input data from the terminal and generates the nodal points on the hull where the force distributions due to wave and rigid body motion will be calculated.

Subroutine FLUID4A calculates the wave loading distribution on the hull in head sea conditions. The calculation procedures are based on the theoretical formulations given in chapters 2 and 3.

Subroutine FLUID4A calls the following subroutines:

1) MOT

2) MOT1

3) COLUMN

4) FLUID3

Subroutine FLUID4A also writes the following data onto output file:

a) The title

b) Summary of the geometrical data

c) Summary of the wave data

d) Summary of the vertical and horizontal forces on the structure in head sea conditions

e) Distribution of the vertical and horizontal forces on the hull in head sea condition

1.2 Subroutine FLUID3

This subroutine calculates wave loading distributions on the hull in beam sea conditions. As with the subroutine FLUID4A, calculation procedures are based on the theoretical formulations given in chapters 2 and 3.

The geometrical and the wave data are transferred from the subroutine FLUID4A to FLUID3A.

Subroutine FLUID3 calls the following subroutines:

1) FLUID

2) COLUMN

3) FRAN1

4) MOT2

Subroutine FLUID3 writes the following data into the output file:

a) Summary of the vertical and the horizontal forces on the structure in beam seas

b) Distribution of the vertical and the horizontal forces on the hull in beam sea conditions

1.3 Subroutine COLUMN

This subroutine generates the nodal points along the columns of the structure (Fig. 1).

It provides the data to subroutine FLUID2 which calculates the wave loading on the columns of the structure.

Subroutine COLUMN writes the following data into the output file:

a) Distribution of drag and inertia coefficients along the nodal points of the columns

b) Distribution of Reynolds and the Keulegan-Carpenter numbers along the nodal points of the columns

c) Distribution of the drag, acceleration and the total forces along the nodal points of the columns

d) Total horizontal column forces and moments (about the free-surface)

Subroutine COLUMN calls the subroutine FLUID2 and returns the calculated values to subroutine FLUID4A and FLUID3.

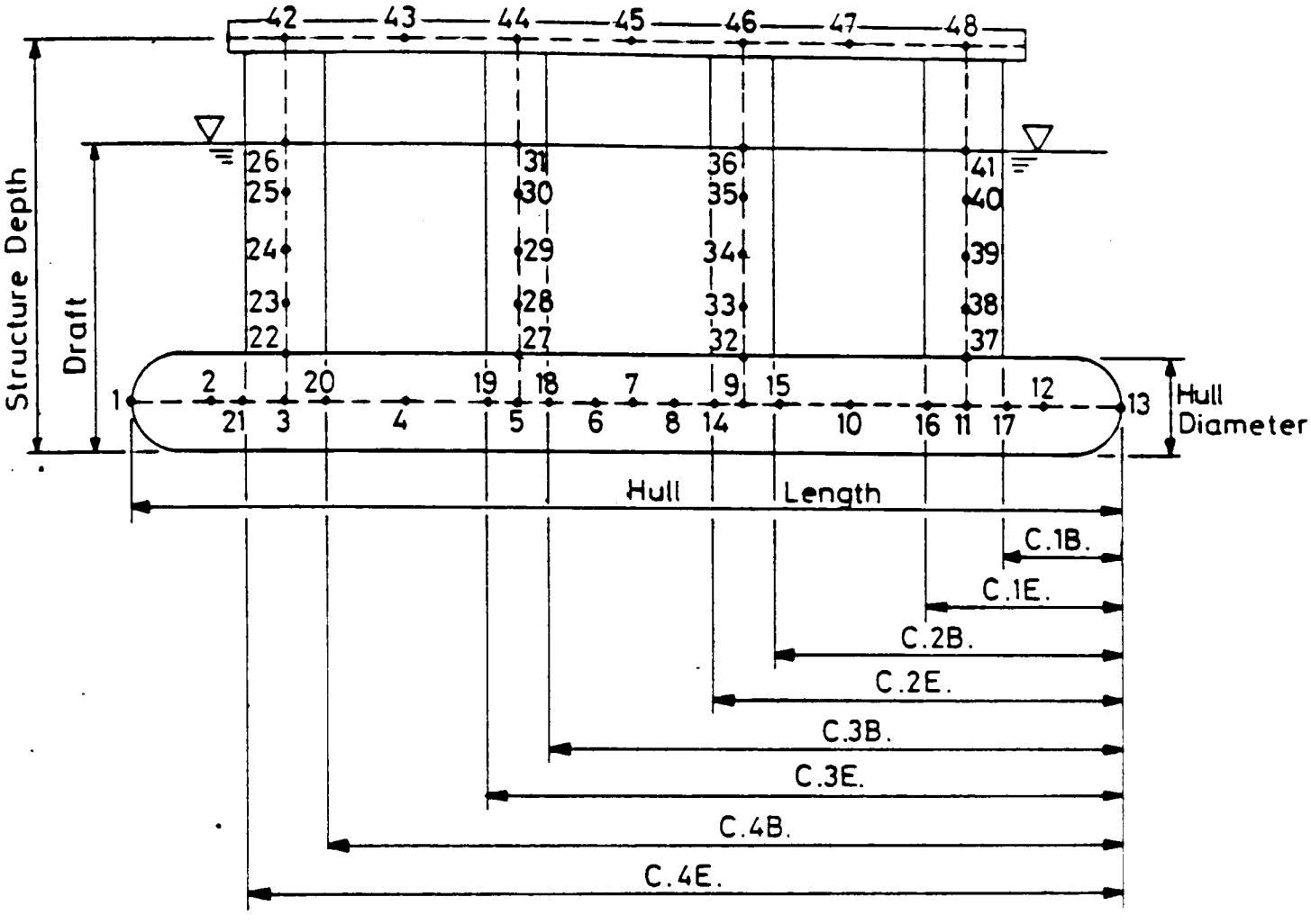

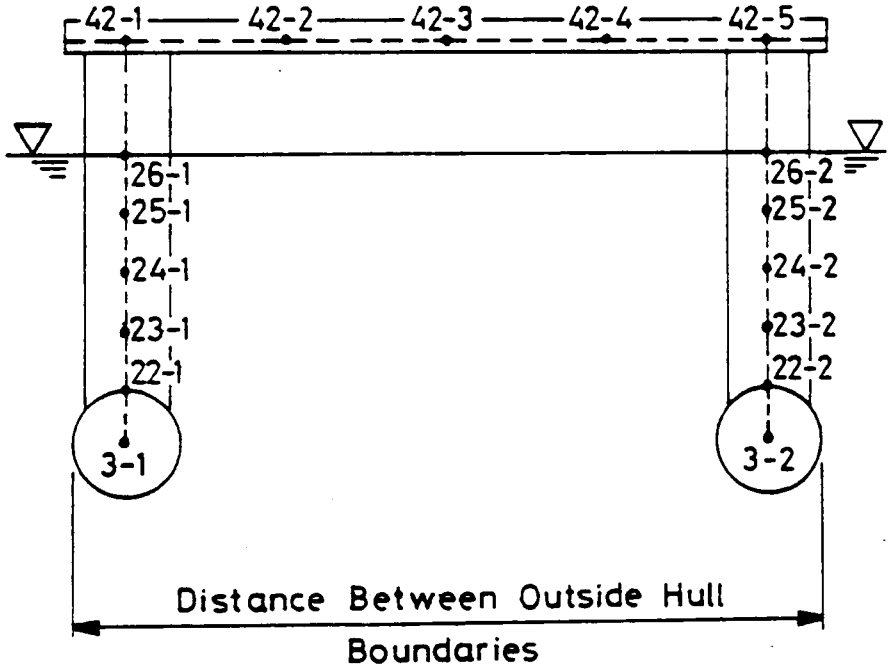


```
>RUN FLUID4A
 ENTER HULL LENTH,HULL DIAMETER *144.5,14.Ø
 ENTER THE DISTANCE BETWEEN OUTSIDE HULL BOUNDARIES *1Ø4.Ø
 ENTER STRUCTURE DEPTH AND DRAFT *57.Ø,38.Ø
 ENTER C1B,C1E,C2B,C2E,C3B,C3E,C4B,C4E *17.1,28.5,51.6,59.9,84.6,92.9,116.Ø,127.4
 ENTER WAVE HEIGTH,WAVE FREQUENCY (RAD/SEC) *1Ø.Ø,3.Ø
 ENTER CENTRE OF GRAVITY OF STRUCTURE FROM BASE LINE *25.Ø
 ENTER  ACCL. OF GRAVITY,DENSITY,VISCOSITY *981.Ø,1.Ø,1.5ØE-Ø2
 ENTER DAMPING COEFFICIENTS IN HEAVE,PITCH,ROLL *Ø.Ø5,Ø.1,Ø.1
```

Fig. 1

1.4 Subroutine FLUID2

This subroutine calculates total wave forces on the vertical circular cylindrical members which are working in any wave loading regime, such as drag, drag + inertia, inertia or diffraction. FLUID2 calls the subroutine LARGE for the wave loading calculations in the diffraction regime. For the circular cylindrical members which are working in drag or drag + inertia regimes FLUID2 divides the vertical column into 20 equal spaces along the length starting from the still water level and calculates wave particle velocity and acceleration as well as Reynolds and Keulegan-Carpenter numbers at each division. Drag coefficients and drag forces are calculated and transferred to FLUID2 by subroutine FLUID.

FLUID2 calculates the inertia coefficients at each division as a function of Keulegan-Carpenter number and the drag coefficients using the semi-empirical relations given in Figs. 2 and 3.

Once the inertia coefficients are determined FLUID2 calculates the inertia forces and the total inertia and drag forces at each division.

FLUID2 also calculates the total wave force and the moment (about the still water level) on the vertical column by carrying out the integration over the 21 divisions. Simpson's integration rule was used to perform the integrations.

FLUID2 returns the following data to subroutine COLUMN:

a) Drag and inertia coefficients on each division (Total of 21 divisions along the column length under the water)

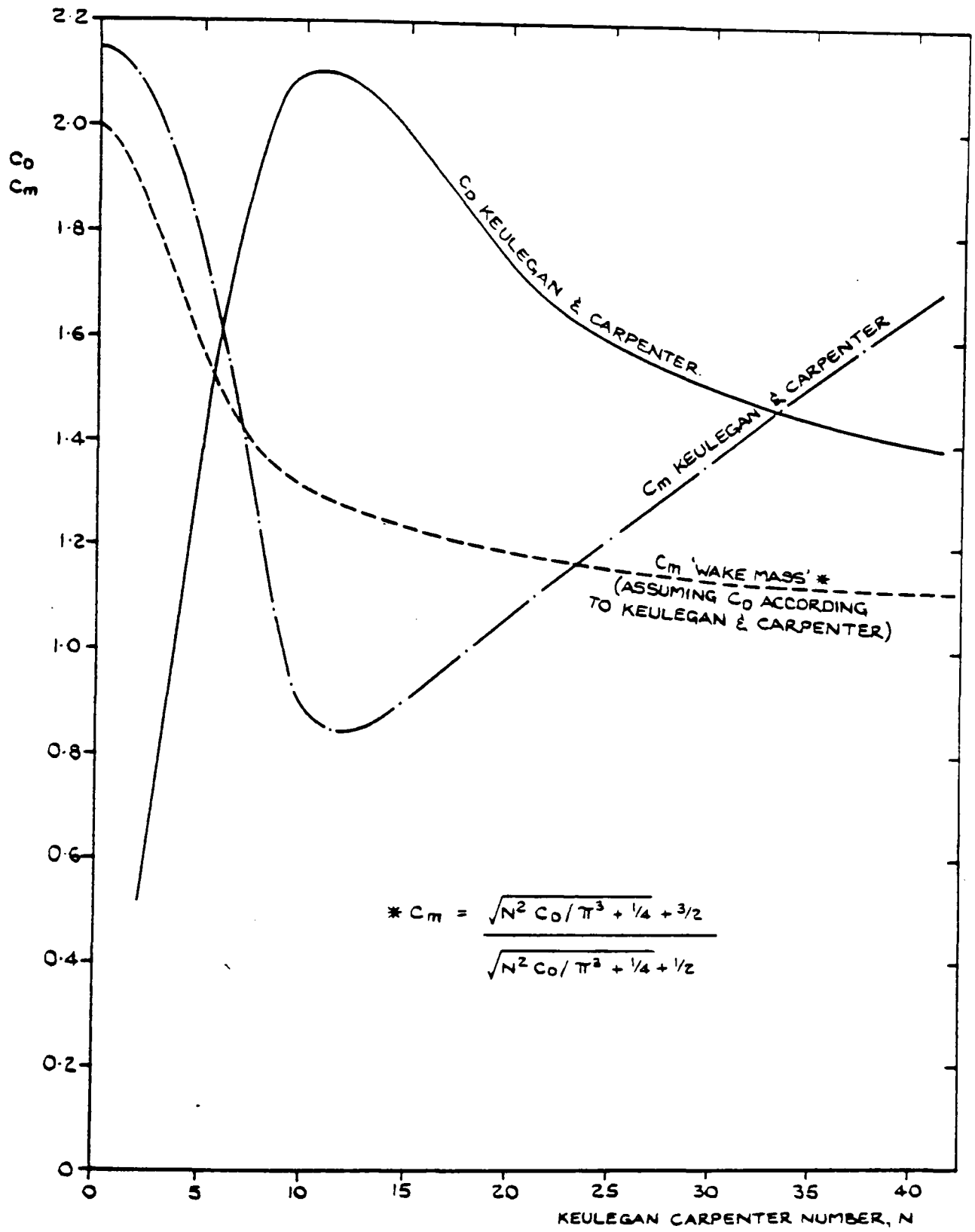

Fig. 2.

RELATION BETWEEN DRAG AND INERTIA COEFFICIENTS.

FROM REFERENCE : 2

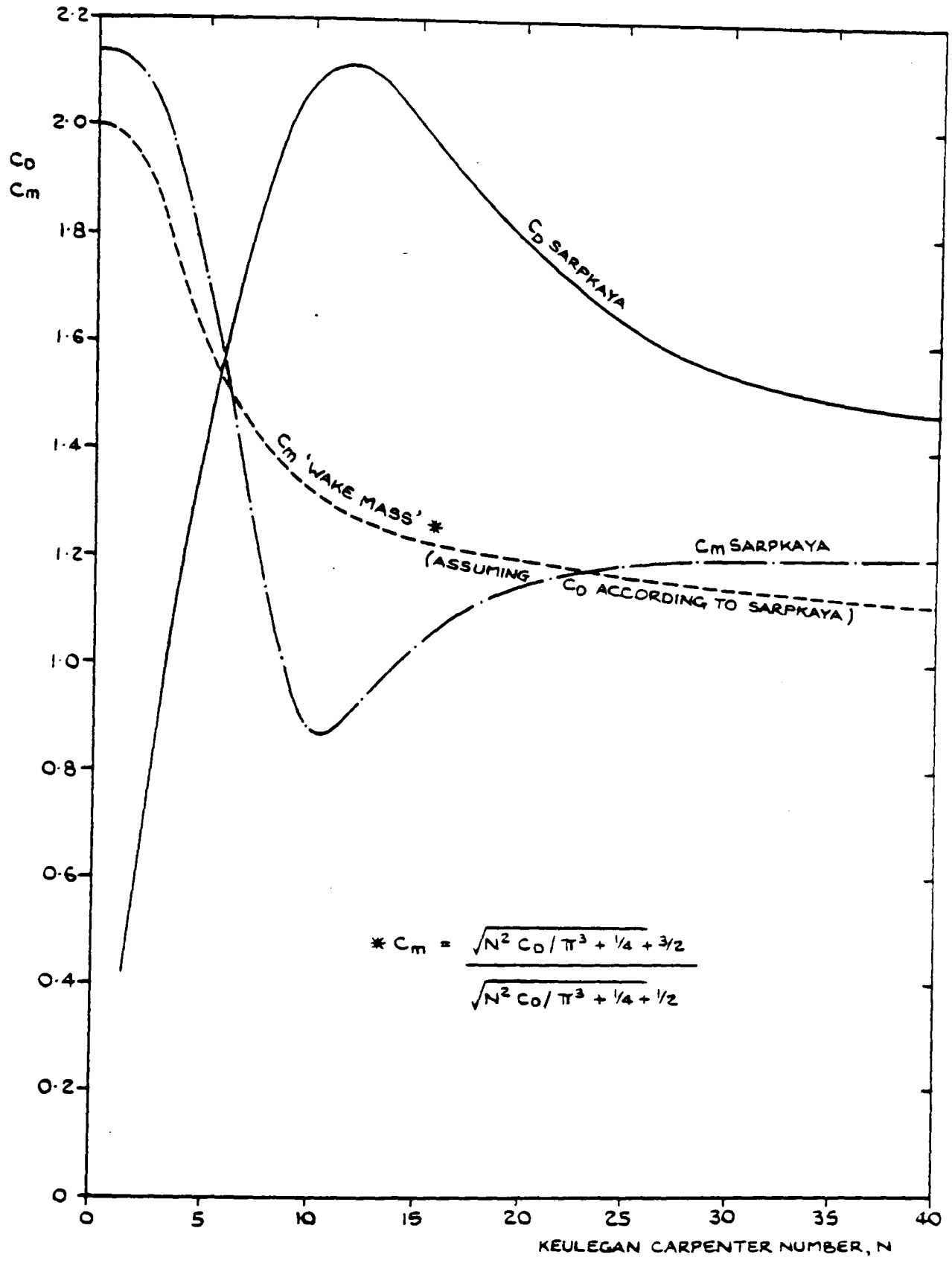

Fig. 3.

RELATION BETWEEN DRAG AND INERTIA COEFFICIENTS.

FROM REFERENCE : 2

b) Reynolds and Keulegan-Carpenter numbers on each division

c) Drag, acceleration and total forces on each division

d) Total force and moment on each vertical column

FLUID2 writes the following data into the output file:

a) Diameter over wave length ratio

b) Total drag force on the vertical column

c) Total inertia force on the vertical column

d) Total drag and inertia force on the vertical column

e) Total moment on the vertical column
(Moment is taken about the still water surface)

f) Centre of total force (from the water surface).

1.5 Subroutine LARGE

When a vertical column is working in the diffraction regime, force calculations are performed by LARGE. This subroutine uses the calculation procedure described in chapter 2 for the large diameter circular cylinders.

LARGE calls the subroutine BESSEL for the determination of the Bessel functions of the first and second kinds.

LARGE subdivides the vertical column into 20 equal spaces and determines the wave coefficients (C_M) and the total forces at each division.

LARGE also calculates the total force and the moment on the vertical large column by integrating the force values calculated on each division. Simpson's integration rule was used to perform the integrations.

LARGE writes the following data into the output file:

a) Diameter over wave length ratio

b) Total force on the large column

c) Total moment on the large column

(Moment is taken about the still water surface)

d) Centre of total force (from water surface)

1.6 Subroutine BESSEL

This subroutine calculates BESSEL functions of the first and second kinds and returns the data to LARGE for the calculation of the wave forces on large diameter circular cylinders.

1.7 Subroutine FLUID

FLUID calculates the drag coefficients and the water particle velocity induced forces on the circular cylindrical members. At the time of the writing of this computer program, the only experimental data on drag coefficients available over a large Reynolds number range, and which took into account the changes in the flow field due to the surface roughness as well as the interference effects between the closely spaced circular cylinders, were steady flow results. This design data, published in Ref. 1, was used to develop subroutine FLUID.

In order to calculate the drag coefficients for a given diameter of cylinder and a given water particle velocity using the design data presented in Ref. 1 FLUID requires the following input:

a) Kinematic viscosity of the fluid domain

b) Surface roughness ratio ε/D where ε is mean surface roughness

c) Angle between the flow velocity vector and the cylinder axis

d) The distance between the circular cylinder on which wave forces are calculated and the neighbouring cylinder which is in close proximity

e) The ratio of the mean square value of the longitudinal component of fluctuating velocity in the flow field over the water particle velocity, i.e. $\sqrt{\overline{u^2}}/V_{oo}$

f) The ratio of the diameter of a circular cylinder over the lateral integral of free-stream turbulence i.e. D/L_s.

Input requirements defined in (e) and (f) can be found in Ref. 1 for various environmental conditions.

Subroutine FLUID calculates the drag coefficients with the following steps:

1) Calculate the Reynold's number

2) If Reynold's number smaller than 10^4 obtain C_D coefficients from Fig. 8 or 9, otherwise continue with step 3

Obtain turbulence factor from Figs. 4 and 5

4) Obtain roughness factor from Fig. 6

5) Obtain C_D coefficient from Fig. 7 using Reynold's number as well as turbulence and the roughness factor

FLUID also corrects the drag coefficients obtained from the measurements taken from the single cylinder in order to take into account the interference, using the information contained in Figs. 22 and 23 of chapter 2.

If this subroutine is to be modified for the calculation of drag forces on full-scale structures, taking the interference into account, the drag coefficients obtained from the experiments which were carried out in the high Reynold's number range need to be used. Extensive model testing carried out with circular cylinder arrangements in a wind tunnel and reported in Ref. 3 could provide substantial data for the modification of this subroutine for the drag force calculations in super-critical Reynold's number ranges. However, the most reliable estimates of drag forces on a full-scale floating structure with a complex geometry could only be obtained from experiments in which the whole complex structure is tested in the super-critical Reynold's number range.

A comparison of the measurements of the forces obtained from a complex offshore structure model and the computer calculations of the forces on the same structure using the available experimental results of the simple member configurations would also provide a reliability margin for the computer calculations.

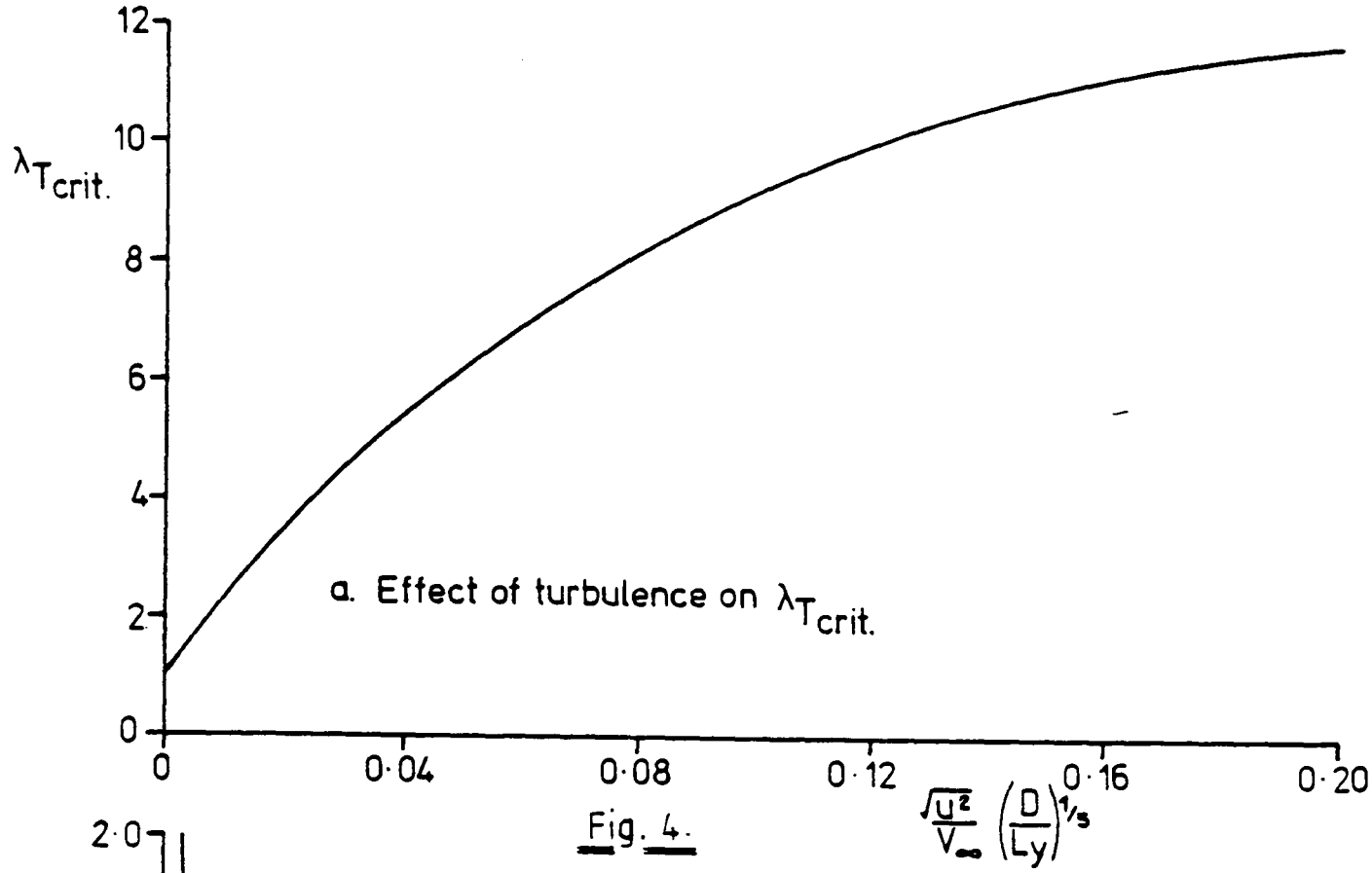

a. Effect of turbulence on $\lambda_{T_{crit.}}$

Fig. 4.

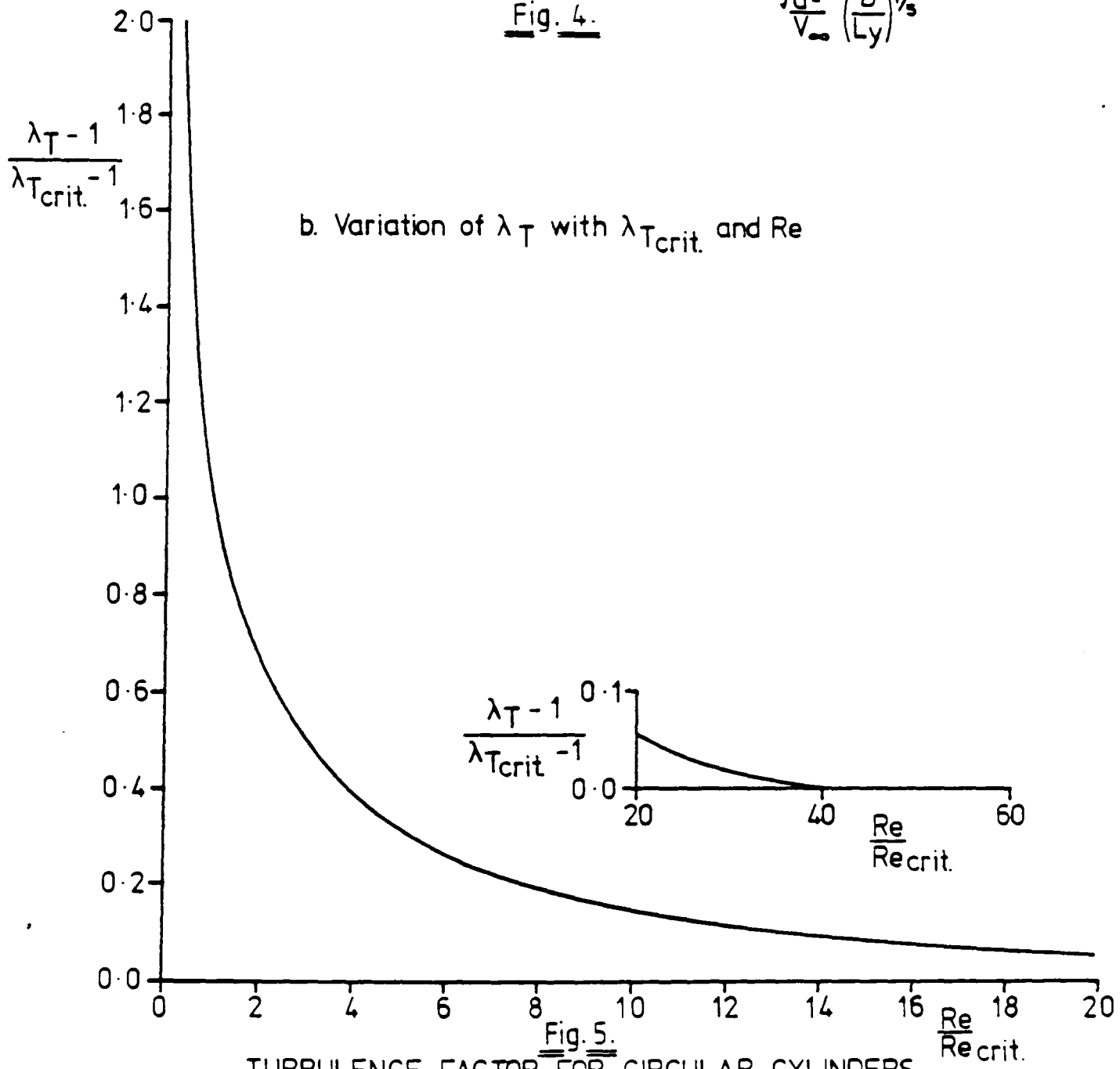

b. Variation of λ_T with $\lambda_{T_{crit.}}$ and Re

Fig. 5.

TURBULENCE FACTOR FOR CIRCULAR CYLINDERS.

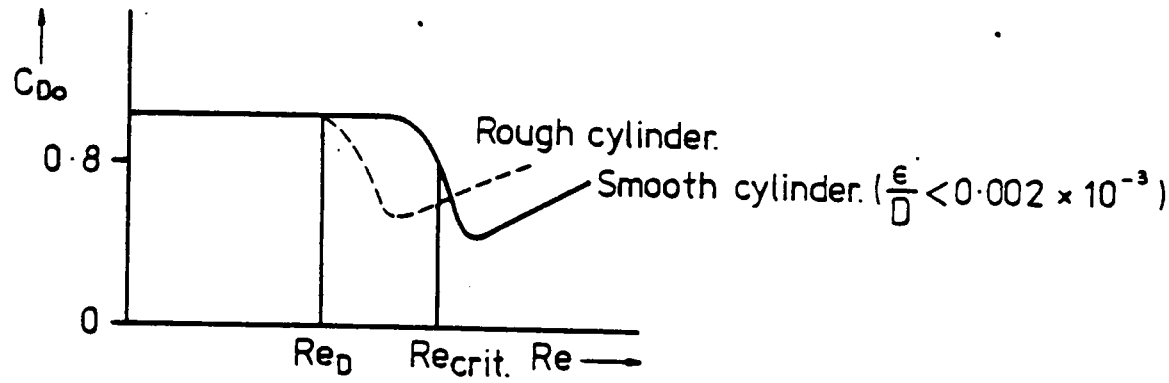

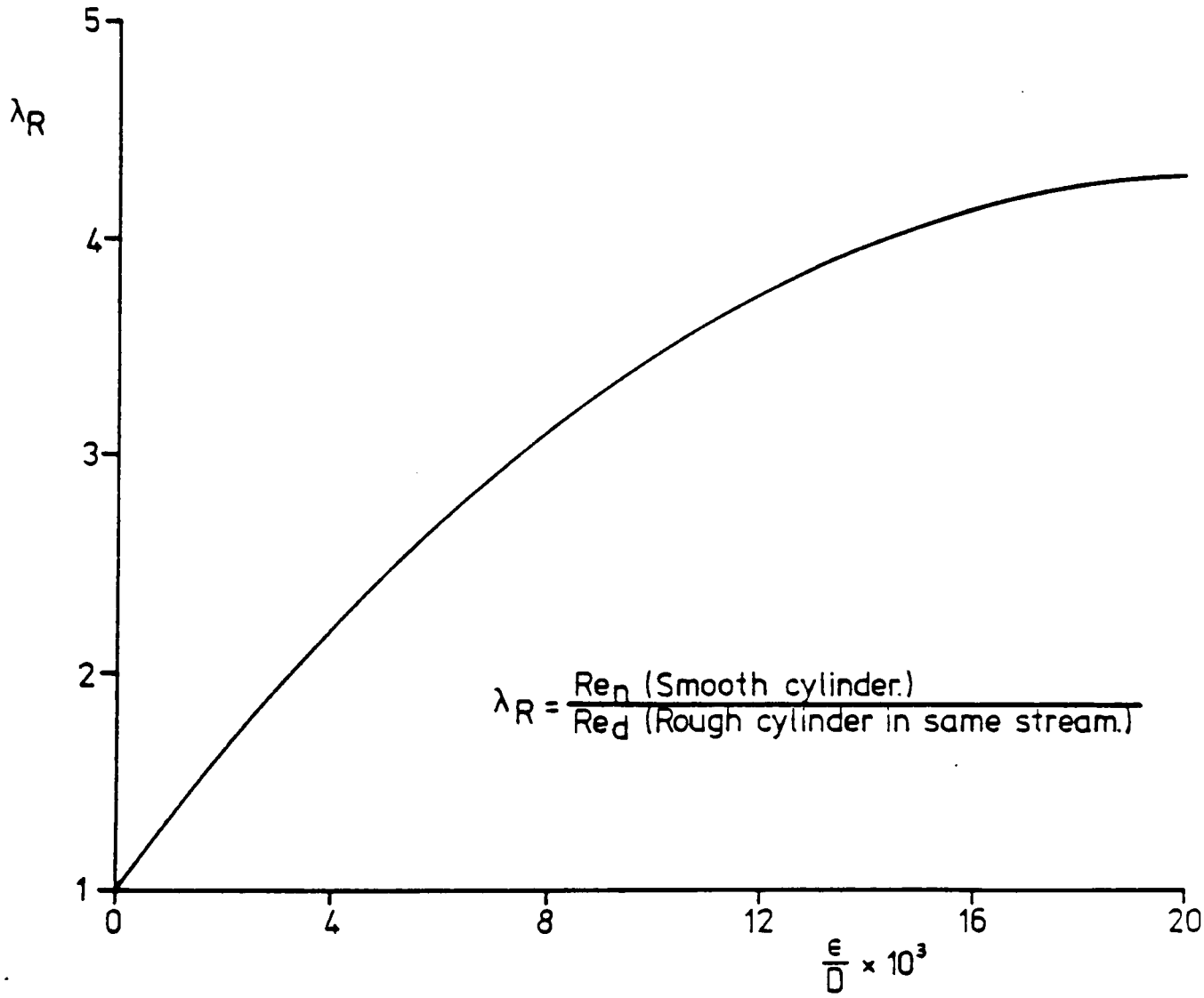

Fig. 6. :- ROUGHNESS FACTOR FOR CIRCULAR CYLINDERS.

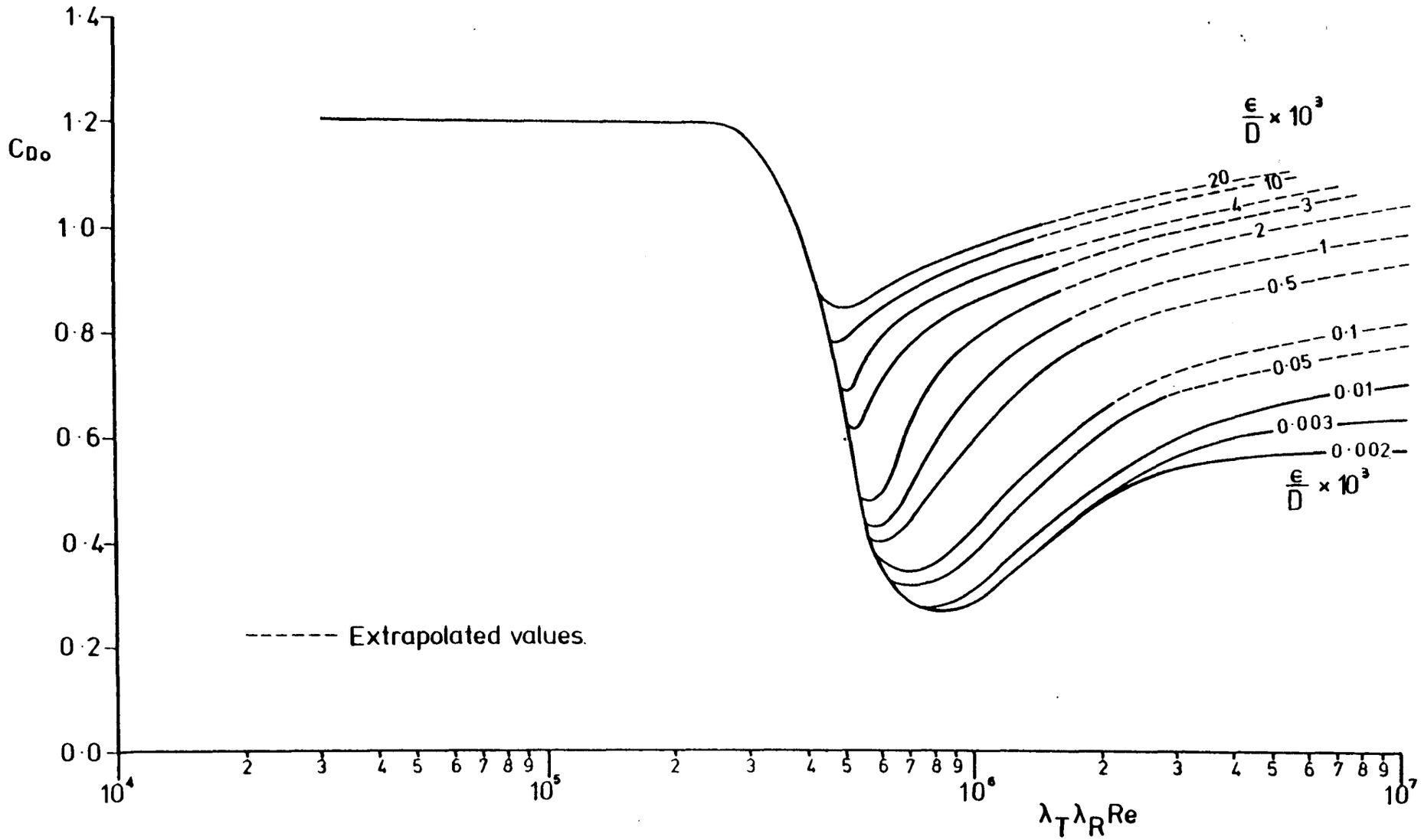

Fig. 7. – VARIATION OF C_{Do} WITH $\lambda_T \lambda_R Re$ FOR $3 \times 10^4 < \lambda_T \lambda_R Re < 10^7$

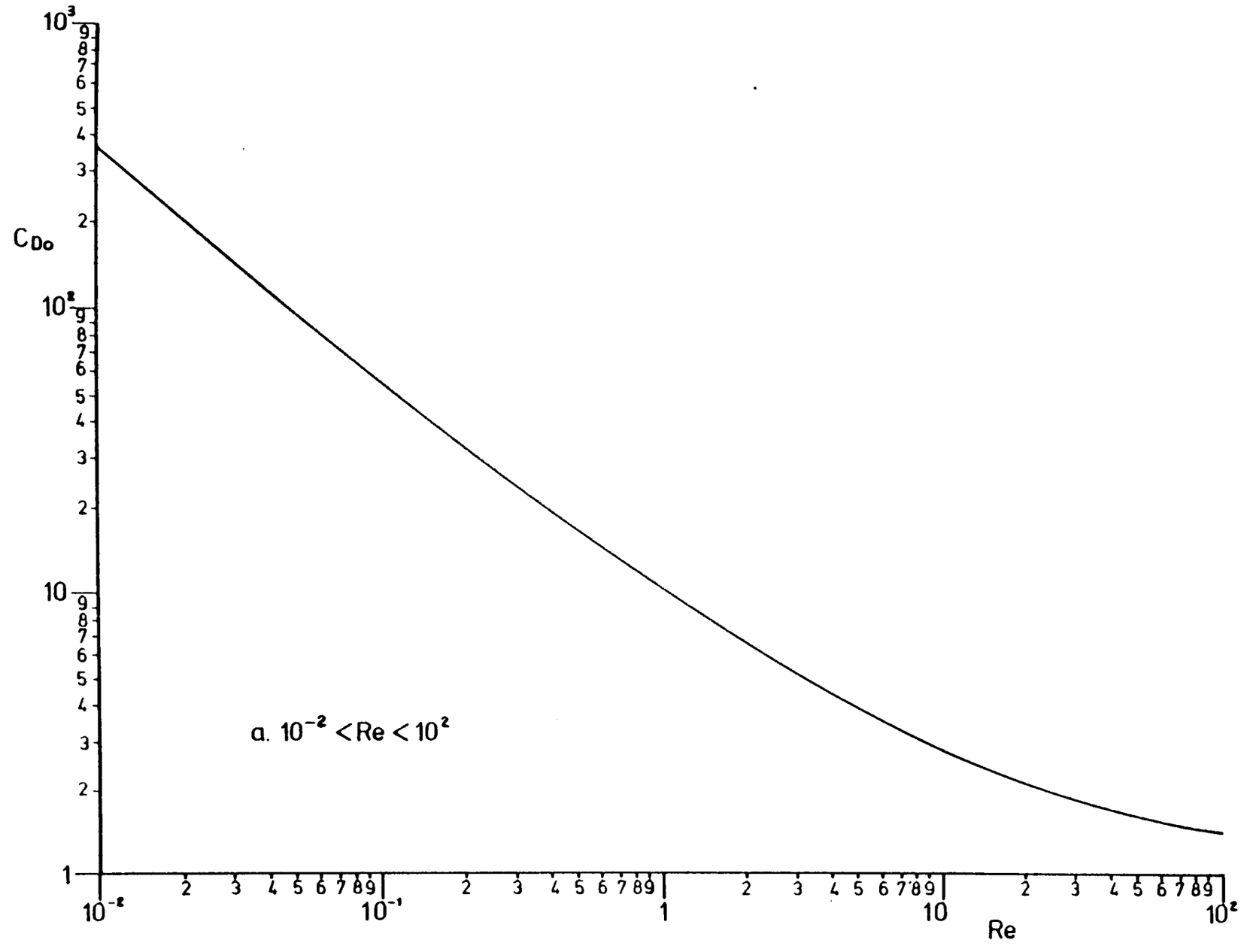

Fig. 8. - VARIATION OF C_{Do} WITH Re FOR A CIRCULAR CYLINDER.

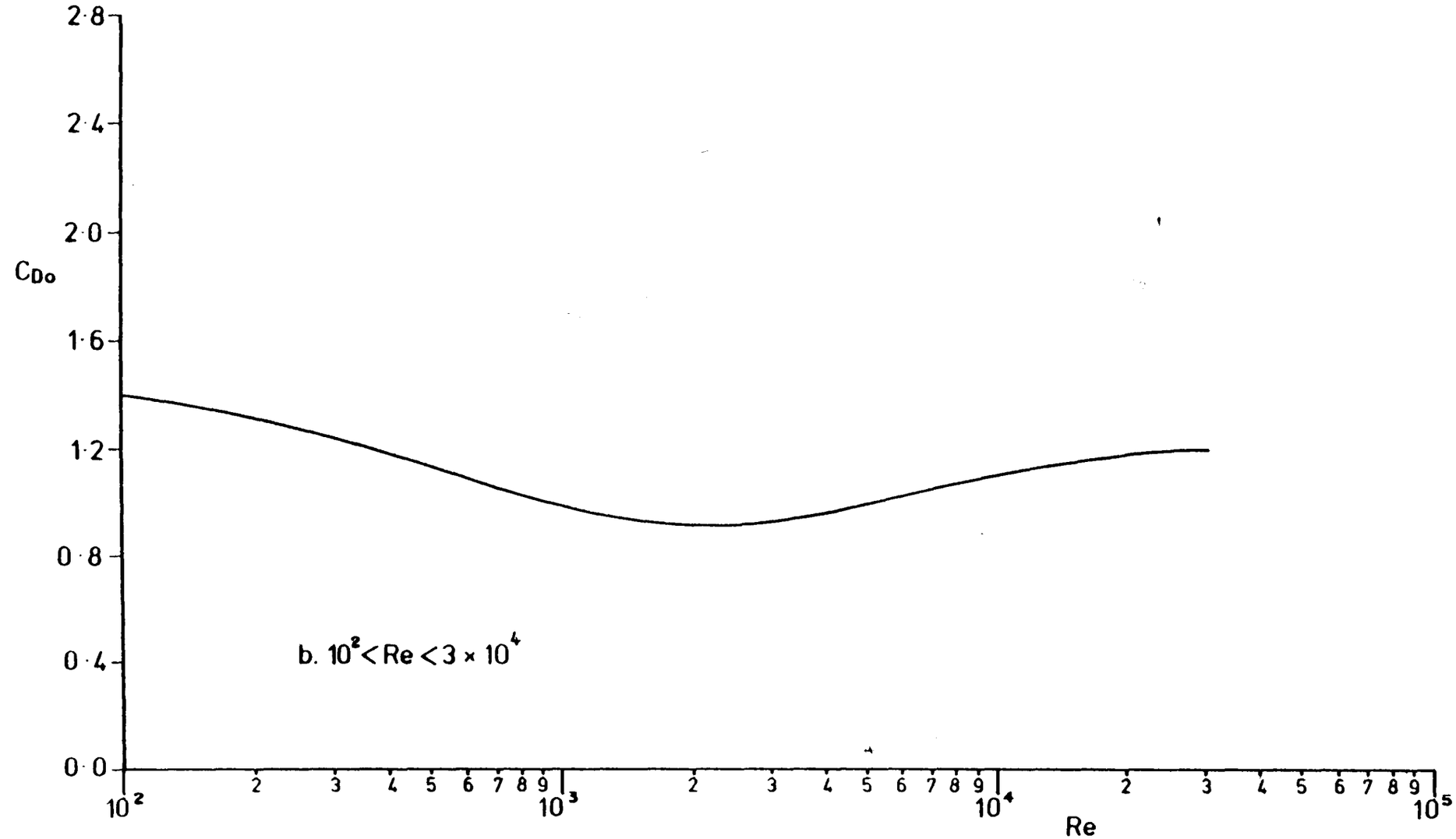

Fig. 9. (Continued)

FLUID calls the following subroutines:

1) FACE

2) REAR1, REAR2, REAR3, REAR4, REAR5

Subroutine FLUID returns the drag coefficient to the subroutine FLUID2 and writes the following data into the output file if required:

a) Reynold's number of a single cylinder, the critical Reynold's number and the corrected Reynold's number

b) A single cylinder's drag coefficient, and the drag coefficient corrected for interference

c) Total drag force on the single cylinder, and the drag force corrected for interference

1.8 Subroutine FACE

FACE calculates relative roughness (roughness height/cylinder diameter) in order to call appropriate subroutines which contain C_D values of Fig. 7. When the relative roughness value in a particular case is different for the value which is plotted in Fig. 7, FACE carries out the linear interpolation between the two C_D curves whose relative surface roughness parameters are close to the relative roughness of the particular case in question.

Subroutine FACE calls the following subroutines:

INTER1, INTER2, INTER3, INTER4, INTER5, INTER6, INTER7, INTER8, INTER9, INTR10, INTR11, INTR12.

Subroutine FACE returns the drag coefficients of a single cylinder to subroutine FLUID.

1.9 Subroutines INTER1, INTER2, INTER3, INTER4, INTER5, INTER6, INTER7, INTER8, INTER9, INTR10, INTR11, INTR12

These subroutines contain the drag coefficients for the twelve different relative surface roughness parameters given in Fig. 7. In each of these subroutines 28 drag coefficients, corresponding to Reynold's numbers which are modified by the surface roughness and the turbulence factors, were stores. These subroutines call subroutine INTER and return the single cylinder's drag coefficients to subroutine FACE.

1.10 Subroutine INTER

INTER carries out the linear interpolation between stored drag coefficients for a given modified Reynold's number and returns the interpolated value to a subroutine which calls INTER.

1.11 Subroutines REAR1, REAR2, REAR3, REAR4, REAR5

The drag coefficients of a cylinder situated behind another cylinder in a steady flow for five difference Reynold's numbers (Fig. 22 of chapter 2) are stored, for varying spacings between the cylinders, in subroutines REAR1, REAR2, REAR3, REAR4, REAR5.

When the Reynold's number of a particular cylinder is different from the value plotted in Fig. 22 of chapter 2, these subroutines carry out a linear interpolation between the two C_D curves whose Reynold's number parameters are close to the Reynold's number of the particular cylinder in question.

These subroutines return the drag coefficients of a rear cylinder to subroutine FLUID.

For the purpose of linear interpolation between the Reynold's numbers REAR2 calls REAR1, REAR3 calls REAR2, REAR4 calls REAR3 and REAR5 calls REAR4.

1.12 Subroutine MOT

This subroutine basically re-arranges the geometrical data to be used for subroutines HYDROS and NAT. The geometrical particulars of the semi-submersible are passed to MOT from FLUID4.

MOT calls subroutines HYDROS and NAT and returns the calculated values to FLUID4A and to NAT.

1.13 Subroutine HYDROS

Subroutine HYDROS was written in order to generate data for the construction of the hydrostatic curves of a twin-circular hulled semi-submersible with 8 columns and bracings (see Table 1). HYDROS divides the draft into 20 equal levels and it calculates the following variables at each level:

a) Cubic displacement

b) Mass displacement

c) Vertical centre of buoyancy

d) Longitudinal centre of buoyancy

e) Transverse BM

f) Longitudinal BM

g) Water plane area

h) Total wetted surface area

HYDROS calls the subroutine HYDRO and returns the calculated values to subroutine MOT.

HEIGHT	DISPLACEMENT (CM*3)	DISPLACEMENT (GRS)	KB	LCB
2.25	4612.95	4728.27	1.33	72.25
4.50	12337.11	12645.54	2.64	72.25
6.75	21221.49	21752.02	3.89	72.25
9.00	26335.95	26994.34	4.56	72.25
11.25	31472.25	32259.06	4.62	72.25
13.50	39092.08	40069.38	5.48	72.25
15.75	45558.22	46697.17	7.19	72.25
18.00	46963.09	48137.17	7.48	72.25
20.25	48367.97	49577.17	7.82	72.25
22.50	49772.84	51017.16	8.20	72.25
24.75	51177.72	52457.16	8.62	72.25
27.00	52582.60	53897.16	9.08	72.25
29.25	53987.47	55337.16	9.58	72.25
31.50	55392.35	56777.16	10.11	72.25
33.75	56797.22	58217.15	10.66	72.25
36.00	58202.10	59657.15	11.25	72.25
38.25	59606.97	61097.14	11.86	72.25
40.50	61011.85	62537.14	12.49	72.25
42.75	62416.72	63977.14	13.15	72.25
45.00	63821.60	65417.14	13.82	72.25

HEIGHT	BM	BML	WATER PLANE AREA	TOTAL SURFACE AREA
2.25	2689.01	4484.09	2971.93	3334.65
4.50	544.72	533.01	3779.17	4874.59
6.75	339.21	331.53	4043.42	6207.69
9.00	261.92	256.18	3877.34	7524.56
11.25	181.25	177.74	3214.92	8992.07
13.50	67.85	66.84	1501.69	11169.17
15.75	23.97	23.34	624.39	13137.45
18.00	23.26	22.64	624.39	13694.17
20.25	22.58	21.98	624.39	14250.89
22.50	21.94	21.36	624.39	14807.61
24.75	21.34	20.78	624.39	15364.33
27.00	20.77	20.22	624.39	15921.06
29.25	20.23	19.70	624.39	16477.78
31.50	19.72	19.20	624.39	17034.50
33.75	19.23	18.72	624.39	17591.22
36.00	18.77	18.27	624.39	18147.95
38.25	18.32	17.84	624.39	18704.67
40.50	17.90	17.43	624.39	19261.39
42.75	17.50	17.04	624.39	19818.11
45.00	17.11	16.66	624.39	20374.83

TABLE 1

1.14 Subroutine HYDRO

Subroutine HYDRO calculates the hydrostatic variables listed in section 1.13 for a given draft level. In addition for the whole structure, if required, HYDRO writes the following information into the data file for each member of a semi-submersible:

a) Co-ordinates

b) Volume

c) Volume centre

d) Wetted surface area

HYDRO returns the calculated values to subroutine HYDROS.

1.15 Subroutine NAT

Subroutine NAT calculates the added-mass in the heave mode and the mass moment of inertia, as well as the added mass moment of inertia in the roll and pitch modes, using the formulations given in chapter 4.

NAT also calculates the natural frequency of the structure in the heave, roll and pitch modes using the hydrostatic data calculated by HYDROS.

NAT calls the subroutine FIT and returns the calculated values to MOT.

1.16 Subroutine FIT

Subroutine FIT contains the curve-fit form of the added-mass and added-mass moment of inertia data for vertically oscillating rectangular strips in unbounded fluid. FIT returns the added-mass and added-mass moment of inertia coefficients to subrountine NAT.

1.17 Subroutine MOT1

Subroutine MOT1 calculates the heave and the pitch responses of a twin circular hulled semi-submersible in head sea condition. In addition to the response values, it also calculates the heave and pitch rigid-body accelerations and the phase angles between the exciting force and the motion. MOT1 is based on the calculation procedure to determine the motion response of single degree of freedom system which was discussed in chapter 4.

Subroutine MOT1 writes the following data into the output file:

a) Heave response and translational rigid-body acceleration of centre of rotation in head sea condition

b) Pitch response and rotational rigid-body acceleration in head sea condition

c) Motion response operators, i.e. Heave response/ wave height, Pitch response/wave height

d) Phase angle between the heave force and heave response and phase angle between the pitching moment and pitch response.

1.18 Subroutine MOT2

Similarly to MOT1, subroutine MOT2 calculates the heave and roll responses of a twin circular hulled semi-submersible in beam sea condition.

MOT2 writes the following data into the output file:

a) Heave response and translational rigid-body acceleration of the centre of rotation in beam sea condition

b) Roll response and rotational rigid-body acceleration in beam sea condition

c) Motion response operators, i.e. Heave response/wave height, Roll response/wave height

1.19 Subroutine FRAN1

Subroutine FRAN1 calculates the maximum axial force, shear force and bending moment values at the deck of a twin circular hulled semi-submersible model. The model represents a determinate structure and FRAN1 uses the formulation given in chapter 5 for a determinate structure with restrained boundary conditions.

FRAN1 writes the following data into the output file:

a) Maximum axial force on the deck

b) Maximum shear force on the deck

c) Maximum bending moment on the deck

d) Maximum bending moment/wave height

Table 2 summarises overlay tree of program FLUID4.

As more data on wave coefficients become available from either laboratory experiments or full-scale measurements, relevant subroutine modules can easily be replaced with improved ones for better simulation of the motion and structural response of twin circular hulled semi-submersibles.

TABLE 2

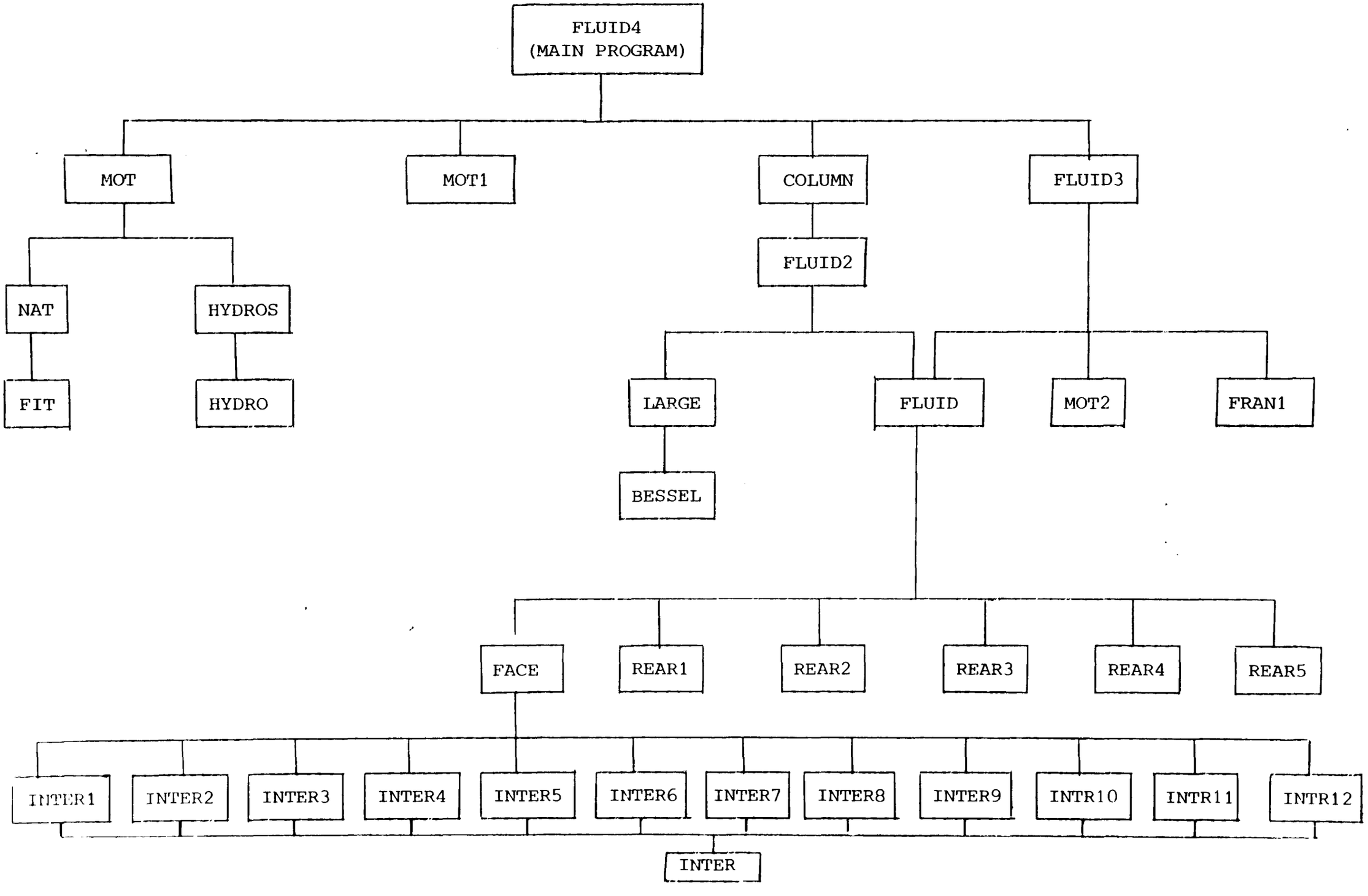
FLUID4
(MAIN PROGRAM)
MOT
MOT1
COLUMN
FLUID3
NAT
HYDROS
FLUID2
FIT
HYDRO
LARGE
FLUID
MOT2
FRAN1
BESSEL
FACE
REAR1
REAR2
REAR3
REAR4
REAR5
INTER1
INTER2
INTER3
INTER4
INTER5
INTER6
INTER7
INTER8
INTER9
INTR10
INTR11
INTR12
INTER

Subroutine FLUID2 and the associated subroutine modules can be easily adopted to any other program with which the calculation of wave loading on a circular cylinder is sought. Similarly, subroutine FLUID and the associated subroutine modules can be adapted to any other program with which the current-drag or wind-drag forces on circular cylinders are to be predicted.

2. DESCRIPTION OF INPUT AND OUTPUT DATA

2.1 Input Data

The input data consists of the geometrical characteristics of the platform, as well as the wave particulars. Additional data in relation to the flow field and the control parameters for the output files were included as fixed data in FLUID4A in order to minimise the input information for frequency domain calculations. The variables of fixed data are defined as follows:

U : Control number. If U = 1.0, subroutine FLUID writes the data described in seciton 1.7 into the output file. If U = 2.0, this data is not written into the output file.

TF : Turbulence factor which is defined as the mean square value of the longitudinal component of the fluctuating velocity in the flow field over the water particle velocity. Appropriate values for TF can be found in Table I of Ref. 1.

TS : Turbulence scale which is defined as the ratio of the diameter of the circular cylinder over the lateral integral of free-stream turbulence. Appropriate values for TS can also be found in Table I of Ref. 1.

A : The angle between the axis of a circular cylinder and the flow direction.

AS : The distance between the circular cylinder on which wave forces are calculated and the nearest neighbouring circular cylinder.

SR : Surface roughness ratio. This value can be calculated using the typical effective roughness height of various materials given in Table II of Ref. 1.

PC : Control number to identify the position of the cylinder for drag force calculations by taking the interference into account. If PC = 1.0, cylinders are situated one behind the other, and if PC = 2.0, cylinders are situated side by side.

The units system used in the program is summarised in Table 3. The input data should be compatible with these units.

UNIT		FULL-SCALE	MODEL-SCALE
LENGTH	:	Meters	Centimeters
AREA	:	Meter-square	Cms-square
DISPLACEMENT (CUBIC)	:	Meter-cub	Cms-cub
DISPLACEMENT (MASS)	:	Tons	Grams
ACCELERATION	:	m/sn^2	cm/sn^2
DENSITY	:	$Tons/m^3$	Grs/cm^3
VISCOSITY	:	m^2/sn	cm^2/sn
DAMPING COEFFICIENTS	:	Non-dimensional	
FREQUENCY	:	Rad./sec.	Rad./sec.
FORCE	:	K-Newtons	Dyns
MOMENT	:	KN-Meters	Dyn-cms

TABLE 3

The input data required to run FLUID4A is prompted by the main programme on the user's terminal as seen in Fig. 1. The user has to enter the data after the asterisks.

2.2 Output Data

FLUID4A was run for the geometry of twin circular hulled semi-submersible model whose details are given in Appendix 1. The typical output of this run is shown in Table 4. The motion and the structural response values calculated using FLUID4A were shown in chapters 4 and 5.respectively.

The variable names used in the output can be interpreted as follows:

T_1/T : The ratio of instantaneous time during a wave cycle to the wave period

VHPF : Vertical wave pressure force on the hull

VHAF : Vertical wave acceleration force on the hull

THF : Total wave force on the hull

VCF : Total wave force on the column

TF : Total vertical wave force on the hull and column (Head sea condition)

THFI : Integration of TF along the hull length

HHPF : Horizontal wave pressure force on the hull

HHAF : Horizontal wave acceleration force on the hull

HHVF : Horizontal wave velocity force on the hull

THHF : Total horizontal wave force on the hull (Beam Sea condition)

TVF	:	Total vertical wave force on the hull and column (Beam sea condition)
CD	:	Drag coefficient
CM	:	Inertia coefficient
REN	:	Reynold's number
CKN	:	Keulegan-Carpenter number

WAVE LOADING, MOTION AND STRUCTURAL RESPONSE CALCULATIONS
FOR TWIN HULL TYPE SEMI-SUBMERSIBLES

GEOMETRICAL DATA:

LENGTH OF STRUCTURE=144.50 DEPTH OF STRUCTURE= 57.00
WIDTH OF STRUCTURE=104.00
DRAFT= 38.00 PONTOON DIAMETER= 14.00
DIAMETER OF COLUMNS= 11.40, 8.30
DISPT= 59606.82 GM= 6.22 GML= 4.44
NATURAL HEAVING FREQUENCY= 2.36
NATURAL ROLLING FREQUENCY= 1.15
NATURAL PITCHING FREQUENCY= 1.12
WAVE DATA:

WAVE HEIGHT= 10.00
WAVE FREQUENCY= 3.00 (RAD/SEC)
ACCL.OF GRAVITY=981.00
DENSITY= 1.00
VISCOSITY=0.15E-01
W A V E L O A D I N G

H E A D S E A S

TOTAL VERTICAL FORCES AND MOMENTS ON THE HULL

TABLE 4

T1/T=0.000

TOTAL HULL FORCE= -1396991.37
TOTAL COLUMN FORCE= 1181472.75
TOTAL HULL+COLUMN FORCE= -215518.63
CENTRE OF TOTAL FORCE= -0.00
TOTAL FORCES ON THE STRUCTURE= -431037.25
TOTAL MOMENT ON THE STRUCTURE= 12.00

NODES	VHPF	VHAF	THF	VCF	TF	THFI	THMI
1	-4106.62	-4106.62	-8213.24	0.00	-8213.24	0.00	0.00
2	-4418.87	-4418.87	-8837.74	0.00	-8837.74	-97190.59	6447744.00
21	-4557.08	-4557.08	-9114.16	32833.75	23719.59	-148353.50	9412948.00
3	-4682.83	-4682.83	-9365.65	32833.75	23468.09	-201020.97	12165414.00
20	-4795.77	-4795.77	-9591.54	32833.75	23242.20	-255049.00	14681285.00
4	-4984.15	-4984.15	-9968.30	0.00	-9968.30	-368007.09	18958304.00
19	-5116.61	-5116.61	-10233.23	26076.08	15842.86	-484670.91	22032310.00
5	-5150.25	-5150.25	-10300.50	26076.08	15775.58	-527278.44	22823454.00
18	-5176.42	-5176.42	-10352.84	26076.08	15723.24	-570134.13	23441422.00
6	-5194.91	-5194.91	-10389.82	0.00	-10389.82	-612656.56	23879248.00
7	-5209.83	-5209.83	-10419.65	0.00	-10419.65	-698495.69	24232826.00
8	-5194.91	-5194.91	-10389.82	0.00	-10389.82	-784334.81	23879248.00
14	-5176.42	-5176.42	-10352.84	26076.08	15723.24	-826857.25	23441422.00
9	-5150.25	-5150.25	-10300.50	26076.08	15775.58	-869712.94	22823454.00
15	-5116.61	-5116.61	-10233.23	26076.08	15842.86	-912320.44	22032310.00
10	-4984.15	-4984.15	-9968.30	0.00	-9968.30	-1028984.25	18958306.00
16	-4795.77	-4795.77	-9591.54	32833.75	23242.21	-1141942.37	14681288.00
11	-4682.83	-4682.83	-9365.65	32833.75	23468.10	-1195970.37	12165417.00
17	-4557.08	-4557.08	-9114.15	32833.75	23719.60	-1248637.87	9412952.00
12	-4418.87	-4418.87	-8837.74	0.00	-8837.74	-1299800.75	6447749.00
13	-4106.62	-4106.62	-8213.24	0.00	-8213.24	-1396991.37	6.00

COLUMN NUMBER=1

NODES	CD	CM	REN	CKN
22	1.08	1.87	9147.04	2.21
23	1.09	1.86	9664.66	2.34
24	1.10	1.84	10211.57	2.47
25	1.12	1.83	10789.44	2.61
26	1.13	1.82	11400.00	2.75

NODES	TDF	TAF	TCF
22	720.45	-3020.18	-2299.73
23	813.57	-3169.72	-2356.15
24	918.60	-3325.02	-2406.41
25	1037.09	-3486.18	-2449.09
26	1170.38	-3653.39	-2483.00

DIAMETER/WAVE LENGTH= 0.02
SINCE D/L<0.2 MORISON EQ. IS USED
DRAG FORCE ON THE CIRCULAR CYLINDER= 22260.982
ACCL. FORCE ON THE CIRCULAR CYLINDER= -79894.438
TOTAL FORCE ON THE CIRCULAR CYLINDER= -57633.453
TOTAL MOMENT ON THE CIRCULAR CYLINDER= -682734.312
CENTRE OF TOTAL FORCE= 11.846 (FROM WATER SURFACE)

COLUMN NUMBER=2

NODES	CD	CM	REN	CKN
27	1.01	1.80	6659.69	3.04
28	1.02	1.79	7036.55	3.21
29	1.03	1.77	7434.74	3.39
30	1.05	1.75	7855.47	3.58
31	1.06	1.74	8300.00	3.78

NODES	TDF	TAF	TCF
27	594.93	-531.42	63.50
28	671.24	-556.44	114.79
29	757.69	-582.33	175.36
30	855.42	-609.12	246.30
31	965.91	-636.84	329.07

DIAMETER/WAVE LENGTH= 0.01
SINCE D/L<0.2 MORISON EQ. IS USED
DRAG FORCE ON THE CIRCULAR CYLINDER= 18365.928
ACCL. FORCE ON THE CIRCULAR CYLINDER= -13990.322
TOTAL FORCE ON THE CIRCULAR CYLINDER= 4375.605
TOTAL MOMENT ON THE CIRCULAR CYLINDER= 39829.582
CENTRE OF TOTAL FORCE= 9.103 (FROM WATER SURFACE)

TABLE 4 (Cont'd)

COLUMN NUMBER=3

NODES	CD	CM	REN	CKN
32	1.01	1.80	6659.69	3.04
33	1.02	1.79	7036.55	3.21
34	1.03	1.77	7434.74	3.39
35	1.05	1.75	7855.47	3.58
36	1.06	1.74	8300.00	3.78

NODES	TDF	TAF	TCF
32	594.93	531.42	1126.35
33	671.24	556.44	1227.68
34	757.69	582.33	1340.02
35	855.42	609.12	1464.54
36	965.91	636.84	1602.75

DIAMETER/WAVE LENGTH= 0.01
SINCE D/L<0.2 MORISON EQ. IS USED
DRAG FORCE ON THE CIRCULAR CYLINDER= 18365.928
ACCL. FORCE ON THE CIRCULAR CYLINDER= 13990.322
TOTAL FORCE ON THE CIRCULAR CYLINDER= 32356.248
TOTAL MOMENT ON THE CIRCULAR CYLINDER= 365479.625
CENTRE OF TOTAL FORCE= 11.295 (FROM WATER SURFACE)

COLUMN NUMBER=4

NODES	CD	CM	REN	CKN
37	1.08	1.87	9147.04	2.21
38	1.09	1.86	9664.66	2.34
39	1.10	1.84	10211.57	2.47
40	1.12	1.83	10789.44	2.61
41	1.13	1.82	11400.00	2.75

NODES	TDF	TAF	TCF
37	720.45	3020.18	3740.63
38	813.57	3169.72	3983.28
39	918.60	3325.02	4243.62
40	1037.09	3486.18	4523.27
41	1170.39	3653.39	4823.77

DIAMETER/WAVE LENGTH= 0.02
SINCE D/L<0.2 MORISON EQ. IS USED
DRAG FORCE ON THE CIRCULAR CYLINDER= 22260.984
ACCL. FORCE ON THE CIRCULAR CYLINDER= 79894.438
TOTAL FORCE ON THE CIRCULAR CYLINDER= 102155.430
TOTAL MOMENT ON THE CIRCULAR CYLINDER= 1173957.625
CENTRE OF TOTAL FORCE= 11.492 (FROM WATER SURFACE)

TOTAL HORIZONTAL COLUMN FORCES= 81253.83
TOTAL HORIZONTAL COLUMN MOMENTS= 896532.50

TOTAL COLUMN FORCE ON THE STRUCTURES= 162507.66
TOTAL COLUMN MOMENT ON THE STRUCTURES= 1793065.00
CENTRE OF TOTAL FORCE= 11.03

M O T I O N R E S P O N S E

HEAVE RESPONSE=	-1.23	PITCH RESPONSE=	0.01
HEAVE ACCELERATION=	11.07	PITCH ACCELERATION=	-0.00
HEAVE RESPONSE/H=	-0.12	PITCH RESPONSE/H=	0.00
PHASE ANGLE B.F.H=	-11.71	PHASE ANGLE B.F.P=	-4.95

TABLE 4 (Cont'd)

B E A M S E A S

TOTAL FORCES AND MOMENTS ON THE HULLS

T1/T=0.000

TOTAL VERTICAL HULL FORCE= -2758283.00
TOTAL VERTICAL COLUMN FORCE= 2327931.50
TOTAL HULL+COLUMN FORCES= -430351.50

TOTAL HORIZONTAL HULL FORCE= 240434.44
TOTAL HORIZONTAL HULL MOMENT= 7453467.50
CENTRE OF TOTAL HORIZONTAL FORCE= 31.00 (FROM WATER SURFACE)

HULL NUMBER=1

NODES	VHPF	VHAF	TVHF	VCF	TVF
1	-4772.12	-4772.12	-9544.23	0.00	-9544.23
2	-4772.12	-4772.12	-9544.23	0.00	-9544.23
21	-4772.12	-4772.12	-9544.23	33459.80	23915.57
3	-4772.12	-4772.12	-9544.23	33459.80	23915.57
20	-4772.12	-4772.12	-9544.23	33459.80	23915.57
4	-4772.12	-4772.12	-9544.23	0.00	-9544.23
19	-4772.12	-4772.12	-9544.23	24161.56	14617.33
5	-4772.12	-4772.12	-9544.23	24161.56	14617.33
18	-4772.12	-4772.12	-9544.23	24161.56	14617.33
6	-4772.12	-4772.12	-9544.23	0.00	-9544.23
7	-4772.12	-4772.12	-9544.23	0.00	-9544.23
8	-4772.12	-4772.12	-9544.23	0.00	-9544.23
14	-4772.12	-4772.12	-9544.23	24161.56	14617.33
9	-4772.12	-4772.12	-9544.23	24161.56	14617.33
15	-4772.12	-4772.12	-9544.23	24161.56	14617.33
10	-4772.12	-4772.12	-9544.23	0.00	-9544.23
16	-4772.12	-4772.12	-9544.23	33459.80	23915.57
11	-4772.12	-4772.12	-9544.23	33459.80	23915.57
17	-4772.12	-4772.12	-9544.23	33459.80	23915.57
12	-4772.12	-4772.12	-9544.23	0.00	-9544.23
13	-4772.12	-4772.12	-9544.23	0.00	-9544.23

NODES	HHPF	HHAF	HHVF	THHF
1	2090.27	2090.27	831.95	5012.49
2	2090.27	2090.27	831.95	5012.49
21	2090.27	2090.27	831.95	5012.49
3	2090.27	2090.27	831.95	5012.49
20	2090.27	2090.27	831.95	5012.49
4	2090.27	2090.27	831.95	5012.49
19	2090.27	2090.27	831.95	5012.49
5	2090.27	2090.27	831.95	5012.49
18	2090.27	2090.27	831.95	5012.49
6	2090.27	2090.27	831.95	5012.49
7	2090.27	2090.27	831.95	5012.49
8	2090.27	2090.27	831.95	5012.49
14	2090.27	2090.27	831.95	5012.49
9	2090.27	2090.27	831.95	5012.49
15	2090.27	2090.27	831.95	5012.49
10	2090.27	2090.27	831.95	5012.49
16	2090.27	2090.27	831.95	5012.49
11	2090.27	2090.27	831.95	5012.49
17	2090.27	2090.27	831.95	5012.49
12	2090.27	2090.27	831.95	5012.49
13	2090.27	2090.27	831.95	5012.49

TABLE 4 (Cont'd)

HULL NUMBER=1

COLUMN NUMBER=1

NODES	CD	CM	REN	CKN
22	1.08	1.87	9147.04	2.21
23	1.09	1.86	9664.66	2.34
24	1.10	1.84	10211.57	2.47
25	1.12	1.83	10789.44	2.61
26	1.13	1.82	11400.00	2.75

NODES	TDF	TAF	TCF
22	748.19	2764.86	3513.04
23	844.89	2901.75	3746.64
24	953.97	3043.92	3997.89
25	1077.01	3191.46	4268.47
26	1215.44	3344.53	4559.97

COLUMN NUMBER=2

NODES	CD	CM	REN	CKN
27	1.01	1.80	6659.69	3.04
28	1.02	1.79	7036.55	3.21
29	1.03	1.77	7434.74	3.39
30	1.05	1.75	7855.47	3.58
31	1.06	1.74	8300.00	3.78

NODES	TDF	TAF	TCF
27	510.77	1413.90	1924.67
28	576.29	1480.47	2056.76
29	650.51	1549.35	2199.86
30	734.42	1620.63	2355.05
31	829.28	1694.38	2523.66

COLUMN NUMBER=1

DIAMETER/WAVE LENGTH= 0.02
SINCE D/L<0.2 MORISON EQ. IS USED
DRAG FORCE ON THE CIRCULAR CYLINDER= 23117.990
ACCL. FORCE ON THE CIRCULAR CYLINDER= 73140.188
TOTAL FORCE ON THE CIRCULAR CYLINDER= 96258.180
TOTAL MOMENT ON THE CIRCULAR CYLINDER= 1104931.000
CENTRE OF TOTAL FORCE= 11.479 (FROM WATER SURFACE)

COLUMN NUMBER=2

DIAMETER/WAVE LENGTH= 0.01
SINCE D/L<0.2 MORISON EQ. IS USED
DRAG FORCE ON THE CIRCULAR CYLINDER= 15768.054
ACCL. FORCE ON THE CIRCULAR CYLINDER= 37222.750
TOTAL FORCE ON THE CIRCULAR CYLINDER= 52990.801
TOTAL MOMENT ON THE CIRCULAR CYLINDER= 607202.437
CENTRE OF TOTAL FORCE= 11.459 (FROM WATER SURFACE)

TABLE 4 (Cont'd)

COLUMN NUMBER=3

NODES	CD	CM	REN	CKN
32	1.01	1.80	6659.69	3.04
33	1.02	1.79	7036.55	3.21
34	1.03	1.77	7434.74	3.39
35	1.05	1.75	7855.47	3.58
36	1.06	1.74	8300.00	3.78
NODES	TDF	TAF	TCF	
32	510.77	1413.90	1924.67	
33	576.29	1480.47	2056.76	
34	650.51	1549.35	2199.86	
35	734.42	1620.63	2355.05	
36	829.28	1694.38	2523.66	

COLUMN NUMBER=4

NODES	CD	CM	REN	CKN
37	1.08	1.87	9147.04	2.21
38	1.09	1.86	9664.66	2.34
39	1.10	1.84	10211.57	2.47
40	1.12	1.83	10789.44	2.61
41	1.13	1.82	11400.00	2.75
NODES	TDF	TAF	TCF	
37	748.19	2764.86	3513.04	
38	844.89	2901.75	3746.64	
39	953.97	3043.92	3997.89	
40	1077.01	3191.46	4268.47	
41	1215.44	3344.53	4559.97	

COLUMN NUMBER=3

DIAMETER/WAVE LENGTH= 0.01
SINCE D/L<0.2 MORISON EQ. IS USED
DRAG FORCE ON THE CIRCULAR CYLINDER= 15768.054
ACCL. FORCE ON THE CIRCULAR CYLINDER= 37222.750
TOTAL FORCE ON THE CIRCULAR CYLINDER= 52990.801
TOTAL MOMENT ON THE CIRCULAR CYLINDER= 607202.437
CENTRE OF TOTAL FORCE= 11.459 (FROM WATER SURFACE)

COLUMN NUMBER=4

DIAMETER/WAVE LENGTH= 0.02
SINCE D/L<0.2 MORISON EQ. IS USED
DRAG FORCE ON THE CIRCULAR CYLINDER= 23117.990
ACCL. FORCE ON THE CIRCULAR CYLINDER= 73140.188
TOTAL FORCE ON THE CIRCULAR CYLINDER= 96258.180
TOTAL MOMENT ON THE CIRCULAR CYLINDER= 1104931.000
CENTRE OF TOTAL FORCE= 11.479 (FROM WATER SURFACE)

TOTAL HORIZONTAL COLUMN FORCES= 298497.97
TOTAL HORIZONTAL COLUMN MOMENTS= 3424267.00

TABLE 4 (Cont'd)

HULL NUMBER=2

NODES	VHPF	VHAF	TVHF	VCF	TVF
1	-4772.12	-4772.12	-9544.23	0.00	-9544.23
2	-4772.12	-4772.12	-9544.23	0.00	-9544.23
21	-4772.12	-4772.12	-9544.23	33459.80	23915.57
3	-4772.12	-4772.12	-9544.23	33459.80	23915.57
20	-4772.12	-4772.12	-9544.23	33459.80	23915.57
4	-4772.12	-4772.12	-9544.23	0.00	-9544.23
19	-4772.12	-4772.12	-9544.23	24161.56	14617.33
5	-4772.12	-4772.12	-9544.23	24161.56	14617.33
18	-4772.12	-4772.12	-9544.23	24161.56	14617.33
6	-4772.12	-4772.12	-9544.23	0.00	-9544.23
7	-4772.12	-4772.12	-9544.23	0.00	-9544.23
8	-4772.12	-4772.12	-9544.23	0.00	-9544.23
14	-4772.12	-4772.12	-9544.23	24161.56	14617.33
9	-4772.12	-4772.12	-9544.23	24161.56	14617.33
15	-4772.12	-4772.12	-9544.23	24161.56	14617.33
10	-4772.12	-4772.12	-9544.23	0.00	-9544.23
16	-4772.12	-4772.12	-9544.23	33459.80	23915.57
11	-4772.12	-4772.12	-9544.23	33459.80	23915.57
17	-4772.12	-4772.12	-9544.23	33459.80	23915.57
12	-4772.12	-4772.12	-9544.23	0.00	-9544.23
13	-4772.12	-4772.12	-9544.23	0.00	-9544.23

NODES	HHPF	HHAF	HHVF	THHF
1	2090.27	2090.27	831.95	5012.49
2	2090.27	2090.27	831.95	5012.49
21	2090.27	2090.27	831.95	5012.49
3	2090.27	2090.27	831.95	5012.49
20	2090.27	2090.27	831.95	5012.49
4	2090.27	2090.27	831.95	5012.49
19	2090.27	2090.27	831.95	5012.49
5	2090.27	2090.27	831.95	5012.49
18	2090.27	2090.27	831.95	5012.49
6	2090.27	2090.27	831.95	5012.49
7	2090.27	2090.27	831.95	5012.49
8	2090.27	2090.27	831.95	5012.49
14	2090.27	2090.27	831.95	5012.49
9	2090.27	2090.27	831.95	5012.49
15	2090.27	2090.27	831.95	5012.49
10	2090.27	2090.27	831.95	5012.49
16	2090.27	2090.27	831.95	5012.49
11	2090.27	2090.27	831.95	5012.49
17	2090.27	2090.27	831.95	5012.49
12	2090.27	2090.27	831.95	5012.49
13	2090.27	2090.27	831.95	5012.49

TABLE 4 (Cont'd)

HULL NUMBER=2

COLUMN NUMBER=1

NODES	CD	CM	REN	CKN
22	1.08	1.87	9147.04	2.21
23	1.09	1.86	9664.66	2.34
24	1.10	1.84	10211.57	2.47
25	1.12	1.83	10789.44	2.61
26	1.13	1.82	11400.00	2.75

NODES	TDF	TAF	TCF
22	748.19	-2764.86	-2016.67
23	844.89	-2901.75	-2056.86
24	953.97	-3043.92	-2089.95
25	1077.01	-3191.46	-2114.45
26	1215.44	-3344.53	-2129.09

COLUMN NUMBER=2

NODES	CD	CM	REN	CKN
27	1.01	1.80	6659.69	3.04
28	1.02	1.79	7036.55	3.21
29	1.03	1.77	7434.74	3.39
30	1.05	1.75	7855.47	3.58
31	1.06	1.74	8300.00	3.78

NODES	TDF	TAF	TCF
27	510.77	-1413.90	-903.13
28	576.29	-1480.47	-904.18
29	650.51	-1549.35	-898.84
30	734.42	-1620.63	-886.21
31	829.28	-1694.38	-865.10

COLUMN NUMBER=1

DIAMETER/WAVE LENGTH= 0.02
SINCE D/L<0.2 MORISON EQ. IS USED
DRAG FORCE ON THE CIRCULAR CYLINDER= 23117.990
ACCL. FORCE ON THE CIRCULAR CYLINDER= -73140.188
TOTAL FORCE ON THE CIRCULAR CYLINDER= -50022.191
TOTAL MOMENT ON THE CIRCULAR CYLINDER= -594796.500
CENTRE OF TOTAL FORCE= 11.891 (FROM WATER SURFA

COLUMN NUMBER=2

DIAMETER/WAVE LENGTH= 0.01
SINCE D/L<0.2 MORISON EQ. IS USED
DRAG FORCE ON THE CIRCULAR CYLINDER= 15768.054
ACCL. FORCE ON THE CIRCULAR CYLINDER= -37222.750
TOTAL FORCE ON THE CIRCULAR CYLINDER= -21454.695
TOTAL MOMENT ON THE CIRCULAR CYLINDER= -259224.422
CENTRE OF TOTAL FORCE= 12.082 (FROM WATER SURFACE)

TABLE 4 (Cont'd)

COLUMN NUMBER=3

NODES	CD	CM	REN	CKN
32	1.01	1.80	6659.69	3.04
33	1.02	1.79	7036.55	3.21
34	1.03	1.77	7434.74	3.39
35	1.05	1.75	7855.47	3.58
36	1.06	1.74	8300.00	3.78

NODES	TDF	TAF	TCF
32	510.77	-1413.90	-903.13
33	576.29	-1480.47	-904.18
34	650.51	-1549.35	-898.84
35	734.42	-1620.63	-886.21
36	829.28	-1694.38	-865.10

COLUMN NUMBER=4

NODES	CD	CM	REN	CKN
37	1.08	1.87	9147.04	2.21
38	1.09	1.86	9664.66	2.34
39	1.10	1.84	10211.57	2.47
40	1.12	1.83	10789.44	2.61
41	1.13	1.82	11400.00	2.75

NODES	TDF	TAF	TCF
37	748.19	-2764.86	-2016.67
38	844.89	-2901.75	-2056.86
39	953.97	-3043.92	-2089.95
40	1077.01	-3191.46	-2114.45
41	1215.44	-3344.53	-2129.09

COLUMN NUMBER=3

```
DIAMETER/WAVE LENGTH= 0.01
SINCE D/L<0.2 MORISON EQ. IS USED
DRAG FORCE ON THE CIRCULAR CYLINDER=    15768.054
ACCL. FORCE ON THE CIRCULAR CYLINDER=  -37222.750
TOTAL FORCE ON THE CIRCULAR CYLINDER=  -21454.695
TOTAL MOMENT ON THE CIRCULAR CYLINDER= -259224.422
CENTRE OF TOTAL FORCE=       12.082  (FROM WATER SURFACE)
```

COLUMN NUMBER=4

```
DIAMETER/WAVE LENGTH= 0.02
SINCE D/L<0.2 MORISON EQ. IS USED
DRAG FORCE ON THE CIRCULAR CYLINDER=    23117.990
ACCL. FORCE ON THE CIRCULAR CYLINDER=  -73140.188
TOTAL FORCE ON THE CIRCULAR CYLINDER=  -50022.191
TOTAL MOMENT ON THE CIRCULAR CYLINDER= -594796.500
CENTRE OF TOTAL FORCE=       11.891  (FROM WATER SURFACE)

    TOTAL HORIZONTAL COLUMN FORCES=  -142953.78
   TOTAL HORIZONTAL COLUMN MOMENTS= -1708041.87
```


TABLE 4 (Cont'd)

```
TOTAL COLUMN FORCES ON THE STRUCTURE= 155544.19
TOTAL COLUMN MOMENTS ON THE STRUCTURE=  1716225.12
CENTRE OF TOTAL FORCE=     11.Ø3  (FROM WATER SURFACE)
TOTAL HORIZONTAL FORCE ON THE STRUCTURE= 395978.63
-----------------------------------------------------------------


S T R U C T U R A L  R E S P O N S E
-----------------------------------
MAXIMUM AXIAL FORCE AT THE DECK  (STRUCTURE HAS NO BRACINGS)
                    AF=    1649625.75
MAXIMUM SHEAR FORCE AT THE DECK  (STRUCTURE HAS NO BRACINGS)
                    SF=    1ØØ8174.ØØ
MAXIMUM AXIAL FORCE AT THE DECK  (STRUCTURE HAS NO BRACINGS)
MAXIMUM BENDING MOMENT AT THE DECK  (STRUCTURE HAS NO BRACINGS)
                BM=   36964296.ØØ
                HR=    3696429.5Ø  (BENDING MOMENT/WAVE HEIGHT)
-------------------------------------------------------------------------------
M O T I O N  R E S P O N S E
---------------------------
HEAVE RESPONSE=           -1.23  ROLL RESPONSE=          -Ø.34
HEAVE ACCELERATION=       11.Ø5  ROLL ACCELERATION=       Ø.Ø5
HEAVE RESPONSE/H=         -Ø.12  ROLL RESPONSE/H=        -Ø.Ø3

PHASE ANGLE B.F.H=       -11.71  PHASE ANGLE B.F.R=      -5.11
-----------------------------------------------------------
-----------------------------------------------------------------
```

TABLE 4 (Cont'd)

Chapter 7: CONCLUSIONS

1. CONCLUSIONS OF CHAPTER 2

In this chapter, a review of the basic hydrodynamic principles for calculating the wave forces on circular cylinders in the drag, drag + inertia and diffraction regimes have been presented.

An approximate method has been given in order to take into account the interference between circular cylinders which are dominantly subject to wave inertia forces.

Under the light of existing theoretical and experimental knowledge it is believed that further experimental studies with large size of models are essential in order to determine correct wave coefficients taking the interference effects into account properly for the structures which are dominantly subject to drag or drag + inertia forces, i.e. jacket structures, guyed towers, etc.

Analytical procedures have been presented for calculating the second-order forces on circular cylinders. Since these forces may occur at the frequencies near to the natural frequency of surge or sway mode of rigid-body motion of the floating structure they must be taken into account during the design of riser or mooring systems. Second-order vertical time independent forces would also cause undesirable steady-tilt angles as was experienced during the model tests with semi-submersible designs in regular waves.

The effect of non-linear free-surface and the second-order time dependent forces was found to cause an increase in wave loading on circular cylinders by an amount of 20%.

A formulation of the wave loading on a circular cylinder which is working in the inertia or in the diffraction regime has been presented using the Stokes' fifth-order wave theory for the shallow water applications.

2. CONCLUSIONS OF CHAPTER 3

A general method and a computer program have been devised to calculate the wave force and moments on the circular cylindrical members of fixed and of floating offshore structures. In the computer calculations the following points were not taken into account due to the limitations in capacity of the computer (PDP 11/40) on which WAVLOA was developed.

(a) The effects of non-linear boundary conditions and second-order forces. However, one may determine these effects manually using the appropriate graphs presented in Chapter 2, or integrate WAVLOA with additional subroutines which could be written using the calculation procedures presented in Chapter 2 on a larger capacity computer.

(b) The variation of drag and inertia coefficients along the length of a member. This can easily be taken into account by compiling WAVLOA with subroutine FLUID2 on a larger capacity computer. FLUID2, which is described in Chapter 6, calculates the variation of drag and inertia coefficients along the length of a member.

It is hoped that the developed computer program WAVLOA will provide a basic tool to the designer, who can select and vary the configuration of the floating or fixed offshore structure on which he calculates the wave loading without any restriction.

As described in Chapter 4, WAVLOA forms a basic part in the calculation method developed for the non-linear, coupled motion response of a floating offshore platform.

Finally, it is hoped that the method and the computer program developed here will be used in further investigations of the force and moment measurements on randomly oriented yawed cylinders for the better understanding of the inertia and the drag forces.

3. CONCLUSIONS OF CHAPTER 4

In this chapter a general method to obtain the rigid-body motion induced loading on the circular cylindrical members of floating offshore structures has been derived. Rigid-body motion induced loading and wave forces are combined to obtain motion equations. Linear, uncoupled single degree of freedom system equations are applied to the model and a full scale semi-submersible type floating offshore platform to predict the motion responses. Comparisons between the predictions and the model test results show reasonably good agreement for small amplitude motions. The general method has been extended to include large amplitude motions by deriving non-linear, coupled motion equations in a six degrees of freedom system. A solution procedure for these equations has been discussed.

The formulations derived in this chapter also provide an efficient tool to study the non-linear dynamic stability of floating structures in waves.

4. CONCLUSIONS OF CHAPTER 5

1. Calculation procedures were developed in order to predict the structural response values for determinate and indeterminate floating platforms. These procedures were applied to model and full-scale semi-submersible design. The comparisons between the theoretical predictions and the test measurements indicate an acceptable level of agreement. However, the comparison of the theoretical predictions which were made using the restrained mathematical model and the experimental results obtained from the free-floating model suggests that wave coefficients should be higher than the values used in these predictions. It is believed that better agreement should be obtained between the theoretical predictions which employ the free-floating mathematical model and the experimental results if the solutions of the linear uncoupled motion response equations are replaced with the solutions of non-linear coupled motion response solutions.

2. At the initial stage of the floating platform design, structural response calculations need to be performed for each member several times by varying the wave frequencies, wave heading angles and the structural properties of the members before the final decision on the scantlings of members is reached.

3. The analysis carried out with the restrained and the free-floating mathematical models showed that the difference in magnitude of response between these two cases had a maximum of ± 20% in the operational region. The free-floating mathematical model uses the solutions of the linear uncoupled motion response equations. Since the rigid body motion-induced loading tends to decrease the structural

response values over a large frequency region, the use of a restrained structural model was found to lead to more accurate calculations and affords a factor of safety in design.

4. In the case of floating platforms, unlike in the ship case, it is not possible to define a critical wave length/structural length ratio at which maximum structural load occurs in waves. Thus in order to define maximum design loads structural response calculations should be carried out in the frequency domain for various wave heading angles. The probabilistic values of design loads can also be obtained readily from these frequency domain calculations by employing the methods of spectral analysis.

5. Since the bracing members reduce the structural response values considerably, extreme design load calculations for the individual strength members should include consideration of a failure or an accident involving the bracing members.

6. Maximum structural response values on the longitudinal and on the transverse strength elements of twin circular hulled design semi-submersibles occurred in beam seas. Again, for the same type of design, the maximum structural response in the strength members of the deck was dominated by the wave loading on the hulls.

7. The effect of the non-linear free surface and the second-order forces induces a maximum increase of 10% in the bending moment values on the transverse deck beam of a model structure. An increase of the same order was found for the restrained and the free-floating model cases.

8. It may generally be said that floating platforms can be accepted as rigid structures; therefore, structural response calculations can be carried out under quasi-static loading for overall structural response. However, structural response under dynamic loading may become important for flexible support members, such as bracings or columns in the case of a failure or an accident involving those flexible members. Similarly, impact loads due to wave breaking can be important for the dynamic loading analysis. These cases suggest that a redundancy analysis should be incorporated into the dynamic analysis.

9. A simplified method has been suggested to determine the structural response values under dynamic loading. The bending moment values on the flexible deck connections of the semi-submersible model given by this method agree better with the experimental measurements than the quasi-static case where response values reach a peak.

5. CONCLUSIONS OF CHAPTER 6

Various computer routines for the prediction of structural loading and response of a twin circular hulled semi-submersible geometry were described. Although the entire FLUID4A program is restricted to a twin circular hulled semi-submersible geometry, various routines can be separately integrated with other programs in order to calculate wave, current and wind drag forces on circular cylinders as well as hydrostatic characteristics.

Since, at the time of the writing of these routines, the only experimental data on drag coefficients available over a large

Reynold's number range was steady flow results, these were used in the appropriate subroutines. However, as more experimental data on drag, inertia and lift coefficients obtained from oscillating water column tests, wave tank tests, or from full scale measurements (see also Chapter 2) become available, the relevant subroutines which could make use of this new information should be updated.

One may also study the sensitivity of these coefficients obtained from steady, oscillating or wavy flow, to the structural loading and response by adding appropriate subroutines which contain new data to the FLUID4A main program.

Finally, when FLUID4A is run for a twin circular hulled semi-submersible which is floating near to the free-surface, routines which calculate added-mass and added-moment of inertia values for the columns and the hulls should be modified to include frequency dependent effects.

6. CONCLUSIONS OF APPENDIX 1

The set up for the measurements of the motion and the structural response of the twin circular-hulled semi-submersible model in regular waves has been described. Considering the regularity obtained in the time domain records and the consistency of the amplitude measurements plotted in the frequency domain, it may be concluded that the set up was reliable enough for the measurements discussed in the Appendix.

The initial aim of these experiments was to compare the calculated motion and the structural response predictions with the measurements. Although reasonable agreement was found between the theoretical predictions and the experimental measurements, in the light of the conclusions drawn in Chapters 4 and 5 it is still believed that further testing is essential for a thorough understanding of the following points:

(1) The effect of the harnesses which stop the model drifting along the tank. The motion and the structural response values should be measured as the location of the harnesses on the model is varied. Measurement of the forces exerted by the harnesses would also be very helpful.

(2) The effect of the interference between the following elements of the model:

    (a) two hulls

    (b) two vertical columns

    (c) one hull and one vertical column.

(3) The effect of structural dynamics. It is necessary to carry out further tests with the complete semi-submersible model restrained against rigid-body movements and designed and instrumented in such a way that the dynamic effects in waves, especially in the condition whereby a bracing has failed, are easily measured. A comparison of such measurements with the summed measurements obtained from the individual components under (2) above will clarify the difference between the quasi-

static and dynamic loading (provided that the force measurements under (2) are carried out with a rigid mounting system). These tests would also provide a comparison between the structural response calculations which were carried out for the restrained model and the measurements.

Items (2) and (3) should be repeated by oscillating the model in calm water in order to determine the motion induced loading.

(4) The effects of the orientation of the model in waves as it is displaced during roll and pitch motion. The model can be fixed at typical configurations, i.e. the model may be fixed as it is heeled at a certain angle of roll, and force and moment measurements can be carried out.

Appendix 1: DESCRIPTION OF MOTION AND STRUCTURAL RESPONSE EXPERIMENTS

INTRODUCTION

In order to compare the calculation procedures developed for the prediction of motion and structural response with the experimental measurements, model tests were carried out. A twin circular hulled semi-submersible model, as shown in Fig. 1-A, was tested in regular waves by varying the range of frequencies from 1 rad/sec to 8 rad/sec and wave heights from 5 cms to 15 cms in the 77 x 4.6 x 2.4 (metres) testing tank at Glasgow University.

The tests were performed in order to measure the heave and roll response of the model, as well as the bending moments at the centre of the transverse beams and the axial forces on the inclined bracings in beam sea conditions.

1. DESCRIPTION OF MODEL

A twin circular hulled semi-submersible model was constructed in two halves and, at the first stage, connected with two transverse beams to represent a determinate structure (Figs. 1-A and 1-B). At the second stage, inclined and horizontal bracings were added to the model to represent an indeterminate structure (Fig. 1-D).

The following materials were used during the construction of the elements of the model:

Elements	Material
Hulls	P.V.C. Tubes
Columns	P.V.C. Tubes
Decks	P.V.C. and Aluminium Sheets (Fig. 1-c)
Transverse Beams	Squared section aluminium beams
Horizontal and Inclined Bracings	Brass Tubes (Fig. 1-D)

All elements of the model were constructed using the workshop machinery at Glasgow University's test tank. Care was taken to ensure the even and symmetrical distribution of element masses throughout the model.

The P.V.C. parts were connected to each other with P.V.C. welding. Aluminium and P.V.C. elements, as well as all aluminium elements, were bolted to each other (Fig. 1-C).

At the second stage of the experiments, inclined and horizontal bracings were bolted to the model.

The bracing elements can easily be mounted on and dismounted from the model.

The model was ballasted to the desired draft level using special ballast containers placed in each corner column. These containers restricted the movement of the ballast during the motions of the model.

Harnesses were attached between the model and the tank walls so that the model could be stopped from drifting along the tank. The location of the harnesses on the model was at about the centre of gravity of the model.

The mass distribution of the model is summarised in Table 1. The structural properties of the elements used in the construction of the model are also given in Table 2.

Picture 1 shows the model during the test in regular waves.

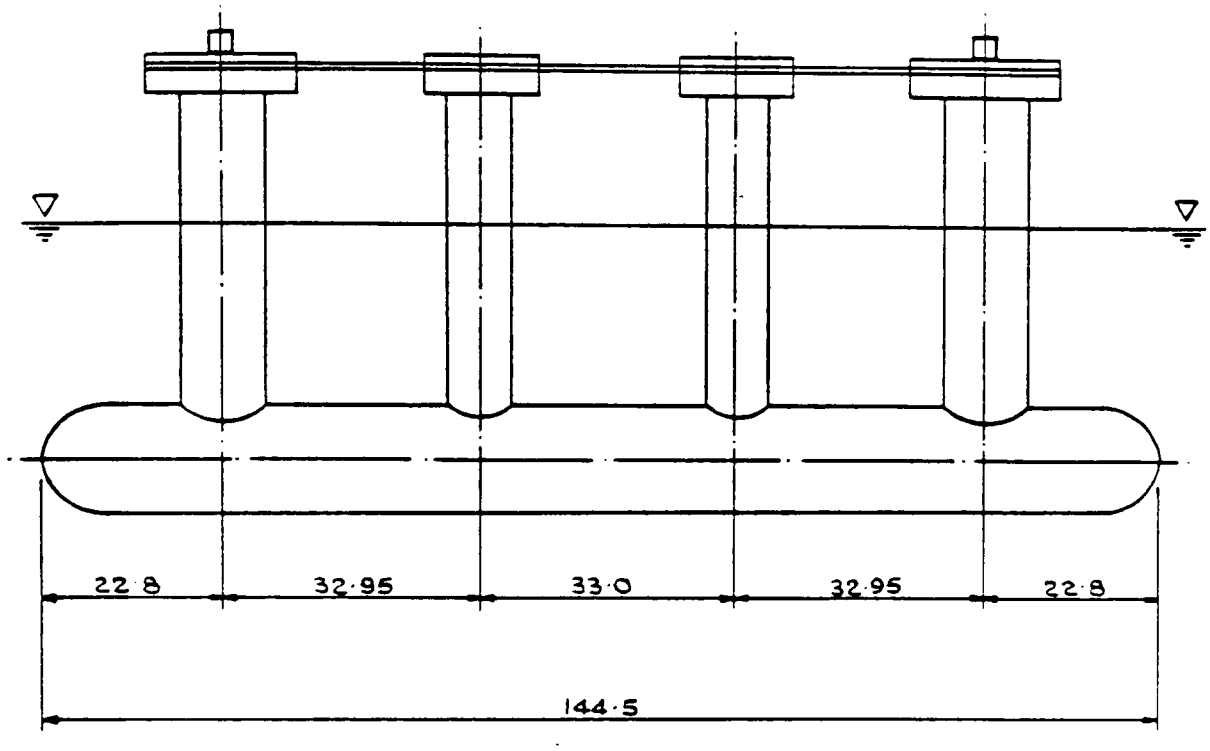

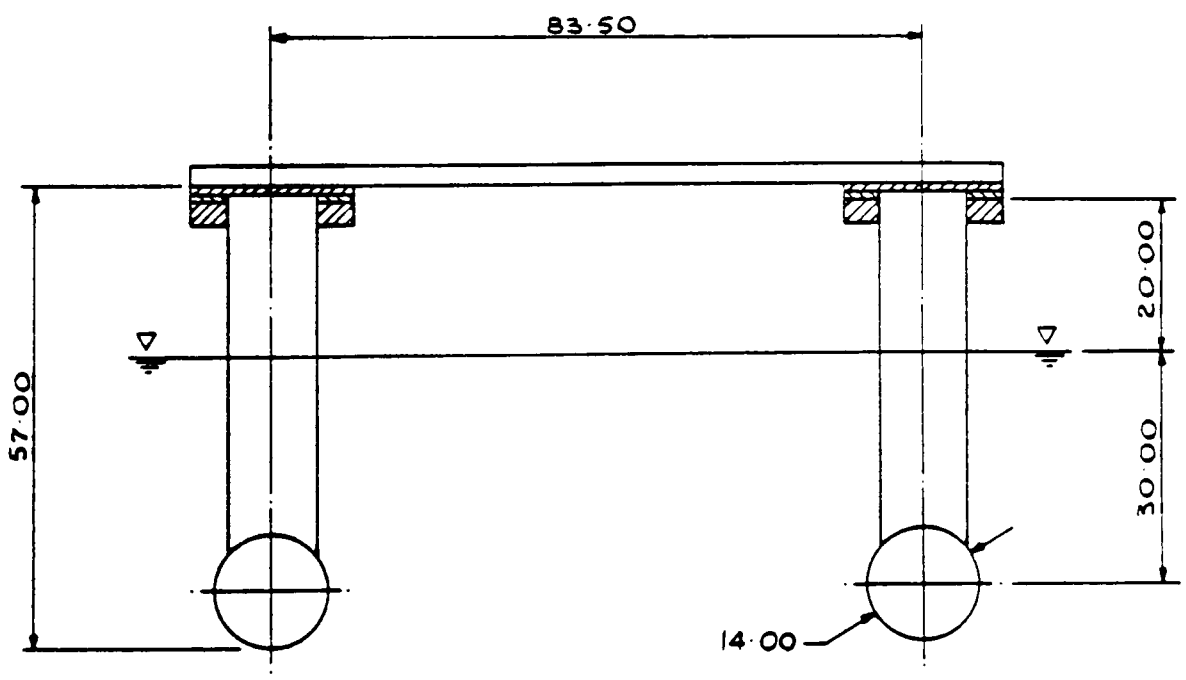

GENERAL ARRANGEMENT OF TWIN HULLED SEMI-SUBMERSIBLE MODEL FOR STRUCTURAL RESPONSE EXPERIMENT.

Fig. 1-A

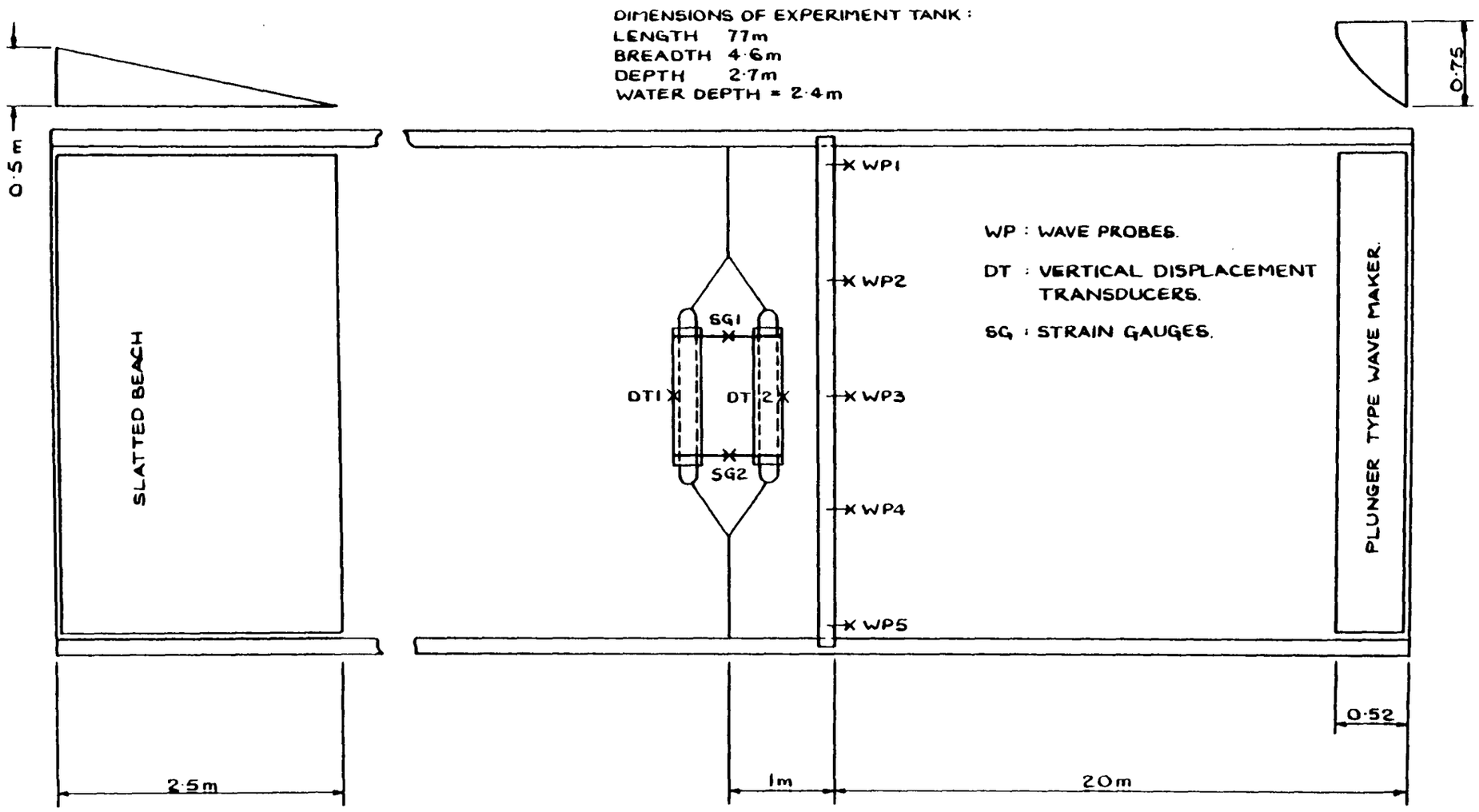

GENERAL ARRANGEMENT FOR MOTION AND STRUCTURAL RESPONSE EXPERIMENT WITH TWIN CIRCULAR HULLED SEMI-SUBMERSIBLE MODEL.

Fig. 2.

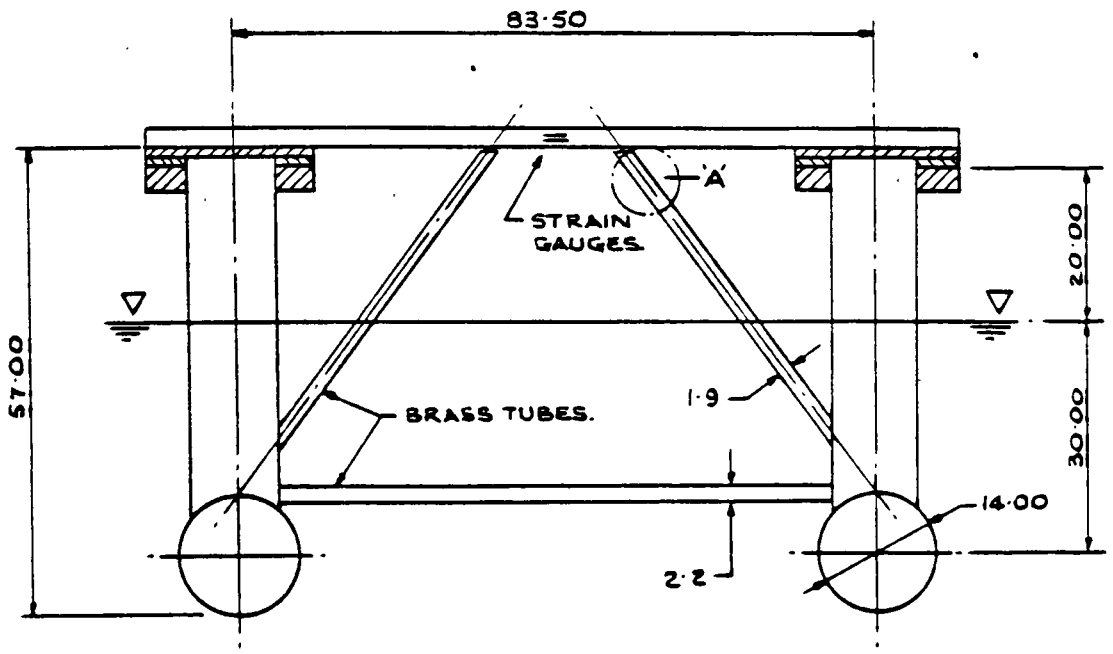

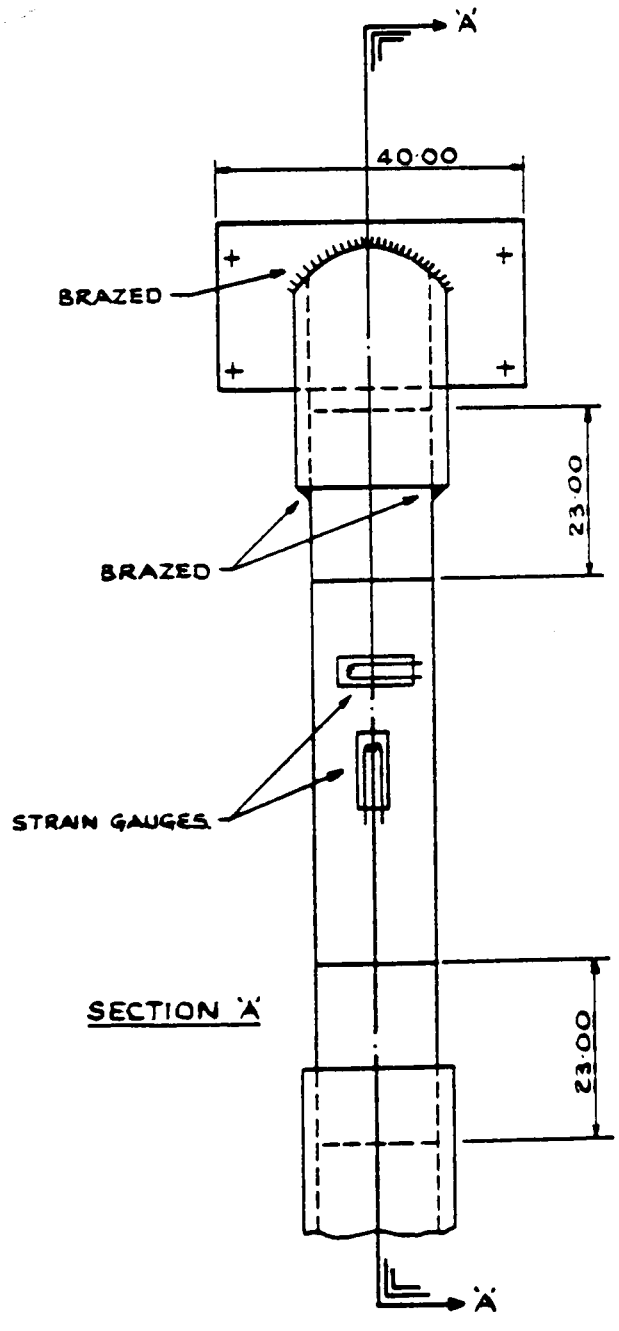

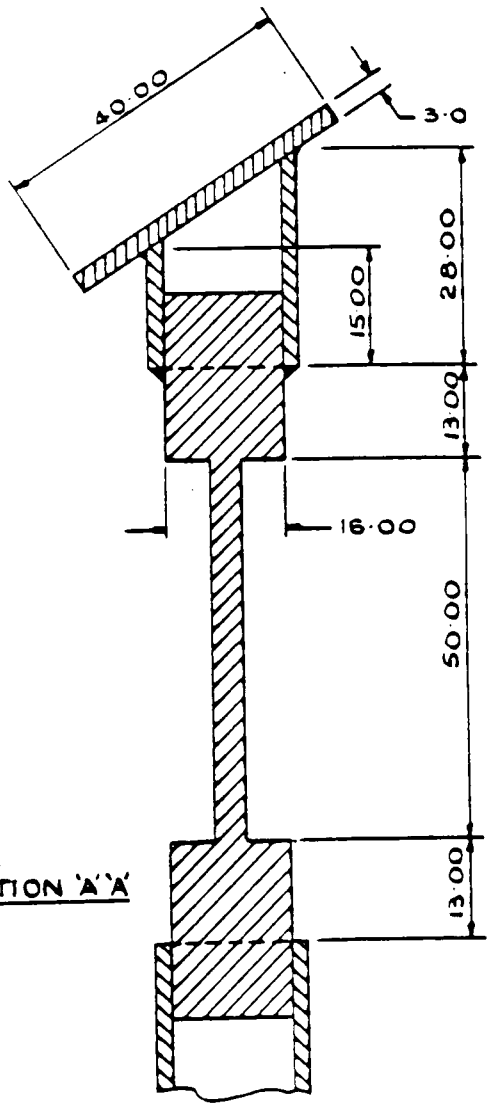

DETAILS OF THE BRACING ARRANGEMENT

Fig. 1-D.

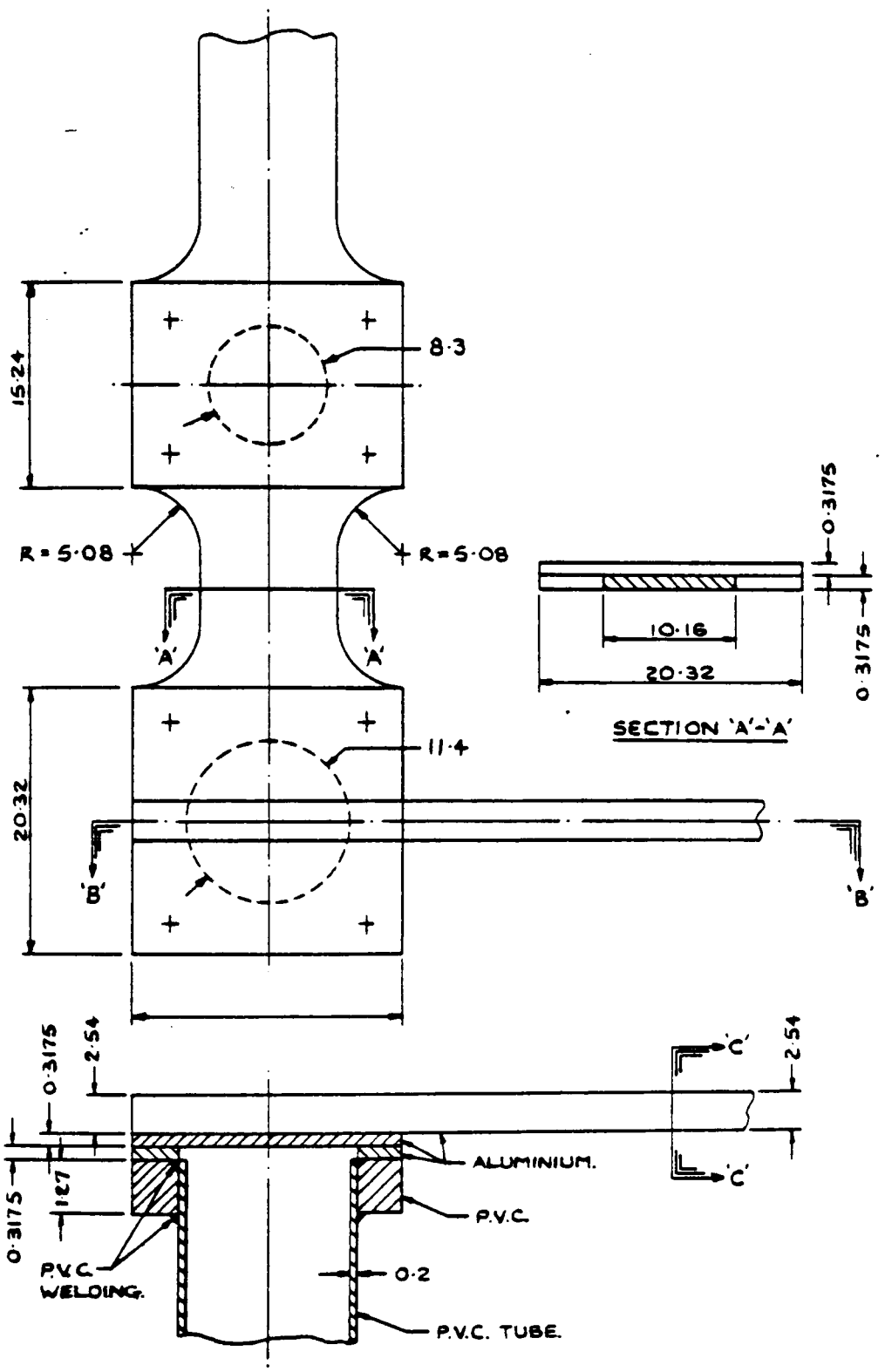

DETAILED DECK ARRANGEMENT OF TWIN HULLED SEMI-SUBMERSIBLE MODEL FOR STRUCTURAL RESPONSE EXPERIMENT.

Fig. 1-C.

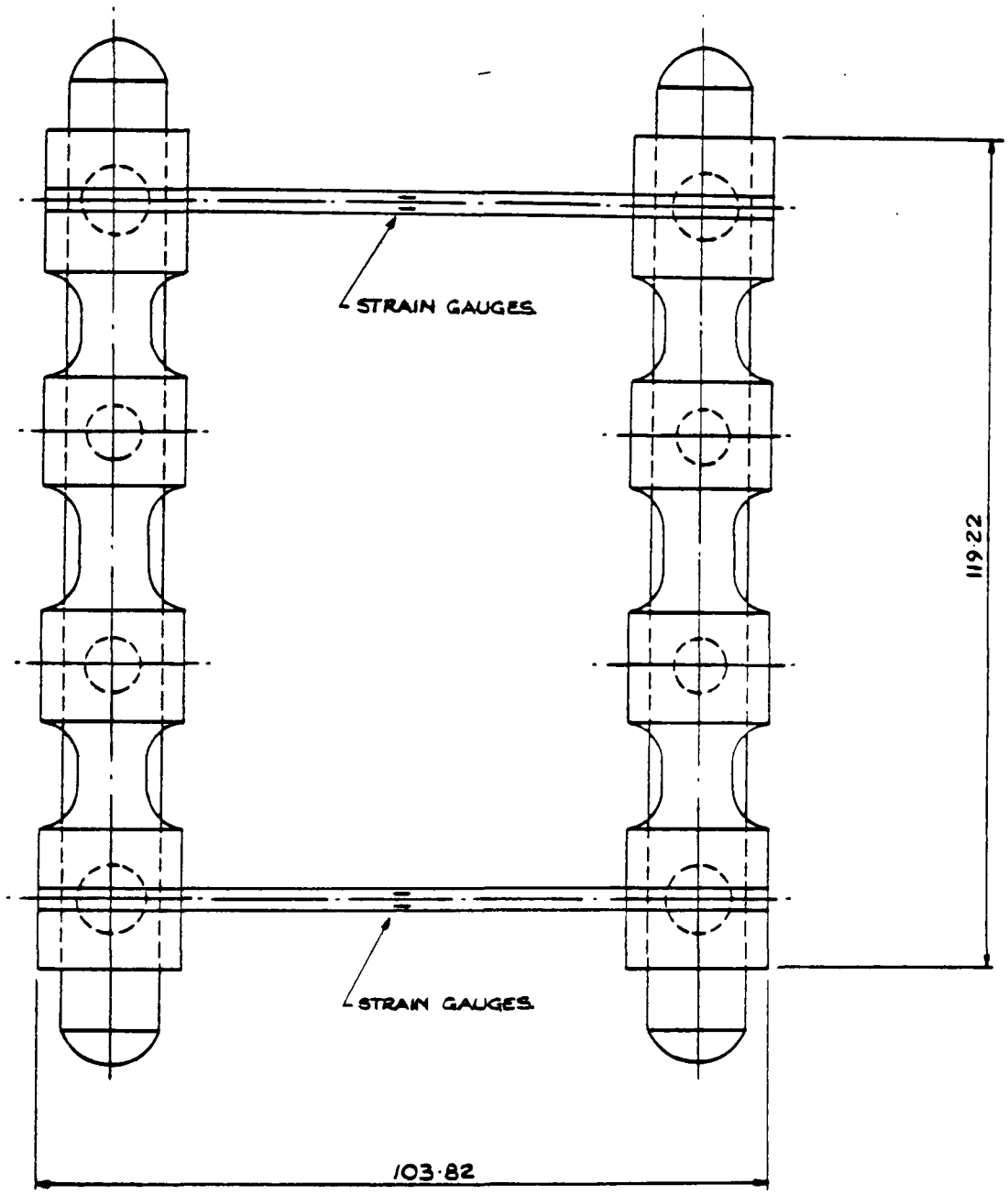

GENERAL ARRANGEMENT OF TWIN HULLED SEMI-SUBMERSIBLE MODEL FOR STRUCTURAL RESPONSE EXPERIMENT

Fig. 1-B

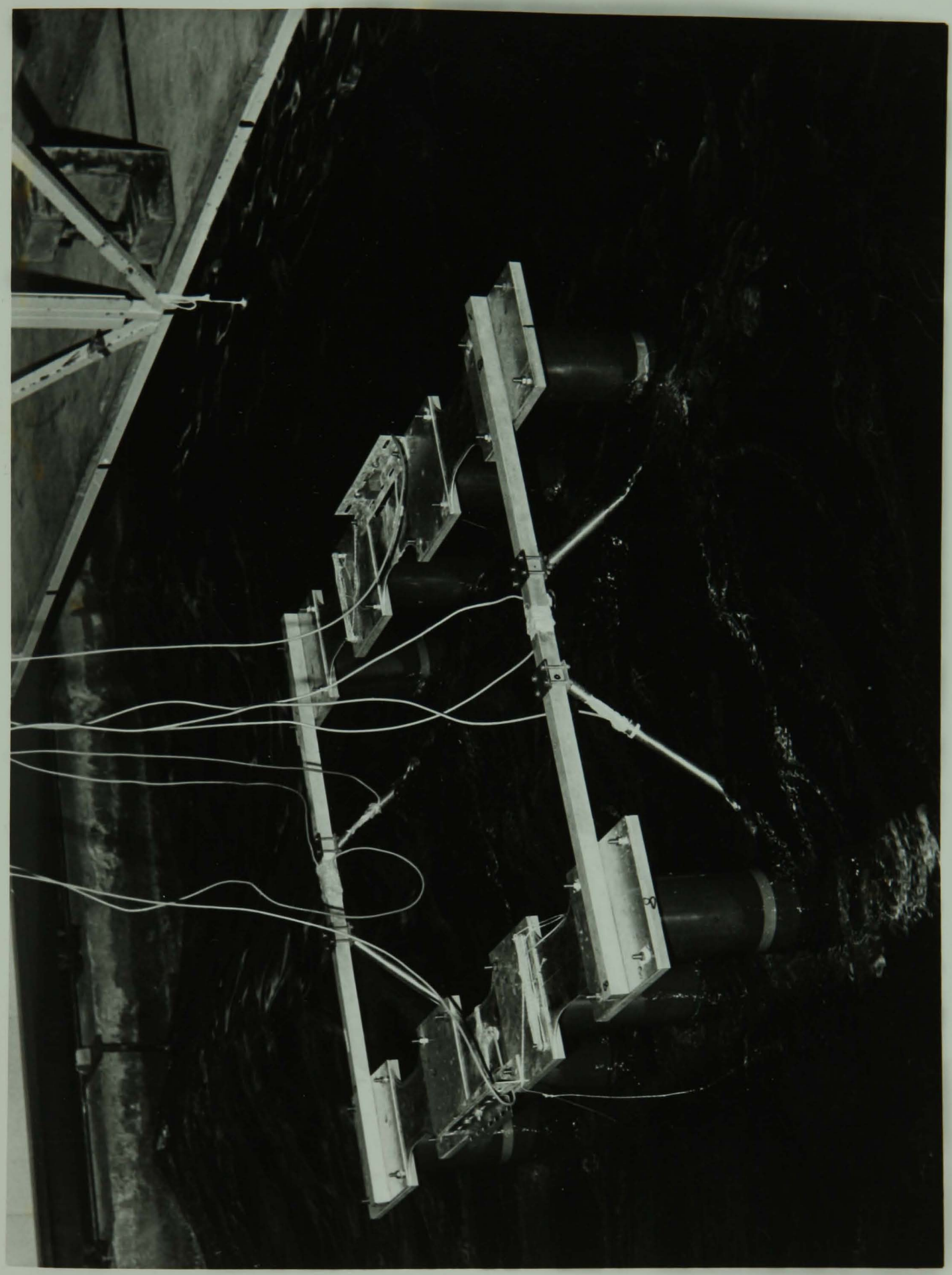

Picture 1

TABLE 1

MASS DISTRIBUTION OF THE TWIN CIRCULAR HULLED SEMI-SUBMERSIBLE

Element	Number	Mass (Kgs)	Distance from Base Line (cms)
Hull	2	6.55	7.00
Vertical Column	8	1.0	35.50
Deck	2	4.7	57.00
Transverse Beam	2	0.82	58.25
Empty Ballast Container	4	0.635	17.13
Ballast	4	6.25	9.88
Inclined Bracing	4	0.451	41.00
Horizontal Bracing	2	0.601	14.70

TABLE 2

STRUCTURAL PROPERTIES OF THE TWIN-CIRCULAR-HULLED SEMI-SUBMERSIBLE

Element	Cross Sectional Area (cm^2)	Second Moment of Area (cm^4)	Elasticity Modulus (N/mm^2)
Hull	17.10	1582.	34.76×10^3
Vertical Column (large diameter)	12.15	742.5	34.76×10^3
Vertical Column (small diameter)	12.25	374.2	34.76×10^3
Deck	3.22	0.03	7.2×10^4
Transverse Beam	2.84	2.16	7.2×10^4
Empty Ballast Container	12.25	374.2	34.76×10^3
Inclined Bracing	1.64	3.10	10.03×10^4
Horizontal Bracing	1.93	8.16	10.03×10^4

2. INSTRUMENTATION

2.1 Instrumentation for Motion Response Experiments

During the motion response tests, the instrumentation was set to record the amplitudes of the regular wave trains as well as the amplitude of the heave and roll motions of the model.

Regular waves were created by a plunger type wave-maker driven by an electronically controlled hydraulic pump (Fig. 2).

Across the tank width 5 resistance-type wave probes were installed. These probes induce an electrical signal whose strength changes as the waves pass the probes. These signals were amplified and recorded on the pen recorder. The pen recorder draws the variation of wave elevation versus the real time.

The heave and roll motions of the model were recorded with a pair of gravity-type linear vertical transducers. They were attached to the sub-carriage and connected to the deck of the model with piano wires suspended over a pair of pulleys. The weights of the vertical displacement transducers were balanced in order to avoid any acceleration being induced on the transducers during the motion of the model. The signals induced as a result of the model's motion in regular waves were sent to the pen recorder via an amplifie to record heave and roll displacements versus real time. Since the motion signals received from the model were the total displacements due to heave and roll (pitch) motion a special amplifier was used to add the signals received from the transducers to obtain a heave signal and to subtract to obtain a roll (pitch) signal.

2.2 Instrumentation for Structural Response Test

During the structural response experiment, the instrumentation was set to record the amplitudes of the regular wave trains as well as bending moment variations at the centre of the transverse beams and the variation in axial force on the inclined bracings.

In order to measure the bending moments, two pairs of strain-gauges were mounted on the top and bottom surfaces of the framework beams, as seen in Fig. 3.

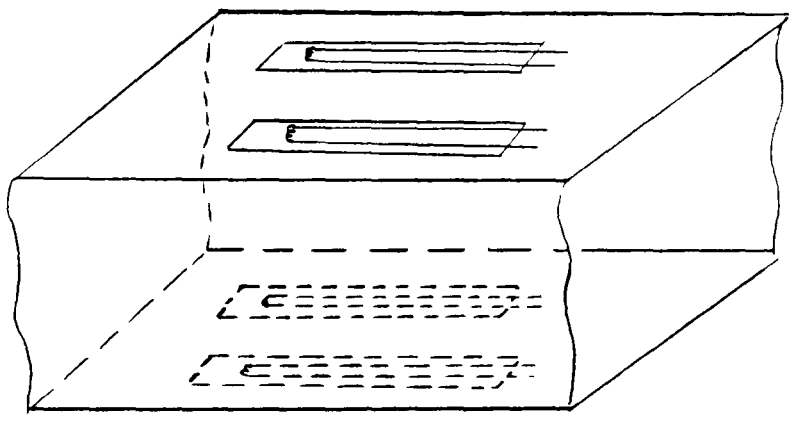

Fig. 3: Strain Gauges on Transverse Beam

The strain gauges were connected such that when the beam was, simultaneously, subject to bending moments and axial forces, they could induce signals only due to the bending moments. Details of this type of strain-gauge instrumentation can be found in Reference 1.

Similarly, in order to measure the axial forces on the inclined bracings, two pairs of strain-gauges were mounted on the brass tubes, as shown in Figs. 1-D and 4.

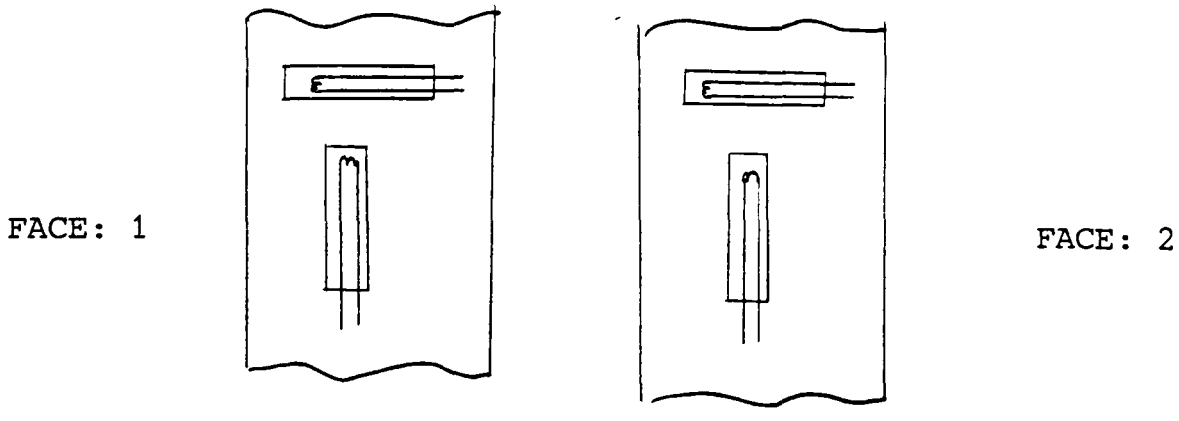

Fig. 4: Strain Gauges on Brass Tube

These strain gauges were also connected such that they could induce signals only due to the axial forces when the bracing were subject to both axial forces and bending moments. Details of this type of strain-gauge instrumentation can also be found in Reference 1.

The signals received from the strain-gauges were sent to the pen recorder via strain-gauge amplifiers to record bending moment or axial force values versus time.

Picture 2 shows the recording instruments.

3. DESCRIPTION OF CALIBRATION PROCEDURES

3.1 Calibration of Wave Probes

All wave probes were submerged up to 3/4 of their lengths into the tank when the water was calm and zero readings on the wave probe amplifiers were taken. At the same time, the pens' positions corresponding to the zero wave elevation was marked on the recorder.

The calibration process was continued, by lifting the wave probes gradually at 5 cms intervals up to 15 cms, and at each step the pens' new positions were marked on the recorder. From the calibration records a linear relationship was found between the displacements of the wave probes and the pens' displacements on the recorder.

Finally, the slope of the calibration curve was calculated as:

$$CFW = \frac{\text{Probe displacement (=wave elevation) [cms]}}{\text{Pen displacement [cms]}} = \frac{2.5}{1.0}$$

3.2 Calibration of Linear Displacement Transducers

The model was floated at the required draft level in the calm water and the displacement transducers were attached to the deck at both sides of the model (Fig. 2).

First, zero readings were taken from both transducers and corresponding zero lines were marked on the pen recorder.

Secondly, the transducers were displaced $\pm$ 10 cms using a vertical vernier attached to the piano wire which connects the model to the transducer. At the same time, the pen's position corresponding to the displacement of the transducer was marked. The same procedure was carried out with the second transducer.

From the calibration records it was found that the responses of both transducers were identical and linear within the range of calibration.

The slope of the calibration curve was calculated as:

$$CDF = \frac{\text{Transducer displacement (= model's displacement) [cms]}}{\text{Pen displacement [cms]}} = \frac{2.0}{1.0}$$

3.3 Calibration of Strain-Gauges on the Transverse Beams

In order to read direct bending moment values from the records, the strain-gauges were calibrated on the actual model. The model was set for calibration in calm water, as seen in Fig. 5.

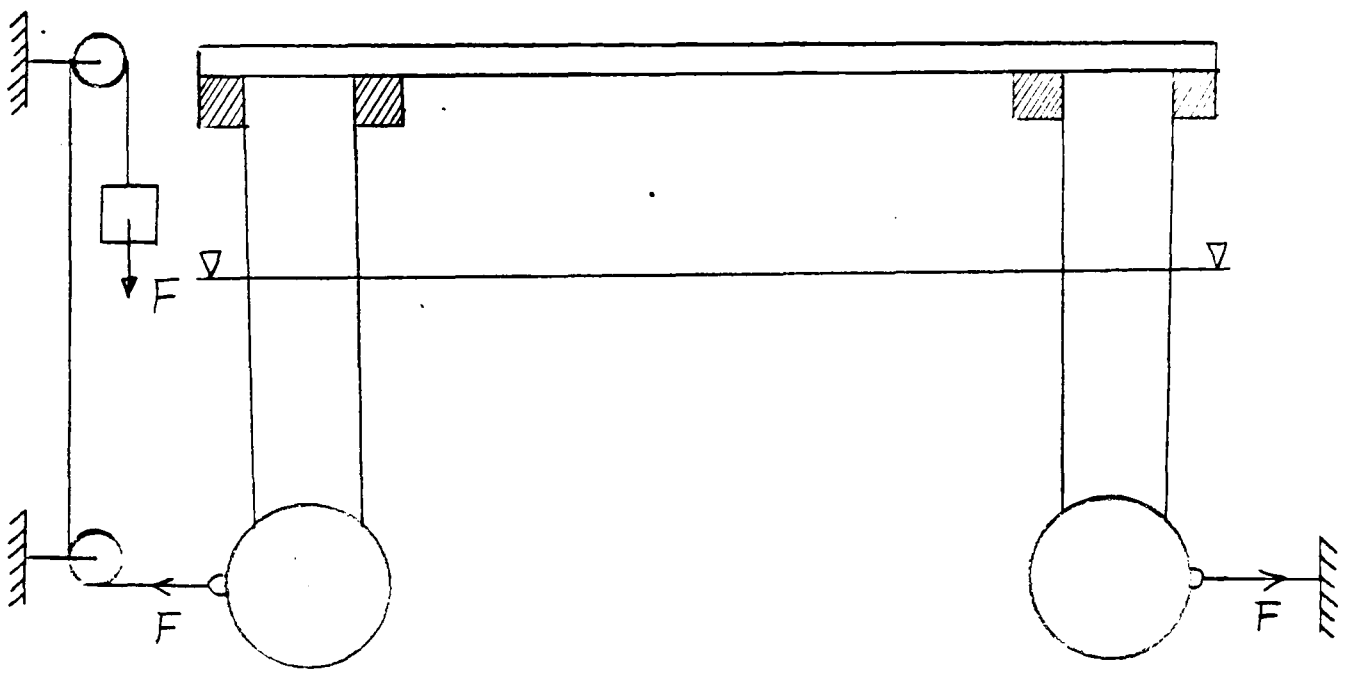

Fig. 5: Calibration of Strain-Gauges on the transverse deck

After taking the zero readings from the strain-gauges mounted on both transverse beams, the bending moment values on the beams were step by step increased by increasing the applied force on the hulls from 1 kgf to 8 kgf. During this process, displacements of the pens corresponding to the applied moment values were marked on the pen recorder at each 1 kgf increase of the applied

force. The responses of the strain-gauges were found to be linear. It was also found that there was a small difference in the slopes of the calibration curves belonging to the first and the second beams. The difference may be due to a slight difference in alignment and/or to a difference in the adhesion of the strain-gauges during mounting.

The slope of the calibration curve for bending moment measurements recorded from both transverse beams was calculated by taking the average value as follows:

$$CFS = \frac{1}{2}\left[\left(\frac{\text{Bending Moment [N cms]}}{\text{Pen dispmacement [cms]}}\right)_{\text{BEAM 1}} + \left(\frac{\text{Bending Moment [N cms]}}{\text{Pen displacement [cms]}}\right)_{\text{BEAM 2}}\right]$$

3.4 Calibration of Strain-Gauges on the Inclined Bracings

In order to calibrate the strain-gauges mounted on the bracings, the simple set-up shown in Fig. 6 was prepared:

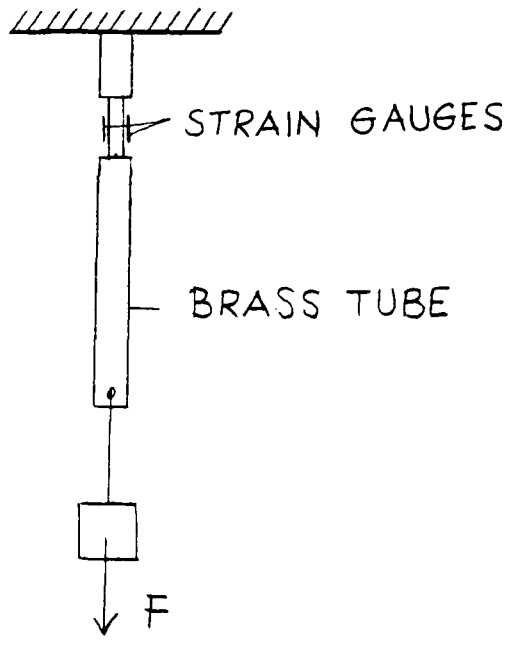

Fig. 6

The calibration process to record axial force versus pen displacements on the recorder was the same as that described in the previous section.

The responses of the strain-gauges were found to be linear and as with the case mentioned in the previous section, there was a small difference in the responses of the strain-gauges mounted on the first and the second bracings.

The slope of the calibration curve used for the axial force measurements recorded from both bracings was calculated taking the average value as follows:

$$CFSB = \frac{1}{2}\left[\left(\frac{\text{Axial Force [N]}}{\text{Pen displacement}}\right)_{\text{BRACING 1}} + \left(\frac{\text{Axial Force [N]}}{\text{Pen displacement}}\right)_{\text{BRACING 2}}\right]$$

4. DESCRIPTION OF THE RECORDS

Three groups of tests were carried out with the twin circular hulled semi-submersible model in regular beam seas.

During the first group of experiments, wave, heave and roll displacements versus real time were recorded.(Figs. 6, 6-A and 6-B). Each run was continued until the first wave train reached the slotted beach (Fig. 2) in order to avoid any possible wave reflection between the transverse tank walls and any wave resonance.

In order to find the motion and wave amplitudes at each test frequency, each record was analysed manually by taking the average of 5 amplitude readings.

These values were plotted as wave frequencies versus response amplitudes in Chapter 4.

Before the model was tested in waves for the measurements of motion amplitudes, free motion experiments were carried out using the same set up as for the motion response experiments. During these experiments the natural heave and roll period, as well as the heave and roll damping coefficients, were measured.

These values are shown in the following table:

TABLE 3

Mode of Motion	Natural Period (Sec)		Damping Coefficients
	Calct.	Measured	
Heave	2.66	2.4	0.075
Roll	5.46	3.9	0.071

A second group of experiments was carried out to measure the amplitudes of the waves and the bending moments at the centre of the transverse beams. During this group of experiments bracings were not mounted on the model. Some records from this group's runs are shown in Figs. 7-(8-A).

The analysis of the measurements recorded during the second group of runs was performed in the same way as that described for the first group. The results of the analysis were plotted as wave frequency versus bending moment/wave amplitude in Chapter 5.

In the final group of experiments, the semi-submersible model with inclined and horizontal bracings was tested in order to measure the amplitudes of bending moment at the centre of the transverse beams, of axial forces on the inclined bracings and of wave amplitudes at each wave frequency. Some records from this group's runs are shown in Figs. 9 and 9-A.

The records of this group of runs were analysed in the same way as described earlier for the first and second group of runs. This group's measurements were plotted as wave frequency versus bending moment/wave amplitude and wave frequency versus axial force/ wave amplitude in Chapter 5.

Picture 2

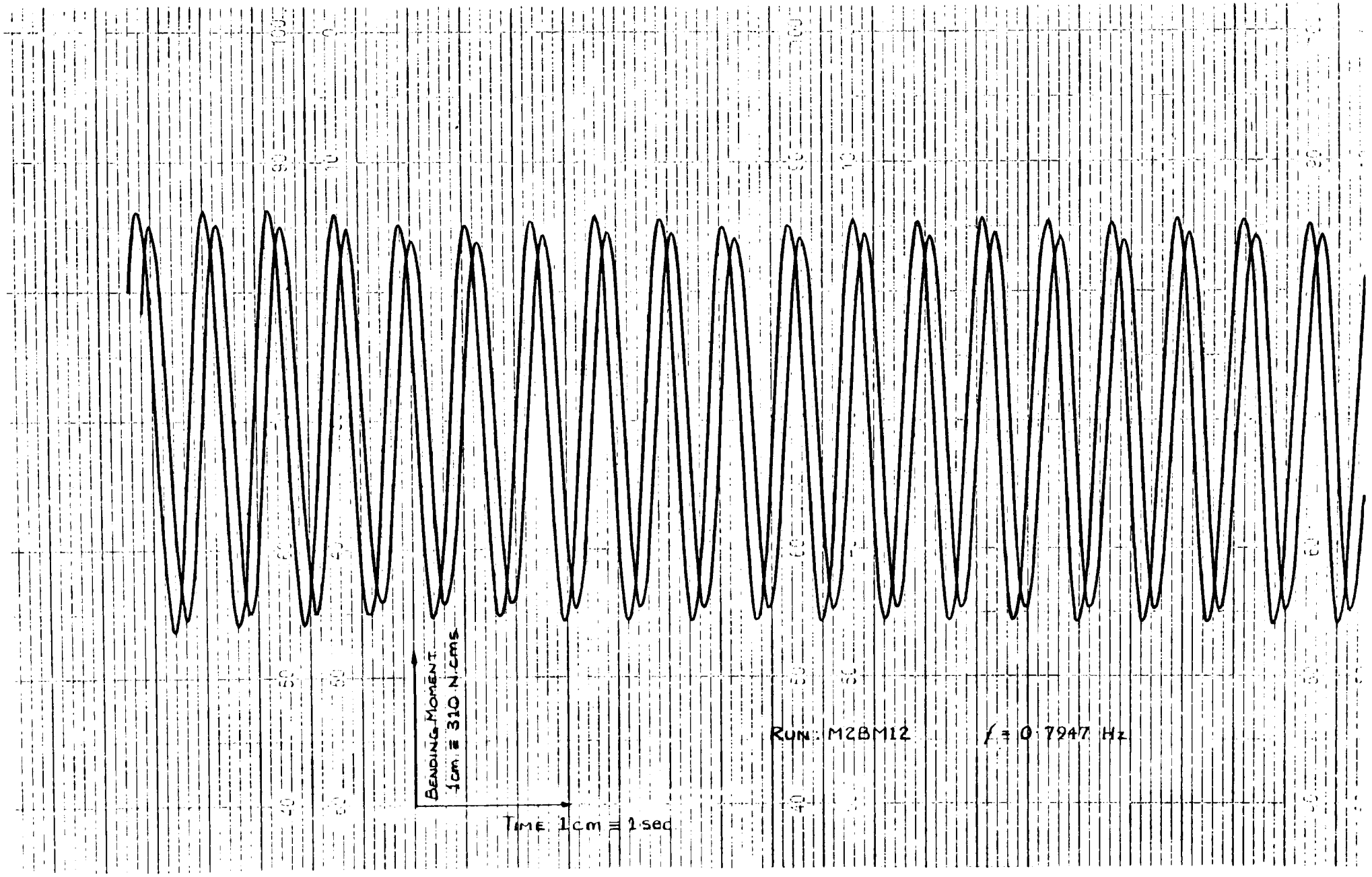
BENDING MOMENT
1cm ≡ 310 N.cms
TIME 1cm ≡ 1 sec
RUN: M2BM12
f = 0·7947 Hz

FIG. 8 -A

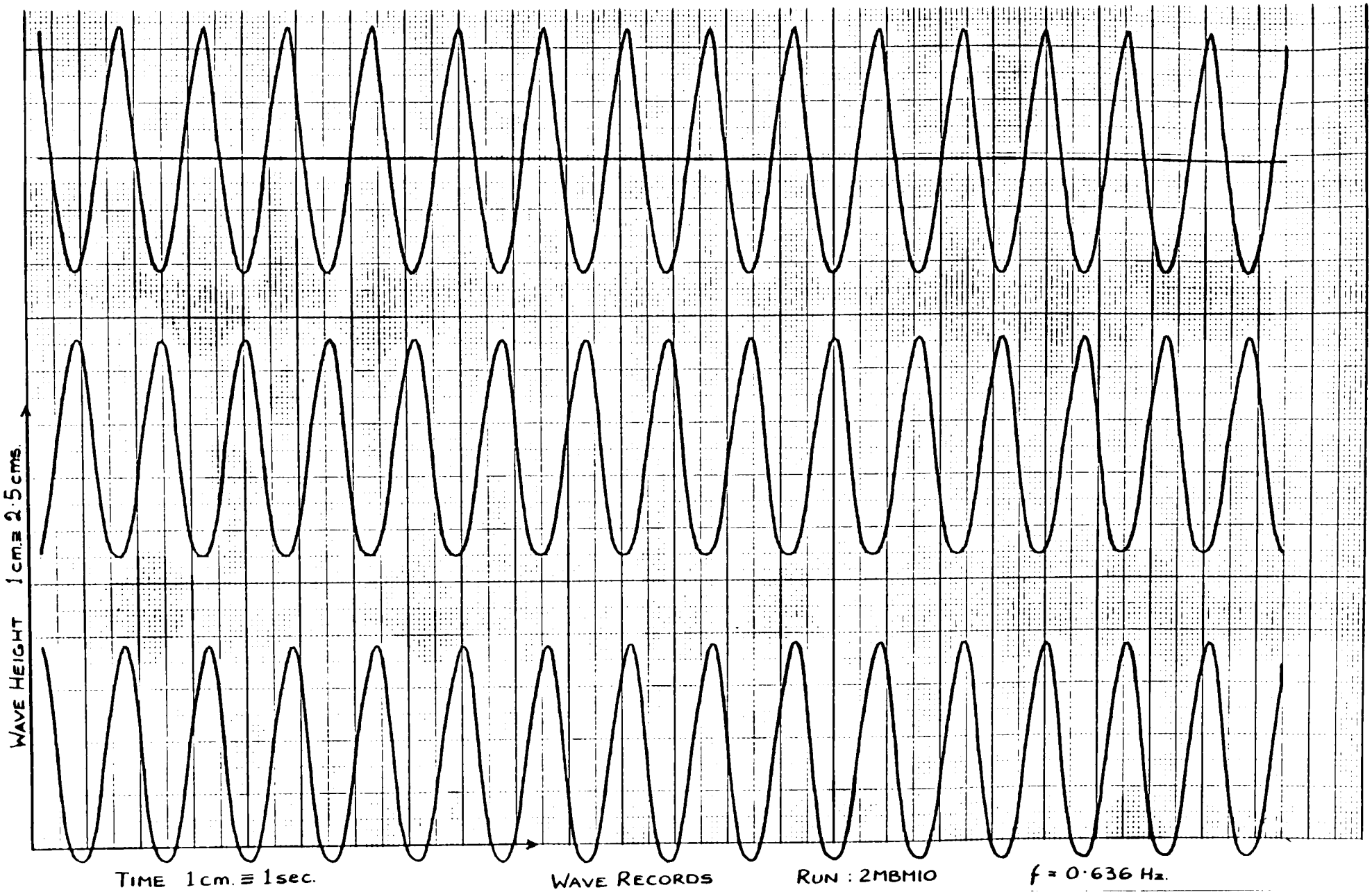
WAVE HEIGHT 1cm.≡ 2·5cms.
TIME 1cm. ≡ 1sec.
WAVE RECORDS
RUN : 2MBM10
f = 0·636 Hz.

FIG. 9

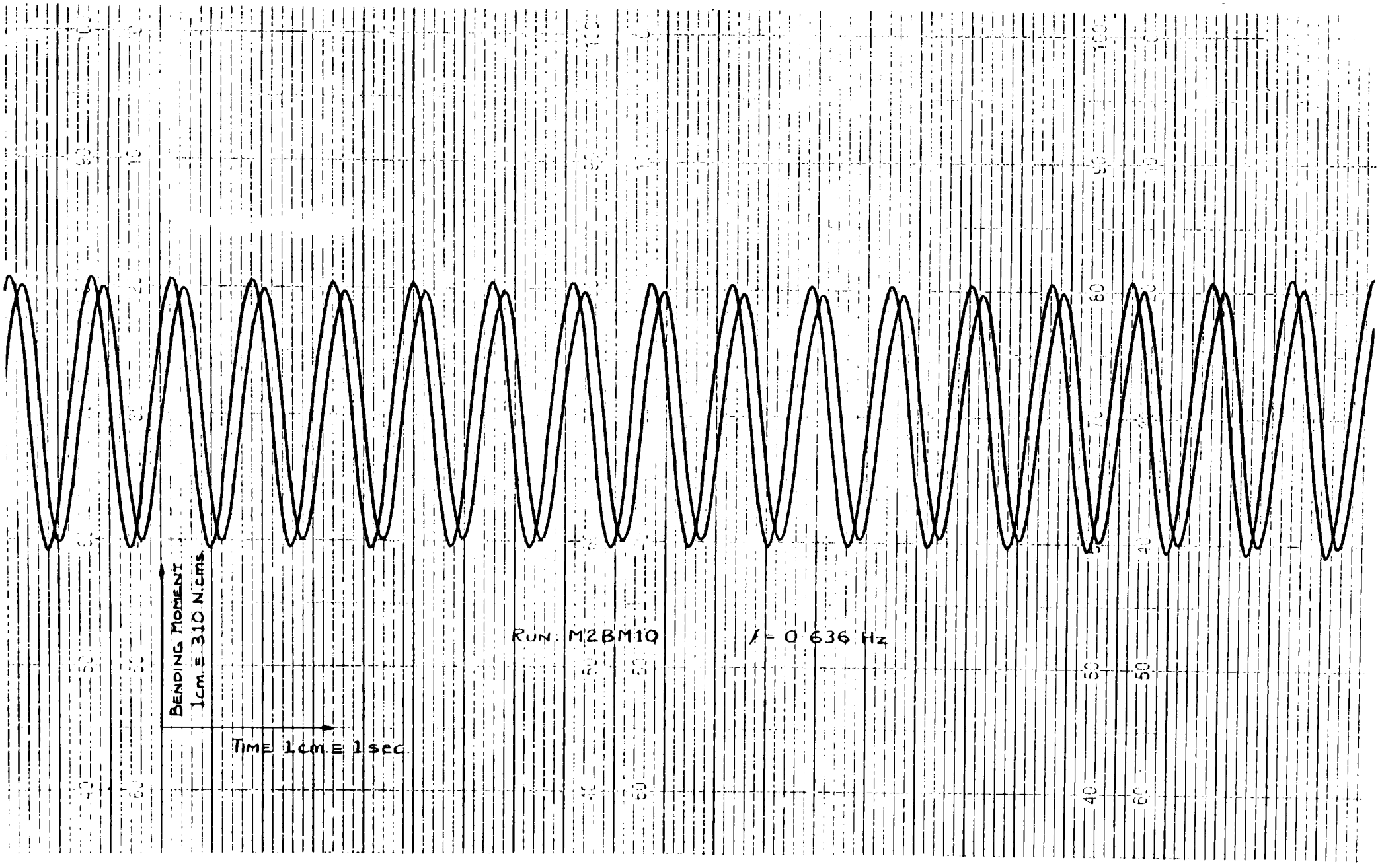
BENDING MOMENT
1cm.≡ 310 N.cms.
TIME 1cm.≡ 1sec
RUN M2BM10
f = 0 636 Hz

FIG. 9-A

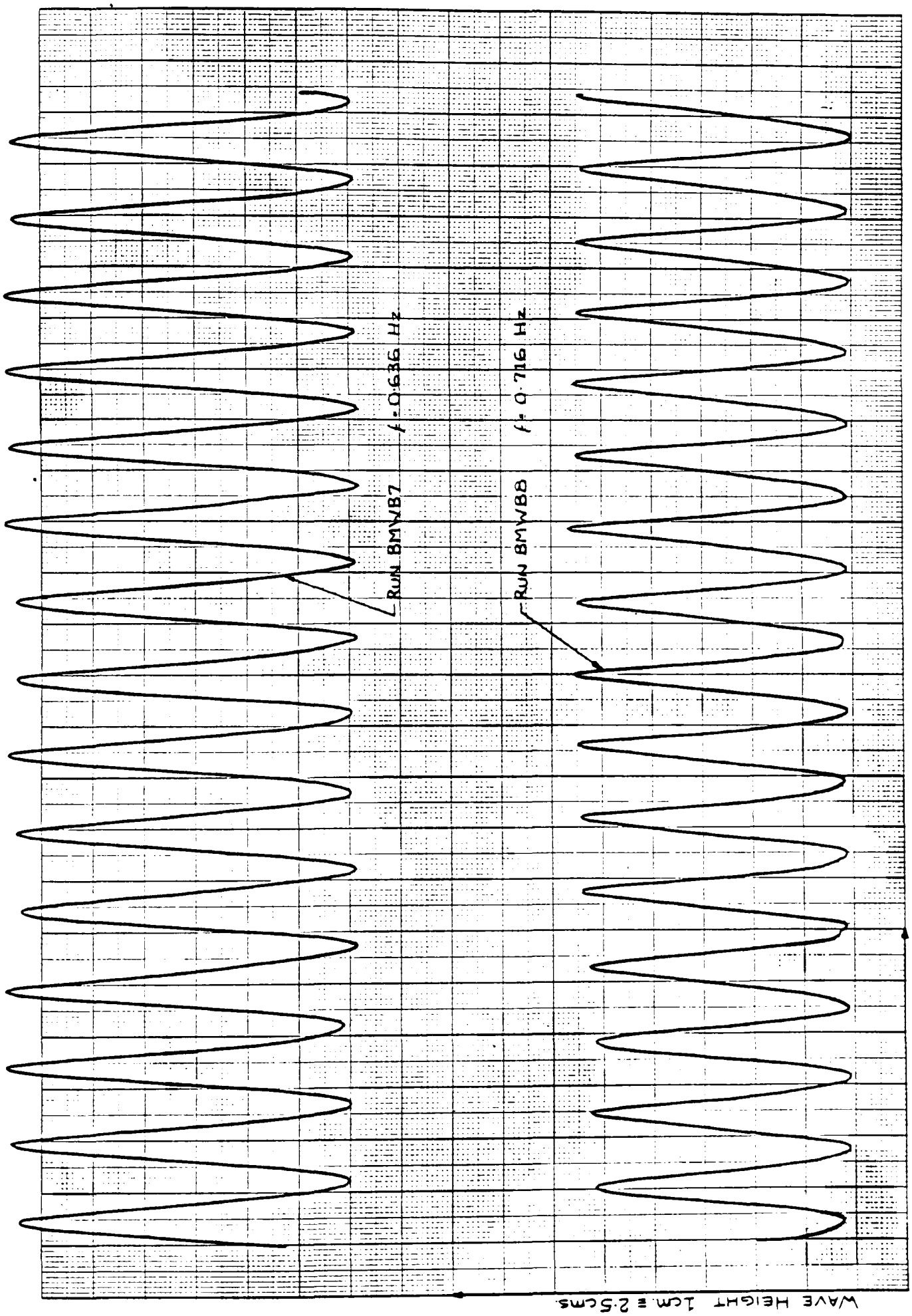

WAVE RECORDS

FIG. 10

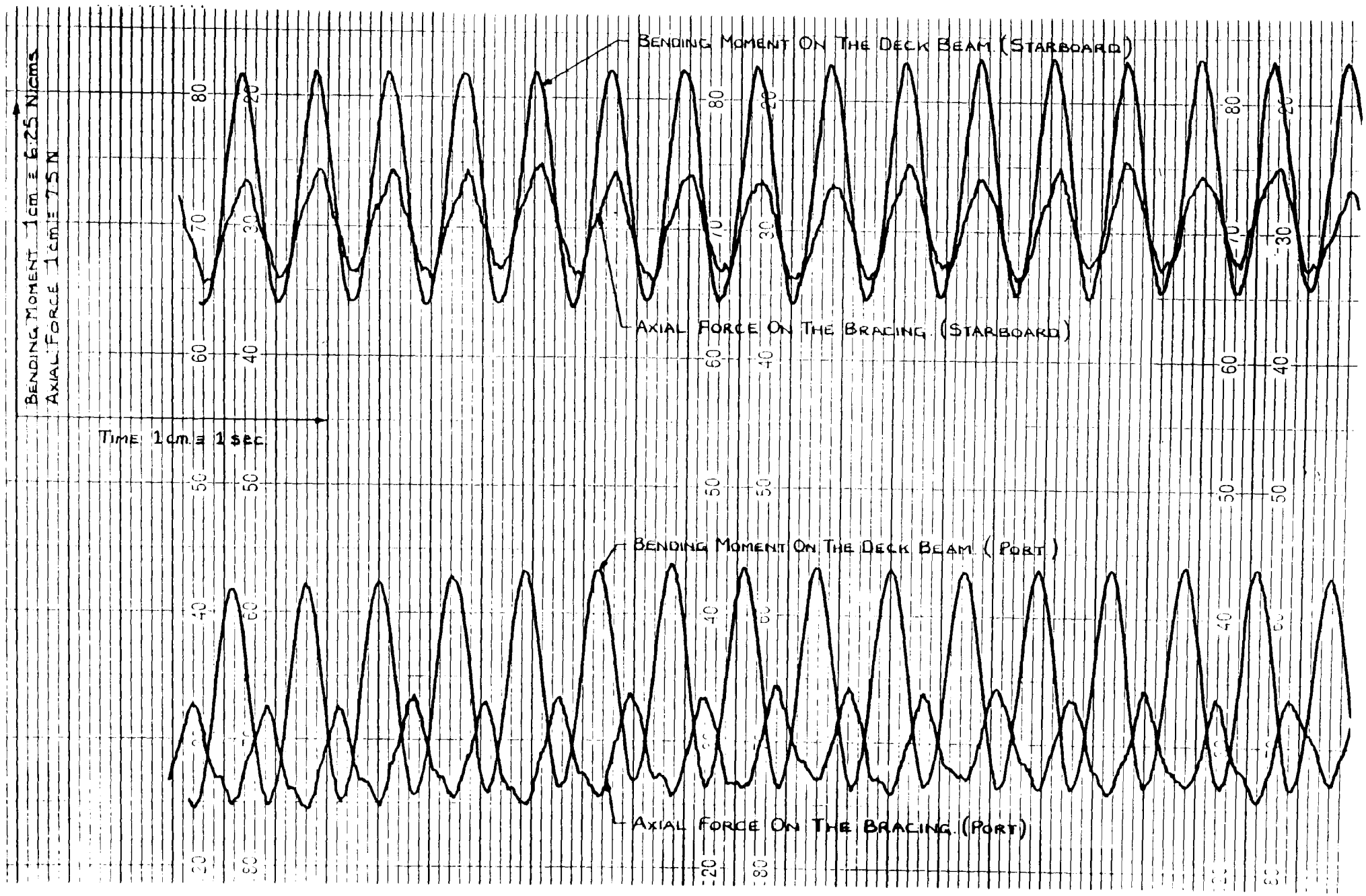
BENDING MOMENT ON THE DECK BEAM (STARBOARD)
AXIAL FORCE ON THE BRACING (STARBOARD)
BENDING MOMENT 1cm = 6.25 N/cms
AXIAL FORCE 1cm = 7.5 N
TIME 1cm = 1 sec.
BENDING MOMENT ON THE DECK BEAM (PORT)
AXIAL FORCE ON THE BRACING (PORT)

FIG. 10-A

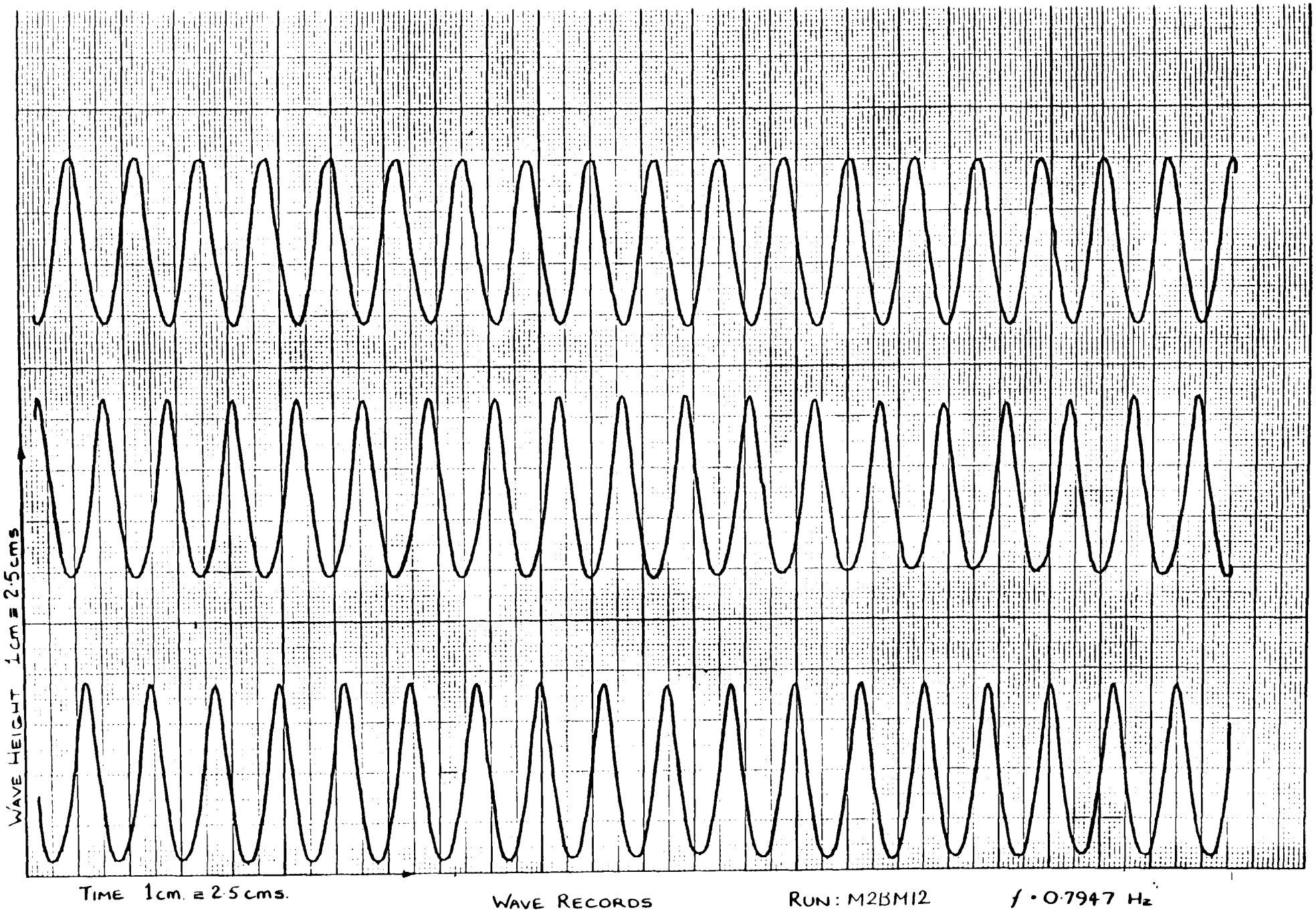
WAVE HEIGHT 1cm = 2.5cms
TIME 1cm = 2.5 cms.
WAVE RECORDS
RUN: M2BM12
f = 0.7947 Hz

FIG. 8

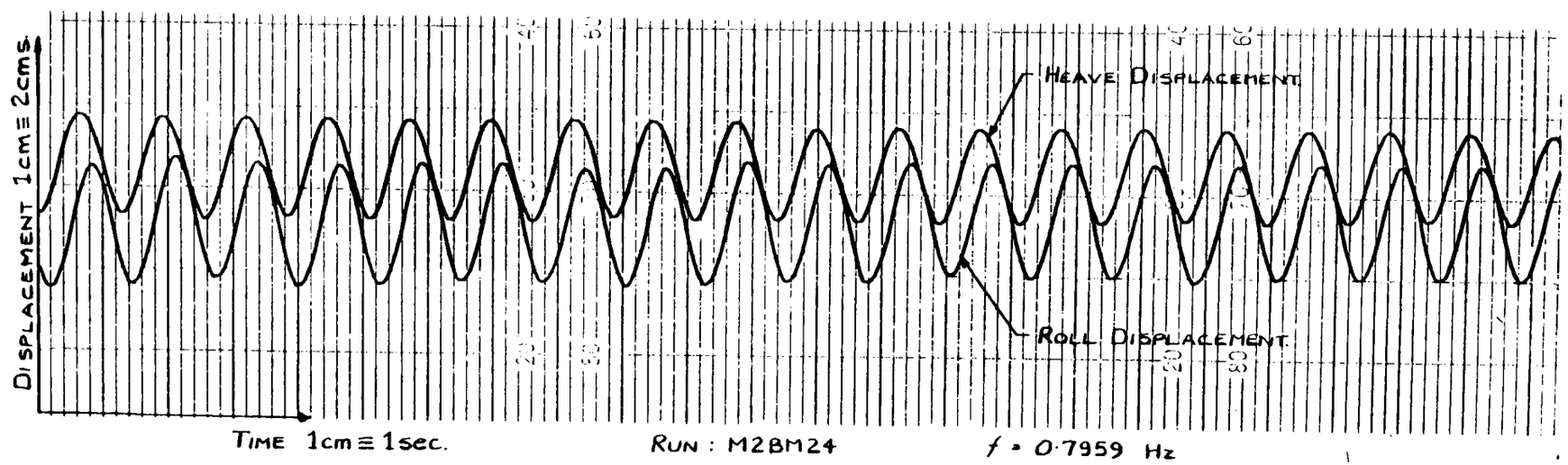
DISPLACEMENT 1cm ≡ 2cms
HEAVE DISPLACEMENT
ROLL DISPLACEMENT
TIME 1cm ≡ 1sec.
RUN : M2BM24
f = 0·7959 Hz

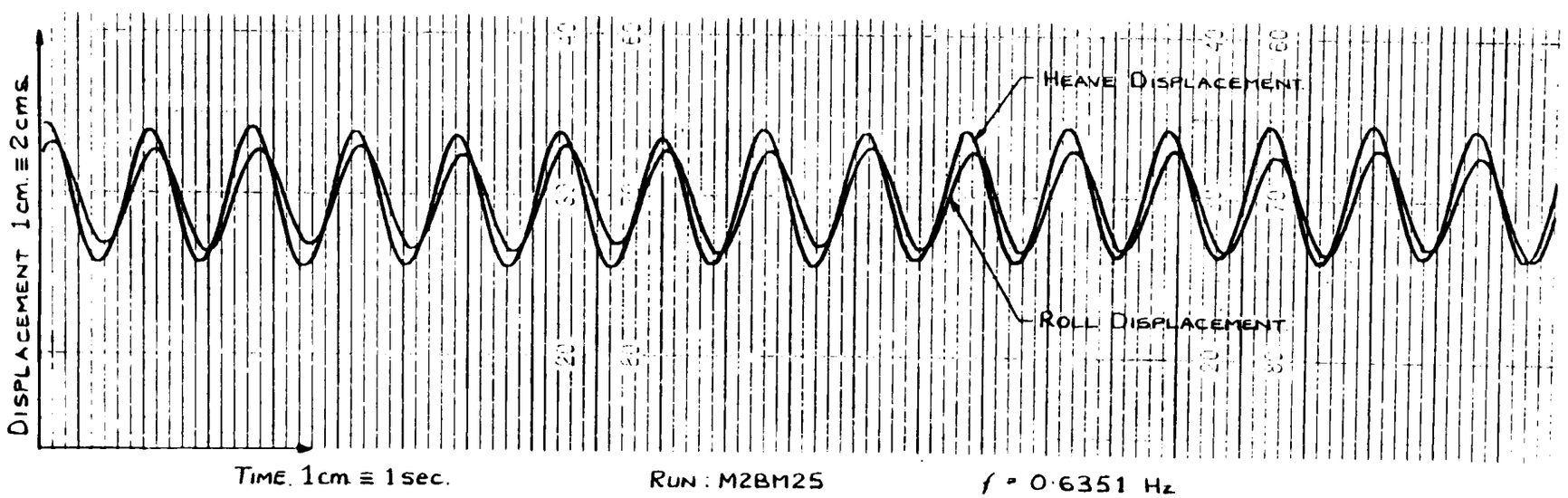
DISPLACEMENT 1cm. ≡ 2cms.
HEAVE DISPLACEMENT
ROLL DISPLACEMENT
TIME. 1cm ≡ 1sec.
RUN : M2BM25
f = 0·6351 Hz

FIG. 7-B

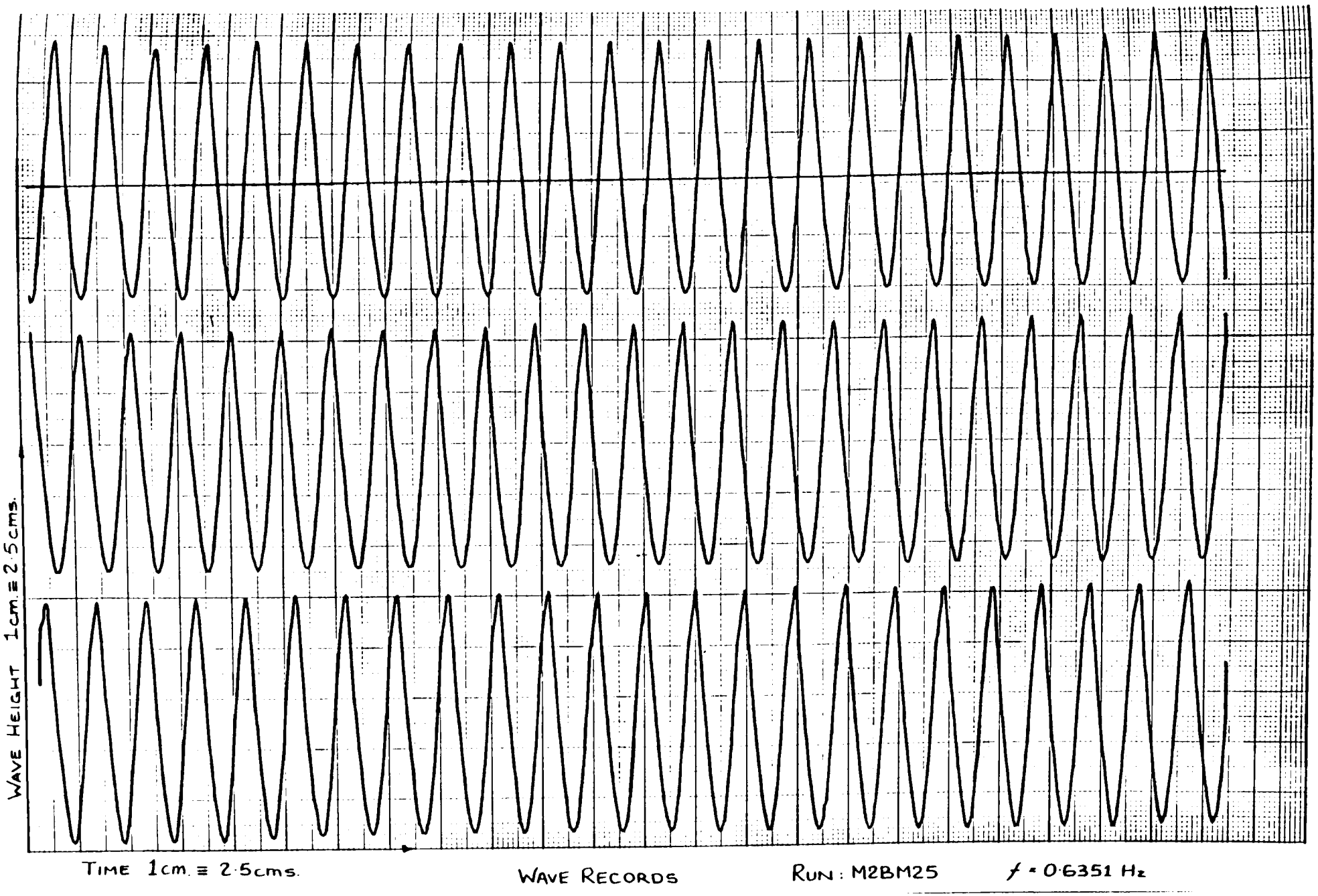
WAVE HEIGHT 1cm. ≡ 2·5cms.
TIME 1cm. ≡ 2·5cms.
WAVE RECORDS
RUN : M2BM25
f = 0·6351 Hz

FIG. 7-A

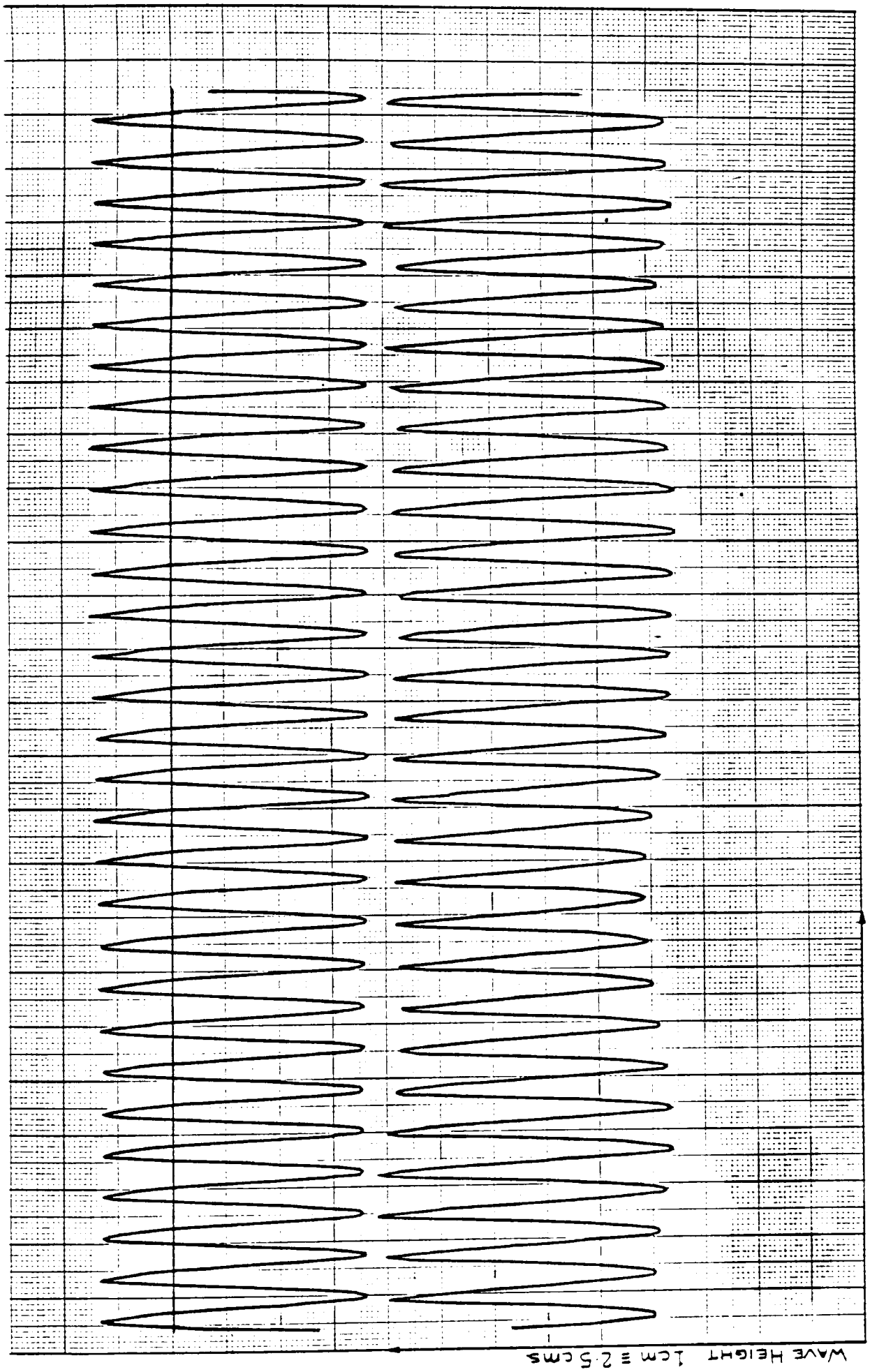
WAVE HEIGHT 1cm = 2.5 cms
TIME 1cm = 1 sec.
WAVE RECORDS
RUN : M2 BM24 f = 0.7959 Hz

FIG. 7

REFERENCES OF CHAPTER 1

1. BURKE, B.G.: "The Analysis of Motions of Semi-submersible Drilling Vessels in Waves", Society of Petroleum Engineers Journal, 1970. (Also published in the Proceedings of Offshore Technology Conference, Houston, 1969).

2. HOOFT, J.P.: "A Mathematical Method of Determining Hydrodynamically Induced Forces on a Semi-submersible", Transactions of the Society of Naval Architects and Marine Engineers, vol. 79, pp 28-70, 1971.

3. OO, K.M., MILLER, N.S.: "Semi-submersible Design: The Effect of Different Geometries on Heaving Response and Stability", Transactions of the Royal Institution of Naval Architects, 1976.

4. KORVIN-KROUKOVSKY, B.V.: "Investigation of Ship Motions in Regular Waves", Transactions of the Society of Naval Architects and Marine Engineers, vol. 63, 1955.

5. MOTORA, A.: "Stripwise Calculations of Hydrodynamic Forces due to Beam Seas", Journal of Ship Research, vol. 8, 1964.

6. GERRITSMA, J., BEUKELMAN, W.: "Analysis of the Modified Strip Theory for the Calculation of Ship Motions and Wave Bending Moments", Netherlands Ship Research Centre: TNO Report No. 96S, 1967.

7. HORTON, E.E., McCAMMON, L.B., MURTHA, J.P., PAULLING, J.R.: "Optimisation of Stable Platform Characteristics", Proceedings of Offshore Technology Conference, Houston, 1972.

8. MILLER, N.S.: "Comparison of Wave Excited Forces and Motion Response for a Series of Designs of Semi-submersibles and Tension Leg Platforms, Part I - General Background to and Description of Programme", Department of Naval Architecture and Ocean Engineering, Report No. SRC-NAI-02, Glasgow University, 1977.

9. De SOUZA, P.M., MILLER, N.S.: "Designs Based on Circular Caisson, Part II", Department of Naval Architecture and Ocean Engineering, Report No. SRC-NAI-03, Glasgow University, 1977.

10. BASSIOUNY, A.H., MILLER, N.S.: "Designs Based on Twin Rectangular Hulls with Two or More Columns per Hull - Part III", Department of Naval Architecture and Ocean Engineering, Report No. SRC-NAI-05, Glasgow University, 1977.

11. STRAHAN, J., MILLER, N.S.: "Designs Based on Twin Circular Columns with Two or More Columns per Hull - Part IV", Department of Naval Architecture and Ocean Engineering, Report No. SRC-NAI-06, Glasgow University, 1977.

12. KAMEL, H.A.: "An Automated Approach to Ship Structure Analysis", Transactions of the Society of Naval Architects and Marine Engineers, vol. 72, 1972.

13. MacNEAL, R.H., McCORMICK, C.W.: "The NASTRAN Computer Program for Structural Analysis", The Journal of Computers & Structures, vol. 1, 1971.

14. ZIENKIEWICZ, O.C. and CHEUNG, Y.K.: "The Finite Element Method in Structural and Continuum Mechanics", McGraw-Hill, 1967.

15. GOREN, Y., SPRINGEFT, C.N.: "Selection and Design of a Semi-Submersible Drilling Vessel", Proceedings of R.I.N.A. Symposium on Offshore Engineering, 1974.

16. BELL, A.O., WALKER, R.C.: "Stresses Experienced by an Offshore Mobile Drilling Unit", Proceedings of Offshore Technology Conference, Houston, 1971.

17. PEDERSEN, B., EGELAND, O., LANGFELDT, J.N.: "Calculation of Long Term Values for Motions and Structural Response of Mobile Drilling Rigs", Proceedings of Offshore Technology Conference, Houston, 1973.

18. PAULLING, J.R.: "Elastic Response of Stable Platform Structures to Wave Loading", Proceedings of the International Symposium on the Dynamics of Marine Vehicles and Structures in Waves, London, 1974.

19. YOSHIDA, K., ISHIKAWA, K., IADA, K.: "Periodic Response Analysis of Floating Framed Structures", Jornal of the Society of Naval Architects of Japan, Part 1, vol. 136, 1974, and Part 2, vol. 138, 1975.

20. PLANEIX, J.M., BELL, C.R., HUARD, G.: "Environment, Statistics and the Computer in the Design of Offshore Units, Particularly Semi-Submersible Ones", Proceedings of Oceanology International, Brighton, 1975.

21. ROBSON, J.D.: "An Introduction to Random Vibrations", Edinburgh University Press, 1963.

22. OCHI, M.K.: "On Prediction of Extreme Values", Journal of Ship Research, 1973.

23. MICHEL, W.H.: "Sea Spectra Simplified", Proceedings of Marine Technology, vol. 5, 1968.

24. STIANSEN, S.G., CHEN, H.H., LEE, F.H.: "Structural Response of a Twin Hull Semi-Submersible Platform in Waves", Gulf Section, Soceity of Naval Architects and Marine Engineers, 1978.

25. FUJISHIMA, K., ISHIDA, M., SATAKE, M., KATAYAMA, M.: "On the Design and Construction of Semi-Submersible Offshore Structures", Technical Review of Mitsubishi Heavy Industries Ltd., 1977.

26. SNIDER, W.D., BUFFLEBEN, G.J., HARRALD, J.R., BISHOP, K.F., CARD, J.C.: "Management of Mid-Atlantic Offshore Development Risks", Proceedings of Marine Technology, vol 14, 1977.

27. MOAN, T., HOLAND, I.: "Risk Assessment of Offshore Structures Experience and Principles", Proceedings of the 3rd International Conference on Structural Safety and Reliability, Trondheim, 1981.

REFERENCES OF CHAPTER 2

1. LAMB, H., "Hydrodynamics" 6th edition, Cambridge. Cambridge University Press, 1945.

2. WIEGEL, R.L., "Oceanographical Engineering", Prentice-Hall Inc., Englewood Cliff, New-Jersey, 1964.

3. WEHAUSEN, J.V. and LAITONE, E.V., "Surface Waves", Encyclopedia of Physics, Vol. 9, Springer-Verlag, Berlin, 446-778, 1960.

4. JOHN, F., "On the Motion of Floating Bodies", Comn. in Pure and Applied Mathematics, p.I, 1949.

5. GARRISON, C.Y., and CHOW, P.Y., "Wave Forces on Submerged Bodies" Journal of the Waterways, Harbors and Coastal Engineering Divisic Proc. ASCE, Vol. 98, No. WW3, pp.375-392, Aug. 1972.

6. HAVELOCK, T.H., "The Pressure of Water Waves upon a Fixed Obstacl Proceedings of the Royal Society A175, 1940.

7. STOKES, G.G., "On the Theory of Oscillatory Waves", Mathematical and Physical paper Vol. 1, Cambridge, Cambridge University Press, 1880.

8. SKJELBREIA, L., HENDRICKSON, J.A., "Fifth Order Gravity Wave Thec Proceedings Seventh Conference on Coastal Engineering, Vol. 1, Ch 10, 1961.

9. LIGHTHILL, J., "Waves and Hydrodynamic Loading", Opening Address Proceedings BOSS '79, London, 1979.

10. NEWMAN, J.N., "Marine Hydrodynamics", M.I.T. Press Cambridge, Massachusetts, 1977.

11. KENNARD, E.H., "Irrotational Flow of Frictionless Fluids, Mostly Invariable Density", David Taylor Model Basic Report : 2299, 1967

12. MORISON, J.R., O'BRIEN, M.P., JOHNSON, J.W., and SCHAAF, S.A., "T Force Exerted by Surface Waves on Piles", Petroleum Transactions, AIEM, Vol. 189, 1950.

13. KEULEGAN, G.R., CARPENTER, L.H., "Forces on Cylinders and Plates an Oscillating Fluid", Journal of Research of the National Bureau of Standards, Vol. 60, No. 5, May 1958.

14. SARPKAYA, T., "Vortex Shedding and Resistance in Harmonic Flow Ab Smooth and Rough Circular Cylinders at High Reynolds Numbers", Na Postgraduate School Technical Report No. NPS-59SL76021, 1976.

15. SARPKAYA, T., "In Line and Transverse Forces on Smooth and Sand-Roughened Cylinders in Oscillatory Flow at High Reynolds Numbers" Naval Postgraduate School Technical Report No. NPS-69SL76062, 197

16. HOGBEN, N., MILLER, B.L., SEARLE, J.W., and WARG, G., "Estimation Fluid Loading on Offshore Structures", NMI Report NMI R11, 1977.

17. ROSHKO, A., "Experiments on the Flow Past a Circular Cylinder at Very High Reynolds Number", Journal of Fluid Mechanics, No. 10 : 345-356, 1961.

18. BIDDE, D.D., "Wave Forces on a Circular Pile due to Eddy Shedding Ph.D. Thesis, University of California, Berkeley, California Technical Report No. HEL-9-16, 1970.

19. BASSET, A.B., "Treatise on Hydrodynamics", Vol. I, 1888.

20. BIERMANN, D., HERRNSTEIN, W.H., "The Interference Between Struts in Various Combinations", NACA Rep. 468, 1933.

21. GREKOUSSIS, C., MILLER, N.S., "The Resistance of Semi-Submersible I.E.S.S. Proceedings, Paper No. 1413, 1978.

22. BUSHNELL, M.J., "Forces on Cylinder Arrays in Oscillating Flow", Offshore Technology Conference Paper No : 2903, 1977.

23. SARPKAYA, T., "Wave Loading in the Drag/Inertia Regime with Particular Reference to Groups of Cylinders", Proceedings of Symposium on Mechanics of Wave-Induced Forces on Cylinders, Vol. 1978.

24. ROSS, C.W., "Large Scale Tests of Wave Forces on Piling", U.S. Co: of Engineers Beach Erosion Board, Tech. Mem. No. 11, 1959.

25. IPPEN, A.T., "Estuary and Coastline Hydrodynamics", McGraw-Hill B Co., 1966.

26. BORGMAN, L.E., "Computation of the Ocean-Wave Forces on Inclined Cylinders", Journal of Geophysical Research, Trans., AGU, Vol. 39 No. 5, 1958.

27. CHAKRABARTI, S.K., TAM, W.L., WOLBERT, A.L., "Total Forces on a Submerged Randomly Oriented Tube Due to Waves", Offshore Technolo Conference Paper No : 2495, 1976.

28. INCECIK, A., "A General Method for Calculating Wave Forces and Moments on Circular Cylinders", Department of Naval Architecture and Ocean Engineering, Glasgow University, Report No : NAOE-HL-79- 1979. (See also Chapter 2.)

29. BURSNALL, W.J., LOFTIN, W.J., "Experimental Investigation of the Pressure Distribution About a Yawed Circular Cylinder in the Crit: Reynolds Number Range", NACA TN-2463, 1951.

30. INCECIK, A., "Computer Programs for the Prediction of Structural Loads on Semi-Submersibles", Department of Naval Architecture and Ocean Engineering, Glasgow University, Report No : NAOE-HL-80-17, 1980. (See also Chapter 6.)

31. ACHENBACH, E., "Influence of Surface Roughness on the Cross-Flow Around a Circular Cylinder", Journal of Fluid Mechanics, Vol. 46, Pt. 2, 1971.

32. MILLER, B.L., "The Hydrodynamic Drag of Roughened Circular Cylind Proceedings of R.I.N.A., 1976.

33. MILLER, N.S., "OSFLAG 8 - Note on Wind Heeling Moments on Semi-Submersibles", Department of Naval Architecture and Ocean Enginee: Glasgow University, NAOE-HL-76-04,,1976.

34. OGILVIE, T.F., "First- and Second-Order Forces on a Cylinder Submerged under a Free Surface", Journal of Fluid Mechanics, Vol. 1963.

35. ABRAMOWITZ, M., STEGUN, I.A., "Handbook of Mathematical Functions with Formulas, Graphs, and Mathematical Tables", National Bureau Standards, 1964.

36. MILNE-THOMSON, L.M., "Theoretical Hydrodynamics", The MacMillan Press Ltd., 5th Edition, 1968.

37. SOMMERFELD, A., "Partial Differential Equations in Physics", Acad Press, New York, 1949.

38. ERINGEN, A.C., "Mechanics of Continua", John Wiley and Sons Ltd., 1967.

39. NICHOLSON, J.W., "The Pressure of Radiation on a Cylindrical Obstacle", Proceedings of Royal London Mathematical Society", No : 11, 1912.

40. MacCAMY, R.C., and FUCHS, R.A., "Wave Forces on Piles : A Diffraction Theory", Technical Memorandum No : 69, Beach Erosion Board, Corps of Engineers.

REFERENCES OF CHAPTER 3

1. HOOFT, J.P., "Hydrodynamic Aspects of Semi-Submersible Platforms". Ph.D. Thesis, Netherlands Ship Model Basin, Publication No. 400, Wageningen, 1972.

2. MILLER, N.S., "Effect of Geometry and Dimensions on Natural Heaving Period" in 'Semi-Submersibles and Tethered Buoyant Platforms - Some Design Considerations', Lecture notes for a course given 26-30th September, 1977, in Department of Naval Architecture and Ocean Engineering, Glasgow University, 1977.

3. SPIEGEL, MURRAY, R., "Vector Analysis". Shaum's Outline Series, McGraw-Hill Book Company, 1974.

REFERENCES OF CHAPTER 4

1. URSELL, F., "On the Heaving Motion of a Circular Cylinder on the Surface of a Fluid", Quarterly Journal of Mechanics and Applied Mathematics, Vol. II, Pt.2, 1949.

2. URSELL, F., "On the Rolling Motion of Cylinders in the Surface of a Fluid", Quarterly Journal of Mechanics and Applied Mathematics, Vol. II, Pt.3, 1949.

3. LEE, C.M., JONES, H., BEDEL, J.W., "Added Mass and Damping Coefficients of Heaving Twin Cylinders in a Free Surface", Naval Ship Research and Development Centre, Report No. 3695, 1971.

4. WEHAUSEN, J.V., "The Motion of Floating Bodies", Annual Review of Fluid Mechanics, Vol. 3, 1971.

5. VUGTS, J.H., "The Hydrodynamic Coefficients for Swaying, Heaving and Rolling Cylinders in a Free Surface", Netherlands Ship Research Centre TNO Report No: 112S., 1968.

6. RAWSON, K.J., TUPPER, E.C., "Basic Ship Theory", Logmans Publication, 1968.

7. YAMAMOTO, Y., "On the Oscillating Body Below the Water Surface", Journal of Zosen Kio Koi, Vol. 77, July, 1955.

8. NEWMAN, J.N., "The Damping of an Oscillating Ellipsoid Near a Free Surface", Journal of Ship Research, Vol. 5, no. 3, 1961.

9. NEWMAN, J.N., "The Exciting Forces on Fixed Bodies in Waves", Journal of Ship Research, Vol. 6, 1962.

10. BLAGOVESHCHENSKY, S.N., "Theory of Ship Motions", Dover, 1962.

11. KIM, C.H., and CHOU, F., "Motions of a Semi-submersible Drilling Platform in Head Seas", Marine Technology, 1973.

12. AMEY, H.B., and POMONIK, G., "Added Mass and Damping of Submerged Bodies Oscillating Near the Surface", Proceedings of Offshore Technology Conference, 1972.

13. FRANK, W., "Oscillation of Cylinders In or Below the Free Surface of Deep Fluids", David Taylor Model Basin Report No. 2375, Washington, D.C., 1967.

14. SALVADORI, M.G., and BARON, M.L., "Numerical Methods in Engineering Prentice Hall, 1952.

15. KREYSZIG, E., "Advanced Engineering Mathematics", John Wiley & Sons, Fourth Edition, 1979.

16. BATHE, K.J. and WILSON, E.L., "Stability and Accuracy Analysis of Direct Integration Methods", Intl. Jnl of Earthquake Engineering & Structural Dynamics, Vol. 1, No. 2, 1973.

17. NEWMARK, N.M., "A Method of Computation for Structural Dynamics", Jnl of the Engineering Mechanics Division, Proc. of the American Society of Civil Engineers, Vol. 85, No. EM 3, July, 1959.

18. "NAG" Fortran Library Manual, Vol. 1, Numerical Algorithms Group, Oxford, U.K., 1978.

REFERENCES OF CHAPTER 5

1. JACOBS, W.R., "The Analytical Calculation of Ship Bending Moments in Regular Waves", Journal of Ship Research, 1958.

2. JACOBS, W.R., DALZELL, J., "Theory and Experiment in the Evaluation of Bending Moments in Regular Waves", International Shipbuilding Progress Report, 1960.

3. OGILVIE, T.F., "On the Computation of Wave-Induced Bending and Torsion Moments", Journal of Ship Research, 1971.

4. CLOUGH, R.W., PENZIEN, J., "Dynamics of Structures", McGraw-Hill Ltd., 1975.

5. BISHOP, R.E.D., TAYLOR, R.E., JACKSON, K.L., "On the Structural Dynamics of Ship Hulls in Waves", Proceedings of R.I.N.A., 1973.

6. BISHOP, R.E.D., PRICE, W.S., "Hydroelasticity of Ships", Cambridge University Press, 1979.

7. TAYLOR, R.E., "Structural Dynamics of Fixed and Floating Platforms in Waves", Proceedings of the International Symposium on the Dynamics of Marine Vehicles and Structures in Waves, London, 1974.

8. DUNCAN, P.E., "Simple Models for the Dynamics of Deepwater Gravity Platforms", Engineering Seructures, Vol. 1979.

9. DUNKERLEY, S., "On the Whirling and Vibration of Shafts", Philosophical Transaction of the Royal Society, A Vol. 185, 1895.

10. THOMSON, W.T., "Vibration Theory and Applications", Prentice Hall Inc., 1965.

11. SANDSTROM, R.E., SMITH, N.P., "Eigenvalue Analysis as an Approach to the Prediction of Global Vibration of Deckhouse Structures", Marine Technology, Vol. 17, No. 3, 1980.

12. NASH, W.A., "Strength of Materials", Schaum's Outline Series, McGraw Hill Book Company, 1972.

13. GREGORY, M.S., "Linear Framed Structures", Longmans Green & Co. Ltd., 1966.

14. RUBINSTEIN, M.F., "Matrix Computer Analysis of Structures", Prentice Hall Series in Engineering of the Physical Sciences, 1966.

15. WILSON, E.L., BATHE, K.I., PETERSON, F.E., "SAP IV, A Structural Analysis Program for Static and Dynamic Response of Lsnear Systems", Report EERC-73-11 University of California, Berkeley, 1974.

16. ARALDSON, P.O., EGELAND, O., "General Description of SESAM-69", Practical Application of the Finite Element Method, NTH, Trondheim, 1971.

17. LIVESLEY, R.K., "Analysis of Rigid Frames by an Electronic Digital Computer", Engineering, Aug. 1957.

18. LIVESLEY, R.K., "Matrix Methods and Structural Analysis", Pergamon Press, 1964.

19. KATAYAMA, M., UNOKI, K., HATAKENAKA, K., TAKASUMI, U., "On Structural Response Analysis of Semi-Submersible Offshore Structures in Waves", Technical Review of Mitsubishi Heavy Industries Ltd., June, 1978.

20. OSTERGAARD, C. and PAYER, H., "Rationale Beurteilung der Festigkeit von Halbtauchern", Jahrbuch der Schiffbautechnischen Gesellschaft, 67 Band, 1973.

21. Correspondence with Norwegian Constructors, June 1980.

REFERENCES OF CHAPTER 6

1. "Fluid Forces Acting on Circular Cylinders for Application in General Engineering, Part 1: Long Cylinders in Two-Dimensional Flow", Engineering Sciences Data Item No. 70013, 1970.

2. HOGBEN, N., "Wave Loads on Structures", Proceedings of the behaviour of Offshore Structures Conference, Trondheim, 1976.

3. GREKOUSSIS, C. and MILLER, N.S., "Interference Drag Effects between Circular Cylinders with Particular Reference to Semi-Submersible Design", Department of Naval Architecture and Ocean Engineering Report No. NAOE-HL-09, Glasgow University, 1976.

REFERENCES OF APPENDIX 1

1. DALLY, J.M. and RILEY, W.F., "Experimental Stress Analysis", McGraw Hill Book Company, 1978.

NOMENCLATURE OF CHAPTER 2

x,y,z : Co-ordinates in the wave reference system

X,Y,Z : Co-ordinates in the structure reference system

$\vec{r}$: Space co-ordinate vector, $(= x\vec{i} + y\vec{j} + z\vec{k})$

$\vec{U}$: Velocity vector of the fluid particles

$\dot{\vec{U}}$: Acceleration vector of the fluid particles

X_i : Rigid-body motion of the structure

U_i : Components of velocity vector of the structure

$\dot{U}_i$: Components of the acceleration vector of the structure

$S(x,y,z)$: Mathematical description of a member surface

dS : Surface area element

w : Complex velocity potential of fluid

$\Phi,\Phi,\Phi_{F,L}$: Velocity potential of fluid

ϕ_o : Velocity potential of oncoming waves

ϕ_s : Velocity potential of scattered waves

ϕ_j : Velocity potential due to rigid body motion in j mode

ϕ_A : $\phi_o + \phi_s$

ψ : Stream function

$\vec{i},\vec{j},\vec{k}$: Orthogonal unit vectors of the structure reference system

∇ : The vector differential operator

$$= \frac{\partial}{\partial x}\vec{i} + \frac{\partial}{\partial y}\vec{j} + \frac{\partial}{\partial z}\vec{k} \quad \text{or}$$

$$= \frac{\partial}{\partial r}\vec{e}_r + \frac{1}{r}\frac{\partial}{\partial \theta}\vec{e}_\theta + \frac{\partial}{\partial y}\vec{j}$$

$\vec{e}_r,\vec{e}_\theta,\vec{j}$: Orthogonal unit vectors of the cylindrical co-ordinate system

F_x,F_y,F_z : Wave loading on a member along x, y, z axes respectively

A_s : Cross-sectional area of a member

Re : Real part of a complex equation

ω : Wave or motion frequency (Rad/Sec)

t	:	Time
T	:	Wave period
g	:	Gravitational acceleration
ρ	:	Density of fluid
H_w	:	Wave height
λ	:	Wave length
k	:	Wave number ($= 2\pi/\lambda$)
$\vec{n}$	:	Normal vector of the surface of a member
C	:	Wave celevity ($= \lambda/T$)
ξ,η,ζ	:	Co-ordinates of a point on the surface of a member
G	:	Green function given
A_m	:	Numerical constant to define the scattering potential
J_m	:	Bessel function of the first kind
Y_m	:	Bessel function of the second kind
$H_m^{(\ )}$	:	Hankel function of the first kind ($= J_m + i\ Y_m$)
I_m	:	Modified Bessel function
p	:	Hydrodynamic pressure
p_A	:	Atmospheric pressure
D	:	Diameter of a circular cylinder
R	:	Radius of a circular cylinder
S_M	:	Surface of a member
S_c	:	Surface of a control volume
m_{ij}	:	Added-mass tensor
V	:	Volume of a member
T	:	Kinetic energy of fluid
A_{ij}	:	Dipole moments defined in equation (43)
Γ	:	Circulation
k_{ij}	:	Added-mass coefficient tensor
C_M	:	Inertia coefficient ($= 1 + K_{ii}$)
F_I	:	Inertia Force

C_D : Drag coefficient

F_D : Drag force

A_L : Projected area

ν : Kinematic viscosity

F_T : Total inertia and drag force

k : Roughness

A_n, B_n : Fourier coefficients

C_L : Lift coefficients

f_v : Vortex shedding frequency (Hz)

ℓ : Length of a member

d : Depth of a member; it is also used as the distance between two cylinders

h : Water depth, or distance between water surface and a cylinder axis

η : Wave elevation

E : Extensional motion of fluid particles defined in equation (108)

α_m : Coefficients used in equation (138-A)

N_m, θ_m : Variables defined in equations (149) and (149-A) respectively

f_D : A function used in equation (151)

$\Phi_{o,s}, \Phi_{o,s}$: Velocity potential of oncoming waves in shallow water

$\Phi_{s,s}$: Velocity potential of scattered waves in shallow water

η_s : Wave elevation in shallow water

C_s : Wave celevity in shallow water

k_s : Wave number in shallow water

p_s : Hydrodynamic pressure in shallow water

ε_n : Coefficients defined in equation (160)

$\alpha, \beta, \alpha', \beta'$: Coefficients used in equations (77 - 79) and (83 - 85)

(s) : Subscripts (s) are used in the second-order force equations

NOMENCLATURE OF CHAPTER 3

x,y,z	:	Co-ordinates in the wave reference system
X,Y,Z	:	Co-ordinates in the structure reference system
u,v,w	:	Co-ordinates in a member reference system
F_y	:	Hydrodynamic force on a circular disk due to rigid-body acceleration of the disk oscillating along y axis
U_x,U_y,U_z	:	Components of the velocity vector of the fluid particles in x,y,z directions respectively
$\dot{U}_x,\dot{U}_y,\dot{U}_z$	:	Components of the accelaration vector of the fluid particles in x,y,z directions respectively
p	:	Hydrodynamic pressure
R	:	Radius of a circular cylinder
D	:	Diameter
ρ	:	Density of fluid
g	:	Gravitational acceleration
K_1	:	A coefficient defined in equation (2) in order to take the effect of three dimensionality into account
k_{ij}	:	Added-mass coefficient tensor
C_D	:	Drag coefficient
β_{ij}	:	Coefficients of a tensor defined in equation (6) in order to transfer the co-ordinates defined in the wave reference system to the structure reference system
α_{ij}	:	Coefficients of a tensor defined in equation (9) in order to transfer the co-ordinates defined in the structure reference system to a member reference system
X_o,Y_o,Z_o	:	Co-ordinates of the origin of the structure reference system

$\vec{i},\vec{j},\vec{k}$	:	Orthogonal unit vectors of the structure reference system
$\vec{e}_1,\vec{e}_2,\vec{e}_3$	:	Orthogonal unit vectors of the member reference system
X_1,Y_1,Z_1,X_2,Y_2,Z_2	:	Ends co-ordinates of a member defined in the structure reference system
ℓ	:	Member length
H_w	:	Wave height
ω	:	Wave frequency (Rad./Sec.)
k	:	Wave number ($= 2\pi/\lambda$)
λ	:	Wave length
G	:	Centre of gravity of the structure
$\vec{n}$	:	Normal unit vector of the surface of a member
$\vec{AB},\vec{GB},\vec{GA},\vec{AP}$	:	Space vectors defined in equation (10)
$[Q]$	:	Equation of a plane defined in equations (12) and (13)
r,θ,u	:	Polar co-ordinates in a member reference system
∇	:	The vector differential operator $= \frac{\partial}{\partial u}\vec{e}_1 + \frac{\partial}{\partial v}\vec{e}_2 + \frac{\partial}{\partial w}\vec{e}_3$
A,B,C	:	Variables defined in equation (17)
A',B',C'	:	Variables defined in equation (21-1)
FP	:	Wave pressure force
FA	:	Wave acceleration force
FV	:	Wave velocity force
$\vec{FT}$	:	Total wave force vector
$\vec{M}$	:	Total moment vector due to the wave forces on the structure
$\vec{m}_A$	:	Moment vector calculated about the origin of the member reference system

m_G	:	Moment vector calculated about the origin of the structure reference system
$\vec{r}$	:	Position vector shown in figure 2
a,b,c	:	Coefficients of the moment vector defined in equation (46)
$[A],[B],[C],[T]$	:	Matrices defined in equation (47)

Subscripts u,v,w denote the forces calculated along u,v,w axes respectively.

Subscript (m) denotes the forces and moments expressed in a member reference system.

Subscript (s) denotes the forces and moments expressed in the structure reference system.

(i) denotes the calculations carried out on an individual member.

NOMENCLATURE OF CHAPTER 4

X,Y,Z	:	Co-ordinates in the structure reference system
u,v,w	:	Co-ordinates in a member reference system
$\vec{k},\vec{j},\vec{k}$	:	Orthogonal unit vectors of the structure reference system
$\vec{e}_1,\vec{e}_2,\vec{e}_3$	:	Orthogonal unit vectors of the member reference system
X_j	:	Components of the rigid-body motion vector
U_j	:	Components of the rigid-body velocity vector
$\dot{U}_j$	:	Components of the rigid-body acceleration vector
ω	:	Motion frequency (Rad./Sec.)
Φ	:	Velocity potential of fluid due to rigid-body motion

ϕ_j : Velocity potential of fluid due to unit rigid-body motion

$\vec{n}$: Normal unit vector of the surface of a member

$\vec{u}$: Rigid-body translational velocity vector

$\vec{\Omega}$: Rigid-body rotational velocity vector

$\vec{r}, \vec{r}', \vec{r}_o$: Space co-ordinate vectors shown in figure 1

R_e : Real part of a complex equation

ρ : Density of fluid

$\vec{F}$: Hydrodynamic force vector due to rigid-body motion

$\vec{M}$: Hydrodynamic moment vector due to rigid-body motion

F_i : Hydrodynamic force and moment vector components

C_{ij} : Coefficients defined in equations (9), (10) and (13)

m_{ij} : Added-mass tensor of a body oscillating in an unbounded fluid

a_{ij} : Added-mass tensor of a body oscillating near or on the free-surface

b_{ij} : Damping coefficients tensor of a body oscillating near or on the free-surface

$\vec{R}, \vec{r}, \vec{AC}$: Space co-ordinate vectors defined in figure 3

α_{ij} : Coefficients of a tensor used in equations (18-A), (19) and (20) in order to transfer the co-ordinates defined in the structure reference system to a member reference system

A(u), B(u), C(u)
Al(u), Bl(u), Cl(u) : Variables defined in equation (23)

$\dot{A}(u), \dot{B}(u), \dot{C}(u)$
$\dot{A}l(u), \dot{B}l(u), \dot{C}l(u)$: Variables defined in equation (24)

a, b, c, F1, F2, F3 : Coefficients of the force vector defined in equation (28)

d, e, f, a', b', c',
M_2, M_3 : Coefficients of the moment vector defined in equation (28-A)

$[T], [AM], [AT], [AlF], [DM]$	:	Matrices defined in equation (29)
Q_1, Q_2	:	Operators defined in equation (29)
$[TM], [Ml], [G], [BT], [AlM]$	:	Matrices defined in equation (30)
g	:	Graviational acceleration
R	:	Radius of cylinder
k_{ij}	:	Coefficients of added-mass tensor of a body oscillating in an unbounded fluid
ℓ	:	Length of member
X_1, Y_1, Z_1	:	End co-ordinates of a member defined in the structure reference system
$[FT]$	:	Total hydrodynamic force matrix
$[MT]$	:	Total hydrodynamic moment matrix
$S(x,y,z)$	:	Mathematical description of a member surface
dS	:	Surface area element
G	:	Green's function defined in equation (13)
f	:	Source strength defined in equation (13)
α	:	A variable defined in equation (45)
a,b	:	Variables defined in equation (48)
k	:	Wave number $(=2\pi/\lambda)$
λ	:	Wave length
H_w	:	Wave height
β	:	Angle of oncoming wave propagation
C_D	:	Damping coefficient
A_w	:	Total water plane area of surface piercing members
∇	:	Displacement of the floating structure
GM_T, GM_L	:	Transverse and longitudinal metacentric heights respectively
KB	:	Centre of immersed volume
BM	:	I/∇

I_T : Total moment of inertia of the water plane area of surface piercing members about X axis

I_L : Total moment of inertia of the water plane area of surface piercing members about Z axis

K_G : Centre of gravity of the floating structure

ρ_M : Mass density

M : Total mass of the structure

$\vec{r}_i, \vec{r}_A, \vec{r}_G$: Position vectors shown in figure 8

I_{XX}, I_{YY}, I_{ZZ} : Mass moment of inertia about X,Y,Z axes respectively

$I_{XY}, I_{YX}, I_{XZ}, I_{ZX}$ I_{YZ}, I_{ZY} : Mass moment of inertia values defined in eqautions (61-D),(61-E),(61-F)

$i_{XX}, i_{XY}, i_{ZZ}, i_{XY}$ i_{XZ}, i_{YZ} : Mass moment of inertia values defined in equations (65-A) - (65-F)

[M],[C],[BM],[MH1] [MH2],[CH1],[CH2] : Matrices defined in equation (68)

[K] : The restoring force matrix defined in equation (22)

$[\ddot{X}] = |\dot{U}|$: Column matrix of acceleration of the structure

[X] : Column matrix of translational and rotational displacements of the structure

ω_n : Natural frequency (Rad./Sec.)

α : Phase angle between the force (or moment) and the rigid-body motion

d : A constant defined in equation (71-D)

Q : Magnification factor defined in equation (72)

a,b,c : Co-ordinates of a point A on the structure given in the structure reference system

[RC] : Matrix defined in equation (83)

[MC],[CC],[X]* : Matrices defined in equation (83-A)

$[F_W]$: Wave force matrix

$[\Delta f_1], [\Delta f_2], [\Delta f_3]$: Incremental form of equation of motion defined in equation (86)

Δt	:	Time increment
ΔX	:	Displacement increment
τ	:	Time
$[\Delta P_w]$	:	Wave load increment matrix
$[\bar{K}]$	:	Stiffness increment matrix

Subscripts (M) denotes the velocities, accelerations, forces and moments expressed in a member reference system.

Subscripts (S) denotes the velocities, acceler ations, forces and moments expressed in the structure reference system.

Subscripts (T) denotes translational acceleration and velocity vector components.

Subscripts (R) denotes rotational acceleration and velocity vector components.

NOMENCLATURE OF CHAPTER 5

M(X)	:	Mass distribution of the ship along X axis
p(X,t)	:	Structural load distribution along the ship length
SF(X,t)	:	Shear force distribution along the ship length
BM(X,t)	:	Bending moment distribution along the ship length
ℓ	:	Ship length
E	:	Elasticity modulus
A	:	Sectional areas
I	:	Moment of inertia of ship cross-sections

$f_w(X,t)$	:	Distribution of wave loading along the ship length
$M'_{22}(X)$	:	Distribution of added-mass of the ship in heave mode of motion
$C_{22}(X)$	:	Distribution of damping coefficients of ship sections in heave mode of motion
$K_{22}(X)$	:	Distribution of restoring coefficients of ship sections in heave mode of motion
$y_d(X,t)$	:	Vertical displacements due to dynamic loading on the ship
$\phi(X)$	:	Shape function
$T(t)$	:	Variation of amplitude of the vertical displacements of the ship
ω	:	Natural frequency of rigid body oscillations of the ship (Rad./Sec.)
A_1, A_2, A_3, A_4	:	The coefficients defined in equation (14)
$SF(u,t)$	:	Shear force distribution along the members of the floating structure shown in Fig. 2
$BM(u,t)$	:	Bending moment distribution along the members of the floating structure shown in Fig. 2
$AF(u,t)$	:	Axial force distribution along the members of the floating structure shown in Fig. 2
u,v,α	:	Local co-ordinates shown in Fig. 3
H,B,D	:	Height, beam and draft of the floating structure shown in Fig. 2 respectively
Δu	:	Increments along the u axis
f_u, f_v, f_w	:	Wave forces along u,v and w axes respectively
$\overline{SF}, \overline{BM}, \overline{AF}$	:	Average shear force, bending moment and axial force respectively
X,Y,Z	:	Co-ordinates in the structure reference system

$\vec{i},\vec{j},\vec{k}$	:	Orthogonal unit vectors of the structure reference system
X_i	:	Translational and rotational rigid-body displacements
M	:	Mass of the floating structure shown in Fig. 2
M'_{22}	:	Added-mass of the floating structure shown in Fig. 2 in heave mode of motion
C_{22}	:	Damping coefficient of the structure shown in Fig. 2 in heave mode of motion
K_{22}	:	Restoring coefficient of the structure shown in Fig. 2 in heave mode of motion
F_1,F_2,F_3,F_4,F_5	:	Mass-inertia, hydrodynamic and restoring forces on the structure shown in Fig. 2 respectively
I_{XX}	:	Mass moment of inertia of the structure shown in Fig. 2 in roll mode of motion
I'_{XX}	:	Added-mass moment of inertia of the structure shown in Fig. 2 in roll mode of motion
C_{44}	:	Damping coefficient of the structure shown in Fig. 2 in roll mode of motion
K_{44}	:	Restoring coefficient of the structure shown in Fig. 2 in roll mode of motion
$\vec{M}_1,\vec{M}_2$	:	Moment vectors due to rigid-body inertia force and hydrodynamic forces respectively
b_{ij}	:	Damping coefficients tensor of a body oscillating near or on the free-surface
$U_i,\dot{U}_i$	:	Components of rigid-body velocity and acceleration vector respectively
E	:	The distance between the centre of gravity of the structure shown in Fig. 2 and the base line. (See also Fig. 15.)
g	:	Gravitational acceleration

ρ	:	Density of fluid
R	:	Radius of the columns of the structure shown in Fig. 2
GM_T	:	Transverse metacentric height
∇	:	Displacement of the structure shown in Fig. 2
ε	:	Constant defined in equations (56),(58),(62),(64)
a_{ij}	:	Added-mass tensor of a body oscillating near or on the free-surface
$F_{1,u}, F_{1,v}$	:	Rigid-body motion induced forces on mass (A) shown in Fig. 28 in u and v directions respectively
α,β,γ	:	Phase angles defined in equation (66)
m	:	Mass of object A
m'_{ii}	:	Added-mass tensor of object A
k_{ii}	:	Stiffness of the beam shown in Fig. 18
$\omega_{n,ii}$	:	Natural frequencies of the beam-mass system shown in Figs 18 and 19
$Q_{n,ii}$	:	Magnification factors defined in equation (72)
$m_i, m''_{i,jj}$	:	Masses and added-masses of the system shown in Fig. 21 respectively
k_{ij}	:	Stiffness coefficients of the system shown in Fig. 21
δ_{ij}	:	Flexibility influence coefficients of the system shown in Fig. 21
$\omega_{n,j}$	:	Natural frequencies of the system shown in Fig. 21
M_i	:	$m_i + m'_{i,jj}$
$M_i + M''_{i,jj}$	:	Masses and added-masses of the structure shown in Fig. 22
A_w	:	Water plane area of the structure shown in Fig. 22

[f] : Member force matrix of the member shown in Fig. 35. (Defined in the member reference system.)

[k] : Stiffness matrix of the member shown in Fig. 35

[d] : Displacement matrix of the member shown in Fig. 35. (Defined in the member reference system.)

[F] : Member force matrix of the member shown in Fig. 35. (Defined in the structural reference system.)

[Δ] : Displacement matrix of the member shown in Fig. 35. (Defined in the structural reference system.)

[T] : Transformation matrix which converts forces and displacements defined in the member reference system to the structural reference system

[S] : Matrix defined in equation (124)

R : Reaction forces on the structure shown in Fig. 39